National Research Council Canada
Conseil national de recherches Canada

PROCEEDINGS
VOLUME I

SYMPOSIUM/WORKSHOP ON SERVICEABILITY OF BUILDINGS (MOVEMENTS, DEFORMATIONS, VIBRATIONS)

May 16-18, 1988

University of Ottawa
Ottawa, Ontario, Canada

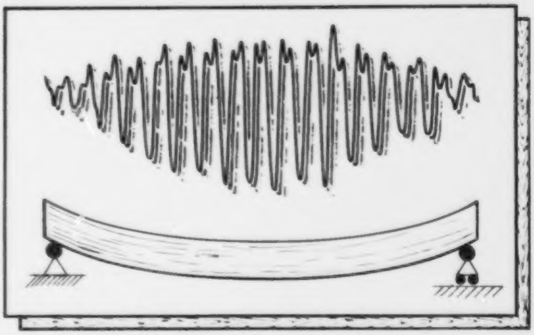

COMPTE RENDU
VOLUME I

COLLOQUE-ATELIER SUR LA TENUE EN SERVICE DES BÂTIMENTS (MOUVEMENTS, DÉFORMATIONS, VIBRATIONS)

16 au 18 mai 1988

Université d'Ottawa
Ottawa (Ontario), Canada

Canadä

Sold by:

Publication Sales & Distribution
National Research Council Canada
Ottawa, ON, Canada
K1A 0R6

Price: $50.00 (Vols. I & II)

DSS: NR15-31/1988E
ISBN: 0-660-12788-1 (set)
NRCC: 28822

Vendu par:

Vente et diffusion des publications
Conseil national de recherches Canada
Ottawa, ON, Canada
K1A 0R6

Prix: 50,00 $ (Vols. I & II)

MAS: NR15-31/1988E
ISBN: 0-660-12788-1 (série)
CNRC: 28822

PROCEEDINGS

VOLUME I

SYMPOSIUM/WORKSHOP ON SERVICEABILITY OF BUILDINGS

(MOVEMENTS, DEFORMATIONS, VIBRATIONS)

May 16-18, 1988

University of Ottawa
Ottawa, Ontario, Canada

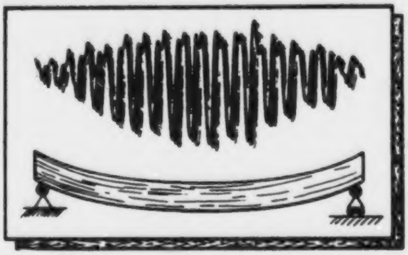

COMPTE RENDU

VOLUME I

COLLOQUE-ATELIER SUR LA TENUE EN SERVICE DES BÂTIMENTS

(MOUVEMENTS, DÉFORMATIONS, VIBRATIONS)

16 au 18 mai 1988

Université d'Ottawa
Ottawa (Ontario), Canada

89-04914/

ORGANIZING COMMITTEE/COMITÉ ORGANISATEUR

D.E. Allen Co-chairman/Coprésident	National Research Council Canada, Ottawa/Conseil national de recherches Canada, Ottawa
J.H. Rainer Co-chairman/Coprésident	National Research Council Canada, Ottawa/Conseil national de recherches Canada, Ottawa
R. Bergmann	M.S. Yolles and Partners Ltd., Toronto
B. Ellingwood	The John Hopkins University, Baltimore
R. Green	University of Waterloo, Waterloo/Université de Waterloo, Waterloo
F. Knoll	Nicolet, Chartrand, Knoll & Assoc., Montreal
C.J. Montgomery	Lamb McManus Associates Ltd., Edmonton
M. Saatcioglu	University of Ottawa, Ottawa/Université d'Ottawa, Ottawa

SPONSORS/ORGANISMES PROMOTEURS

Institute for Research in Construction, National Research Council Canada/
Institut de recherche en construction, Conseil national de recherches Canada

University of Ottawa/Université d'Ottawa

Canadian Society for Civil Engineering/
Société canadienne de génie civil

American Society of Civil Engineers

Canadian Group of the International Association for Bridge
& Structural Engineering/
Le groupe canadien de l'Association internationale
des ponts et charpentes

International Council for Building Research (CIB)/
Conseil international du bâtiment pour la recherche (CIB)

SECRETARIAT/SECRÉTARIAT

Mike Boroczki
Conference Services/Service des conférences
National Research Council Canada/Conseil national de recherches Canada
Ottawa, Ontario, Canada K1A 0R6

Telephone/Téléphone: (613) 993-9009
Facsimile: (613) 993-0603
Telex/Télex: 053-3145

PREFACE

Buildings and building components—despite their apparent stability and rigidity—move, deform and vibrate. Such movements are of concern if they result in damage to the building, discomfort to occupants, or inability to carry out activities within the building. In structural practice the conditions which describe these functional requirements of the building are termed the "serviceability limit states" or, more generally, "performance requirements". Lighter and more flexibile building structures made compositely and with fewer non-structural attachments, has resulted in an increasing number of problems associated with movements, deformations and vibrations.

This Symposium/Workshop brings together designers, builders and researchers to review current experience with such problems, to exchange knowledge recently developed for avoiding such problems, and to make recommendations for the future. Volume I of the proceedings contains the papers prepared for the symposium. Volume II contains the discussion and recommendations from the workshop sessions.

The Organizing Committee wishes to thank all the authors, discussers and workshop participants for their contributions, and the sponsors of the symposium for their assistance. Special thanks go to the members of the Secretariat, Conference Services of National Research Council Canada, for making the physical arrangements, providing secretarial services, and producing the proceedings.

PRÉFACE

En dépit de leur stabilité et leur rigidité apparentes, les bâtiments et leurs éléments de construction se déplacent, se déforment et vibrent. De tels mouvements suscitent une certaine inquiétude lorsqu'ils causent des dommages au bâtiment, qu'ils incommodent les occupants ou qu'ils entravent les activités normalement réalisées à l'intérieur du bâtiment. Sur le plan structural, les conditions qui décrivent les exigences fonctionnelles du bâtiment sont appelées "états limits d'utilisation" ou, de façon plus générale, "exigences de performance". L'avènement de structures de bâtiment plus légères et plus flexibles fabriquées à partir de matériaux composites et comportant moins de pièces de fixation non structurales a donné lieu à un nombre croissant de problèmes associés aux mouvements, aux déformations et aux vibrations.

Le présent colloque-atelier met en rapport des concepteurs, des constructeurs et des chercheurs pour passer en revue l'expérience acquise jusqu'à de jour en ce qui a trait à ces problèmes, pour échanger les connaissances acquises récemment pour éviter ce genre de problèmes et pour faire des recommandations pour l'avenir. Le volume I du compte rendu contient toutes les communications préparées pour le colloque. Le volume II renferme les discussions et les recommandations découlant des séances d'atelier.

Le comité organisateur désire remercier les auteurs ainsi que les participants aux discussions et aux ateliers de leurs contributions, de même que les organismes qui ont parrainé le colloque. Il désire remercier tout particulièrement les membres du Secrétariat, Services de conférence, du Conseil national de recherches Canada, d'avoir fait les arrangements physiques, assuré les services de secrétariat et préparé le compte rendu.

TABLE OF CONTENTS/TABLE DES MATIÈRES

Page

Organizing Committee/Comité organisateur ii
Sponsors/Organismes Promoteurs ii
Secretariat/Secrétariat ii
Preface iii
Préface iv

KEYNOTE LECTURES/DISCOURS PRINCIPAUX

General Serviceability - Deflections, Differential Movement and Cracking
J.G. MacGREGOR 3

Vibrations - The Designer's Perspective
R.L. TOMASETTI 7

SESSION A/SÉANCE A
GENERAL SERVICEABILITY/TENUE EN SERVICE GÉNÉRALE

Performance Criteria for Small Buildings
G. NAWAR 11

Fuzzy Concept of Serviceability Limit States
M. HOLICKY 19

Structural Serviceability and Concrete in Compression
E.F.P. BURNETT, P.F. KELLY 32

Probabilistic Design for Serviceability Related to Excessive Deformation
D.M. FRANGOPOL 49

Reliability of Serviceability Limit States for Engineered Wood Structures
J.J. SALINAS, R.G. GILLARD 62

Serviceability of Buildings - Probabilistic Approach
F. BLJUGER 73

Industrial Case Study of an Extensive Structural Floor Slab Replacement
K.N. SMITH 86

SESSION B/SÉANCE B
DEFLECTIONS/FLÉCHISSEMENTS

A Practical View on Deflections and Cracks
F. KNOLL 91

Design, Construction and Deflection of Two-way Slabs
C.J. MONTGOMERY, R.G. BROCKBANK, M.J. STEPHENS, G. KRYWIAK 101

Comparison of Field Measured Floor Slab Deflections for Two Reinforced Concrete Buildings
E.P. JOKINEN, A. SCANLON, G.J. BURGHARDT 112

Page

Effect of Elastic and Time-Dependent Concrete Properties on Construction Loads in Multistory Two-way Slab Construction
A.F. SHAIKH, S.K. GHOSH, M.M. MEHTA 124

Proposed Code Provisions for Slab Span Thickness Limitations Including Construction Loads
N.J. GARDNER 126

Serviceability of Reinforced Concrete Two-way Floor Slab Systems
S.G. PINJARKAR 137

Calculations of Short-term and Long-term Deflections of Reinforced Concrete Beams
K. MAHMOOD, S.I. AL-NOURY 152

Serviceability Problems of Department Store - Case Study
M. HOLICKY 166

SESSION C/SÉANCE C
WIND-INDUCED VIBRATIONS/VIBRATIONS CAUSÉES PAR LE VENT

Measured Motions of Tall Buildings in Wind and Their Evaluation
N. ISYUMOV, A. MASCIANTONIO, A.G. DAVENPORT 181

Wind-induced Motions of Buildings
P.A. IRWIN, V. FERRARO, G.K. STONE 200

Fundamental Study on Tuned Liquid Damper (TLD) - A New Damper for Building Vibrations
Y. FUJINO, B.M. PACHECO, P. CHAISERI, L.M. SUN 214

Wind-induced Vibration of Tall Towers and Practical Applications of Tuned Sloshing Damper
Y. TAMURA, K. FUJII, T. SATO, T. WAKAHARA, M. KOSUGI 228

Devices for Damping Lateral Vibrations in Tall Structures
D.W. HUST 242

Probabilistic Criteria for Human Perception of Low-frequency Horizontal Motions
J. KANDA, Y. TAMURA, K. FUJII 260

Human Response to Wind-induced Vibration of Tall Buildings
M. FUJIMOTO, T. OHKUMA, T. TAMURA 270

SESSION D/SÉANCE D
DIFFERENTIAL MOVEMENT/MOUVEMENT DIFFÉRENTIEL

Structural Serviceability Aspects of Building Envelopes in Tall Buildings
R. BERGMANN 293

Page

The Design of Wall Cladding: National Aviation Museum
M. SOMMERSTEIN 323

Vérification de l'état d'utilisation des colonnes sous déformations imposées
D.B. NAJDANOVIC 337

Experimental Analysis of the Deformability of Partition Walls and Brittle Coverings
É. NEMESTOTHY, Gy. VISNOVITZ 348

Foundation Problems and Their Effect on the Serviceability of Buildings
J.R. SCHURING, D. RAGHU, E.G. DAUENHEIMER 360

A Simple Design Aid for Predicting Shrinkage and Creep Strains in Buildings
P. ARUMUGASAAMY, R.N. SWAMY 378

Relaxation of Restraint Effect Caused by Temperature Difference or Settlement of a Support in Long Term Tests
J. JOKELA 396

Effect of Differential Settlement on the Performance of a Continuous Truss
H.P. NIU 406

Investigation of the Service Tower Movements at the Jock Hardy Arena
S. ROBINS 411

SESSION E/SÉANCE E
VIBRATIONS FROM HUMAN ACTIVITY/VIBRATIONS CAUSÉES PAR L'ACTIVITÉ HUMAINE

Practical Cases of Structures with Man-induced Vibrations
H. BACHMANN 419

Ten Years of Floor Vibration Research - A Review of Aspects and Some Results
S.V. OHLSSON 435

Crowd-induced Dynamic Loads
A. EBRAHIMPOUR, R.L. SACK 451

Dynamic Study of a Stub Girder Floor System
C.M. MATTHEWS, C.J. MONTGOMERY 465

Performance and Acceptability of Wood Floors - Forintek Studies
D.M. ONYSKO 477

Practical Aspects of Floor Serviceability Design
T.M. MURRAY 495

Page

Dynamic Footfall Loading from Groups of Walking People
P.-E. ERIKSSON, S.V. OHLSSON 497

A Serviceability Criterion to Avoid Human Discomfort for Light-weight Wooden Floors
Y. H. CHUI, I. SMITH 512

Vibration Response of a Ribbed Slab Floor to Dancing
I. ROSENTHAL, M. ITSKOVITCH 526

A Dance Floor with Unsatisfactory Dynamic Response
C.M. MATTHEWS, C.J. MONTGOMERY 533

Serviceability Calculations for Timber Building Components with Mechanical Connections
I. SMITH, Y. H. CHUI 547

An Automated Approach to Floor Vibration Analysis
R.A. TOLAYMAT 558

Dynamic Response of Floors Due to People in Motion
J.H. RAINER, D.E. ALLEN, G. PERNICA 566

SESSION F/SÉANCE F
GROUND-TRANSMITTED AND MACHINERY-INDUCED VIBRATIONS/
VIBRATIONS CAUSÉES PAR LES MACHINES ET LES TRANSPORTS

Control of Building Vibration from Ground-borne Excitation
D.L. ALLEN, B. HOWE 575

SWD Criteria for Building Damage from Ground Vibratious
R. CIESIELSKI, J. KAWECKI, E. MACIAG 579

Micro-Vibration Control Procedure for High-Tech Facilities
K. SHIOYA, K. MAEBAYASHI 589

Effect of Train-induced Vibrations on Houses - A Case Study
J.H. RAINER, G. PERNICA, A.H.P. MAURENBRECHER,
K.T. LAW, D.E. ALLEN 603

Case Study: Effect of Rail Traffic Vibrations on Jail Structure
T.B. MORRIS 615

On Shock Effects in Structures Due to Pile Driving - Case Study
S. UMINSKI, Z. CYWINSKI 618

Author Index/Index des auteurs 627

KEYNOTE LECTURES/DISCOURS PRINCIPAUX

GENERAL SERVICEABILITY -
DEFLECTIONS, DIFFERENTIAL MOVEMENT AND CRACKING

J.G. MacGregor
Department of Civil Engineering
University of Alberta
Edmonton, Alberta, Canada
T6G 2G7

ABSTRACT: The concept of limit states design is reviewed to illustrate the differences between design for ultimate limit states and serviceability limit states. The characteristics of limit states of deflection, differential movement and cracking are reviewed. It is shown that for a given limit state there is no unique limiting value for all applications. The limiting values are functions of a number of aspects of behavior and damage done.

1. INTRODUCTION

All structures deflect under load, most, if not all, foundations settle under load and most, if not all, reinforced concrete structures crack under load. In most cases these deflections, settlements or cracks go unnoticed because they have no adverse effect on the serviceability of the structure. When they are noticed, however, they frequently lead to concern by owners and users, repairs and litigation. To quote Hardy Cross[1], "Strength is essential but otherwise unimportant."

Although structural deformations have always been a problem the advent of new and lighter methods of construction has lead to thinner, longer spans which deflect more. In the past 50 years the allowable service load stress for reinforcing in flat slab floors has increased from 18000 psi (124 MPa) in slabs designed by the 1936 ACI Code to 36000 psi (250 MPa) in slabs designed by the current Canadian and American codes. Similar increases have occurred in other structures. Since steel stress directly affects the curvature of a member and this in turn is directly related to deflections, there has been a tendency for structures that deflect more. Modern construction methods emphasize speed of construction. In concrete structures this means form removal and reshoring when the concrete is very young. As a result, the heaviest loads many slabs ever experience come on them in the first two weeks, before the concrete reaches its full strength. The increased cracking leads to increased deflections. All these things have led to an increased focus on serviceability in design.

This paper will deal with static or long time deformations. It will not deal with the equally important problem of vibrations and dynamic problems in buildings. The discussion will be limited to building structures.

2. LIMIT STATES DESIGN

Increasingly, modern design codes are being recast in a limit states design format. A "limit state" is defined as a state during the life of the structure when the structure ceases to fulfill its intended purpose.

Limit states design is a process in which the designer: (a) enumerates all the possible modes of failure (limit states) for a structure and (b) considers each of the limit states in turn during his design. In most cases a code writing body has already set limits on strengths in the form of load and resistance factors, and on deflections, etc. in the form of allowable deflections, crack widths and the like. Frequently the load and resistance factors are derived probabilistically. Generally the deflection and crack width limits are empirical deterministic values.

In limit states design, design is based on one or more primary limit states. Following this the remaining limit states are checked with calculations, or with deemed-to-satisfy rules. In the case of a low building, strength is the primary limit state. This is considered first in the design, followed by checks of vibration, deflection, etc. In the case of a tall building there are two primary limit states: wind vibration and strength. These control the selection of the structure which is subsequently checked for floor deflections and so on. In the case of a water tank, the primary limit state is watertightness, followed closely by strength.

The strength design methods of the Canadian and American concrete and steel codes are a particular subset of limit states design in which the strength limit state is always assumed to be the primary limit state.

The limit states are generally divided into two groups: "ultimate limit states" corresponding to collapse of part or all of the structure and "serviceability limit states" corresponding to loss of function but not collapse. The characteristics of these two groups and our strategies in dealing with them differ.

2.1 Ultimate Limit States. Ultimate limit states include rigid body sliding or tipping of the structure, rupture or buckling of parts of the structure, formation of plastic mechanisms and similar states corresponding to collapse of part or all of the structure.

Ultimate limit states tend to approach a binary yes-no definition of failure. A concrete beam has either failed due to excessive moment or it hasn't. Furthermore, the associated calculation models are generally clearly understood. This allows a straight forward probabilistic treatment to select load and resistance factors for design.

2.2 Serviceability Limit States. For buildings the major serviceability limit states are:

(a) Vertical deflections of floors. These are a problem if they are unsightly or if they cause damage to partitions, windows and so on.

(b) Horizontal deflections of frames. These are closely linked to wind vibrations.

(c) Differential deflections due to uneven settlement of foundations, unequal shortening of columns or temperature differences between the exterior and interior of a building.

(d) Cracks which are unsightly or allow leakage of air, water or other materials.

(e) Vibrations: vertical vibration or floors, sway vibration of frames and vibrations induced by machinery.

The definition of when a serviceability limit state is reached is highly subjective in most cases because the detection of the limit state frequently depends on the sensitivity of the observer. Furthermore, the limit on acceptable deformation may vary from structure to structure depending on its use or loading.

The calculation models available for estimating deflections, settlements and crack widths are much poorer than the strength calculation models. This is particularly true for deflections of concrete structures with service loads close to the cracking loads.[2]

As a result, the treatment of serviceability in design is at a much less sophisticated level than the treatment of structural safety. Very few comprehensive studies have dealt with this problem. Reid and Turkstra[3] have approached this from an optimization standpoint. Galambos and Ellingwood[4] have calculated safety indices corresponding to various return periods of live loads on simple structures.

3. CHARACTERISTICS OF STRUCTURAL DEFORMATIONS

Before one can propose limits on deformations or design strategies for dealing with them, it is desirable to classify them with respect to how they are detected, their causes, and their effects since different classes may require different limits. Excellent reviews of structural deformations are presented in References 5, 6 and 7.

Floor deflections and foundation settlements consist of two parts, an elastic part which occurs as the load is applied and for some materials a creep component which gradually increases as the load is sustained. The first is recoverable when load is removed, the second is largely irrecoverable.

Differential deflections in a frame may occur due to daily temperature fluctuations causing cyclic differences in the temperature of the core relative to the outside columns, or they may occur due to differing amounts of creep in the columns or different settlements of the foundations. If these lead to damage to partitions, a more stringent limit might be imposed on deformations which cycle on a daily or monthly basis than would be imposed if the damage occurred once in the life of the building, due for example to creep deflections, and could be repaired easily.

In setting limits on deflections or crack widths it is important to note whether the deformation is

(a) Rapidly occurring or slowly occurring,

(b) Recoverable or not,
(c) Frequent, infrequent or permanent,
(d) Causes damage that is transitory, permanent, or repairable at a reasonable cost.

It is also important to note whether the deformation is detected by a human response (visual, feeling vibration) in which case the limit at which it is detected is fuzzy, or whether it is detected by damage or malfunction which may be easier to define mathematically.

REFERENCES

1. Cross, H. Engineers and Ivory Towers, McGraw-Hill.

2. Ramsey, R., Mirza, S.A. and MacGregor, J.G., "Variability of Deflections of Reinforced Concrete Beams", ACI Journal, Proceedings, Vol. 76, No. 8, August 1979, pp. 897-918.

3. Reid, S. and Turkstra, C., "Codified Design for Serviceability", Elsevier, 1981, pp. 583-592.

4. Galambos, T.V. and Ellingwood, B., "Serviceability Limit States: Deflection", Journal of Structural Engineering, Proceedings ASCE, Vol. 112, No. 1, January 1986, pp. 67-84.

5. International Organization for Standardization, "Bases for the Design of Structures - Deformation of Buildings at the Serviceability Limit States", Draft International Standard ISO/DIS 4356, 1976, 20 pp.

6. "Deformation Requirements for Buildings", Steelbuilding Association (SG), Rotterdam and the Concrete Association (CUR), Zoetermeer, SG-CUR Report No. 2, Delft, 1975, 138 pp. NRC Technical Translation TT-1969, Ottawa, 1980.

7. Burland, J.B. and Wroth, C.P., "Settlement of Buildings and Associated Damage", Settlement of Structures, Halsted Press, John Wiley and Sons, 1975, pp. 611-654.

8. Mayer, H. and Rüsch, H., "Damage to Buildings Resulting from Deflection of Reinforced Concrete Members", Deutscher Ausschuss für Stahlbeton, Bulletin 193, Wilhelm Ernst, Berlin, 1967, 90 pp; English translation: Technical Translation 1412, National Research Council of Canada, Ottawa, 1970, 115 pp.

VIBRATIONS - THE DESIGNER'S PERSPECTIVE

R.L. Tomasetti
Thornton-Tomasetti, P.C.
New York, NY, USA

This paper will emphasize the practicing engineer's point of view concerning vibration problems and their solution in buildings. Emphasis will be placed on an overview of related topics and their practical considerations.

Topics to be covered will include:

1. Education of design engineers in the area of building vibrations - at the University - and afterwards.
2. Awareness of vibration considerations during the design process. When is it considered? How thoroughly is it considered?
3. Where the designer typically gets into trouble - long spans, height restrictions, low natural frequency, minimum damping.
4. Research needs and guidelines required to assist in predicting and avoiding vibration problems in buildings.
5. Approaches to solving vibration problems existing in buildings through analysis and testing.

The discussion will relate to different types of vibrations including wind induced and those associated with human activities, machinery and/or transportation. Particular examples concerning design will be covered, as well as solutions to vibration problems.

SESSION A/SÉANCE A

GENERAL SERVICEABILITY/TENUE EN SERVICE GÉNÉRALE

PERFORMANCE CRITERIA FOR SMALL BUILDINGS

George Nawar

The University of New South Wales
Australia

ABSTRACT: The performance of small buildings is defined in terms of design objectives and divided into various design parameters. The sensitivity of serviceability functions to the different design parameters is examined in order to develop a decision model for designs based on serviceability limit state.

1. INTRODUCTION

Small buildings (also sometimes referred to as low rise buildings) may be defined in terms of its height, footing loads and materials of construction. In terms of building height, small buildings are assumed to be up to say 7.2 metres ± 10% above ground level and consisting of one or two storeys, excluding basement. Typical footing loads range from 1kN/m under internal walls of single storey clad frame superstructures with truss roofs, to 100kN/m below internal walls of double storey, full masonry superstructures with basement, concrete floors and conventional roofs. Approximately 80% of buildings in Australia fall within these values with a wide range of functions including residential, commercial and institutional applications.

Unlike other types of construction, small buildings have the following characteristics which govern their engineering objectives.

1. Buildings are mostly occupied by their owners and this tends to develop a bias towards high initial cost for disproportional improvement in serviceability.
2. Buildings represent a large portion of their owners' financial assets and this reflects on their utility towards changes in building value. "Risk avoidance".
3. The inability of users to assess the relationship between stability and serviceability narrows their tolerance of acceptable performance.

4. The implication of performance on prestige, status and quality of life is very high for certain types of buildings.

5. A relatively large array of government agencies, professionals and tradesmen involved in the control, design and construction of small buildings tend to restrict the optimisation of engineering decisions.

6. There is an increasing consumer tendency to rely on litigation for the settlement of disputes.

7. There is greater involvement of the insurance industry.

These factors amongst others create an urgent need to develop equitable parameters, related to basic objectives by which the engineering performance of small buildings may be assessed and measured.

2. DERIVATION OF PERFORMANCE CRITERIA

Many attempts have been made to establish some performance criteria; most of these attempts related only to one factor or a very narrow range of applications. A more general and commonly accepted method by the Building Research Station[1] employs six performance categories related to negligible, very slight, slight, moderate, severe and very severe degrees of damage. These degrees of damage are based on a specific range of crack widths in walls and floors with a corresponding scenario of typical damage and ease of repair for each category.

While this method simplifies the assessment process, it tends to relate subjective estimates of performance to objective categories with inflexible boundaries and this could result in inadequate assessment of localised conditions leading to corrosion, leakage or structural failure.

A more equitable assessment should relate performance criteria to the engineering objective of buildings. Generally a common objective could be stated as the provision of SHELTER to enable certain USAGE. A Building's performance as a SHELTER measures its capacity to sustain the occupant's life and contents against natural hazards such as floods, cyclones, tremors, and other disasters, as well as its resistance to environmental conditions such as rain, snow, wind, vibration, etc, for which the design parameters include ductility, stability and strength in various degrees.

Building performance for USAGE, should measure user's satisfaction in terms of the building's capacity to sustain various operating loads, delivery of function at a desired quality, all within the economic and social constraints. Design parameters for these conditions include resistance, serviceability, cost and value of both material and design arrangement which are measured in terms of tilt, crack width, insulation capacity and repair cost, as well as any other criteria related to the building's specific function.

Table 1 shows the derivation of performance parameters from the building's basic objectives. The table is set up in some order of significance from the top down, such that items high on the list need to be satisfied in order to achieve satisfactory performance of lower items.

Similarly, items on the right-hand side of the list are functions of those to the left, but not rigidly linked. The relationship of such linkage may be defined for individual buildings depending on their sensitivity to various design parameters.

The performance of small buildings is less sensitive than tall buildings to the upper design parameters such as stability or strength but is more sensitive to serviceability and cost which are dependent on all other parameters to a lesser degree.

This means that less effort is warranted in small buildings for the investigation and analysis of individual design parameters and that effort should be directed towards the definition of a collective relationship between all parameters.

3. ANALYSIS OF PERFORMANCE CRITERIA

The performance of small buildings can be conveniently rated into seven grades (Table 2), representing subjective assessment and corresponding to the inverse of the degree of damage and categories as defined in References [1] and [2].

By superimposing the objective function and design parameters, from Table 1, USAGE function could loosely correspond to the first three categories which also define the acceptable performance range. Serviceability is then viewed as the minimum acceptable parameter and used to define the boundary between USAGE and SHELTER. Such cross relationships are possible because of the subjective nature and definition of these parameters. The anomalies become apparent when these parameters are quantified in terms of measurable parameters such as tilt and crack width. Figures 1 and 2 illustrate the relationship between tilt, crack width and performance criteria as defined in References [1] and [2]. It could be argued that the relationship between these parameters is not objective and at best only represent subjective community standards and utility.

Other parameters such as cost of repairs and the probability of occurrence can only provide further objective tools for the description of subjective standards.

The linkage of suitable criteria is often necessary to develop codes of practice and standards for engineering applications. Unless these applications are very narrowly defined (such is not the case for small buildings), performance criteria must be statistically based and time related in order to be equitable and representative of community utility. Even then the risks of misrepresentation cannot be completely avoided.

An ideal format would allow the development of performance criteria to be based on the prevailing conditions of each individual application.

Such a format is now more feasible by the application of expert system ideas and decision models.

REFERENCES

1. Digest 251, 1981. Building Research Station, Graston, Watford, WD27JR.
2. Australian Standard 2870-1986. Residential slabs and footings.
3. Ingles, O.G. and Nawar, G. An evaluation of engineering experience in Australia. Proc. IABSE Conf. Quality assurance in the building process (RIG 1, 1983) 111-116.
4. Nawar, G. Performance of masonry buildings under ground movement. Proc. IEA Conf. Concrete 85 (Brisbane, 1985) 26-31.
5. Nawar, G. Q.A. of buildings in area subject to ground movement. Proc. IABSE Conf. Quality assurance in the building process (Tokyo, 1986) 197-206.

TABLE 1 - PERFORMANCE PARAMETERS AS RELATED TO OBJECTIVES

OBJECTIVE	DESIGN CONDITIONS			DESIGN PARAMETERS		PERFORMANCE CRITERIA	
				material selection	size & arrang't		
		FLOODS					
		CYCLONES		DUCTILITY			
	NATURAL HAZARDS	TREMORS					
		BUSH FIRE			STABILITY		WALL
		LANDSLIDE				TILT or SLOPE	FLOOR
		(OTHER)					OTHER
SHELTER		RAIN					
		SNOW		STRENGTH			
		WIND	SLOPE STABILITY				
	ENVIRONMENT CONDITIONS	VIBRATION	REACTIVE SOIL		FLEXIBILITY		
		GROUND CND.	MADE GROUND				WALLS
		VEGETATION	COLLAPSABLE SOIL			CRACK WIDTH	FLOORS
		SERVICE LINES	EXCAVATION				OTHER
		MINING SUBS	U/G COAL				
		(OTHER)	PUMPING WELLS		RELIABILITY		
	LOADING	LIVE LOADS	DEWATERING				
		DEAD LOADS					
		SERVICE LOADS		RESISTANCE			FIRE
		CONSTRUCTION LOADS				INSULATION CAPACITY	TEMP
							SOUND
		OCCATIONAL LOADS			SERVICEABILITY		MOIST
		(OTHER)					
		SOUND INS.					
USAGE	FUNCTION & QUALITY	TEMP. INS.		DURABILITY			
		DEFLECTION					
		CRACKING					
		WEAR & TEAR				RUNNING COST	OPERATION MAINTENANCE REPAIR
		(OTHER)		VALUE (cost effectiveness)			
	SOCIO-ECONOMIC	SOCIAL ACCEPTANCE		AESTHETICS			
		COST (OTHER)		QUALITY OF LIFE			

TABLE 2 - ANALYSIS OF PERFORMANCE CRITERIA

PERFORMANCE RATING	V.GOOD	GOOD	FAIR	POOR	V.POOR	DANGER	FATAL	
OBJECTIVE	← USAGE →			← SHELTER →				
DEGREE OF DAMAGE [1&2]	NEG.	SLIGHT	MODERATE	SEVERE	V.SEVERE	←	TOTAL	→
DESIGN PARAMETER "LIMIT STATE"	QUALITY OF LIFE	AESTHETICS	UTILITY	SERVICEABILITY	RELIABILITY	STABILITY	DUCTILITY	
CATEGORY OF DAMAGE [1]	0	1	2	3	4	5	6*	7*
EXTENT OF DAMAGE	VERY LOCALISED	LOCALISED	ISOLATED	GENERAL	EXTENSIVE	____	DOMINANT	____
MOVEMENT (TILT %) 1 WALL	0.25%	0.33%	0.5%	0.66%	1%	2%	4%	6.6%
MOVEMENT (TILT %) 2 FLOOR [2]	0.26%	0.33%	0.5%	0.83%	1%	1.25%	1.6%	3.3%
DEFORMATION I (CRACK WIDTH mm) 1 WALL [1&2]	0.1	1	5	5-15	15-25	25		....
DEFORMATION I (CRACK WIDTH mm) 2 FLOOR [1]	0	0	1	5	5-15	15		....
DEFORMATION I (CRACK WIDTH mm) 3 FLOOR [2]	0.3	1.0	2	3	4	5	....	....
COST OF MAINTENANCE AND REPAIR (% OF REPLACEMENT COST)	0.1	1	2	5	10	25	....	....
PROBABILITY OF OCCURRANCE (IN NSW) INCIDENCE PER STRUCTURE PER ANNUM [3,4 & 5]		$5x10^{-1}$	$5x10^{-2}$	$3x10^{-3}$	$5x10^{-4}$	$5x10^{-5}$	$5x10^{-6}$	

*ADDITIONAL CATEGORIES NOT IN REF [1]

FIG. 1 PERFORMANCE CRITERIA AS RELATED TO WALL AND FLOOR TILT

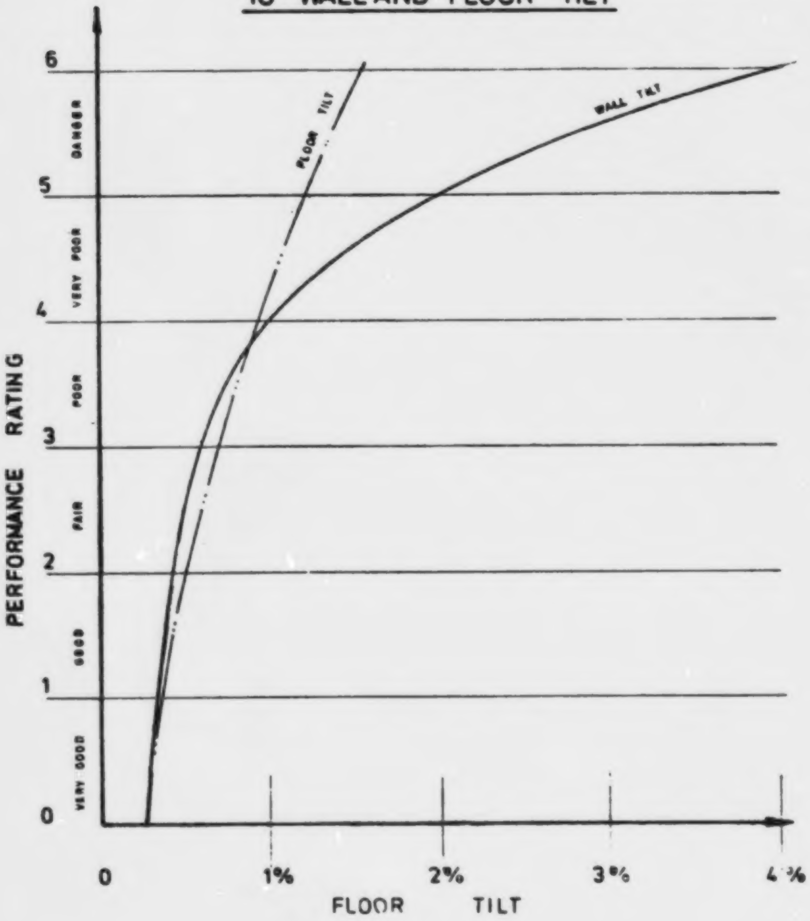

FIG. 2 PERFORMANCE CRITERIA AS RELATED TO CRACK WIDTH

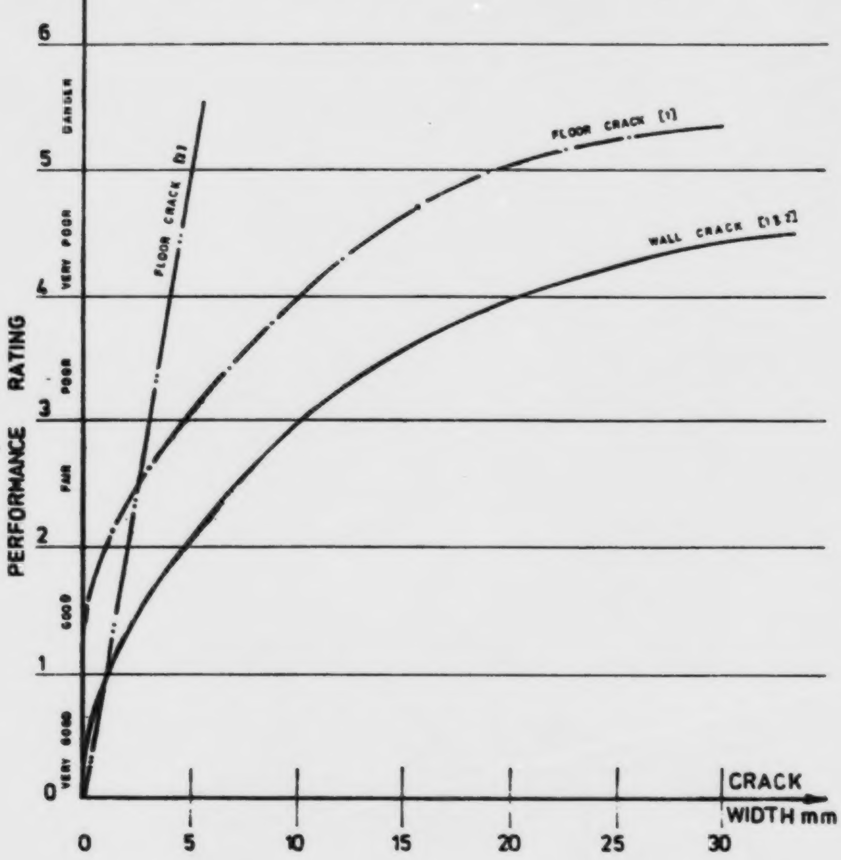

FUZZY CONCEPT OF SERVICEABILITY LIMIT STATES

Milan Holický

Building Research Institute
Technical University of Prague
Prague, Czechoslovakia

ABSTRACT: Fuzzy concept of serviceability limit states of building structures takes into account common reality that suitability of a structure for normal use is not completely lost when its deformation (acceleration, crack width, etc.) exceeds certain limit value, but rather it gradually decreases with increasing deformation from top level to full disability. Thus, generally there is no crisp but more or less fuzzy definitions of functional requirements. The level of ability of a structure to comply with the functional requirements is described by membership function, known from the fuzzy set theory; in the range from one to zero it gives the level of support for the structure to be a member of the set of fully suitable structures. Proposed definition for characteristic value of limit deformation is based on fundamental characteristics of appropriate membership function and on admissible cumulative damage of a structure. Furthermore, probabilistic analysis of functional requirements yield conditions for admissible statistical characteristics of structural deformations garanteeing sufficiently low fuzzy - probability of serviceability failure. Fuzzy set theory seems to be useful tool in solving various practical problems of serviceability limit states of building structures.

1. INTRODUCTION

Serviceability limit state of building structures are becoming more and more important due to increasing flexibility of bearing components and also due to more severe functional requirements imposed on modern buildings. Present methods of design are based on verification of serviceability conditions, according to which expected (deterministic) structural deformations (deflections, accelerations, crack widths etc.) must comply with admissible limiting values. These values should represent appropriate functional requirements, i.e. structural, operational, physiological and appearance requirements guaranteeing "normal use" of structures.

The most frequently applied serviceability condition may be written in a simple form

$$z \leq 1 , \qquad (1)$$

where z denotes structural deformation which is normally dependent on number of basic variables describing mechanical and geometric characteristics of the structure and properties of load, l denotes admissible limit deformation, which is generally dependent on various quantities describing appropriate functional requirements. It is well recognized /1, 2/, that the deterministic approach of the present design methods does not take into account random variability of basic variables and the resulting quantities z and l .

There are some experimental /3 to 5/ and theoretical /5 to 7/ results concerning random behaviour of actual structural deformation z , but very little and rather vague information exist /8 to 10/ on limit deformation l . Admissible or limiting values of l , introduced in various codes, are usually taken as "customary values", which has "worked well in the past". Appropriate rational analysis is however very difficult, since relevant functional requirements are often represented imprecisely or merely in liguistic form, where subjective evaluation and engineering judgement may play considerable role.

It appears, therefore, that serviceability problems of building structures involve various incertitudes, which may be devided into two groups. First natural randomness, which causes statistical uncertainty (for example of structural deflection) and secondly imprecision, which causes fuzziness (for example of limit deflections). While the more familiar randomness can be handled mathematically through the well established theory of probability, less familiar concept of imprecision and vagueness seems to be a subject, which could be handled by the newly developing theory of fuzzy sets /11 to 15/.

An attempt is made in this paper to apply fuzzy sets theory when analysing some of the basic problems of serviceability limit states. The fundamental concept of membership function, as a measure of imprecision in definition of limit deformation is introduced in the next section. The characteristic value of limit deformation is then defined using proposed concept of the cumulative damage. Further, conditions for satisfactory characteristics of actual structural deformation corresponding to a given admissible fuzzy probability of failure are derived. Finally other possible applications of the fuzzy set theory in analysing serviceability limit states are indicated.

2. MEMBERSHIP FUNCTION

Consider a simple case when fulfilment of all the functional requirements are dependent on a single deformation variable (for example deflection) x . As already mentioned there is no distinct boundary l separating a set of safe (serviceable) S and failed (unserviceable) F structures. As a rule, with increasing deflection x the ability of a structure to comply with specified functional requirements decreases starting from top level, to which the value 1 is assigned, to full disability, expressed by 0. This imprecision or fuzziness as to whether the structure is serviceable and therefore whether is a member of the set S is often expressed by liguistic variables. The following scale may be suitable: fully, almost, medium, little, very little, not at all.

The mathematical measure of this kind of imprecision, suggested by Zadeh /11/ and later applied in civil engineering /12, 13/, is the fuzzy membership function $\mu_S(x)$. As an example, the simpliest tri-linear form, indicated in Fig. 1, is assumed in the following analysis. For a deformation x up to certain limit l_1 the structure is fully serviceable without any restrictions and objections; then its serviceability decreases and at a certain limit l_2 vanishes, i.e. the structure becomes entirely unserviceable. The set of unserviceable, failed structures, F may be mathematically defined by relationships

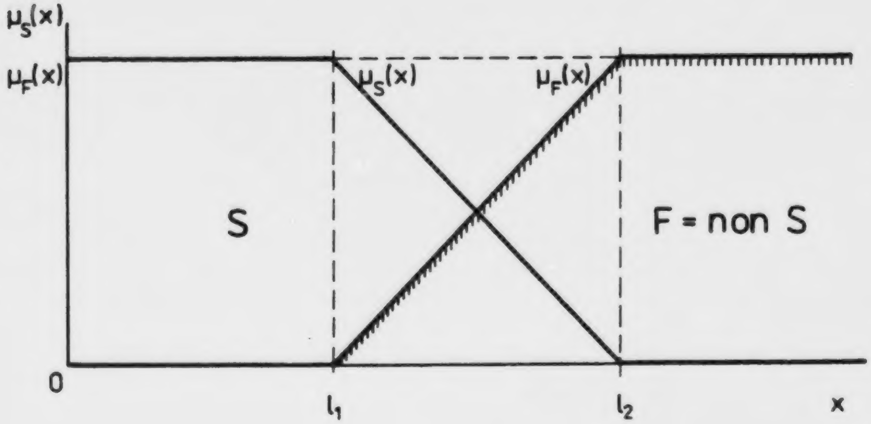

Fig. 1. Membership functions $\mu_S(x)$ and $\mu_F(x)$

$$F = \text{non } S, \qquad \mu_F(x) = 1 - \mu_S(x). \tag{2}$$

The membership function $\mu_F(x)$, shown in Fig. 1, is described by the following formulas

$$\mu_F(x) = 0 \quad \text{for } x < l_1 ,$$

$$\mu_F(x) = \frac{x - l_1}{l_2 - l_1} \quad \text{for } l_1 < x < l_2 ,$$

$$\mu_F(x) = 1 \quad \text{for } x > l_2 . \tag{3}$$

It should be noted, that this simple model represents only an acceptable envision, not based on any concrete data. Other possible shapes of the membership function $\mu_F(x)$ are also conceivable. In any case "transition zone" where a structure is gradually becoming unserviceable, is limited by two boundaries l_1 and l_2, which characterize fuzziness of considered functional requirements.

Furthermore, due to variability of adjacent structural components (in case of structural requirements), or technological appliance (operational requirements) or sensitivity of users (physiological and appearance requirements), estimates

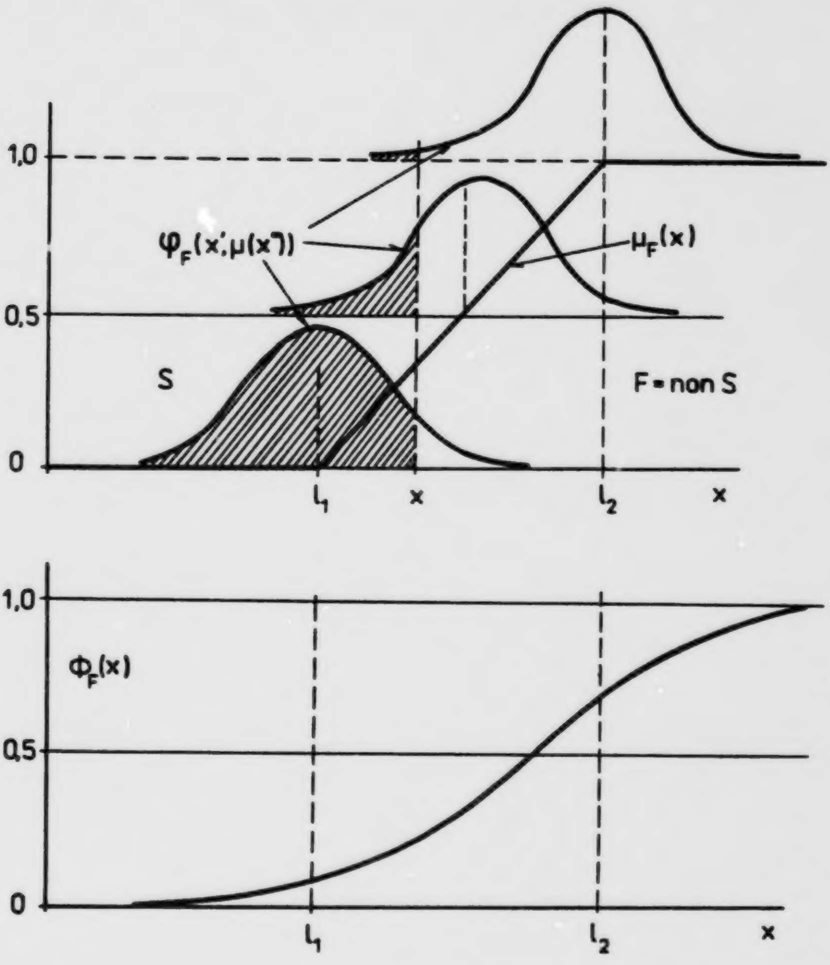

Fig. 2. Cumulative damage function $\Phi_F(x)$

for both values l_1 and l_2 and corresponding membership function may have considerable scatter (see Fig. 2). Let the probability density function of a certain value $\mu_F(x")$ be $\varphi_F(x', \mu_F(x"))$, where x' and x" are generic points of the variable x. In the following a normal distribution having the mean equal to $\mu(x'')$ and a constant standard deviation σ_F is considered, i.e.

$$\varphi_F(x'; \mu_F(x'')) = \frac{1}{\sqrt{2\pi}\,\sigma_F} \exp\left(- \frac{(x' - \mu_F(x''))^2}{2\sigma_F^2}\right), \tag{4}$$

Therefore, the membership function $\mu_F(x)$ is generally dependent on three characteristics: boundaries of transition zone l_1 and l_2, characterizing fuzziness, and standard deviation σ_F, characterizing randomness of appropriate functional requirements. These three basic characteristics are required for practical application of the following analysis. Available data /8 to 10/ may be used for such an estimation. However, as the previous investigations have not intentionally searched for these characteristics their estimation will not be straightforward procedure. This part of research is still in very early stage but it appears that there will be less difficulties with estimating the bounds l_1 and l_2, than with assessing the standard deviation σ_F. If there is no randomness but fuzziness only, the standard deviation σ_F vanishes. In case of technological and structural serviceability requirements lower values of σ_F may be expected than in case of aesthetical and physiological requirements. For the purpose of practical examples in the following analysis it will be assumed that $l_2 \doteq 2l_1$ and $\sigma_F \doteq 0{,}25(l_2 - l_1)$.

3. CHARACTERISTIC VALUE OF LIMIT DEFORMATION

Assume, that the structural deformation z is deterministic quantity, which should satisfy the reliability condition (1) with a required level of reliability. As indicated in previous section the limit deformation l is a fuzzy variable, which generally involves two types of incertitudes; fuzziness expressed by boundaries l_1 and l_2, and randomness expressed by standard deviation σ_F. It follows from Fig. 2, that for a certain value l, cumulative level of failure or cumulative damage of structures satisfying the inequality (1), may be determined by the integral

$$\Phi_F(x) = \frac{1}{K} \int_{l_1}^{l_2} (\mu_F(x'') \int_{-\infty}^{x} \varphi_F(x', \mu_F(x''))\, dx'\, dx'' , \tag{5}$$

where the normalizing factor

$$K = \int_{l_1}^{l_2} (\mu_F(x'') \int_{-\infty}^{\infty} \varphi_F(x', \mu_F(x''))\, dx'\, dx'' \tag{6}$$

is used in order to ensure unique resulting internal $\langle 0,1 \rangle$ for the quantity $\Phi_F(x)$ independently of assumed type of membership and probability density function. The formula (5) may be also seen as an application of fuzzy Bayes theorem /13/. Assuming the membership function (3) and probability density function (4), the corresponding cumulative damage function $\Phi_F(x)$ for selected values of the ratio $\sigma_F/(l_2 - l_1)$, is shown in Fig. 3.

It may be seen that the cumulative damage function $\Phi_F(x)$ may be used in optimization procedure similarly as cumulative distribution function in purely random case. If the cost of failure (unserviceability)of a structure is C_f and cost

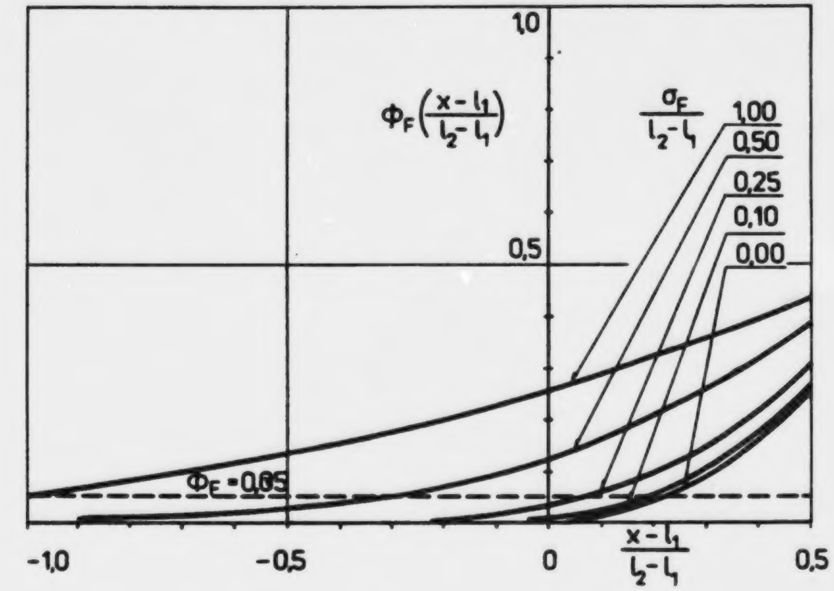

Fig. 3. Cumulative damage function $\Phi_F(x)$

of lower level of serviceability of this structure due to its deformation x is $\mu_F(x)C_f$, then expected cost of lower serviceability of all structures satisfying the reliability condition (1) is given by the multiple $\Phi_F(l)C_f$. For that reason reliability of structures to comply with functional requirements is henceforth expressed by the cumulative damage function $\Phi_F(x)$ similarly as in purely random case by cumulative distribution function. The characteristic value of limit deformation is defined similarly as the characteristic strength of materials.

For a given admissible value of the cumulative damage function $\Phi_F(x)$ denoted simply Φ_F , the characteristic value l is defined by the relation

$$\Phi_F(l) = \Phi_F . \qquad (7)$$

Consider, for example, the value $\Phi_F = 0,05$, shown in Fig. 4 by dashed line. The characteristic values l corresponding to various σ_F , are given by points of intersection of the dashed line with curves $\Phi_F(l)$. For representative admissible values $\Phi_F = 0,001; 0,005; 0,010; 0,050; 0,100; 0,200$ and previously considered values of the ratio $\sigma_F/(l_2 - l_1)$, characteristic values of l

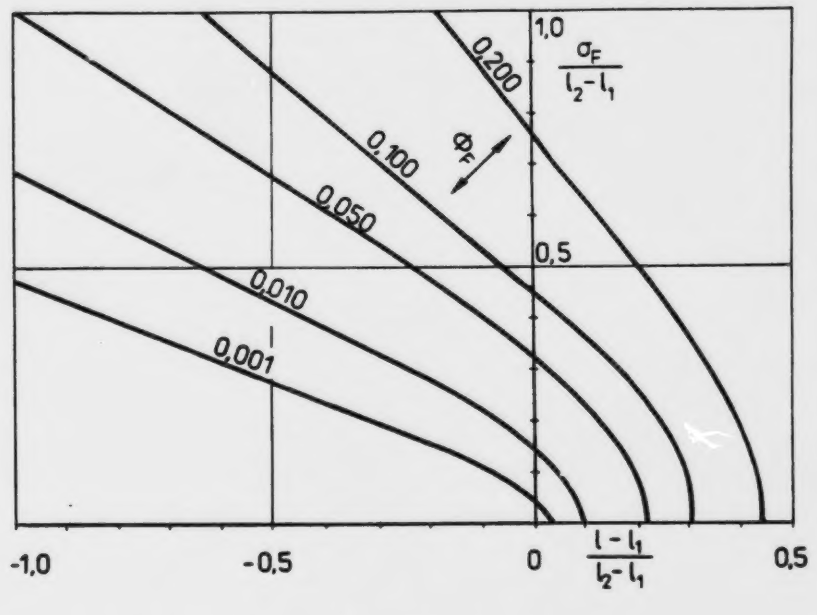

Fig. 4. Characteristic value of limit deformation l

Table 1. Characteristic values of limit deformation l for admissible cumulative damage $\Phi_F(l)$ and the standard deviation σ_F. Indicated values hold for the ratio $(l - l_1)/(l_2 - l_1)$

$\Phi_F(l)$	$\sigma_F/(l_2 - l_1)$				
	0,00	0,10	0,25	0,50	1,00
0,001	0,03	-0,08	-0,41	-1,04	∼ -2,5
0,010	0,10	0,05	-0,16	-0,63	∼ -1,7
0,050	0,22	0,20	0,08	-0,25	-1,00
0,100	0,32	0,29	0,21	-0,06	-0,63
0,200	0,45	0,43	0,38	0,20	-0,18

related to the bounds l_1 and l_2 are given in Table 1.

To indicate the practical application of obtained results consider limit deflection of floor components of the span L. If

$$l_1 = \frac{L}{400} = 0{,}0025L,$$

$$l_2 = \frac{L}{400} = 0{,}0050L,$$

$$\sigma_F = 0{,}25(l_2 - l_1) = 0{,}000625L,$$

and admissible cumulative damage $\Phi_F = 0{,}05$, then (see Fig. 4 and Table 1) it follows

$$l = l_1 + 0{,}08(l_2 - l_1) = 0{,}0027L = \frac{L}{370},$$

which is close to the famous historical values L/360.

4. FUZZY PROBABILITY OF FAILURE

Structural deformation z is random quantity with considerable variability /3 to 5/. Normal and log-normal distributions $\varphi_z(x)$ are, in accordance with results of previous research /6, 7/ considered in the following analysis. The mean $\bar{z}$ and standard deviation σ_z are generally related to the bounds l_1 and l_2, the coefficient of skewness for the log-normal distribution is, for the sake of simplicity, considered by the single value +1.

Fuzzy probability of failure is formally defined in the same way as in the case of purely random variables;

$$p_f = P\{z > l\} , \tag{8}$$

where l is described by the cumulative damage function $\Phi_F(x)$. In view of discussion in previous section, the fuzzy probability of failure may be determined by convolution integral

$$p_f = \int_{-\infty}^{\infty} \varphi_z(x)\Phi_F(x)dx . \tag{9}$$

Note that quantity p_f is generally a multiple of probability and fuzziness and this is a reason for the term fuzzy probability of failure.

Fig. 5 shows fuzzy probability p_f as a function of the mean $\bar{z}$ and standard deviation σ_z, both related to the bounds l_1 and l_2. As already indicated, it is assumed that $\sigma_F = 0{,}25(l_2 - l_1)$. Within the range $p_f \le 0{,}10$, slightly higher probability of failure correspond to log-normal that to normal distribution of structural deformation z. Fig. 6 shows correponding restrictions imposed on the mean $\bar{z}$ and standard deviation σ_z by admissible value of the probability of failure $p_f = 0{,}001; 0{,}010; 0{,}050$ and 0,100. Satisfactory combinations of both characteristics are always located left of an appropriate curve. Under the assumption that $l_2 = 2l_1$ and therefore the point $\bar{z} = 0$ correspond to the relative value $(\bar{z} - l_1)/(l_2 - l_1) = -1$ dot-and-dash lines in Fig. 6 indicate a constant value of the coefficient of variation

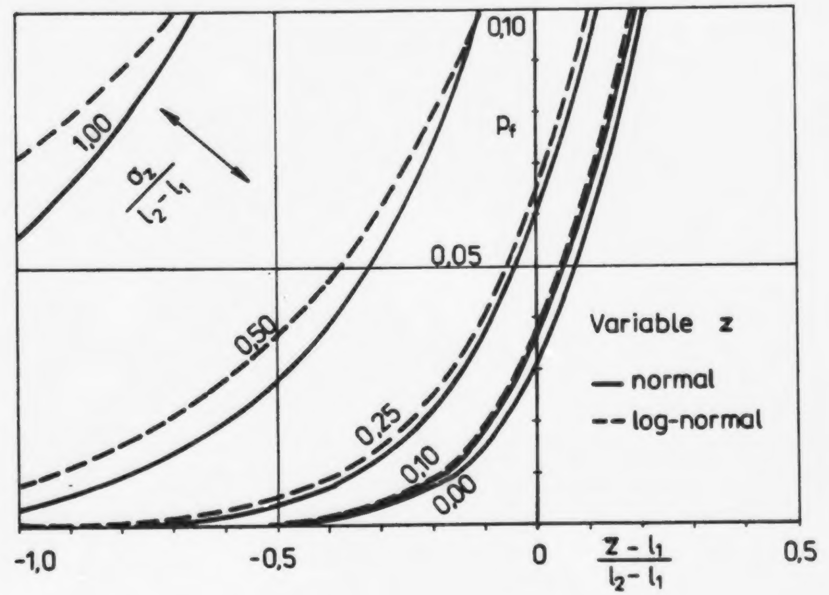

Fig. 5. Fuzzy probability of failure p_f for $\sigma_F = 0,25(l_1 - l_1)$

$v_z = \sigma_z/m_z$ for the structural deformation z . If the coefficient of variation $v_z = 0,30$ then the maximum mean $\bar{z}$ corresponding to the admissible fuzzy probability $p_f = 0,050$ is given by the value $l_1 - 0,1(l_2 - l_1)$ (approximately for both types of distribution); when $p_f = 0,001$, then
$\bar{z} \leq l_1 - 0,50(l_2 - l_1)$ in case of normal distribution and
$\bar{z} \leq l_1 - 0,56(l_2 - l_1)$ in case of log-normal distribution.

5. OTHER APPLICATIONS OF FUZZY SET THEORY

Functional requirements may involve several attributes (for example deflection of floor, cracking of supported partition walls etc.) each of which may be decisive for partial serviceability S_i and failure $F_i = \text{non } S_i$, with the corresponding membership functions μ_{S_i} and $\mu_{F_i} = 1 - \mu_{S_i}$. The total serviceability of the structure is then fuzzy intersection

$$S = \bigcap_i S_i \ , \qquad (10)$$

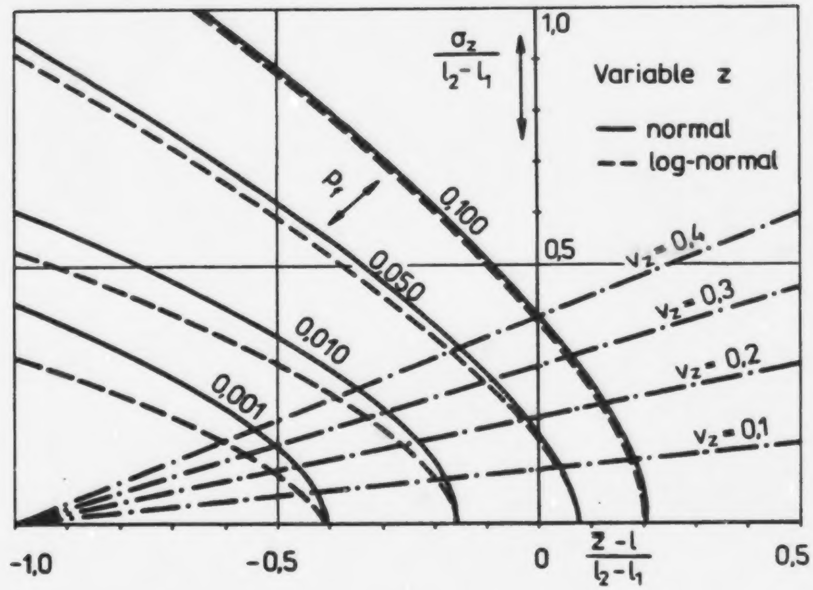

Fig. 6. Admissible statistical characteristics of deformation z for $\sigma_F = 0,25(l_2 - l_1)$

and the membership function given as

$$\mu_S = \bigwedge_i \mu_{S_i} \ , \tag{11}$$

where $\bigwedge_i$ denotes the minimum of the membership functions μ_{S_i} with respect to all attributes i . Fuzzy set of failed structures F = non S is given as union

$$F = \bigcup_i F_i \tag{12}$$

with the membership function

$$\mu_F = \bigvee_i \mu_{F_i} \ , \tag{13}$$

where $\bigvee_i$ denotes the maximum of all membership functions μ_{F_i}

Following the ideas of the paper /10, 11/ assume that the attribute i applies for j distinct components of the structures (for example girders). Failure of the component j due to the attributes i is denoted F_{ij}. The fuzzy set F_i is now given as algebraic sum

$$F_i = \sum_j F_{ij}$$

with the membership function

$$\mu_{F_i} = 1 - \prod_j (1 - \mu_{F_{ij}}) . \tag{14}$$

As an example consider a structure, where F_1 denotes serviceability failure due to deflection, F_2 serviceability failure due to partition wall cracking. If there are four components with recorded deflection, where $\mu_{11} = 0{,}4$; $\mu_{12} = 0{,}3$; $\mu_{13} = 0{,}5$ and $\mu_{14} = 0{,}2$, then $\mu_1 = 0{,}83$. Let the cracking of partition walls be registered in three cases: $\mu_{21} = 0{,}8$; $\mu_{22} = 0{,}2$ and $\mu_{23} = 0{,}6$ then it follows from the equation (14), that $\mu_2 = 0{,}94$. Now, using equation (13) the resulting support for membership of the structure to the set of unserviceable structures F is $\mu_F = \max(\mu_{F1}, \mu_{F2}) = \max(0{,}83;\ 0{,}94) = 0{,}94$.

Significance of various deformation effects could be analysed by fuzzy relation and composition. Consider a set of effects $X = \{x_1, \ldots, x_k\}$ for example x_1 - deflection, x_2 - cracking of partition walls, x_3 - floor vibration, x_4 - cracking of cladding and set of functional requirements $Y = \{y_1, \ldots, y_m\}$ for example y_1 - structural requirements, y_2 - operational requirements, y_3 - physiological requirements and y_4 - appearance requirements. Assume that there is a fuzzy relation R (from X to Y) and T (from Y to F); then the composition $C = R \,.\, T$ indicates relation of X and F. As an example consider the following membership values $\mu_R(x_i, y_j)$ and $\mu_T(y_j)$ of the relations R and T:

$\mu_R(x_i,y_j)$	y_1	y_2	y_3	y_4
x_1	0,2	0,4	0,0	0,5
x_2	0,6	0,2	0,0	0,8
x_3	0,4	0,6	0,9	0,0
x_4	0,7	0,0	0,0	0,6

$\mu_T(y_j)$	y_1	y_2	y_3	y_4
F	1,0	0,8	1,0	0,7

For the composition $C = R \,.\, T$ it holds /13/

$$\mu_C(x_i) = \bigvee_{y_j} [\mu_T(y_j) \wedge \mu_R(x_i, y_j)] , \tag{15}$$

Using this formula it follows

$\mu_c(x_i)$	F
x_1	0,5
x_2	0,7
x_3	0,9
x_4	0,7

In this way determined relation between the fuzzy sets X and F indicates relative significance of various deformation effects x_i in damage assessment of the structure. Floor vibration x_3 leads to the highest support 0,9, that the structure is unserviceable, cracking of partition walls x_2 and cracking of cladding x_4 seems to be slightly less significant (support 0,7), while the lowest support 0,5 is due to deflection x_1. It is expected that similar analysis in design stage would yield information enabling reliability differentiation of various serviceability limit states and/or redesign of critical structural details.

6. CONCLUSIONS

1) Serviceability problems of building structures involve two types of incertitudes:

- natural randomness which causes statistical uncertainty, and
- imprecisions or vagueness, which causes fuzziness.

It is important to distinguish them and to apply appropriate mathematical models.

2) Due to imprecision and vagueness in definition of serviceability limit states, there is no crisp but fuzzy boundary separating set of safe (serviceable) and failed (unserviceable) structures. Trilinear membership function for failed structures, characterized by two boundaries of transition zone and their standard deviation, may be used as an acceptable model.

3) Characteristic value of limit deformation may be defined using the concept of cumulative damage, which is generalization of cumulative distribution function. For a given cumulative damage characteristic value is dependent on a given membership function and its characteristics.

4) Reliability of serviceability limit states may be measured by fuzzy probability of failure defined by convolution integral of probability density function of structural deformation and cumulative damage function. Derived restrictions for admissible characteristics of structural deformation, corresponding to a given fuzzy probability of failure, may be easily applied in design calculation.

5) Fuzzy set theory seems to be most useful tool in solving various problems of serviceability limit state of building structures. The research is, however, in its early stage and further investigation is needed to precise some fundamental mathematical models and their characteristics.

REFERENCES

/1/ Holický, M., Tichý, M. and Vorlíček, M., "Statistical Serviceability Conditions for Concrete Structures", Stavebnícky časopis, Vol.XX, 1972/7.

/2/ Holický, M. and Tichý, M., "Statistische Untersuchung der Gebrauchsfähigkeit von Betonbauten", In: Sicherheit von Betonbauten, Deutscher Beton-Verein, Wiesbaden, 1973.

/3/ ACI Committee 435 "Variability of Deflections of Simply Supported Reinforced Concrete Beams", ACI Journal, January 1972, pp. 29-35.

/4/ Beeby, A.W., "A note on an aspect of the variability of deflections", Magazine of Concrete Research, Vol.26, No.88, September 1974, pp. 161-168.

/5/ Ramsay, R.J., Mirza, S.A. and MacGregor, J.G., "Monte Carlo Study of Short Time Deflections of Reinforced Concrete Beams", ACI Journal 1979, pp. 897-917.

/6/ Holický, M., "Theoretical Analysis of Random Structural Deformations", Acta Technica ČSAV, No.5, 1975, pp. 521-529.

/7/ Holický, M. and Bouška, P., "Random Behaviour of Concrete Beam Deflection", Acta Polytechnica, Vol.11., No.I,2,1986, pp. 67-75.

/8/ Mayer, H. and Rüsch, H., "Bauschäden als Folge der Durchbiegung von Stahlbeton-Bauteilen", Deutscher Ausschuß für Stahlbeton, Heft 193, Berlin 1967, 90 p. ("Building Damage Caused by Deflection of Reinforced Concrete Building Components", translated by Reiner, J.H., NRC Ottawa, 1970).

/9/ SG - CUR Report No.2., "Vorvormingseisen voor bouwconstructies", Waltman Delft, 1975, 138 p. (Deformation requirements for buildings, translated by Maurenbrecher, A.H.P., NRC Ottawa, 1980).

/10/ "Structural Deflections. A Literature and State-of-the-Art Survey". U.S. Department of Commerce, National Bureau of Standards, October 1973.

/11/ Zadeh, L., "Fuzzy Sets", Information and Control, Vol.8, 1965, pp.338-353.

/12/ Blockley, D.I., "The Nature of Structural Design and Safety," Ellis Horwood Ltd., Chichester, England, 1980.

/13/ Brown, C.B. and Yao, J.T.P., "Fuzzy Sets and Structural Engineering", Journal of the Structural Engineering, Vol.109, No.5, May,1983, pp.1211-1225.

/14/ Yao, J.T.P., "Damage Assessment of Existing Structures", Journal of the Engineering Mechanics Division, ASCE, Vol.106, No.EM4, Aug., 1980, pp.785-799.

/15/ Shiraschi, N. and Furata, H., "Structural Design Process as Fuzzy Decision Model". In: Fourth International Conference on Applications of Statistics and Probability in Soil and Structural Engineering, Universita di Firenze (Italy), 1983, Pitagora Editrice.

STRUCTURAL SERVICEABILITY AND CONCRETE IN COMPRESSION

E.F.P. Burnett[1] and P.F. Kelly[2]

1. Building Engineering Group, Civil Engineering Dept.
University of Waterloo
Waterloo, Ontario
2. Adjeleian, Allen, Rubeli Ltd. Consulting Engineers
Toronto, Ontario

ABSTRACT

In the analysis and design of reinforced concrete structures, it is necessary to make numerous assumptions, rationalizations and approximations. Of the two materials involved, the actual properties and likely response of the steel reinforcement is much better understood than those of the concrete. It is for this reason that the in-service performance and safety of structural concrete elements are largely predicated on the likely behaviour of the steel. For example, yield is an upper limit on service load response, and "plastic" yielding is the basis for so-called "ultimate strength" calculations. For these and other reasons there is a tendency, in structural design, to lose sight of the fact that concrete response in compression can, in certain circumstances, be critical. This is indeed the case when considering service response.

The objective of this paper is to discuss the relative importance of concrete in compression and to demonstrate the need for a specific serviceability criterion for concrete in flexural compression.

The provisions of the current Canadian Code are considered. It is demonstrated that there are many instances where compression overstress occurs under service loads. Certain anomalies that exist as a consequence of the recent code changes are identified and discussed. A serviceability criterion for concrete in compression is recommended.

1. INTRODUCTION

In general, everyone involved with a building has a stake in ensuring that each and every component comprising the building performs satisfactorily. It is generally expected that the actual performance of the building, in part and as a whole, will be better than (or at least comparable to) some explicit or even implicit standard of performance. Insofar as it is possible to do so, this general expectation may be expressed in the form of the following conditional criterion:

$$[P^r_{c,w} \geq P^s_{c,w}]^{B_{max}}_{\$_{min}} \qquad (1)$$

where

$P^r_{c,w}$ represents the actual or computed response (r) of each and every component (c) under each and every possible loading situation (w)

$P^s_{c,w}$ represents the desired response (s) of the relevant component (c) for each and every situation that could be construed as a loading

B_{max} represents maximum relevant benefits

$\$_{min}$ represents minimum relevant costs.

All safety and serviceability considerations must be satisfied. In general terms, one could say that the structural system is serviceable if, in part and as a whole, it performs in an essentially repeatable, controllable and calculable manner under service loading.

Serviceability must be confirmed at all levels of in-service response, i.e., the material, section, element, sub-system and system levels of in-service response. A set of serviceability criteria can be developed to apply over the entire range of service loads, i.e., between the minimum and the maximum service load. These are largely deformation-related limits, e.g. sway, deflection or strain.

Some of these serviceability criteria are familiar, e.g., deflection at the sub-system and system level of response or steel strain limits at the material level of response.

In the case of reinforced concrete structural systems, at least two materials are involved: reinforcing steel and concrete. Because of the low tensile strength of concrete, it is necessary to satisfy serviceability criteria that explicitly address issues such as the incidence of tension cracking and the width of cracks, both visible and otherwise. Another serviceability consideration that should be addressed is the performance of the concrete in compression. For example, it is necessary to ensure--everywhere in the system under service loading--that:

$$[\epsilon_{c\,max} \leq \epsilon_{cs}] \qquad (2)$$

where ϵ_{cmax} is the maximum compression strain in the concrete at each and every critical section

and ϵ_{cmax} is a limiting allowable value for the concrete being used at the relevant section.

In practice, this serviceability criterion is rarely addressed explicitly. Neither of the applicable North American codes (CAN 3 A23.3, AC1 318) specifies a limiting strain or stress for concrete in compression. At best, there is an expectation that this serviceability consideration is implicitly satisfied.

In this paper the objectives are:

(i) to evaluate and discuss the implications of current practice with regard to compression in the concrete under service loads, and
(ii) to develop a serviceability criterion for compression in the concrete and to illustrate its relevance for reinforced concrete buildings.

2. CURRENT PRACTICE

Probably the most common calculation in designing reinforced concrete structures is satisfying the safety criterion for bending, namely:

$$[M_r \geq M_f] \qquad (3)$$

where M_r is the maximum computed flexural strength of the critical section in any element, and

M_f is the maximum bending moment that is likely to occur at this section.

In accordance with CAN 3 A23.3 M84, the right-hand side of the criterion will involve a factored or ultimate load, w_f, which is derived as follows:

Type of Loading	Service Load	Factor	Factored or "Ultimate" Load
Dead Load (W_d)	w	1.25	1.25 w
Live Load (W_l) (for $W_l/W_d = m$)	mw	1.50	1.50 mw
	$w_w = w(1+m)$		$w(1.25+1.5\ m)=w_f$

Given that analysis at the system and sub-system levels is based upon the assumption of linear elastic response and some non-varying distribution of flexural stiffness, the magnitude of the relevant applied moments is:

$$M_f = w_f L^2 F \alpha (1.25 + 1.5m) \tag{4}$$

$$M_w = M_d + M_l = w_w L^2 F \alpha (1 + m) \tag{5}$$

$$M_d = wL^2 F \alpha 1 \tag{6}$$

$$M_l = mw L^2 F \alpha m \tag{7}$$

The left-hand side of the criterion involves the computation of the moment of resistance at the appropriate critical section. For under-reinforced and essentially rectangular, singly reinforced elements the current Canadian code suggests:

$$M_r = \phi_s f_y A_s (d - a/2) \tag{8}$$

and $$a = \frac{\phi_s f_y A_s}{\phi_c .85 f_c' b} = \frac{\phi_s}{\phi_c} \frac{f_y}{f_c'} \rho \frac{d}{.85} \tag{9}$$

for $\rho = \frac{A_s}{bd}$

$$M_r = \phi_s f_y \rho\, bd^2 \left(1 - \frac{\phi_s}{\phi_c}\frac{f_y}{f_c'}\frac{\rho}{1.7}\right) \qquad (10)$$

The code superimposes two reinforcement limits on the use of this expression, namely:

$A_s \geq 0.002\, A_g$, for slabs.

$$\rho \geq \frac{1.4}{f_y} \qquad (11)$$

$$\rho \leq \frac{\phi_c f_c' \beta_1\, 510}{\phi_s f_y (600 + f_y)}, \text{ for beams and slabs} \qquad (12)$$

For any specified set of dimensions, i.e., b, d and h, and choice of materials, e.g., a steel with $f_y = 400$ MPa and a specific f_c' value, it follows that for any value of ρ the relevant value for M_r can be determined.

Similarly, it follows that if $M_r = M_f$, then the value of the moment at maximum service load is:

$$M_w = M_r \frac{(1+m)}{(1.25 + 1.5m)} \qquad (13)$$

Under service loading, it is usually presumed that although the section may be cracked, response is both linear and elastic. It follows that the extreme fibre stress (for singly reinforced sections) may be determined from the following expressions:

$$f_{c\,max} = \frac{2M_w}{bd^2 k\left(1 - \frac{k}{3}\right)} \qquad (14)$$

where $k = \sqrt{n^2\rho^2 + 2n\rho} - n\rho$, for $n = \frac{E_s}{E_c} = \frac{200{,}000}{5{,}000\sqrt{f_c'}}$

$$\text{hence } f_{c\,max} = \frac{2(1+m)\,\phi_s f_y \rho \left(1 - \frac{\phi_s}{\phi_c}\frac{f_y}{f_c'}\frac{\rho}{1.7}\right)}{(1.25 + 1.5m)\,k\left(1 - \frac{k}{3}\right)}$$

$$= 2\,\phi_s f_y \rho \,\frac{(1+m)}{(1.25 + 1.5m)}\,\frac{\left(1 - \frac{\phi_s}{\phi_c}\frac{f_y}{f_c'}\frac{\rho}{1.7}\right)}{k\left(1 - \frac{k}{3}\right)} \qquad (15)$$

Equation 15 is a general expression for the maximum concrete stress in compression for a singly reinforced rectangular concrete section.

Hence, for various values of m it, is, in theory, relatively simple to calculate this maximum compression stress under service loading. For example, Figure 1a shows a graph of $f_{c\ max}$ versus ρ for any singly reinforced rectangular section with $f_y = 400$ MPa and $f_c' = 25$ MPa and for live-to dead-load ratios ranging from 0.5 to 2.0. It is evident that the value of the maximum compression stress will vary as a function of ρ. Similar graphs can be developed for sections with 30, 35 and 45 MPa concrete (i.e. Figures 1b, 1c, and 1d).

3. THE CONCRETE COMPRESSION SERVICE LIMIT STATE

The serviceability criterion for compression in the concrete was previously stated, namely:

$$[\epsilon_{c\,max} \leq \epsilon_{cs}] \qquad (16)$$

If the usual assumption of linear elasticity under service loading is made, then it follows that the left-hand side of this conditional criterion may be evaluated from the stress value:

$$\epsilon_{c\,max} = \frac{f_{c\,max}}{E_c} \qquad (17)$$

$$\epsilon_{c\,max} = \frac{2\,\phi_s f_y \rho\,(1+m)\left(1 - \frac{\phi_s}{\phi_c}\frac{f_y}{f_c'}\frac{\rho}{1.7}\right)}{5000\sqrt{f_c'}\,(1.25 + 1.5m)\,k\left(1 - \frac{k}{3}\right)} \qquad (18)$$

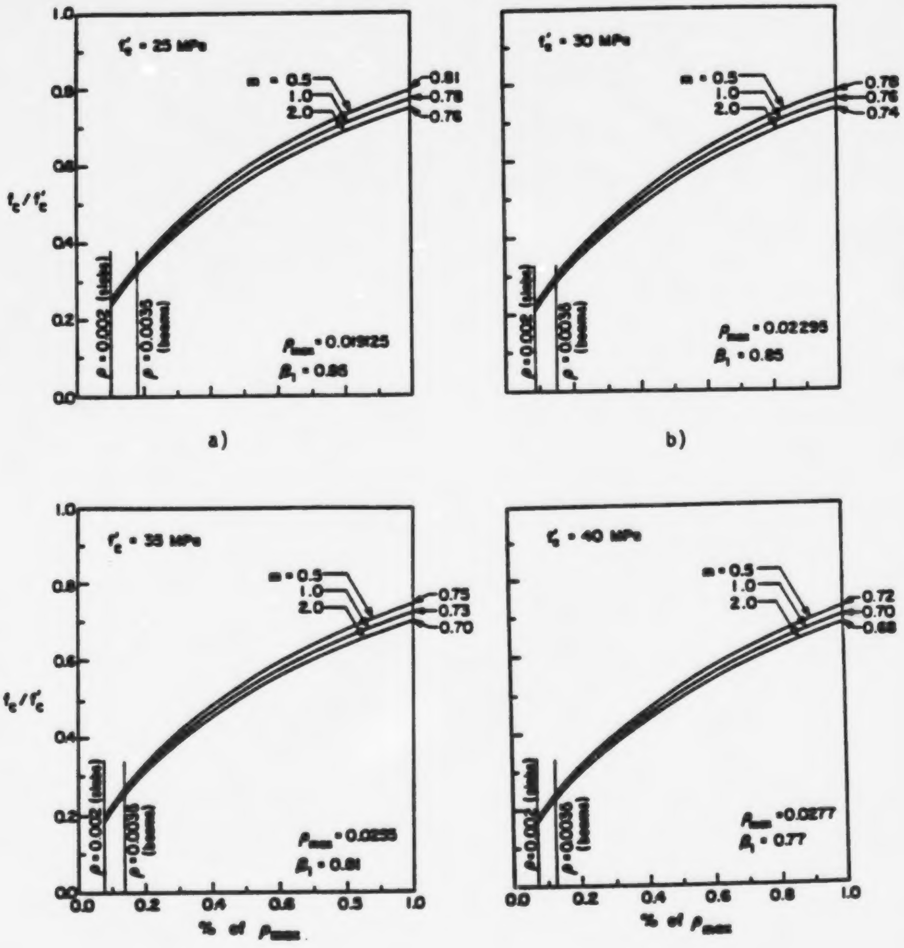

a)

b)

c)

d)

FIGURE 1: MAXIMUM FLEXURAL COMPRESSION STRESS UNDER SERVICE LOADS VERSUS PROPORTION OF TENSION REINFORCEMENT.

The right-hand side of the conditional criterion is not specified in CAN 3 A23.3. In fact, it is difficult to find any reference to a service load limit for concrete in compression. Consider the representative stress-strain relationships for concrete in compression shown in Figure 2. Tests on a standard cylinder are customarily used to provide a model of the relationship between stress and strain, at least up to maximum strengh, f_c'. The secant modulus of elasticity

$$E_c = 5000\sqrt{f_c'}$$

for normal density concrete is variously stated to cut this curve at somewhere between $0.45f_c'$ and $0.5f_c'$. If there is constraining reinforcement in the compression zone (both ties and longitudinal bars), then there will be two curves--one for the cover or the shell and another for the constrained concrete or the core.

In order to ensure that under service loading the compression zone performs in a reasonably repeatable, controllable and calculable manner, it is evident that, as far as possible, linear elasticity should be preserved. To do so, consider the following:

(i) The initiation of shell-core separation must be avoided so that the concrete in the shell and within the core behaves in a similar manner and normal linear elastic flexural theory is applicable. Sargin, on the basis of strain measurements, reported that the ties become effective in confining the core at a stress of between 60 to 70 percent of f_c' [2]. As shown in Figure 2, the behaviour of the compression zone is relatively complex.

(ii) To calculate the "ultimate" flexural resistance of a section, i.e., M_r, the basic assumptions as to concrete compression response are shown in Figure 3. Instead of the "actual" stress-strain curve, an overly simple stress-factored version is currently used in the Canadian code. In other words the maximum permissible stress for safety calculations would appear to be $0.6\ f_c'$.

At the "ultimate-limit" state, the designer's primary concern is to avoid a low-probability calamitous event. For the service-limit state, the designer is concerned with a highly probable event, one that might occur many times. The object is to avoid or minimize perturbation, cumulative deformation, or other effects that might affect the in-service performance of the building. Using a similar logic, it follows that under service loads compression stress should be limited to a value somewhat less than $0.6\ f_c'$.

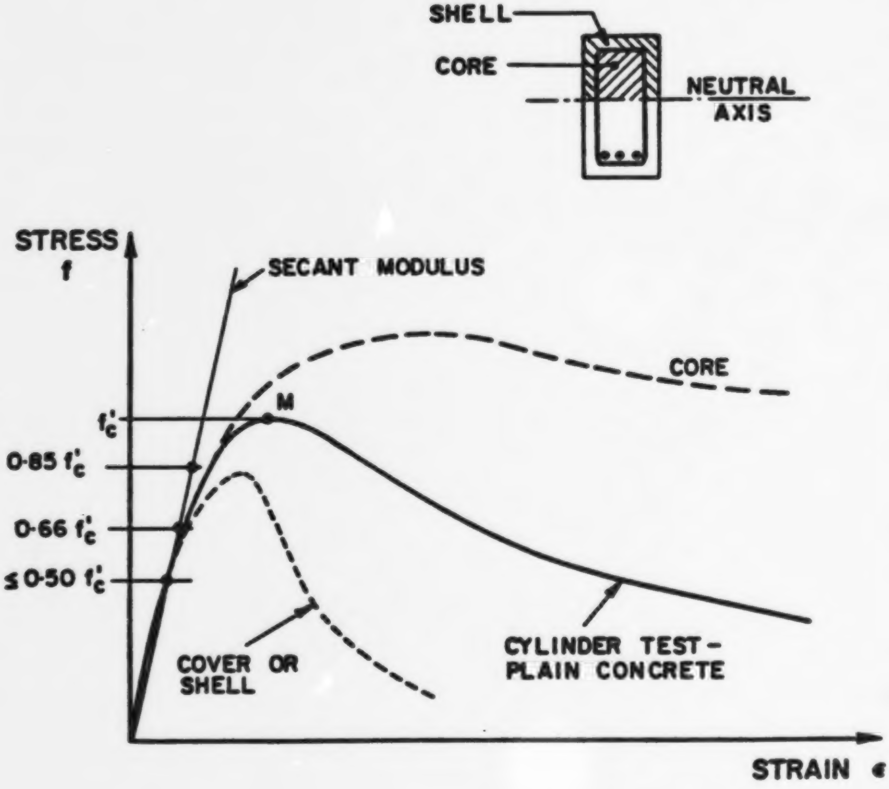

FIGURE 2: STRESS STRAIN CURVES FOR CONCRETE IN FLEXURAL COMPRESSION.

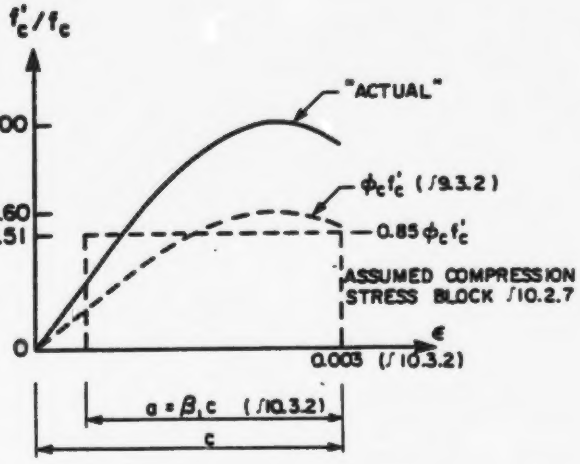

FIGURE 3: ASSUMED STRESS - STRAIN DISTRIBUTION FOR CONCRETE IN FLEXURAL COMPRESSION (CAN 3 A23.3-M84)

In fact, the rationale for the use of 0.6 f_c' as an ultimate limit state would seem to make it illogical for a stress greater than 0.6 f_c' to be tolerated at service load.

(iii) Various texts suggest that the secant modulus, E_c, intersects the compression stress-strain curve at either 0.45 f_c' or 0.5 f_c'. In numerical terms, the use of the straight-line relationship provides a good model for concrete response up to a maximum compression stress of about 0.6 f_c'. After this point, the non-conservative effects tend to exceed the conservative effects and the strains start to diverge significantly.

(iv) Service loads involve both sustained and removable loads. Under sustained loading, creep relaxation occurs--especially in the concrete in compression. The immediate consequence is increased strain, followed, perhaps, by a relatively small decrease in compression stress. In addition, serviceability criteria apply at the start as well as the end of the service life of the building, i.e., starting from the date of commissioning. Furthermore, the non-sustained proportion of the loads can be applied at any time and, in buildings, this is often a large proportion of the total service load. It follows that because strain values are significantly affected by creep, it is better to work in stress rather than strain terms for this serviceability criterion.

(v) Service loading involves repeated application of load. Figure 4, based on tests on standard cylinders (Kelly 1986), shows what happens to the stress-strain relationship after a cylinder has been subjected to 10,000 cycles of the same loading; for the two cases shown the upper limit of the cyclic load was .5 f_c' and .6 f_c'. In both cases the reloading path is offset from the initial loading path, and the reloading path converges with the initial path at a point greater than the cyclic limit, i.e., .5 f_c' and .6 f_c' respectively. It is also clear that the higher the level of cyclic loading, the greater the divergence from the initial stress strain curve. Most of this divergence occurs well before 1000 cycles have been applied. On the evidence of these simple tests it is clear that better performance (less divergence, greater stability, less computational error) is obtained when the maximum level of repeated loading is kept relatively low: preferably below .6 f_c'.

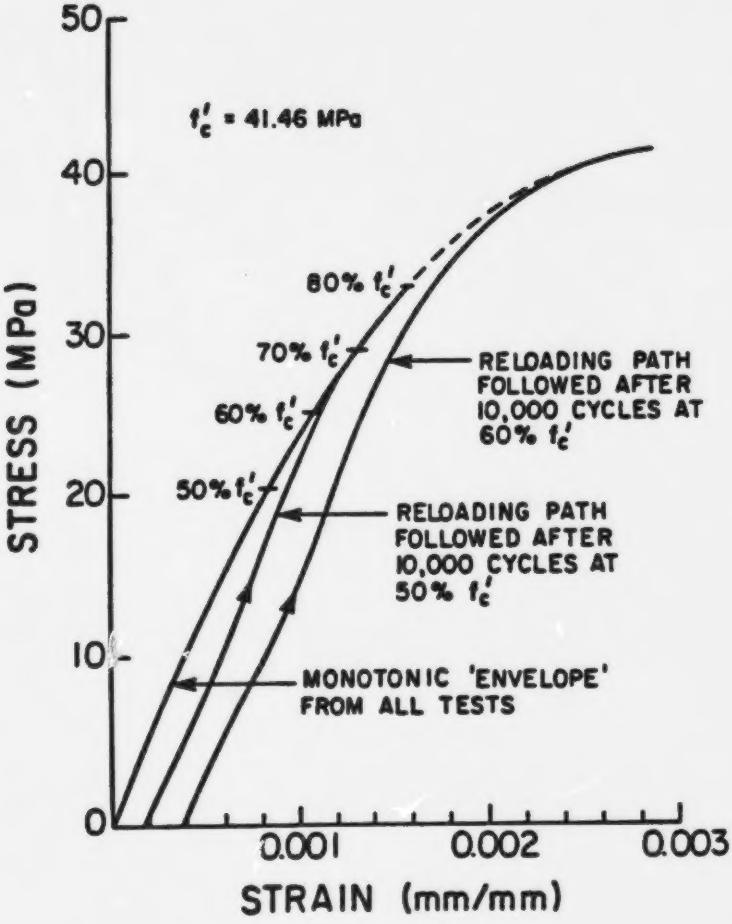

FIGURE 4: STRESS-STRAIN RELATIONSHIP FOR CONCRETE CYLINDERS SUBJECTED TO REPEATED LOADING

A much more comprehensive study on cylinders, beams and columns under fatigue loading was carried out by Aas-Jakobsen (Aas-Jakobsen 1970). Some of his findings were as follows:

- Prisms, beams or columns of the type tested will not fail during one million load cycles due to fatigue if the moment (or stress) is less than 60 per cent of the ultimate moment (or stress) found in short-time tests.

- Repeated load has little influence on the ultimate load if the specimen does not fail due to fatigue.

- Inelastic strains due to creep and repeated loads are not independent of each other.

- The increase in deformation due to 1 million load cycles for beams ranged from 40 to 80 per cent of the initial deformation. Furthermore, the results indicated a linear relationship between increased deformation and the ratio of the maximum moment to the ultimate moment, i.e., the amount of increase in deformation is directly proportional to the ratio of the maximum applied cyclic moment to the ultimate moment of the member.

It is therefore evident that the serviceability criterion in service limit state for concrete in compression (irrespective of whether there is constraining reinforcement) might be:

$$[f_{c\,max} \leq 0.55\, f_c'] \qquad (19)$$

A limiting value of 0.55 f_c' has been chosen. While there are a number of reasons why a value greater than 0.6 f_c' should not be used, there is little data to support any particular value less than 0.6 f_c'. A value of 0.55 f_c' has been chosen in order to allow for combined action of all the time-dependent effects such as creep, repeated loading, wear and tear, etc., and to provide some reserve against a level of 0.6 f_c' being exceeded. It is worth noting that in the old days of "Working Stress Design", a value of 0.45 f_c' was used as the limit of compression response for the concrete.

4. IMPLICATIONS FOR DESIGN

To illustrate the impact of introducing this serviceability criterion for concrete in compression, consider the representative sections for which the relationship between the maximum compression stress and proportion of reinforcement is shown in Figure 1. Figure 5 is a reproduction of Figure 1 with the limiting stress value of 0.55 f_c' added.

It is evident that:

(i) This serviceability criterion would severely restrict the amount of reinforcement that could be used. For $f_c' = 25$ MPa and a live-to-dead-load ratio of 0.5, the maximum proportion of reinforcement would be 42 per cent of the code-permitted amount; and for a live-to-dead-load ratio of 2.0, no more than 48 percent of the current maximum would be permitted. With a stronger concrete or a higher live-to-dead-load ratio, the maximum allowable reinforcement ratio increases.

(ii) Figure 5 clearly shows that many members designed and built in accordance with the current Canadian code could be performing non-linearly and inelastically under service loads. In other words, their response is non-repeatable (inelastic), uncontrollable (cumulative deformations) and impossible to compute (non-linear and dependent upon loading history).

(iii) Of obvious concern is the effect of a compression stress limit on the flexural capacity of a reinforced concrete member. In Table 1 the maximum proportions of reinforcement are listed for both the current code and a 0.55 limit on service load compression stress in the concrete. In addition, the ratio of the associated values for maximum moment (Mf) for each criterion is listed. Clearly the reduction is significant, and with low strength concretes this serviceability criterion could be restrictive. One advantage of using higher strength concrete is evident in Table 1. However, some other benefits from using higher strength concrete are:

- higher cracking moment
- a stiffer section, i.e., greater E_c
- reduced deformation

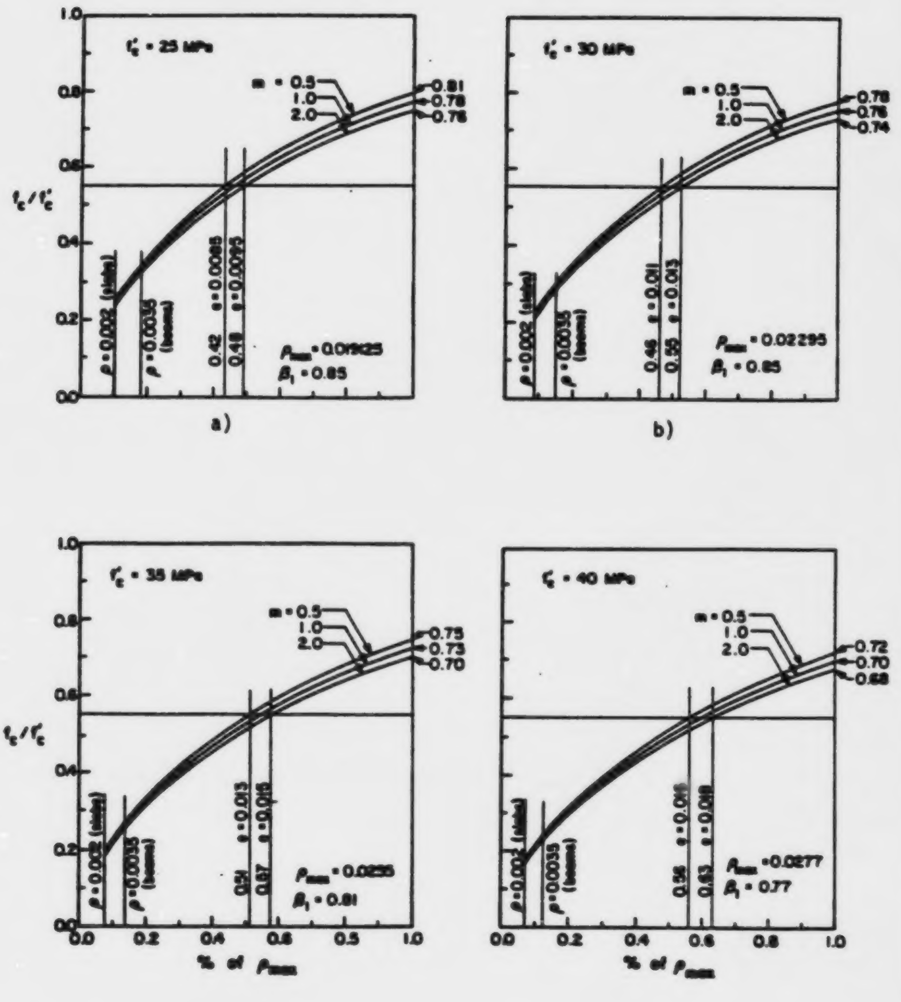

a)

b)

c)

d)

FIGURE 5: REINFORCEMENT LIMITS FOR A LIMITING COMPRESSION STRESS DESIGN CRITERION.

- greater shear strength
- greater ductility

TABLE 1 RATIO OF MAXIMUM MOMENT VALUES BASED ON RECOMMENDED AND CURRENT LIMITS ON REINFORCEMENT

f_c' (MPa)	ρ_{max} [1.] A 23.3-M84	$m = 0.5$		$m = 1.0$		$m = 2.0$	
		ρ_{max} [2.]	Ratio	ρ_{max} [2.]	Ratio	ρ_{max} [2.]	Ratio
25	0.019125	0.0085	.50	0.009	.55	0.0095	.58
30	0.02295	0.0105	.54	0.011	.57	0.012	.61
35	0.025515	0.013	.59	0.014	.63	0.015	.67
40	0.02772	0.0155	.63	0.0165	.66	0.0175	.70

1. for $c = \frac{600\,d}{(600 + f_y)}$ and $f_y = 400$ MPa
2. for $f_c = 0.55\,f_c'$ at maximum service load.

In simple economic terms, the use of this compression stress limit is not likely to have much impact since most practical reinforced concrete sections have reinforcement proportions that are much lower than the maximum permissible amount. The proposed limit would ensure that the reinforcement ratio lay within an economic range and would provide a good reason for doing so.

Perhaps the most important benefit would be the improved service life performance of reinforced concrete members, especially beams with high reinforcement ratios, e.g., members subject to hogging moment.

(iv) In pedagogical terms, there is an advantage in removing one of the many anomalies inherent in the latest Canadian Code. It is both illogical and unnecessary to limit reinforcement indirectly by referring to an improbable and undesirable condition, i.e., the balanced section, and in doing so to permit non-linear, inelastic service load response of the concrete and, thus, of the structure. To explain this provision to an undergraduate engineering student is an unnecessary challenge.

5. CONCLUSIONS

The serviceability criterion proposed in the paper ensures that greater attention is paid to the role and the relative significance of the concrete in design. Secondly, a much better--and more logical--upper limit on tension reinforcement is introduced. The current limit, based on the so-called "balanced" condition, has always been problematic in that it is presumed that the tension reinforcement attains its proportional or elastic limit at the same instant as the concrete compression zone attains it maximum contribution to flexural resistance. By satisfying two material serviceability criteria, namely:

$[\epsilon_s \le \epsilon_y]$ for the tension reinforcement and

$[f_c \le 0.55\, f_c']$ for the concrete in compression

it follows that a consistently logical limit on tension reinforcement is provided. This is a by-product of addressing the in-service performance of reinforced concrete in a more rational and systematic manner.

REFERENCES

Aas-Jakobsen, Knut, "Fatigue of Concrete Beams and Columns", The University of Trondheim, Norway, Sept. 1970.

Kelly, Peter, "Flexural Stiffness Considerations in Reinforced Concrete Buildings" M.Sc. Thesis, University of Waterloo, 1986,.331.p.

PROBABILISTIC DESIGN FOR SERVICEABILITY RELATED TO EXCESSIVE DEFORMATION

Dan M. Frangopol
Department of Civil, Environmental
and Architectural Engineering
University of Colorado at Boulder
Boulder, Colorado 80309-0428, USA

ABSTRACT: An analytical investigation carried out to assess the reliability of structural steel frame systems with multiple deformation requirements is reported. First-order elastic deformation analysis of deterministic structures acted on by random service loads is used. Safety indices with respect to excessive vertical and lateral displacements due to flexural components of frame deflections are calculated. The computations are made by using a first-order second-moment reliability analysis including imposed deterministic deformation limits and calculated random elastic deformations. Structural system reliability theory is used for computing a system safety index with respect to multiple deformation requirements. Isosafety service loading functions of structural systems are proposed to evaluate excessive deformation requirements from a reliability viewpoint.

1. INTRODUCTION

In recent years, considerable effort has been directed toward the application of reliability concepts and techniques in probability-based limit states design codes. In general, these codes contain requirements to insure that structures remain safe with regard to the occurrence of ultimate limit states. Recently, Galambos and Ellingwood (1986) as well as the Ad Hoc Committee on Serviceability Research (1986) recognized that the current code treatment of serviceability limit-states is inadequate. Today the desire to reduce structural weight without compromising structural performance provides further motivation for the development of probabilistic design for serviceability.

The survey reported by the Ad Hoc Committee on Serviceability Research (1986) indicates that significant serviceability problems related to ordinary building construction are associated with excessive deformation. Also, it was acknowledged (Turkstra and Reid 1981; Galambos and Ellingwood 1986; Ad Hoc Committee on Serviceability Research 1986) that designs of many current structures are controlled by deflection and drift limits rather than by strength requirements. It is, therefore, of practical importance to develop a probabilistic framework in order to examine the serviceability limit-state related to xcessive deformation.

This paper presents a probabilistic treatment of the safety of structural steel frame systems with multiple deformation requirements. First-order elastic deformation analysis of deterministic structures acted on by random service loads is used. Safety indices with respect to excessive vertical and lateral displacements due to flexural components of frame deflections are calculated. The computations are made by using a first-order second-moment reliability analysis including imposed deterministic deformation limits and calculated random elastic deformations. Structural system reliability theory is used for computing a system safety index with respect to multiple deformation requirements. Isosafety service loading functions of structural systems are proposed to evaluate excessive deformation requirements from a reliability viewpoint.

2. ASSUMPTIONS

The basic assumptions adopted herein for the probabilistic design of structures are similar to those presented by Frangopol and Nakib (1987a):

- First-order elastic vertical and lateral displacements correspond to an idealized deterministic structure with fixed geometry and rigidity;
- Only flexural components of frame displacements are considered in the analysis;
- The service static loads acting on the structure are random variables with known statistical properties for a given serviceability reference period (eight years, according to Galambos and Ellingwood 1986);
- The positions of loads are deterministic;
- The allowable (vertical) deflection, Δ_v^a, and the allowable (horizontal) drift, Δ_h^a, are deterministic limits specified by the code or by the designer;
- The statistical dependencies among the service random loads are accounted for through correlation coefficients;
- Consistent with a first-order second-moment reliability theory, the necessary statistical information is given in terms of service load vectors (mean values and coefficients of variation) and service load correlation matrix (coefficients of correlation among loads);
- On the same basis, of a first-order second-moment reliability approach, regardless of the probability distributions of the individual loads, the reliability of the structure with regard to (vertical) displacements is given as

$$\beta_v = \bar{g}_v/\sigma(g_v) \qquad (1)$$

and with regard to (horizontal) drift is given as

$$\beta_h = \bar{g}_h/\sigma(g_h) \qquad (2)$$

where β_v and β_h are safety (reliability) indices with respect to vertical and horizontal displacements, respectively. The deformation safety margins g_v and g_h are defined as

$$g_v = \Delta_v^a - \Delta_v \qquad (3)$$

$$g_h = \Delta_h^a - \Delta_h \qquad (4)$$

where Δ_v and Δ_h are the maximum first-order elastic vertical and lateral deflections due to random service loads. Unserviceability occurs when the functions g_v or g_h, or both, fall below zero. $\bar{g}_i$ and $\sigma(g_i)$ in (1) and (2) are the mean and standard deviation of the deformation safety margin g_i, respectively.

- The global safety (system reliability) index of a structure with respect to excessive deformation due to both (vertical) deflection and (horizontal) drift is given as

$$\beta_{system} = \beta_{v,h} = \bar{g}_{v,h}/\sigma(g_{v,h}) = \bar{g}_{system}/\sigma(g_{system}) \tag{5}$$

where $g_{v,h} = g_{system}$ is the deformation safety margin of the structure with respect to both deflection and drift, and $\bar{g}_{system}$ and $\sigma(g_{system})$ are the mean and standard deviation of the system deformation safety margin, respectively.

3. SYSTEM RELIABILITY EVALUATION ASSOCIATED WITH EXCESSIVE DEFORMATION

The reliability of a system acted on by random service loads with respect to loss of serviceability by excessive deformation is essentially a problem involving multiple deformation requirements.

If a structure under a given service load combination has m critical sections with respect to vertical deflections and n critical sections with respect to lateral deflections (drift), the occurrence of the maximum allowable vertical (Δ_v^a) or lateral (Δ_h^a) deflections, or both, in any of these sections will constitute loss of deformation serviceability of the system. The probability of system unserviceability by excessive deformation, therefore, is:

$$P_{system} = P(E_v \cup E_h) \tag{6}$$

where

$$E_v = \bigcup_{i=1}^{m} A_i \tag{7}$$

and

$$E_h = \bigcup_{j=1}^{n} A_j \tag{8}$$

represent the events associated with loss of serviceability by vertical and horizontal displacements, respectively. The event A_i (A_j) represents the occurrence of the maximum allowable vertical (horizontal) deflection limit Δ_v^a (Δ_h^a) at the critical section i (j); and U = the union of events A_i or A_j. If all random variables are normally distributed, then Eq. 6 becomes

$$P_{system} = \Phi(-\beta_{system}) \tag{9}$$

in which $\Phi(-\beta_{system})$ is the standardized normal distribution function. Alternatively, the system safety index β_{system} may be related to the risk of system unserviceability by excessive deformation as follows

$$\beta_{system} = \Phi^{-1}\,(1-P_{system}) \qquad (10)$$

A portal frame example is given next to illustrate the system reliability evaluation associated with excessive deformation.

4. NUMERICAL RESULTS

The three-member rigid steel frame shown in Fig. 1 is considered. This frame has fixed geometry (span = ℓ = 10m, height = h = 4m) and deterministic flexural rigidity (EI = 20525.6 kNm^2). The structure is subjected to two random concentrated service loads as follows: a lateral load H acting at the top of the left-hand side column, and a gravity load P acting at the distance a from the left-hand side column and b = ℓ-a from the right-hand side column. The two random variables H and P are assumed to be normal distributed and the statistical information (over eight years reference period) is as follows: mean loads ($\bar{H}$ = 100kN, $\bar{P}$ = 30kN), coefficients of variation of loads (V(H) = 0.15, V(P) = 0.20), and coefficient of correlation among loads $\rho(H,P) = 0$. The two critical sections of the frame with respect to loss of serviceability due to excessive flexural deformation by vertical deflection, Δ_v, and drift, Δ_h, are the sections 1 and 2 (see Fig. 1), respectively. Both Δ_v and Δ_h have two components as follows:

$$\Delta_v = \Delta_v^P + \Delta_v^H$$

$$\Delta_h = \Delta_h^H + \Delta_h^P$$

where

Δ_v^P = the first-order elastic vertical deflection due to P; Δ_v^H= the first-order elastic vertical deflection due to H; Δ_h^H = the first-order elastic drift due to H; and Δ_h^P = the first-order elastic drift due to P. The allowable deflection and drift limits are $\Delta_v^a = \ell/300 = 3.33$ cm and $\Delta_h^a = h/200 = 2$cm, respectively.

Figs. 2,3,4 and 5 show the mean values of the displacement components $\bar{\Delta}_v^P$, $\bar{\Delta}_v^H$, $\bar{\Delta}_h^H$, and $\bar{\Delta}_h^P$, respectively, when the gravity load P changes its location from the left-hand side column (i.e., a=0) to the right-hand side column (i.e., a=10m). The negative mean displacements in Fig. 3 (i.e., $\bar{\Delta}_v^H < 0$ for $a > 5$m) and Fig. 5 (i.e., $\bar{\Delta}_h^P < 0$ for $a < 5$m) are due to the fact that for these positions of the gravity load, H and P have opposite effects on Δ_v and Δ_h, respectively. As expected, it appears that changes in the gravity load location have no influence on the mean drift $\bar{\Delta}_h^H$ due to the horizontal load H (see Fig. 4).

Figs. 6 and 7 show the sensitivity of the individual safety indices β_v^P and β_h^H to changes in the gravity load location. In these figures the safety indices β_v^P and β_h^H correspond to the mean displacements $\bar{\Delta}_v^P$ (see Fig. 2) and $\bar{\Delta}_h^H$ (see Fig. 4), respectively.

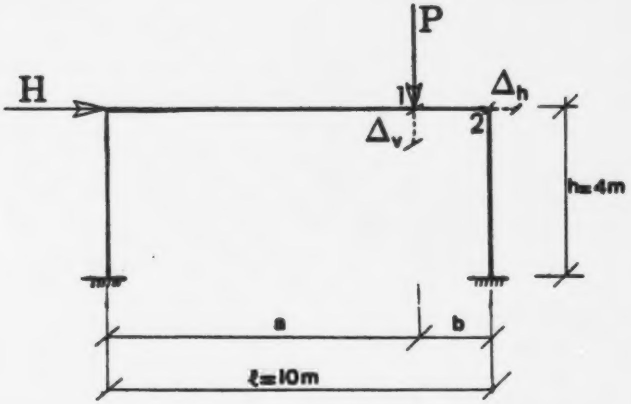

Fig. 1 - Three-member rigid frame.

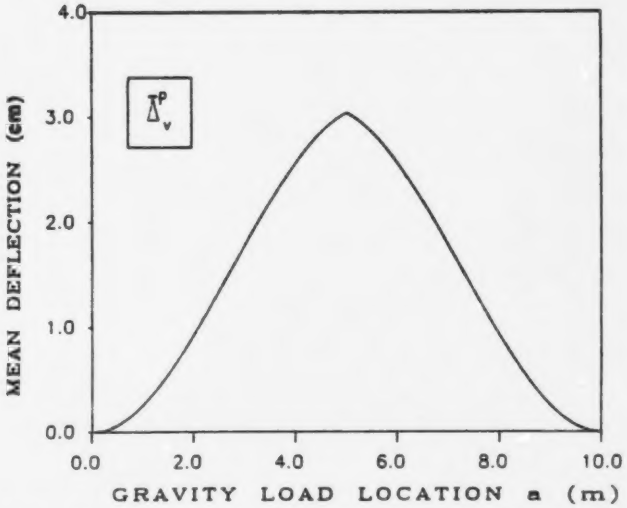

Fig. 2 - Mean vertical displacement due to vertical load P.

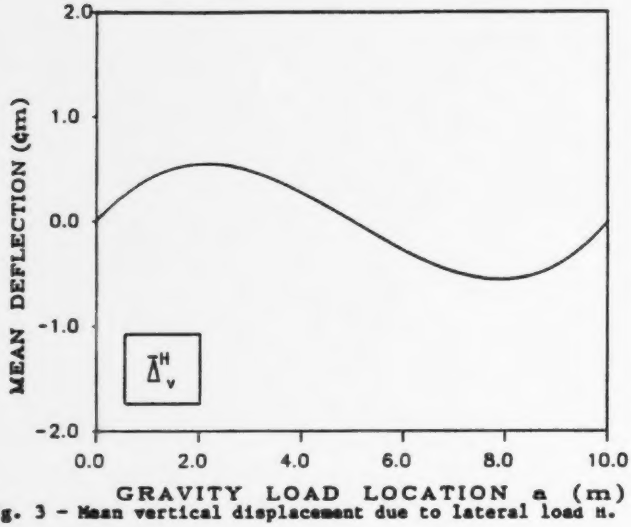

Fig. 3 - Mean vertical displacement due to lateral load H.

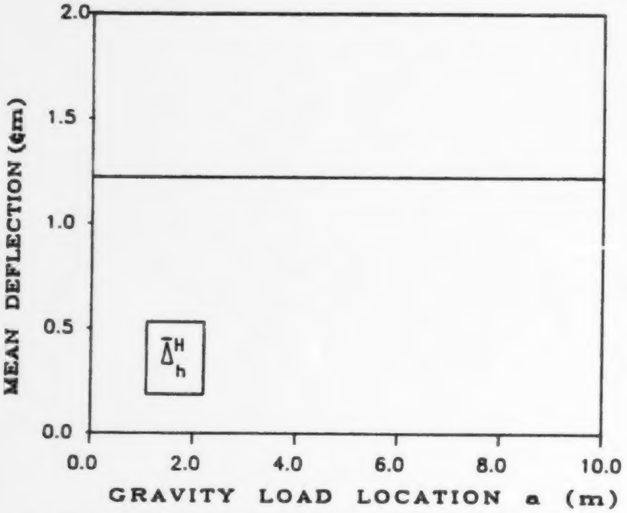

Fig. 4 - Mean horizontal displacement due to lateral load H.

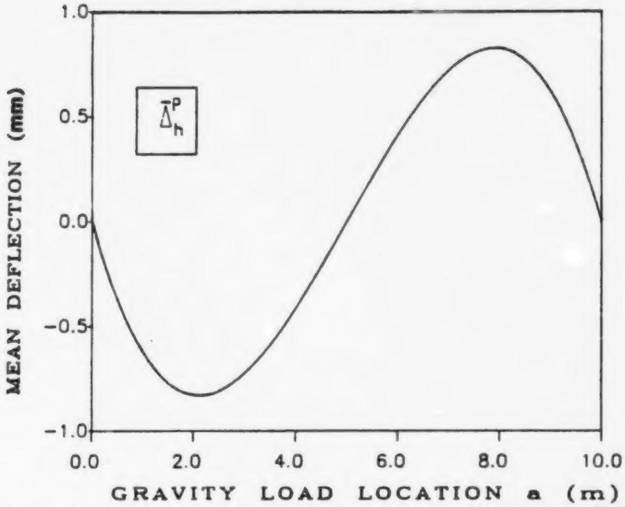

Fig. 5 - Mean horizontal displacement due to vertical load P.

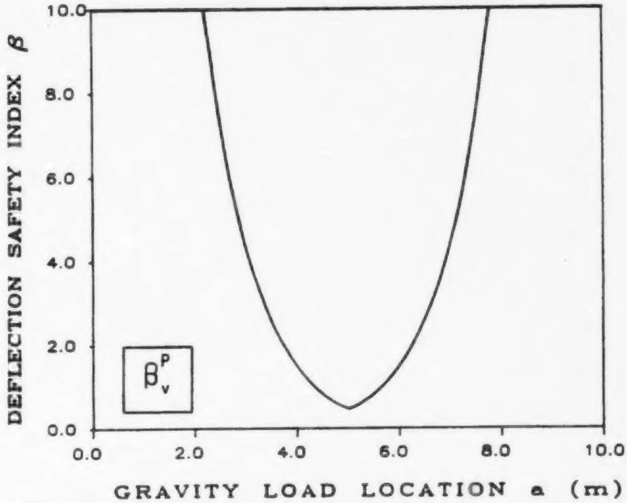

Fig. 6 - Safety index with respect to excessive vertical displacement due to vertical load P.

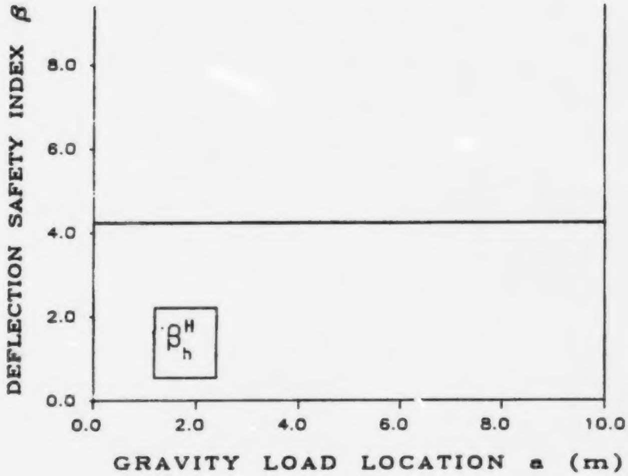

Fig. 7 - Safety index with respect to excessive drift due to horizontal load H.

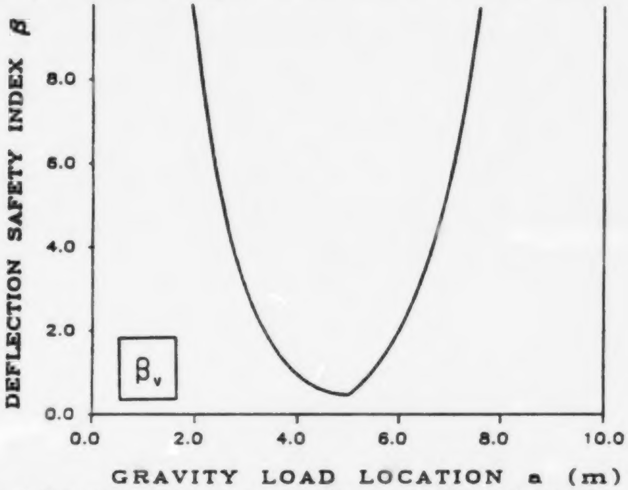

Fig. 8 - Safety index with respect to excessive vertical displacement due to loads P and H.

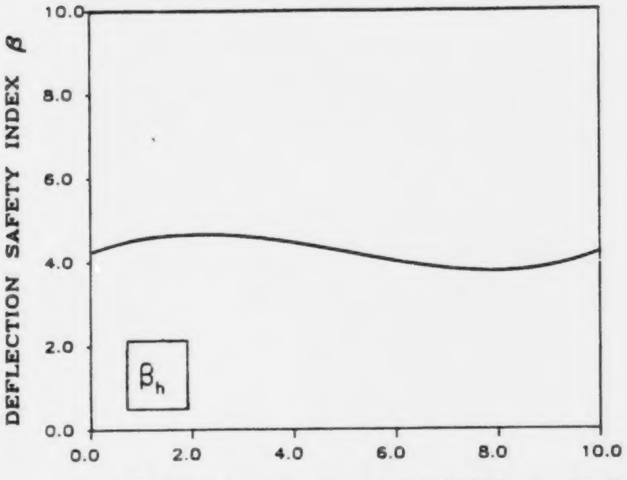

Fig. 9 - Safety index with respect to excessive drift due to loads H and P.

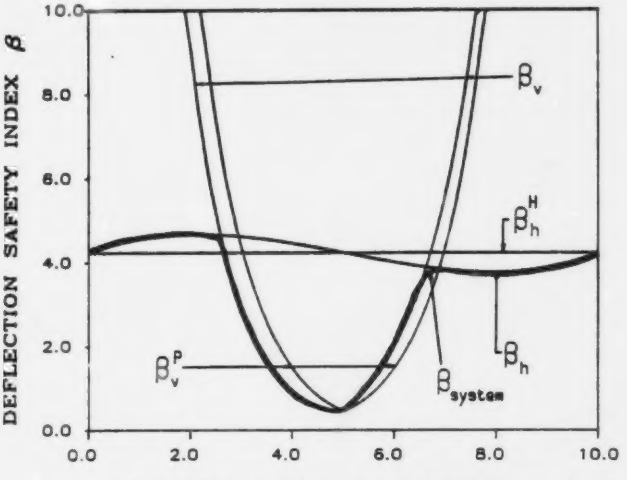

Fig. 10 - Safety indices with respect to excessive displacements.

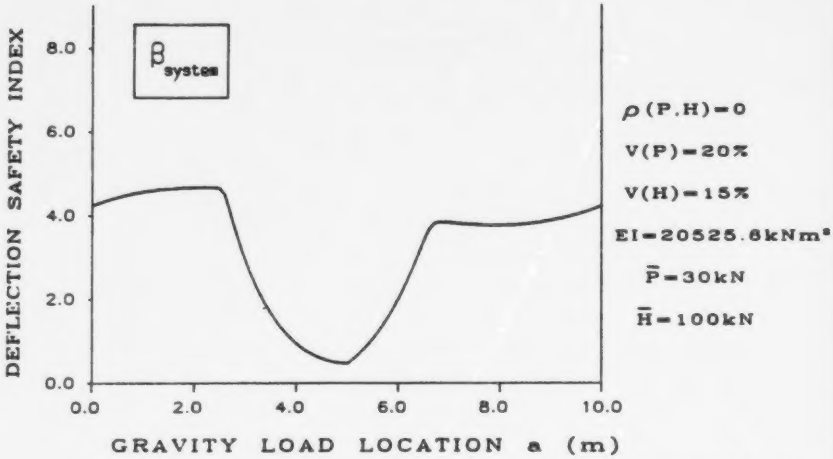

Fig. 11 - Overall system deformation safety index for independent loads.

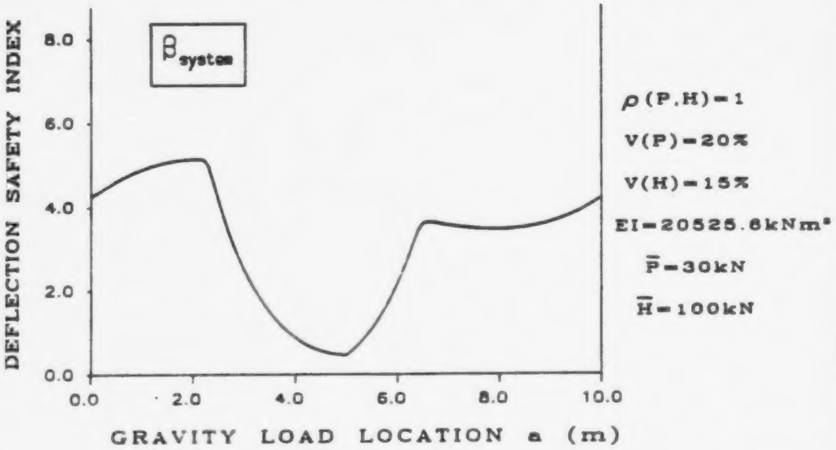

Fig. 12 - Overall system deformation safety index for perfectly positive correlated loads.

The safety indices β_v and β_h including both effects of P and H, are shown in Figs. 8 and 9, respectively. The loads P and H appear to dominate in contributing most to the safety indices β_v and β_h, respectively. It is also interesting to note that the reliability with respect to horizontal displacement is larger for $a < 5m$, and the reliability with respect to vertical displacement is increasing more rapidly for $a > 5m$. The reason for these is that the two service loads considered in this example have opposite effects on Δ_h and Δ_v for $a < 5m$ and $a > 5m$, respectively.

The individual safety indices β_v^P, β_h^H, the global safety indices β_v and β_h, and the overall system safety index β_{system} are illustrated in Fig. 10. The overall system safety index is also shown in Fig. 11; it corresponds to Ditlevsen's upper bound approximation (Ditlevsen 1979). For purposes of comparison the system deformation safety index β_{system} corresponding to perfect positive correlation among loads $\rho(H,P) = 1$ is shown in Fig. 12. Notice that for small values of a (say, $a \leq 2m$), the system safety index increases with increasing the coefficient of correlation $\rho(H,P)$ and for large values of a (say, $a \geq 8m$) decreases. In the central region, (say, $4m < a < 6m$) where the influence of the vertical load appears to dominate in contributing most to the safety of the system with respect to loss of serviceability by excessive deformation, the influence of load correlation is not as significant as it is in the extreme regions.

5. ISOSAFETY SERVICE LOADING FUNCTION

The serviceability limit-state function related to excessive deformation for a structure acted on by random service loads with a given reference period (say, 8 years) is defined here as an isosafety service loading function in the space of mean values of the service loads. Two different points on the same service loading function represent two different combinations of the mean values of the service loads leading to the same value of the probability of system unserviceability for a given reference period. An isosafety service loading function cuts the mean service loading space into two regions: the safe mean service loading region (where $\beta_{system} > \beta_{system}^a$) and the unsafe mean service loading region (where $\beta_{system} < \beta_{system}^a$). The set of mean service loading combinations that satisfy the strict equality $\beta_{system} = \beta_{system}^a$, where β_{system}^a = the allowable overall system safety index, are points on the isosafety service loading function.

Examples of isosafety service loading functions for unserviceability related to excessive deformation of the three-member frame in Fig. 1, due to vertical or lateral displacements, or both, are shown in Figs. 13 and 14. The isosafety service loading functions are obtained from first-order elastic analysis of the two possible deformation modes (i.e., vertical and horizontal deflections associated with sections 1 and 2, respectively). All points on the isosafety service loading functions shown in Figs. 13 and 14 represent different combinations of mean service loads $(\bar{H}, \bar{P})$ leading to the same value of the overall system safety index associated with excessive deformation $\beta_{system} = \beta_{system}^a = 2.32$. It is interesting to note how the safe mean service loading region decreases with increasing both the distance a from the left-hand side column to the vertical load P (see Fig. 13 where $a \leq 5m$) and the distance $b = \ell - a$ from the right-hand side column to the vertical load P (see Fig. 14 where $a \geq 5m$).

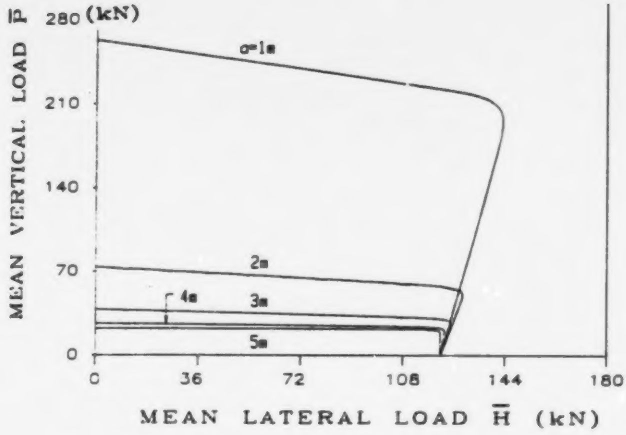

Fig. 13 - Isosafety service loading functions: a ≤ 5m.

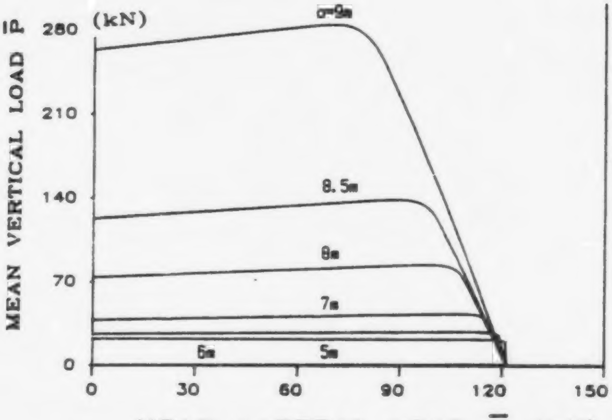

Fig. 14 - Isosafety service loading functions: a ≥ 5m.

6. CLOSURE

Mathematically speaking, probabilistic design for serviceability related to excessive deformation can be regarded as a system reliability problem with multiple deformation requirements, while from an engineering point of view it provides the designer with a systematic tool for considering the risk of system unserviceability. The isosafety service loading functions presented in Section 5 may serve as the rational basis for the formulation of risk-based provisions for efficiently designing structures for proper reliability levels with respect to multiple deformation requirements.

Only first-order elastic analysis of deterministic structures acted on by random service loads have been considered in this paper to illustrate the applicability of system unserviceability approach to static flexural deflections of simple frames. However, this approach has a rich potential far beyond these preliminary applications, and it may be expected to receive increasing attention in reliability-based analysis, design, and optimization of structural systems (Frangopol and Nakib 1987b, Frangopol 1987).

ACKNOWLEDGEMENTS

Support for this research study was received from the National Science Foundation through Grants No. MSM-8618108 and ECE-8609894. The writer is thankful to R. Nakib, graduate student at the University of Colorado at Boulder, for assistance in computations.

REFERENCES

Ad Hoc Committee on Serviceability Research, Committee on Research of the Structural Division. 1986. Structural serviceability: A critical appraisal and research needs. Journal of Structural Engineering. ASCE, 112 (12), pp. 2646-2664.

Ditlevsen, O. 1979. Narrow reliability bounds of structural systems. Journal of Structural Mechanics. 7, pp. 453-472.

Frangopol, D.M. 1987. Unified approach to reliability-based structural optimization. Dynamics of Structures (Ed. J.M. Roesset), ASCE, New York, pp. 156-167.

Frangopol, D.M. and Nakib, R. 1987a. Reliability analysis of deflection-drift limited structures. Reliability and Risk Analysis in Civil Engineering (Ed. N.C. Lind), 1, pp. 456-463.

Frangopol, D.M. and Nakib, R. 1987b. Reliability of structural systems with multiple limit states. Materials and Member Behavior (Ed. D.S. Ellifritt), ASCE, N.Y., pp. 638-646.

Galambos, T.V. and Ellingwood, B. 1986. Serviceability limit states: Deflection. Journal of Structural Engineering. ASCE, 112(1), pp. 67-84.

Turkstra, C.J. and Reid, S.G. 1981. Structural design for serviceability. Probabilistic Methods in Structural Engineering (Eds. M. Shinozuka and J.T.P., Yao), ASCE, N.Y., pp. 81-101.

RELIABILITY OF SERVICEABILITY LIMIT STATES FOR ENGINEERED WOOD STRUCTURES

J.J. Salinas
Department of Civil Engineering
Carleton University
Ottawa, Canada

R.G. Gillard
Manhire–Cunliffe Partnership
Engineering Consultants
Ottawa, Canada

ABSTRACT: The performance of engineered wood products is examined and assessed in terms of the probability of failure to satisfy serviceability requirements. The safety of the system is characterised by the *reliability index*, β, which is calculated for a range of values of the permissible mid-span deflection under service loads. The results of tests on two different types of building structures have been used to compare the behaviour of conventional wood systems with that of new designs and new products. The levels of safety against failure for serviceability limit states found in this study indicate the existance of a *size effect* in long-span light wood roof trusses.

The level of safety against excessive deflections of conventional solid lumber joists has been compared with that of waferboard I beams. Both products show acceptable levels of the reliability index, β, for allowable deflections near or above $\frac{SPAN}{360}$ but fail to meet the more strict criteria imposed by CMHC.

1. INTRODUCTION

CSA–S408–1981 defines *Serviceability limit states* as those which restrict the normal use and occupancy of a building or affect its durability. These limit states include excesive deflections affecting the function of the structure or its appearance as well as the function of equipment or other non–structural components. Excesive local damage such as cracking, splitting, spalling, connection slip, etc. are also undesirable limit states.

More recently, with the increased use of high strength materials, smaller sizes are adequate to resist the loads but the stiffness or mass of the resulting structural system in many cases are inadequate to avoid excesive deflections or vibrations. Therefore, excesive vibration that affects the comfort of the occupants or the operation of equipment is also an undesirable limit state.

The rationalization or the origin of the more traditional constraints imposed on deflections — such as the well-known *span/360*— have not been well established, yet these simple rules-of-thumb have received wide acceptance by the profession. Percival (1979) has shed some light as to the origin of this particular requirement.

Unfortunately in many cases, structures satisfying the stiffness requirements still exhibit excesive vibrations. The *Ad Hoc* Committee on Serviceability of ASCE (1986) recognized the importance of developing a system of serviceability guidelines flexible enough to incorporate the various sources of undesirable limit states as well as adaptable enough to encourage the designer to take a closer look at serviceability constraints.

As is the case with most recent advances in code development, this study uses of the concepts of probability-based limit states design to compare the performance of engineered wood structures. The reliability index, β, is used as a measure of the level of safety against failure to meet deflection limits for specific designs of floor and roof systems. First, the performance of Waferboard I beams is compared with that of conventional solid joists. At the same time, the performance of the test itself is examined in an attempt to find faster and more economical test procedures. In the second application, the performance of long-span roof trusses is investigated with respects to seviceability (deflection) requirements. Before the actual applications are presented, the following section discusses briefly the theory behind the approximate formulation of the reliability index.

2. A GENERALIZED FORMULATION

The reliability of a structural system can be defined as the probability that the system will not fail during its expected lifetime. For a serviceability limit state, it is possible to express reliability as the probability that the system will not exceed certain limits imposed on its response to loads. These limits typically consist of maximum allowable deflections or vibration response spectrums under characteristic use and occupancy loads.

The analysis of a single-failure-mode system can be formulated as a 'demand–capacity' problem where the 'demand' is characterized by the flexibility of the system, represented by the variable, Y, and the 'capacity' is represented by the limiting factor Y_a. The performance function for this system is given by:

$$Z = Y_a - Y \tag{1}$$

The limiting performance of the system is given by $Z = 0$ which defines a *limit state* in which there is no failure to meet the specified limits nor excess capacity in the system. The *failure state* is given by $Z < 0$ and the *safe state* by $Z > 0$.

The probability of failure of the system can be calculated by determining the probability of occurrence of the *failure state*, $Z < 0$. Failure occurs when $Y_a < Y$ and for a given demand $Y = u$ the failure event is the joint occurrence of $Y_a < Y$ and $Y = u$. Consequently, the probability of failure is calculated by multiplying the probabilities associated with these two events.

$$P[Y_a \leq Y] = \int_{-\infty}^{Y} f_{Y_a} dY_a \tag{2}$$

where f_{Y_a} = probability density function of the system capacity, Y_a. The probability that the demand will take a particular value, $Y = u$, is given by:

$$P[Y = u] = f_Y(u)dY \tag{3}$$

where f_Y = probability density function of the system demand, Y. The probability of failure must be evaluated for all $-\infty \leq u \leq +\infty$ and is given by:

$$P_f = \int_{u=-\infty}^{u=+\infty} f_Y(u)dY \int_{Y_s=-\infty}^{Y_s=Y=u} f_{Y_s}(u)dY_s \tag{4}$$

Alternatively, the probability density function for Z, f_Z, can be derived from the individual probability density functions for the system flexibility and the capacity, f_Y and f_{Y_s}.

The reliability index, β, can be defined as the ratio of the mean to the standard deviation of the derived distribution for Z.

$$\beta = \frac{m_Z}{\sigma_Z} \tag{5}$$

If f_Z is assumed to follow a normal distribution, the probability of failure and the reliability index are related by:

$$P_f = 1 - \Phi(\beta) \tag{6}$$

where $\Phi(\beta)$ = cumulative distribution function of the standard normal variable, evaluated at β. Table 1 lists the values of β corresponding to various probabilities of failure, according to CSA Special Publication S408-1981. Recommended target values for the reliability index are given in Table 2.

Table 1: Reliability Index and Probability of Failure

β:	1.28	2.33	3.09	3.72	4.26	4.75	5.61
P_f:	10^{-1}	10^{-2}	10^{-3}	10^{-4}	10^{-5}	10^{-6}	10^{-7}

Table 2: Target Reliability Index, β. CSA S408-1981.

	Type of Failure	
Safety Class	Gradual	Sudden
Not Serious	2.5	3.0
Serious (Normal Buildings)	3.5	4.0
Very Serious	4.0	4.5

If the actual probability density functions for the supply and demand variables, Y and Y_s are approximated by log-normal functions that fit in the significant tails, CSA S408-1981 suggests the following approximation for the reliability index:

$$\beta = \frac{\ln(m_{Y_s}/m_Y)}{\sqrt{V_{Y_s}^2 + V_Y^2}} \tag{7}$$

where 'm' refers to the mean and 'V' to the coefficient of variation (standard deviation divided by the mean). This approximation for β is valid for $V \leq 0.30$.

To determine the reliability index using Equation 7 the means and coefficients of variation, m_Y, m_{Y_a}, V_Y and V_{Y_a}, must be determined first. In general, Y and Y_a, can be expressed as functions of other design or geometric parameters, which are considered to be random variables themselves. The following approximation can be used to estimate the mean and variance of a function of several variables.

$$Y = f(X_1, X_2, \ldots, X_n) \tag{8}$$

Ignoring higher order terms, a Taylor series expansion about the mean gives:

$$m_Y = f(m_{X_1}, m_{X_2}, \ldots, m_{X_n}) + \frac{1}{2}\sum_{i=1}^{n}\sum_{j=1}^{n}\frac{\partial^2 f}{\partial x_i \partial x_j}|_m Cov[x_i x_j] \tag{9}$$

and

$$\sigma_Y^2 = \sum_{i=1}^{n}(\frac{\partial f}{\partial x_i}|_m)\sigma_{X_i}^2 \tag{10}$$

where $Cov[x_i x_j]$ = covariance of the pair of variables $[x_i x_j]$ and σ_Y^2 = variance of variable Y. To carry out a theoretical analysis, the expresions for Y and Y_a are used, together with Equations 9 and 10, to evaluate the means and coefficients of variation required for Equation 7 to calculate the reliability index, β. This requires previous knowledge of the mean, variance and correlation coefficient for all individual variables.

Alternatively, an empirical approach would use the results of laboratory tests on a given system, subject to a known load history, and evaluate the required means and variances required by Equation 7.

3. RESIDENTIAL FLOOR SYSTEMS

Acceptance testing of engineered wood products is commonly required to evaluate the performance of floor systems for residential and small buildings. Test procedures currently used must determine the strength as well as the stiffness of structural elements combining two or more constitutive materials like solid lumber, waferboard, plywood, metal plates or metal webs. In this study, the behaviour of Waferboard I beams was compared with that of solid joists in terms of their capacity to satisfy serviceability requirements.

3.1 *Test specimens*.- Commercially available waferboard I beams with solid lumber top and bottom flanges and waferboard webs were used. The flanges were solid Spruce lumber, 38 mm thick; the webs were 9.5 mm thick waferboard, as shown in Figure 1. Solid joists were S-P-F (Spruce) No. 2 grade. A total of 40 specimens were tested and grouped in four series with 10 specimens each as described in Table 3 and Figure 1

3.2 *Test loads* In this study, the standard test procedure recommended by Canada Mortgage and Housing Corporation (CMHC) was used to evaluate the performance of the Wafeboard I beams and compare it with that of the solid lumber joists. In addition two 'accelerated' procedures were used in order to reduce the duration of the test. These load regimes are described graphically in Figure 2.

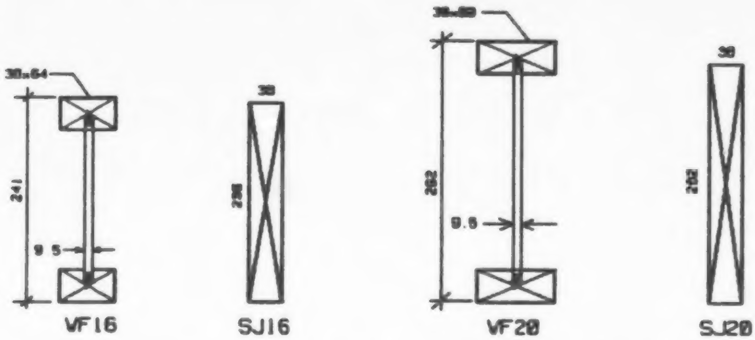

Figure 1: Floor systems. Test series and specimen dimensions

Table 3: Test specimens

SERIES	SYSTEM	DEPTH	SPAN	REMARKS
WF16	Waferboard I beams	241 mm	5 m	Flanges 38 × 64 mm
WF20	Waferboard I beams	292 mm	6 m	Flanges 38 × 89 mm
SJ16	Solid lumber joists	235 mm	5 m	Cross-section 38 × 235
SJ20	Solid lumber joists	282 mm	6 m	Cross-section 38 × 282

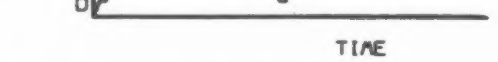

Figure 2: Test Loads. (A = Ramp load; B = Partial CMHC + ramp; C = Standard CMHC + ramp). D = Specified dead load; L = Specified live load.

3.3 *Serviceability analysis.*- In general, the serviceability limit state is asociated with an acceptable level of performance within the functional requirements for the system. Deflections are limited to avoid cracking of ceilings or to reduce discomfort of the user due to excesive vibrations. The mid–span deflection due to live loads is the parameter used in this study to assess the behaviour of the floor system. Limiting deflections are those recommended by the National Building Code of Canada as well as those required by the CMHC test procedure.

The reliability index, β, is calculated using Equation 7 with the following considerations: Y = measured mid–span deflection, with mean and coefficient of variation, m_Y and V_Y, to be determined from tests. Y_a = deterministic variable with mean m_{Y_a} = span/180, span/240, span/360 or 12.7 mm (CMHC recommended value) and coefficient of variation $V_{Y_a} = 0$. Equation 7 becomes:

$$\beta = \frac{\ln(\frac{Y_a}{m_Y})}{V_Y} \tag{11}$$

3.4 *Test results.*- A complete set of test results, including strength and serviceability analysis, has been reported by Gillard (1986) and Salinas and Gillard (1987). A summary is given in Table 4 which shows only the mean and coefficient of variation of 40 tests (four series), grouped into 10 cases according to the loading used, material and span. These values, together with Equation 11 were used to calculate the reliability index, β, for several values of the limiting deflection, Y_a. Figures 3 and 4 show the results of these calculations.

Table 4: Mid–span deflection (mm). Summary of test results for floor systems

SERIES	LOADING *	m_Y	V_Y
WF20	A	17.4	0.09
SJ20	A	14.8	0.14
SJ16	A	12.4	0.13
WF16	A	12.5	0.09
WF20	B	17.3	0.10
SJ20	B	14.4	0.12
SJ16	B	12.3	0.18
WF16	B	14.3	0.14
SJ16	C	13.5	0.16
WF16	C	14.8	0.11

* See Figure 2

3.5 *Observations.*- If a target reliability index for serviceability between 3.00 and 4.00 is accepted, Figures 3 and 4 show the inability of both conventional solid joist systems and the new engineered wood products to meet the more strict deflection limitations (span/360). In practice, however, we seem to have implicitly accepted these systems and their performance and perhaps the target serviceability reliability index should be smaller than that recommended for the strength limit state. In relative terms, Figures 3 and 4 show a significant difference in the behaviour between conventional joist systems and that of wood I beams. The engineered product exhibits a better reliability in complying with the more lax deflection

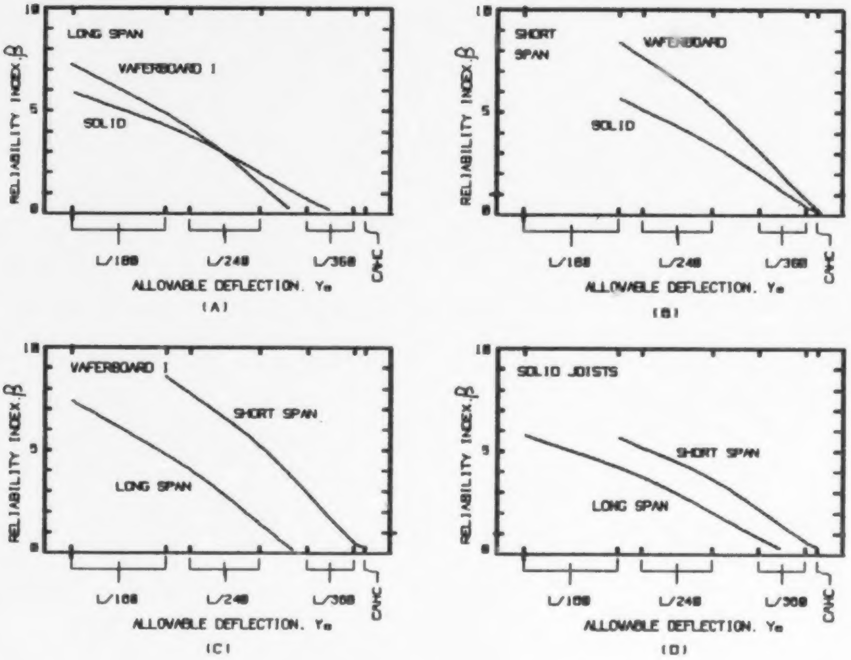

Figure 3: Reliability Index, β, *Vs* Allowable Deflection, Y_a.

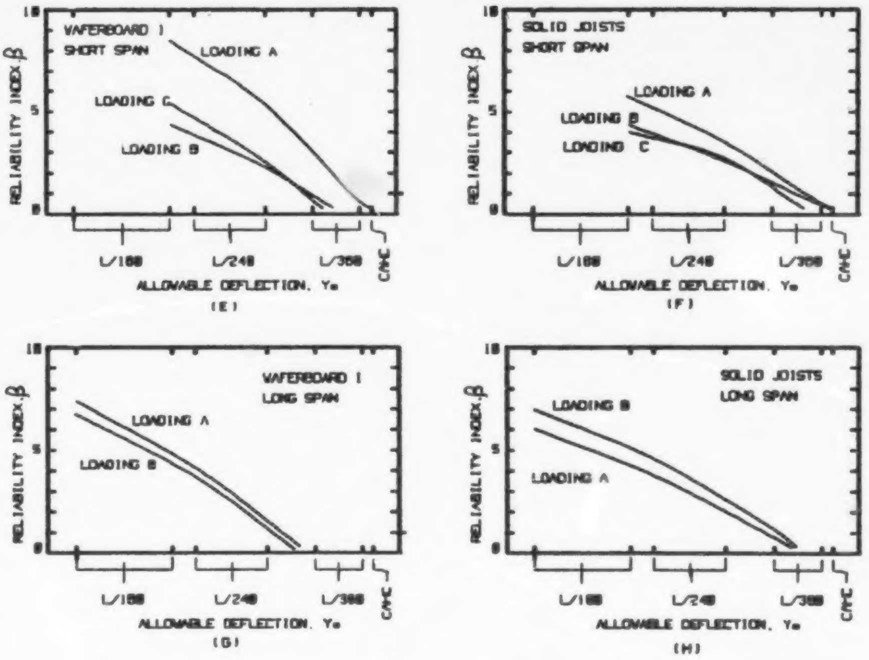

Figure 4: Reliability Index, β, *Vs* Allowable Deflection, Y_a.

limitations (span/240 and span/180) . This superiority seems to disappear at the more strict limitations imposed by CMHC and for span/360. Systems with shorter spans consistently exhibited higher reliability levels than those with longer spans, indicating the existence of a *size effect* commonly associated with wood structures.

The effect of the loading regime used in the tests is clearly manifest in Figure 4. The 5-minute ramp load [loading (A)] resulted in smaller deflections with a higher level of reliability against failure to meet the deflection limits. This could be a manifestation of the *duration of load effect* widely acknowledged for wood products but usually associated only with the strength limit state. This effect seems to be masked by the size effect as indicated by the results from tests on solid joist systems with long span, as shown in Figure 4 (H)

It is also apparent that loadings (B) and (C) give similar results and therefore an 'accelerated', 1-hour+ test load like (C), can be used instead of the longer (48-hour) CMHC standard test procedure with significant economy.

4. ROOF TRUSSES

Testing of full-size prototypes is commonly required to assess new designs of light wood roof trusses with metal plate connectors. Standard test procedures recommended by CSA S-307 (Canadian Standards Association, 1977) establish minimum strength and deflection limitations to ensure acceptable levels of safety. To verify certain assumptions made for the design of long-span trusses, 75 specimens were tested to failure and the results used to evaluate their safety. These tests are described in detail by Salinas *et al* (1985). The specimens were grouped according to span length and chord size as described in Table 5.

Table 5: Roof trusses. Case studies

	Span		Chord Size		Design Load (kPa)		Test Results*	
Case	Long	Short	Large	Small	Dead	Live (Snow)	m_Y	V_Y
1	21 m		38 × 286		0.48	1.84	36.1	0.12
2	21 m			38 × 235	0.48	0.86	27.3	0.22
3		12 m	38 × 286		0.48	2.41	19.5	0.09
4		12 m		38 × 235	0.48	1.15	15.0	0.24

* Mean and coefficient of variation of mid-span deflection (mm)

The different combinations of span and chord size listed in Table 5 are considered to be representative of construction practices for this type of systems. The snow loads are representative of design values found for a large number of geographical locations across Canada. The mid-span deflection results were used with Equation 11 to calculate the reliability index for several values of deflection limits. Figure 5 summarizes the results.

4.1 *Observations.-* In the study by Salinas *et al* (1985) it was reported that most long span trusses tested failed to meet acceptable levels of safety with regards to strength. However, all trusses tested met deflection limits without any difficulties. As can be observed in Figure 5 β was above 3.00 for all cases and deflection limits. In relative terms, it can be observed

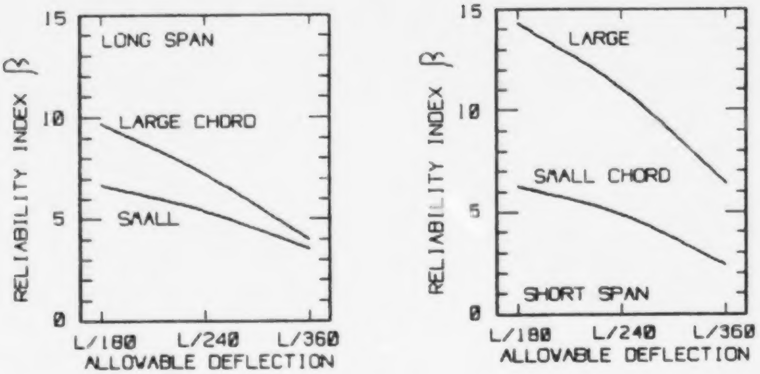

Figure 5: Reliability Index *Vs* Allowable Deflection for roof trusses

that there is a significant difference in the level of safety against failure to meet serviceability criteria for long and short spans. This seems to be another indication of a *size effect*.

5. RECOMMENDATIONS AND CONCLUSIONS

Taken as a convenient measure of safety, the reliability index, β, serves as an indicator of the *relative* importance of the various parameters affecting the performance of engineered wood products. As an absolute measure of the likelihood of failure, the approximate approach used in this investigation should be refined to incorporate more information about material properties and the variability of service loads.

Target reliability values for serviceability conditions must be examined and compared with those assigned to strength limit states. A program of calibration against observed behaviour in the field would be an important step towards the development of more realistic target reliability levels for serviceability of engineered wood products.

6. ACKNOWLEDGEMENTS

The financial support of the Natural Sciences and Engineering Research Council of Canada, in the form of an operating grant to the senior author, is gratefully acknowledged.

7. REFERENCES

AD-HOC COMMITTEE ON SERVICEABILITY RESEARCH. 1986. *Structural Serviceability: A critical appraisal and research needs.* Committee on Research, Structural Division, ASCE. Journal of Structural Engineering, Vol 112, No 12. December, 1986. pp. 2646–2664.

CANADA MORTGAGE AND HOUSING CORPORATION. 1983. *Load test procedure for floor framing systems for houses and small buildings.* ME–8309. CMHC, 682 Montreal Rd., Ottawa, Ont., 12 p.

CANADIAN STANDARDS ASSOCIATION. 1981. *Guidelines for the development of limit states design.* CSA Special Publication S408–1981. CSA, Rexdale, Ont., 33 p.

CANADIAN STANDARDS ASSOCIATION. 1977. *Load test procedures for wood trusses for houses and small buildings.* CSA–S307. Rexdale, Ont., 17 p.

GILLARD, R.G. 1986. *Reliability analysis of Waferboard I beams. A damage accumulation approach.* M. Eng Thesis. Department of Civil Engineering, Carleton University, Ottawa, Ont., 141 p.

PERCIVAL, D.H. 1979. *History of L/360.* Forest Products Research Society, Forest Products Journal, August 1979. pp 26–27.

SALINAS, J.J. and R.G. GILLARD. 1987. *Equivalent criteria in acceptance testing.* Proceedings of the 5th International Conference on Applications of Statistics and Probability in Soil and Structural Engineering (ICASP5). University of British Columbia, Vancouver, B.C. Canada, May 25–29, 1987. pp 325–332.

SALINAS, J.J. and R.G. GILLARD. 1985. *Strength and structural safety of long-span light wood trusses.* Canadian Journal of Civil Engineering, 12, 114–125.

SERVICEABILITY OF BUILDINGS - PROBABILISTIC APPROACH

F. Bljuger

Building Research Station
Technion - Israel Institute of Technology
Haifa, Israel

ABSTRACT: Structural serviceability of buildings is assured by a semi-probabilistic design method, dispensing with a uniform reliability level for all structures. Probabilistic analysis of serviceability of a structure may yield the probability function of limit states, which should not exceed the criterion function.

The probabilistic approach to evaluation of expected distributions of crack appearance and deflections is illustrated on examples of R.C. structures. Variation of the mean tensile strength of concrete in the member population, the lengthwise variation of the concrete strength, and the load variation - are all taken into account.

The probabilistic approach permits to obtain different structures with the specified reliability, and may also be used for definition of new deterministic criteria in traditional structural design.

The codes should be supplemented by suitable initial statistical data and probabilistic limitations.

1. INTRODUCTION

The engineer's task is to prevent occurrence of the serviceability limit state with specific probability. In practice the serviceability of structures is assured by a semi-probabilistic design method with limitations on the appearance - or excessive width - of cracks and on excessive deflections or displacements. The deterministic criterion for the design limit state of structural serviceability is based on the probabilistic characteristics of certain parameters (load, concrete strength), dispensing with a uniform reliability level for all structures having the same purpose [1-3]. In reality, however, crack appearance - or the limiting deformation - in a structure complies with a particular probability. Design crack appearance, or the expected deformation, should be characterized by probabilistic functions, and the design criteria for structural serviceability should be a probabilistic limit or limiting function. The design check for serviceability of a structure can thus be based on its probabilistic analysis.

The variable characteristics of the structure parameters may be given in terms of distributions, and the attendant calculation difficulties can be overcome by recourse to a computer.

In probabilistic serviceability analysis of R.C. structures, the main characteristics are the lengthwise variation of concrete strength over the structure, and the mean concrete strength of the members within their general population. Probabilistic analysis of the bearing capacity of walls and columns based on above approach was applied in [4-5], and the probabilistic approach - to estimation of crack appearance in [6-7] and to deflection evaluation in [8]. According to [7], initially the probability of crack appearance in a section is evaluated, and subsequently the probability of crack appearance in the considered member with specific mean concrete strength and in a member with a given grade of concrete (in the population of given structures). On the basis of obtained probabilistic functions the load complying with 5% probability may be found or, for a given load, the probability of crack appearance may be evaluated and compared with the given probability.

The above reasoning, however, is not relevant to deflection analysis, as appearance of a single crack is not associated with drastic changes in the deflection pattern, even in a member with a very small reinforcement ratio, only if the mean tensile strength of the concrete significantly exceeds the characteristic one. Probabilistic deflection calls for a different approach. In this paper, variability of the load is also taken into account in all problems.

2. CRACK APPEARANCE

The probabilistic serviceability analysis of R.C. structures relative to crack appearance is considered in [5-7]. Potential cracks in the considered model of a member in bending (Fig. 1) may appear with 40mm spacing in its middle part between x_1 and x_2.

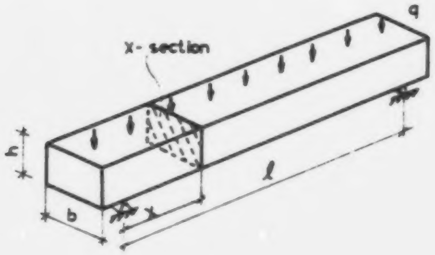

Fig. 1 - Member for cracking analysis.

The probability of crack appearance in the x-section is:

$$P_x = \frac{\Delta i}{\sqrt{2\pi}} \sum_{i=-3}^{j} \exp(-i^2/2) \qquad (1)$$

where Δ_i is the summation step (taken as 0.3), i is an independent parameter, j is given by:

$$j = [(\frac{M_x}{W} - f_p)/f_{cm} - 1]/C_{vl} \quad (2)$$

and the moment M_x in the x-section for a uniformly distributed load p is:

$$M_x = \frac{p}{2} (\ell x - x^2) \quad (3)$$

f_p - residual prestress in most stressed fibre.
f_{cm} - mean concrete strength in member.
C_{vl} - coefficient of lengthwise strength variation.

The probability of crack appearance in the considered member with specific mean concrete strength is:

$$P_{rm} = 1 - \prod_{x_1}^{x_2} (1 - P_x) \quad (4)$$

The probability of crack appearance in a member with a given grade of concrete is evaluated by:

$$P_r = \sum_m P_{rm} . P_m \quad (5)$$

where

P_m - probability of occurrence of the specific mean concrete strength, namely:

$$P_m = \frac{\Delta_m}{\sqrt{2\pi}} \exp (-m^2/2) \quad (6)$$

The mean concrete strength is defined as:

$$f_{cm} = f_{cmm} (1 + m C_{vo}) \quad (7)$$

where

f_{cmm} - mean flextural tensile strength for given grade of concrete,
C_{vo} - variation coefficient of above mean concrete strength in member population,
m - independent parameter.

Where no specific data are available for C_{vo}, it may be taken as recommended by [4,7]: $C_{vo} = C_v/\sqrt{2}$, with $C_v = \sqrt{C_{vo} + C_{vl}}$ - coefficient of variation of tensile concrete strength in general population. From [1] the following initial statistical data can be drawn:

Concrete grade f_{ck} [MPa]	20	30	40	50
Mean tensile strength of concrete f_{ctm}	2.2	2.8	3.4	4
Coefficient of variation C_v	0.165	0.174	0.179	0.183

The results of numerical probabilistic analysis of the members with different concrete strength variation (C_{vo}), shown in Fig. 1 (h=.2m, b=.3m) made of C-30 grade concrete, under .0024 MN/m non-variable load [8] are presented in Fig. 2. For the specified load (.0024 MN/m) have widely differing probabilities of crack appearance (from 5.3% to 32.1%), and for its specified probability (5%) we have differing "characteristic" loads according to variation of the mean concrete strength in the member (C_{vo}).

Let us consider the probability of crack appearance as function of the load variation. When the load deviates from the specified value in both directions with equal probability, the probability increases with the variation coefficient. Fig. 3 presents the relevant results for beams made of different grades of concrete. As deterministic analysis is based

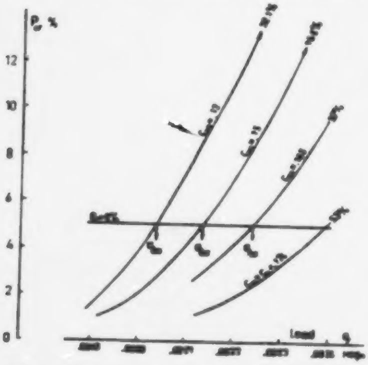

Fig. 2 - Probabilities of crack appearance in beams with different variabilities of mean concrete strength.

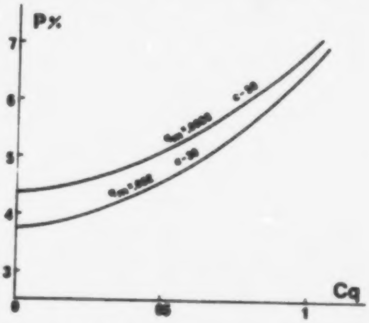

Fig. 3 - Probabilities of crack appearance in beams made of C-30 and C-50 grade concrete versus coefficient of load variation at appropriate mean loads (.002 MN/m and .0028 MN/m).

on specification of characteristic loads, the structure should be analyzed for a mean load smaller than the characteristic one according to load variability. For example, if the probability of the characteristic load is 5% ($q_{.05}$), the mean load is given by:

$$q_m = \frac{q_{.05}}{1 + 1.645\, C_q} \tag{8}$$

where

C_q = coefficient of load variation, given by:

$$C_q = \frac{\sqrt{\sum_i (C_{qi} \cdot q_{mi})^2}}{q_m} \tag{9}$$

C_{qi} = coefficients of variation of i loads,
q_{mi} = mean values of i loads, $q_m = \Sigma\, q_m$:

The real probabilities of crack appearance for the beam in question (C.30, C_v=.174, C_{vo}=.123), are calculated for different mean loads, according to (8):

C_q	0	.02	.05	.1
q_m	.0024	.002324	.002218	.002061
P_{cr}%	32.1	22.2	15.8	10

Thus, on the assumption that the lengthwise variation of concrete strength is the same as that of the mean strength in the member population (C_{v1}=C_{vo}), the traditional approach yields the expected probabilities of crack appearance between 32.1% and 10%, depending on the variation coefficient of load, varied between 0 and 0.1. Note that the design strength of the concrete is taken into consideration with only 5% probability (see Fig. 2).

Fig. 4 shows the probabilities of crack appearance under two specified characteristic loads for the beam in question, versus their coefficient of variation.

The above probabilities are evaluated by:

$$P = \sum_{m_1} P_r \cdot P_q \tag{10}$$

where the probabilities P_r are evaluated by (5) for the relevant load

$$q = q_n(1+m_1 \cdot C_q) \tag{11}$$

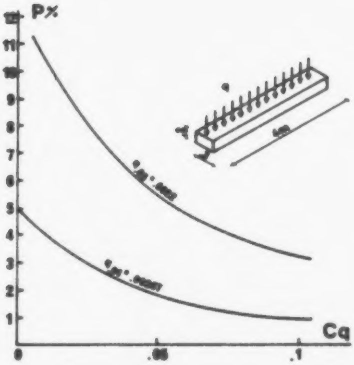

Fig. 4 - Probabilities of crack appearance in two beams made of C-30 grade of concrete under two different characteristic loads (.0022 MN/m and .00207 MN/m) versus coefficient of load variation.

$$P_q = \frac{\Delta_{m1}}{\sqrt{2\pi}} \exp\left(-m_1^2/2\right) \qquad (12)$$

m_1 - independent parameter.

The probabilities of crack appearance are much lower, and may be excessive or reasonable according to the specified variation of the loads.

For statically indeterminate structures, the probabilities of crack appearance in certain zones should be taken into account, as well as the moment M_x (3) according to the relevant formula.

In conclusion, in principle, the cracking resistance of a structure can be objectively estimated only on the basis of probabilistic structural analysis, including application of the probabilistic criterion of crack appearance. In the process, the variation of the concrete strength - both in the mean and lengthwise - should be taken into account, and in many cases - the load variability as well.

3. DEFLECTION

As noted, state of R.C. structures considered above is, as a rule, not critical in relation to the deflection, and characterized only by crack appearance in a member representing the population of structures. In practice, according to [1,3], the deflection is evaluated as the sum of curvatures multiplied by the coordinate x from the support to the considered part of the member.

If only one crack appears, only the curvature of one part of the structure changes; in these circumstances the effect on the deflection is negligible, and only subsequent cracks may cause a significant deflection (Fig. 5). As cracks form variously in sections of unequal strength, the deflection can be evaluated with reference to the mean concrete strength in the member under consideration. Such an approach yields incorrect data only for loads causing not more than two-three cracks along the structure. In the light of the above, Ref. [8] recommends the mean concrete strength as basis.

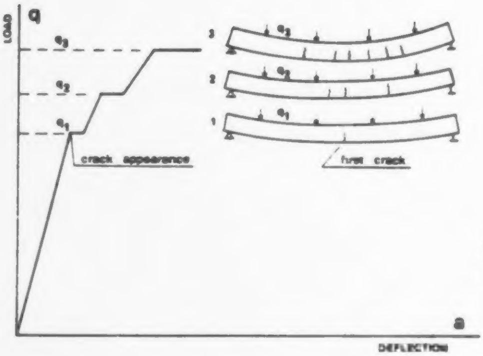

Fig. 5 - Deflection vs. load for member in bending (schematic), and illustration of crack development.

Of the two possible design models for evaluation of the deflection (one - based on the characteristic cracking moment [2], and the other - on the curvature [1,3,9]), the second is preferable. It permits more exact evaluation of the deflection with partial cracking allowed for. This is important for statically indeterminate structures with cracked support areas.

For the purpose of analysis, a member with height h, consisting of $2n_1$ parts with possibly differing stiffness, each of length about h (Fig. 6)

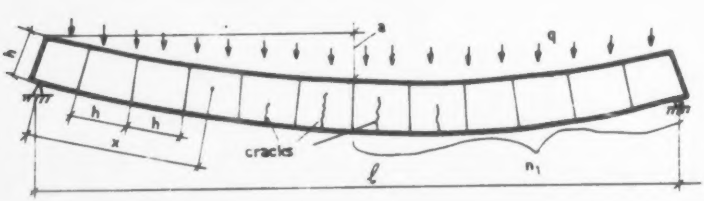

Fig. 6 - Model of structure for evaluation of deflection

is considered. The number of parts in one half-span is:

$$n_1 = \ell/2h \qquad (13)$$

In the general case the deflection is computed by summation of the appropriate products (from $x = h/2$ to $\ell/2-h/2$):

$$a = \ell\cdot\Sigma(k_x.x)/2n_1 \qquad (14)$$

where k_x - curvature of x-part.

The curvature of the cracked part is evaluated by [3]:

$$k_x = \frac{M_x}{d(d-x_c/3)} \left(\frac{\phi}{E_s A_s} + \frac{0.9}{x_c b E_c \nu}\right) \qquad (15)$$

where ϕ - bond coefficient between concrete and reinforcing steel

$$\phi = 1.25 - S \cdot M_{cr}/M_x \qquad (16)$$

$$M_{cr} = W \cdot f_{cm} \qquad (17)$$

d - distance from extreme compressed fiber to centroid of tension reinforcement,
x_c - height of compressed part of section,
f_{cm} - tensile flexural strength of concrete under consideration, for short-term loads: $S = 1.1$, $\nu = .45$.

The deflection distribution for a structure population may be evaluated in the following manner:

The "elastic" deflection of a member is evaluated by:

$$a_{e\ell} = .0153\, q\ell^4/E_c I \qquad (18)$$

Next, for different values of mean concrete strength in a member, evaluated by (7) with probability of crack appearance (P_m) as per (6), the appropriate cracking moment is calculated:

$$M_{cr} = W.f_{cm} \qquad (19)$$

Finally, $M_x = (q/2)(\ell x - x^2)$ is calculated from $x = \ell_s/2$ to $x = 1/2 - \ell_s/2$ with step ℓ_s.

If $M_x/M_{cr} > 1$, the curvature of the considered part is evaluated by (15). The variable coefficient ϕ, depending on M_{cr}, is a function of the variability f_{cm}. The deflection for a specific member under specific load q is found by summation of the "elastic" deflection and the differences due to possible cracking of the relevant parts.

Each evaluated deflection is subject to the probability:

$$P = P_m \cdot P_q \qquad (20)$$

The overall probability pattern is obtained by summation of the probabilities obtained for closely spaced deflections.

The influence of concrete strength variability on the expected deflection distribution is shown in [8]. For structures with low reinforcement ratio, the characteristic deflection may change by a factor of two for different variations of mean concrete strength, from $C_{vo}=.17$ to $C_{vo}=.12$ (Fig. 7). Here, in numerical analysis both the variation of the concrete strength and the load variability are taken into account.

Members with 1m width and 120mm height, made of C-50 grade concrete, are analysed ($C_v=.183$, $C_{vo}=C_v/\sqrt{2}$). Two types of member are considered: one - 3.6m span under 6.5 kN/m load with $5\phi 8$mm reinforcement, the other 4m span under 5.5 kN/m load with $5\phi 10$mm reinforcement. For the first type we have, under the same mean load of 6.5 kN/m, with different variations (C_q), different distributions of deflection probabilities (Fig. 8). Note that the figure shows the probabilities of deflections exceeding a. If the characteristic value of the deflection is defined for 5% - probability ($a_{.05}$), it is a function of the coefficient of load variation, varied from 7mm to 10mm (Fig. 9). Bearing in mind that for the same characterstic

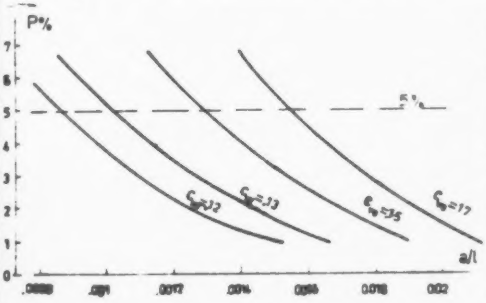

Fig. 7 - Probability functions of relative deflections in member with 0.3% reinforcement ratio (h=.15m, l=4m) under non-variable load [7].

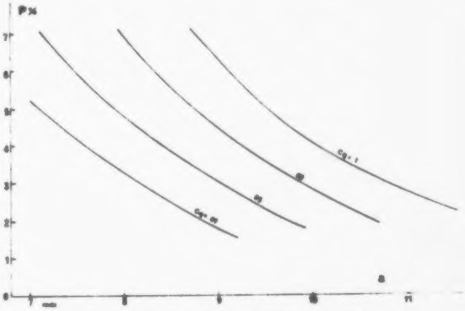

Fig. 8 - Probability functions of deflections of analyzed member for 3.6m span under .0065 MN/m - mean load with different load variations.

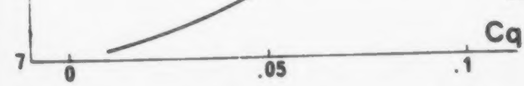

Fig. 9 - Characteristic values of deflections of member under .0065 MN/m - mean load versus coefficient of load variation C_q.

load, the mean load value differs, depending on the load variation, the appropriate mean load may be evaluated according to the above expression (8). These mean loads are:

Coeff. of load var. C_q	0	.02	.03	.05	.07
Mean load q_m: (a) for 3.6m span	.0065	.006293	.006194	.006	.005829
(b) for 4m span	.0055	.00532	.005241	.005082	.004932

Figs. 10 and 11 show the appropriate probability functions of the deflections at different load variabilities (for the same characteristic value of the load), covering the interval between 2 and 6%. The deflections with 5% probability ($a_{.05}$) versus the coefficient of load

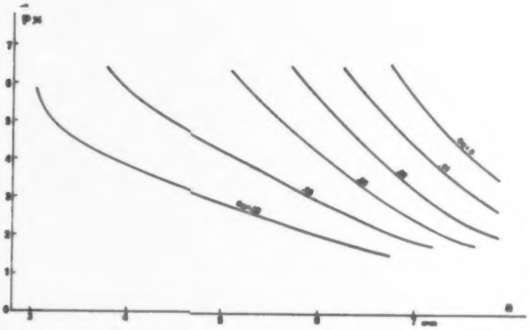

Fig. 10 - Probability functions (P) for deflections (a) in 3.6 m - span member for different coefficients of load variation (C_q).

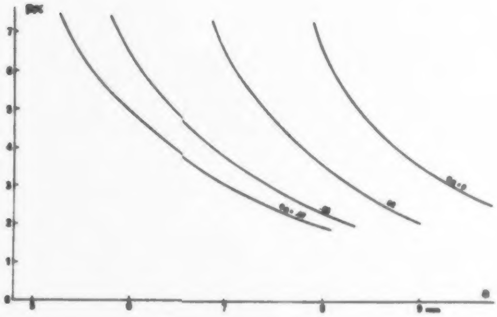

Fig. 11 - Probability functions (P) of deflections (a) in 4m - span member for different coefficients of load variation (C_q).

variation are shown in Figs. 12 and 13. In the first case the 5% deflection varies between 1/1100 and 1/500 of the span, in the second - between 1/670 and 1/480, depending on the coefficient of load variation, varied between 0 and 0.07.

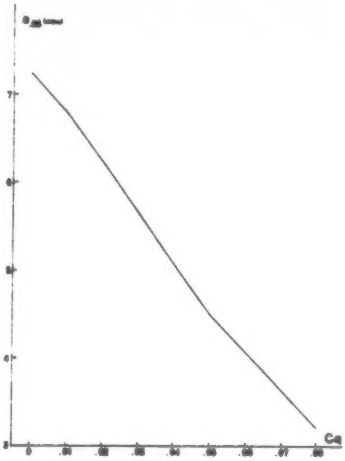

Fig. 12 - 5% - deflections vs. coefficient of load variation for 3.6m - span member.

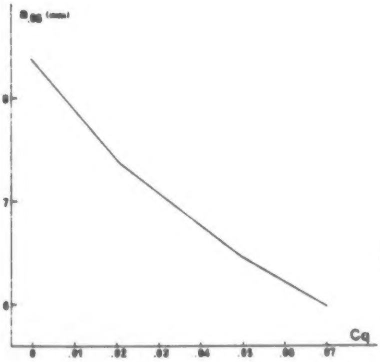

Fig. 13 - 5% - deflections vs. coefficient of load variation for 4m - span member.

The deflections, due to characteristic loads, were also estimated for the same two cases by the traditional design approach, with the characteristic tensile strength of the concrete taken into account (5% - probability strength - $f_{ctk.05}$). The appropriate characteristic values of the deflections were 10.71mm and 11.05mm respectively (1/336 and 1/362 of span), significantly in excess of the 5% values for these members. This numerical procedure permits evaluation of the expected probability of determined deflections by the traditional approach. The results are presented in Fig. 14. The probabilities are varied between 0.5% and 0.05% depending on the load variation. Characteristic value of concrete along the member, that is, in essence, the mean concrete strength in the considered member. The probability of such a case may be evaluated on the basis of a reduced coefficient of variation of concrete strength - for example by a factor of $\sqrt{2}$ [4]. The argument of the Gaussian function should then be: $u=1.645\times\sqrt{2} = 2.326$ and $P=99\%$. The true moment distribution further reduces the probability of crack appearance below 1% and together with the variability of loads brings about the results presented above.

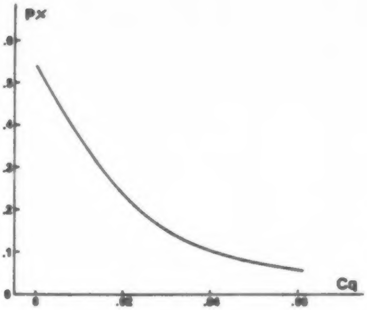

Fig. 14 - Probabilities of deflections calculated by traditional approach for analyzed members, depending on coefficient of load variation.

CONCLUSION

The traditional estimation approach of structural serviceability yields significantly different reliabilities regarding crack appearance and excessive deformation. The variability of mean concrete strength in the member population and its lengthwise variation, as well as load variability, may play a very important role in evaluating the probabilities of the two effects.

In any event, probabilistic criteria should be specified in advance for all types of design structural serviceability, namely limiting probabilities of crack appearance or crack width, and limiting deflections complying with a definite probability of their appearance in the considered type of structural system.

The probabilistic approach makes possible different structures with the same specified reliability; at the same time, different probabilistic criteria may be applied for dissimilar structures and buildings.

The probabilistic approach may also be used for definition of new deterministic criteria in traditional structural design.

It should be particularly emphasized that the probabilistic approach calls for supplementation of codes by suitable statistical data for materials, as well as for loads affecting the serviceability characteristics, and by probabilistic limitations.

REFERENCES

1. CEB-FIP, 1978. Code for Concrete Structures, 3rd Edition, Comité Euro-International du Beton/Féderation Internationale de la Précontrainte, Paris, 471 pp.

2. ACI Standard, 1983. Building Code Requirements for Reinforced Concrete (ACI 318-77), ACI Manual of Concrete Practice, part 3, Detroit, Michigan, pp. 218-330.

3. SNiP 2.03.01-84, 1985. Building Code for Design of Reinforced and Non-Reinforced Concrete Structures, S.I., Moscow, 79 pp. (in Russian).

4. Sementsov, S.A., 1972. Influence of Irregular Concrete Heterogeneity in an Element (Column, Panel) on its Strength, ZNIISK, Strength of Precast Panel and Masonry Structures, S.I., Moscow, pp. 22-35 (in Russian).

5. Bljuger, F., 1987. Probabilistic Analysis of R.C. Columns and Walls in Buckling, ACI Structural Journal, pp. 124-131.

6. Bljuger, F., 1985. Cracking Resistance of Concrete Members in Bending, ACI Journal, pp. 467-474.

7. Bljuger, F., 1985. Reliability Cracking Analysis of Two-way Concrete Slabs, Proc. of 4th Intern. Conf. on Structural Safety and Reliability, Kobe, Japan, pp. III-652-658.

8. Bljuger, F., 1987. Probabilistic Serviceability Analysis of R.C. Structures, Proc. of 5th Intern. Conf. on Applications of Statistics and Probability in Soil and Struct. Engineering, V.1, Vancouver, Canada, pp. 63-70.

9. Carreira, D.J. and Kugang-Han Chu, 1986. The Moment-Curvature Relationship of R.C. Members, ACI Journal, pp. 191-198.

INDUSTRIAL CASE STUDY OF AN EXTENSIVE STRUCTURAL FLOOR SLAB REPLACEMENT

Kenneth, N. Smith
McNeely Engineering & Structures Limited
Kingston, Canada

ABSTRACT: This case study involves the replacement, in stages, of 6000 square metres of floor slab in an industrial building. This replacement took place over the past nine years. The existing floor system was precast lightweight concrete channel slabs supported by steel beams and was constructed about 1958. The floor carries manufacturing machines and is subjected to the associated vibrations. Numerous signs of structural distress and serviceability problems have been observed such as spalling, local failures, and hundreds of random cracks.

In recent years, heavier new machines have been installed and the material transport system has been changed; coincident with this, the floor is being replaced by a cast-in-place reinforced concrete slab suitable for high concentrated loads and lateral load distribution.

In this case the original selection of an articulated lightweight floor system is questionable for the intended use. The changing use requirements were not unreasonable for an industrial situation and suitable provisions in this regard might have been made in the initial design criteria.

1. INTRODUCTION

An industrial building has had 6000 square metres of structural floor slab replaced in stages over the past nine years. This is a brief case study of the project.

The relevant construction and the structural distress in the existing precast floor will be described. A change in use which evolved and the renovations which were then carried out will be given. Finally, there will be a discussion to present some conclusions from this case history.

2. EXISTING CONSTRUCTION AND OBSERVED DISTRESS

This structure was built about 1958. The floor system in question was designed for a single room over 6000 square metres in area on the second floor of a two storey building. The floor was constructed of precast lightweight concrete channel slabs, 125 mm deep, 450 mm wide, spanning about 2,300 mm, with 50 mm concrete topping. Figure 1 shows the cross section. These slabs were supported by steel beams and precast concrete columns. A small portion of the floor was cast-in-place reinforced concrete slab for supporting a conveyor system employed in transporting material horizontally. The floor is subjected to continual vibrations from manufacturing machines.

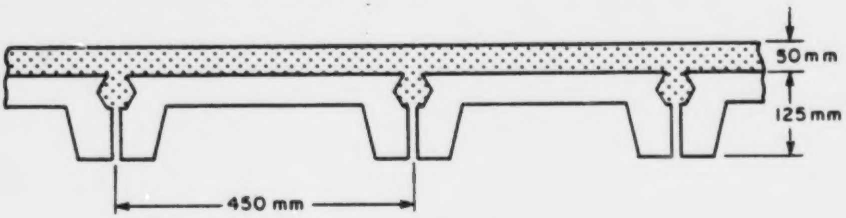

Figure I : Existing floor

The following problems had developed in the concrete floor system:

(a) The number of cracks and their random distribution were extraordinary. There were many hundreds of cracks in random directions and locations in the precast channel slabs. Some cracks in the horizontal part of the channel sections were thought to be the result of dropping objects on the floor.

(b) A few members exhibited substantial spalling, shear cracks, or splitting along the bottom reinforcing steel.

(c) Some "reflection" cracks were observed in the floor over supports.

(d) Various local failures had occured in the past requiring replacement of members or other remedial measures.

3. LOADS AND ANALYSIS

To update the manufacturing process the existing machines on the floor were scheduled to be replaced by new, heavier machines, the heaviest weighing 45 kN. In addition, the horizontal conveyor system was to be replaced by fork lift vehicles. The gross weight of a fork lift truck was 54 kN.

The floor was originally designed for 12 kN/m^2 (250 psi) live load. Due to the new machines a live load of 14.4 kN/m^2 was considered appropriate. In addition, a dynamic load allowance of 20% was used in the investigation. For a lift truck load of 54 kN, the building code requires that the floor be adequate for a concentrated load of 36 kN spread over an area 750 mm by 750 mm. In addition to considering the above loads, an analysis was also carried out for individual machine loads using the actual average pressures under the machines.

Structural analysis demonstrated that the floor was particularly inadequate for shear and also less than adequate for flexure. This conclusion was consistent with previous analysis and load testing that had been carried out in previous years due to the structural distress exhibited by the floor members.

4. RENOVATION

Each year for the past nine years a portion of the floor has been replaced by a 175 mm thick reinforced concrete slab. The area involved each year generally coincided with the area where machines and equipment were to be changed. In order to reduce shrinkage cracking in the new work, the reinforced concrete slab is quite heavily reinforced and is interupted by construction joints over some of the supports. For simplicity, and to protect equipment below, the new slab is placed on metal deck formwork. This solid slab has high strength locally and good lateral load distribution and therefore is inherently suitable for large concentrated loads.

As previously mentioned, there were small portions of the floor area in which solid cast-in-place reinforced concrete slabs were used originally. Analysis of some of these areas was hampered by the fact that the owner did not have complete data on the reinforcing steel. The ability to make renovations and analyze for new loads on the basis of new codes are aspects of serviceability. For this, adequate information on reinforcing steel should be on file and the owner should have a copy of the placing drawings.

5. DISCUSSION

In addition to the heavy vibratory machine loads in this case, it is to be expected that such an industrial floor will also be subjected at times to high local loads. The original selection of an articulated lightweight floor system is questionable for these various conditions.

The change in use involved the installation of somewhat heavier production machines and a different method of horizontal material transport, i.e., lift trucks instead of fixed conveyors. It should be noted, however, that the gross lift truck weight of 54 kN is little different from the heaviest new machine weighing 45 kN. The changing use requirements in this case were reasonable for an industrial situation and suitable provisions in this regard might have been made in the initial design criteria.

SESSION B/SÉANCE B

DEFLECTIONS/FLÉCHISSEMENTS

A PRACTICAL VIEW ON DEFLECTIONS AND CRACKS

Franz Knoll, Dr. Sc.

Nicolet, Chartrand, Knoll Ltd.
Montreal, Canada

ABSTRACT: A simplified model is presented to demonstrate the direct relationship of cracks and deflections, independent of loading and elastic theory. A review of causes relating to cracking is given along with their correlation to crack formation, propagation and expansion. Three cases of field experience follow, illustrating the complexity of interpretation of causes and effects in practice. The conclusion is that excessive deflections often occur due to cracking induced by restrained contraction, with deformations accumulating locally, near zones of reduced tensile strength.

In over twenty years of work as a practising engineer I have become convinced that every deflection problem in concrete structures has an explanation relating to some extreme or extraordinary situation in the history of the structure: Ordinary, normal, regular structures, reasonably designed, built and used just do not have any reason to deflect excessively.

Only, sometimes they do, to everybody's surprise -well, almost everybody's. For somebody among the participants is usually not or ought not to be surprised because his action or inaction is at the root of the problem.

It is not always easy in retrospect to pinpoint who or what exactly was the cause of the problem as records may not have been kept and the people concerned may no longer be around to account. This is no proof that nothing extraordinary has happened:

It takes only a moment of overloading a freshly stripped slab for a healthy deflection to occur, and many opportunies are available for it. First, when the forms have been removed but the reshoring under the slab is not installed yet, or when the shoring above the slab is removed and it becomes available for depositing loads such as a number of pallets of brick or a few loads of gypsum board. Sometimes the deflection is announcing itself through cracks and the brick mover will become induced to deposit the load elsewhere. While the slab will remain deflected, nobody save the man with the brick pallets will know the cause. This sort of scenario, with minor variations, is repeating itself over and over.

Before presenting some cases from the real world, let me suggest a very simple and simplistic model which will at once demonstrate the direct relationship of cracks and deflections:

a slab with cracks

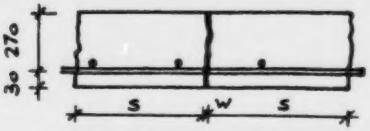

which is loaded in bending

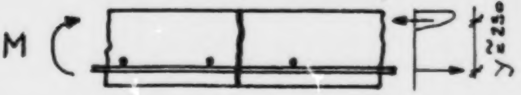

will rotate because in the compression zone, contact will reestablish itself

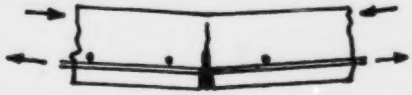

This when integrated over a simple span, amounts to a deflection of roughly:

$$\delta = \frac{w}{s} \cdot \frac{l^2}{8y}$$

If the crack originates for instance from restrained shrinkage, or from some physical phenomenon producing similar effects such as cold temperature, then one can put numbers to it due to shrinkage alone, and with full restraint and a shrinkage rate of, say

$$\varepsilon_{sh} = \frac{w}{s} = 0.0003$$

we obtain for a slab of 9 m (30ft) span and a thickness of 300 mm (12") a deflection of about

$$\delta = 0.0003 \cdot \frac{9000^2}{230} = 13\text{mm}$$

from shrinkage alone.

Other factors will of course influence this result such as discontinuities, or the accumulation of shrinkage deformation of a large piece of concrete in one particular, but much smaller area. Fracture mechanics teaches that in a condition like this, involving tension imposed by restrained contraction, separations (= cracks) already existing in a brittle material will open wider, rather than new cracks forming since the separation is where the least energy will be needed to provide for deformations imposed and to reestablish equilibrium and compatibility.

If one were, e.g., to accumulate the shrinkage of a slab extending over 5 bays in one of the bays one would be looking, with a reduction factor for continuity of, say 50%, at a deflection of about

$$\delta = 50\% \times 5 \times 13 = 32\text{mm}$$

from shrinkage which, if added up with other effects, will certainly exceed practically acceptable limits. Again, in normal circumstances, this will not usually occur. But every experienced builder has seen similar things happen every now and then, and in many cases, explanations akin to what the little model suggests, may have applied:

A slab well within the geometric limits such as those stipulated by codes, or as suggested by much practical experience, surprisingly sagged much more than expected because it was fully or partially restrained by stiff resisting elements at either end of its extent, and thus prevented from contracting as a whole. Eventually, the tendency to contract will prevail over the tensile resistance of the concrete, and cracks will open. This of course, will occur in the weakest region of the slab, most likely in a zone where cracking - perhaps invisible and **with different causes** - has already occurred - and there the geometric change will be accumulated, causing the particular span to sag. It is often impossible to establish why it happened in a particular place as there are at least two dozen different possibilities for cracks to form, several of which may be present simultaneously as illustrated by Table 1.

TABLE I

	Crack initiation	Crack propagation	Crack opening
Tension, load controlled	+	+	++
Tension, deformation controlled	+	+	+
Restrained shrinkage especially with concentrated restraints	++	++	++
Cold temperature, especially on young concrete	++	+	+
Differential settlement, externally imposed deformations	±	+	++
Absence of sufficient reinforcing transverse to cracks	±	+	++
Temperature gradients in time and space, together with restraints	+	+	+
Construction joints (pour joints)	++	±	±
Sudden changes in stress or cross section	++	+	+
Temporary overloading	++	±	±
Permanent overload	+	++	+
Concentrated loads eg. Prestress, Anchorages	+	++	++
Dynamic or cyclic loads	±	++	+

(Table I continued)

	Crack inititation	Crack propagation	Crack opening
Reversal of load or deformation condition	+	+	++
Rust of embedded steel	+	+	++
Cavities, openings reentrant corners	++	+	±
Hydrostatic pressure in crack	+	++	+
Freeze and thaw action in crack	+	++	++
Chemical attack or incompatibility e.g. chlorides, sulphates, alkali reaction	++	+	+
Trapped heat e.g. from hydration	++	+	±
Abrupt changes in thickness, rate of reinforcement	+	±	++
High water content	+	±	±
Premature drying of concrete	+	±	±
High cement content	+	±	±
Freezing of green concrete	++	±	±
Settlement of formwork	++	±	±
Disturbance of green concrete	++	±	±

Legend:
++ Strong correlation
+ Positive correlation
± Negligible effects

This table highlights, without any attempt at precision and neglecting the fact that some of the items listed are obviously interrelated, some of the multitude of possible circumstances which will help cracks to form and to grow. It must be kept in mind that it does not follow that one and the same cause effects a crack to start, and subsequently to open wide and long. As a matter of fact, most often, combinations of two or more parameters are at work, separate in time, space and physical origin.

If one wants to follow the typical little drama through a few more scenes: sometime after the construction of the slab in question, cracks are discovered and the building team is presented with the fact that the product of their efforts has not, after all, turned out to be perfect. Now everybody proceeds to become worried and apprehensive about his own relation to the possible causes and effects of the cracking. Usually the structural engineer is then asked to elaborate, whereupon he performs some detective work, digging out field reports about the weather, the performance of the various parties and devices involved and records about the concrete, and comes up with an opinion which will be accepted by the parties it does not put at fault, and rejected by the ones it does.

Usually it is quite impossible to find unequivocal, let alone complete answers as there are many gaps in the records, as well as due to the fact that the quantitative evalution of the combined effects of several interrelated causes is much too complex for any precise analysis. However, the application of very simplified models may sometimes yield "plausible" or reasonable explanations which may point to measures to be taken towards whatever deleterious effects the cracks could produce (deflections, leakage, cracking of partitions or floor tiles, unsightliness etc). Also as life is a learning process, lessons can be derived for future use, always with a goodly number of grains of salt. A reasonable recipe for the interpretation of a crack situation seems to be the following sequence of questions:

- A crack has formed, there must be one or several physical causes for it. List possibilities, evaluate likelyhood of each one.
- The crack represents a discontinuity in the structure which was supposed to transmit forces from the portion this side of the crack to the one opposite. What happened to these forces and/or what will the structure do or has done already to find a new state of equilibrium and compatibility.
- What will be the future of the crack, will it continue to open, stay the same, or close or do cyclic movements, and what will be the consequences for whatever else in the building may be related.
- If measures are to be taken towards preventing some undesirable effects, what will their consequences be in view of the above questions and answers, and in time. Will cosmetic measures do, like filling the crack, or must the causes be dealt with ?

Typically, all questions cannot be answered clearly and to the satisfaction of all, and the more adversary the climate within the building team, the less acceptance will be found for whatever is offered towards explanation and preventive strategy. Therefore, as always, technical and physical problems can only be solved when the human problems have been solved first.

Seen like this, the little drama appears to want to become a tragedy, and some comfort seems to be called for. Codes and Standards, as well as numerous learned publications do provide some advice towards controlling cracks, and numerous recipes and expressions are offered, attempting to link the physical parameters thought to be involved, with methods and measures to counteract their ill effects, mostly demanding considerable amounts of reinforcing steel.

To say the least, these attempts are controversial and laboratory-conceived, and their application in practice often leads to grotesque and bizarre consequences which sometimes cannot be executed even at great cost, especially in situations where apprehension guides the actions of the builders. Other design or construction measures could perhaps have been taken to counteract the tendency to crack. To illustrate his, Table 2 lists, in a qualitative manner, some positive measures and their relationship to crack control. A bit more philosophically and generally perhaps, the approach can be summarized in the following way: Given the fact that excessive cracking and deflections very often relate to situations of direct tension acting on the (reinforced) concrete, this tension situation is really what should be avoided, or if this is impossible to do, managed in such a way as to distribute the problem in space or time, thereby "thinning" it out to acceptable proportions. In the case of tension induced by incompatibility of deformations, ways should be found to avoid local concentration of these effects, e.g. by placing the restraining elements in a suitable manner such as in the central area, or distributed evenly.

TABLE 2

	Prevention of initial crack formation	Stopping of cracks	Control of crack width
Extended wet curing	++	±	+
Low steel stresses	±	+	++
Reinforcing transverse to cracks	±	++	+
Reduction of bar spacing	+	±	++
Prestressing transverse to cracks	++	+	±
Cooling of massive concrete(1)	+	±	+
Insulation to prevent high temperature gradients (1)	++	±	+
Sealing of existing cracks	±	±	+
Grouting of cracks	(2)	(2)	(2)
Control joints, expansion joints, expecially during curing (3)	++	+	++
Care	++	++	++

(1) The management of temperature and heat must be carefully considered throughout all the stages in the production and service life of the structure, lest measures such as insulation or cooling may become counterproductive.

(2) The filling or grouting of cracks is a purely symptomatic measure.

(3) Joints of any kind represent discontinuities in the structure which may themselves become the cause of problems if not properly managed. Consider e.g. the possibility of water penetration, with subsequent chemical attack or ice formation. Control joints (pouring gaps) which have been closed later will leave construction (cold) joints in the concrete which may consequently enhance the expansion of single concentrated cracks, rather than an even distribution of smaller cracks. They should be so arranged as to avoid zones of high tensile stress and shear.

THREE PRACTICAL CASES

1. For compelling reasons, unrelated to structural considerations, a structural slab was built in two parts, with a time lag of about half a year between the two. The portion to be constructed first forms a frame type rectangle in plan, with the infill added at the second stage (Fig. 1). Time was of the essence, especially in the second phase as this was late on the critical path and curing of this concrete had to be kept to the minimum time, with wet curing impossible, because leakage to below could not be allowed.

In time, some portions of the slab showed deflections up to 60 mm (2 1/2 inches) which with a column spacing of 7.50 m (25 ft) and a slab thickness of 200 + 100 (drop panels) is quite excessive. A change of tenant permitted to remove carpet and tiles and extensive cracking in the central part of the slab could be observed, with no visible cracking in the portion built first.

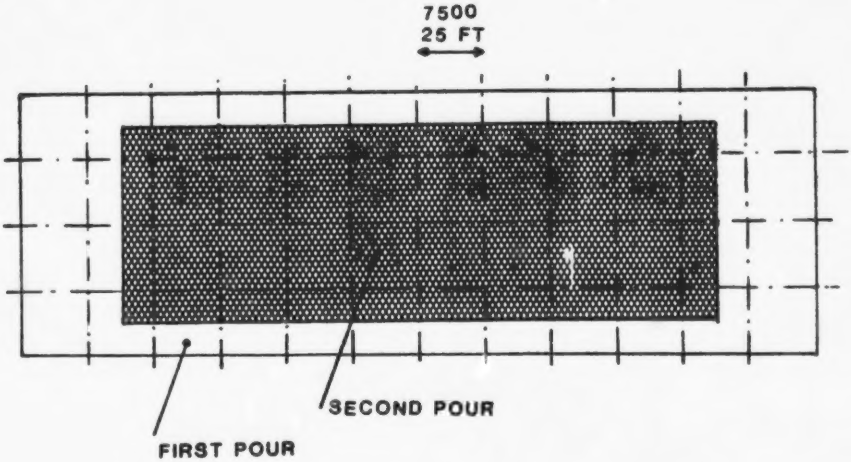

Plan view, schematic
Fig. 1.

Clearly, in this case, differential shrinkage of the 2nd phase concrete which was restrained by the first phase which had already experienced most of its shrinkage contraction, was the main cause of the cracking and consequently the deflections, probably aggravated by the quick and minimal curing of the concrete in the 2nd phase. The crack width and deflections varied widely, from imperceptible to the maximum. The reasons for this were never established in detail. They have probably something to do with the early loading history of the slab where some cracks were initiated, thereby producing weak zones which then attracted deformations due to shrinkage which have a tendency to concentrate in areas where the tensile resistance of the concrete is already reduced.

2. This concerns a long 12 storey apartment building which was built with a 180 mm (7") flat plate on a column spacing of 6 m (20 ft) or so, a standard design for this kind of construction. Gypsum partitions had been tightly mounted at top and bottom, for economic reasons brought forward by the contractor. After some five years, many of the partitions

showed signs of distress and measurements of slab deflections were taken. These amounted to 38 mm (1 1/2" maximum, not in themselves very serious but far beyond anything that could be predicted analytically with traditional calculations. As well, related to the rigid fixing mode of the partitions, they caused considerable damage which, due to bankruptcy of the contractor, had to be borne among the surviving parties.

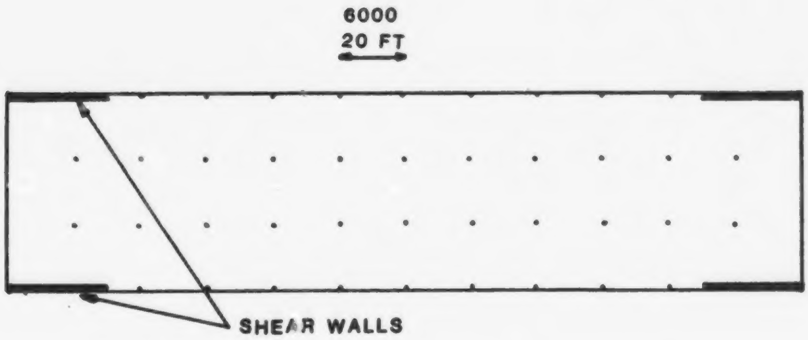

Plan view, schematic
Fig. 2.

Some cracking was seen but no one was alarmed since none of the cracks were wide enough to cause apprehension. The principal cause of the problem was thought to be the two sets of shear walls the building has in order to resist seismic loads and which were arranged at either end of the long building, providing almost complete restraint against longitudinal contraction from shrinkage. The slabs therefore had no choice but to absorb this deformation by forming cracks to relieve the tension. Presumably this occurred mostly in the weakest section where a construction joint, some previous loading history, a truck load of weaker concrete, shorter laps of the reinforcing, an opening or one or several of numerous other reasons existed to trigger the first cracks. These weakened the particular section, so that now most of the contraction accumulated here, causing this bay to deflect - it did not happen in the same location on all the floors of the 12 storey building.

If one looks once more at the little numerical calculation at the beginning, one realizes that it does not take large cracks to produce a serious deflection, e.g. with $\varepsilon_{sh} = 0.0003$ and a crack spacing of 300 mm, one finds an average crack width of

$$W = 0.0003 \times 300 = 0.09 \text{ mm } (4/1000 \text{ in})$$

a fine hairline crack which is easy to overlook, especially if one wants to .

However, a slab with cracks of this size may already sag considerably and with some other circumstances helping, cause embarrassment, and perhaps repair costs and liability problems.

3. A slab belonging to an underground structure about 150 m (500 ft) long had been built in three sections, each making up for about 1/3 of the total length. The dates of concreting of the three sections were one to several months apart, and in addition artifical discontinuities involving a piece of wood and a separation made with expanded metal had been used as a measure towards crack control (see Fig. 3).

While successful in attracting deformations due to contraction from shrinkage and temperature drop in the rest of the large building structure (90,000 sq. m.) these control joints:

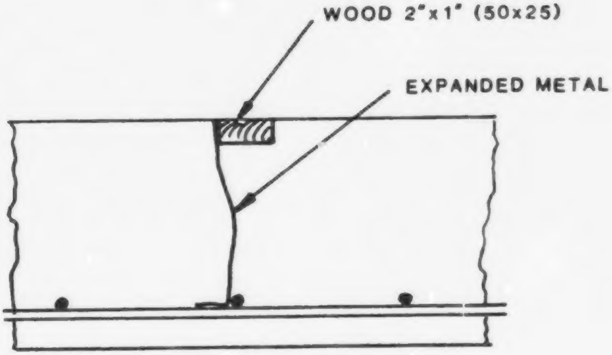

Fig. 3.

failed to prevent random cracking in one particular area near the center of the building. Cracks in this location were seen opening from unnoticeable in the subsequent summer to the maximum width of about 1 1/2 mm in the following winter. A search of the construction records of the various participants turned up the following elements:

- due to extreme pressure from the owner regarding the time schedule, as well as less than benevolent weather, the curing of the particular piece of slab had not been beyond reproach in several aspects
- The slab was built in the wintertime which means that after its curing period, it became exposed to very low temperatures (-30°C or so).
- the compaction of the crushed stone backfill under the scaffolding (this was the first suspended basement slab) was less than perfect. As well, a cycle of freezing and subsequent thawing -when heat was introduced under the slab - may have had something to do with the necessity to adjust the scaffolding supports upward during and immediately after the concreting in order to bring the slab back to its desired level.
- A somewhat controversial record was found regarding the depositing of several pallets of concrete block early in the history of the slab.

- The treatment of the top surface of the slab involved blasting it with little steel particles (similar to sand blasting). This of course exaggerated the appearance of the cracks at the top surface, every crack, visible or not, being made into a major groove, to the great alarm of some participants.
- Deflections did not appear to represent a problem in this case, as they were thought to have already occurred when finishes were applied.

What should be the conclusion of this story then which is, if not in its details, then certainly in a general way quite typical ? And if claims arise from it, who shall be called to account ?

CONCLUSION

A direct relationship between cracks and deflections exists but not necessarily between cracking and loading. Often other causes are the major source of this class of serviceability problems, and in many cases attempts at interpretation must focus on the effects of restrained contraction due to shrinkage or cooling. These can not always be prevented with the classical methods of crack control such as the ones listed in codes and literature which invariably lead to important amounts of extra reinforcing steel. Other measures are needed relating to conceptual design, or to the construction procedure. If restrained shrinkage or temperature contraction cannot be avoided, their effects can perhaps be directed towards locations were they are harmless or easy to deal with, or spread more evenly to make them stay within acceptable limits.

While no hope exists that precise interpretation of cracking and deflections of concrete structures will ever be possible, qualitative study of all parameters using simplistic models may in many cases help the search for the right thing to do.

DESIGN, CONSTRUCTION AND DEFLECTION OF TWO-WAY SLABS

C. J. Montgomery (1), R. G. Brockbank (2),
M. J. Stephens (1), G. Krywiak (1)

(1) Lamb McManus Associates Ltd.
(2) PCL Construction Group Inc.
Edmonton, Alberta, Canada

ABSTRACT: The deflections of reinforced concrete two-way slabs are of concern to owners, designers and contractors. Slab deflections can be excessive if the designer does a poor job of communicating the requirements for camber control and shoring removal to the contractor. Two case histories are presented to illustrate the problems that can occur if these requirements are not properly considered. A third case history is presented to give an example of a properly constructed slab. Finally, recommendations are made for improvements in the design, specification and construction of two-way slabs.

1. INTRODUCTION

Owners expect that the floors in their buildings will be flat and level. To achieve flat and level floors with reinforced concrete two-way slab construction, slabs should be cast on cambered formwork. It is assumed that these built-in cambers will offset the short and long-time deflections of the floor slabs.

Often the behavior of two-way slabs is not consistent with expectations and excessive deflections occur. These excessive floor deflections are sometimes attributed to a lack of quality control by the contractor during construction. However, when the design procedures and floor construction methods are reviewed for a problem floor slab, it is often found that the designer did a poor job of communicating the requirements for camber control and shoring removal to the contractor.

The purpose of this paper is to provide recommendations to designers and contractors relative to the control of deflections for reinforced concrete two-way slabs.

Three case histories are presented to document field measurements of slab deflections. Two of these case histories illustrate the problems that can occur if camber and shoring requirements are not properly considered. The other case history provides data for a properly constructed floor slab. In the final portion of the paper, recommendations are made for improvements in the design, specification and construction of reinforced concrete two-way slabs.

2. CASE HISTORY I - SLAB WHICH WAS NOT CAMBERED

2.1 General: Table 1 presents the geometry and properties for a typical interior panel of a two-way slab which forms the second floor of a two-storey department store. The roof above the second floor was constructed from structural steel. The slab was not cambered during construction.

Other than the lack of camber, there was nothing unusual about the design or construction of the two-way slab. The design satisfied the strength and minimum thickness requirements of the applicable Canadian design codes and standards. Construction was completed during the winter in Calgary, Alberta, with adequate heating and hoarding. Construction records indicated that measured concrete compressive strengths and slumps were acceptable. Shoring for the slab was removed after the concrete was 28 days old.

2.2 Observed Deflections: The owner of the department store complained that the deflections of the second floor slab were excessive. The histograms shown in Figures 1 and 2 record deflection measurements made by the contractor when the slab was on average 16 months old.

The mean measured deflections at the centre of panels (Figure 1) and at midspan along column lines (Figure 2) were 30.3 mm and 19.8 mm, respectively. As indicated by the relatively high coefficients of variation, the measured deflections were quite variable. Since the deflections were measured with a surveyor's level several months after the shoring was removed, some of the observed variability likely occurred because the floor was not finished perfectly flat.

2.3 Calculated Deflections: Calculated deflections for the floor slab are summarized in Table 2. These deflections were evaluated in part by the ADOSS computer program [Canadian Portland Cement Association (1987)], which determines the cracked section properties and the short term deflections of the slab using the procedure outlined in Canadian Standards Association (1984). To account for the influence of restrained shrinkage, the recommendations of Scanlon and Murray (1982) were followed in calculating the cracked moments of inertia for the slab. By their recommendations, the modulus of rupture of the concrete is reduced from the value in the standard to $0.32\sqrt{f'_c}$ in units of MPa, where f'_c is the specified compressive strength of concrete in units of MPa. Long-time deflections of the slab were evaluated using the graphical recommendations of Canadian Portland Cement Association (1985).

Other methods are available to calculate the deflections of two-way concrete slabs [see, for example, Ghali and Favre (1986), Rangan and McMullen (1978) and Rangan (1976)]. The various methods give similar results provided that the inevitable cracking of concrete owing to stresses and restrained shrinkage is properly taken into account.

Because floors are rarely subjected to full design loadings, the deflections given in Table 2(a) are best compared to the measured deflections. The mean measured deflections (Figures 1 and 2) were about the same as the calculated deflections at age 16 months.

The calculated instantaneous deflections under specified live load [Table 2(b)] were slightly more than the Canadian Standards Association (1984) allowable value of 1/360 times the span. However, because the thickness of the slab exceeded the minimum value specified by the standard, it would not have been necessary for the design engineer to check deflections. The calculated differential deflections after the attachment of architectural finishes were smaller than the standard allowable of 1/240 times the span required when finishes are not sensitive to deflections.

In summary, since the calculated and measured deflections were about the same, neither the building owner, designer or contractor should have been surprised at the observed deflections. However, camber at the time of casting should have been used to achieve a flat floor in the long term.

3. CASE HISTORY II - SLAB WHICH WAS CAMBERED IMPROPERLY

3.1 General: The geometry and properties for an interior panel of a two-way slab which forms the third floor of a highrise tower in Edmonton, Alberta are summarized in Table 3. The contractor advised that camber for each slab panel was obtained by jacking up the formwork approximately 15 mm at the centre of the panel and at midspan along two opposite column lines to obtain a one-way sloped surface. The slab panels were jacked up after concrete was screeded on the forms.

The slab design was in general conformance with the requirements of the applicable Canadian design codes and standards, although top steel was not specified for the central 3 m portion of middle strips. Complete details of the construction procedures for the slab were not available to the authors.

3.2 Observed Deflections: Measured deflections for the floor slab were quite variable. Typical results are presented in Figure 3 for a panel of the slab at an age of approximately 24 months. Measurements were made by the contractor with a surveyor's level.

As illustrated in Figure 3, cracks were typically observed at midspan bottoms, and around drop panels at the top of the floor slab. These cracks were generally less than 1 mm wide.

3.3 Calculated Deflections: The calculated deflection of the floor slab at age 24 months under self-weight plus a sustained load of 1.0 kN/m^2 was 27 mm at the centre of the panel. This deflection compares favorably with the measured value of 33 mm (Figure 3).

In the approximate procedure used to assess deflections, it was assumed that the floor consisted of an imaginary strip of one-way slab at the centre of the panel spanning from imaginary beams running between columns. To account for two-way action, one-half of the supported load was used when calculating the deflection of the one-way slab and the reactions of the slab on the supporting beams. With this model, the total deflection at the centre of the panel is equal to the average of the centreline deflections of the supporting beams plus the centreline deflection of the strip of one-way slab relative to the supporting beams.

Camber was neglected in calculations. Since slab cambers were jacked into the formwork after the concrete was placed, extensive micro-cracking likely occurred as a direct result of the cambering procedure. These cracks would have closed when the shoring was removed, and a majority of the camber would have been lost.

In calculations, the partial cracking of the slab owing to shrinkage and temporary construction loading was accounted for by adjusting moments of inertia. The effective moments of inertia were calculated using the appropriate Canadian Standards Association (1984) equation and the reduced modulus of rupture of concrete recommended by Scanlon and Murray (1982), as previously discussed for Case History I. Long-term deflection multipliers were determined using the method described for Case History I.

In summary, the excessive deflections observed for this floor slab occurred because the contractor and the designer's field inspector did not pay proper attention to cambering procedures. Had the formwork been cambered prior to the placing of concrete and the top of the floor screeded parallel to the formwork, then the slab deflections could have been reduced by the magnitude of the initial camber.

4. CASE HISTORY III - SLAB WHICH WAS CONSTRUCTED PROPERLY

4.1 General: Table 4 presents the geometry and properties for a typical interior panel of a two-way slab which forms the second floor of a two-storey department store. Similar to Case History I, the roof above the second floor was constructed from structural steel. The slab was cambered during construction.

The design of the slab satisfied the strength and minimum thickness requirements of current Canadian design codes and standards. Construction was completed during the late summer and early fall in Edmonton, Alberta. Construction records indicated that measured concrete compressive strengths and slumps were acceptable. Shoring for the slab was removed when the concrete was between 21 and 28 days old.

4.2 Observed Deflections: Elevations at the top of slab were measured with a surveyor's level prior to the removal of shoring and after stripping when the slab was between 2 and 4 months old. The mean measured cambers prior to removal of shoring were 23.7 mm with a coefficient of variation of 0.46 and 15.8 mm with a coefficient of variation of 0.58 at the centre of panels and at midspan along column lines, respectively. The mean measured deflections after removal of shoring were 9.6 mm with a coefficient of variation of 0.45 and 5.8 mm with a coefficient of variation of 0.57 at the centre of panels and at midspan along column lines, respectively.

It is believed that the slab elevation measurements were made with care by the contractor. The relatively high coefficients of variation for these measurements were likely the result of uneven formwork settlement, variations in the age of the slab at form removal and normal construction tolerances.

4.3 Calculated Deflections: Slab deflection calculations were carried out using the computer program and procedures described for Case History I. A summary of the calculated results is presented in Table 5.

The mean measured deflections, although less than the calculated deflections at age 3 months [Table 5(a)], followed the predicted trends. Measured deflections that were less than the calculated values are probably the result of actual sustained live loads being less than the assumed load of 1.0 kN/m^2. The calculated deflections for the cases of Table 5(b) and (c) satisfied the requirements of Canadian Standards Association (1984). Note that the total deflections recorded in Table 5(a) at an age 5 years would be nearly offset by the initial slab cambers.

In summary, the owner of the building described by this case history can expect a relatively flat floor in the long term. Deflection assessment and camber control were a high priority of both the designer and the contractor.

5. RECOMMENDATIONS FOR IMPROVED DESIGN, SPECIFICATION AND CONSTRUCTION OF SLABS

5.1 Design: Engineers can improve the performance of reinforced concrete two-way slabs by using available procedures to calculate realistic deflections at the design stage, even if deflection calculations are not required by governing design standards and codes. These calculated deflections should be compared to allowable values specified in codes and standards. Camber requirements should be shown on drawings. If important to other trades (for example, the suppliers of non-structural elements likely to be damaged by large deflections), estimates of the portions of total deflections occurring after the attachment of non-structural elements should also be shown on the drawings.

Designers should avoid specifying cambers which are excessive. Slabs should only be cambered for self-weight plus a realistic estimate of superimposed dead loads plus an estimate of the sustained live loads.

5.2 Specification: In writing specifications, designers should require that the contractor check cambers and measure deflections as follows:

(a) The camber of formwork and heights of screed boards should be recorded prior to casting concrete.
(b) The camber of the slab should be monitored immediately prior to the removal of shoring.
(c) The deflection of the slab immediately after the removal of formwork and shoring should be recorded.

Although the deflection monitoring described above may increase the cost of the project slightly, precise field measurements will be of great assistance in determining who is responsible - the designer or contractor - if problems occur. In addition, a monitoring program helps to convince owners that floors in buildings actually do deflect.

On large projects, experience with cambers and deflections measured near the beginning can be used to improve performance later on in the project.

Specifications should note that the camber shown on drawings must be added to allowances made for the deflection and settlement of shoring. Hurd and ACI Committee 347 (1973) indicate that an allowance of 6 mm per 3 m of the span is reasonable for the deflection and settlement of shoring.

Specifications should point out that the early removal of shoring will increase the magnitude and variability of slab deflections.

Under normal conditions, the specifications should require that both the underside and top of the slabs be cambered so that the structural thicknesses shown on the drawings are maintained.

5.3 Construction: Contractors should recognize that slab deflections are influenced by construction methods. Formwork must be used which can be adjusted for camber prior to the placement of concrete. If early shoring removal is required by the construction schedule, special precautions must be taken [see, for example, ACI Committee 435 (1985)].

It is the designer's responsibility to review the contractor's proposed methods of camber control and shoring.

6. SUMMARY AND CONCLUSIONS

Reinforced concrete two-way slabs deflect as a result of the effects of loads, and the long-time creep and shrinkage of concrete. Floors satisfying the requirements of owners for flatness can be achieved if designers and contractors work together to develop satisfactory procedures for camber control and shoring removal.

To achieve flat and level floors, the designer must make realistic estimates of deflections and specify camber requirements. The contractor must use formwork which can be adjusted for camber, prior to the placement of concrete, and take care in finishing operations. The contractor's proposal for camber control and shoring design and removal must be reviewed by the designer.

7. REFERENCES

ACI Committee 435. 1985. Observed deflections of reinforced concrete slab systems, and causes of large deflections. In American Concrete Institute SP-86, ACI, Detroit, Michigan, pp. 15-61.

Canadian Portland Cement Association. 1985. Concrete design handbook. Part I, CPCA, Ottawa, Ontario, pp. 1-485.

Canadian Portland Cement Association. 1987. ADOSS (Analysis and design of slab systems). CPCA, Ottawa, Ontario.

Canadian Standards Association. 1984. Design of concrete structures for buildings. CAN3-A23.3-M84, CSA, Rexdale, Ontario, 281 p.

Ghali, A. and Favre, R. 1986. Concrete structures: stresses and deformations. Chapman and Hall Ltd., London, England, 352 p.

Hurd, M. K. and ACI Committee 347. 1973. Formwork for concrete. 3rd Edition, American Concrete Institute SP-4, ACI, Detroit, Michigan, 363 p.

Rangan, B. V. 1976. Prediction of long-term deflections of flat plates and slabs. ACI Journal, V. 73, No. 4, pp. 223-226.

Rangan, B. V. and McMullen, A. E. 1978. A rational approach to control of slab deflections. ACI Journal, V. 75, No. 6, pp. 256-262.

Scanlon, A. and Murray, D. W. 1982. Practical calculation of two-way slab deflections. Concrete International, V. 4, No. 11, pp. 43-50.

Table 1: Slab which was not cambered

(a) Geometry	
Spans	7315 mm x 7315 mm
Slab thickness	203 mm
Capital dimensions	610 mm x 610 mm x 229 mm thick
Column size	356 mm x 356 mm
Storey to storey height	5330 mm
(b) Reinforcing Steel (Each Way)	
Column strip - Top	7500 mm^2
Bottom	2400 mm^2
Middle strip - Top	0 mm^2
- Bottom	2400 mm^2
(c) Specified Material Properties	
Concrete compressive strength	25 MPa
Reinforcement yield strength	400 MPa
(d) Specified Loads	
Live	4.8 kN/m^2
Superimposed dead	0.5 kN/m^2

Table 2: Calculated deflections for slab described in Table 1

Description	Centre of Panel		Midspan Along Column Lines	
	Deflection (mm)	Deflection / Diagonal Span	Deflection (mm)	Deflection / Span
(a) Total deflection under slab weight plus 0.5 kN/m^2 superimposed dead plus 0.96 kN/m^2 sustained live				
Age 16 months	30.5	1/339	20.3	1/360
Age 5 years	36.6	1/282	24.4	1/300
(b) Instantaneous deflection under specified live	32.2	1/321	21.6	1/339
(c) Differential deflection after attachment of finishes at age 8 months	36.1	1/286	24.1	1/304

Table 3: Slab which was cambered improperly

(a) Geometry	
Spans	9000 mm x 9000 mm
Slab thickness	220 mm
Drop panel dimensions	3000 mm x 3000 mm x 180 mm thick
Column size	560 mm x 560 mm
Storey to storey height	5500 mm
(b) Reinforcing Steel (Each Way)	
Column strip - Top	7500 mm^2
Bottom	3000 mm^2
Middle strip - Top	1800 mm^2
- Bottom	2800 mm^2
(c) Specified Material Properties	
Concrete compressive strength	30 MPa
Reinforcement yield strength	400 MPa
(d) Specified Loads	
Live	4.8 kN/m^2
Superimposed dead	1.0 kN/m^2

Table 4: Slab which was constructed properly

(a) Geometry	
Spans	8534 mm x 8534 mm
Slab thickness	229 mm
Drop panel dimensions	2845 mm x 2845 mm x 178 mm thick
Column size	457 mm x 457mm
Storey to storey height	5486 mm
(b) Reinforcing Steel (Each Way)	
Column strip - Top	5000 mm^2
Bottom	4000 mm^2
Middle strip - Top	3600 mm^2
- Bottom	2600 mm^2
(c) Specified Material Properties	
Concrete compressive strength	25 MPa
Reinforcement yield strength	400 MPa
(d) Specified Loads	
Live	4.8 kN/m^2
Superimposed dead	0.5 kN/m^2

Table 5: Calculated Deflections For Slab Described In Table 4

Description	Centre of Panel		Midspan Along Column Lines	
	Deflection (mm)	Deflection / Diagonal Span	Deflection (mm)	Deflection / Span
(a) Total deflection under slab weight plus 0.5 kN/m^2 superimposed dead plus 1.0 kN/m^2 sustained live				
Age 3 months	20.3	1/595	13.7	1/623
Age 5 years	30.4	1/397	20.5	1/416
(b) Instantaneous deflection under specified live	22.7	1/532	15.2	1/561
(c) Differential deflection after attachment of finishes at age 6 months	26.3	1/459	17.7	1/482

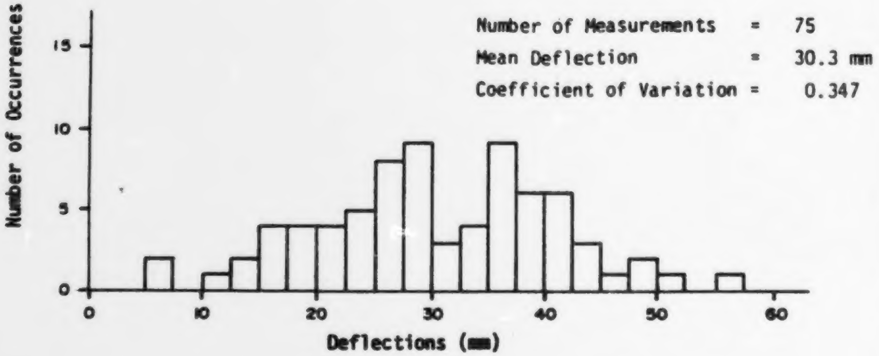

Figure 1: Measured deflections at centre of panels for slab described in Table 1

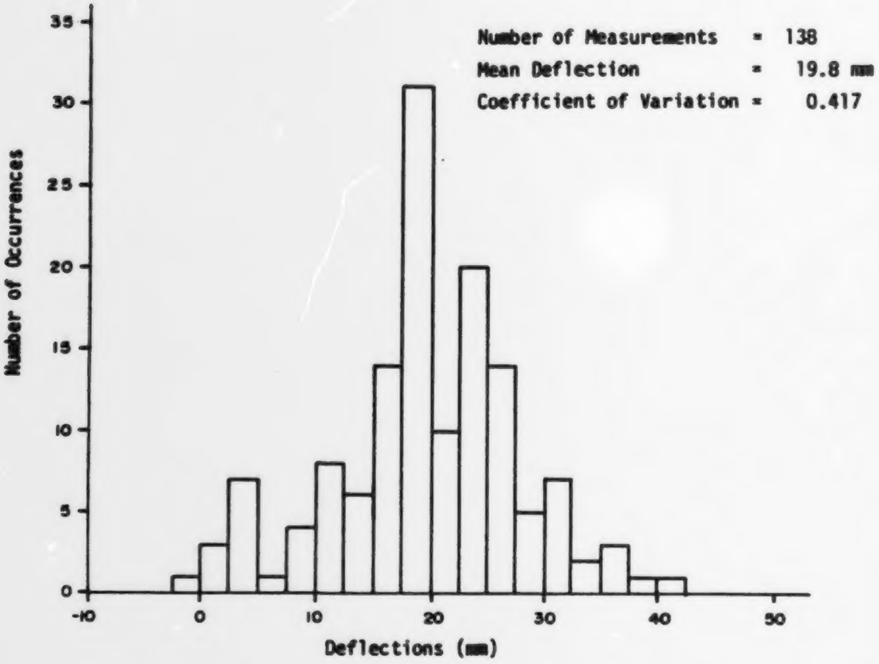

Figure 2: Measured deflections at mid-span along column lines for slab described in Table 1

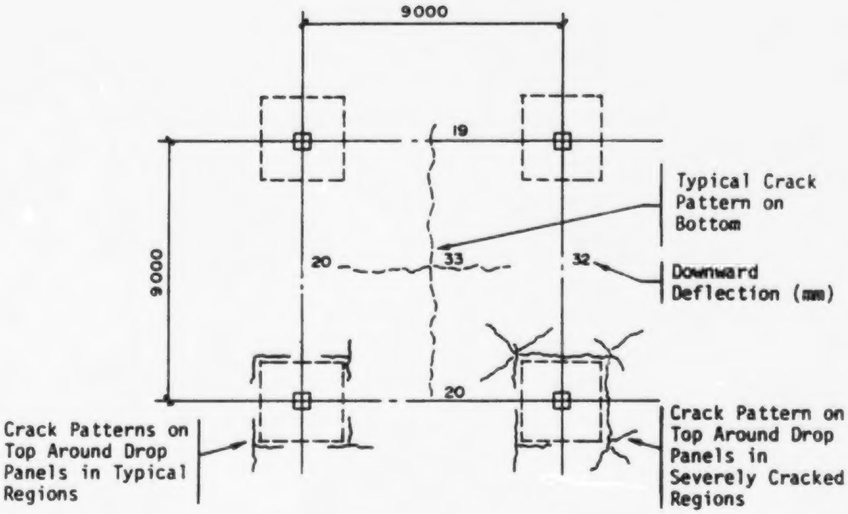
9000
9000
19
20
33
32
20
Typical Crack Pattern on Bottom
Downward Deflection (mm)
Crack Patterns on Top Around Drop Panels in Typical Regions
Crack Pattern on Top Around Drop Panels in Severely Cracked Regions

Figure 3: Measured deflections and observed crack pattern for slab described in Table 3

COMPARISON OF FIELD MEASURED FLOOR SLAB DEFLECTIONS FOR TWO REINFORCED CONCRETE BUILDINGS

E. P. Jokinen
Eric P. Jokinen Associates Ltd., Edmonton, Canada

A. Scanlon
The Pennsylvania State University, University Park, PA 16802 USA

G. J. Burghardt
University of Alberta, Edmonton, Canada

ABSTRACT: Field measured floor slab deflections for two buildings are compared. The slabs have similar span dimensions but different thicknesses. Measured deflections are compared with calculated deflections. Recommendations are included for modifying code calculation procedures.

1. INTRODUCTION

Code provisions for deflection control are empirical and based on experience obtained over the years. In order to assess the adequacy of these code provisions, data obtained from field measurements are required because of the wide range of variables that influence deflections in building structures. Very few case studies involving deflection measurements in North America have been reported. This paper compares measured deflections for two slab systems with similar span arrangements but different slab thicknesses.

2. BUILDING DESCRIPTIONS

Both buildings are of cast-in-place reinforced concrete construction. In each case the floor system consists of two-way flat slabs with column capitals and drop panels. Span length center to center of columns is 9000mm for each building. However in Building A, a 28-story commercial office tower, the slab thickness is 200mm while for Building B, a five-story government building, the slab thickness is 230mm. Details of the slab systems are listed in Table 1.

It should be noted that the slab thickness for Building A is less than the code empirical minimum thickness for which deflections need not be calculated. Deflection calculations based on CSA A23.3 (1984) procedures indicated that the specified permissible deflection limits were satisfied. The slab thickness for Building B exceeds the code empirical minimum thickness.

As shown in Figure 1(a) Building A has an L-shaped floor plan and all slab panels are either edge panels or corner panels. The layout of one floor level of Building B is shown in Figure 1(b). This floor system contains interior panels as well as edge and corner panels. Building A has no edge beams. Building B has 400x810 edge beams. Both buildings were constructed using shoring and re-shoring.

3. DEFLECTION SURVEYS

Slab deflection measurements were taken during construction for both buildings as part of the construction quality control process. Details of the deflection measurement survey for Building A are reported elsewhere (Jokinen and Scanlon 1987.)

For Building B, top of formwork elevations were taken prior to placing concrete. Top of slab elevations were then established after the concrete was placed and had hardened. Elevations were measured adjacent to columns, at mid-span along column lines, and at mid-panel. These measurements provide data on slab thickness provided and amount of initial camber provided. Data on slab thickness and camber provided are shown in Figures 2 and 3. On average the slab thickness provided was just slightly less than specified. The camber provided was an average about 33% less than specified.

3.1 Deflection Measurements: For Building A, deflections were measured during construction using standard leveling techniques and at one year using a string line stretched between columns. The one year measurements do not therefore include any camber provided. A mid-panel camber of 15mm was specified. However in most cases the camber provided was less than 15mm. Part of the variability in the one-year measured deflections can be attributed to variability in camber. An example of deflection measurements for a corner panel is shown in Figure 4.

Deflection measurements for Building B were taken at about 4.5 months after placing concrete and again at about 4 years. In both cases standard leveling techniques were used. For the deflections at 4.5 months top of slab elevations were measured relative to the same benchmark, immediately after placing concrete and at 4.5 months, to obtain the total deflection. Deflections at 4 years were obtained by adding the initial camber to the net deflection relative to the slab elevation adjacent to columns. The effects of camber are therefore included in these measurements. Plots of interior, edge, and corner panel deflections vs time are shown in Figure 5. The deflection statistics are shown in Table 2.

3.2 Comparison Between Building A and Building B: Direct comparison of deflection measurements between the two buildings is not possible because the measurements were made at different ages, and because the 1-year deflections for Building A do not include the effects of initial camber. In addition Building A has no interior panels.

Mean deflections are summarized for the two buildings in Table 3. Deflections at 28 days in Building A exceed those at 4.5 months in Building B, while the 1 year deflections of Building A (not including camber) are similar to the 4-year deflections in Building B. No significant differences are found between corner, edge, and interior panel deflections for each building.

The coefficient of variation of measured deflections in Building A was found to be of the order of 30% both at 4 weeks and at one year (Jokinen and Scanlon 1987.) For Building B the coefficient of variation was found to be of the order of 15% as indicated in Table 2.

These results suggest that the smaller slab thickness leads not only to larger deflections but higher variability also.

4. DEFLECTION CALCULATIONS

Deflection calculations were made using the crossing beam procedure described in the CPCA Design Handbook (1985). Effective moment of inertia values were computed for each span using the procedures outlined in CSA A23.3 (1984). Using the code-specified value of $f_r = 0.6\sqrt{f'c}$ and appropriate long time multipliers reflecting the age at which deflections were measured, the calculated deflections are significantly smaller than the mean measured deflections as shown in Table 4.

With a reduced effective modulus of rupture ($f_r = 0.3\sqrt{f'c}$) good agreement was obtained between measured and calculated deflections for interior panels, but edge and corner panel deflections were overestimated. These calculated deflections were based on an average I_e value for the end span given by
I_e (ave) = 0.25 I_e (int. neg.) + 0.75 I_e (int. pos)

Better agreement was obtained when the average I_e value for exterior spans was calculated from
I_e (ave) = 0.10 I_e (ext. neg) + 0.30 I_e (int. neg) + 0.6I_e (int. pos)

Calculated deflections are summarized on Table 4 which also lists mean measured deflections.

5. SUMMARY AND CONCLUSIONS

Results of deflection surveys for two reinforced concrete buildings have been presented. In Building A the floor slab thickness was less than the code empirical minimum thickness and in Building B a slab thickness equal to the code empirical minimum value was provided. As would be expected, deflections for Building A were generally significantly greater than for Building B. In addition, the deflections for Building A were generally more variable than for Building B.

Deflection calculations based on the code provisions underestimated the mean deflections for both buildings. Much better correlation between mean measured deflection and computed deflection was obtained when a reduced modulus of rupture $f_r = 0.3\sqrt{f'c}$ MPa was used in the computation of effective modulus of inertia. In conjunction with this value of f_r, a method for computing the weighted average Ie for exterior spans is suggested that provides reasonable agreement between computed and measured deflections for exterior spans.

REFERENCES

Canadian Standards Association 1984. Code for the Design of Concrete Structures for Buildings, CAN3-A23.3-M84.

Canadian Portland Cement Association 1985. Concrete Design Handbook.

Jokinen, E.P.and Scanlon A. 1987. Field Measured Two Way Slab Deflections. Canadian Journal of Civil Engineering 14(4).

Table 1: Slab Details

	Building A	Building B
Slab Thickness	200mm	230mm
h_{min}	230mm	210mm
Drop Panel Thickness	350mm	350mm
Column Capital Size	1520mm	1500mm
Edge Beam Size	—	400x810mm
Span (Column Centres)	9000mm	9000mm
Specified Camber (Mid-Panel)	15mm	25mm
f'c (28 days)	30MPa	30MPa

Table 2: Deflection Statistics for Building B

Slab Type	Interior		Edge		Corner	
Age (months)	4.4	48	4.3	48	5.1	48
Number of Panels	16	13	18	16	8	6
Mean Deflection (mm)	20.25	38.27	21.44	36.16	17.75	38.08
Standard Deviation (mm)	1.95	5.12	3.31	5.74	3.11	4.03
Coefficient of Variation (%)	9.6	13.4	15.4	15.9	17.5	10.6

Table 3: Summary of Mean Deflections for Buildings A and B

	Mean Mid-Panel Deflection (mm)					
Panel Location	Corner		Edge		Interior	
Building	A	B	A	B	A	B
28 days	27.33	--	23.75	--	—	—
4.5 months	—	17.7	--	21.44	--	20.25
1 year (1)	32.53	--	33.43	--	—	—
4 years	—	38.08	--	36.16	--	38.27

Note: (1) Initial camber not included

Table 4: Measured and Calculated Deflections

		Building A		Building B		
	fr	Edge	Corner	Interior	Edge	Corner
Time (months)		12	12	4.4	4.3	5.1
Measured Mean Deflection (mm)		35.24	32.53	20.25	21.44	17.75
Calculated Deflections (mm)						
a) $I_e = I_{e1}$	$0.6\sqrt{f'c}$	16.41	23.81	7.05	11.06	11.94
b) $I_e = I_{e1}$	$0.3\sqrt{f'c}$	37.12	55.73	20.12	28.81	24.45
c) $I_e = I_{e2}$	$0.3\sqrt{f'c}$	27.43	36.45	20.12	22.25	18.82

Note

Weighted Average I_e values for exterior span

$I_{e1} = 0.25\ I_e$ (int. neg.) + $0.75 I_e$ (int. pos)

$I_{e2} = 0.10\ I_e$ (ext. neg.) + $0.30\ I_e$ (int. neg.) + $0.6\ I_e$ (int. pos)

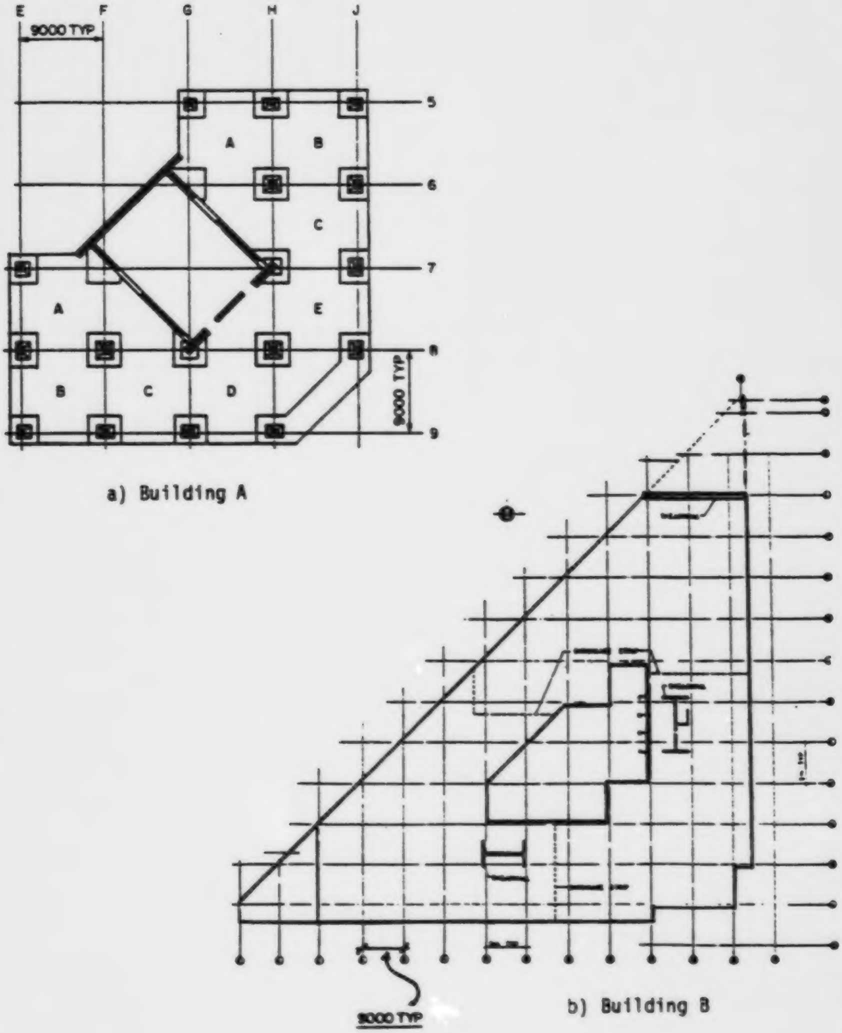

a) Building A

b) Building B

Figure 1 Floor Slab Layouts

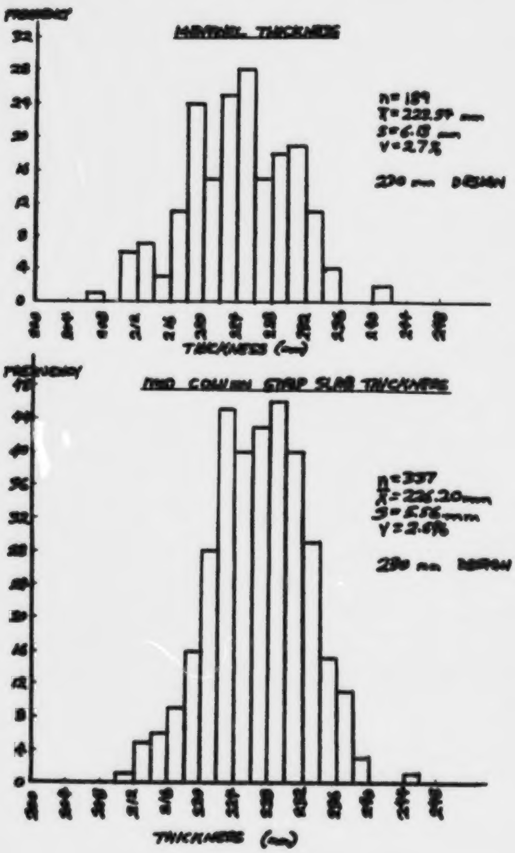

Figure 2 Building B - Measured Slab Thicknesses

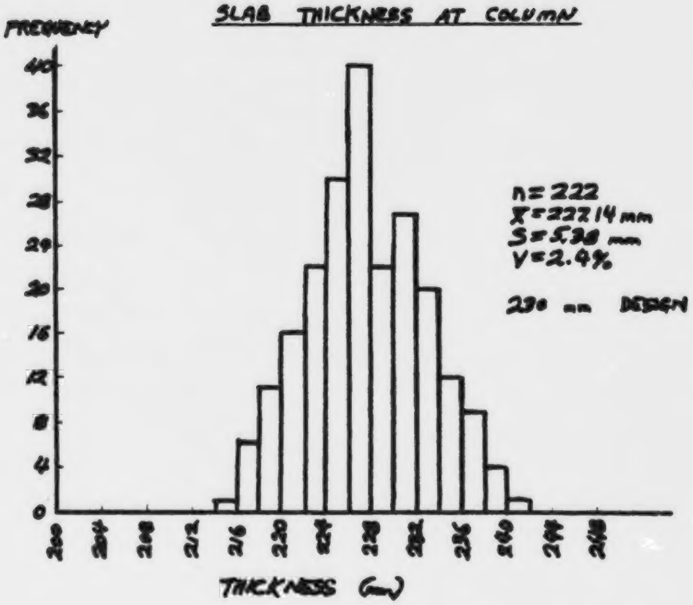

Figure 2 Building B - Measured Slab Thicknesses (Cont'd.)

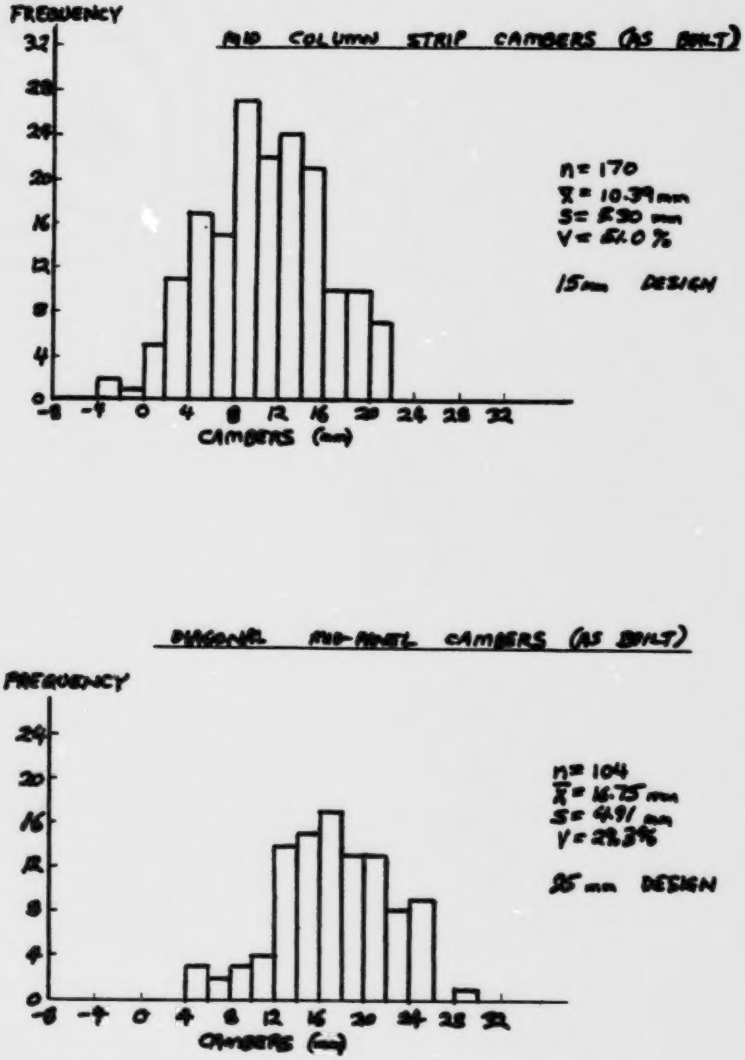

Figure 3 Building B - Measured Initial Camber

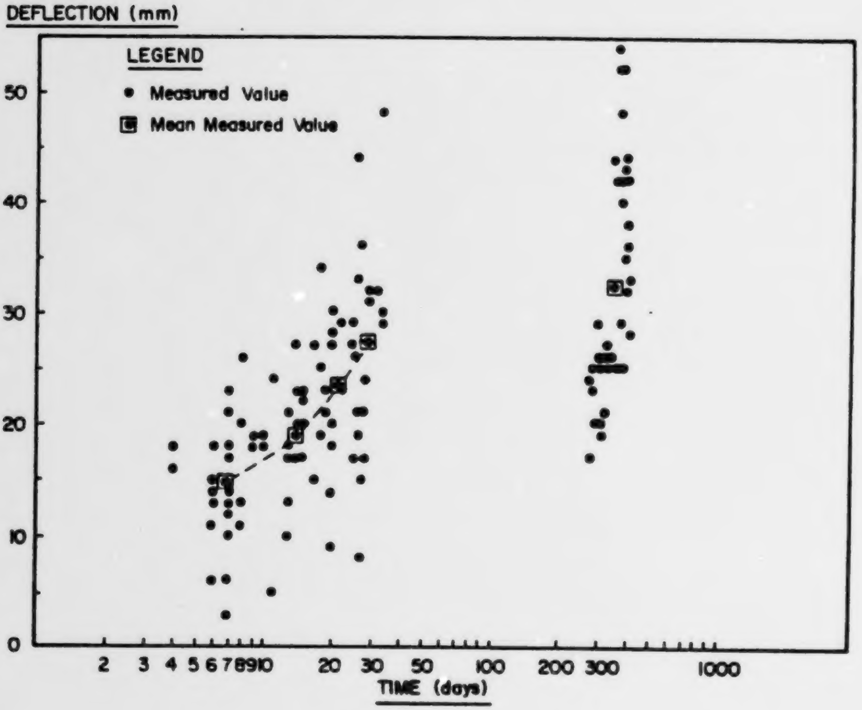

Figure 4 Building A - Measured Deflections for Corner Panel

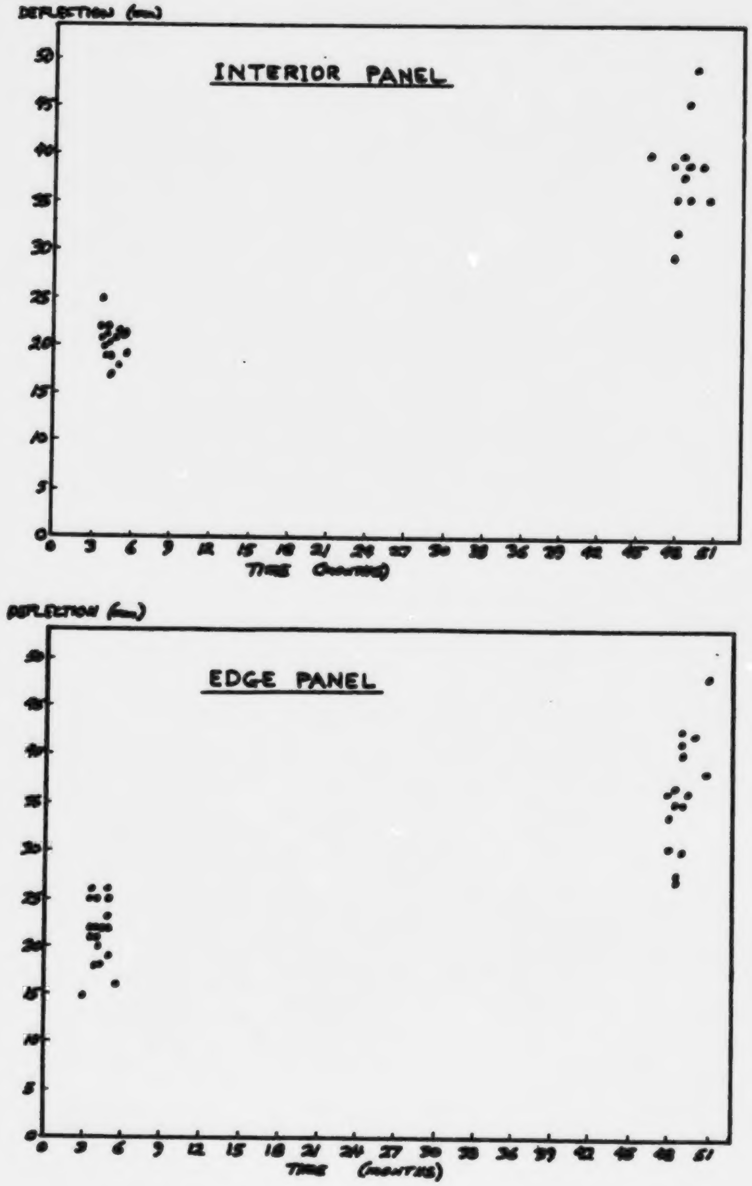

Figure 5 Building B - Measured Deflections at Mid-panel

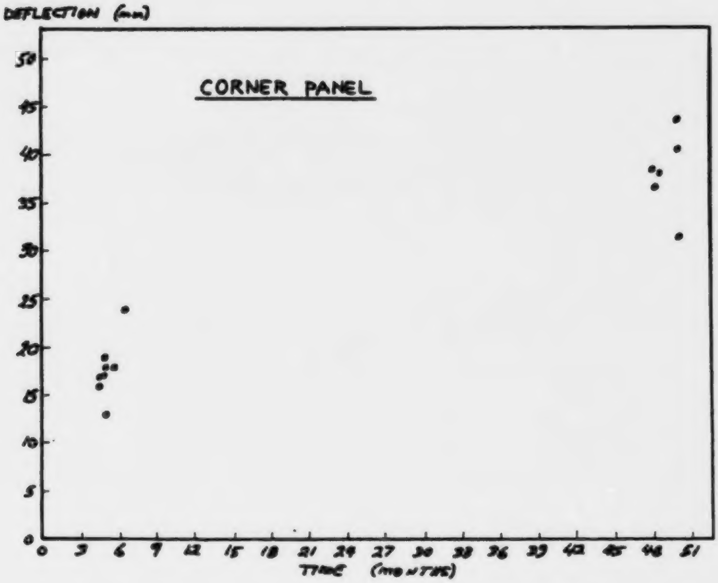

Figure 5 Building B - Measured Deflections at Mid-panel (Cont'd.)

Effect of Elastic and Time-Dependent Concrete Properties on Construction Loads in Multistory Two-Way Slab Construction

A. F. Shaikh[1], S. K. Ghosh[2], and M. M. Mehta[3]

During construction of multistory two-way slab buildings, the floor slabs generally get overloaded due to the practice of casting a new floor by supporting it on a number of previously cast floor slabs. The magnitude of the overloads depends on the rate of construction i.e. number of floors cast per week, the construction scheme i.e. the number of floors used to support a new floor, and the total dead and construction live loads in a scheme.

These construction loads can be greater than the design service loads (in rare cases even the design ultimate loads) for these floors, resulting in excessive deflections and high stresses in the floor slabs. Thus, to assure the safety of the structure during construction an accurate analysis is required to calculate the construction load distribution between various floors.

Analyses were carried out of the distribution of construction loads as affected by cracking in floor slabs and concrete properties such as compressive strength, modulus of elasticity and modulus of rupture and the variation in these properties during the period of construction. Analyses also included the effects of creep and shrinkage in concrete.

The cracking of floor slabs was found to have significant effect on the load distribution on floor slabs, resulting in reduction of the load ratios (load induced on a slab/(dead load of the slab + weight of formwork) by approximately 20%. Due to the effect of cracking, the lower slabs have a lower flexural stiffness as compared to the upper slabs of a scheme. Thus at different load stages a larger portion of the load is distributed to upper slabs as compared to lower slabs. Although the lower slabs still carry the major portion of the total load (i.e. dead load of the slabs, formwork and other construction loads), the load redistribution due to cracking reduces the likelihood of failure of lower floor slabs. Thus it is possible in most cases to have a faster rate of construction in multistory two way slab buildings, without endangering the safety of the building.

[1] Professor of Civil Engineering and Associate Dean for Graduate Studies and Research, [3] Former Graduate Student, University of Wisconsin-Milwaukee, Milwaukee, Wisconsin 53201, [2] Manager, Engineered Structures Program, Portland Cement Association, Skokie, Illinois, 60077

The effect of creep and shrinkage was found to be negligible on load distribution. Construction loads are sustained for a very short period of time and the total creep and shrinkage deformations during that short period of time are small. But due to the early removal of the formwork ultimate creep and shrinkage deflections will be large.

A shoring-reshoring scheduling computer program has been developed. The program determines the schedule of construction subject to safety and serviceability criteria, by evaluating strength and deflections, as per ACI 318 code requirements.

PROPOSED CODE PROVISIONS FOR SLAB SPAN THICKNESS LIMITATIONS INCLUDING CONSTRUCTION LOADS.

N. J. Gardner

Department of Civil Engineering
University of Ottawa
Ottawa, Canada

Abstract: Relatively large construction loads applied to immature slabs will cause large initial elastic deflections. The high applied stress/developed strength ratio will cause significant creep deflections resulting in large long term deflections. Currant code provisions permit slabs to be designed without calculating deflections provided the slabs have a minimum thickness. Current code provisions for minimum slab thicknesses need to be modified to accomodate construction load effects.

Keywords; Concrete construction; deflections; flat plates; multi-storey buildings; loads (forces); code provisions.

1. INTRODUCTION

Reinforced concrete flat slab structures are frequently used for apartment buildings and office buildings and comprise a significant fraction of rentable construction. Flat slabs are generally constructed using flying forms and reshores which is a very rapid and repetitive construction process.

The typical construction procedure involves casting the new slab onto forms which are supported on one or more previously cast floors. The loads occurring on the supporting slabs during construction, which are uniquely determined by the construction schedule, are large and can exceed the supporting structures design capacity. An added complication is that these construction loads are applied to slabs which have not achieved their design strength.

Fig. 1 shows the construction of a multi-floor flat slab building using one level of forms and three levels of reshores. To reduce the load on the slabs supporting the forms these slabs can be supported by reshores. In a slab/form/reshore system failure can occur by failure of one or more floors or failure of the forms or reshores.

The loads applied to the slabs, forms, and reshores are dependent upon the number of forms, number of reshores and the sequence of stripping the forms and reshores.

The problem now separates into two phases, or limit states, a short term construction safety limit state and a long term deflection serviceability limit state.

To avoid a collapse during construction the design and formwork engineers must ensure that the stength available is greater than that required at all stages of construction. Catastrophic failure of flat slabs is usually caused by failure due to punching shear. The punching shear capacity available is dependant upon the shear perimeter available, the developed concrete strength, reinforcement ratio and the assumed or code specified relationship between shear strength and concrete strength.

Relatively large construction loads applied to immature slabs with their low elastic moduli will cause large initial elastic deflections. The high applied stress/developed strength ratio will cause significant creep, generally non-recoverable, resulting in large long term deflections. Shrinkage, while not related to construction loads, also contributes to long term deflections. The concrete strength developed is dependant upon rate of construction or age, construction temperature, type of cement and chemical or mineral admixtures used. The elastic,creep and shrinkage deflections are related to structural detail, reinforcement ratio, the developed concrete strength, and hence temperature and humidity, and load history.

Fu and Gardner 1985 reviewed the literature reporting measured long term deflections and the results of a detailed laboratory study. Unfortunately most published work does not report the construction schedule. Table 1 presents a summary of the published ratios of measured long term deflection to initial deflections. The summary shows clearly that the long term deflections cannot be ignored in the design process and the work of Sbarounis 1984, Graham and Scanlon 1986, and Fu and Gardner 1985 show that the contribution of the effects of construction loads on long term deflections cannot be ignored.

In summary the long term deflection serviceability is dependant upon load history imposed during construction in addition to the 28 day design provision. The influence of the construction loads on the long term deflection serviceability means that the construction process cannot be independant of the design considerations. Fundamental to both the safety limit state and the deflection limit state is a knowledge of the load history and the probable concrete properties given the age-temperature profile.

However many building codes specify maximum span thickness ratios for which deflections need not be considered. Using published information this paper presents a method for calculating long term deflections and using reasonable assumptions calculates limiting slab span/thickness ratios below which deflections need not be calculated.

The loads applied to the slabs, forms and reshores can be calculated knowing the number of forms and reshores. A detailed description of the method to calculate construction loads was given by Agarwal and Gardner 1974.

2. LONG TERM DEFLECTIONS

The long term deflection of a concrete member will include a deflection due to shrinkage of the concrete and the elastic deflections caused by the various dead and live loads plus creep deflections calculated for each of the loads taking account of the age at loading.

2.1 Creep

ACI 209 1971 suggested the creep of concrete in compression could be represented by the following expression.

$$Ct = 1.25 * to^{-.118} \frac{(t-to)^{0.60}}{10 + (t-to)^{0.60}} * Cu$$

where Cu = ultimate creep coefficient
Ct = creep coefficient at time t
to = age at loading

The ultimate Creep Coefficient can be taken as 2.35 in absence of experimental data.

2.2 Creep Deflection

ACI 209 proposed the following empirical equation for calculating the additional deflection due to creep for slabs with a low ratio of compression steel.

$$\delta c = [1/(1 + 50p')] * Ct\,\delta i > 0.4 * \delta i$$

where δc = additional deflection due to creep
δi = elastic initial deflection
Ct = creep coefficient
p' = compression steel ratio

2.3 Shrinkage

ACI 209 1971 proposed, that in the absence of specific data,that an ultimate concrete shrinkage strain of 780 x 10^{-6} could be used and correction factors were given for humidity, size effects etc..

2.4 Deflection due to shrinkage

Branson and Christiason 1971 proposed that the long term deflection due to shrinkage could be calculated from the following expression.

$$\delta_{shrinkage} = Kw * \phi sh * L$$

where Kw = boundary constant dependant upon boundary restraints

$$\phi sh = 0.7 \frac{\varepsilon sh}{h} [(p - p')^{1/3}] \sqrt{\left(\frac{p - p'}{p}\right)} \text{ for } (p-p') < 3 \text{ percent}$$

p = percentage of tension steel
p'= percentage of compression steel
h = slab thickness
ε_{shu} = ultimate shrinkage strain
ϕ_{sh} = shrinkage curvature
L = span

2.5 Long term deflection

Approximate methods to calculate the long term deflections have been given by ACI 209, Sbarounis, Fu and Gardner and Gardner and Fu 1987.

ACI209

$$\delta_{total} = \delta_{elastic} (1 + Ct) + \delta_{shrinkage}$$

Sbarounis

$$\delta_{long\ term} = \delta_{service} \times \text{factor}$$

$$\delta_{service} = \frac{\text{service load}}{\text{construction load}} \times \delta_{construction}$$

$$\text{factor} = 1 + 2.8 \frac{Cu}{2.35} + 1.2 \frac{\varepsilon_{shu}}{800}$$

where Cu is the ultimate creep coefficient and ε_{shu} the ultimate shrinkage in millionths.

Fu and Gardner 1985

$$\delta_{long\ term} = \delta_{elastic} (1 + C.C.) + \delta_{sh}$$

where C.C.= [3.3 + 5.5 * (plf - 0.55)]

$$plf = \text{peak load factor} = \frac{Pmax}{Pult} \sqrt{\frac{f'c}{fc}}$$

Pmax = maximum load during construction
Pult = 28 day design ultimate load
f'c = 28 day concrete strength
fc = concrete when Pmax is applied

Gardner and Fu 1985

$$\delta_{total} = \delta_{sh} + \delta_{sus} \left[1 + Ct\left(1 + \frac{CL}{UL}\right)\right]$$

where δ_{sh} = Deflection due to shrinkage calculated by Branson et al
CL = maximum construction load in multiples of slab dead load
UL = 1.4*D + 1.7*L

δ_{sus} = deflection due to service load
Ct = ACI creep coefficient

Both the ACI 209 method and Sbarounis' method involve calculating the deflections at each application of load and are not too convenient for calculating span thickness ratios.

3. Simplified Method

Fu and Gardner 1985 reported the results of an experimental study of the effects of early age loads on the deflections of one-way slabs subjected to different load histories. Figures 2, 3 and 4 taken from Fu and Gardner show the applied load histories and the resulting measured deflections and clearly show the importance of construction load effects on long term serviceability. Using the results taken from this paper a simplified equation is developed to calculate the long term deflections and subsequently limiting slab span/thickness criteria were calculated.

Any long term deflection calculations should include deflection due to construction loads and creep effects, deflection due to sustained live load and associated creep and deflection due to shrinkage.

3.1 Shrinkage Deflection

Gardner and Fu 1987 reported that Branson's equation for calculating deflection due to shrinkage gave reasonable prediction of their experimental results.

3.2 Construction Deflection

From observation of Figure 3 it can be noted that the 28 day deflection of the shore + 3 reshores system is slightly larger than the 28 day deflection of the dead load only case and that the shore plus reshore method of construction results in the smallest long term total deflection of all the load histories considered. Consequently the alternating load case of the shore + reshore load case need not be calculated exactly. Probably the more common shoring system is to use one shore and three levels of reshores. The maximum construction load, excluding construction live loads effects, for the chosen system is 1.35 times slab dead load. The modulus of elasticity to be used should be the modulus appropriate to the slab age at which the load is applied and creep effects should be calculated from the age of loading.

$$\delta_{constuction} = \frac{K1*1.35*D*L^4}{Econ*h^3/12} \, (1 + 1.25*tc^{-.118}Cu)$$

where Econ = modulus of elasticity at casting
K1 = boundary coefficient constant
Cu = ultimate creep coefficient
D = slab dead load
L = diagonal span for slab panels
tc = age at casting

3.3 Sustained Load Deflection

The live load to be used in sustained load calculations should be less than than the design live load; it is suggested that 0.25 times the live load be used.

$$\delta_{sustained} = \frac{K1*D*L^4 (0.25*Live/Dead)}{Eservice*h^3/12} (1 + Cu(1 - \frac{ts^{0.561}}{a + ts^{0.561}}))$$

where Eservice = Modulus of elasticity at 28 days
a = size dependant constant taken from Bryant 1987.
ts = 28 days

3.4 Creep Coeficient

Recent work by Bryant and Vadhanavikkit 1987 recomends that the creep equations given by ACI 209 be modified as given below to better accomodate size effects.

$$Ct = \frac{t^{0.561}}{a + t^{0.561}} Cu$$

where $a = 161*Td^{1.18}$
and Td = equivalent thickness

In addition the recomended ultimate creep coeficient given is 4.6 compared with the value of 2.35 recomended by ACI 209.

3.5 Calculations

Deflections were calculated for several span/thickness ratios for slab casting cycles of 3, 7, 14 and 28 days for slabs designed for live load/ dead load ratios of 0.5, unity and 2. The moduli of elasticity used are given in Table 2 taken from experimental work at Ottawa using air-entrained Type 10 cement concrete cast and cured at 16 C with a 28 day strength of 25 MPa.. (It is assumed that the shear perimeter provided is adequate to prevent failure by punching shear.)

It was assumed that for interior flat slab panels the diagonal span was appropiate and Kw = 1.2/16 and Kl = 2/384. It was also assumed that the limiting total deflection should be span/240.

Table 3 shows results calculated for live load/dead load ratios of unity which are typical of all live load/dead load ratios. It can be seen that for a specified limiting deflection at a single construction rate several span /thickness ratios give acceptable deflections. However the parameter $L^{3/4}/h$ (with h and L expressed in metres) seems to be approximately constant for each construction time.

Using $L^{3/4}/h$ as the thickness parameter Table 4 gives the appropiate values for live/dead load ratios of 0.5, unity and 2 for construction ages of 3, 7, 14 and 28 days for creep factors of 2.35 (ACI) and 4.6 (Bryant) respectively for interior flat slab panels. For exterior slab panels the minimum thickness calculated from Table 4 should be increased by 10%.

3.6 Discussion

The calculations presented assumed that the gross concrete second moment of area was acceptably accurate.

The ultimate concrete shrinkage recommended by ACI 209 is considerably greater than that recommended by CEB; why?

The difference in the numerical values of creep coefficients given by ACI 209 and Bryant 1987 should be resolved.

4 CONCLUSIONS

The current code provisions for maximum span/thickness ratios are too simplistic and should include terms relating to construction rate and slab design live load /dead load ratio.

A new method of specifying span thickness ratios is presented but consensus is required over the appropiate creep coefficient that should be used.

For all slabs a minimum thickness of 150 mm should be required.

REFERENCES

ACI Committee 209 1971. "Prediction of creep,shrinkage and temperature effects in concrete structures",ACI Special Publication SP-27 Creep, Shrinkage and Temperature Effects.

Agarwal R.K., and Gardner N.J. 1974. "Form and shore requirements for multistorey buildings". ACI Journal Proceedings V.71,pp.559-569

Branson D.E. and Christiason M.L. 1971. "Time dependent concrete properties relating to design strength and elastic properties: creep and Shrinkage", ACI Special Publication SP-27,pp257-277

Bryant A.H. and Vadhanavikkit C. 1987. "Creep, Shrinkage size and age at loading effects" ACI Materials Journal, Vol.84,No2, pp117-124

Fu H.C. and Gardner N.J. 1986. "Effect of Construction loads on the long term behaviour of slab structures" ACI Special Publication SP95 Concrete at Early Ages, Special Publication SP-95,pp173-200.

Gardner N. J. and Fu H.C. 1987. "Effects of high construction loads on long term deflections of flat slabs" ACI Structural Journal V.84 No.4,pp 349-360.

Graham C. J. and Scanlon A. 1986. "Long term multipliers for estimating two-way slab deflections" ACI Journal V.83 pp899-908.

Sbarounis J.A. 1984. "Multistory flat plate building; effect of construction loads in long term deflections" ACI Concrete International pp.62-70.

Source	Year	Age of Initial Deflection	Age of Final Deflection	Deflection Ratio
Washa	1947	28 days	5 years	3.9
CSIRO	1961	10 days	8 months	12
Taylor & Heiman	1970	14 days	2.5 years	6-8
Taylor	1971	56 days	1 year	3.9
			3.5 years	6.3
			8 years	6.7
Heiman & Taylor	1972	17 days	610 days	2.2
			3.5 years	2.5
Jenkins	1972	10 days	1 year	2.6
Yamamoto	1982	1-28 days	112 days	4.4-6.4
Sbarounis	1984		1 year	4.2-6.4

Table 1. Summary of long-term deflection ratios

Age	3 days	7 days	14 days	28 days
Modulus of Elasticity (GPa)	14.6	16.8	21.1	25.0

Table 2. Variation of Modulus of Elasticity with age
Type 10 cement, water/cement =0.55, 16°C

L/h	span (m)	thickness (m)	live/dead	age (days)	defl L/δ	$L^{3/4}/h$
25	9.125	0.365	1.00	3	240.9	75.5
27	7.695	0.285	1.00	3	240.7	74.9
33	4.950	0.150	1.00	3	239.3	73.4
25	10.000	0.400	1.00	7	240.2	79.1
27	8.370	0.310	1.00	7	241.7	78.1
33	5.445	0.165	1.00	7	239.8	77.0
27	9.180	0.340	1.00	14	240.7	81.8
30	7.350	0.245	1.00	14	239.6	81.3
33	5.940	0.180	1.00	14	241.2	80.4
27	9.990	0.372	1.00	28	240.0	85.3
30	7.950	0.265	1.00	28	241.0	84.6

Table 3. Limiting Span/thickness ratios satisfying deflection limit of span/240. (C_u=2.35 and $\varepsilon_{shu}=800\times10^{-6}$)

Creep Coef.	Live / Dead	Casting Cycle (days)			
		3	7	14	28
		Shrinkage 800×10^{-6} (400×10^{-6})			
2.35	0.5	75 (83)	78 (87)	82 (91)	85 (94)
	1.0	73 (81)	76 (85)	80 (88)	84 (92)
	2.0	71 (78)	74 (82)	78 (86)	82 (90)
4.60	0.5	60 (65)	63 (69)	67 (72)	70 (75)
	1.0	58 (63)	62 (67)	65 (70)	68 (73)
	2.0	67 (61)	60 (65)	64 (68)	67 (72)

Table 4. Span-thickness coefficient to satisfy span/240 limit.

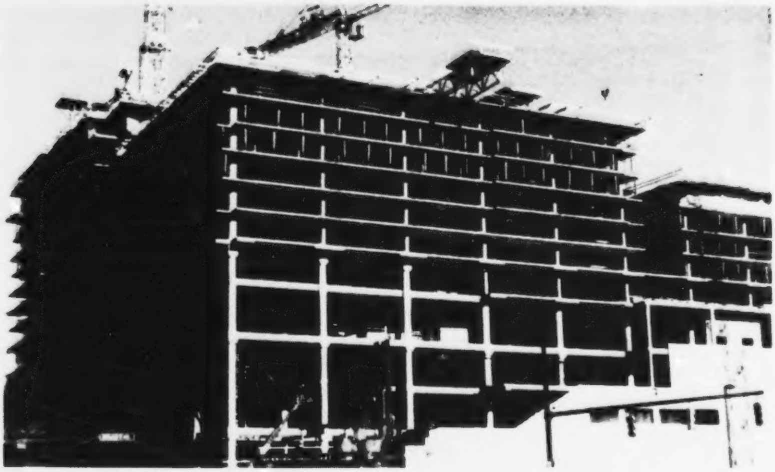

Figure 1. Typical form-reshore construction using one level of forms plus three levels of reshores

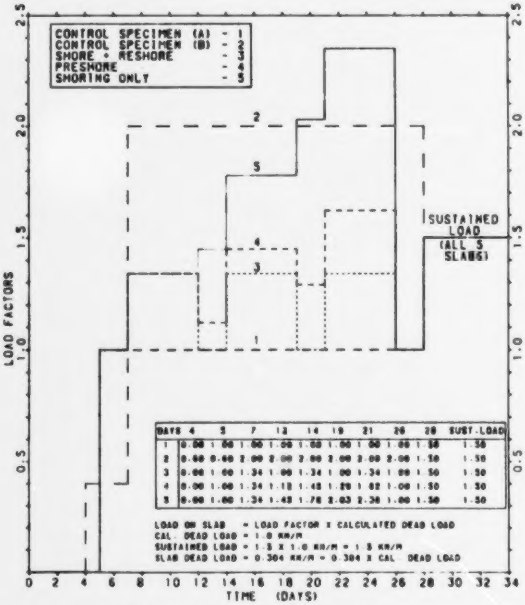

Figure 2. Load history on slab models

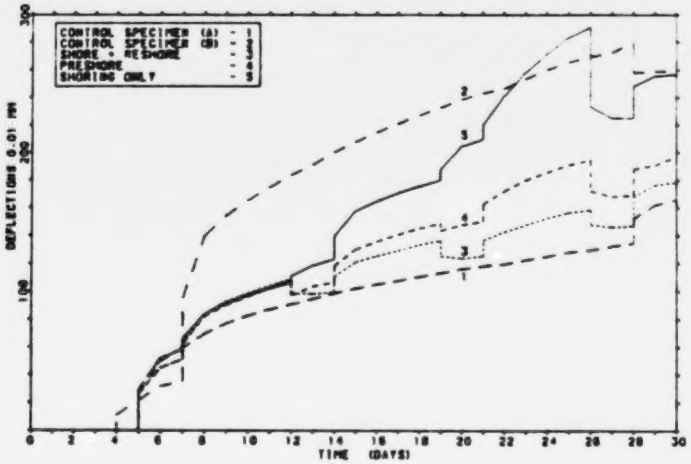

Figure 3. Measured deflections due to construction loads up to 28 days.

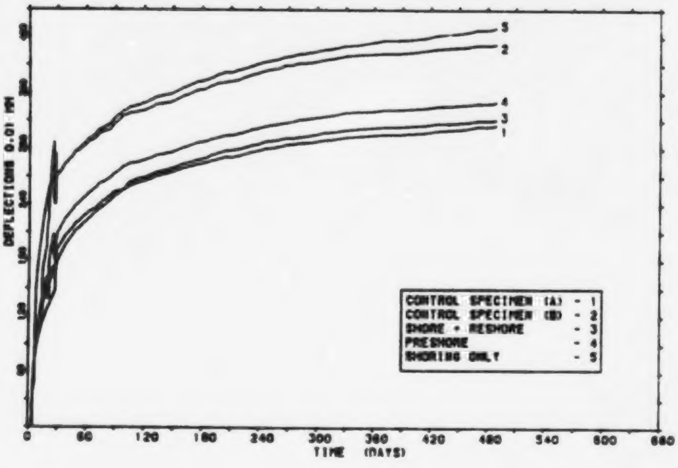

Figure 4. Long term measured deflections

SERVICEABILITY OF REINFORCED CONCRETE TWO-WAY FLOOR SLAB SYSTEMS

Suresh G. Pinjarkar

Raths, Raths & Johnson, Inc.
Chicago, Illinois, U.S.A.

ABSTRACT: Serviceability of two-way floor slab systems is influenced by design requirements, construction practices, and exposure conditions. Serviceability distress is primarily associated with deflections, cracking, and concrete durability. Factors affecting serviceability include concrete strength, loading history, intensity of loadings, concrete cover, distribution of steel reinforcement, and building maintenance. Examples are included showing various types of serviceability problems. Recommendations to improve serviceability and service life should include not only sound design and construction practices, but a cost-benefit analysis of various options for use by the owners.

1. INTRODUCTION

Serviceability of building structures has become an important issue in recent years. The current crisis with infrastructure deterioration and maintenance has led engineers to focus more attention to design for service life, in addition to strength. All building codes contain explicit requirements for strength and safety. However, requirements for serviceability are limited to guidelines and are generally non-enforceable. Often, serviceability guidelines are in conflict with strength requirements with the latter taking the precedent. In addition, the designers are reluctant to incorporate serviceability-related features into the design due to short-term economic considerations. Among all structural building components, two-way concrete slabs are more affected by serviceability-related issues.

By definition, serviceability means that the building component will fulfill its intended function under normal usage during its useful life. It means that the structure will perform its intended function as envisioned by the designer and the owner. Since there are no explicit serviceability requirements in the building codes, this usually becomes a responsibility of the owner. In addition, the serviceability-related issues often crop up long after the building is built and may have undergone changes in ownership. From the owner's or user's perspective, loss of serviceability may include the following:

- Esthetic and visually objectionable problems.
- Excessive deflections causing sagging, gaps and ponding.
- Damaged partitions, windows, and door frames.
- Cracked plaster and finishes.
- Cracking, spalling, and loose concrete.
- Rust staining, corroded and exposed reinforcement.
- Cracking and debonding of floor tiles.
- Water leakage and damage.
- Increased maintenance and user complaints.

Often, continued neglect of serviceability-related problems could eventually lead to structural distress, loss of strength, safety hazards requiring load posting, reduced usage, and extensive structural repairs.

2. CODE REQUIREMENTS

For two-way slab systems, the building codes (Ref. 1, 2, 3, 4, 5) contain requirements to assure serviceability in an indirect way. These requirements pertain to design, construction, and material properties to include the following:

- Minimum slab thickness or maximum span/depth ratio.
- Maximum permissible deflections.
- Maximum suggested crack width.
- Minimum spacing and amount of reinforcement.
- Requirements for distribution of reinforcement.
- Minimum concrete cover.
- Maximum suggested crack width.
- Tolerances on reinforcement placement, concrete cover, effective depth, slab thickness, and level grade.
- Requirements for strength, water-cement ratio, air content, and chloride content based on exposure conditions.

It is assumed that if the minimum code requirements are satisfied, serviceability will be assured.

3. FACTORS AFFECTING SERVICEABILITY

Serviceability-related distress in two-way floor slabs is primarily associated with deflections, cracking, and concrete durability. Unfortunately, there are a number of factors which have a detrimental effect on the in-service behavior of floor systems. In addition, various factors are interrelated and often contradict each other. For example, maximum concrete cover is required to prevent corrosion damage due to severe environmental exposure conditions to increase the service life. However, minimum concrete cover is necessary to reduce and limit the crack widths. A designer must evaluate the various factors which affect the serviceability and perform a cost-benefit analysis, including maintenance aspects, for consideration by the owner. A brief discussion of factors affecting serviceability of two-way slab systems is given below.

3.1 **Deflections**: The building codes generally require that members subjected to flexure shall be designed to have adequate stiffness to limit the deflections or deformations that may adversely affect strength and serviceability of a structure. However, there is a high degree of uncertainty involved in computing the slab deflections and the selection of acceptable limiting values to assure adequate strength and serviceability. Because of this, most building codes (Ref. 1, 2, 3, 5) follow an indirect rule-of-thumb approach, based largely upon past experience, to control the slab deflections. In varying forms, this approach consists of specifying either minimum slab thickness or effective depth, or maximum span/effective depth or span/thickness ratios. In addition, the codes also provide approximate methods to compute deflections based again on experience and compare them with the specified allowable deflections (also based on experience) to satisfy the serviceability requirements. This procedure often creates contradictory (unintended) situations where the measured deflections exceed the allowable limits, although the slab thickness or span/thickness ratios meet the code requirements.

Field measurements (Ref. 6) have shown that long-time measured deflections can be 4 to 12 times the calculated initial deflection. The long-time deflections of slabs are influenced by several factors which are difficult to allow for in the calculations. These factors include loading history, form removal, re-shoring, and other construction practices, estimates of end restraints, magnitude and location of cracking, concrete strength and quality, effect of partitions, etc. In addition, within the same structure, measured deflections can vary substantially making deflection computations less reliable. The factors listed here must be logically accounted for in any serviceability-based design. For example, suitable movement joints should be provided between floors and partitions, if these partitions are likely to be damaged by expected slab deflections. Without such provisions, the partitions may be subjected to heavy loads and suffer severe cracking. The same is true for window frames and sliding doors attached to the floor slabs.

Measurements reported by Sbarounis (Ref. 7) indicated one-year deflections of a flat plate slab ranging from 0.53 to 2.16 inches (13.5 to 54.3 mm). The deflections averaged 1.35 inch (34.3 mm) with a standard deviation of 0.29 inch (7.37 mm). Measurements made by the author, of a 12-year old flat plate structure, indicated slab deflections varying from 0.8 to 1.62 inches (20.3 to 41.1 mm). Similarly, measurements of a 20-year old flat slab structure by the author indicated deflections varying from 1.3 to 2.5 inches (33.0 to 63.5 mm). Variability of these measurements depict the futility of using maximum allowable deflections as a criteria to evaluate the serviceability of the existing floor slabs. Load tests of existing slabs indicate instantaneous deflections to be consistent with computed deflections with almost full recovery. In many cases, the slabs were cracked and severely deteriorated with rampant corrosion of reinforcement. These observations indicate that slabs with apparent serviceability problems still possess sufficient strength and stiffness to support the design loads.

The minimum slab thickness requirements of the ACI Building Code (Ref. 1) are based upon experience, are empirical in nature, and are probably satisfactory for typical floor loads of 50 psf (2.4 kPa). However, often two-way slab systems are used to support heavy planter loads (100 to 400 psf or 4.8 to 19.2 kPa) and occasional fire truck loading. Such slabs, designed using minimum thickness requirements, have experienced excessive deflections and severe cracking. The minimum thickness requirements of the ACI Building Code may need some modifications to provide better control of cracking and deflections under heavier loads.

3.2 Cracking: Cracks observed in two-way slab systems can be of either a structural or non-structural nature. Cracks of structural significance are indicative of the flexural behavior of the slab system. Structural cracks at the top of the slab are usually around the columns, with radial cracks emanating from a single circumferential crack. Structural cracks, at the underside of the slab, are located at the center of the span and the panels. Although crack patterns remain similar, crack widths depend upon concrete cover, amount of distribution of reinforcement, magnitude of superimposed dead loads, and concrete strength. Other factors that would influence crack widths would be construction loading, concrete strength at the time of initial shore removal, re-shoring, and concrete curing.

Non-structural cracking includes early plastic shrinkage cracks and cracks due to long-term drying shrinkage. Plastic shrinkage cracks generally pass around the aggregate and are in the form of surface crazing or map cracking. Drying shrinkage cracks often appear much later and are caused by restrained volume changes. These cracks often go through the entire slab thickness and their magnitude depends upon the location of construction joints and restraint provided by columns, beams, and walls.

Cracking may affect serviceability depending upon the magnitude of the cracking, type of floor covering, and exposure conditions. For interior exposure, cracking may result in reflective cracking and debonding of tiles and floor coverings and in the areas of kitchens and bathrooms, may lead to corrosion of reinforcement and associated damage. For outdoor exposure, cracking could result in severe serviceability problems. For slabs subjected to deicing salts and alternate freeze/thaw cycles, cracking would accelerate the corrosion damage. Also, similar problems can occur in coastal areas and in buildings exposed to saltwater spray and alternate wetting and drying conditions.

The building codes (Ref. 1 and 2) provide flexural crack control in an indirect way by specifying requirements pertaining to concrete cover, slab thickness, and distribution and reinforcement details. Generally, building codes refrain from specifying absolute limits on crack widths. Some building codes, (Ref. 2) however, provide means of calculating crack widths to evaluate appearance and durability. The British Code of Practice (Ref. 2) recommends maximum surface crack width of 0.012 inch (0.3 mm) for reinforced concrete and 0.004 times the concrete cover to the reinforcement for structures exposed to severe corrosive atmospheres. The ACI Committee 224 (Ref. 8) recommends tolerable crack widths varying from 0.006 inch to 0.016 inch (0.15 mm to 0.41 mm) depending upon the exposure conditions.

3.3 Concrete Cover: Concrete cover over the top reinforcement has both beneficial as well as detrimental effects on long-term serviceability of concrete slab systems. Crack widths are directly proportional to steel stress and concrete cover to the reinforcement. It is a "Catch-22" situation where increased cover provides more protection from severe environmental damage but adds to the cost and weight of the structure. It also contributes to increased cracking and crack widths. Reduced concrete cover, on the contrary, reduces crack widths but provides less protection from severe environmental exposure conditions. There are cases where unintentional high cover has caused severe structural deficiencies in the form of reduced strength and serviceability, due to higher deflections and wider cracks. On the other hand, low cover can cause damage due to corrosion and traffic.

For concrete exposed to weather and external sources of chlorides in service, most building codes (Ref. 1 and 2) recommend a minimum concrete cover of 2 inches (50 mm) for cast-in-place concrete construction. Tolerances for placing reinforcing and finishing would affect the actual cover and would require approximately an additional 1/2 inch (12 mm) of cover. Builders and designers are generally reluctant to adhere to such cover requirements due to the increase in costs resulting in a reduction in serviceability. Such cover requirements, however, would introduce more cracking and increase the crack widths. In such cases, it may be cost effective to use epoxy-coated reinforcement and maintain normal concrete cover.

Cantilever balcony slabs with exterior exposure are occasionally subjected to corrosion-related damage causing severe serviceability problems. As specified by the ACI Building Code (Ref. 1), the minimum concrete cover required for interior exposure is 3/4 inch (19 mm) whereas the cover required for exterior exposure is 1-1/2 inches (38 mm) to 2 inches (50 mm). The designers generally provide 3/4 inch (19 mm) cover for cantilever bars located over the exterior columns. Because of low cover and presence of chlorides in concrete, the concrete undergoes cracking, spalling, and general deterioration. Similarly, the bottom bars are also subjected to corrosion damage due to low cover. Here again, it may be cost effective to use epoxy-coated reinforcement in the balcony areas.

3.4 Concrete Quality: Lower strength concrete is more prone to cracking due to lower tensile strength. Concrete with a high water/cement ratio has generally lower strength, higher shrinkage, more permeability, and less resistance to abrasion. A high quality of concrete is required for two-way slabs exposed to weather, deicing salts, brackish water, seawater or spray from these sources. The building codes generally contain requirements for minimum air entrainment, water/cement ratio, and limits on chloride content for concrete subjected to a corrosive environment. In such an environment durability of concrete can be augmented by using specialty concrete with low permeability, use of surface sealers or coatings, increased cover over reinforcement, and providing adequate drainage.

3.5 Tolerances: Two-way slabs are extremely susceptible to variations due to accepted tolerances on individual portions such as concrete slab thickness, variation from the level or grades indicated on the drawing, placement of reinforcement, and minimum concrete cover. Thin slabs are more sensitive to the cumulative effects of these tolerances which may be individually incompatible. It is recommended that the designer should anticipate this difficulty and specify cumulative performance oriented tolerances to avoid future serviceability-related problems.

The ACI Building Code (Ref. 1) recommends only minus tolerance (to maximize effective depth) on minimum concrete cover. For a typical floor slab, and assuming 3/4 inch (19 mm) design cover, the as-built cover on the bar may be only 1/4 inch (6.4 mm). Considering the durability of concrete, it is recommended that the tolerance limit for concrete cover should include only plus value (+ 1/2 inch or + 12 mm). Both the British and Canadian Codes (Ref. 2 and 4) require plus and minus tolerance limits on concrete cover. Using the ACI (Ref. 9) recommended tolerances on slab thickness and level grade, a difference in slab elevation at column and at the center of the panel, can be approximately 3/4 inch (19 mm). A designer must take into account these factors when specifying concrete cover, minimum effective depth, and minimum slab thickness.

3.6 **Exposure and Usage Conditions**: Concrete exposed to freezing and thawing or deicing chemicals will generally exhibit serviceability-related distress in the form of cracking, spalling, and corrosion of embedded metal. In the past, many parking garages in North America have been built at lower levels of the enclosed buildings. Moisture and salt brought in and deposited by vehicles have caused serious corrosion damage in these structures. Two-way slabs used for vehicular traffic and subjected to a corrosive environment require special features, compared to two-way slabs generally used for residential/office purposes. The ACI State-of-the-Art Report on Parking Structures (Ref. 10) contains specific recommendations on this subject.

Many two-way slab systems are used as plazas and promenades with large planter areas with trees and shrubs. Generally, designers tend to add more steel reinforcement in planter areas to support higher loading. However, this does not prevent higher deflections and severe flexural cracking. Wet soil and clogged drains can substantially increase the loads and may eventually lead to failures. Occasionally, two-way slab system plaza areas surround high-rise buildings requiring access to fire-fighting trucks and equipment. These trucks can weigh as much as 30 tons (267 kN) or even higher than HS-20 highway loading. Such slab systems need to be designed to support the heavy, concentrated wheel loads. Serviceability of plazas and promenades is dependent upon the effectiveness of the waterproofing and, on occasion, has resulted to water leakage through the slab cracks, severe efflorescence, corrosion, and concrete spalling from the underside of the slabs.

3.7 **Construction Practices and Details**: Construction has a direct influence on deflections, cracking, and general serviceability of the two-way slab systems. Removal and re-shoring operations, strength of concrete at the time of shore removal, and construction loading have great influence on initial and long-time slab deflections and cracking. Lower levels of the high-rise buildings are many times used to store building materials such as concrete blocks, bricks, etc. which can add substantial load to the slab and increase initial deflections due to creep under sustained load. Deficiencies in curing can cause plastic shrinkage cracks and increase drying shrinkage of hardened concrete. Drying shrinkage, creep, and temperature drop combine to produce concrete shortening and may cause cracking depending upon the restraints, geometric discontinuities, and location of construction joints.

Occasionally, design details involving bent reinforcing bars or recess in concrete, results in placement of top mat reinforcement much lower than specified. In thin, flat plates, this can substantially reduce the effective depth causing extensive cracking and increase in deflections.

Expansion joints, control joints, and construction joints are often a source of service-related problems such as cracking, spalling, water leakage, etc. The location, design, and installation of these joints are very critical for two-way slabs exposed to weather and a corrosive environment. Many two-way slabs are provided with sliding types of expansion joints, which tend to freeze causing cracking and spalling especially if suitable bearing pads are not provided.

4. EXAMPLES OF SERVICEABILITY-RELATED DAMAGE

The following examples are presented to illustrate serviceability-related distress associated with two-way slab systems. The structures discussed include some built recently and some built 20 years ago. The building code provisions have changed substantially in the last 10 years, especially the requirements pertaining to structures exposed to weather and a corrosive environment. The examples depict service-related distress caused by excess or lack of cover, misplacement of reinforcement, lack of details to accommodate slab movements, etc. Some service-related deficiencies are indicative of structural behavior of the two-way slab systems and are inherent with this type of construction.

Example 1: Fig. 1 shows gaps between the floor and the partition wall, and jamming of the door caused by slab deflection.

Example 2: Cracking of the balcony partition block wall is shown in Fig. 2. Cracking was primarily caused by deflection of the cantilever slab and the lack of a control joint between the blockwall and the slab above, to accommodate vertical displacement.

Example 3: Fig. 3 shows floor weight being transferred to the metal partitions causing buckling of metal studs. Premature installation of metal studs was the primary cause of the distress.

Example 4: Fig. 4 shows concrete spalling, due to the corrosion of reinforcement at the underside of the balcony floor slab. Severe cracking and corrosion of reinforcement was also observed at the top of the slab. Measured concrete cover was less than 3/4 inch. These balconies were located in a hot and humid ocean-side environment exposed to saltwater spray.

Example 5: Fig. 5 shows a 10-year old waffle slab supporting the injection molding machines. Fig. 6 shows cracking at the top surface around the column supporting the slab. The design slab thickness was 13 inches (330 mm), which was increased to 15-1/2 inches (394 mm) at some locations to allow a 2-1/2 inch (64 mm) deep recess for terrazo floor in the corridor. This resulted in increased concrete cover varying from 3 to 6-1/2 inches (75 to 165 mm) over the top steel at some column locations. Measured crack widths varied from 0.04 inch to 0.08 inch (1 mm to 2.0 mm) and the depths of the cracks varied from 3 inches to 6.5 inches (75 mm to 160 mm).

The measured natural frequency of the slab system was 12.90 cps in an area of a 15-1/2 inch (394 mm) thick slab and 11.4 cps in a 13-inch (330 mm) thick slab area. Calculated damping varied from 6 to 7 percent of critical damping. The slab system was found to have sufficient strength to support the static and dynamic loading. Observed cracking was due to excess concrete cover over the top reinforcement. Remedial recommendations included newer types of machines with less vibrations and the sealing of slab cracks using a flexible joint sealant.

Example 6: Fig. 7 shows cracking at the top surface around the column of a cantilever balcony floor slab. Concrete cover over the cantilever steel was found to vary from 2 inches to 3.5 inches (50 mm to 90 mm) and the maximum measured crack width corresponding to the maximum concrete cover varied from approximately 0.02 inch to 0.04 inch (0.5 mm to 1.00 mm). Maximum measured deflections at the end of an 8-foot (2.4-meter) long cantilever slab was approximately 2 inches (50 mm). Reflective cracking observed in the floor tiles is shown in Fig. 8.

Example 7: Fig. 9 and Fig. 10 show deterioration of concrete in an enclosed 20-year old flat slab structure. Deterioration was in the form of cracking, spalling, exposed and loose corroded reinforcement, and severe efflorescence. Portions of the garage exhibited serious serviceability problems due to large areas of loose concrete and exposed reinforcement, causing traffic and safety hazards. The primary cause of the deterioration is the lack of sufficient concrete cover, and the corrosion of reinforcement due to the exposure to chlorides. Although the garage is enclosed, salt and moisture are brought in by motor vehicles and deposited on the slab.

5. RECOMMENDATIONS

The serviceability of two-way slab systems can be improved, provided adequate design provisions are made to avoid the problems discussed here. The serviceability criteria should be discussed with the owner, during the design phase, and should include a cost-benefit analysis of various options, including maintenance methods and schedules. The owner should be made aware of various factors affecting the serviceability to avoid future problems and possible litigation. The following are general recommendations to improve the serviceability of two-way slab systems:

5.1. Incorporate design features to minimize deflections, cracking, and crack widths. The design documents must include specific details showing slab thicknesses, geometry, location and distribution of reinforcement, and concrete cover, taking into account various tolerance limits.

5.2. Increase slab thickness or provide additional support where two-way slabs are used to support heavy planter or fire truck loads. Also, provide adequate and reliable drainage, and increase safety factors to account for possible extra loads due to clogged drains.

5.3. Compute slab deflections using assumptions which will take into account in-place material strengths, construction practices, and tolerances to give reasonable results. Considering variability of deflections, use L/150 as an approximate guide for computing maximum long-term deflection to design non-structural attachments.

5.4. Provide structural details to permit controlled relative movement between adjacent structural and non-structural parts without impairing the functional integrity of the structure. Provide suitable movement joints between floors and partitions to accommodate deflections. Provide suitable expansion joints to accommodate both expansion and contraction of the structure. The joints should not only allow free movements, but should be durable, weatherproof, and remain functional at all times.

5.5. Provide properly designed and sealed control joints and construction joints to minimize volume change deformations.

5.6. Provide concrete cover and concrete quality consistent with exposure conditions. Check position of top reinforcement before and during concreting with particular attention to cantilever sections.

5.7. In a corrosive environment, use epoxy-coated reinforcement and provide protective concrete surface coatings to prevent moisture penetration.

5.8. Provide adequate curing to minimize shrinkage cracking.

5.9 Provide maintenance schedule and methods, when appropriate. For exposed concrete surfaces in a corrosive environment, this may include periodic re-application of surface coatings or, in the case of slabs supporting planters, it may include periodic inspection of drains.

6. SUMMARY AND CONCLUSIONS

Serviceability of two-way slab systems is affected by concrete cover, location and placement of reinforcement, concrete quality and exposure conditions. Various factors affecting serviceability are discussed in terms of code requirements, construction practices, and field observations. Recommendations are presented to improve serviceability and service life to include special design provisions, and construction practices. Also, recommendations are presented to include cost-benefit analyses discussing various design options, maintenance methods, and schedules for the benefit of the building owners.

REFERENCES

1. American Concrete Institute, "Building Code Requirements for Reinforced Concrete", ACI 318-83, American Concrete Institute, Detroit, Michigan, 1983.

2. British Standards Institution, "Code of Practice for the Structural Use of Concrete, Part 1: Design, Materials and Workmanship", CP110, British Standards Institution, London, 1972.

3. Canadian Standards Association CSA Standard, CAN3-A23.3, Code for the Design of Concrete Structures for Buildings.

4. Canadian Standards Association CSA Standard, CAN3-A23.1, Concrete Materials and Methods of Concrete Construction.

5. Clark, C. V., Neville A. M., Houghton-Evans, W., "Deflections - Problems and Treatment in Various Countries", ACI Publication SP-43, Deflection of Concrete Structures, 1974.

6. ACI Committee 435 Report, "Observed Deflections of Reinforced Concrete Slab Systems, and Causes of Large Deflections", ACI Publication SP-86, Deflection of Concrete Structures, American Concrete Institute, Detroit, Michigan, 1985.

7. Sbarnounis, J. A., "Multistory Flat Plates - Measured and Computed One-Year Deflections", ACI Concrete International, August 1984, pp. 31 - 35.

8. ACI Committee 224 Report, "Control of Cracking in Concrete Structures", ACI Concrete International, October 1980, pp. 36 - 76.

9. ACI Committee 117 Report, "Standard Tolerances for Concrete Construction and Materials", American Concrete Institute, Detroit, Michigan, 1981.

10. ACI Committee 362 Report, "State-of-the-Art Report on parking Structures", American Concrete Institute, ACI Journal, July - August, 1985, pp. 544 - 578.

SGP/car

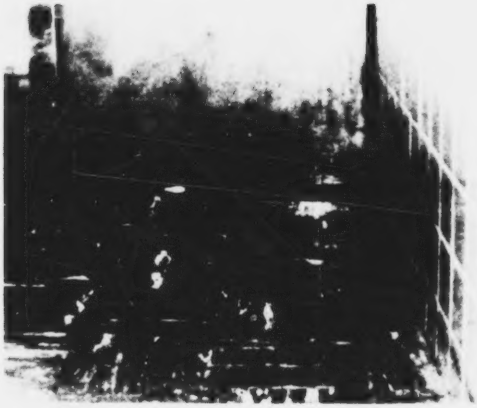

Fig. 1 Problems associated with excessive deflection of floor slab relative to partition wall and door.

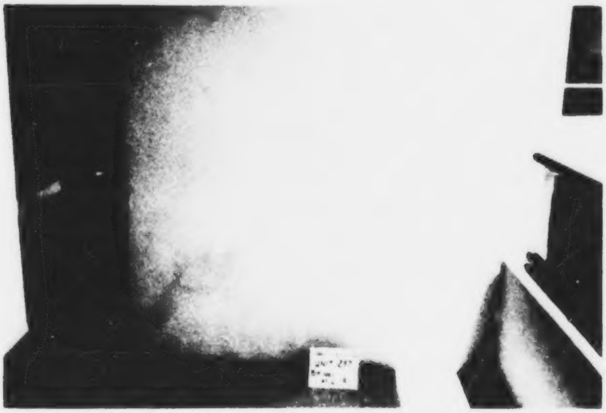

Fig. 2 Cracking of cantilever balcony partition wall.

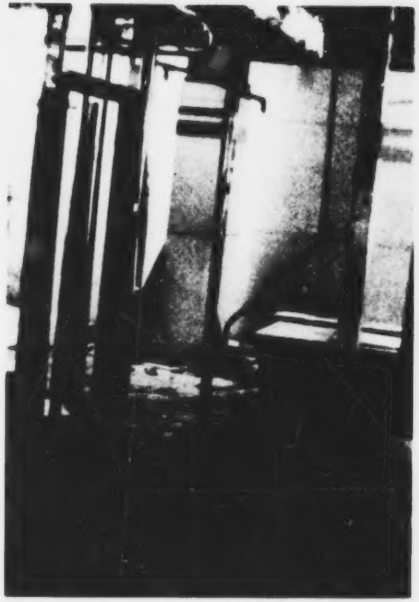

Fig. 3 Buckling of metal stud wall caused by slab deflection.

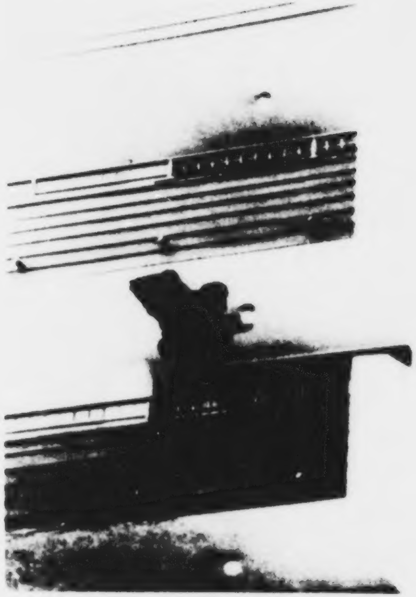

Fig. 4 Concrete spalling underneath the balcony floor slab due to corrosion of reinforcement.

Fig 5. Waffle slab floor supporting injection molding machines.

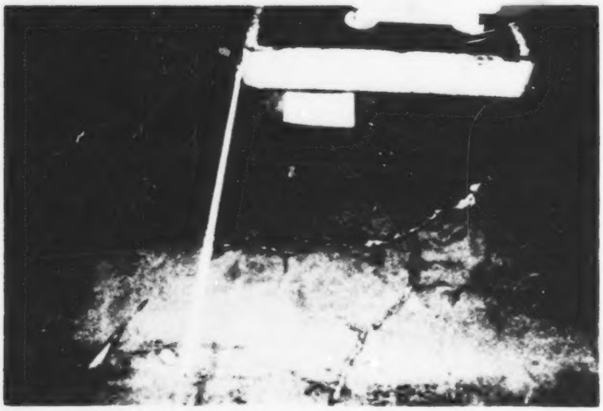

Fig. 6 Cracking around concrete column supporting the waffle slab shown in Fig. 5. Note location of circumferential crack at an approximate location of concrete column capital below.

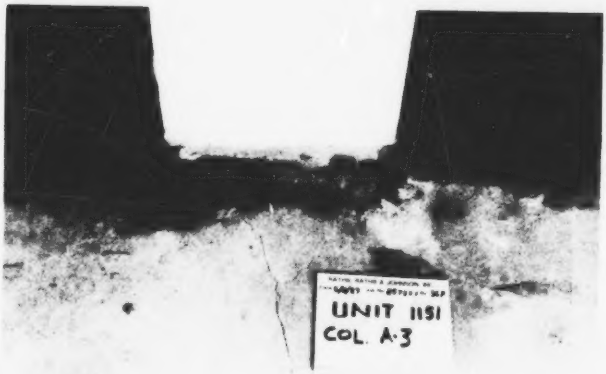

Fig. 7 Cracking around column of a cantilever balcony floor of a flat plate slab system.

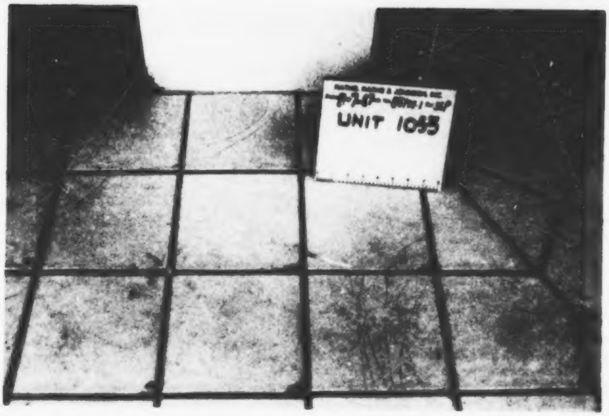

Fig. 8 Cracking of floor tiles as a result of cracking of the concrete slab, similar to that shown in Fig. 7.

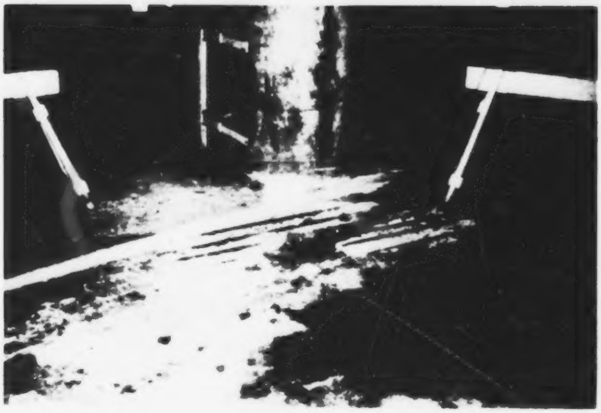

Fig. 9 Concrete surface deterioration of an enclosed, two-way flat slab garage caused by insufficient cover and salt brought in by vehicles.

Fig. 10 Concrete spalling and deterioration at the underside of the garage shown in Fig. 9. Note loose pieces of concrete have fallen from the underside of the slab.

CALCULATIONS OF SHORT-TERM AND LONG-TERM DEFLECTIONS OF REINFORCED CONCRETE BEAMS

K. Mahmood and S.I. Al-Noury
Civil Engineering Department
King Abdul Aziz University
Jeddah, Saudi Arabia

ABSTRACT: The paper presents a method for calculating short-term and long-term deflections of simply supported reinforced concrete beams subjected to symmetrical loads in service range. The calculation procedure for short-term deflection assumes that inelastic curvatures and rotations due to cracking are concentrated at the cracks and their effect on deflection is taken into account by considering a linkage mechanism. Long-term deflection is assumed to be the sum of two components, shrinkage deflection and initial plus creep deflection. It is proposed that shrinkage deflection be calculated by the available methods, while the initial plus creep deflection be calculated by a procedure similar to that developed for the short-term deflection, using a reduced modulus and increased modular ratio approach giving due consideration to compatibility and equilibrium conditions. The expressions developed for simply supported beams have been applied to the available experimental and theoretical data to indicate the suitability of the proposed method.

1. INTRODUCTION

In reinforced concrete design serviceability limit state of deflection requires a check of short-term and long-term deflections of beams under working loads. Short-term or instantaneous deflections are influenced by the magnitude and distribution of loads, span and conditions of constraints, section properties, material properties and degree of cracking in a beam(1). Long-term deflections occur due to the effects of shrinkage and creep and are therefore time-dependant deformations. Long-term deflection of a member is affected by the stresses in the concrete, amount of tension and compression reinforcement, size of the member, environmental conditions, age of concrete at time of loading and duration of loading(1). Experimental studies(2,3) show that, depending on these factors, long-term deflections may be 2 to 3 times the corresponding instantaneous values.

Present codes of practice recommend simplified methods for predicting deflections of reinforced concrete beams in order to check the serviceability criteria. ACI Code 318-83(4), for example, recommends the use of an effective moment of inertia for computing short-term deflections. The long-term deflections under sustained loading are then obtained(4) by multiplying the corresponding short-term deflections by a coefficient which depends only upon the ratio of compressive to tensile reinforcement. Using a moment-curvature approach based on the provisions of the CEB-FIP Model Code(5), the CEB Manual on Cracking and Deformation(6) presents rigorous and simplified methods for calculating deflections and recommends the simplified methods for the design office use. The simplified code methods generally predict deflections within an accuracy of ± 20% when compared with experimental results.

The objective of this paper is to develop a procedure for calculating short-term and long-term deflections of reinforced concrete beams under serivce loads by taking into account most of the abovementioned factors affecting deflections. In the case of simply supported beams under symmetrical loads the proposed method yields expressions which can be conveniently used to calculate the two types of deflections while checking the serviceability criteria in the design of reinforced concrete beams.

2. SHORT-TERM DEFLECTIONS

For a cracked beam loaded in the service range, the short-term deflection a_o, at time $t = 0$, can be considered to be the sum of two components a_{eo} and a_i, i.e.,

$$a_o = a_{eo} + a_i \qquad (1)$$

where a_{eo} is the elastic component of the deflection and can be calculated by assuming the beam to be uncracked along the span with flexural rigidity equal to $E_{co}\, I_{uo}$ (E_{co} is the modulus of elasticity of the concrete under short-term loading and I_{uo} is the moment of inertia of uncracked transformed section). The deflection component a_i is due to inelastic curvatures occurring at the cracks and can be calculated from a knowledge of moment-curvature relationship, cracking pattern and curvature distribution.

Fig. 1 shows moment-(average) curvature relationship(M-k_m relationship), under short-term loading for a small element, composed of two parts, cracked and uncracked, and subjected to a bending moment M. Referring to Fig. 1, k_{eo} is the curvature in uncracked state and is equal to $M/E_{co}I_{uo}$ and k_{co} is the curvature in cracked state and is equal to $M/E_{co}I_{co}$ (I_{co} is the moment of inertia of cracked transformed section). The distribution ratio between the cracked and uncracked states is denoted by c (Fig. 1) and is expressed as follows in the CEB -FIP Model Code(5) and the CEB Manual(6):

$$\begin{aligned} c &= 1 - \beta_1\beta_2(M_c/M)^2 \qquad (2) \\ &= 0 \text{ for } M < M_c \end{aligned}$$

where M_c is the cracking moment and β_1 and β_2 are constants defind in the Model Code(5). Putting in the code values of these coefficients for a reinforced concrete beam having deformed bars and subjected to short-term loading, the distribution ratio c_j for jth element in the beam, subjected to a bending moment M_j, becomes:

$$c_j = 1 - (M_c/M_j)^2 \tag{3}$$

In developing expression for deflection, in the present study, the above equation for c_j has been modified as follows:

$$c_j = 1 - \frac{M_c^2}{M_j.M_o} \tag{4}$$

where M_o is the bending moment at the critical (midspan) section of a simply supported beam.

Fig. 2 shows typical crack pattern and curvature distribution for a simply supported beam under symmetrical loading. A symmetrical crack pattern with a crack spacing s and a crack at midspan is assumed in the cracking length L_c(= r.L, where r is a constant which depends on the loading pattern and L is the span length). Considering $(k_{co}-k_{eo})c_j$ as the inelastic component of the average curvature (Fig. 1) for jth element of length s, the inelastic rotation at the jth crack is:

$$\theta_j = (k_{co}-k_{eo})c_j.s \tag{5}$$

$$\text{or} \quad \theta_j = \left(\frac{1}{E_{co}I_{co}} - \frac{1}{E_{co}I_{no}}\right)M_j.c_j.s \tag{5a}$$

The expression for a_i, the deflection component due to inelastic curvatures at cracks, can now be written in the following form by considering a linkage mechanism (Fig. 3) and assuming that the inelastic rotations thus produced are concentrated at the cracks:

$$a_i = \frac{L\theta_o}{4} + \left(\frac{L}{2} - s\right)\theta_1 + \left(\frac{L}{2} - 2s\right)\theta_2 \tag{6}$$

where θ_o, θ_1 and θ_2 are inelastic rotations at the midspan crack and cracks 1 and 2 respectively. Extending it to n cracks in one half of a beam subjected to symmetrical loading, the general equation for a_i is,

$$a_i = \frac{L\theta_o}{4} + \sum_{j=1}^{n} \left(\frac{L}{2} - j.s\right)\theta_j \tag{7}$$

Substituting Eq.(5) into Eq.(7) in terms of bending moments M_j and distribution ratios c_j at various cracks for a particular loding condition and introducing the simplifications $2ns \simeq (2n+1)s$ $L_c = rL$ and $ns \simeq (n+1)s \simeq L c/2 = rL/2$, the expression for a_i becomes,

$$a_i = (a_{co} - a_{eo})z \tag{8}$$

where a_{co} is the deflection estimate based on the flexural rigidity $E_{co}I_{co}$ of cracked transformed section and z is a coefficient which depends on the loading pattern and shape of the moment-curvature relationship. Substituting the value of a_i in Eq.(1), the general expression for short-term deflection, a_o, becomes,

$$a_o = (1-z)a_{eo} + z.a_{co} \tag{9}$$

The coefficient z in Eq.(9) can be defined, on the analogy of the definition of coefficient c, as the distribution ratio between the cracked and uncracked states in a beam under a particular loading condition. Table 1 shows formulae for r and z for simply supported beams subjected to various type of symmetrical loadings, based on the moment-curvature relationship shown in Fig. 1.

For calculating deflection estimates a_{eo} and a_{co} the moments of inertia of uncracked and cracked transformed sections (I_{uo} and I_{co}) is calculated by considering that the modular ratio under short-term loading n_o, is equal to E_s/E_{co}, where E_s is the modulus of elasticity of steel.

3. LONG-TERM DEFLECTIONS

As mentioned earlier, long-term deflections occur primarily due to the effect of creep and shrinkage properties of the concrete. Therefore, at time t, the total deflection a_t, in a reinforced concrete beam under sustained loading can be considered to be the sum of two components a_{cp} and a_{sh}, i.e.,

$$a_t = a_{cp} + a_{sh} \tag{10}$$

where a_{cp} is the initial plus creep deflection and a_{sh} is the shrinkage deflection at time t after initial loading.

In developing the calculation procedure for long-term deflections in this paper, it is suggested that the shrinkage deflection, a_{sh}, be determined by the following equation given by Branson(1,7):

$$a_{sh} = K_{sh}.k_{sh}.L^2 \tag{11}$$

where K_{sh} is a coefficient which depends on the support conditions and k_{sh} is shrinkage curvature and can be calculated from a knowledge of the shrinkage properties of the concrete by using the available formulae(1, 7).

The deflection component a_{cp} is calculated by considering an expression similar to Eq.(9) for short-term deflection a_o. Therefore, rewritting Eq.(9) in terms of a_{cp}:

$$a_{cp} = (1-z)a_{et}+z.a_{ct} \tag{12}$$

where a_{et} and a_{ct} are deflection estimates based on the flexural rigidities of uncracked and cracked transformed sections, respectively, at time t. These flexural rigidities can be obtained by reduced modulus and increased modular ratio approach. Branson(7) has discussed the limitations of simple quasi-elastic methods based on the increased modular ratio approach for calculating time-dependent deflections. Therefore due consideration has been given to the compatibility and equilibrium conditions while using this approach in the present study.

Due to additional cracking under sustained loading, the value of z may change with time. However, this change will not be significant, and therefore, the value of z obtained for short-term deflections may be used for calculating a_{cp}.

Modular ratio is defined as the ratio of modulus of elasticity of steel to that of concrete and is obtained by equating steel and concrete strains at a section assuming perfect bond(8). The concept of modular ratio and transformed area is used for uncracked as well as cracked sections, in the short-term service load analysis, because only hairline cracks appear in a member and the assumption of perfect bond between steel and concrete is valid at the cracked section. Under sustained loading, deformations increase with time affecting also the bond between steel and concrete and therefore the concept of modular ratio does not remain valid for tension steel at a cracked section. However, this concept is still applicable at an uncracked section and for compression steel at a cracked section and can therefore be made basis for calculating creep deformations.

Fig. 4 shows strain distributions at an uncracked section immediately after loading and at time t under the influence of creep. For the extreme fibre in compression the strain ε_{ut} at time t is $(1+C)\varepsilon_{uo}$, where ε_{uo} is the instantaneous strain and C is the creep multiplier. Assuming that stresses and strains are within elastic range and that the modulus of elasticity of concrete I_{ct} (reduced modulus) at time t is equal to $E_{co}/(1+C_t)$, where C_t is the creep coefficient, the following equation results:

$$1 + C = (1+C_t)\,\frac{y_{ut} I_{uo}}{y_{uo} I_{ut}} \tag{13}$$

Here y_{uo} and y_{ut} are the distances of the neutral axis for the two strain distributions shown in Fig. 4 and I_{uo} and I_{uf} are the moments of inertia of the uncracked transformed section immediately after loading and at time t respectively. The values of y_{ut} and I_{ut} are obtained by considering that the modular ratio n_t, at time t is equal to $(1+C_t)n_o$.

Now consider stresses and strains at a cracked section (Fig. 5) immediately after loading and at time t under the influence of creep. It is assumed here that the creep multiplier C for the concrete strains in the cracked state is the same as that for the uncracked state and has been expressed by the Eq. 13. Taking moments about the tension steel in Fig. 5a, for the stress distribution immediately after loading,

$$M = \frac{1}{6}f_{co}k_o bd^2(3-k_o)+\rho' bd^2 n_o f_{co} \frac{k_o-d'}{k_o}(1-d') \tag{14}$$

or

$$\frac{M}{f_{co}bd^2} = \frac{3k_o-k_o^2}{6} + \rho' n_o \frac{k_o-d'}{k_o}(1-d') = m(\text{constant}) \tag{15}$$

Similarly, from the stress distribution at time t(Fig.5b),

$$\frac{M}{f_{co}bd^2} = \left[\frac{3k_t-k_t^2}{6} + \rho' n_t \frac{k_t-d'}{k_t}(1-d')\right] \left(\frac{1+C}{1+C_t}\right) \tag{16}$$

where f_{co} is the stress in the concrete at the extreme fibre in compression, immediately after loading. k_o and k_t are the neutral axis depth factors ummediately after loading and at time t, respectively. ρ' is the compression steel ratio, b is the width and d is the effective depth of the section. d' is a factor which defines the depth of the compression steel A_s' with respect to that of tension steel A_s. M is the bending moment at the cracked section and remains constant under sustained load in the case of a simply supported beam.

Equating the right hand sides of Eqs. 14 and 15, and rearranging,

$$\frac{3k_t-kt^2}{6} + \rho' n_t(1-d')\frac{(k_t-d')}{k_t} = m\left(\frac{1+C_t}{1+C}\right) \tag{17}$$

Trial and error solution of Eq.16 will yield the value of k_t, the neutral axis depth factor for a doubly reinforced rectangular section at time t. In the case of a singly reinforced rectangular section, Eq. 17 reduces to a quadratic equation, whose solution yields the following expression for k_t:

$$k_t = 1.5 \pm \sqrt{2.25-\left(\frac{1+C_t}{1+C}\right)(3k_o-k_o^2)} \tag{18}$$

Considering the tracked transformed section at time t (Fig. 5c), the expression for the transformed area multiplier for tension steel, n_{tt}, is obtained by taking moments of areas about the neutral axis and rearranging terms:

$$n_{tt} = \frac{k_t^2 + 2(n_t-1)\rho'(k_t-d')}{2\rho(1 - k_t)} \tag{19}$$

In the case of a singly reinforced rectangular section, Eq.(19) reduces to the following form:

$$n_{tt} = \frac{k_t^2}{2\rho(1-k_t)} \qquad (20)$$

With the values of k_t and n_{tt} known, the moment of inertial of cracked transformed section I_{ct}, at time t, and initial plus creep deflection a_{cp} can be computed.

4. TEST RESULTS AND DISCUSSION

Short-term and long-term deflections calculated by the method proposed in the paper have been compared with the experimentally observed deflections for a number of simple span beams. In the calculation of these deflections, cracking moment M_c has been computed by using uncracked transformed section with modulus of rupture equal to $0.7\sqrt{f'_c}$ (MPa), where f'_c is cylinder compressive strength of the concrete in MPa. The modulus of elasticity for concrete, under short-term loading E_{co}, has been taken equal to $4700\sqrt{f'_c}$ (MPa) and the modulus of elasticity for steel E_s has been equal to 200,000 MPa. The creep coefficient C_t at time t has been taken from the available test data for the beams.

A report by Beeby (9) contains data and experimentally observed short-term deflections at different load levels in service range for some 300 singly and doubly reinforced rectangular beams and T-beams subjected to uniformly distributed load, centrally applied load or two-point symmetrical loading. The proposed method was used to compute short-term deflections for these beams and the results were compared with the observed deflections. Fig. 6 shows histogram of computed to observed deflection ratio for 500 test results for these beams. Fig. 6 shows that 86 percent of the results have the ratio of computed to observed deflections in the range of 0.80 to 1.20 and 52 percent in the range of 0.90 to 1.10. These results therefore indicate that the proposed method can be used to predict, within acceptable limits, short-term deflections of simply supported reinforced concrete beams in service load range.

Table 2 shows a comparison of short-term and long-term deflections, computed by the exact method of CEB's Manual (6) and the proposed method, for the beams data given in Section 3.8.1 (Example 1) of the Manual. The results in Table 2 show that the two methods give a very close estimate of short-term deflections. However, in the case of long-term deflections, the values obtained by the proposed method are greater than those obtained by the exact method of the Manual. This is because of the difference in the assumptions in the two methods. In the calculation of moment of inertia of cracked transformed section I_{ct} at time t, in the proposed method, two different values of transformed area multipliers n_t and n_{tt} are used for compression and tension steels respectively. An analysis of results for various beams shows that n_{tt} is smaller n_t and therefore a lower estimate of I_{ct} (and a higher estimate of a_{cp}) is obtained with these values when compared with the value of I_{ct} calculated on the basis of n_t for compression and tension steels.

The validity of this assumption of using different transformed area multipliers for compression and tension areas becomes clear from the results in Table 3 which shows the computed values of n_t, n_{tt} and C as well as a comparison of measured and calculated short-term and long-term deflections for the rectangular beams of Washa and Fluck(2). The results in Table 3 show that n_{tt} is smaller than n_t and the values of C and n_{tt} are influenced by the size of the member and the amount of tension and compression reinforcements. By using the bending formula and the computed section properties, an analysis of stresses for these beams (results not presents in the paper) shows that, due to the effect of creep, stress increases with time in the tension steel at uncracked section, but remain almost constant at cracked section. In the case of compression steel, stress increases with time at cracked as well as uncracked section.

Further analysis of results for the beams in Table 3 shows that the ratio I_{ut}/I_{ct} for each beam at time t is equal to I_{uc}/I_{co} under short-term loading and this leads to a simple method for estimating initial plus creep deflection a_{cp} from the short-term deflection a_o by using the following expression:

$$a_{cp} = a_o(1+C_t)I_{uo}/I_{ut} \qquad (21)$$

Table 4 shows measured and calculated short-term and long-term deflections for T-beams reported by Yu and Winter(3). For each beam the short-term deflections has been computed by Eq. 9 while the initial plus creep deflection component a_{cp} has been calculated by Eq.21. The results in Table 4 indicate that a good comparison exists between computed and measured deflections and that Eq.21 can be used to predict initial plus creep deflection a_{cp} of simply supported beams.

5. CONCLUSIONS

In the development of the proposed method a crack pattern consisting of flexural cracks was considered. While calculating deflections by the proposed method, it is therefore assumed that the beam has been adequately designed for shear and that only flexural cracks occur under service loads.

A comparison of the computed short-term and long-term deflections with the available data from various sources indicates that the proposed method can be used to predict the two types of deflection for checking serviceability criteria. The method takes into account most factors affecting deflections of reinforced concrete beams and results into simple expressions for simply supported beams subjected to symmetrical loads. For design office use graphical aids can also be prepared for the solution of the expressions developed in the paper to facilitate serviceability checks.

REFERENCES

1. ACI Committee 435, "Deflections of Reinforced Concrete Fluxtural Members," ACI Journal, Proceedings, V. 63, No. 6, 1966, pp. 637-674.

2. Washa, G.W., and Fluck, P.G. "Effect of Compression Reinforcement on the Plastic Flow of Reinforced Concrete Beams, "ACI Journal, Proceedings V. 49, No. 8, Oct. 1952, pp. 89-108.

3. Yu W.W., and Winter, G. "Instantaneous and Long-Time Deflections of Reinforced Concrete Beams under Working Loads," ACI Journal, Proceedings V. 57, No. 1, July 1960, pp. 29-50.

4. "Building Code Requirements for Reinforced Concrete" (ACI 318-83), American Concrete Institute, Detroit, 1983.

5. "CEB-FIP Model Code for Concrete Structures," Information Bulletin No. 124/125-F, 1978.

6. CEB Manual "Cracking and Deformation", Ecole Polytechnique Federale de Lansanne, 1985.

7. Branson, D.E., "Deformation of Concrete Structures," McGraw Hill, New York, 1977.

8. Winter, G., and Nilson, A.H., "Design of Reinforced Concrete Structures," 9th Ed. 1978, McGraw Hill, New York.

9. Beeby, A.W., "Short-term Deformations of Reinforced Concrete Members," Technical Report TRA408, Cement and Concrete Association, London, 1968.

Table 1: Proposed Formulae for Cracking Length Factor r and Distribution Ratio z Between Cracked and uncracked States in a Beam.

Loading Condition		r	z
Uniformly distributed load		$\sqrt{1-M_c/M_o}$	$\frac{20r^3-9r^4-12r^5+6r^6}{5}$
Centrally applied load		$1 - M_c/M_o$	$\frac{9r^2-10r^3+3r^4}{2}$
Two point symmetrical loading*	$\alpha = 1/2$	$1-0.5M_c/M_o$	$\frac{12r^2-11r^3+3r^4-3r-0.3125}{0.69}$
	$\alpha = 1/3$	$1-0.67M_c/M_o$	$\frac{11r^2-10.67r^3+3r^4-2r-0.19}{1.14}$

* α=distance between the two load points.

$$r=1-(1-\alpha)M_c/M_o; \quad z = \frac{(9+6\alpha)r^2-(10+2\alpha)r^3+3r^4-6\alpha r-3\alpha^2+4\alpha^3-\alpha^4}{(1-\alpha)^2\,(2+2\alpha-\alpha^2)}$$

Table 2: Comparison of the Deflections Calculated by the CEB Manual's Exact Method and the Proposed Method*

ρ	$\frac{\rho'}{\rho}$	$q^{\dagger}$ KN/m	CEB Manual's Exact Method		Proposed Method			
			a_o	a_t	a_o		a_t^{++}	
			mm	mm	mm	%**	mm	%**
0.003	0	8.9	4.2	10.9	4.2	100	11.7	108
0.006	0	16.9	10.0	16.2	10.3	103	27.3	169
	0.25		10.0	15.5	10.2	102	26.1	168
	0.5		9.9	14.9	10.0	101	24.9	167
0.009	0	25.0	12.0	19.2	12.3	102	31.2	163

* See Example 3.8.1 in CEB's Manual(6) for beams data.

† q = Uniformly distributed load

** Expressed as percentage of the corresponding value by the Exact Method

++ C_t = 2.0

Table 3 : Computed Values of n_t, n_{tt} and C and Comparison of Measured and Calculated Deflections for Simply Supported Rectangular Beams(2)*

Beam Designation	n_t^+	n_{tt}	C	Measured Deflection		Calculated Deflection			
				a_o	a_t^{**}	a_o		a_t^+	
				mm	mm	mm	%++	mm	%++
A1, A4	29.6	14.0	1.14	13.5	25.2	13.2	98	27.9	111
A2, A5	29.6	13.3	1.51	15.2	35.1	14.0	92	36.3	103
A3, A6	29.6	11.4	2.17	17.0	49.3	14.7	87	47.5	96
B1, B4	31.8	14.8	1.42	23.4	55.6	22.4	96	54.1	97
B2, B5	31.8	12.6	1.74	24.9	71.6	22.9	92	65.3	91
B3, B6	31.8	11.0	2.32	26.4	96.3	23.6	89	82.3	86
C1, C4	33.0	14.8	1.27	40.1	86.3	38.4	96	86.9	101
C2, C5	33.0	13.8	1.61	43.4	110.0	39.6	91	112.3	103
C3, C6	33.0	11.7	2.26	47.7	155.7	41.2	86	139.7	90
D1, D4	33.0	14.8	1.26	11.9	30.2	13.7	115	31.0	103
D2, D5	33.0	13.8	1.60	14.2	36.1	14.5	102	39.1	108
D3, D6	31.5	11.3	2.27	17.8	53.6	14.5	82	49.3	92
E1, E4	32.6	14.9	1.46	59.4	134.4	46.5	78	114.3	85
E2, E5	32.6	12.9	1.77	55.9	140.7	47.5	85	138.4	98
E3, E6	32.6	10.9	2.33	63.0	205.0	48.5	77	172.5	84

*See reference 2 and 1 for beam details and test results — beams subjected to uniformly distributed load for a period of 30 months.

**Projected 20 year (ultimate) deflections(1) from the measured long-term deflections in 30 months.

+C_t = 2.5 (ultimate creep coefficient). Shrinkage deflection component a_{sh} calculated by Branson's method(1, 7).

++Expressed as percentage of the corresponding measured deflection.

Table 4 : Comparison of Measured and Calculated Deflections for Simply Supported T - beams (3)*

Beam Designation	Measured Deflection		Calculated Deflection			
	a_o	a_t^{**}	a_o		a_t^{+}	
	mm	mm	mm	%[++]	mm	%[++]
A	34.0	81.0	28.7	84	79.5	98
B	31.5	66.7	28.7	91	71.1	107
C	30.2	67.8	29.0	96	70.6	104
D	32.3	81.3	35.2	109	80.8	99
E	13.0	35.8	14.0	108	40.6	113
F	55.9	118.6	50.8	91	139.8	118

*See reference 3 and 1 for beam details and test results — beams subjected to uniformly distributed loads for a period of 6 months.

**Projected 20-year (ultimate) deflections(1) from the measured long-term deflections in 6 months.

+C_t = 2.0 (ultimate creep coefficient). Shrinkage deflection component a_{sh} calculated by Branson's method (1,7).

++Expressed as percentage of the corresponding measured deflection.

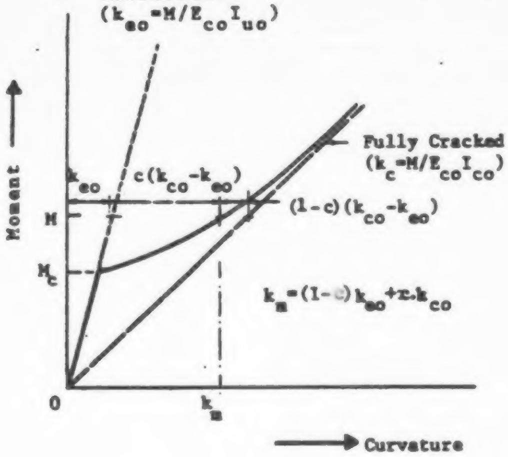

Fig. 1 : Assumed Moment-(Average)Curvature Relationship.

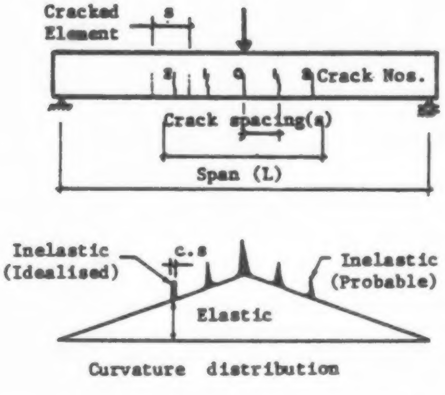

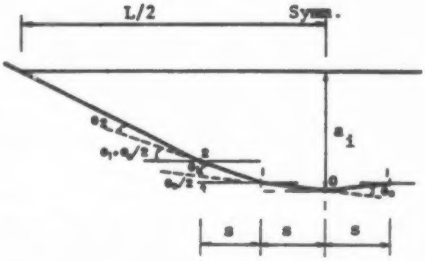

Fig. 2 : Crack Pattern and Curvature Distribution in a Reinforced Concrete Beam.

Fig. 3 : Inelastic Deflections and Rotation Cracks.

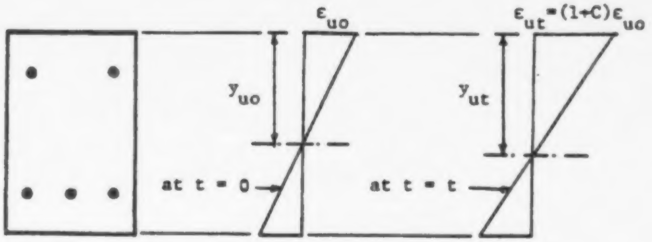

Fig. 4 : Strain Distributions at Uncracked Section.

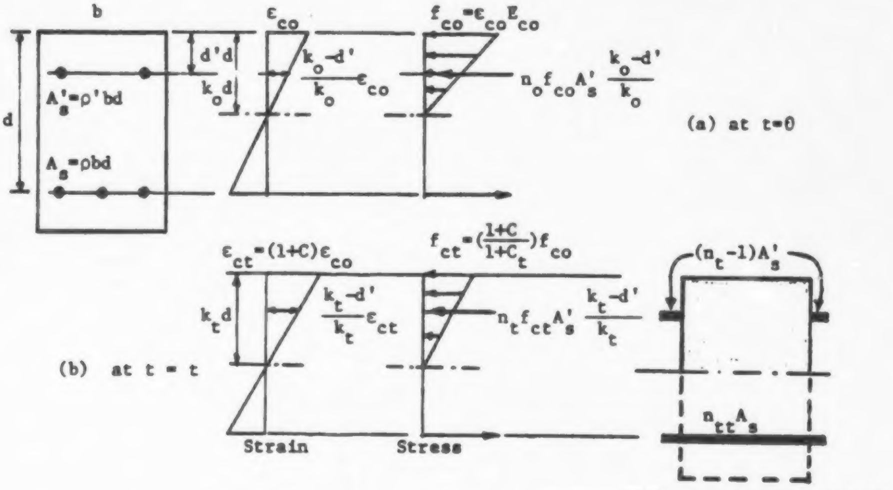
b
d
d'd
k_od
$A'_s=\rho' bd$
$A_s=\rho bd$
ε_{co}
$\frac{k_o-d'}{k_o}\varepsilon_{co}$
$f_{co}=\varepsilon_{co}E_{co}$
$n_of_{co}A'_s\,\frac{k_o-d'}{k_o}$
(a) at t=0
$\varepsilon_{ct}=(1+C)\varepsilon_{co}$
k_td
$\frac{k_t-d'}{k_t}\varepsilon_{ct}$
$f_{ct}=(\frac{1+C}{1+C_t})f_{co}$
$n_tf_{ct}A'_s\,\frac{k_t-d'}{k_t}$
(b) at t = t
$(n_t-1)A'_s$
$n_{tt}A_s$
Strain
Stress

(c) Transformed Section

Fig. 5 : Cracked Section

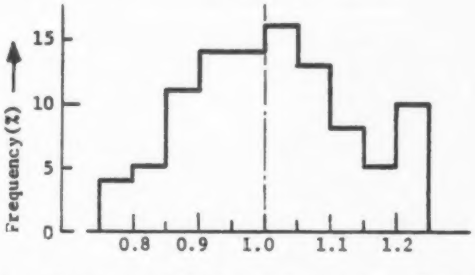

Fig. 6 : Histogram of Ratio of Computed to Observed Deflections.

SERVICEABILITY PROBLEMS OF DEPARTMENT STORE - CASE STUDY

Milan Holický

Building Research Institute
Technical University of Prague
Prague, Czechoslovakia

ABSTRACT: Load bearing structure of the new two-storeyed department store in Prague consists of reinforced concrete coffer slabs supported directly on columns within span distances 12 x 12 m. Slabs above the first and second storey cantilever out beyond edge columns by 3 m. After few years in service serious performance problems concerning cladding as well as interior partitions and other elements have been observed. At present the second storey is closed and the building is subjected to reconstruction. Analyses of load effects show that although the structure is safe, large span cantilevered slabs have insufficient stiffness. Serviceability failure of the second storey is primarily due to lack of consideration in design of deflection caused above all by permanent load and shrinkage. Construction faults have however enhanced unfavourable deformation effects. Theory of fuzzy relation and composition seems to provide an effective tool to analyse significance of various defects for damage assessment of the building.

1. INTRODUCTION

Recently built department store in a new suburban town is one of the most important social facilities of the large urban locality in Prague. Public building of this type should naturally comply with all functional requirements, including serviceability conditions, with relevant high level of reliability. Unfortunately, shortly after its completion, several structural defects (cracks, deflections) have been observed. Incidentally at the same time another department store of the same user collapsed and this was perhaps partly the reason why all the performance problems of the new building have been watchfully recorded and publicly reported, although the collapsed department store was a steel structure and its failure was due to well recognized reasons. This unfavourable psychological situation seems to play a significant role in the subsequent assessment of structural damage. Observed defects were often exaggerated and interpreted as structural condition indicating insufficient safety against collapse, not just serviceability defects. At present, after less than 10 years in service, the second storey of the two-storeyed building is closed and damaged non-bearing components are subjected to reconstruction.

2. LOAD BEARING STRUCTURE

Plan view of the building of the gross area 78 x 53 m is schematically indicated in Fig. 1. Load-bearing structure consists of reinforced concrete coffered (double ribbed) slabs of the total thickness 0,45 m (see Fig. 2) supported directly on columns of the cross section 0,5 x 0,5 m or 0,7 x 0,7 m located within span distances 12 x 12 m (see Fig. 1 and 3). The slabs above the columns are provided by hidden heads of the plan view dimensions 1,65 x 1,65 m (mostly edge columns) and 3,35 x 3,35 m (mostly interior columns), where the coffer ceiling is replaced by solid slab. In the remaining part of the slab ribbs of the cross section 0,18 x 0,38 m, which form regular orthogonal grid of interior spans 0,8 x 0,8 m, support thin plate of the thickness 0,07 m. Equivalent thickness of the solid slab having the same rigidity would be 0,34 m only, which indicates that stiffness of the structure is very low. Moreover, slabs above the first and second storey cantilever out beyond edge columns by 3 m (see Fig. 2).

Design loads of the slab above the first storey considred in the original analysis consist of permanent part 7,0 kN/m^2 and temporary part 4,0 kN/m^2, corresponding values for the second storey slab are 7,2 kN/m^2 and 1,5 kN/m^2. However, actual permanent load of the slab above the second storey is due to roof composition and ceiling greater and could be as high as 10 kN/m^2. Nevertheless, the ultimate strength of the slab is, according to the revised Czechoslovak standard /1/ "Design of concrete structures" and new standard /2/ "Design and assessment of building structures subjected to reconstruction", sufficient, and therefore the load bearing structure need not any strengthening. The whole reconstruction then concerns merely the damaged non-bearing structures.

3. NON-BEARING STRUCTURES

Non-bearing structures of the second storey, which were affected by deformations of bearing structures consist of circumferential cladding, interior partition walls and interior built-in components like glass walls, and shelf stands. Cladding of the building consists of large glass windows, brick walls and window pillars, located within regular distances of 2,4 m. The window pillars, reinforced by steel ties anchored into floor and ceiling, were built in the bearing slabs without any expansion joints. Similarly all interior masonry partition walls, reinforced by rolled steel elements of I- and U-section were constructed without any separation from roof slab. Also all the interior built-in components were not provided by expansion joints. All of these non-bearing structures were evidently designed without desirable consideration of different deflection of both floor and ceiling slabs due to their different stiffness and loading.

4. PERFORMANCE PROBLEMS

After few years in service serious performance problems concerning cladding as well as interior non-bearing structures have been observed.

The most alarming were perhaps defects appearing in non-bearing structures: cracks of partition walls (see Fig. 4 and 5), deformed door frames and buckled shelf stand, which were especially apparent and impressive. Also elements of circumferential cladding were damaged. Tensile cracks of window pillars were especially pronounced near to the exterior corners of the building (see Fig. 6

and 7).

There were also sporadic shear cracks in slab ribbs close to hidden column heads found, however, mostly near to construction joints only. These cracks, which were perhaps less important for the overall damage assessment of the building, were the only detected defects of the load bearing structure. All other performance problems concern merely non-bearing structures.

5. DEFECTS CAUSES

All of the defects of non-bearing structures in the second storey are caused by different deflection of the floor slab (above the first storey) from deflection of the roof slab, primarily due to permanent load and shrinkage. As mentioned above the permanent load of the more flexible roof is by 3 kN/m^2 greater than that of slightly less flexible floor slab. This could lead to considerable difference in midspan deflection (shortening up to 30 mm) as well as cantilever deflection (extension up to 5 mm, at exterior corner up to 10 mm). Also shrinkage may lead to similar mutual differences in slab deflections; midspan shortening and cantilever extension may reach 5 mm (extension at exterior corners may be 10 mm). Deformations due to temporary load and temperature are less important and may cause the maximum midspan extension 6 mm and shortening 1 mm, cantilever extension or shortening less than 1 mm. Observed deformation effects well correlate with theoretical results. However no calculation of structural deformation has been made in original design documentation. This was partly due to inadequate provisions provided by contemporary Czechoslovak standard.

The only measure taken in design, which could limit structural deformation, consists of steel ties, primarily assumed to reinforce window pillars of cladding structure. Owing to their insufficient stiffness the ties could not effectively limit cantilever deformation, irrespective of the fact, that some of them were not properly anchored into the lower slab.

Another construction fault mentioned above concerns permanent load of the roof slab. Due to actual own weight of the ceiling and roof (slope concrete layers) the permanent load of the slab is by 30 % greater than that assumed in design calculation. However this discrepancy is also due to negligence of some load components in design calculation. Also actual permanent load of the slab above the first storey may be slightly greater than that considered in design. Even though the deformation effects would be considerably lower if the actual load equals the assumed load, many of serviceability defects would anyhow appear. This concerns above all cracks in cladding especially at the exterior corners of two-way cantilevered slabs.

It follows, that most of the observed defects were primarily due to lack of consideration in design of deflection and due to inaccurate determination of design load. Construction errors have,however, considerably enhanced unfavourable deformation effects.

6. RECONSTRUCTION

Although there were almost no defects apparent on load bearing structural components (except sporadic shear cracks in ribs), it has been decided to close the second storey and to reconstruct most damaged interior partitions and other non-bearing structural components as well as cladding components. Interior partitions including reinforcing steel elements has been separated from the ceiling and new expansion joints have been covered by panel strip. Cantilevered slabs have been mutually tied up by new ties located near window pillars. These measures have been accepted by the designer, even though additionally made analysis show that expected deformations due to temporary load and temperature (as mentioned above) are limited, and in some cases could be admitted without any modification of non-bearing structures.

7. SIGNIFICANCE OF DEFORMATION EFFECTS

An attempt has been made to analyse significance of detected deformation effects and consequent malfunctions of structural components using the theory of fuzzy relation and composition /3/ as suggested in /4/. The following analyses have been carried out after the department store had been partly closed and therefore had no effect on its original design and current reconstruction.

Consider simplified set of deformation effects $X = \{x_1, x_2, x_3, x_4\}$ with the following components

x_1 - cracks in cladding,

x_2 - deformation and cracking of partition walls,

x_3 - deformation and buckling of built-in components,

x_4 - cracks in ribs.

In the first step of the analysis the basic set of functional requirements $Y=\{y_1, y_2, y_3, y_4\}$ is considered; where the components are in accordance with Czechoslovak standard taken as

y_1 - structural requirements,

y_2 - operational requirements,

y_3 - physiological requirements,

y_4 - appearance requirements.

The folowing membership values $\mu_R(x,y)$ concerning the given department store has been estimated for the fuzzy relation R of the fuzzy sets X and Y:

$\mu_R(x,y)$	y_1	y_2	y_3	y_4
x_1	0,5	0,2	0	0,6
x_2	0,5	0,7	0	0,8
x_3	0,2	0,8	0	0,9
x_4	0,8	0	0	0

and the following values $\mu_T(y)$ for the fuzzy relation T of Y and F, where F denotes set of unserviceable (failed) structures:

$\mu_T(y)$	y_1	y_2	y_3	y_4
F	0,4	0,7	0,5	0,8

The fuzzy relation C between the set of deformation effects X and set of unserviceable structures F is now given by the composition C = R . T , where /3/

$$\mu_C(x) = \bigvee_y \{\mu_R(x,y) \wedge \mu_T(y)\}$$

Using this formula it follows for the membership values $\mu_C(x)$:

$$\mu_C(x) = \begin{array}{c|c} x_1 & 0,6 \\ x_2 & 0,8 \\ x_3 & 0,8 \\ x_4 & 0,4 \end{array}$$

In this way determined relation between deformation effects and set of failed structures shows that deformation and cracks of partition walls and built-in components lead to the highest support (0,8), that the structure is unserviceable; lower support is due to cracks in cladding (0,6) while cracks in ribs seem to be even less important (0,4). It should be mentioned that the highest significance of defects observed in partition walls and built-in components is caused by violation of appearance requirements, which is (due to psychlogical aspects) assessed in the relation R by relatively high support 0,8 and 0,9. However, it should be noted that subjective assessments of some other specialists may differ from that presented above.

In the next step in the significance analysis more detailed classifications of the fuzzy sets X and Y may be applied and possible weights of various deformations effects could be considered. It is expected that such an analysis in design stage may indicate relative significance of various effects enabling reliability differentiation of corresponding serviceability limit states and/ or redesign of critical structural details.

8. CONCLUSIONS

Serviceability failure of a new department store in Prague was primarily due to lack of consideration in design of deflection caused above all by permanent load and shrinkage; less significant were effects of temporary load and temperature. Construction faults (greater permanent load and imperfect anchoring of cantilever ties) have however significantly enhanced unfavourable deformation effects.

Coincident collapse of another department store of the same user significantly affected damage assessment of the new building and subsequent decision made by constructor and other building authorities.

Theory of fuzzy set relation and composition seems to provide an effective tool to analyse significance of various deformation effects, which may yield background material for differentiation of required reliability and/or redesign of critical structural details. It could be used in design or in assessment of damage state of existing structures.

REFERENCES

/1/ ČSN 73 1201 "Navrhování betonových konstrukcí" (Design of concrete structures), ÚNM Prague, 1987.

/2/ ČSN 73 0038 "Navrhování a posuzování stavebních konstrukcí při přestavbách" (Design and assessment of building structures subjected to reconstruction), ÚNM Prague, 1986

/3/ Brown, C.B., Yao, J.T.P., "Fuzzy Sets and Structural Engineering", Journal of Structural Engineering, ASCE, Vol. 109, No 5, May, 1983, pp.1211 - 1225.

/4/ Yao, J.T.P., "Damage Assessment of Existing Structures," Journal of the Engineering Mechanics Division, ASCE, Vol. 106, No EM4, Aug., 1980, pp.785 - 799.

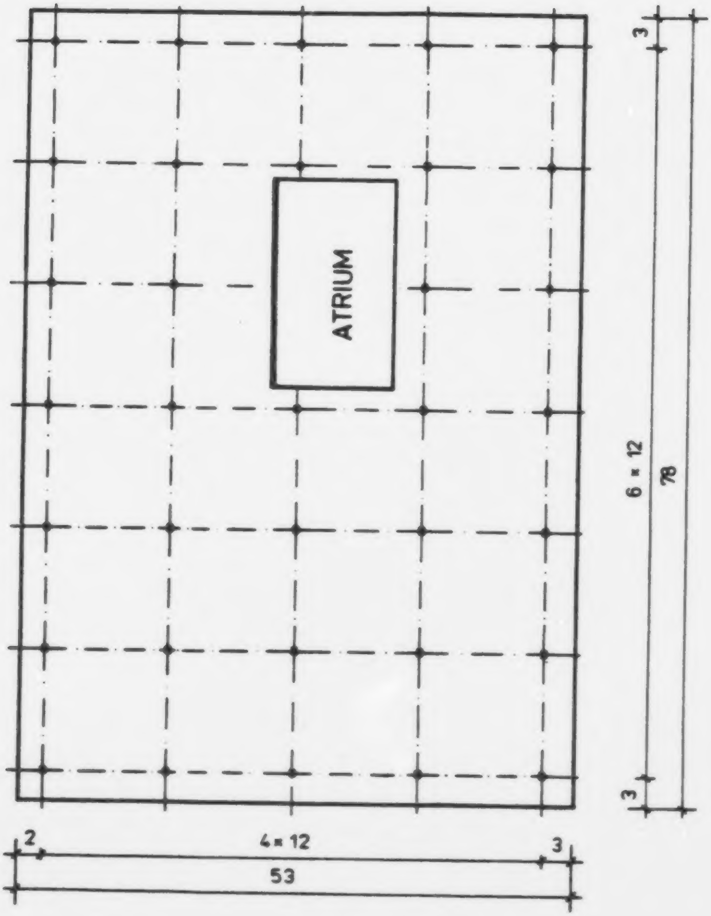

Figure 1 : Plan view

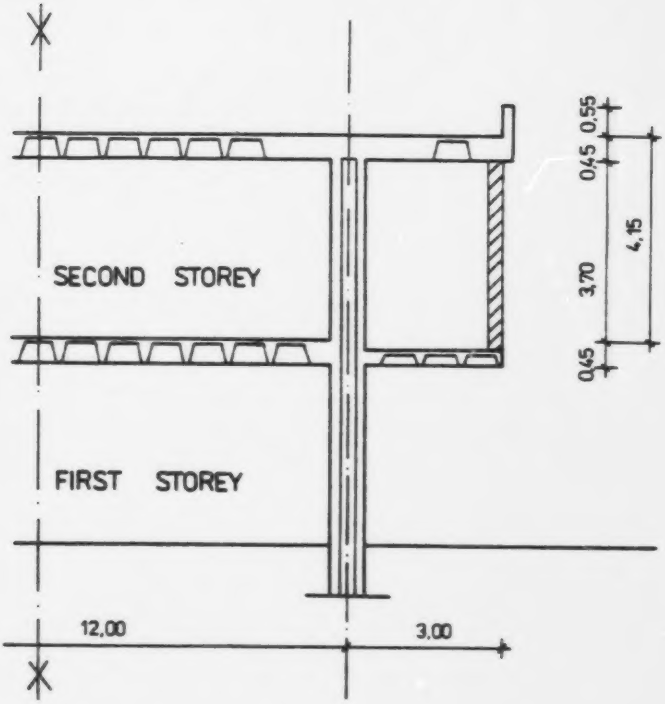

Figure 2 : Section view

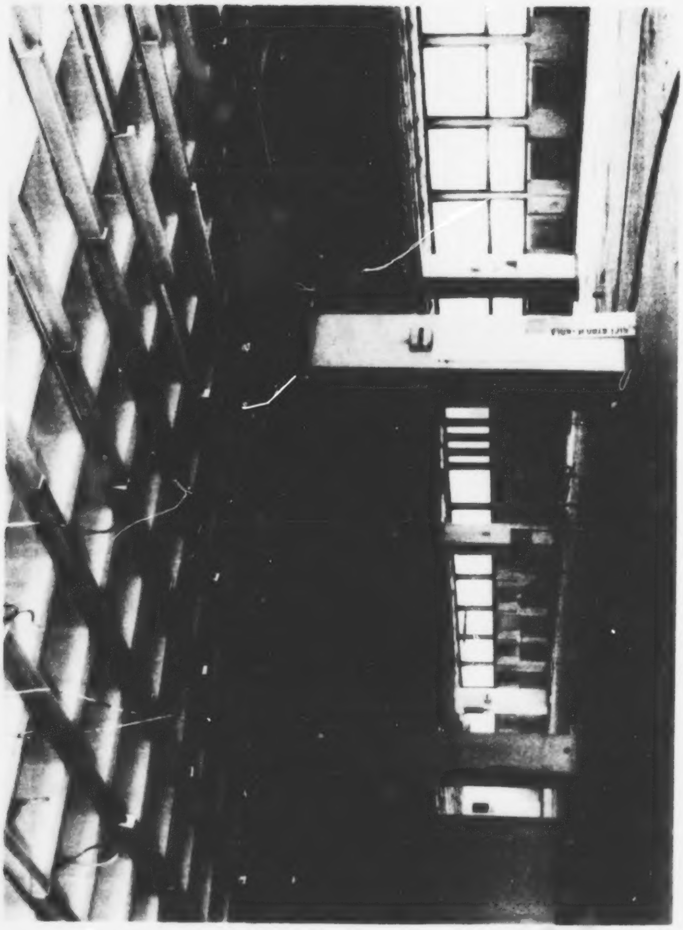

Figure 3 : Interior View

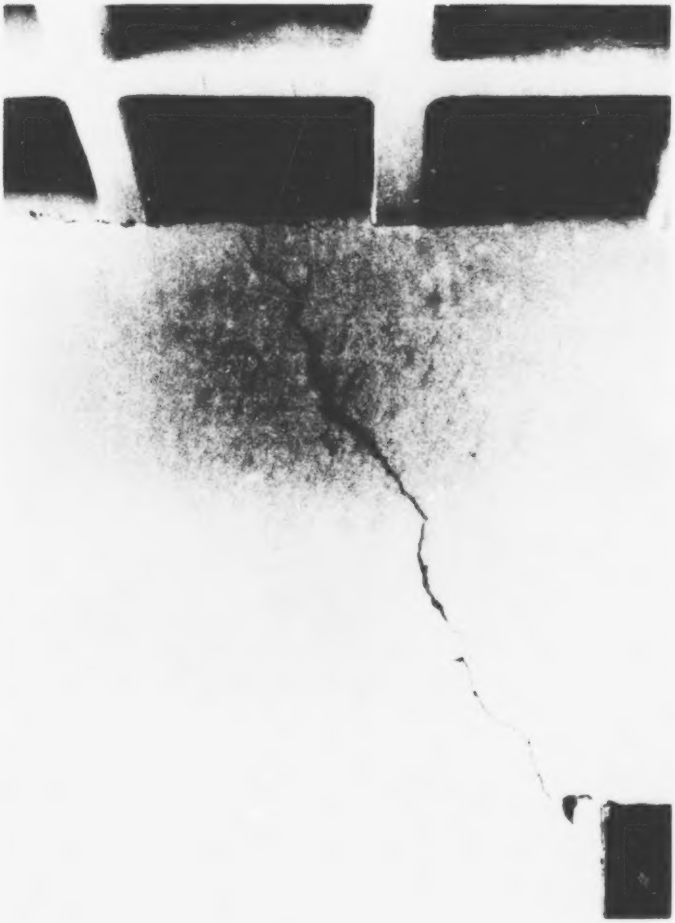

Figure 4 : Cracks in partition walls

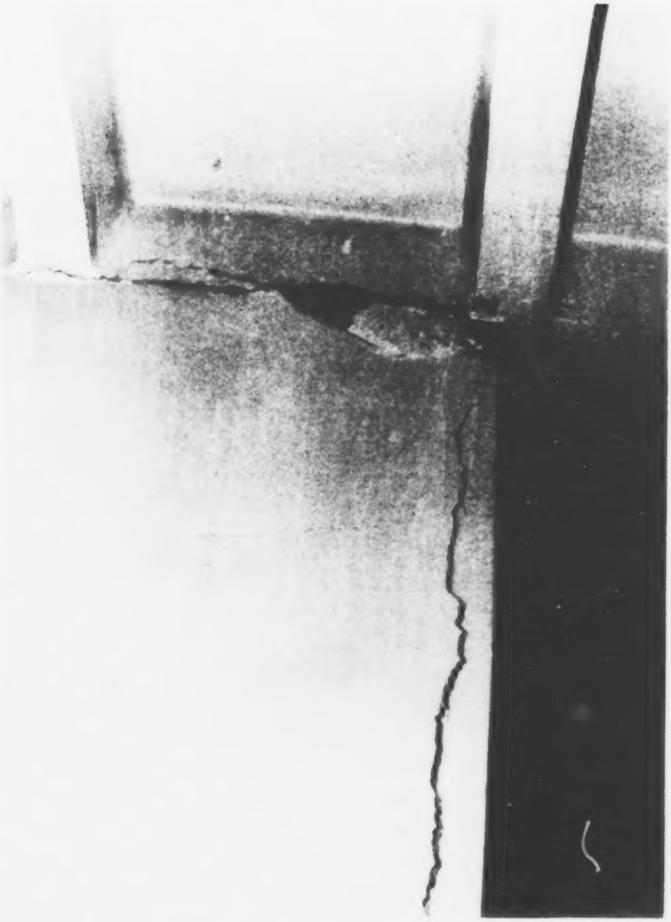

Figure 5 : Buckled steel component reinforcing partition wall

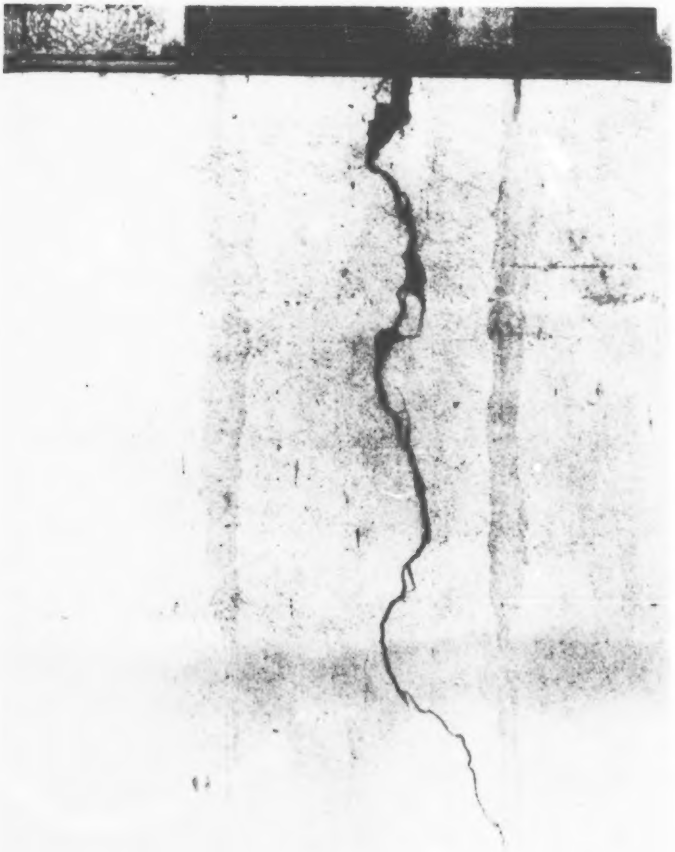

Figure 6 : Cracks in cladding near to exterior two-way cantilevered corner

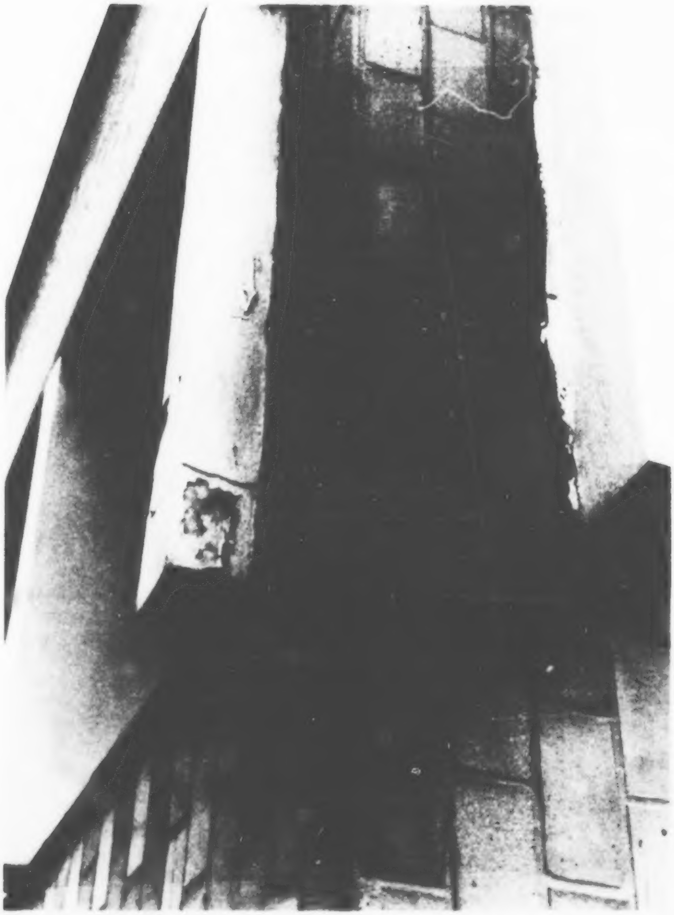

Figure 7 : Cracks in cladding at the exterior two-way cantilever corner

SESSION C/SÉANCE C

WIND-INDUCED VIBRATIONS/VIBRATIONS CAUSÉES PAR LE VENT

MEASURED MOTIONS OF TALL BUILDINGS IN WIND AND THEIR EVALUATION

N. Isyumov, A. Masciantonio and A.G. Davenport

Boundary Layer Wind Tunnel Laboratory
The University of Western Ontario
London, Ontario N6A 5B9 Canada

ABSTRACT: This paper describes some of the more noteworthy contributions of full-scale measurements towards the understanding of the performance of wind-sensitive structures. The paper continues to present a number of Case Studies, describing specific programmes of full-scale monitoring and their validation of both analytical and wind tunnel procedures for estimating the wind-induced response.

INTRODUCTION

Technological advances and innovation, including improved analysis procedures made possible by computers, the availability of high-strength materials, and improved fabrication and construction methods have produced more efficient but lighter, more flexible and more lightly damped structures. As a consequence, modern buildings and structures have become more sensitive to the dynamic action of wind. This has resulted in a greater emphasis on predicting the wind-induced response of modern tall buildings and structures at the design stage and wind tunnel model studies have become the norm for many wind-sensitive structures. Also, there has been more full-scale monitoring. These observations have improved the understanding of the behaviour of buildings and structures under wind action. Some provided information to clarify unknown aspects of wind within the atmospheric boundary layer and its action on structures. Others have provided valuable confirmations of expected behaviour and added confidence to the design process.

This paper provides a number of examples of full-scale observations, both historic and recent. These are provided to illustrate the diversity of reasons for such measurements and approches taken. The information provided by such studies and the lessons learned have made valuable contributions to the state-of-the-art of wind engineering of today.

BACKGROUND

A number of early observations of wind-induced behaviour provided information on the nature of boundary layer winds and underscored the importance of the dynamic response of tall buildings and structures. Some of the more noteworthy historic and contemporary contributions include:

The Eiffel Tower: Full-scale measurements of the wind-induced response of tall buildings date back some 100 years. The 300-metre Eiffel Tower became the first tall structure to be instrumented as Gustaf Eiffel began experiments shortly after its completion in 1889. These included measurements of wind speed and the movements of the tower, using a vertical telescope aimed at a target on the top level of the tower (1). Examples of the results of these historic measurements are shown in Figure 1. These important measurements showed that the wind speed at the top of the Eiffel Tower was on average 2 or 3 times greater than that at the Bureau of Meteorology taken at a height of 20 metres. This provided an early indication of the variation of the mean wind speed and hence velocity pressure within the atmospheric boundary layer and supported Eiffel's assumption that the wind pressure increases with height from the base of the tower.

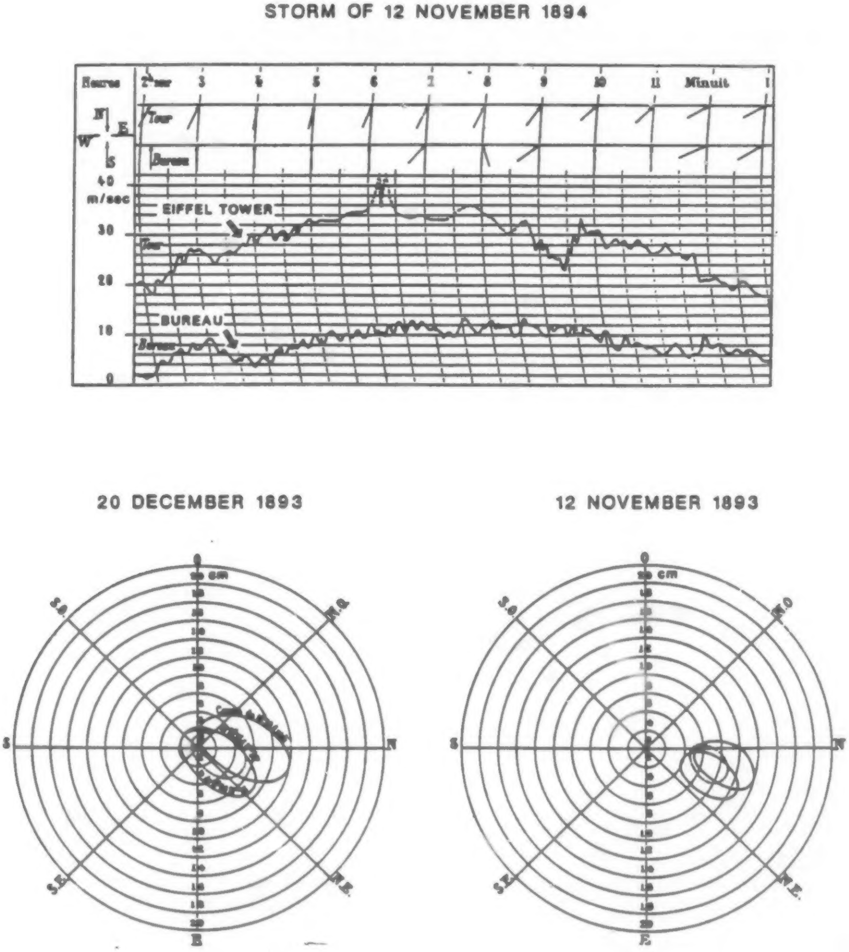

Figure 1: Records of Wind Speed and Motion of Eiffel Tower (after Ref. 2)

The observations of the tower motion show elliptical envelopes of the time-varying deflection, offset from the centre of the target by the static displacement. The major axes of these envelopes point approximately towards the centre of the target suggesting greater motion in the along-wind or drag direction. The ratio of the maximum to the mean deflection, from these traces appears to be of the order of 1.4 to 1.7. While these early benchmark measurements clearly demonstrated that the action of wind is both static and dynamic, engineers, until quite recently, continued to treat wind as a static loading.

Early U.S. Skyscraper: Observations of the wind-induced motion of tall buildings date back to the end of the 19th century. A transit and a plumb bob suspended in a stairwell were used to observe the wind-induced movements of the 17-storey Monadnock Building in Chicago during a violent wind storm in 1884. Davenport in his re-examination of these data (2), suggests that the resonant dynamic response of this broad, heavy masonry building was relatively small and that the measured dynamic response was largely due to the quasi-static background excitation by turbulence. The wind-induced responses of a number of New York skyscrapers were measured in the 1930's (2,3). These clearly revealed the presence of resonant or oscillatory dynamic motions of tall buildings under wind action. The conclusions drawn were that building frames of tall buildings must be designed to resist wind-induced pressures, as well as have a sufficient stiffness to keep wind-induced vibrations within limits which would assure occupant confidence in the integrity of the structure. It is noteworthy that while the pioneers of the New York skyscraper boom were aware and concerned about wind-induced building motions, the current New York Wind Code does not limit the wind-induced drift nor the resulting building accelerations.

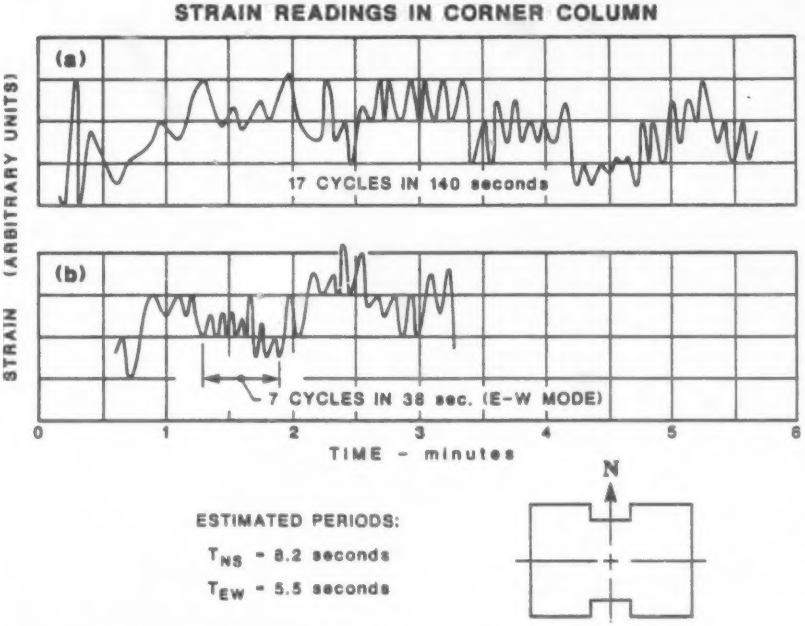

Figure 2: Wind-Induced Response of Empire State Building (after Ref. 2)

The most significant study of full-scale behaviour of traditional skyscrapers was carried out for the Empire State Building by Rathbun (4). The work of Rathbun was a major full-scale monitoring programme for its time. The instrumentation included an anemometer, 30 manometers to measure wind pressures on the exterior of the building, 28 cameras with remote operating mechanisms, 22 extensometors, 1 collimator and target and a plumb bob. A re-examination of Rathbun's study (2), has led to a number of significant findings. As observed some 50 years earlier by Eiffel, Rathbun's data clearly demonstrated the significant reduction in the mean wind speed at lower heights in an urban area. Records of the wind-induced strain of the Empire State Building, given in Figure 2, clearly show the dynamic nature of the wind-loading process. There are resonant vibrations at the fundamental sway periods as well as a quasi-static variation attributed to the action of large gusts. Davenport's revisit of the Empire State Building, which also included follow-up force balance wind tunnel model measurements (5), brought forth other interesting aspects of the behaviour of this building. The ratio of the maximum to the mean response, referred to as the gust effect factor in the National Building Code approach, was estimated to be about 1.6. Furthermore, the wind-induced accelerations near the top of the building, predicted for a recurrence interval of 10 years, were estimated to be somewhat under 10 milli-g. Both of these findings are indicative of a building with a lesser sensitivity to wind-induced resonant vibrations in comparison to modern tall buildings. This is largely attributed to the extensive masonry infill and heavy stone facade which result in relatively high building mass (average building density of 19 lb/cu.ft.) and in a likely higher effective damping.

Contemporary Buildings and Structures

The World Trade Center Towers

The design of the twin World Trade Center Towers in Lower Manhattan brought about radical departures from previously-accepted practice. Wind tunnel model tests were carried out in flows which representatively simulated the turbulent boundary layer characteristics of natural wind. The analytical procedures developed took into account the random buffeting effects of turbulence. The design of these two tall slender buildings was a turning point both in the wind tunnel testing of wind-sensitive structures and in the development of design methods to allow for the dynamic action of wind (2). Monitoring of the visco-elastic dampers, included in the design of the Towers to assure their behaviour under wind action, was started after installation in 1969. This monitoring programme was expanded to include measurements of building accelerations and is continuing. Results reported to-date (6) indicate that the towers are performing as expected.

John Hancock Tower, Chicago

The analysis of accelerometer records taken near the top of the John Hancock Tower in Chicago in the late 1960's provided a valuable confirmation of the predominance of the resonant response in the fundamental modes of vibration for a tall building. Another important outcome, was the realization that the inherent structural damping of modern steel structures can be well below commonly accepted values (7).

Commerce Court Plaza

The Commerce Court Plaza Building in Toronto, Ontario was instrumented by the National Research Council in the early 1970's to provide information on building accelerations and exterior and interior wind-induced pressures (8,9,10). This was the first major study of the full-scale behaviour of a tall building in Canada. It provided valuable comparisons with the results of wind tunnel model studies and made significant contributions towards the understanding of the action of wind both on the overall structure and on components of the exterior envelope.

John Hancock Building, Boston

An extensive programme of full-scale monitoring was undertaken for the John Hancock Building in Boston, shortly after its construction. This programme, operated during 1973 to 1975, examined the behaviour of the curtain wall systems, as well as the wind-induced motions of the structural frame. Information on the enormous data base acquired during this programme (some 20,000 transducer hours) is now emerging in the literature (11).

CN Tower, Toronto

The 555m high CN Communications Tower in Toronto remains the world's tallest free-standing structure. A programme of full-scale observations was started in 1976 shortly after its completion. The objectives were to examine the expected behaviour of the structure which was extensively wind tunnel tested and which represented a major extension of technology. The results of the study provided important confirmations of the dynamic properties of the Tower, its behaviour under wind action and the structure of the atmospheric boundary layer (12). This major programme is discussed as a "Case Study" below.

Allied Bank Plaza, Houston

Hurricane Alicia in August of 1983 subjected the then recently completed Allied Bank Plaza in Houston, Texas to winds of design severity. The building at the time was instrumented with 2 accelerometers in order to ascertain the effective structural damping. This provided a unique record of the response of a major building exposed to hurricane-intensity winds for a period approaching two hours (13,14). Further details of these measurements, which provide an important validation of wind tunnel predictions, are given below.

MONITORING PROGRAMMES AND INFORMATION GAINED

As seen from the above examples, there are many reasons for monitoring the full-scale behaviour of structures. In addition to scientific curiosity, the more clearly identifiable ones include:

i) Validations of Methodology and Assurance of Expected Behaviour

For unusual structures or in situations of new technology, the monitoring of structural behaviour after construction can provide important validations of design procedures and an assurance of acceptable behaviour.

ii) Diagnostic Tools

Full-scale measurements are valuable diagnostic tools for identifying the potential for unacceptable behaviour. One example are measurements made to determine the inherent effective damping in situations where there are concerns for dynamic effects. Others are the monitoring of the structural response for operational requirements or to provide an early warning of potential structural distress.

iii) Assistance to Designers Dealing With the Rehabilitation of Structures

The properties of as-built structures are important to designers involved in additions to or rehabilitations of existing structures. In such situations, information on the insitu mass, stiffness and damping, derived from full-scale observations, can improve both economy and reliability.

Clearly, the range of effort and hence cost of full-scale measurements is large. Some of the most significant measurements of full-scale behaviour have been obtained with relatively simple and inexpensive methods. It has been the author's experience that the dynamic response of wind-sensitive structures can be determined by measuring the wind-induced acceleration at a number of well selected locations. Accelerometers along with relatively simple data recording methods can provide information on periods of vibration, the orientation of the principle axes of stiffness, the effective damping and comparisons with structural behaviour predicted from wind tunnel studies. A brief summary of information obtained with such measurements and an indication of the order of their difficulty are given in Table 1. There are clear advantages in maintaining the instrumentation simple and in attempting to only capture key measures of the dynamic response during a significant wind storm. With current technology it is relatively inexpensive to expand such instrumentation systems to include automatic recording above some pre-set threshold value.

In contrast, some full-scale monitoring programmes have tended to attempt detailed measurements of many parameters over long periods of time. Such programmes, to be effective, require continuous maintenance, scrutiny and evaluation of the quality of the data base. The costs involved therefore can become enormous.

Table 1: Types of Measurements of Dynamic Structural Behaviour

Objective	Complexity	Monitoring Effort	Essential Additional Information Needed
- Measurements of periods of vibration	- Very simple	- Typically 1 hour	None
- Information on mode shapes; alignment of principle axes of stiffness	- Relatively simple	- Typically 1 hour per set-up	None
- Estimates of Damping	- Difficult	- Many hours required to achieve necessary frequency resolution; desirable that the excitation remain stationary	None
- To obtain definitions of structural response for comparison with predicted behaviour	- More difficult	- Many hours at several wind speeds and wind directions	Wind speed and direction seen by structure; these can be estimated from winds aloft or at anemometer stations; the alternative is measured well above building

RECENT CASE STUDIES

Several recent studies of full-scale behaviour of tall buildings and structures are given below. These have been selected to illustrate differences in objectives, instrumentation systems and results obtained. All case studies involve structures studied at the Boundary Layer Wind Tunnel Laboratory.

Observations Of CN Tower Response

Measurements of the response of the CN Tower in Toronto were made after the completion of the concrete shaft which extends some 450m (1480 ft.) above ground. These measurements of the partially-erected Tower were carried out in order to confirm the anticipated stiffness and damping of the structure. This confirmation was judged important for the final interpretation of the findings of the aeroelastic wind tunnel model study used to provide information on overall wind-induced loads and responses.

Measurements of strain of an instrumented reinforcing bar at the base of the Tower were made during wind conditions with a gradient wind speed of about 20 m/sec. (45 mph). These measurements (15), indicated that the Youngs modulus of the concrete was approximately 4.3×10^4 MPa (6.3×10^6 psi). The initially expected value was 3.4×10^4 MPa (5×10^6 psi). The effective structural damping for the first mode of vibration was estimated to be in the range of 0.5 to 1.0 percent of critical from these observations. This confirmed the structural damping assumed in the wind tunnel tests.

The programme of monitoring and recording the wind-induced response and some meteorological parameters was started after the completion of the Tower and continued for several years. Participants in this study were the Department of Civil Engineering of the University of Toronto, the Atmospheric Environment Service of Canada, the Division of Building Research of the National Research Council and the Boundary Layer Wind Tunnel Laboratory. In its normal mode of operation, the instrumentation system sampled 80 channels of data at a rate of 5 Hz and logged calculated 10-minute average statistical data. During strong winds, all data were recorded on magnetic tape. The instrumentation included sets of three anemometers and directional vanes located on booms at three levels along the Tower and a single anemometer and vane at the very top. Other instrumentation included accelerometers, Optron optical tracking device, strain gauges, temperature probes and gas analyzers. Details of this programme can be found elsewhere (12, 16, 17, 18). The maintenance and operation of the various sensors in a relatively hostile environment proved to be highly demanding. Not all of the instrumentation functioned throughout the programme and the subsequent analysis was complicated by uncertainties about data quality. Some of the more significant findings of this major programme are given below.

The dynamic properties of the completed structure were found to correspond well to anticipated values, once the stiffness characteristics of the concrete shaft were determined. Table 2 provides a comparison of the measured and predicted periods of vibration for the first seven modes. The agreement is good. Measurements of the Tower frequencies to-date have not indicated any significant changes with time or with wind speed. The damping of the structure in its fundamental mode of vibrations has been found to be somewhat below 1% of critical. The overall response of the structure to wind action was found to be in good agreement with wind tunnel predictions. Of the various instrumentation, accelerometers were found to be most reliable. Figure 3 shows resultant rms accelerations at the top of the Tower and at the restaurant level. These data are from a number of observations with different wind speeds and wind directions from NW ±11.25°. As expected, there is considerable scatter at low wind speeds. For higher winds, however, the observations tend to approach values predicted from the aeroelastic wind tunnel model study. Measurements of the properties of the wind towards the top of the Tower proved interesting. The turbulent boundary layer appears to be somewhat deeper and the turbulence intensities near the top of the Tower somewhat higher than conventionally assumed. The intensity of turbulence at the top anemometer was typically about 10 and 5% respectively for off-the-land and off-the-lake directions.

Table 2: Comparison of Measured and Predicted Periods of Vibration of CN Tower, Toronto, Ontario

Mode of Vibration	Period (sec.)	
	Analytical Estimate	Full-Scale Observations
1	8.06	7.87
2	3.76	3.36
3	2.06	2.07
4	1.23	1.23
5	0.97	0.98
6	0.55	0.56
7	0.50	0.49

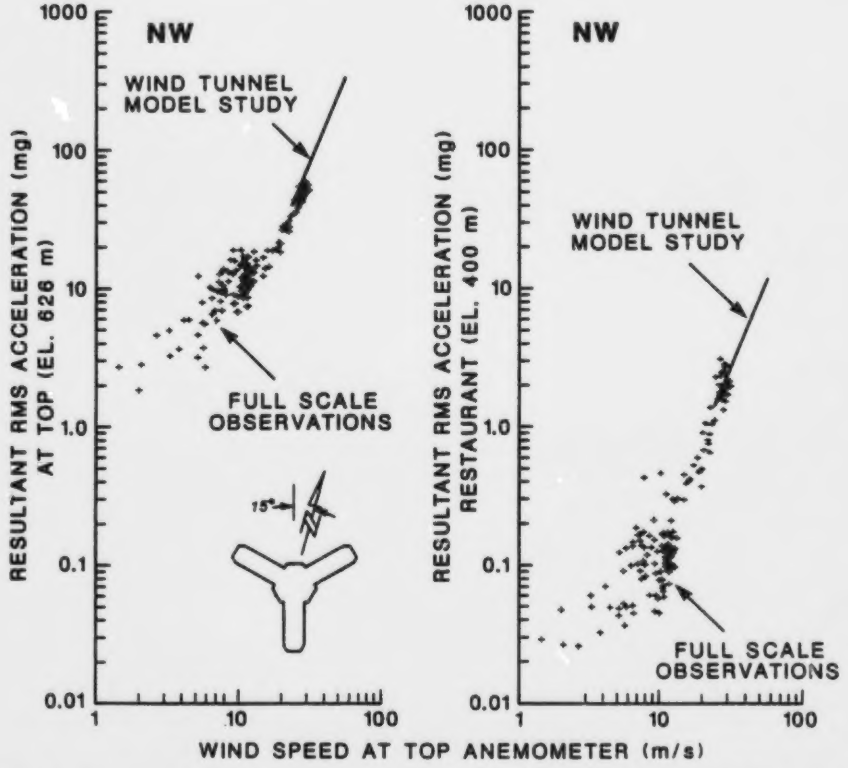

Figure 3: Resultant RMS Accelerations v.s. Wind Speed at the CN-Tower - Full Scale and Model Study

The programme clearly showed that while a significant "glimpse" of the wind-induced response is obtained relatively readily from measurements during one or two significant wind storms, a detailed description of the response is much more difficult. A long period of time, with fully functioning instrumentation, is required in order to experience wind storms with a significant range of speeds and direction.

The Response of the Allied Bank Plaza during Hurricane Alicia

The approximately 980-ft. Allied Bank Plaza Building in Houston, Texas was wind tunnel tested at its design stage. A programme of monitoring the dynamic response was started in October 1982. The primary objective was to confirm the dynamic properties of the Tower after construction. The instrumentation comprised two (2) manually-operated accelerometers located at the 71st floor (top of the building). There was no wind sensing equipment and reliance was placed on estimates of wind speed and wind direction from local weather stations.

Hurricane Alicia struck downtown Houston in the early hours of August 18, 1983. The recording system was turned on by the senior partner of Skidmore, Owings & Merrill, architects and engineers for the building, who braved the storm and was able to reach the top of the building. The recording continued over a period of about 90 minutes near the peak of the storm. This has provided the only existing record of the response of a major building in winds of hurricane intensity.

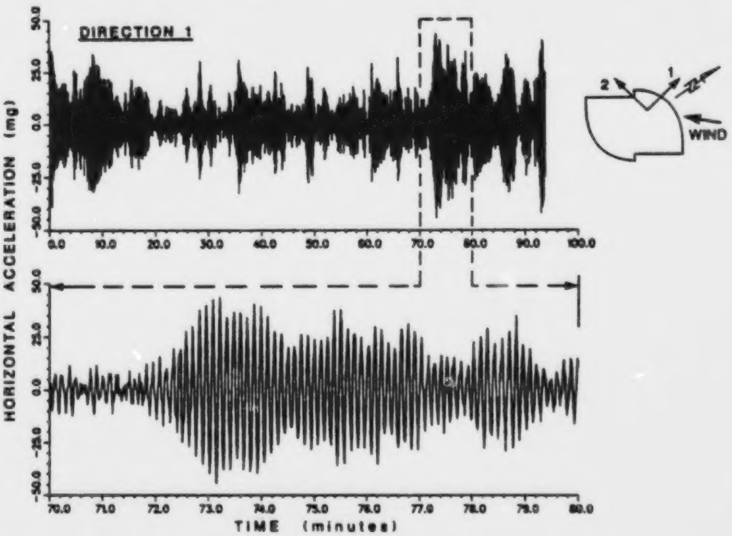

Figure 4: Time History of Horizontal Acceleration At the Top Floor of the Allied Bank Plaza During Hurricane Alicia (after Ref. 13)

Figure 4 shows the time history of horizontal accelerations of the Allied Bank Plaza along one of its principle axes of stiffness. Corresponding data for Direction 2, see Figure 4, is not shown. In addition to showing the entire time history, Figure 4 shows an expanded version of a 10-minute interval containing the highest recorded peak acceleration of about

43 milli-g. This corresponds to a dynamic peak deflection of about ±2 ft. The corresponding peak acceleration in the other principle sway direction was around 20 milli-g. Further details on the analysis of these records, is provided elsewhere (13, 14).

As expected from the aeroelastic model study, the building response was primarily in the two fundamental sway modes of vibration. This is clearly seen from the power spectra shown in Figure 5. Accelerometer 1 was aligned along principle axes 1 and has a power spectrum with a single-dominant peak at the fundamental sway mode in that direction. Accelerometer 2 was aligned in a direction parallel to the second principle axes of stiffness and at a distance of 45 ft. from the centre of stiffness. The power spectrum for this accelerometer has a dominant peak at the second fundamental sway mode with smaller peaks at a frequency corresponding to the first sway mode and the fundamental torsional mode. The small peak at the first mode of vibration frequency is attributed to the combined effects of a slight misalignment of accelerometer 2 and its sensitivity to mode 1 vibrations due to the warping of the floor slab. The torsional wind-induced motions of the building, as expected, are relatively small. The measured periods of first and second sway modes and in the fundamental torsional mode are 7.7, 6.4 and 3.6 seconds respectively, see Figure 5. The corresponding calculated periods were 7.4, 6.4 and 3.5 seconds. These are in good agreement, with the largest difference between calculated and measured values of about 4% for the first fundamental sway mode.

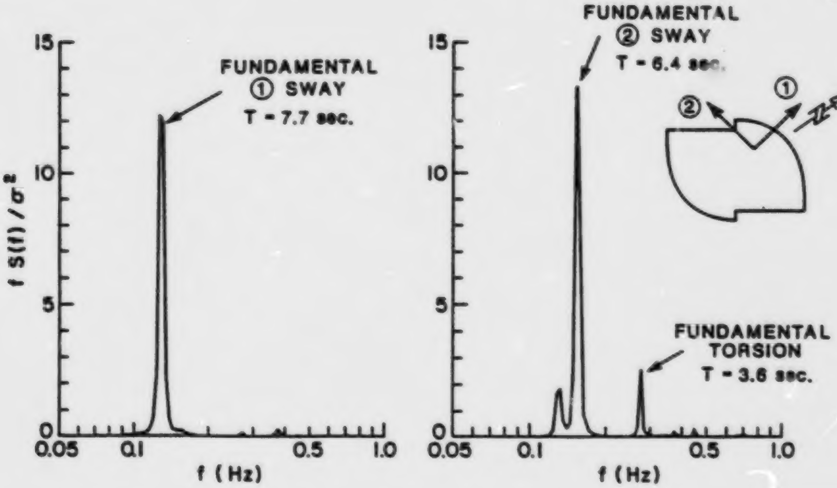

Figure 5: Power Spectra of the Acceleration of the Allied Bank During Hurricane Alicia (after ref. 13)

The damping of the Tower in its first and second fundamental sway modes was estimated to be about 1.6 and 1.4% respectively. The aerodynamic damping, estimated from the aeroelastic wind tunnel model study, was relatively small (13) and as a result, most of this measured damping is attributed to the energy dissipation in the structure and its foundation. The estimated effective structural damping was assumed as 1.5% of critical at the design stage.

The recorded response of the Allied Bank Plaza provided a unique opportunity for comparison with the response predicted from the aeroelastic wind tunnel model study. Such a comparison required information on the strength and direction of the wind, as seen by the building during the storm. This was obtained through a reconstruction of the wind field, using all available meteorological information for the storm. From this, it was estimated that during the 90-minute recording period the mean wind speed at gradient height gradually increased from about 36 to about 44 m/s. The wind direction during this interval is estimated to have been from the NE to E (13, 19, 20). This estimated wind speed corresponds to an event with a return period somewhat in excess of 50 years. Having estimated the time history of wind speed and wind direction during the storm, the variation of the Tower accelerations was reconstructed from the results of the wind tunnel study. The latter had evaluated the response for all wind directions and all practicable wind speeds.

Figure 6 shows the time history of the likely peak resultant acceleration obtained from this analysis. To allow for the uncertainties in the reconstruction of the actual wind field, it was assumed to accept a ±5 mph variation in the wind speed and a ±5° variation in the reconstructed wind direction. The band shown in Figure 6 corresponds to the resulting upper and lower bound estimates of the 10-minute peak resultant accelerations at the top floor of the building. The best estimate is approximately in the middle of this range. Plotted on the same graph are the actually observed 10-minute maximum resultant accelerations. The agreement is excellent as most points fall near the middle of the estimated range.

Observations of the Allied Bank Plaza during Hurricane Alicia also provided valuable information on the human response to building motion. As reported by Mr. R.A. Halvorson, who took the observations (14),

> "the motion was clearly perceptable and comparable to being on the deck of a very large ship. Some effort was required to balance oneself against lateral forces and walking required concentration".

In addition, there were various visual cues which accentuated the sensation of building motion.

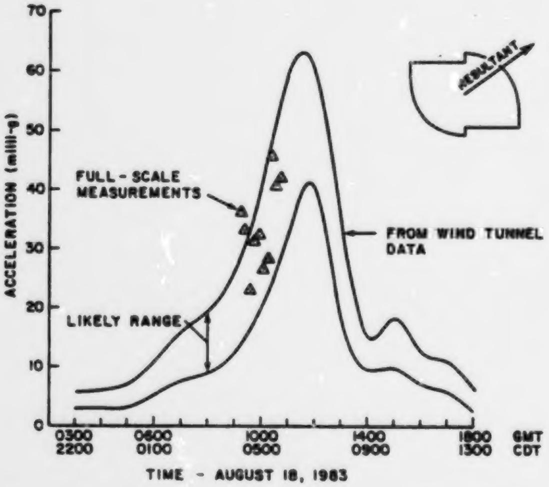

Figure 6: Measured Peak Accelerations at the Top Floor of the Allied Bank and Comparisons With Values Anticipated From Wind Tunnel Model Study (after ref. 13)

The observed motions were entirely consistent with the design objective of limiting the building acceleration to approximately 20 milli-g during 10-year return period storms. During a rare event such as Hurricane Alicia, higher acceleration levels are acceptable as structural integrity and minimizing damage become the primary concerns. The building experienced no visible damage to the structure nor its interior finishes. The drift index of the peak deflection, including an allowance for static effects, was approximately 1:400 in direction 1. There was extensive damage to the window glass; however, this was totally attributed to impact damage from flying roof gravel and debris.

Full-Scale Observations of Citi-Corp Building, New York, N.Y.

This approximately 910-ft. Office Tower was extensively wind tunnel tested during its design stage (21). The innovative structural system and the high strength materials used resulted in a relatively light building and there was an early commitment to equip the Tower with a tuned-mass damper (TMD) in order to control its wind-induced dynamic motions and to assure the comfort of its occupants (22, 23, 24, 25). The approach followed was to use the TMD only to assure occupant comfort and not to rely on its beneficial effects for the structural integrity in extreme winds.

The TMD installation was instrumented to provide information on the acelerations of the building in its two principle sway directions and the relative sway motions of the 410 ton concrete mass block with respect to the building. The purpose of this instrumentation was to provide operational information for the TMD system. The system was designed to start up automatically whenever the maximum acceleration for two successive cycles of the building exceeds 2 milli-g. Once activated, the TMD system continues to operate as long as the building motions continue and only stops ½-hour after the last pair of building cycles for which the maximum acceleration is greater than 0.75 milli-g. Experience with the system for a period approaching 10 years indicates that operation in this automatic start-up mode is typically for around 300 hours per year. When on standby, the TMD system is continuously powered, however, records of the response are only made during its operation. These records, taken on FM-tape provided an important opportunity to examine the building response and to make comparisons with anticipated behaviour (26).

Figure 7 shows time histories of the 63rd floor sway accelerations during Hurricane David on September 6, 1979. The TMD system was operational for approximately 6 hours and clearly show the passage of the storm. The maximum single component acceleration, recorded in the Y-direction, was around 10 milli-g. The maximum resultant translational acceleration was approximately 12 milli-g. Power spectra of the X and Y accelerations during different parts of the storm are also shown in Figure 7. These clearly demonstrate the predominance of the dynamic response in the fundamental modes of vibration. Contributions from higher modes are seen to be relatively small. This confirms current approaches which assume that the responses in the fundamental modes of vibration dominate the effective static wind forces, the building displacements and the horizontal accelerations.

The variation of the fundamental building periods over the course of the storm, demonstrate the amplitude dependence of the stiffness of the building. During the operation of the TMD, the fundamental mode of vibration is replaced by two closely-spaced modes of the combined building - TMD system. This can be seen from the spectra in Figure 7 which in some cases, show two closely-spaced peaks. The spectral analysis did not allow a frequency resolution fine enough to distinguish between these two peaks. Slight variations in these peak from hour to hour are due to the inherent variability of spectral estimates. The amplitude dependence of the building periods complicates estimates of the damping and conventional statistical methods, such as the logarithmic decrement or the half-power bandwidth techniques lead to overestimates (26).

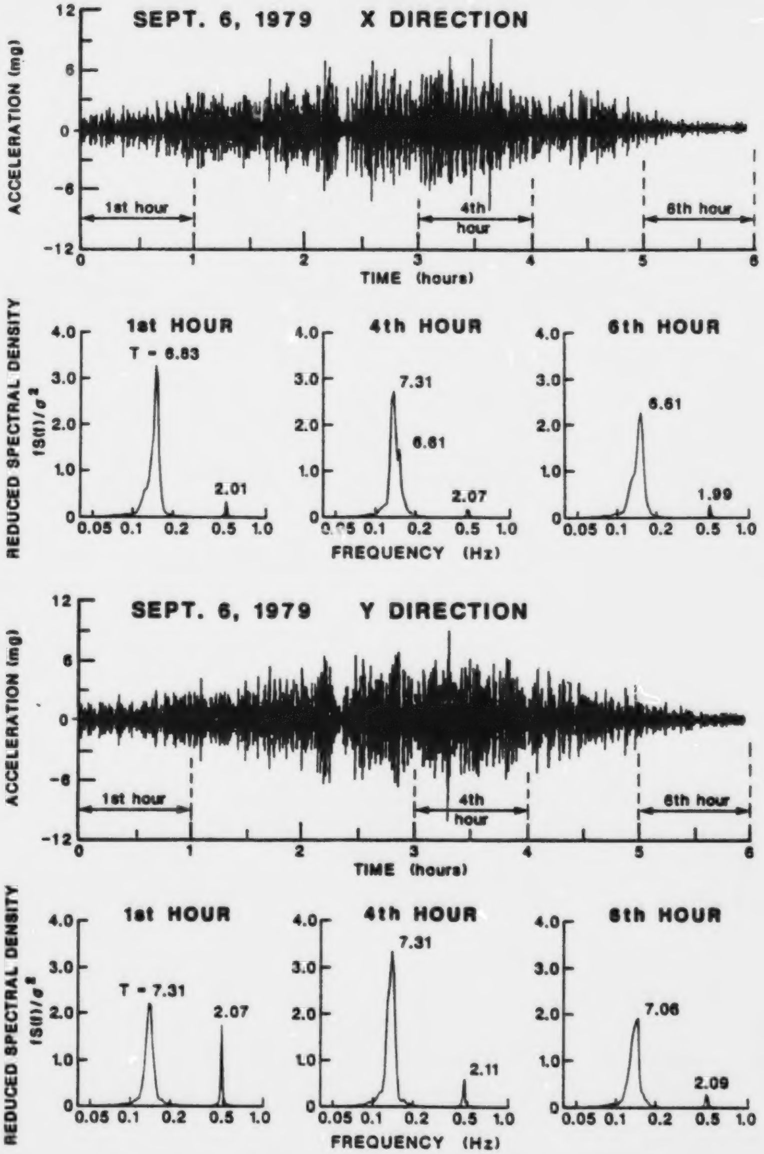

Figure 7: Time Records of Building Acceleration and Corresponding Power Spectra for the Citi-Corp Building During Hurricane David

The building accelerations recorded during Hurricane David were compared with estimates predicted from the aeroelastic wind tunnel model study. One difficulty in these comparisons was the estimation of the wind speed and wind direction actually experienced by the building during the storm. There were no wind sensing instruments on top of the building and the gradient wind speed had to be estimated from available weather data. Unfortunately, the balloon measurements regularly taken at the John F. Kennedy Airport were discontinued for the most windy portion of Hurricane David. As a result, it became necessary to rely on records from surface anemometers at the Newark, LaGuardia and the John F. Kennedy Airports. Best estimates of the variation of the gradient wind speed and wind direction during the storm are shown in Figure 8. During the peak of the storm, winds were from the south with a gradient wind speed in excess of 80 mph (36 m/sec).

The corresponding X and Y rms accelerations at the 63rd floor, estimated from wind tunnel data, are shown in Figure 8 for effective structural damping values of 1 and 4%. The 1% data indicate the hypothetical response of the building with a nominal structural damping of 1% of critical and without the beneficial effects of the TMD. The 4% data are predictions for the building with the TMD operational. In each case, the wind tunnel predictions are shown as bands in order to reflect the uncertainties in the estimated wind speed and wind direction. The actually measured rms accelerations, averaged over successive 10-minute intervals, are shown as points in Figure 8. The full-scale observations are comparable to the values anticipated from the wind tunnel study for an effective damping of 4%. Comparisons of the wind tunnel predictions for structural damping values of 1 and 4% of critical clearly demonstrate the effectiveness of the TMD in controlling the wind-induced motions of this building.

Studies in Aid of Building Rehabilitation

The previous Case Studies describe situations where full-scale observations were effective in confirming the anticipated behaviour of buildings specifically designed to resist wind-induced effects. Another important application is the use of full-scale observations to assist in the rehabilitation of buildings. This important role is demonstrated by .he following two examples. Observed accelerations of a 43-storey building during a significant wind storm are shown in Figure 9 (27). These results are from a study carried out in order to evaluate its dynamic properties of the building, as required in a wind tunnel model study carried out to ascertain its integrity and performance. As shown in Figure 9, the study used three (3) accelerometers positioned at the 41st floor of the building. Accelerometers 1 and 3 were positioned to record motion in the E-W direction due to vibrations in the E-W sway modes and in torsion. Accelerometer 2 was oriented to only measure accelerations in the N-S direction. The accelerometers were switched on manually and recordings were made on FM-tape cassettes. The programme continued over some six months and produced observations from 11 different events.

The full-scale observations clearly showed the coupling between the E-W sway motions and torque. This was expected in view of the eccentricity provided by the masonry core, located at the north end of the building. Recorded periods of vibration indicated a softening of the building with increased response level. This can be seen from Table 3 which summarizes the periods of vibration in the fundamental sway and torsional modes during low and high wind speeds. At low amplitudes, the effective stiffness is significantly higher due to contributions from non-structural components. During higher wind speeds, the periods tend to approch analytical estimates based on the stiffness of the steel frame. The first mode of the building comprises essentially N-S sway, see spectrum in Figure 9. Modes 2 and 3 however are combinations of E-W sway and torsion. Comparisons of the measured accelerations suggested that rigid diaphragm action of the floors is not necessarily achieved, particularly in older buildings. This has implications on the effective stiffness of the building, and its deformation under dynamic wind action.

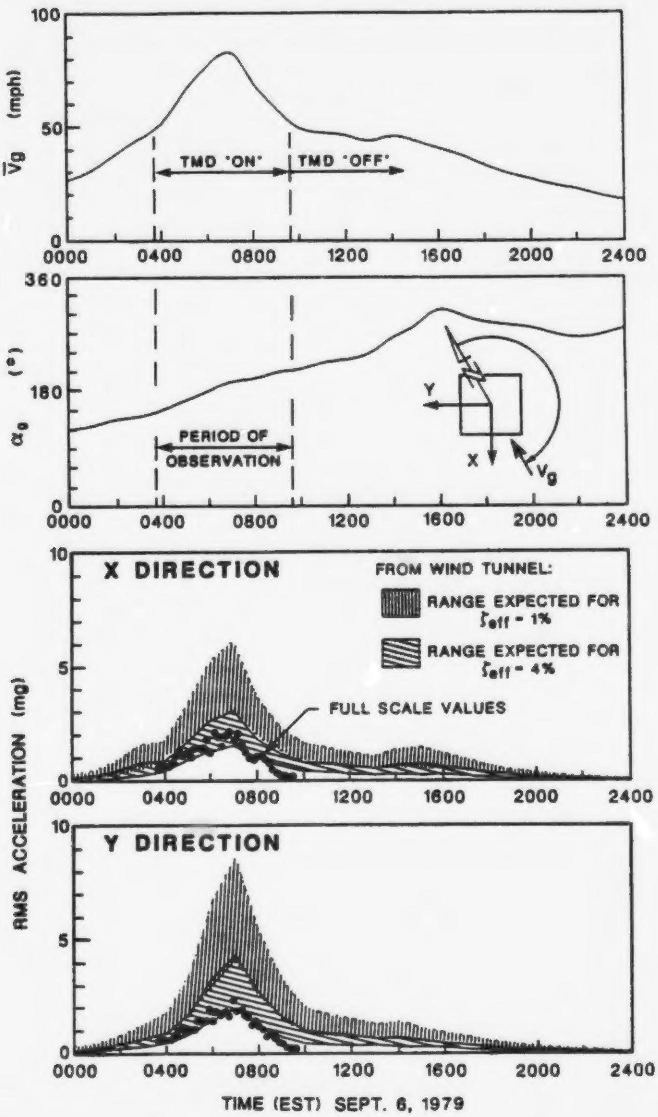

Figure 8: Wind Tunnel and Full Scale Comparisons During Hurricane David - September 6, 1979

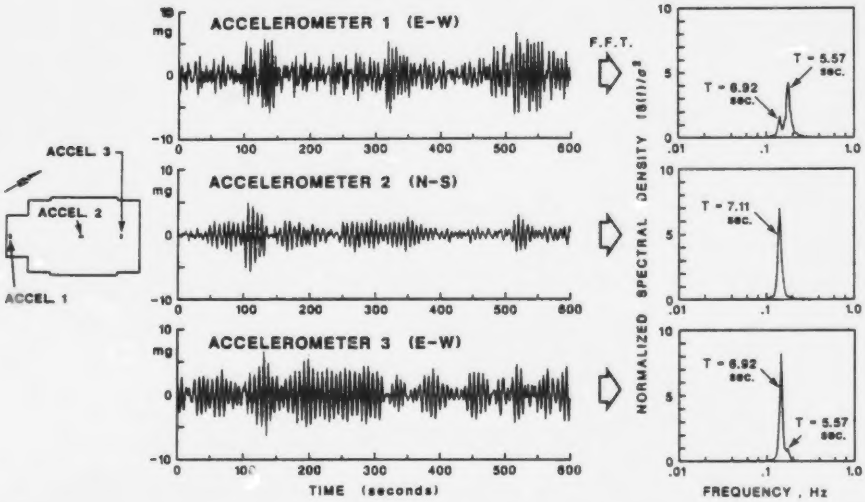

Figure 9: Observed Accelerations and Corresponding Power Spectra of a 43-Storey Building (after ref. 27)

Table 3: Summary of Fundamental Periods of 43-Storey Building (see Figure 9)

Mode	Analytical Estimate (sec)	During Low Winds Ave. (sec)	During Low Winds C. of V. (%)	During High Winds Ave. (sec)	During High Winds C. of V. (%)
1 N-S	9.0	6.26	5.6	7.16	1.4
2 E-W	7.25	6.32	2.4	6.89	1.9
3 Torsion	5.5	4.75	4.0	5.69	3.1

Estimates of the effects of damping were complicated by the coupled E-W and torsion degrees of freedom which made a separation of the second and third modes of vibration very difficult. The structural damping in the first mode, which comprises independent N-S sway, was estimated to be around 3% of critical. This is considered an overestimate in view of the difficulties in obtaining sufficient frequency resolution. Assumptions of stationarity are not valid considering the change in the building periods over the course of a storm. Results of this study illustrated that the dynamic behaviour of a tall building can be determined with a relatively modest instrumentation and monitoring effort. Further details including comparisons of the full-scale response with wind tunnel predictions are given elsewhere (27).

While it is relatively common that the sway and torsional degrees of freedom of a tall building are coupled, in certain situations there can also be coupling between the sway motions. This occurs when the axes of principle stiffness do not correspond to the geometric axes of the building shape. Figure 10 shows the results of full-scale observations for a 33-storey concrete building where the principle axes of stiffness did not correspond to the geometric "long" and "short" directions of the building, as shown. This was clearly noticeable from initial observations with accelerometers oriented along the long and short building axes. To determine the actual alignment of the principle axes of stiffness, two orthogonally oriented accelerometers were systematically rotated by an angle θ_m as shown in Figure 10. Typical spectral estimates of the x_m and y_m accelerations for different values of θ_m are shown in Figure 10. In each case, the spectrum of the measured acceleration contains peaks at the fundamental X and Y-sway modes. The alignment of the principle axes of stiffness X and Y corresponds to the alignment of the accelerometers for which the spectral "cross-talk" between the X and Y-sway modes is a minimum. From this analysis, the principle X axis was approximately 27° clockwise from the long direction of the building.

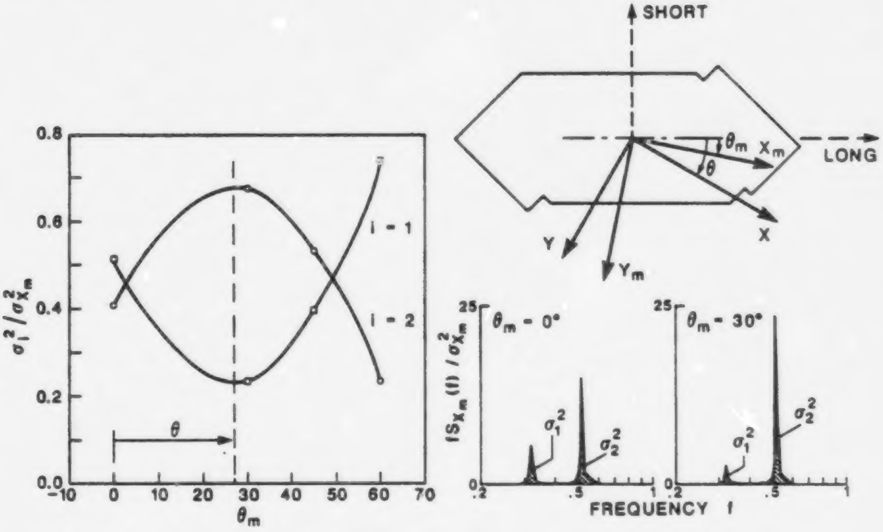

Figure 10: Use of Full Scale Observations to Determine the Principle Axis of Stiffness of a 33-Storey Building

CONCLUDING REMARKS

The paper provided a brief overview of some of the historically noteworthy full-scale observations of buildings and structures under wind action. The objectives of such measurements have varied broadly. Some studies have been highly ambitious with the undertaking to measure many variables over long periods of time. Others have relied on relatively simple instrumentation to capture a few relevant measures of the response. Several case studies were presented to illustrate situations where full-scale measurements have been effective. In some situations, such measurements have provided a valuable reassurance of the performance of a major building or structure. In others, it has added confidence to analytical and wind tunnel procedures used in design. Finally, as demonstrated, full-scale observations can be a valuable design aid in the re-evaluation or rehabilitation of an existing structure.

In the authors' opinion there are clear advantages of keeping the objectives of full-scale measurements simple and uncluttered. The greatest uncertainties usually lie in the wind-induced dynamic response of a structure. Progress can be made in this area by measuring the wind-induced accelerations of the structure and recording them with a manually or automatically activated FM-tape system. Measurements of wind speed and direction are clearly important in situations where comparisons with anticipated response levels are necessary. In the absence of wind data measured well above the aerodynamic influence of the building, progress can be made by estimating the wind speed and wind direction from available weather data.

Finally, it is important to recognize that it is difficult to demonstrate the precise correspondence of full-scale and model. Not only is it difficult to define the complete full-scale input and boundary conditions (wind speed and turbulence for example) but the exact properties of the structure may differ. The long term objective of full scale observations should therefore be to establish a sufficient number of comparisons to indicate general consistency and a general level of reliability. More data are needed to achieve this.

REFERENCES

1. Eiffel, G. Travaux Scientifiques Executes a la Tour de Trois Cents Metres de 1889 a 1900. L. Maretheux, Paris, France.
2. Davenport, A.G. 1986. The Response of Supertall Buildings To Wind. Council on Tall Buildings and Urban Habitat, Second Century of Skyscrapers, Chicago. January.
3. Coyle, D.C. 1931. Measuring the Behaviour of Tall Buildings. Engineering News Records, pp. 310-313.
4. Rathbun, J.G. 1940. Wind Forces on a Tall Building. Trans. ASCE V.105, pp. 1-41.
5. Tschanz, T. and Davenport, A.G. 1983. The Base Balance Technique for the Determination of Dynamic Wind Loads. Paper presented at the 6th International Conference on Wind Engineering, Gold Coast, Australia, March 21-25, 1983, Auckland, New Zealand, April 6-7, 1983, Journal of Wind Engineering and Industrial Aerodynamics, 13(1983), 429-439.
6. Mahmoodi, P., Robertson, L.E., et al. 1987. Performance of Viscoelastic Dampers on World Trade Center Towers. Presented at 6th Annual ASCE Structures Conference, Orlando, Florida, August 17-20.
7. Davenport, A.G., M. Hogan and Vickery, B.J. 1970. An Analysis of Records of Wind-Induced Building Movement and Column Strain Taken at the John Hancock Center (Chicago). Eng. Sc. Res. Rep. BLWT-10-70, The University of Western Ontario, Sept.
8. Dalgliesh, W.A. 1982. Comparison of Model and Full-Scale Tests of Commerce Court Building in Toronto. Proc. International Workshop on Wind Tunnel Modeling in Civil Engineering Applications, Gaithersburg, MD. April.
9. Dalgliesh, W.A., Cooper, K.R., Templin, J.T. 1983. Comparison of Model and Full-Scale Accelerations of a High-Rise Building. Vol. 1 Proc. Sixth International Conference on Wind Engineering, Gold Coast, Australia, March.
10. Dalgliesh, W.A., Rainer, J.H. 1978. Measurements of Wind Induced Displacements and Accelerations of a 57 Storey Building in Toronto, Canada. Proc. 3rd Colloquium on Industrial Aerodynamics, Aachen, Germany, June.
11. Durgin, F.H. and Hansen, R.J. 1987. Full-Scale On-Site Wind-Induced Data From a Tall Building. Presented at 6th Annual ASCE Structures Conference, Orlando, Florida, August 17-20.

12. Isyumov, N., Davenport, A.G. and Monbaliu, J. 1984. CN Tower, Toronto: Model and Full Scale Response to Wind. International Association for Bridge and Structural Engineering (IABSE) 12th Congress, Session VI, September 3-7, Vancouver, B.C.

13. Isyumov, N. and Halvorson, R. 1984. Dynamic Response of Allied Bank Plaza During Alicia. Specialty Conference of the ASCE: Hurricane Alicia: One Year Later. Galveston, Texas, August 16-17.

14. Halvorson, R. and Isyumov, N. 1986. Comparison of Predicted and Measured Dynamic Behaviour of Allied Bank Plaza. Presented at the ASCE Spring Convention, Seattle, Washington, April 7-11.

15. Isyumov, N. and Brignall, J. 1975. Some Full-Scale Measurements of Wind-Induced Response of the CN Tower. Journal of Industrial Aerodynamics, 1 (1975), 213-219.

16. Collins, M.P., Birkemoe, P.C. and Bunjamin, H. 1980. Structural Behaviour of the CN-Tower During a Windstorm. Session 61 on Full-Scale Structural Testing, ASCE, Oct.

17. Monbaliu, J. 1985. Full Scale Observations at the CN-Tower, Toronto, Canada. M.E.Sc Thesis, The University of Western Ontario.

18. Isyumov, N., Monbaliu, J. and Davenport, A.G. 1985. Full-Scale and Wind Tunnel Measurements Relevant To the Wind-Induced Response of the CN-Tower, Toronto, Canada. Presented at 6th Coll. on Industrial Aerodynamics, Aachen, June 19-21.

19. Georgiou, P. 1984. Simulation of Hurricane Wind Speeds. ASCE Specialty Conference 'Hurricane Alicia; One Year Later', August 16-17, Galveston, Texas.

20. Powell, M.D. and Georgiou, P.N. 1987. Response of the Allied Bank Plaza Tower During Hurricane Alicia (1983). Journal of Wind Engineering and Industrial Aerodynamics, 26(1987), 231-254.

21. Isyumov, N., Holmes, J.D., Surry, D. and Davenport, A.G. 1975. A Study of Wind Effects For the First National City Corporation Project - New York, U.S.A. The University of Western Ontario, Engineering Science Research Report, BLWT-SS1-75.

22. McNamara, R.J. 1977. Tuned Mass Dampers For Buildings. ASCE Journal of Structural Division, Vol. 103, Sept.

23. Wiesner, K.B. 1979. Tuned Mass Dampers to Reduce Building Sway. ASCE Boston Convention, April.

24. Petersen, N.R. 1979. Design of Large Scale Tuned Mass Dampers. International IUTAM Symposium on Structural Control, University of Waterloo, Ontario, Canada, June.

25. Petersen, N.R. 1981. Using Servohydraulics to Control Hi-Rise Building Motion - The CityCorp TMD System. U.S. National Conference on Fluid Power, Chicago, October.

26. Masciantonio, A., Isyumov, N. and Petersen, N.R. 1987. Wind-Induced Response of a Tall Building and Comparisons with Wind Tunnel Predictions. Presented at the 6th Annual ASCE Structures Conference, Orlando, Florida, August 17-20.

27. Dobryn, D., Isyumov, N. and Masciantonio, A. 1987. Prediction and Measurement of Wind Response: Case Story of a Wind Sensitive Building. Presented at the 6th Annual ASCE Structures Conference, Orlando, Florida, August 17-20.

WIND INDUCED MOTIONS OF BUILDINGS

PETER A. IRWIN, VINCENT FERRARO AND GARY K. STONE
ROWAN WILLIAMS DAVIES & IRWIN Inc.
650 WOODLAWN ROAD WEST
GUELPH, ONTARIO

ABSTRACT

This paper discusses the state of knowledge of wind induced motions in tall buildings. Existing criteria for occupant comfort and tolerance levels are reviewed. Available techniques to estimate building motions are discussed, including wind tunnel measurements and code based calculations. An alternate calculation technique to the code is presented. Comparisons between calculation and wind tunnel measurements are presented and methods of mitigating excessive building motions are discussed.

1. INTRODUCTION

For tall buildings the magnitude of wind induced motions is an important design consideration. The consequences of excessive motion can be tenants concerned about the motions they perceive and noises they hear, cracking of partitions, slapping of elevator cables and problems with the curtainwall system. Many buildings now being designed are wind tunnel tested and, as part of the wind tunnel investigation, the motions under high wind conditions are assessed. Rowan Williams Davies & Irwin Inc. (RWDI), formerly the wind tunnel division of Morrison Hershfield Limited, has undertaken numerous investigations of this type and in this paper results for over 40 buildings are compared with building accelerations predicted by formulae given in the Commentary to the National Building Code of Canada. In carrying out this comparison some insights into the important parameters governing the building motions, as manifested by the acceleration, are gained. Alternate formulae for predicting accelerations are also examined.

In assessing whether a given building has acceptable behaviour it is clearly necessary to compare it with appropriate criteria. Current criteria and their origins are therefore discussed in Section 2. Also, where a building is predicted at the design stage to be headed for a motion problem it is useful to know what options are available for reducing motions. Therefore the final section of the paper reviews this aspect.

2. CRITERIA FOR WIND INDUCED MOTIONS

People sense building motions in three ways: i) horizontal accelerations cause forces on the body which affect the balance organs; ii) motions of the building relative to fixed objects in the distance and motions of objects such as hanging plants can be seen; and iii) the building motions can create noises such as creaking and slapping of elevator cables. Ideally criteria for acceptability would incorporate all these factors but the current state of the art is to base criteria on the magnitude of horizontal accelerations only. It is worth noting that motion is most likely to be detected visually by occupants when there is significant torsional action.

Human sensitivity to horizontal accelerations is highly variable from person to person and depends on their activity. The data of Chen and Robertson(1) indicate that at typical building frequencies, the most sensitive are able to perceive peak acceleration values as low as 2 milli-g while standing and the least sensitive may not perceive accelerations until they exceed 20 milli-g if they are sitting. Thus, it is necessary to base criteria on an average of the population. Chang(2) investigated the question of how to estimate building accelerations and suggested using the 10 year return period wind as the condition under which to do the evaluation.

An important milestone in setting acceleration criteria was the publication of the paper by Hansen, Reed and Vanmarcke(3). They surveyed occupants of two buildings that had experienced wind storms to arrive at a criterion for tolerable motions in a building rather than examining the question of what is merely perceptible. They found, as might be expected, that greater accelerations are tolerable provided they occur on a less frequent basis. Thus their criterion was expressed in the form: "The return period for storms causing an rms horizontal acceleration at the building top, which exceeds $\bar{\sigma}^*$, shall not be less than R^* years". They tentatively set $\bar{\sigma}^*$ at 5 milli-g for $R^* = 6$ years and indicated the rms acceleration that is compared with $\bar{\sigma}^*$ should be a representative average over the top occupied floor. For a building that lies on this criterion it was estimated that 2% of the occupants in the top third of the building would find the building objectionable.

Codes that address building motions appear to rely heavily on these results. The National Building Code of Canada(4) gives a range of 10 to 30 milli-g for the peak acceleration in the 10 year return period wind. Assuming a peak factor of 3.5 to convert from rms to peak acceleration, the middle value of this range, i.e. 20 milli-g, converts to an rms acceleration of 5.7 milli-g. Adjusting for the difference between 10 and 6 year return period one arrives at a value very close to the 5 milli-g value proposed by Hansen et al. The International Organization for Standardization(5) (ISO) proposes criteria very similar to the 5 milli-g, 6 year return period criterion. The ISO document has the criterion varying slowly with building natural frequency and is based on using a 5 year return period. For a typical tall building with natural frequency of 0.2 Hz the criterion is 5 milli-g for the 5 year return period, i.e. close to Hansen et al's 5 milli-g rms value for the 6 year return period.

At RWDI our approach is to use a 10 year return period peak acceleration of 21 milli-g as a guideline for comfort for office buildings. This can be derived from Hansen et al's result by first adjusting their 5 milli-g rms to 6 milli-g to account for the difference between the 6 year and 10 year return periods and then assuming the representative peak acceleration is 3.5 times the rms acceleration (3.5 x 6 = 21 milli-g). In cases where the accelerations exceed the guideline, discussions are initiated with the building owner to indicate that more than 2% of his tenants may find the motion behaviour of the building objectionable and to arrive at a satisfactory compromise between increased structural cost and comfort for tenants. For example, if the 10 year return period acceleration is allowed to be as high as 30 milli-g then the data of Hansen et al would indicate that approximately 5% of the occupants in the top third of the building would object to the general level of wind induced motions of the building. The data of Goto(6) indicate that over 30% of occupants would object to the building if the 10 year peak acceleration was at the 60 milli-g level. For residential buildings there is little data to give guidance to appropriate criteria, but since they are more likely to remain occupied during a severe storm, the criteria should probably be more strict than for office buildings.

3. SUMMARY OF WIND TUNNEL METHODOLOGY

This paper uses building motion predictions obtained from wind tunnel studies employing both aeroelastic and high-frequency force-balance modelling techniques. The intention of this section is to describe briefly the test procedures used in these studies. References are provided for more detailed descriptions.

Aeroelastic models simulate the flexibility, mass and damping of the full scale building. Two basic types of aeroelastic models are used. These are, two-degree-of-freedom, models, which simulate only linear sway vibration modes, and multi-degree-of-freedom aeroelastic models, which simulate the important lower sway and torsional modes of vibration. Descriptions of aeroelastic modelling techniques are by Irwin(7), Isyumov(8) and Templin and Cooper(9). Using this approach, the model motions are a scaled representation of the full scale building motions. Accelerometers are used to measure the individual sway and torsional acceleration components of the models.

The high-frequency force-balance technique is an alternative approach to the aeroelastic model method for determining the dynamic response of a building to the action of wind. This approach is suitable in cases where aerodynamic damping effects are expected to be small and where the main components of the response are attributed to the fundamental vibration modes. In practice, this method is applicable to most building geometries. A lightweight, rigid model of the building's geometry is constructed, involving no further scaling considerations, and mounted on a stiff sensitive flexure system. This approach allows the direct measurement of the aerodynamic load functions in each of the fundamental modes without distortions due to resonant vibrations of the model. Descriptions of the high-frequency force-balance technique have been given by Whitbread(10) and by Tschanz(11). A modal analysis approach, analogous to the gust factor method (as in National Building Code of Canada, for example) is used to predict the responses of the actual structure. The force-balance technique is now used for most wind tunnel dynamic studies instead of the aeroelastic model approach due to economic considerations.

The wind tunnel data presented in this paper are for model studies conducted at geometric scales of either 1:400 or 1:500 in turbulent boundary layer flow conditions . The tests were performed in the presence of detailed models of the structures surrounding each building site within a radius of about 600m. The influence of the terrain upwind of the surrounding models on the wind flow characteristics at each building site was appropriately simulated. The wind simulation techniques are described by Irwin(12).

The wind tunnel measurements were analyzed and combined with the meteorological data appropriate for each building's location in order to determine predicted total acceleration levels. The combining of the wind tunnel data with meteorological data was based on the methods described by Lepage and Irwin (13), Irwin(14) and Davenport(15).

4. COMPARISON OF EMPIRICAL EXPRESSIONS WITH WIND TUNNEL PREDICTIONS

4.1 Comparison with NBCC Expressions The wind tunnel techniques, described in the previous section, represent the most accurate approach currently available to designers for predicting accelerations in buildings. The many factors affecting accelerations can be properly accounted for including exterior shape, effects of surrounding structures and effect of terrain upwind of the site. In the case of the high-frequency force-balance technique the effect of changing essential building parameters, such as damping, mass and frequencies, on accelerations can be assessed quickly and repeatedly. For single or multi degree-of-freedom aeroelastic models, the effect on accelerations of couple mode shapes can be included in the model building's behaviour. Finally, an estimate of torsional motion, previously identified as an important component of occupants' perception of motion, can be obtained.

The purpose of this section is to compare wind tunnel results with the simplified calculations outlined by the National Building Code of Canada (NBCC) and, in Section 4.2, with alternate expressions derived from wind buffeting theory. Although both calculation procedures are based on similar random vibration and buffeting theories, the former uses more simplifications in arriving at the final expressions. Both methods rely to some degree on empirical data.

Acceleration levels for a ten year return period near the top of 43 buildings tested at RWDI's wind tunnel laboratory have been estimated using the expressions for across wind and along wind motions described in the NBCC(3) and listed below.

Across Wind (Lift)

$$a_W = n_W^2\, g_p \sqrt{WD}\,\left(a_r/(\rho_B\, g \sqrt{\beta_W})\right) \tag{1}$$

Along Wind (Drag)

$$a_D = 4\pi^2\, n_D^2\, g_p\, (\Delta/C_g)\, (K\, S\, F/C_e \beta_D)^{1/2} \tag{2}$$

where

n_W, n_D = lift and drag fundamental natural frequencies respectively (Hz)
β_W, β_D = lift and drag damping ratios, respectively
W, D = lift, drag plan dimensions respectively (m)
a_W, a_D= peak lift, drag accelerations respectively (m/s^2)
ρ_B = average building density (kg/m^3)
a_r = $78.5 \times 10^{-3} (V_H/n_W\sqrt{WD})^{3.3}$, N/m^3
V_H = mean wind speed at height, H of the building (m/s)
Δ = maximum wind induced drag deflection at top of building (m)
g = gravity acceleration (m/s^2)
g_p = peak factor
K = surface roughness factor
S = size reduction factor (see Appendix A)
F = gust energy ratio at $n_o = n_D$ (see Appendix A)
C_e = exposure factor (see Appendix A)

C_g = gust factor
q = wind pressure at reference height of 10 metres, Pascal

The resultant peak acceleration $\hat{a}_R$ is obtained simply as

$$\hat{a}_R = \sqrt{a_W^2 + a_D^2} \qquad (3)$$

For each building two values of $\hat{a}_R$ are obtained corresponding to the assumed wind direction being incident to orthogonal building faces. Also, for each building, the code values are plotted in Figure 1 against the resultant acceleration measured in the wind tunnel test. A peak factor, g_p of 3.5 is assumed in all cases. The symbols used in the figure represent the approximate plan form of the top third of each building. These dimensions are chosen because the top third of a building undergoes most of the deflection and motion in responding to wind loading. In Figure 1 the vertical and horizontal axes illustrate calculated (NBCC) values and values determined by wind tunnel test respectively. The 45 degree diagonal line represents the ideal case where code calculations and measured values are equal, i.e. the slope and the ratio = 1.0. The more inclined dashed line with slope of 1.6 represents the actual average ratio for the same 43 buildings. The coefficient of variation (COV) of the ratios relative to the ideal 45 degree line is 0.92 and the COV relative to the actual average is 0.46.

The code formulae are based on numerous approximations not present in the wind tunnel measured values. The most important of these include:

(i) The code does not account for the usually moderating effect of wind direction relative to building orientation, i.e. the directions for which the building is most sensitive often do not coincide with directions for which strong winds are most common.

(ii) The code does not account for variations in building cross sectional shape.

(iii) The code calculations do not have a provision for torsional accelerations.

(iv) Since the peak predicted ten year accelerations in two orthogonal directions do not usually occur simultaneously a reduction factor would be required in calculating the resultant acceleration. The code does not address the issue. The wind tunnel technique used at RWDI automatically includes this factor by measuring instantaneous accelerations in both sway directions and in torsion.

(v) Since the effects of (iii) and (iv) are in opposite senses and are often of similar magnitude, no attempt has been made in this paper to account for either effect in using the code approach.

The results presented in Figure 1 indicate that for most buildings the code is likely to significantly overestimate the actual measured accelerations, sometimes by factors of 2 or more. Although this magnitude of overestimation is partly desirable to account for inherent uncertainty in random behaviour of the wind and lack of exact definition of the surroundings, among other reasons, the scatter is due in part to simplifications used in the governing equations. For instance, the cross sectional building area is approximated by W and D, the correlation length of wind is only approximately included through the size reduction factor, S, and aerodynamic damping is omitted altogether. Although usually a small quantity, aerodynamic damping can make as much as a 20% difference on accelerations of some buildings. With the intent of examining possible improvements in calculation procedure the formulae of the next section are introduced.

4.2 Comparison With Alternate Expressions Based on the theories of random vibrations and wind buffeting of structures, expressions have been derived by RWDI for the estimation of accelerations in across wind, and along wind, directions. The formulae are:

Across Wind (Lift)

$$a_L = 0.1466 \cdot \frac{n_L^2 B^{11/6} F_\varphi^{1/2}}{\bar{M}_L H^{1/2} \zeta^{1/2} L_1^{1/3}} \cdot \frac{\bar{U}^{3.83}}{|\bar{U}+3|} \cdot \frac{I_V |C_L'| F_{AV}}{|1+A_L|^{1/2}} \qquad (4)$$

Along Wind (Drag)

$$a_D = 0.1424 \cdot \frac{n_D^2 W^{11/6} F_\varphi^{1/2}}{\bar{M}_D H^{1/2} \zeta^{1/2} L_1^{1/3}} \cdot \frac{\bar{U}^{3.83}}{|\bar{U}+3|} \cdot \frac{I_U C_D F_{AU}}{|1+A_D|^{1/2}} \qquad (5)$$

where

n_L, n_D = fundamental natural frequencies in lift and drag (Hz)
B, W = depth and width of building near the top third of the building (m)
F_φ = mode shape factor (dimensionless, = 0.333 for linear mode)
$\bar{U}$ = reduced velocity (= $U/(n_L\ B)$ in Eq. 4 and = $U/(n_D\ W)$ in Eq. 5)
U = wind speed at building height (m/s)
H = building height (m)
L_1 = turbulence length scale (see Appendix A)
I_V, I_U = turbulence intensities in across wind and along wind respectively
C_L', C_D = lift curve slope and drag coefficient respectively (see Appendix A)
F_{AV}, F_{AU} = correction factors for correlation length of the wind (see Appendix A)
ζ = structural damping
$\bar{M}_L$, $\bar{M}_D$ = $\rho_s W/(3\rho B)$, $\rho_s B/(3\rho W)$ (see Appendix A for more general expressions)
A_L, A_D = ratio of aerodynamic to structural damping for the lift and drag directions respectively (see Appendix A)

These expressions differ from those of the NBCC in several ways.

(i) The across wind response depends heavily on the lift curve slope ($C_L' = d\,C_L/d\psi$ where ψ = wind direction) and this parameter is specifically identified in the acceleration formula. C_L' is a function largely of building shape. The drag coefficient, also a function of building shape, is specifically identified in the along wind expression.

(ii) The turbulence intensity is specifically identified in its across wind (I_V) and along wind (I_U) components.

(iii) The aerodynamic damping is included in approximate form.

These expressions were combined as in section 4.1 to obtain a peak acceleration $\widehat{a_R}$ from the rms acceleration and this was compared with wind tunnel data in a similar manner to that in Figure 1. The degree of scatter appeared similar but by optimizing C_L' to a value of 2.0 the C.O.V. of the formulae predictions about the wind tunnel predictions was reduced to 0.37. In this investigation, C_D was left set at 1.3.

Comparison of the COV of 0.37 for these results to the COV of the NBCC type of formula i.e. COV = 0.46, indicates a marginal improvement in the ability of the present equations to predict acceleration levels. Further improvements might possibly be obtained by categorizing building shapes with corresponding values of the shape dependent parameters C_L' and C_D and this is currently being investigated.

5. METHODS FOR REDUCTION OF BUILDING MOTION

From the previous section it is clear that key structural factors affecting the building's susceptibility to motions are its natural frequencies, its mass and its damping. By increases in any of these parameters building motions can be reduced. The dependence of the peak acceleration on wind speed and these parameters can be approximately expressed as

$$a = c \frac{U^{\mu}}{M \, n^{\mu-2} \zeta^{1/2}}$$

where

c, μ = constants
U = mean wind speed (averaged over about 10 minutes)
n = natural frequency
ζ = damping ratio
M = mass of the building

If we use the NBCC value of 3.3 for μ for illustrative purposes we can make a number of interesting deductions. For example, if stiffness is added to the structure, thereby increasing n, and if this is done with negligible change in mass M, then the acceleration will be reduced in proportion to $1/n^{1.3}$. On the other hand, if mass is added throughout the building without adding to the stiffness then, since in this situation n goes down as $1/M^{1/2}$, the net result is that the acceleration forces go down as $1/M^{0.35}$. However, if the addition of mass is in the form of structurally active components and is accompanied by a proportional increase in stiffness, then in this case n does not change and the acceleration goes down as 1/M. These cases are somewhat hypothetical but in a real case the above formula is useful during structural design in examining combined changes in mass, stiffness and damping, particularly where initial wind tunnel results have already provided the values of c and μ.

For most buildings it is possible to obtain acceptable performance from the point of view of wind induced motions by adjustments to mass and stiffness. In fact, in the majority of cases the normal application of code loads results in structures that are already adequate from a motion point of view. It is only the more slender and lightweight buildings where such adjustments are sometimes necessary.

However, for the most tall and lightweight buildings the adjustments to mass and stiffness needed to keep wind induced motions under control can become large and costly. In these cases, it is beneficial to consider ways of increasing the damping ratio ζ. A number of methods have been proposed and have been implemented in some buildings. Increasing damping is particularly effective in combating motions induced by vortex shedding. This is illustrated in Figure 2 which shows some results of an exploratory wind tunnel study by RWDI on a 'supertall' building of height 760m and width (in the top portion) 72m. The study was on a 1:600 scale aeroelastic model. Figure 2 shows the peak acceleration as a function of wind speed, solid curves being for assumed natural sway periods in both principal directions of 20 seconds and the broken curves being for sway periods of 15 seconds. Examining the three curves for the 20 second periods it can be seen that at a damping of $\zeta = 0.01$ a high peak acceleration of 60 milli-g occurs at a wind speed of 35 m/s. Shortening the period to 15 seconds, which represents a substantial increase in structural cost, has the effect of moving the peak response to a higher wind speed. However, the accelerations would still be excessive if we apply the 20 milli-g criterion on a once in 10 years basis and assuming the 10 year return period wind speed at the building top to be 41 m/s. A better response would be obtained by leaving the building stiffness (and hence period) unchanged and increasing the damping to $\zeta = 0.04$. At this value of damping the strongly peaked response characteristic of vortex shedding excitation is virtually eliminated.

The question that then arises is: Is it less costly to increase structural stiffness and mass or to build in additional damping? The answer depends greatly on the method by which damping is introduced. Two methods that have been used are:

i) Tuned Mass Dampers, examples being the Citicorp Building in New York for which the damper was built in from the outset, and the John Hancock Building in Boston in which it was retrofitted.

ii) Visco-Elastic Dampers, examples being the World Trade Center towers in New York, and the Columbia Center in Seattle.

The Tuned Mass Damper (TMD) consists essentially of a secondary mass of order 1% of the building's generalized mass that is attached to the main structure near the building's top via a spring suspension system and viscous dampers. The natural frequency of the secondary mass spring damper system is tuned to a value very close to the natural frequency of the mode of vibration of the building it is desired to damp. If the tuning of the damper is optimized such a damper has a similar effect to increasing the viscous type damping of the main structure several fold. An excellent description of the application of a TMD to the Citicorp building has been given by Wiesner(16) of LeMessurier Consultants. In that case the ratio of damper mass (a 373,000 kg concrete block) to building generalized mass was about 0.02 and the damping ratio of the damper itself was 0.14. The springs consisted of pneumatic actuators using compressed nitrogen.

The cost of the Citicorp TMD is understood to have been of the order of \$4M to \$5M illustrating that the cost is not insignificant. In the case of the 72 Storey Interfirst Plaza building, Dallas, the design studies, including aeroelastic model tests at RWDI's wind tunnel laboratory, showed that in that case it was more attractive overall to control motions by adding structural stiffness than a TMD when costs were compared.

Other concepts for TMD's have been examined although they have not yet been implemented on buildings. These include masses hung by cables or a rigid arm, i.e. using pendumlum action, to provide stiffness and hydraulic dampers to provide damping. For a building with a 7 second period the length of the pendulum would need to be approximately $9.81\,(7/2\pi)^2 = 12$m long. Fine tuning of this type of TMD can be achieved by adjusting the pendulum arm length.

Another type of TMD concept that has been proposed uses the damping produced by liquid sloshing, rather as done in ships to reduce rolling. Modi and Welt(17) have published results demonstrating suppression of vortex excitation on a wind tunnel model by this method. The ratio of liquid mass to main mass in their case needed again to be a few percent of the main mass to be effective. It was important to ensure the natural 'sloshing' frequency of the damper coincided with that of the main structural mass.

Besides the mass, stiffness and damping the remaining variables affecting the building response are its shape and surroundings. It is not intended to go into these subjects here. However, it is worth mentioning that some buildings are subject to vortex excitation and this type of excitation is sensitive to details of shape. One way of eliminating vortex excitation is to design openings in the top third of the structure to let the wind pass through. Experience on structures other than buildings indicates that to be effective, the area of the openings should be of order 30% of total area of the top third of the structure which imposes significant constraints on the aesthetic design of the building. Another approach is to incorporate aerodynamic devices such as corner slots, turning vanes, corner stepping or chamfering and spoilers. Recent investigations of these devices are described in References 18 to 20.

References

1.	Chen, P.E. and Robertson, L.E.	"Human Perception Thresholds of Horizontal Acceleration Journal of the Structural Division, ASCE, Vol. 98, ST8, July 1972, pp. 1681 - 1695.
2.	Chang, F.K.	"Human Response to Motions in Tall Buildings", Journal of the Structural Division, ASCE, Vol. 99, No. ST6, 1973, pp. 1259 - 1272.
3.	Hansen, B.J., Reed,J.W. and Vanmarcke,E.H.	"Human Response to Wind-Induced Motion of Buildings", Journal of the Structural Division, ASCE, Vol. 99, ST7, 1973, pp. 1589 -1605.
4.	Associate Committee NBCC, NRC	"The National Building Code of Canada" and "The Supplement to the National Building Code of Canada", 1985.
5.	International Organization for Standardization	"Guide to the Evaluation of the Response of Occupants of Fixed Structures, Especially Buildings and Off-Shore Structures, to Low Frequency Horizontal Motions (0.063 to 1.0 Hz)", ISO, Draft International Standard, 1982.
6.	Goto, T.	"Studies on Wind-Induced Motion of Tall Buildings Based on Occupant Reactions", Proceedings, 6th International Conference on Wind Engineering, Australia and New Zealand, 1983, Session 5, pp. 241-252.
7.	Irwin, P.A.	"Model Studies of the Dynamic Response of Tall Buildings to Wind", Proceedings CSCE Annual Conference, Edmonton, May 27 - 28, 1982.
8.	Isyumov, N.	"Aeroelastic Modelling of Tall Buildings", Proceedings, International Workshop on Wind Tunnel Modelling for Civil Engineering Applications", National Bureau of Standards, Gaithersburg, Cambridge University Press, 1982.

9. Templin, J.T. and Cooper, K.R. "Design and Performance of a Multi-Degree of Freedom Aeroelastic Building Model, 4th Colloquium on Industrial Aerodynamics, Aachen, June 18 - 20 1980, Part 2, pp. 123 - 135.

10. Whitbread, R.E. "The Measurement of Nonsteady Wind Forces on Small Scale Building Models", Proceedings - 5th International Conference on Wind Engineering, Heathrow, 1975.

11. Tschanz, T. "Measurement of Total Dynamic Loads Using Elastic Models of High Natural Frequency", Proceedings, International Workshop on Wind Tunnel Modelling for Civil Engineering, Applications, National Bureau of Standards, Gaithersburg, Cambridge University Press, 1982.

12. Irwin, P.A. "The Design of Spires for Wind Simulations" Journal of Wind Engineering and Industrial Aerodynamics, 7, 1981, pp. 361 - 366.

13. Lepage, M.F. and Irwin, P.A. "A Technique for Combining Historical Wind Data with Wind Tunnel Results to Predict Extreme Wind Loads", Proceedings of the 5th U.S. National Conference on Wind Engineering, Lubbock, Texas, 1985.

14. Irwin, P.A. "Pressure Model Techniques for Cladding Loads", Proceedings 7th International Conference on Wind Engineering, Aachen, 1987.

15. Davenport, A.G. "The Prediction of Risk Under Wind Loading", Proceedings of the 21st Conference on Structural Safety and Reliability, Munich, 1977.

16. Wiesner, K.B. "Tuned Mass Dampers to Reduce Building Motion", ASCE Spring Convention and Exposition, Boston, 1979, Preprint 3510.

17. Modi, V.J., and Welt, F. "Damping of Wind Induced Oscillations through Liquid Sloshing" Proceedings, 7th International Conference on Wind Engineering, Aachen, 1987.

18. Shiraishi, N., Matsumoto, M. Shirato, H. and Ishizaki, H. "On Aerodynamic Stability Effects for Bluff Rectangular Cyclinders by Their Corner Cut", Proceedings 7th International Conference on Wind Engineering, Aachen, 1987.

19. Kwok, K.C.S. "Effect of Building Shape on Wind-Induced Response of Tall Buildings", Proceedings, 7th International Conference on Wind Engineering, Aachen, 1987.

20. Ogawa, K., Sakai, Y., and Sakai, F. "Aerodynamic Device for Suppressing Wind Induced Vibration of Rectangular Section Structures", Proceedings, 7th International Conference on Wind Engineering, Aachen, 1987.

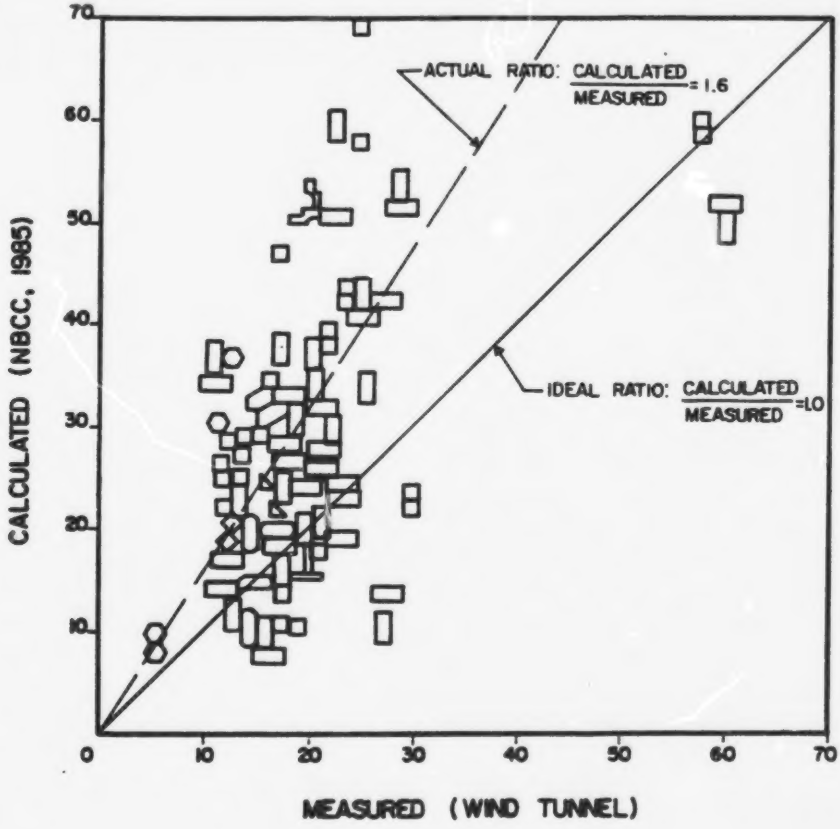

NOTE: SYMBOLS REPRESENT APPROXIMATE BUILDING SHAPES
SYMBOL ORIENTATIONS ARE RELATIVE TO WIND DIRECTION
REPRESENTED BY A HORIZONTAL LINE ON THE PAGE

FIGURE 1

COMPARISON OF CALCULATED TO MEASURED BUILDING ACCELERATIONS (milli-g)

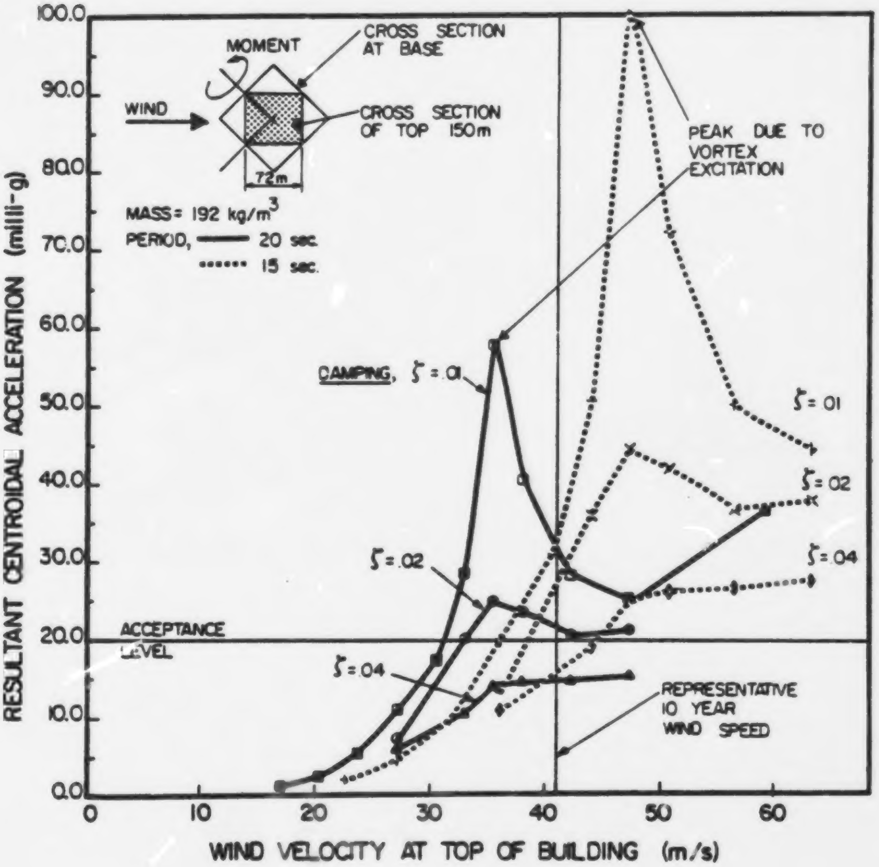

NOTE: WIND TUNNEL RESULTS FOR A PROPOSED 750m HIGH BUILDING

FIGURE 2
EFFECT OF DAMPING AND PERIOD
ON BUILDING ACCELERATIONS

APPENDIX A

ADDITIONAL DETAILS OF EXPRESSIONS IN SECTION 4.1 AND 4.2

$$S = (\pi/3)\left[1/(1 + 8\,n_o\,H/3U)\right]\left[1/(1 + 10\,n_o\,w/U)\right] \tag{A1}$$

$$F = x_o^2/(1 + x_o^2)^{4/3};\ x_o = 1220\,n_o/U \tag{A2}$$

$$C_e = (H/10)^{0.28}\text{: open exposure} \tag{A3}$$

$$C_e = 0.5\,(H/12.7)^{0.5}\text{: suburban exposure} \tag{A4}$$

$$C_e = 0.4\,(H/30)^{0.72}\text{: urban exposure} \tag{A5}$$

$$F_{AV} = (F_{JV}/(1 + 0.0565\,\overline{U}_1^2)^{7/3})^{1/2} \tag{A6}$$

$$F_{JV} = (1 + 0.0173\,\overline{H}^{1.79}\,\overline{U}_H^{2.348})/(1 + 0.357\,\overline{U}_H^{1.189}) \tag{A7}$$

$$F_{AU} = (F_{JU}/(1 + 0.0565\,\overline{U}_1^2)^{1/2}\,(1 + 0.0141\,\overline{U}_1^2)^{5/6}))^{1/2} \tag{A8}$$

$$F_{JU} = (1 + 0.055\,(1 + 1/(2\overline{H}))^{-5}\,\overline{U}_H^P/(1 + 0.055\,\overline{U}_H^{1.734})) \tag{A9}$$

$$I_U = 0.11\,(Z_G/H)^{\alpha} \tag{A10}$$

$$I_V = 0.7\,I_u \tag{A11}$$

$$L_1 = 11.0\sqrt{H}\ \text{,meters} \tag{A12}$$

$$A_L = \overline{U}\,F_{\varphi}\,C_L'/25.1\,\overline{M}\,\zeta \tag{A13}$$

$$A_D = \overline{U}\,F_{\varphi}\,C_D/12.6\,\overline{M}\,\zeta \tag{A14}$$

where in addition to symbols in the main text

$\overline{H} = H/L_1$

$\overline{U}_1 = U/(n_o\,L_1)$; $n_o = n_L$ or n_D

$\overline{U}_H = U/(n_o\,H)$

$P = 2.585\,(1/(2\,\overline{H}) + 0.11)^{0.181}$

z_G = gradient height

α = 0.14, 0.25. 0.36 for open, suburban and urban exposures respectively

NOTE: The full definitions of F_{φ}, $\overline{M}_L$ and $\overline{M}_D$ are

$$F_{\varphi} : \frac{1}{H}\int_0^H \phi^2\,dz$$

$$\overline{M}_L, \overline{M}_D = \int_0^H m\,\phi^2 dz\Big/\left(\rho B^2 H\right)\ ,\ \int_0^H m\,\phi^2 dz\Big/\left(\rho W^2 H\right)$$

where m = mass per unit height, ρ = air density and ϕ = mode shape (= 1.0 at top of building). The expressions in the main text for $\overline{M}_L$ and $\overline{M}_D$ apply strictly only to rectangular shaped buildings with uniform mass distributions and linear mode shapes.

FUNDAMENTAL STUDY ON TUNED LIQUID DAMPER (TLD)
- A New Damper for Building Vibrations -

Y. Fujino, B.M. Pacheco, P. Chaiseri, and L.M. Sun

Department of Civil Engineering
University of Tokyo
Tokyo, Japan

ABSTRACT: A new kind of damper, relying on motion of shallow liquid in a rigid cylinder, is experimentally studied. Prototype-sized containers with diameters 40 cm and 60 cm and partially filled with water are attached to a single-degree-of-freedom structural model with natural period of 2 sec. The damper effect is measured in terms of the increase in the logarithmic rate of decrement of free oscillation of the main structure. It is seen that, for large damping effect at small amplitude of structural vibration, it is necessary to tune the fundamental sloshing period of the liquid to the natural period of structure; hence the name Tuned Liquid Damper. It is found that breaking of surface waves, while highly dependent on structural vibration amplitude, is the main mechanism of energy dissipation. Also investigated are the effects of: ratio of liquid frequency to structure frequency; liquid viscosity; container bottom roughness; container roof height; ratio of liquid mass to structure mass; and container diameter.

1. INTRODUCTION

The growing use of high-strength materials and welded joints leads to relatively light, flexible, and weakly damped structures. Structural vibrations then emerge as a potential problem in serviceability or even safety of buildings, towers, or bridges. One way to control such vibrations is by base isolation in case of ground motions [Reference 1].

Mechanical dampers are another option when isolation is impossible and suppression is required [Reference 2]. Tuned Mass Dampers (TMD) are a class of such devices for absorbing and dissipating vibrational energy. TMD now finds practical application in buildings and bridges but not without problem areas of its own, such as sensitivity of device to external conditions, maintenance requirements, or reliability of automatic activation.

The alternative damper discussed herein and named Tuned Liquid Damper (TLD) [Figure 1] relies on motion of shallow liquid inside a rigid container, for absorbing and dissipating structural vibration energy. Liquid dampers have been in use in space satellites and marine vessels [Figure 2 and References 3 - 6]. Modi and Sato [References 7 and 8] were among the first to suggest their application to ground structures including buildings and towers. A few other recent studies may also be cited [References 9 - 15]. Growing interest in TLD is attributable to several potential advantages, including low cost, easy installation even in already existing structures, few maintenance requirements, and adaptability to temporary use.

Studies on TLD so far indicate its effectiveness; but adequate modelling and clear explanation of its mechanism are lacking. This report presents data and insights from an experiment designed to demonstrate the TLD's fundamental mechanism, with emphasis on parameters that immediately relate to practical implementation.

2. EQUIPMENT AND PROCEDURE OF EXPERIMENT

To simulate a tall flexible building or tower, a steel platform as shown schematically in Figure 3 was designed with a fundamental natural period of 2 sec (or frequency $f_S = 0.5$ hz), and mass ranging from 116 to 440 kg. The structural mass was large enough to keep the ratio of liquid mass to structural mass in the range usually acceptable for dampers, i.e. about 1%.

Unlike in past experiments that employed small models, large prototype-size cylinders (diameters of 40 and 60 cm) were used here as liquid containers, with a view to using multiple identical TLDs in massive actual structures. With mass ratio, dimension, and vibration frequency thus made equal to those of prototype, it was possible to sidestep some dynamic fluid similarity requirements that would be difficult if not impossible to satisfy simultaneously.

The structure, i.e. platform, was essentially a single-degree-of-freedom system. It was given initial displacement while taking care that the liquid in the TLD was quiescent before the structure was released into free vibration. Both structural displacement and liquid surface height at one side of the TLD were electronically recorded.

Damping in the structure (either with or without TLD attached) was calculated as amplitude-dependent locally-averaged logarithmic rate of decrement of oscillation amplitude, $\delta = \delta(A)$:

$$\delta(A_n) = 0.25 \ln(A_{n-2} / A_{n+2}) \tag{1}$$

where A_n is structural vibration amplitude for nth cycle; A_{n-2} is amplitude two cycles before; and A_{n+2} is amplitude two cycles after.

Continuous δ-versus-A curve was fitted to the discrete points obtained by Equation 1. Additional damping due to TLD was then quantified as

$$\Delta\delta = \delta_T - \delta_S \tag{2}$$

where δ_T is logarithmic decrement of structure alone; and δ_S is logarithmic decrement of structure with TLD attached. Thus additional damping Δδ could be experimentally determined as function of structural vibration amplitude A. This approximate procedure was deemed sufficient when Δδ or δ was not very high.

3. PARAMETERS UNDER INVESTIGATION

The following parameters were varied to demonstrate the effect on TLD mechanism and on additional damping Δδ:

- Amplitude of structural vibration, A
- Ratio of natural liquid frequency to structural frequency, $\gamma = f_L / f_S$
- Kinematic viscosity of liquid, ν

- o Roughness of bottom of cylinder [Figure 4]
- o Gap between liquid surface and roof of container, G [Figure 5]
- o Ratio of liquid mass to structural mass, $\mu = m_L / m_S$
- o Diameter of cylinder, Φ

The undamped natural frequency of fundamental mode of sloshing of liquid, f_L, was calculated as:

$$f_L^2 = [\ 1.84\ g\ \tanh(\ 1.84\ h/a\ )\ ] / [\ a\ (\ 2\pi\ )^2\ ] \tag{3}$$

from linear potential theory [Figure 6]. g is gravitational acceleration; h is depth of liquid; and $a = \Phi/2$ is cylinder radius.

4. RESULTS OF EXPERIMENT

Figure 7 shows sample time histories of structural displacement without and with damper. Figure 8 shows the curves fitted to the calculated amplitude-dependent logarithmic decrement of structure without TLD. Additional damping $\Delta\delta$ is shown in Figure 9 for selected cases. It may be pointed out that for buildings the amplitude that is usually relevant to serviceability problems may be about $A = 1$ cm. Experimental data for $A > 1.0$ cm are included here for completeness, as towers and other structures that are not for human occupancy may well involve such large amplitudes. (When not specified, the actual parameter values are: $\Phi = 40$ cm; $m_S = 116$ kg; $A = 1$ cm; the liquid is plain water.)

4.1 Effect of frequency tuning: Each curve of $\Delta\delta$ versus A in Figure 9 corresponds to a different liquid depth h and, accordingly, different frequency ratio γ. On the other hand, each curve of $\Delta\delta$ versus γ in Figure 10 corresponds to a different amplitude A. One thing that is immediately noticeable from Figure 10 is that the liquid in TLD is generally shallow, e.g. the ratio h/a is below 0.1 in most of the cases where additional damping is significant.

As these figures show, high additional damping $\Delta\delta$ is obtainable when the frequency ratio is about $\gamma = 1.0$, which is the nominal tuning condition for the present system. The additional damping at tuned condition is particularly high when the amplitude A is small. In fact $\Delta\delta$ exhibits strong dependence on A when $\gamma = 1.0$, and has a peak at a certain small amplitude.

On the other hand, additional damping $\Delta\delta$ is rather low at frequency ratios that are very different from $\gamma = 1.0$. Indeed, for very high frequency ratio, say $\gamma > 1.5$, and accordingly deep liquid, little $\Delta\delta$ is attainable even as the mass ratio μ is large. It should be pointed out that the peak $\Delta\delta$ mentioned above corresponds to a liquid mass that is only about 1% of structure.

The condition of tuning seems unnecessary, however, for large amplitude A, where the same moderate additional damping $\Delta\delta$ is obtained almost regardless of frequency ratio γ. This may suggest the use of γ less than 1.0, to make the liquid mass ratio μ accordingly lower. Still, γ should be close to 1.0 if high $\Delta\delta$ is to be obtained specially at small A; the name Tuned Liquid Damper is on account of this latter requirement.

As for the sensitivity of γ or f_L to errors or deviations in the liquid depth h, Figure 6 shows that for given $f_L = f_S$ the sensitivity to h is less when the cylinder is bigger, although the required h itself is deeper. This suggests that tuning may be more reliably accomplished with a relatively big cylinder.

4.2 Effect of liquid viscosity: In usual oil or viscous dampers it is preferable to use high-viscosity liquids. For TLD, Figure 11 compares two liquids with the same density but different kinematic viscosities. It turns out that generally higher $\Delta\delta$ is obtained from the less viscous liquid; and there is no significant difference when the amplitude A is very large.

4.3 Effect of roughness of bottom of container: The liquid in TLD being generally shallow, the bottom is the major contact surface and roughness here [Figure 12] may affect the TLD's effectiveness, too. The comparison in Figure 13 shows that the peak $\Delta\delta$ is higher when the container bottom is smooth. Moreover, upon introduction of bottom roughness elements, the h (and accordingly the γ) where peak $\Delta\delta$ is attained is shifted up, indicating that a certain layer of liquid at the bottom is restrained and the effective depth is less than the actual h.

4.4 Effect of gap between liquid and roof of container: With a closed roof, it is possible for the liquid to hit it and dissipate energy in the process. At the same time, if the gap is small, liquid motion may be restrained and the original TLD mechanism may be suppressed. Figure 14 demonstrates the effect of roof in a tuned case, showing that $\Delta\delta$ has a peak at gap ratio $1.0 < G/h < 1.5$ although the increase over the infinite-gap or no-roof case is not much. Instead, the indication is that it is wiser to provide a high roof and avoid restraining the liquid motion.

4.5 Effect of liquid mass ratio and number of dampers: Figure 15 shows the effect on $\Delta\delta$ when, for the same TLD, the structural mass is halved from 232 kg to 116 kg and hence the liquid mass ratio μ is doubled. For doubled mass ratio μ, the additional damping $\Delta\delta$, too, is increased by a factor of approximately 2 when the frequency ratio is about $\gamma = 1.0$. (It is uncertain whether the calculated ratios for $\gamma > 1.5$ are in fact smaller than 2; in this range of γ, the individual $\Delta\delta$ values themselves are very small and prone to errors.)

Mass ratio could also be increased, for the same TLD configuration and same structural mass, by using multiple identical TLDs as done for Figure 16. This in fact may be the way of applying 40 or 60 cm diameter TLDs in prototype structures. Figure 16 shows trends similar to Figure 15. These figures indicate that for as long as the frequency ratio is about $\gamma = 1.0$, additional damping $\Delta\delta$ is practically linearly proportional to the number of identical dampers or to liquid mass ratio.

4.6 Effect of container size: As Equation 3 and Figure 6 show, in tuning the natural frequency of liquid to the frequency of structure, it is possible to choose from among different sizes and their corresponding required liquid depths. The question in practice is whether to use one large TLD or multiple smaller ones.

Firstly, Figure 17 compares single 40 cm and 60 cm TLDs. On comparing the respective peaks of $\Delta\delta$ at about $\gamma = 1.0$ and $\mu = 1.2\%$, it is seen that the larger TLD gives higher peak $\Delta\delta$. Figure 18 compares one large TLD with five small ones, again showing that the peak $\Delta\delta$ is higher for larger TLD, even as almost equal mass ratios correspond to these peaks. Thus for the present case it is indicated that, for the same mass ratio, the bigger TLD is more effective in producing large $\Delta\delta$.

It is not conclusive, however, that still bigger TLDs are better. For given structural period (or frequency) and amplitude, there may be a size that gives an optimal effectiveness. This is further discussed below.

5. INSIGHTS AND DISCUSSIONS

5.1 Liquid motion and additional damping: As Figure 9 illustrated, the additional damping $\Delta\delta$ due to the TLD depended very much on structural vibration amplitude A. It may be recalled that on account of the procedure adopted for the test, the effective motion of the cylinder was forced sinusoidal oscillation with gradually decreasing amplitude. According to excitation frequency and amplitude the liquid motion was expected to vary [References 7 and 16]. In fact the type of liquid motion changed as the amplitude A changed during the free-vibration test, and liquid motion type could be correlated with $\Delta\delta$.

The $\Delta\delta$-vs-A curves of Figure 9 were replotted in Figure 19, together with descriptions of liquid motion. The boundary between types of motion could not be identified exactly, as the classification was done visually; but it was clear that Type III motion consistently corresponded to rather large $\Delta\delta$. Six types of liquid motion were visually identified:

o Type I : two smooth waves travelling back and forth
o Type II : one smooth wave travelling back and forth
o Type III: two waves travelling on half-circles along the wall
o Type IV : similar to III but not as smooth
o Type V : wavy liquid surface moving only vertically
o Type VI : similar to V but smooth

Wave height was also measured at a point near the container wall, on a diameter along the direction of structural motion. Figure 20 shows two example wave records and their corresponding structural displacement records, corresponding to curves (3) and (4) in Figure 9 or 19. These wave records provided a good estimate, even if the recorded positive peaks included some effect of splashing during Type III motion, and even if very low wave troughs could not be recorded at all.

For the case shown in Figure 20(a) and curve (3) in Figure 19, $\Delta\delta$ had a peak value at around $A = 0.25$ cm and dropped drastically for still smaller amplitude. Inspection of the wave record showed that for $A > 0.25$ cm, the wave height H was greater than 1.2 cm which was the depth of liquid h in that TLD. Wave breaking, with the associated turbulence at the wave crest, was to be expected when wave height H reached a value about equal to liquid depth h; indeed turbulence at the wave crest was observed during the experiment.

The same case (Figure 20(a) and curve (3) in Figure 19) also showed, however, that while wave breaking occurred the resulting $\Delta\delta$ would not necessarily be larger or the same at larger amplitude A. This could be understood by recalling that $\Delta\delta$ is proportional to the ratio $\Delta E/E$, where the kinetic energy E in the denominator is proportional to A^2. The per cycle energy dissipation ΔE in the numerator turned out to be nearly proportional to A [Figure 21] rather than A^2, for the range of amplitudes considered.

Wave breaking occurred not only in the above tuned case. It could also be observed during vibration at very large amplitude even when frequency ratio was not $\gamma = 1.0$, e.g. curves (1), (2) and (4) in Figure 19. The threshold wave height in the case of curve (4) and Figure 20(b) was about $H = 1.8$ cm, which matched the corresponding liquid depth h. For $\gamma >> 1.0$, however, liquid motion tended to be smooth sloshing (Type VI) even for large amplitude A; and no significant $\Delta\delta$ could be attained.

For enhancing surface wave development and the subsequent wave breaking, it may well be recalled from Section 4.2 and Figure 11 that, for given liquid density, low viscosity liquid was more effective. From Section 4.4 and Figure 14 it was also learned that sufficient gap between liquid surface and container roof was favorable to the natural development and breaking of high waves.

It may be pointed out here that energy loss per cycle ΔE or additional logarithmic decrement $\Delta\delta$ is a measure of energy extracted from the structure. A tuned-type mechanical damper may, in principle, absorb this energy and, having a dissipation mechanism, also dissipate it into the surrounding environment. For example, a classical tuned mass damper, otherwise called dynamic absorber, would merely absorb energy; whereas TMDs that are supplied with viscous dampers absorb energy and also dissipate it at a rate per cycle that is proportional to A^2.

In the case of TLD, the present experimental evidence indicates that $\Delta\delta$ is attributable to energy dissipation rather than mere absorption by the damper. In other words, $\Delta\delta$ is attributable to dissipation by wave breaking instead of mere transfer of energy into the liquid.

Should simplified mechanical modelling of TLD in terms of mass, spring, and damping elements be attempted, the almost linear relation between per cycle energy loss ΔE and amplitude A [Figure 21] in the amplitude range considered suggests a property of coulomb-type damping instead of viscous.

5.2 Choosing the appropriate size of cylinder: Section 4.6 and Figures 17 and 18 showed that, for the same liquid mass ratio, the bigger (60 cm) TLD was better since higher $\Delta\delta$ was produced.

The advantage of the bigger diameter, for given period of TLD oscillation, may be associated with the manner of liquid motion when it is Type III: two waves develop along half circles and hit together twice per cycle [Figure 19]. Each time that the waves meet, the energy dissipated is proportional to the velocity of the converging waves; this velocity is in turn proportional to the length of the half-circle arc that they traverse every half-cycle.

Energy loss per cycle was plotted versus amplitude A in Figure 21, for 40 cm and 60 cm TLDs at $\gamma = 1.0$. It showed that, at each amplitude A, the energy loss per cycle in the 60 cm TLD was almost 10 times that in the 40 cm TLD. The mass ratio involved in both cases was $\mu = 1.2\%$; but the actual liquid mass in the 60 cm TLD was 4 times more. The ΔE per unit liquid mass was almost 2.5 higher in the larger TLD.

Other considerations may rule out the use of very large TLD, however. Figure 22 illustrates that for tuning to given period (or given frequency), there is a wide range of possible cylinder sizes; each size ϕ has its own corresponding required liquid depth h. The necessary relative liquid depth h/ϕ is not constant, however; instead it increases rapidly in the range of large ϕ. Very high h/ϕ in very large TLD would not be very efficient, as some liquid near the bottom would tend to be immobile and ineffective.

Moreover, the deeper liquid would require a higher wave height H, hence a larger structural amplitude A, before energy dissipation by wave breaking can start. For example, the 40 cm TLD required about $A = 0.5$ cm [Figure 9]; the 60 cm TLD required about $A = 1$ cm.

Therefore it may be presumed that there is an optimal size of TLD for given structural period (or frequency) and amplitude.

6. CONCLUSIONS AND RECOMMENDATIONS

An extensive experiment was performed in order to investigate the fundamental properties of Tuned Liquid Damper (TLD). The experiment was essentially free-oscillation test of a single-degree-of-freedom structure with attached TLD. The main findings are briefly summarized as follows.

(1) The present experiment indicates that energy dissipation in TLD is due mainly to wave breaking. Wave breaking can explain various TLD properties.

(2) Damping is highly dependent on amplitude of vibration. There is no additional damping at very small amplitude, as wave breaking has not started to occur. There is limited additional damping at very large amplitude, as wave breaking, by its very nature, limits the height that liquid waves may reach.

(3) To attain large additional damping specially at small to moderate vibration amplitude, it is necessary to tune the liquid frequency to the natural frequency of the structure. This enhances energy absorption by the TLD, prior to energy dissipation by wave breaking. For very large amplitude, TLD is rather insensitive to tuning; but the additional damping itself is not so large.

(4) Low-viscosity liquid is preferable as it enhances the development of waves which leads to wave breaking.

(5) Making the cylinder bottom rough does not improve TLD effectiveness, as the energy dissipation occurs primarily on the free surface of the liquid.

(6) Closed roof has two counteracting effects: allow energy dissipation through impact of liquid, and restrain the development of waves. The net effect differs only slightly from no-roof condition. A more reliable TLD design is to make the roof sufficiently high.

(7) When liquid mass ratio is small, the additional damping is practically linearly proportional to mass ratio or to number of identical TLDs.

(8) Within the range of parameters considered in the experiment, the larger TLD is more effective. Because of changing liquid condition from shallow to deep, however, for given frequency and amplitude of structure there may be a cylinder diameter that produces optimal amount of additional damping.

The subject of optimal TLD size requires further investigation. As for developing a simple mechanical model for the TLD itself, which may then be interfaced and used in the analysis of complicated structure, a more straightforward experiment would be to measure the interface force between TLD and structure [Reference 12]. The mass, stiffness, and damping elements of the mechanical model would then be easier to identify. Further study is also needed for comparing the present TLD with other shapes, e.g. doughnut-shape [Reference 7], rectangular [References 9 - 11], and spherical [Reference 14], or with dampers completely filled with two immiscible liquids [Reference 15].

ACKNOWLEDGMENT

The authors are grateful to Prof. M. Ito and Asso. Prof. M. Isobe of University of Tokyo, and Mr. K. Fujii and Mr. T. Sato of Shimizu Co. for their very useful comments. Likewise they thank Mr. I. Shino and Mr. P. Warnitchai of University of Tokyo for their help in the experiment. This research was supported partially by a Grant-in-Aid from the Japan Ministry of Education, Science, and Culture.

REFERENCES

(1) Fujita, T. 1985. Earthquake isolation technology for industrial facilities - research, development and applications in Japan. Bul New Zealand Natl Soc Earthq Eng, 18(3), 224-249

(2) Tsuji, M. 1984. Review of various mechanical means for suppressing wind-induced vibration of structures. Japan J Wind Eng, 20, 81-102 (in Japanese)

(3) Alfriend, K. 1974. Partially filled viscous ring nutation damper. J Spacecraft, 11(7), 456-462

(4) Bhuta, P.G. and Koval, L.R. 1966. A viscous ring damper for a freely precessing satellite. Intl J Mech Sci, 8, 383-395

(5) Amieux, J.C. and Dureigne, M. 1972. Analytical design of optimal nutation damper. J Spacecraft, 9(12), 934-936

(6) Watanabe, S. 1969. Methods of vibration reduction. Proc Japan Naval Arch Soc Symp, 156-179 (in Japanese)

(7) Modi, V.J. and Welt, F. 1987. Vibration control using nutation dampers. Proc Intl Conf Flow Induced Vib, England, 369-376

(8) Sato, T. 1987. Tuned sloshing damper. Japan J Wind Eng, 32, 67-68

(9) Miyata, T., Yamada, H., and Saitoh, Y. 1987. Feasibility study on damping of wind-induced vibrations of structures by breaking of sloshing water. Japan J Wind Eng, 32, 65-66 (in Japanese)

(10) Noji, T. et al. 1987. Study on a vibration damper system using hydrodynamic force of sloshing (Parts 1,2,3). Proc Conf Arch Inst Japan, 867-872 (in Japanese)

(11) Matsuura, Y. et al. 1986. On a mean to reduce excited-vibration with the sloshing in a tank. Proc Japan Naval Arch Soc, 160, 424-432 (in Japanese)

(12) Fujii, K., Sato, T., and Otsuki, T. 1987. Damper using liquid sloshing motion - tuned sloshing damper. Proc Conf Arch Inst Japan, 1483-1484 (in Japanese)

(13) Chaiseri, P., Pacheco, B., Fujino, Y. and Sun, L. 1987. Damper for bridge tower - utilizing water motion as energy dissipator. Proc Intl Conf Cable-stayed Bridges, Bangkok, 1, 545-556

(14) Sayar, B. and Baumgarten, J. 1982. Linear and nonlinear analysis of fluid slosh dampers. Amer Inst Aero Astro J, 20(11), 1534-1538

(15) Bauer, H. 1984. Oscillations of immiscible liquids in a rectangular container: a new damper for excited structures. J Sound Vib, 93(1), 117-133

(16) Hashimoto, H. 1986. Future trend and topics of liquid sloshing. J Japan Soc Mech Engr, 89(810), 512-517

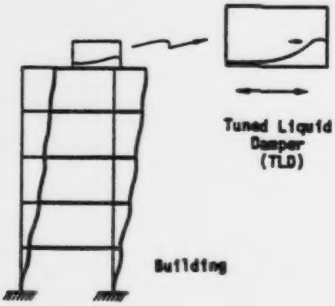

Figure 1: TLD installed on a building (TLD and building not to same scale)

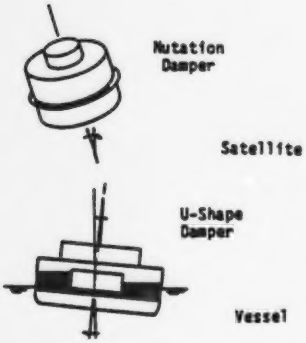

Figure 2: Other liquid dampers

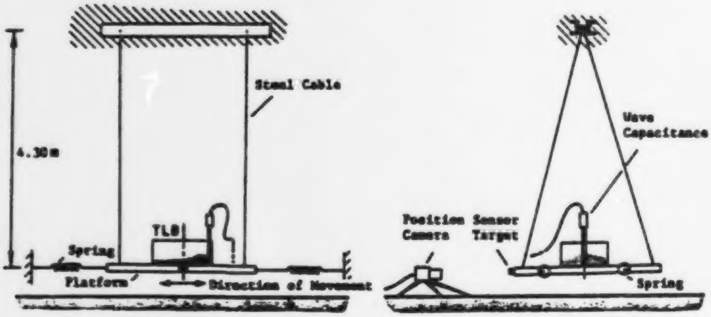

Figure 3: Single-degree-of-freedom structural model with TLD

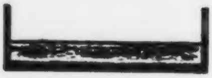

Figure 4: Roughness of container bottom

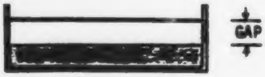

Figure 5: Gap with container roof

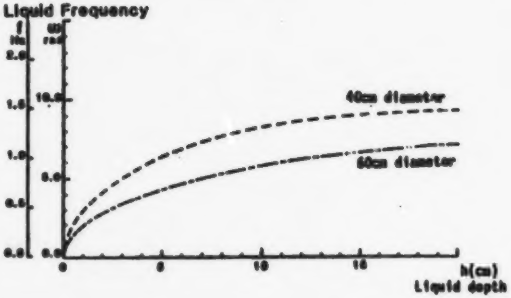

Figure 6: Natural frequency versus depth of liquid

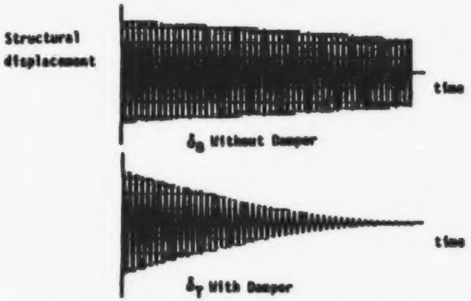

Figure 7: Structural displacement histories

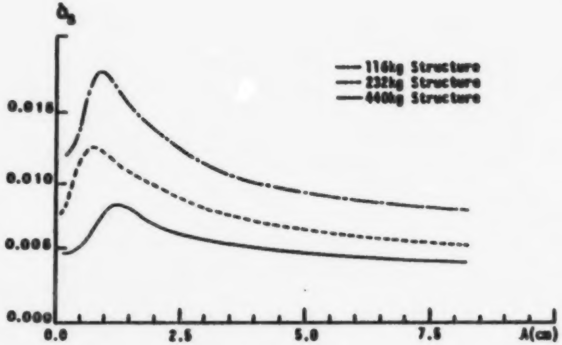

Figure 8: Logarithmic decrement of structure without TLD

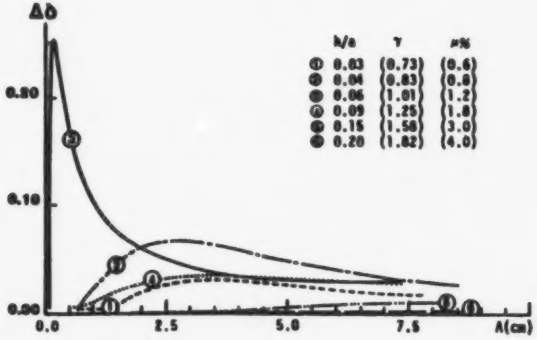

Figure 9: Additional damping due to TLD

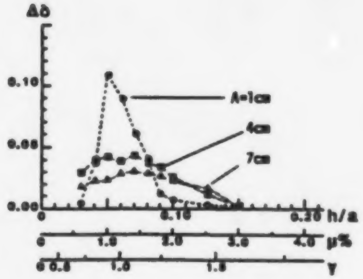

Figure 10: Additional damping versus frequency ratio

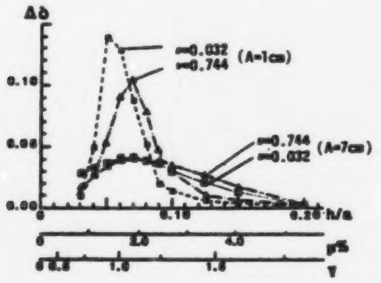

Figure 11: Effect of liquid kinematic viscosity ν (ν = 0.032 $CaCl_2$ solution; ν = 0.744 Sugar solution)

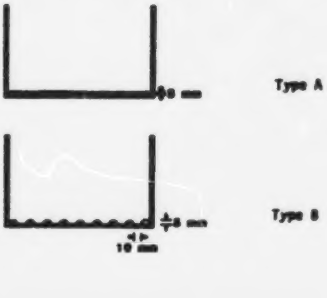

Figure 12: Semispheres as roughness elements at container bottom

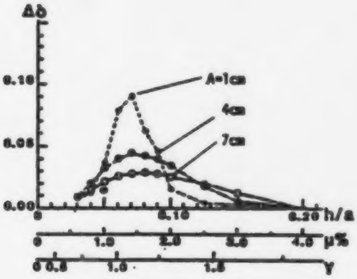

(a) With Type A roughness

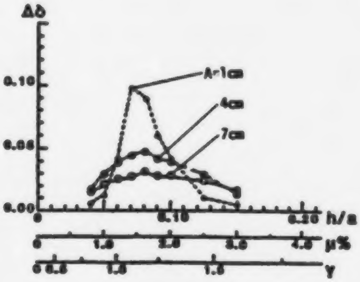

(b) With Type B roughness

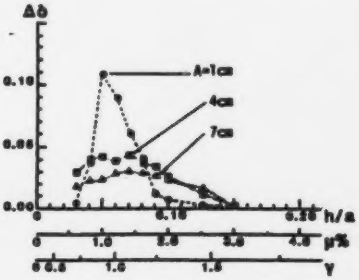

(c) Smooth

Figure 13: Effect of bottom roughness on additional damping

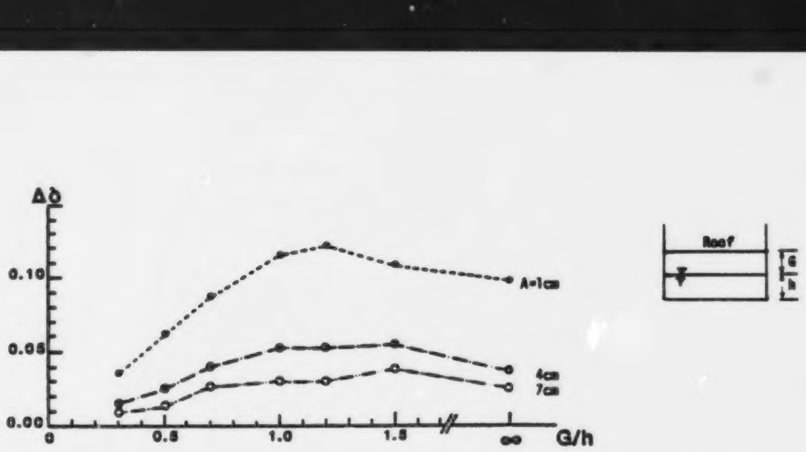

Figure 14: Effect of roof height on additional damping (γ = 1.0)

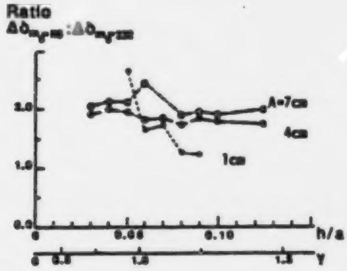

Figure 15: Effect of mass ratio on additional damping

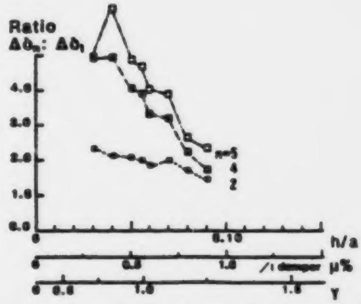

Figure 16: Effect of number n of TLDs on additional damping (232 kg structure)

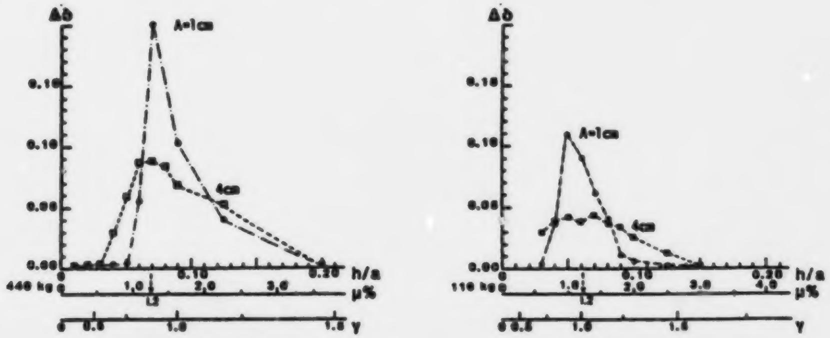

(a) Diameter = 60 cm

(b) Diameter = 40 cm

Figure 17: Comparison of single large TLD and single small TLD

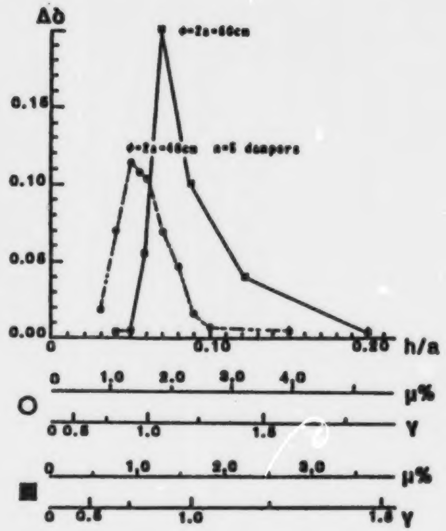

Figure 18: Comparison of one large and five small TLDs (440 kg structure)

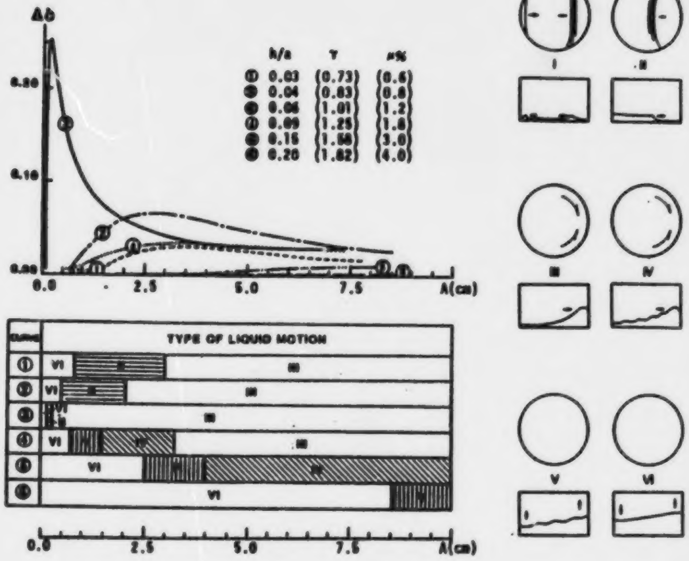

Figure 19: Visual classification of type of liquid motion

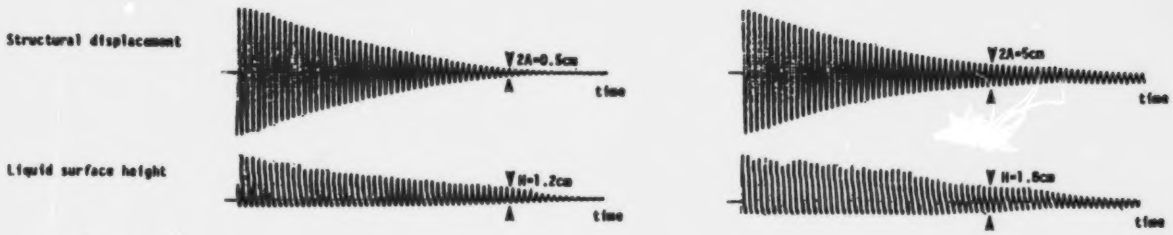

(a) Case 3 in Figure 19
(γ = 1.0; h = 1.2 cm)

(b) Case 4 in Figure 19
(γ = 1.25; h = 1.8 cm)

Figure 20: Histories of structural displacement and liquid surface height at one side of TLD

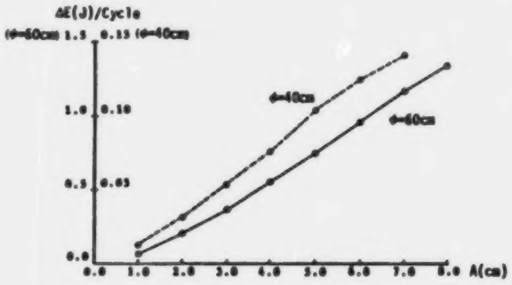

Figure 21: Energy loss per cycle versus vibration amplitude

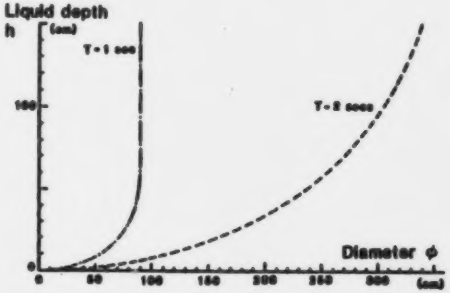

Figure 22: Required depth versus container diameter for specified natural period (or frequency)

WIND-INDUCED VIBRATION OF TALL TOWERS AND PRACTICAL APPLICATIONS OF TUNED SLOSHING DAMPER

Y. Tamura*, K. Fujii, T. Sato**,
T. Wakahara**, M. Kosugi*****

* Tokyo Institute of Polytechnics, Iiyama, Atsugi, Kanagawa, Japan
** Institute of Technology Shimizu Corporation, Ecchujima, Koto-ku, Tokyo, Japan
*** Azusa Sekkei Co. Ltd., Nishigotanda, Shinagawa-ku, Tokyo, Japan

ABSTRACT: Wind-induced vibration of two actual tall towers were reduced to about half upon installation of newly developed Tuned Sloshing Damper, which utilizes liquid motion in circular container. Vibration at Nagasaki Airport Tower (height 42m) and Yokohama Marine Tower (height 101m) were measured during gusty days, before and after installation of the damper. The reduced vibration levels after installation were in the range acceptable from the view point of comfort and serviceability. To further estimate the effects of Tuned Sloshing Damper, the dynamic force frequency response function of TSD was experimentally determined. Using this frequency response function, numerical simulation on gust responses was conducted. The results indicate that the amplitude level is reduced to about half and this qualitatively agree well with those observation in the Yokohama Marine Tower.

1. INTRODUCTION

Since a tall, steel structure is light and its mechanical damping is small, it is vulnerable to vibration caused by wind. Airport towers in Japan are mostly steel structures, and furthermore, the runways are being expanded and higher airport towers are being constructed even at local airports. Therefore, not only from the viewpoint of wind resistance design but also from the viewpoint of serviceability and comfort of the air traffic controllers who work on the top floor of the airport tower, the problem of vibration has become an important topic for discussion[1].

The number of observation towers is also increasing. Business or service is stopped in some of these towers if most of the people at the tower perceive strong vibrations. Wind-induced vibration greatly affects the tower's serviceability.

Although this paper focuses on tower structures made of steel, as some projects on high-rise office buildings with the heights of 400-500m or high-rise residential buildings are drawn up in Japan, the problem of the relation between building vibration caused by wind and serviceability will definitely increase in importance.

In order to improve the serviceability of a tower or building on a gusty day, a damper which can reduce vibration is necessary. As examples of actual buildings with dampers, John Hancock Tower[2], Citicorp Center[3], and Sydney Tower[4] are given. In these buildings, the Tuned Mass Damper with a mechanical system is used. The damping device used in the present study is different from such a mechanical system damper. We call it the "Tuned Sloshing Damper" (TSD hereafter), because a frequency of the sloshing motion in a container has to be tuned to a particular natural frequency of a structure. The TSD absorbs and dissipates vibration energy through the sloshing of liquid in a container. In the field of spacecraft, a Nutation Damper, which utilizes liquid, has been used for space stations and satellite spin stabilization[5][6]. Also, in the field of shipbuilding, an application of the liquid damper is being conducted by using the sloshing in a tank[7]. V.J.Modi[8] is one of the pioneers in the research for the application of nutation dampers to the structures in the field of civil engineering. The TSD introduced in this paper was invented by one of the authors, T.Sato[9][10], and it is the first of its kind actually applied to a tower structure. The frequency response function of the TSD has a dependency on amplitude and indicates different characteristics from those of the mechanical TMD.

In this paper, we measured the characteristics of the wind-induced vibrations of actual airport tower and observation tower, and made inquiries about the vibration perception to air traffic controllers. We also confirmed the effects of TSD with these two towers. We investigated the basic characteristics of the TSD.

2. FULL-SCALE MEASUREMENTS AND QUESTIONNAIRE STUDIES AT NAGASAKI AIRPORT TOWER

2.1 Nagasaki Airport Tower: The Nagasaki Airport is located on a flat island surrounded by the sea. The airport tower is a steel framed tower placed on a low-rise reinforced concrete building with a height of 4m as its base. The total height of the entire tower is 42.0m above the ground (Fig.1). The tower body has a 5.15m square cross section. An air traffic control room with a 7.4m square plan is located at the top of the tower (Fig.2). The height of the air traffic control room floor is 38.5m above the ground. The total mass of the tower is about 170000kg and the lowest natural frequency of the bending vibration is 1.07Hz for both x and y axis. The damping ratio is 0.93%.

2.2 Measurements: Windspeed as well as wind direction was measured by 3-cups anemometer at the northeast corner at a height of 1.5m above the air traffic control roof (43.5m above the ground) as shown in Fig.1. Four displacement pick-ups and two accelerometers were installed on the floor of the air traffic control room as shown in Fig.2. As far as wind speed, displacement, acceleration are concerned, the data were sampled with a frequency of about 40Hz and with an averaging time of about 100s. The displacement records were analyzed and converted to the torsional angles and the displacements of x and y directions at the centroid of the air traffic control room floor.

2.3 TSD Placement: The TSD installed onto the airport tower was a vinyl chloride cylinder with a height of about 50cm and a diameter of 38cm. It was divided into 7 layers at every 7cm. Into the respective layers, 4.8cm depth water was poured. The lowest natural frequency of the motion of the sloshing in the respective layers was almost tuned with the natural frequency of the fundamental mode of the control tower. The water mass of one TSD was about 40kg. As Fig.1 indicates, 12 TSDs were placed on the air traffic control room floor in a dispersed manner and several on each of the stair landings, making a total of 25 TSDs (total water mass: about 1000kg, which is 1.6% of the fundamental generalized mass or 0.59% of the total mass of the airport tower).

2.4 Characteristics of the Wind-Induced Vibrations of the Airport Tower: Here, we show the results of the responses of the tower under gusty wind in the direction N which had the most abundant records. In this case, the y axis of the tower is longitudinal direction and the x axis is the transverse direction to the wind. The tower vibrates mainly with the lowest natural frequency of bending vibration. Fig.3 shows the variation of measured rms displacements with the mean windspeed. It can be seen that the rms displacements at low windspeed are scattered, but those at high windspeed lie along one straight line. The lines in the figure are the regression lines obtained by the least square method using the data exceeding the windspeed of 8m/s. "A" in the figure is the slope of the regression line and "B" is the intercept indicating the power index when the response, R(cm/s² or cm), is expressed with mean windspeed, V(m/s), as,

$$R=10^{B}V^{A}. \tag{1}$$

In most cases, the transverse response is greater than longitudinal response; the difference is especially significant at high windspeed range. Fig.4 shows the variation of the rms acceleration with windspeed.

2.5 Questionnaire Study on Vibration Perception by Air Traffic Controllers: When we consider the comfort and serviceability in the air traffic control room, we should definitely understand how the controllers feel towards vibration on gusty days. Thus, we requested the controllers to answer questionnaires at the time of vibration measurement, and studied the correspondence with the measured response acceleration of the tower. We handed our questionnaires to the controllers at the time of shift change on gusty days and collected them later. The questions had to do with the time they perceive the vibration, its duration, the degree of vibration perceived, the cause of the vibration perception, and so on. The questionnaire studies were executed 12 times, and a total of 35 air traffic controllers submitted the answers. All were male and 25 persons of them were in their 30s and 10 persons in their 40s. Most of them were sitting when they perceived the vibration.
As the acceleration level of the tower corresponding to the time survey was taken, the maximum peak among all the x and y direction accelerations observed at the time of the questionnaires was adopted. Fig.5 shows the results obtained after some adjustment because the answers were somewhat scattered. The figure also shows the threshold curves for vibration perception reported by various researchers[11][12][13][14]. As the curves are for the amplitudes of sinusoidal steady state acceleration, the maximum peak accelerations corresponding to the questionnaires were converted into the equivalent amplitudes by dividing them by the peak factor (assuming 3.5) and then multiplying them by $\sqrt{2}$. The maximum peak acceleration observed actually at the control tower was about 2.5 times greater than the value plotted in the figure. According to the questionnaire results, the air traffic controllers begin to perceive the vibration from 0.8cm/s² (the actual maximum peak acceleration of the tower is about 2.0cm/s²), and perceive it clearly over 1.2cm/s², and strongly perceive vibration over 2.0cm/s². The minimum acceleration level to perceive at 0.8cm/s² almost corresponds to the threshold curves for vibration perception in the figure.

2.6 Effects of TSD: On calm days, we executed free vibrations test of the tower both with the TSDs and without the TSD. When all of 25 TSDs were installed, the damping greatly differed from that of the tower without TSD. With TSDs, the amplitude of the free vibration was rapidly reduced initially, and then, gradually reducing amplitude modulation appeared. The damping ratio in the case with 25 TSDs calculated from the initial amplitude reduction is about 4.7%, which is about 5 times greater than that in the case without TSD (Fig.6).

Fig.7(a) and (b) show the variations of longitudinal rms displacement y and the transverse rms displacement x with windspeed in the case of wind direction N. The white plots indicate the case without TSD and the black plots the case with 25 TSDs. According to the regression lines, the transverse rms displacements are reduced to 35% due to the effects of TSDs at windspeed around 20m/s, and these effects become more significant at the higher windspeed. The longitudinal rms displacements are reduced to 50% due to the TSDs effects at windspeed around 20m/s. Thus, the response of the tower may be reduced to as small as 1/3, at high windspeed. However, in the case with TSDs, as there are not so much data obtained for high windspeed, the reliability of the regression line at high windspeed range is somewhat low.

We calculated the maximum accelerations of several return periods by using the regression lines obtained from full-scale measurements at the airport tower and the past meteorological data at the airport. Fig.8 shows the maximum accelerations for various return periods both for with TSDs and without TSD. The acceptable levels of vibration in the codes and regulations[15][16][17][18] are also shown in the figure. Here, as the acceptable levels of the ISO standards are based on the rms accelerations, they are multiplied by 3.5 (peak factor) in order to adjust to other standards. When the TSD is not installed, the vibration levels of the tower satisfied the standards of Canada and Australia for office buildings, but they don't necessarily satisfy the acceptable levels of vibration for the Canadian standard or the ISO standard for residential buildings. On the other hand, when the TSDs are installed, the vibration levels of the tower satisfy all of these standards, and the effectiveness of TSD to improve the serviceability of the tower is clearly recognized.

3. FULL-SCALE MEASUREMENTS AT YOKOHAMA MARINE TOWER

3.1 Yokohama Marine Tower: The Yokohama Marine Tower (height 101m), the symbol of Yokohama Port, was built in January of 1961, and is a steel truss structure. On the top of the tower, the highest light house in the world has been installed (Fig.9). There is an observation room under the light house and it attracts a great number of tourists every day. The cross section of the tower is decagonal. The lowest natural frequency of the tower is 0.55Hz and the second natural frequency is 2.5Hz; torsional frequency is 1.4Hz. The damping ratio is 0.6%. The total mass is 540000kg and the generalized mass is 157000kg.

3.2 Measurements: The wind direction and windspeed were measured at 105m above ground on top of the tower roof. The anemometer is a 3-cups anemometer and the wind direction meter is a wind vane type. Two servo-type accelerometers were installed at 99m in the light house to measure x and y axis sway vibrations and torsional vibration. The records of the acceleration, the wind direction and the windspeed were stored in a tape recorder. The data were sampled with a frequency of 25Hz and with an averaging time of 180s.

3.3 TSD Placement: The installed TSD was an acryl cylinder container with a height of about 50cm and a diameter of 49cm. The cylinder was divided into 10 layers every 5cm. The respective layers had water with a depth of 2.1cm. The sloshing frequency of the respective layers was tuned with the lowest natural frequency of the tower (0.55Hz). Water mass was 41kg per TSD, or 1600kg for 39 TSDs, which was a total of 1% of the generalized mass of the tower. These TSD were placed in the light house at the top floor of the tower (Fig.10).

3.4 Characteristics of the Wind-Induced Vibrations and Perception Level at the Marine Tower: Fig.11 indicates the frequency spectrum of the Marine Tower. Analyzing the power spectrum from the data on a gusty day, the tower almost vibrates with the lowest frequency in sway mode response, and the torsional response was under 10% of sway.
With a strong wind of 15-21m/s at the top of the tower, the maximum rms value of the longitudinal acceleration was 1.8cm/s^2 (Fig.12), and that of the transverse acceleration was 2.6cm/s^2 (Fig.13). According to ISO standards, the average threshold for vibration perception is about 2cm/s^2 at the frequency of 0.55Hz. Therefore, we can assume that most visitors sense the vibration of the tower.

3.5 Effects of TSD: In the free vibration test, the damping ratio was found to be 4.5% with the TSD installed, which was 7 times that in the case without the damper.
The tower vibration was greater in the transverse direction than the longitudinal direction. We observed the average damping effect from the regression lines calculated between 8m/s and 18m/s (Fig.12 and 13). The rms acceleration of the tower with TSD was about half of that without TSD between 10m/s and 15m/s. As response shown in Fig.13 are rather scattered, the response values for windspeed range of 1m/s interval were grouped and averaged. The results are shown in Fig.14. Around windspeed 18m/s the rms acceleration was 0.9cm/s^2 without TSD; with TSD this was reduced to 0.3 cm/s^2, which was about 1/3 of the former (Fig.14).
According to the ISO standard, with a frequency 0.55Hz, the minimum perception range in which a sensitive person would perceive vibration is about 0.5cm/s^2, while the average perception range in which most of the people would perceive vibration is about 2cm/s^2. Without TSD, when the wind speed was at about 15m/s, the rms acceleration rose over the minimum perception range, and the windspeed was about 24m/s, it rose over the average perception range (Fig.12 and 13). On the other hand, with the TSD, the value rise slightly over the minimum perception range at the windspeed of 18m/s, up to 20m/s, it would not surpass the average perception range. Also, according to the 2.7-hour long data at the windspeed range 15-18m/s, the acceleration was over the ISO standard for about 36% of the total time in the case without TSD, while in the case with TSD it was over the standard only about 1% of the total time.
Fig.15 shows representative sample time histories of transverse acceleration of the tower and the ISO standard level. Thus, the TSD proved to have an extremely significant damping effect. According to the personnels actually working in the tower, they evaluated that the TSD damped the vibration down to less than 50%.

4. CHARACTERISTICS OF THE TUNED SLOSHING DAMPER (TSD)

The TSD employs the sloshing of liquid inside a container, is an extremely simple device and can easily be mounted onto actual existing towers. Here, we describe basic characteristics of the TSD cylinder container, which we have studied for application to the Yokohama Marine Tower. We also describe the mechanical frequency response function of a structure when the TSD is installed.

4.1 Frequency Response Function of a TSD: In a model vibration experiment, a simple steel bar with TSD was used, and a significant vibration damping effect was obtained when the lowest natural frequency of the liquid inside the TSD was tuned to the steel bar's natural frequency[10]. A similar Tuned Liquid Damper (TLD) experiment executed by Fujino et al.[19] had a similar result. Therefore, in this study, the TSD's natural frequency was tuned to the structure's natural frequency, and we measured the TSD vibration characteristics by executing vibration experiment.

We used in the experiment a cylinder container identical to the TSDs used at Yokohama Marine Tower. The liquid inside the container was water. The internal diameter of the container was 38.9cm and it was made of acryl. The lowest natural frequency f_1 of the sloshing of the water inside the container was calculated based on the eq.(2) from the potential theory[20]. Here, g; acceleration of gravity, a; radius of a container, H: water depth.

$$f_1 = \frac{1}{2\pi}\sqrt{\varepsilon_1\left(\frac{g}{R}\right)\tanh\left(\varepsilon_1\frac{H}{R}\right)} \quad , \qquad \varepsilon_1 = 1.837 \tag{2}$$

In the Yokohama Marine Tower, the water depth was 2.1cm to correspond to the natural frequency of 0.55Hz. The container was placed on the shaking table and shaken at various frequencies ranging from 0.1-1.0Hz. A load cell measuring inertia force by liquid motion was set between the container and the shaking table (Fig.16). The inertia force of the container itself was canceled by another load cell. By dividing the inertia force generated through the liquid motion by [(the water mass inside the container)×(shaking table acceleration)], the frequency response function of a container was obtained (Fig.17). According to the results of the full-scale data in the Yokohama marine Tower, the double amplitude of the displacement of the tower with TSD was nearly 0.1cm in strong wind (windspeed 15-20m/s). In the shaking table test, when the double amplitude was 0.1cm, the TSD frequency response function showed a sharp peak. The damping ratio estimated by curve fitting to an equivalent single-degree-of-freedom (SDOF) system was 2.4%. However, when the double amplitude was 0.4cm, the height and shape of the peak of the response function changed, and could not be fitted anymore with SDOF curve. In the later case, the wave crest inside the container was complex. Fujino et al.[19] analyzed the liquid motion and the relation between the water motion and energy dissipation. In this paper, we have directly measured the total inertia force in the form of a frequency response function. Thus, the frequency response function of the TSD depending on the amplitude shows nonlinear property. In this reason, the TSD was different from the conventional TMD. For actual tower we install a number of such containers. The TSD frequency response function has been proved to be the same, both in the case of a container with only one layer and in the case of a container with 10 layers. Therefore, for given amplitude, the TSD can be considered as a multiple damper which can be added linearly.

4.2 Frequency Response Function of a Building with TSDs: We calculated the frequency response function by the Lumped Mass System using the TSD frequency response function. As Fig.18 indicates, the analytical model is a multiple damper with a number of TSDs.
The frequency response function of a structure with TSDs is as given by eq.(3). Here we define ω_0: natural frequency of the structure, h_0: damping ratio of the structure, M_0: generalized mass of the structure, $H_j(\omega)$: frequency response function of a TSD, m_j: mass of a TSD, j: number of TSD.

$$H_0(\omega) = \frac{1 + i2h_0(\omega/\omega_0)}{1 - (\omega/\omega_0)^2 + i2h_0(\omega/\omega_0) + (\omega/\omega_0)^2\sum_{j=1}^{N}\left(\frac{m_j}{M_0}\right)H_j(\omega)} \tag{3}$$

In the case of 0.1cm(p-p) amplitude, the structure's frequency response function (hereafter TSD model) was almost identical to that using the conventional amplitude-independent TMD model (Fig.19(a)). However, in the case of 0.4cm(p-p) amplitude, the TMD model could not be applied. Hence, we calculated the structure's frequency response function by using eq.(3). It is shown in Fig.19(b). The amplitude and phase of the frequency response function around the tuned frequency (0.55Hz) were different for the 0.4cm(p-p) and the 0.1cm(p-p) cases.

The amplitude in the case of Yokohama Marine Tower is about 0.1cm. Although either the TMD model or the TSD model may be used at such a low amplitude level, the TSD model was employed in the succeeding simulation of acceleration response. When a random external force equivalent to the wind load is input into the tower's frequency response function estimated in the TSD model, the tower's response was reduced by about 50% in terms of rms, compared with the case of the tower without the TSD installation (Fig.20).

5. CONCLUSIONS

1) According to the response measurements of Nagasaki Airport Tower with a height of 42m and Yokohama Marine Tower with a height of 103m, the transverse vibration was greater than the longitudinal vibration. Also, in both towers, vibration could be perceived by occupants at wind speed of over 15m/s.

2) According to the questionnaires given to the air traffic controllers, they perceive vibration when the maximum acceleration of the tower is 2.0cm/s^2 (equivalent to sinusoidal acceleration amplitude 0.8cm/s^2).

3) When the Tuned Sloshing Dampers were installed onto the airport tower, the displacements on gusty days were reduced to less than 50%. The acceleration responses of these towers with TSDs may be reduced to as small as 1/3 at high windspeed.

4) When the TSDs were installed, the wind induced vibration at the Nagasaki Airport Tower satisfied all the codes and regulations of the main countries considered. Also, at the Yokohama Marine Tower, the TSD effect was so great in improving serviceability that the vibration was reduced to the point that most people did not sense the vibration up to the windspeed of 20m/s.

5) We have studied the TSD using water sloshing in order to reduce tower vibration. The natural frequency of the water inside the container of TSD was tuned to that of the structure. To further study the effect of the TSD, the dynamic force frequency response function of TSD was experimentally determined. When we measured the TSD frequency response function, we found that to be dependent on the amplitude.

6) Numerical simulation of acceleration response of the Yokohama Marine Tower was also conducted, using the TSD model. The results showed that the amplitude level well with the full-scale measurements.

7) Through the present study, we have proven that the TSD can be used in actual existing towers. Our future task is to be a parameter study and design the optimal TSD for individual structures. Also, we need to understand the mechanism of the TSD energy absorption and dissipation which depends on the amplitude.

ACKNOWLEDGMENTS

The authors would like to express its deepest gratitude to Dr.Y.Fujino and Dr.B.M.Pacheco of Tokyo University, who has been studying the TLD, a damper similar to the TSD, for his valuable advice. We would also like to sincerely thank Mr.T.Otsuki and Mr.K.Shimada of the Institute of Technology, Shimizu Corporation and Mr.I.Nishimura of Waseda University for their assistance in the full-scale measurements, TSD experiments and discussions.

REFERENCES

[1] Y.Tamura, M.Kosugi, I.Nishimura, Wind-induced response of control tower of airport (Part-1), National Conference of AIJ, October 1987 (in Japanese)
[2] Hancock Tower Now to Get Dampers, Engineering News Record, October 1975
[3] R.J.Mcnamara, Tuned Mass Dampers for Buildings, Journal of the Structural Division, ASCE, 1985
[4] K.C.S.Kwok, Fullscale measurements of wind-induced response of Sydney Tower, Proceedings of the 6th International Conference on Wind Engineering, 1983
[5] P.G.Bhuta, L.R.Koval, A viscous ring damper for a freely precessing satellite, Int. J. Mech. Sci., 1966
[6] J.C.Amieux, M.Dureigne, Analytical Design of Optimal Nutation Damper, Journal of Spacecraft, 1972
[7] G.Matsuura, K.Matsumoto, et al., On a mean to reduce excited-vibration with the sloshing in a tank, Journal of the Society of Naval Architects of Japan, 1986
[8] V.J.Modi, F.Welt, Vibration controlling nutation dampers, International Conference on Flow Induced Vibrations, May 1987
[9] T.Sato, Tuned sloshing damper, Journal of Wind Engineering, Japan, No.32, 1987
[10] T.Sato, Tuned sloshing damper, National Conference of JSCE, 1987 (in Japanese)
[11] M.Ishimoto, M.Ootsuka, Determination de la limite perceptible des secousses, Reports of Seismic Laboratory of University of Tokyo, 1933
[12] M.Fujimoto, T.Ohkuma, et al., Occupant's vibration perception under low frequency excitations, National Conference of AIJ, 1979 (in Japanese)
[13] M.Ohshima, Effects of vibration on human body, Journal of Biomechanism Association, 1984
[14] F.J.Meister, Die meßtechnische Bewertung der Wahrnehmung-sstarke bei der Schwingungsbelastung des Menschen, Zeit schrift fur Larmbekampfung, 30, 1983
[15] ISO 6897, First edition, 1984-8-15
[16] European Convention for Constructional Steel Work; Recommendations for the Calculation of Wind Effects on Buildings and Structures, Technical Committee T12: Wind Effects, 1978
[17] National Building Code of Canada, Part 4, Design 4.1.8, 1980
[18] Australian Standard, Rules for Minimum Design Loads on Structures, Part 2, 1975
[19] Y.Fujino, B.M.Pacheco, P.Chaiseri, L.M.Sun, Fundamental study on Tuned Liquid Damper(TLD) - A new damper for building vibration -, Symposium/Workshop on Serviceability of Buildings, 1987
[20] C.W.Housner, Dynamic pressure on accelerated fluid containers, Bulletin of the Seismological Society of America, 1957

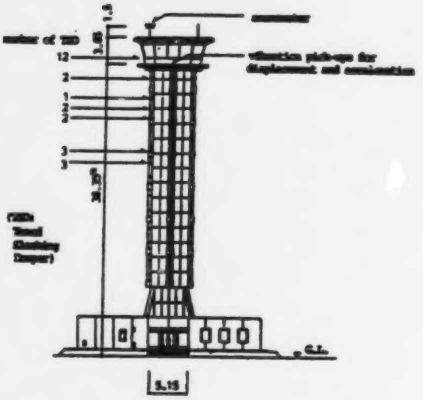

Fig.1 Elevation of the Nagasaki Airport Tower.

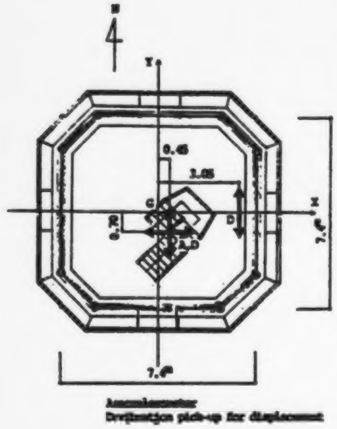

Fig.2 Arrangements of vibration pick-ups for displacement and acceleration in the air traffic control room.

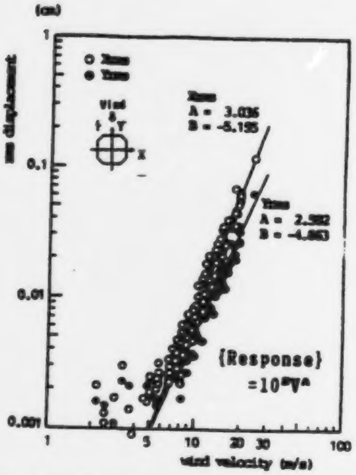

Fig.3 Variations of rms displacements of the airport tower with windspeed.

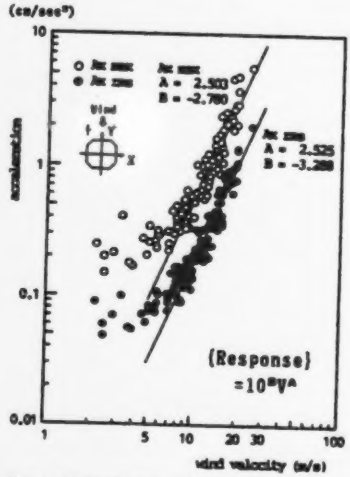

Fig.4 Variations of accelerations of the airport tower with windspeed.

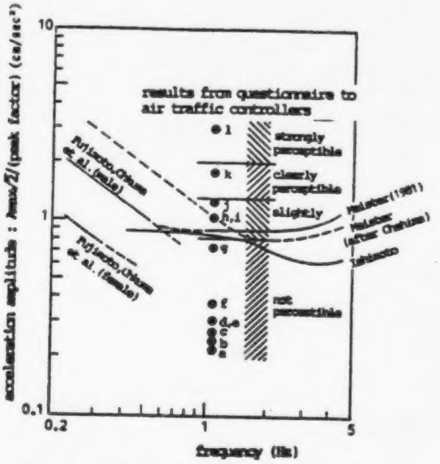

Fig.5 Vibration perception of the air traffic controllers determined by the question-naire study and the threshold curves reported by several researchers.

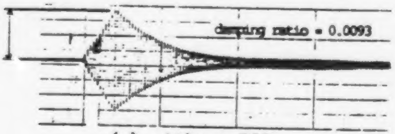

(a) without TSD

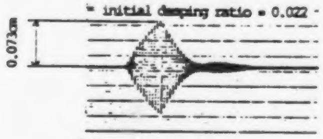

(b) with 7 TSDs

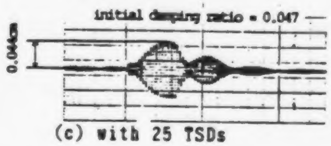

(c) with 25 TSDs

Fig.6 Free vibrations of the airport tower without and with TSDs.

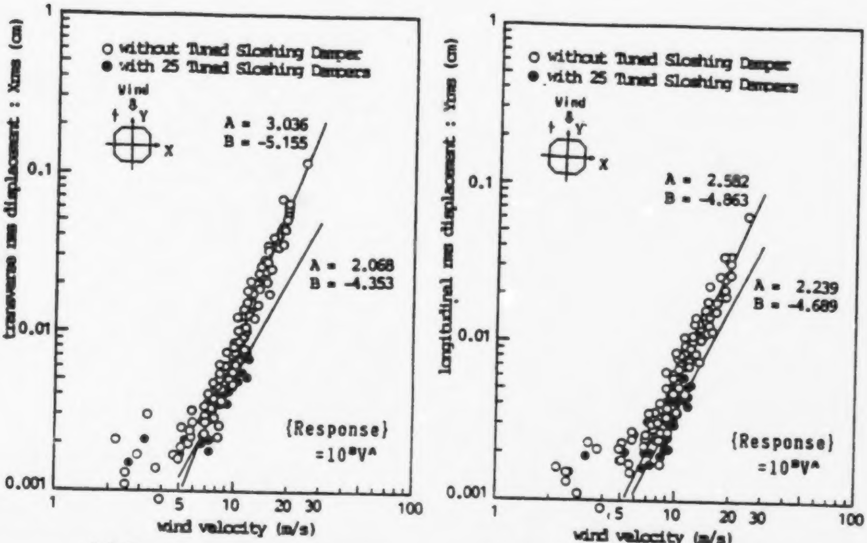

(a) Transverse rms displacements (b) Longitudinal rms displacements

Fig.7 Effects of the TSDs on the response of the airport tower.

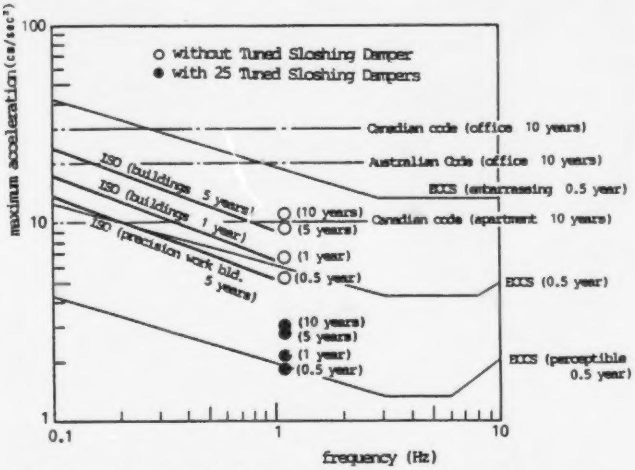

Fig.8 Maximum accelerations of the airport tower for several return periods and comparisons with the levels of vibration acceptable by codes and regulations.

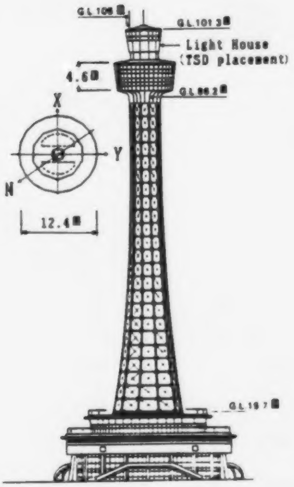

Fig.9 Elevation of the Yokohama Marine Tower

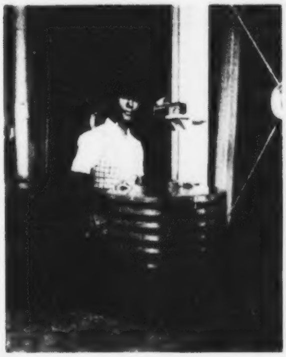

Fig.10 Tuned Sloshing Damper (TSD)

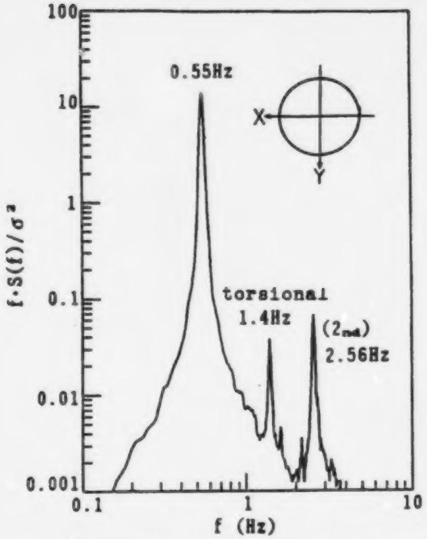

Fig.11 Power spectral density of the acceleration of the Marine Tower.

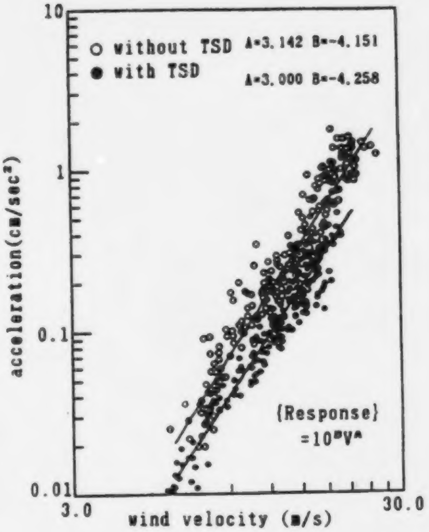

Fig.12 Effects of the TSDs on the longitudinal acceleration of the Marine Tower.

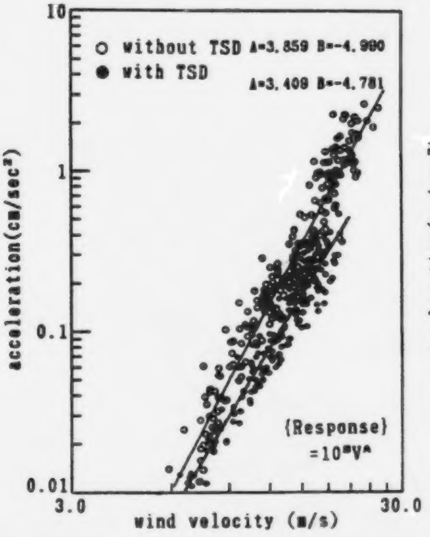

Fig.13 Effects of the TSDs on the transverse acceleration of the Marine Tower.

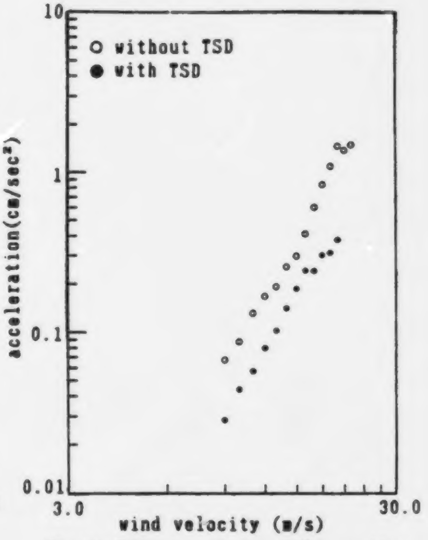

Fig.14 Effects of the TSDs on the average value of rms acceleration of the Marine Tower.

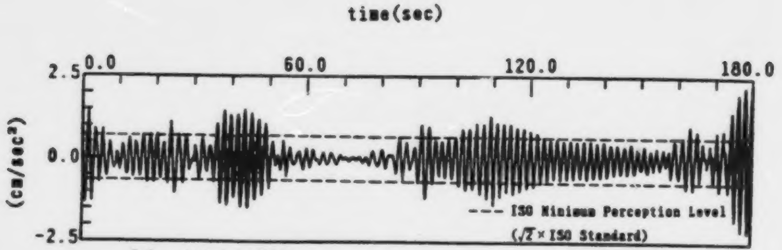

(a) without TSD

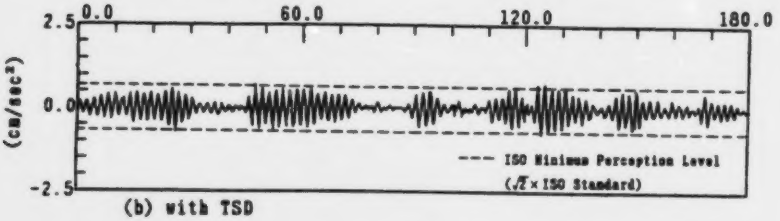

(b) with TSD

Fig.15 Samples of the transverse accelerations of the Marine Tower both without and with TSDs.

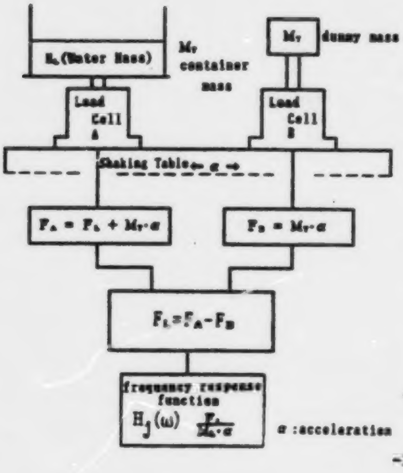

Fig.16 Measuring system of the frequency response function of a TSD.

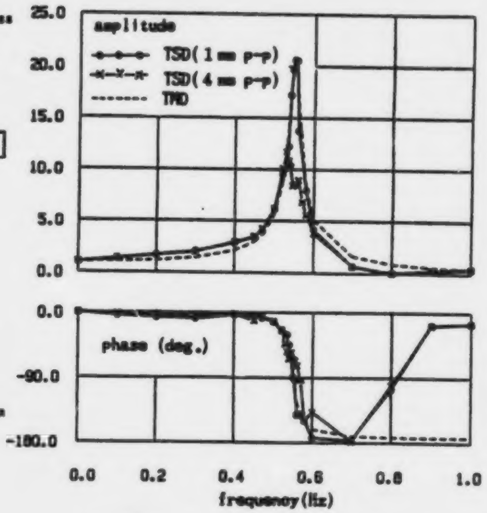

Fig.17 Frequency response function of a TSD.

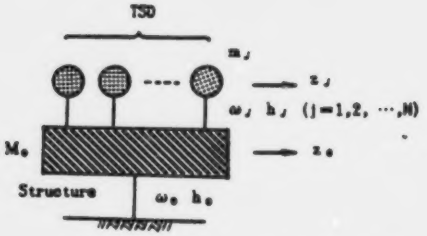

Fig.18 Model of the multiple damper.

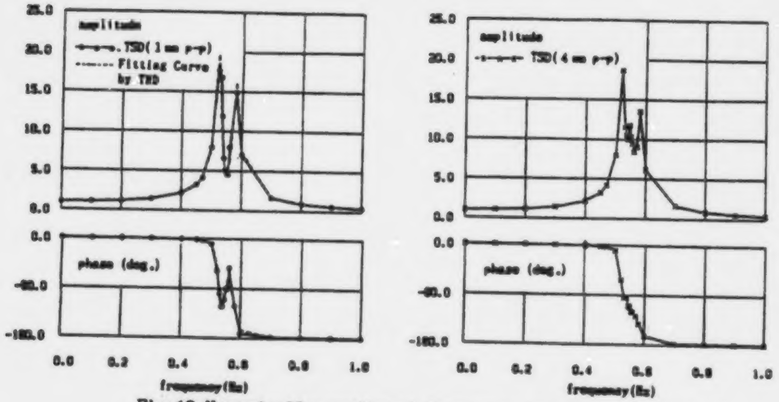

Fig.19 Numerically predicted frequency response function of the Marine Tower using the Lumped Mass System.

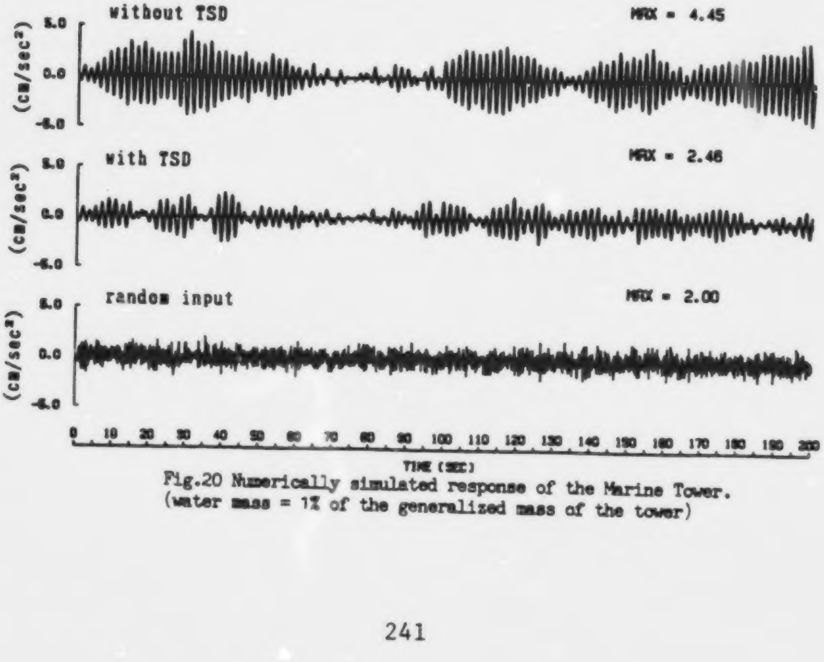

Fig.20 Numerically simulated response of the Marine Tower.
(water mass = 1% of the generalized mass of the tower)

DEVICES FOR DAMPING LATERAL VIBRATIONS IN TALL STRUCTURES

Darren W. Hust

McGill University
Montreal, Canada

ABSTRACT: The combination of lighter construction materials and increasing height, makes modern skyscrapers highly susceptible to lateral forces. While they may be structurally sound, many buildings subject occupants to uncomfortable accelerations, and can damage non-structural elements of the building.

This condition and its subsequent results can be remedied by incorporating damping devices into the structure, which absorb and dissipate vibrational energy.

While the use of various devices is frequently employed, damping of tall building vibration is a quantity which does not readily lend itself to theoretical deduction. For this reason, studies on full-scale structures continue in order to gain data on which theories about structural damping can be based.

1. INTRODUCTION

As buildings increase in height, horizontal loads causing lateral deflections become increasingly hard to resist. With the trend towards lighter, more economic buildings, more efficient methods of resisting these lateral loads must also be sought. Early skyscrapers such as the Empire State Building, completed in 1930, use much more steel (206.5 kg/m^2) than contemporary buildings of similar height such as the John Hancock Center in Chicago (145.3 kg/m^2). [2] This difference in weight is largely due to more innovative and efficient designs, higher strength steels, and the use of welding for fastening instead of bolts which often require angles and gusset plates to make connections possible. There have also been gradual increases in allowable stresses on the basis of ongoing research as well as a reduction in the weight of construction materials, permitting the use of lighter steel frames. [2].

This reduction in weight, however, makes today's skyscrapers much more flexible than previous ones. While the Empire State Building sways only seven or eight centimeters in a strong wind, the World Trade Center (completed in 1972) sways up to 90 cm., very close to the limit of 1/500 prescribed by the Building Code.

Very often, occupants are adversely affected by this lateral movement, even though the building is still structurally safe.

To build taller skyscrapers that remain serviceable, structural engineers have developed various methods of stabilizing them which can be grouped under two basic categories. The first is to rely solely on the structure of the building to limit lateral deflection. These methods, as illustrated in Figure 1, vary in efficiency (compared to a monolithic vertical cantilever) from 25-30% for the Empire State Building to about 90% for the proposed trussed tube design. The frame tube and modular tube designs both have a cantilever efficiency of about 80%. [1] The other proposed designs have undetermined efficiencies at the present time.

To increase building stiffness by even 5-10% can be quite expensive, which has led many structural engineers to find alternate methods of resisting lateral loads. This second category, which is the topic of this paper, consists of various methods of limiting building oscillations aside from merely increasing the building's stiffness. These include tuned mass dampers, passive mass dampers, impact dampers, aerodynamic dampers, viscoelastic (or neoprene) dampers, friction dampers and also a fully active damping system which utilizes cable bracing, now in the development stage.

2. TYPES OF DAMPING DEVICES

Damping of a building may come from structure, from its foundations, from aerodynamic forces or from added damping devices. [3] These devices include viscoelastic dampers, friction dampers, passive dampers, tuned mass dampers, aerodynamic dampers, impact dampers, as well as a proposed fully active cable bracing system. Very often these devices are more effective and efficient than attempting to increase the building stiffness, which has a negligible effect on acceleration, the main cause of human discomfort. [7]

2.1 Viscoelastic Dampers:

2.1.1 **Background:** Layers of viscoelastic material may be used to augment the inherent damping of structures in two basic ways, as illustrated in Figure 2. The first method, as seen in Figure 2a, is where a thin layer of stiff polymer is used to coat the base structure (most often a beam or plate). Within certain temperature and frequency limits, the inherent damping of the viscoelastic material can be many times that of the underlying metal. [11] When the structure deforms due to externally applied loads, the viscoelastic material undergoes stretching and compression, moving with reluctance. This decreases lateral movement, converting the energy from the swaying structure into harmless heat. Maximum damping is achieved using as stiff a coating as possible. [11]

Figure 2b illustrates the other way in which viscoelastic material is used to increase structural damping. This time the material is sandwiched between two steel plates. When these plates vibrate or move with respect to one another, the damping layer undergoes oscillatory shear which results in energy dissipation. Contrary to the first method, the use of a constrained viscoelastic layer requires a relatively soft type of neoprene or related polymer for maximum damping. This second method produces more damping per unit of added weight than the free layer treatment, and is consequently used more often. [11] The World Trade Center (Figure 3) has this type of damper separating the walls from the floors. [5]

2.1.2 Effectiveness of Viscoelastic Dampers: Evaluations of the damping of structures utilizing a viscoelastic material are most often made in terms of a parameter known as a loss factor. The loss factor is a quantity associated with steady state sinusoidal vibration and can be expressed as follows:

$$\eta = \frac{1}{2\pi}\left[\frac{\text{energy dissipated per cycle at resonance}}{\text{peak energy stored at resonance}}\right] \qquad (1)$$

Loss factors for typical viscoelastic materials can be as high as 10 with values between 1.0 and 2.0 being regarded as very good. [11] An example of equipment commercially available for the measurement of loss factors is the Model 830 Elastomer Test System manufactured by MTS Systems Corporation, which measures stiffness and damping over the ranges 5 to 100 Hz and 15 to 175 C. Comparatively, a metal structure with practical joints or supports would have a loss factor in the range 0.01 to 0.10.

Equation 1 shows that besides measuring the inherent damping of a structure, the loss factor depends on other parameters of the structure. It is important therefore to distinguish between the loss factor η of the viscoelastic material and the loss factor η_s of the structure as a whole. Hence, in Equation 1, the energy terms refer to the viscoelastic material only if η is the desired loss factor. [11]

To maximize the loss factor for the entire structure, it makes sense to apply the viscoelastic material where there is the largest amount of stored energy. For example, in a beam exhibiting flexural vibration, the damping material is most effective placed as far from the neutral axis as possible. This is because most of the stored energy is concentrated in the flange area. Formulas for the design of structures utilizing viscoelastic dampers can be found in Reference 15.

2.2 Friction Dampers: Friction dampers are particularly useful in damping vibrations caused by seismic forces, although they may also be used to damp wind forces. [10] These types of dampers as used in steel framed buildings will be discussed under two main subsections, rigid frames and braced frames.

2.2.1 Rigid Frame Friction Dampers: Friction dampers can be used in rigid frames to provide real plastic hinges which yield under the appropriate moment. [10] This avoids having to rely on beams to provide plasticity and the subsequent permanent damage which results.

Suitable solutions, as given by Marsh and Pall in Figure 4, are ones in which the beams continue to transmit shear as the hinges rotate (columns will remain elastic). Rigid frames incorporating these types of dampers are analyzed using existing procedures for plastic analysis.

Any permanent distortion of a building, subsequent to an earthquake can be eliminated by loosening and retightening any bolts in joints which have moved. The essential elasticity of the building frame will return the structure to its original shape. [10]

2.2.2 **Braced Frame Friction Dampers:** In braced frames, the use of diagonal bracing which slips at a predetermined stress value is employed. Once the diagonal bracing has slipped, there must be an increase in the shear force carrying capacity by some other part of the structure so as to force slippage of successive diagonals in a vertical panel of the building. This will return the building to its original position as the earthquake passes. A second vertical panel of bracing, which does not slip, will limit the travel in the slip joints to the elastic strains in the diagonals of the second panel. [10]

When a combination of tension and compression diagonals are used to resist lateral loads, the sliding devices can be incorporated in their joints which will allow simultaneous slippage. This will prevent the occurrence of any secondary bending moments in the structure. Figure 5 illustrates how the sliding motion occurs either along the diagonals and the beams or columns, as well as the mode of slippage for various forms of two way bracing. [10]

Very often it is desirable to use a tension only cross bracing system to avoid having to use heavy compression members. In this case, it is essential that only the tension diagonal is loaded (or that the compression remains as small as required in the other diagonal), regardless of the direction of the lateral force. [10] Figure 6 shows some friction damping devices which allow this type of tension only system.

The friction dampers discussed above are ideal for the damping of seismic vibrations because they have a predictable slip load and also due to their uniform hysteretic behavior. They permit plastic behavior by replacing yielding as a means of providing non-linearity while allowing the structure itself to remain elastic. [10]

2.3 Tuned Mass Dampers:

2.3.1 **Introduction:** Another damping device, which is used very often, is known as a tuned mass damper (TMD). Frequently applied in machinery, automative and aircraft engines, the use of large-scale tuned mass dampers has come about only recently in structures such as the Centrepoint Tower in Sydney, the CN Tower in Toronto, Boston's John Hancock Tower and the Citicorp Center in New York City. [14]

The TMD as used in structures consists of a large mass which moves ninety degrees out of phase to the swaying building, hence inertially damping any lateral movement. [5] The CN Tower (Figure 7) uses two small tuned mass dampers to reduce the second and fourth modes of vibration in order to minimize antenna bending loads. [12] Two TMD's, 67 meters (220 ft.) apart in Boston's John Hancock Tower (Figure 8) decrease wind induced twisting. [5] Prior to their installation, this twisting motion caused many windows to crack and fall out of this building. The large TMD installed in the Citicorp Center in Manhattan to control first mode bending, offers insight into state of the art design and operation of tuned mass dampers and will subsequently be discussed in some detail.

2.3.2 Citicorp Center Tuned Mass Damper:

2.3.2.1 **Configuration and Basic Operation:** Installed on the 63rd floor of New York's Citicorp Center (Figure 9) is a 363,000 kg (410 ton) concrete block 9.1m (30 ft.) square by 2.7m (9 ft.) high (Figure 10).

Since the TMD is used for building occupant comfort, it is automatically activated by accelerations between 0.001g to 0.003g which are below the threshold of human perception. [5,12] These minute horizontal accelerations are detected by accelerometers bolted to the frame of the building.

Upon activation of the system, the concrete block is hydraulically raised, enabling the building to move back and forth under the block. As this happens, the block's movement is inhibited by two nitrogen charged springs, tuned to the natural oscillation period of the building. Next, two computer controlled hydraulic actuators push and pull the concrete block back and forth, in two directions simultaneously, inertially damping the sway of the building. [5]

2.3.2.2 **Mass Block Support Bearings:** When not in operation, the mass block of the TMD rests on a set of phenolic blocks with rubber springs to prevent unnecessary load concentration on the floor. Upon activation of the system, the block is raised about 19 mm (3/4 in.) and the damper is operable in about three minutes. While in operation, the mass block is supported on a series of twelve, 55.9 cm (22 in.) diameter hydraulic pressure balanced bearings (PBB - Figure 11).

The twelve bearings sit on two 19 mm (3/4 in.) thick hot rolled steel plates 3.6 m by 9.1 m (12 x 30 ft.) which were polished on site to a local flatness of 1.6 mm (1/16 in.) so as to minimize oil leakage through the elastomeric seals. The individual bearings are hydraulically coupled together as illustrated in Figure 12, with each group containing its own height control valve so that the bearings evenly distribute the floor loading despite any unevenness present in the bearing plates. The overall achieved coefficient of friction for the PBB installation is about 0.003 requiring an actuator force of about 10.6 kN (2,400 lbs.) to overcome frictional losses.

2.3.2.3 **Control Actuators:** Simultaneous movement of the block in the E-W and N-S directions is provided by two double acting equal area hydraulic actuators. Designed for a maximum velocity of 1.72 m/sec (68 in/sec) with a piston area of 83.9 cm^2 (13 in.^{2}), each actuator provides a maximum damping force of 209 kN (47 kips) as shown in Figure 13. From this diagram it can also be seen that at zero actuator force the maximum driving velocity is 71 cm/sec (28 in/sec) and that at velocities greater than this, the control actuator must absorb energy from the forcing device. [12] Each actuator has an operating stroke of 2.75 m (108 in.) at which the system allows a free motion of 218 cm (86 in.) after which hydraulic overtravel snubbers attached to the block, come into contact with concrete abutments formed as part of the floor. These snubbers allow an overtravel of 5 cm (2 in.), after which the TMD automatically shuts down.

The TMD also shuts down when thirty minutes have elapsed in which building sway has not exceeded 0.00075g in either axis. As another safety feature, the block is also constrained from rotational motion by an anti-yaw assembly (see Figure 10). [12]

2.3.2.4 **Passive Spring System:** Due to the overall size of the tuned mass damper used in the Citicorp Center, new technology was required in the design of a passive spring system. Earlier TMD's used the concept of torsion bars to absorb energy, which would have been impractically large and expensive if applied to the Citicorp TMD (305 mm in diameter and 41.1 m long for each axis of the system). This problem was overcome by using two opposed pneumatically precharged cylinders as shown in Figure 14. Deflections occurring perpendicular to the axis of the cylinders cause a very linear force-deflection relationship since the inherent non-linearity of adiabatic gas compression in a closed vessel is almost exactly compensated by the geometric considerations. [12]

This linear relationship (Figure 15) and the compactness of the system made it the ideal solution for the TMD. The operating precharge of the Citicorp TMD is about 5,865 kN/m^2 (850 psi) of dry nitrogen and can be easily adjusted to vary the spring rate if necessary. The previous torsion bar concept involved the use of torsion bars with varying length arms to change the spring rate in order to vary the natural frequency.

2.3.3 Efficiency of the TMD: The Citicorp TMD system uses four main hydraulic pumps which supply fluid from a 0.76 m^3 (200 gal.) tank at a pressure of 4,830 kN/m^2 (700 psi). Generally one pump is sufficient to operate the system with three units being necessary under the most severe excitation conditions. [12]

A recent study [14] conducted by Tanaka and Mak (1983) showed that a properly tuned damper will reduce building response by 30-60%. They found too, that the narrower the band width of excitation frequency, the more effective the damper can be. Maximum effective damping occurs when the TMD is tuned close to the building frequency but not necessarily exactly the same. [14]

The tuned mass damper in the Citicorp Center reduces the rms building sway amplitude by 45-50%. [5,12] This is equivalent to raising the basic structural damping to about 4%. Engineers estimate that the Citicorp damper produces an improvement equivalent to quadrupling the structural bracing of the building, a saving of nearly four million dollars. [5]

2.4 Fully Active System: Despite the fairly high efficiency of tuned mass dampers, experiments are being carried out to produce a fully active system. One such system in the development stages at State University in Buffalo, New York has sensors and jacks which operate a cable bracing system. [5] Such a system, as illustrated in Figure 16, could be particularly effective under earthquake loading. The beauty of a fully active system is that deflections could be reduced completely to zero.

One objective of the ongoing study is to determine how many sensors, cables and controllers are needed, and where they should go. Once this has been done, researchers feel that the ideas will be applied first to television towers and eventually to bridges and buildings. Whether or not a fully active system applied to a large structure would be economically feasible, remains to be seen. Also questionable, is the necessity to eliminate, completely, deflections caused by accelerations below the human threshold of perception.

2.5 Other Types of Damping Devices: In addition to the previously discussed types of damping devices, the following merit brief mention.

The first of these is the passive mass damper. The basis behind this type of damper is similar to that of the tuned mass damper in that a mass resists motion and hence inertially damps the structure. One example of a passive system would be a TMD without the actuators moving the block contrary to the building movement. A water tank located at the top of a building contributes to the damping of a structure in the form of a passive damper. To analyze this type of damping requires a theoretical derivation of the natural frequencies of the free surface waves in the tank. [9] Passive dampers, however, lack the accuracy, dynamic range and flexibility found in active systems such as a tuned mass damper. [12]

Another type of damping device, used to counter the problem of vortex shedding, is the aerodynamic spoiler. [8] Vortex shedding causes tall, slender stacks to vibrate in a plane perpendicular to the direction of the wind. At critical wind speeds, vortices are shed at regular intervals alternately on each side as the wind passes the structure, causing pressure differentials which create the lateral vibration. [4,6] An aerodynamic spoiler, which is a continuous metal plate ledge spiralling the stack, does not allow air to flow directly past the stack, eliminating vortex shedding, and hence damping the structural vibrations.

Another class of damping devices is the impact damper. This type of damper can be applied to antennas and smoke stacks, consisting most often of a rubber encased chain hanging inside a vertical channel in the structure. When the structure vibrates, the chain periodically impacts the channel walls, dissipating the vibrational energy of the structure. A comprehensive study of these types of dampers is given by Reed [13].

3. SUMMARY AND CONCLUSIONS

As a building's height increases and its weight decreases, due to lighter and stronger construction materials, it also becomes more flexible. Modern structures deflect more under lateral loads than earlier skyscrapers because of this increased flexibility.

Although today's tall buildings are structurally safe, they may not be entirely serviceable to people inhabiting them, under severe lateral loading conditions. Building codes stipulate that the drift ratio must be limited to 1/500, but investigations into human comfort suggest that this ratio is not a satisfactory indicator of the effect of building sway on its occupants. Several studies have found that acceleration is the main reason people perceive movement in structures. These same studies give guidelines to providing tall but comfortable structures based on acceleration criteria, but building codes still rely merely on the drift ratio.

To prevent any undesirable physiological and psychological effects on building occupants and also damage to non-structural elements of the building, engineers can increase the stiffness of the structure. This is very costly and, while it will prevent damage to non-structural materials, it has a negligible affect on acceleration and hence does not significantly improve human comfort.

A more effective method of decreasing building sway and counteracting rms acceleration is to use a damping device. These include viscoelastic dampers, passive dampers, aerodynamic dampers, impact dampers, friction dampers and tuned mass dampers. These devices damp building vibrations by absorbing and dissipating the energy of the swaying building. At present, engineers are attempting to perfect a fully active system which would completely eliminate lateral movement of tall structures. This system's potential for application to television towers and masts appears promising, but its suitability and cost efficiency as applied to large buildings is questionable.

Damping of structures is a quantity which does not lend itself to theoretical deduction. For this reason, the most reliable method of obtaining information of a structure's damping characteristics is to conduct vibration tests. From results of these tests, engineers hope to be able to establish concrete theories about structural damping. The tuned mass damper has proven very effective in several structures.

Damping of tall structure vibrations is a topic on which much attention, both theoretical and practical, is and will be focussed in the future.

REFERENCES

1. Ashley, S., "Superskyscrapers", in Popular Science, December 1985, pp. 62-65.
2. Donahue, M.A. (Ed), "Less Steel Per Square Foot", in Modern Steel Construction, 12:1, March 1972, pp. 8-9.
3. Etkin, B. and J.S. Hansen, "Effect of a Damper on the Wind-Induced Oscillations of a Tall Mast", in Journal of Wind Engineering and Industrial Aerodynamics, Vol. 17, 1984, pp. 11-15.
4. Etkin and Hansen, pp. 17-20.
5. Gannon, R., "Buildings That Keep Their Balance", in Popular Science, August 1985, pp. 58-62.
6. Gaylord, C.N. and M. Watabe (Eds), Monograph on Planning and Design of Tall Buildings (Volume SB) Structural Design of Tall Steel Buildings (New York: ASCE, 1979), pp. 86-87.
7. Gaylord and Watabe, pp. 395-396.
8. Gould, P.L. and S.H. Abu-Sitta, Dynamic Response of Structures to Wind and Earthquake Loading (New York: John Wiley and Sons Inc., 1980), pp. 122-123.
9. Kolousek, V. and others, Wind Effects on Civil Engineering Structures (Oxford: Elsevier, 1984), pp. 277-279.
10. Marsh, C. and A.S. Pall, Friction Devices to Control Seismic Response, Conference on Dynamic Response of Structures, Atlanta, Georgia, January 15-16, 1981.
11. Nelson, F.C., "The Use of Viscoelastic Material to Damp Vibration in Buildings and Large Structures", in Engineering Journal, 5:2, April 1968, pp. 72-78.
12. Petersen, N.R., "Design of Large Scale Tuned Mass Dampers" in Structural Control (North Holland Publishing Company, 1980), pp. 581-596.

13. Reed, W.H., Hanging Chain Impact Dampers: A Simple Method for Damping Tall Flexible Structures, Proceedings Vol. II from Conference on Wind Effects on Buildings and Structures, Ottawa, September 11-15, 1967.

14. Tanaka, H. and C.Y. Mak, "Effect of Tuned Mass Dampers on Wind Induced Response of Tall Buildings", in Journal of Wind Engineering and Industrial Aerodynamics, Vol. 14, 1983, pp. 357-368.

15. Ungar, E.E., "A Guide to Designing Highly Damped Structures Using Layers of Viscoelastic Material", in Machine Design, February 1963, pp. 162-168.

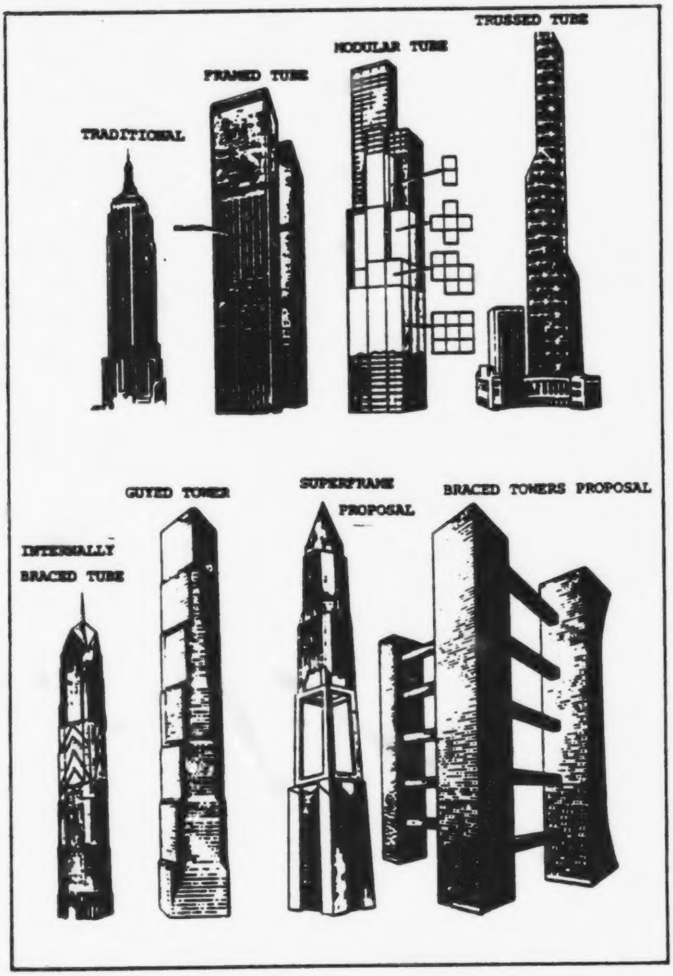

Figure 1: Types of lateral load resisting structures [1]

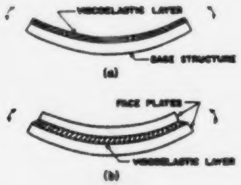

Figure 2: Use of viscoelastic material
to damp flexural vibration [11]

Figure 3: World Trade
Center

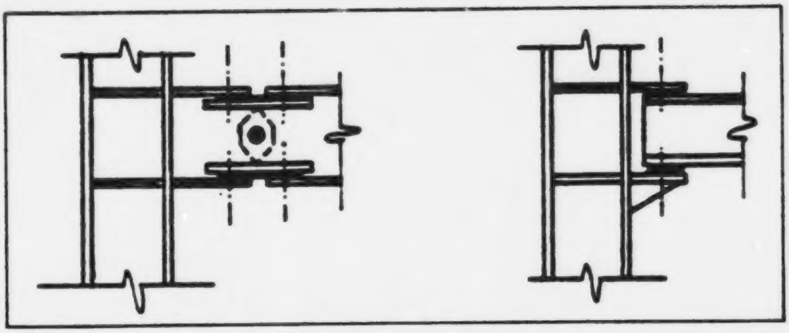

Figure 4: Rigid frame friction dampers [10]

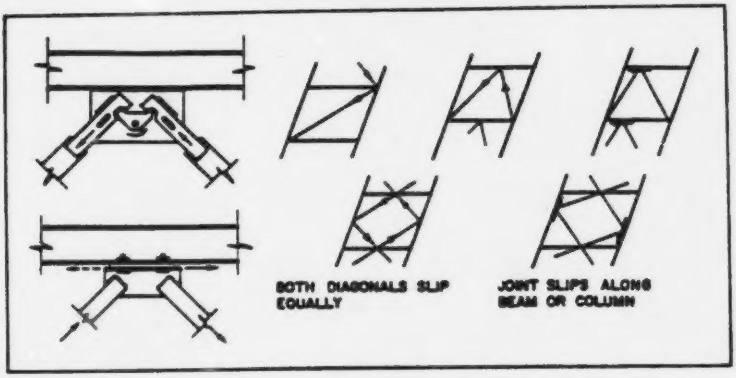

Figure 5: Sliding bracing [10]

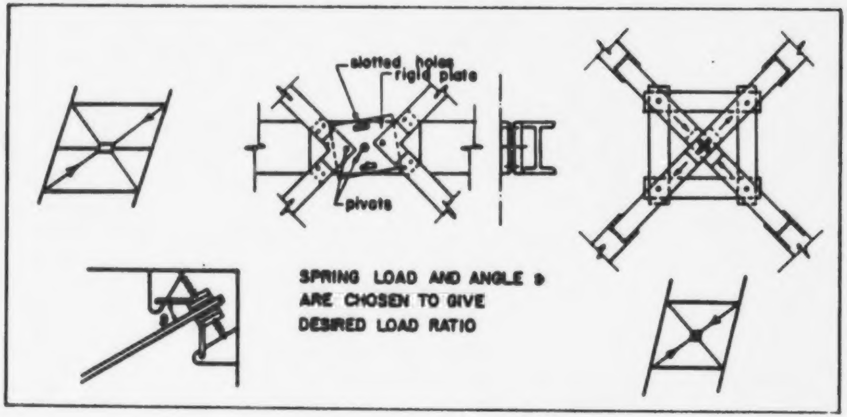

Figure 6: High tension, low compression bracing [10]

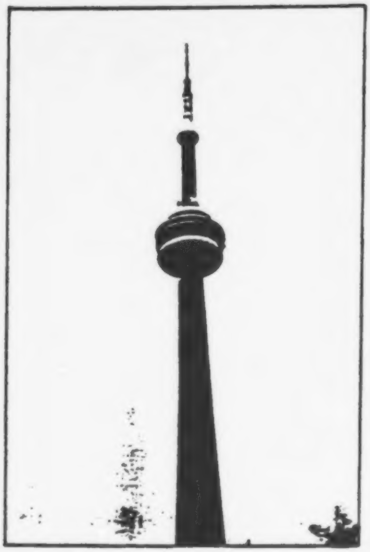

Figure 7: CN Tower

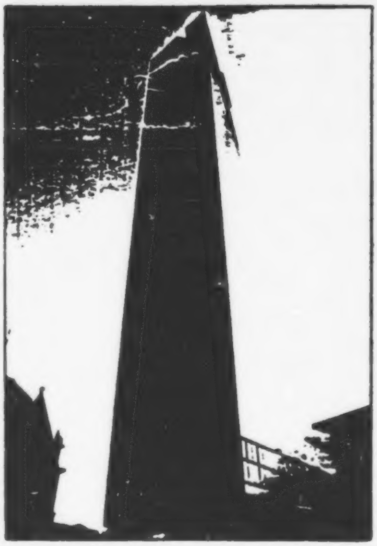

Figure 8: John Hancock Tower

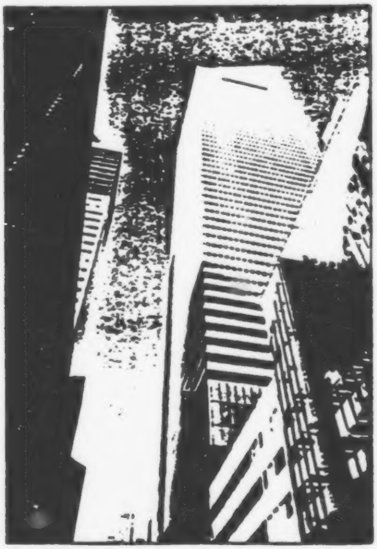

Figure 9: Citicorp Center

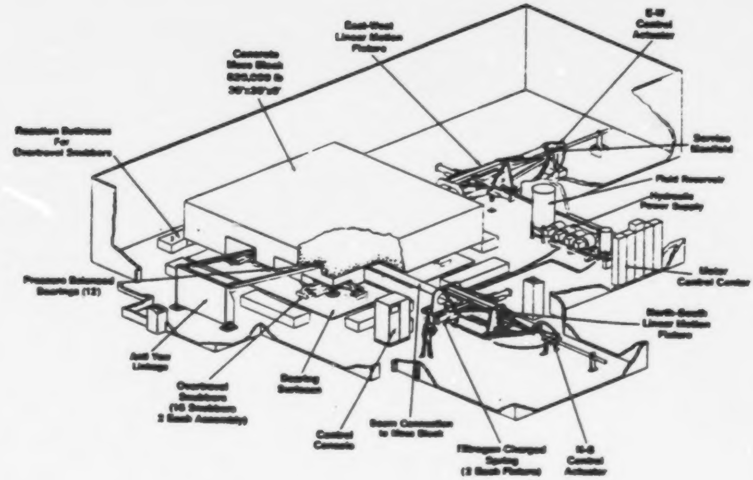
East-West Linear Motion Fixture
E-W Control Actuator
Concrete Mass Block 820,000 lb 30'x30'x8'
Reaction Buttresses For Overboard Snubbers
Service Manifold
Fluid Reservoir
Hydraulic Power Supply
Motor Control Center
Pressure Balanced Bearings (12)
North-South Linear Motion Fixture
Anti Yaw Linkage
Overboard Snubbers (16 Snubbers 2 Each Assembly)
Bearing Surfaces
Control Console
Beam Connection to Mass Block
Nitrogen Charged Spring (2 Each Fixture)
N-S Control Actuator

Figure 10: 63rd floor of Citicorp Center [12]

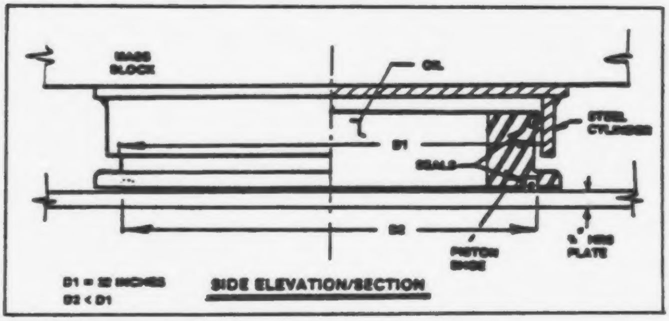

Figure 11: Pressure balanced bearing [12]

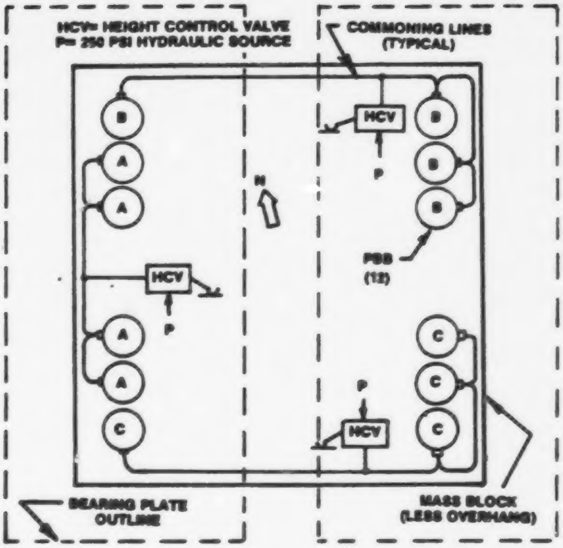

Figure 12: PBB system [12]

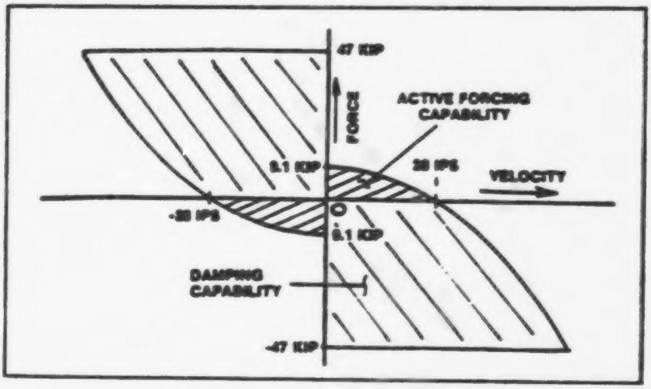

Figure 13: Control actuator force/
velocity capabilities [12]

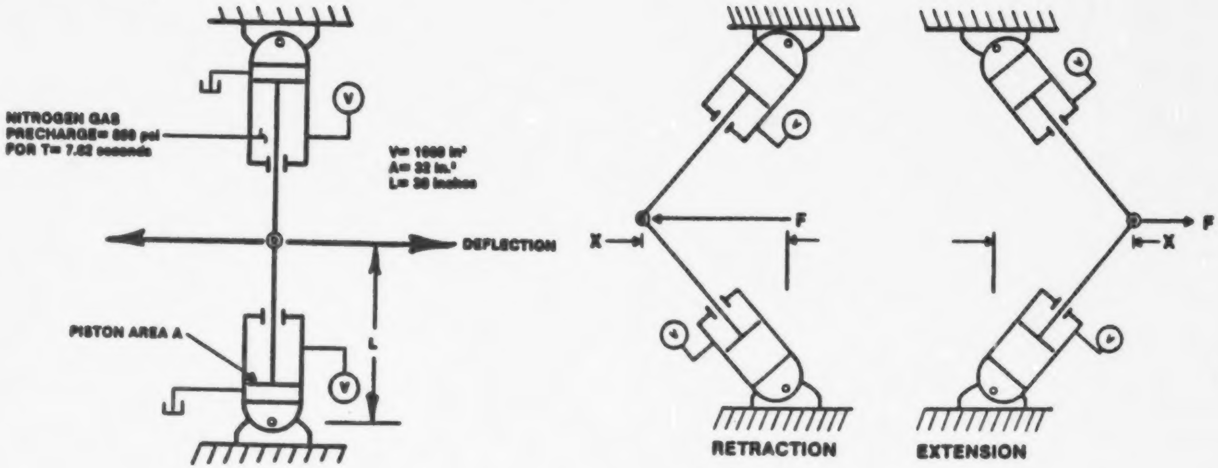

Figure 14: Passive spring operation [12]

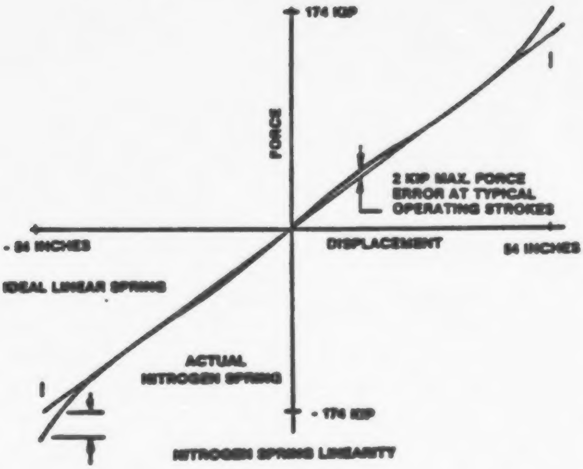

Figure 15: Nitrogen spring linearity [12]

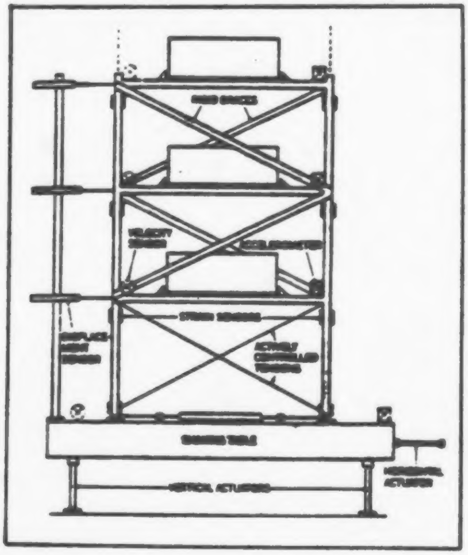

Figure 16: Fully active system [5]

PROBABILISTIC CRITERIA FOR HUMAN PERCEPTION OF LOW-FREQUENCY HORIZONTAL MOTIONS

J. Kanda
University of Tokyo, Tokyo, Japan
Y. Tamura
Tokyo Insitute of Polytechnics, Atsugi, Japan
and K. Fujii
Institute of Technology,
Shimizu Construction Co., Ltd., Tokyo, Japan

ABSTRACT: The serviceability criteria for tall residential buildings against strong winds tends to be determined by the human perception limit of low-frequency horizontal motions. Although there have been various reports and proposals published for human perception limits of these, existing experimental results are seldom sufficient to discuss their statistical nature especially for a low frequency region.

A new spring pendulum shaking simulater (S.P.S.S.) was designed and constructed to provide a realistic residential space and to produce controlled acceleration time histories for human perception tests. Sinusoidal step-by-syep waves were successfully re-produced with acceleration amplitudes ranging from 0.0002 to 0.008 g for a frequency region between 0.3 and 2.0 Hz. Experiments were repeated for over one hundred subjects.

The results were compared with existing proposals and discussed by applying log-normal probability distributions to each group of human responses for two body orientations, various age and sex categories. Statistics for human perception limits were reduced to a preliminary proposal for serviceability criteria of probability-based design for tall residential buildings against strong winds.

1. INTRODOCTION

There have been quite a few reports and proposals for horizontal vibration criteria since 1930's. [1,2,3,4,5] In spite of those amounts of data, objective comparisons have not sufficiently been made and so not only the societial consensus but consensus among engineers seem not to be reached yet concerning the rational serviceability criteria for the low-frequency horizontal motion of buildings.

Data sources are due to either vibration simulater tests or vibrations of actual buildings. The former tends to have some difficulties in the simulation of vibration environment including the realistic setting of interior surroundings and the accurate representation of aimed motions. Problems for the latter case are the limitation of samples and repeatability. These are major reasons for the difficulty in objective comparisons of human perception criteria.

So far most codes and standards including ISO specifying the vibration criteria tend to give some descriptions for the human response. However the variability of individual responses is fairly large [6], and so the descriptions are not always applicable to individuals. Moreover, annoyance criteria are easily changed by some social and economical situations and human experiences, while the perception criteria seems to be less sensitve against the change of situations. In tall residential buildings in Japan, claims by occupants seem to occur because he/she often feels the vibration but not because he/she can not bear the level of vibration. In order to reach some consensus in the serviceability limit state of horizontal motion, it is essential to discuss the probabilistic nature of human perception of the motion.

The purpose of this paper is to provide fairly large number of data for the human perception criteria of low-frequency horizontal vibrations and to evaluate the variability of human perception considering various human factors for a typical body posture.

2. EXPERIMENTAL METHOD

2.1 Spring Pendulum Shaking Simulator: A new spring pendulum shaking simulater (S.P.S.S.) was designed and constructed in order to achieve the accuracy in the representation of low level acceleration time history. S.P.S.S. is composed of the pendulum (the length of vertical rod is 4 m hinged at both ends), the test room (width: 2.4 m, length 3.7 m, height 2.4 m), an electro-magnetic type oscillator (maximum input force : 1900 N, maximum stroke ± 12.5 mm) and the connecting spring (spring constant : 11920 N/m). The schematic view of S.P.S.S. is shown in Fig. 1.

The system is meant to be one mass and dual spring system with one degree of freedom. The higher frequency motion from the oscillator is diminished by the existence of connecting spring. Measured and calculated response characteristics in terms of the ratio of response acceleration amplitude to the input displacement amplitude are shown in Fig. 2. The agreement is satisfactory. The natural frequency is 0.442 Hz for the empty condition of test room, the effective mass is 2268 kg and the damping ratio is 0.04.

The interior of test room is simulated to be a realistic sample. A screen painted in blue was attached to the outside of a large window. Small windows are blind type so that subjects can not obtain visual clues through a view from windows. The space is wide enough for two persons. The plan of test room is shown in Fig. 3.

2.2 Test Procedure: As a typical body posture sitting on a fairly rigid chair was selected. By setting two chairs in two directions as shown in Fig. 3, two body orientations, fore-and-aft and side-to-side, can be tested at one time. The range of frequency was chosen to be 0.33 Hz, 0.5 Hz, 0.8 Hz, 1.25 Hz and 2.0 Hz. Sinusoidal step-by-step waves were reproduced with acceleration amplitudes ranging from 0.0002 g to 0.008 g. Each time history is simulated to be continuous ten step ascending level motions and ten step descending level motions with a duration time of six mimutes.

The maximum level of amplitude was determimed to be greater than the average level of perception limit described in ISO guidelines [7]. An example of input

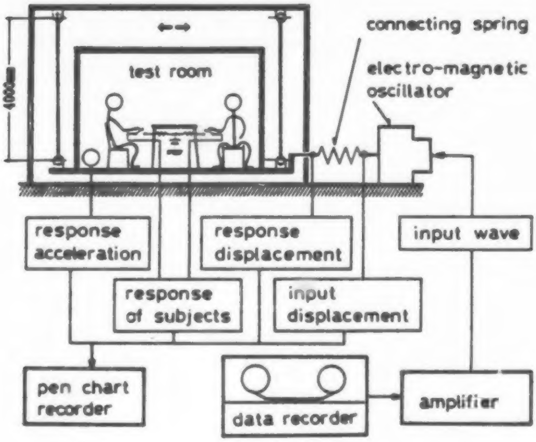

Fig. 1 Schematic view of S.P.S.S. and measurement diagram.

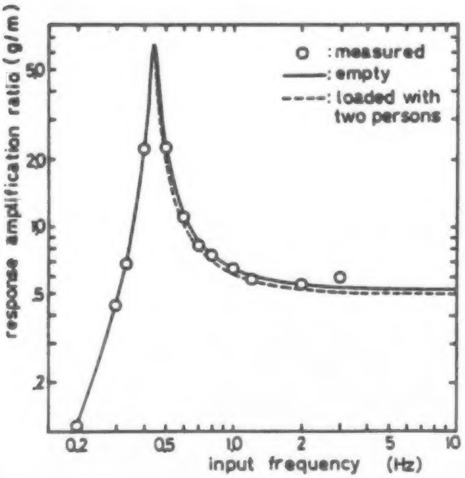

Fig. 2 Measured and calculated response amplification.

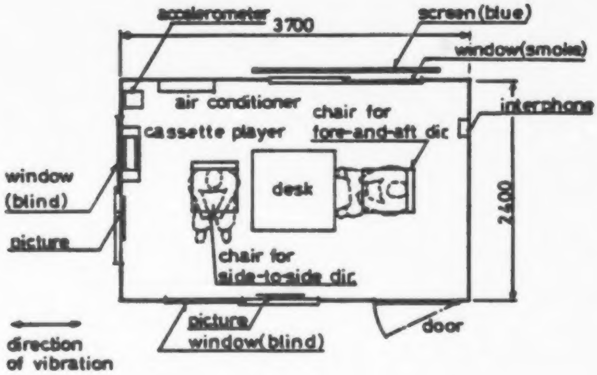

Fig. 3 Plan of S.P.S.S. test room.

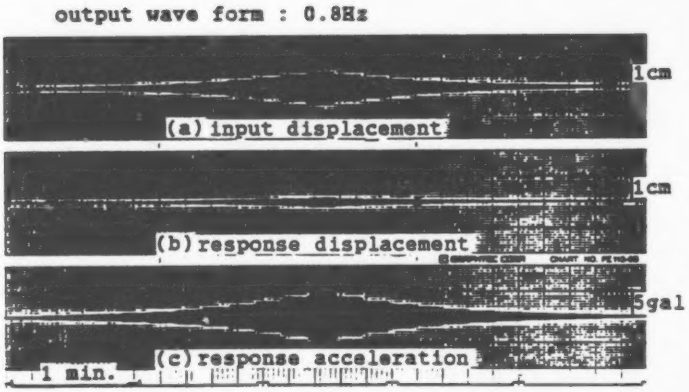

Fig. 4 Example of input and output time histories.

Table 1 Number of tested subjects

sex age	male	female	total
20's	24	20	44
30's	31	9	40
40's over	25	10	35
total	80	39	119

and output time histories are shown in Fig. 4.

The detection of the subjective perception is obtained through a holding type switch with a pilot lamp and recorded simultaneously with the input and output motions. Each subject is directed to switch on when he/she begins to feel vibration and to switch off when he/she ends to feel. One test cycle is composed of five sets of motions with randomly ordered various frequencies. Each subject takes two cycles of test by exchanging the position to change the body orientation to the motion direction. Compulsory time for a subject is approximately 80 minutes including a prepapratory test and answering the enquiry. Number of subjects are 119 as listed in Tabel 1. Age and sex distribution is also tabulated.

3. EXPERIMENTAL RESULTS

3.1 Overall Results: All data were plotted in Fig. 5 for the fore-and-aft direction and in Fig. 6 for the side-to-side direction. Figures 5(a) and Fig. 6(a) are the cases of increasing amplitude, i.e. beginning of perception and Fig. 5(b) and Fig. 6(b) are those of decreasing amplitude, i.e. ending of

Table 2 Statistics of perception criterea

(a) increasing amplitude, fore-and-aft direction

frequency	0.33	0.5	0.8	1.25	2.0
mean ($\times 10^{-3}$g)	2.59	2.11	1.52	1.25	0.86
c.o.v.	0.55	0.50	0.53	0.50	0.59

(b) decreasing amplitude, fore-and-aft direction

frequency	0.33	0.5	0.8	1.25	2.0
mean ($\times 10^{-3}$g)	2.07	1.54	1.25	1.04	0.82
c.o.v.	0.44	0.44	0.44	0.50	0.45

(c) increasing amplitude, side-to-side direction

frequency	0.33	0.5	0.8	1.25	2.0
mean ($\times 10^{-3}$g)	2.07	1.82	1.22	0.98	0.75
c.o.v.	0.60	0.51	0.49	0.51	0.56

(d) decreasing amplitude, side-to-side direction

frequency	0.33	0.5	0.8	1.25	2.0
mean ($\times 10^{-3}$g)	2.06	1.45	1.15	0.88	0.77
c.o.v.	0.44	0.44	0.37	0.44	0.45

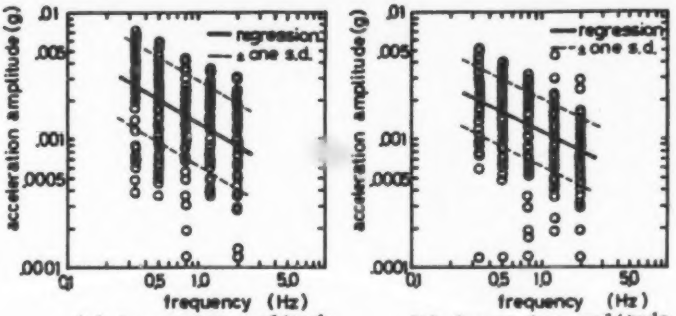

(a) increasing amplitude (b) decreasing amplitude

Fig. 5 Perception plots for the fore-and-aft direction.

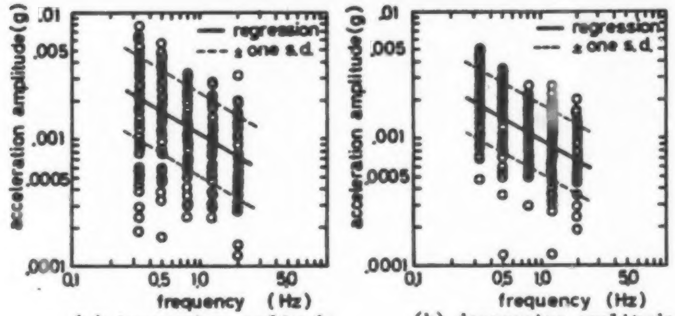

(a) increasing amplitude (b) decreasing amplitude

Fig. 6 Perception plots for the side-to-side direction.

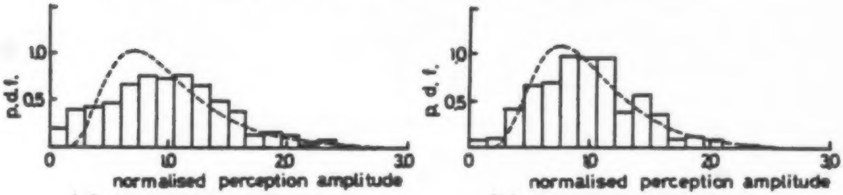

(a) increasing amplitude (b) decreasing amplitude

Fig. 7 Perception histogram for the fore-and-aft direction.

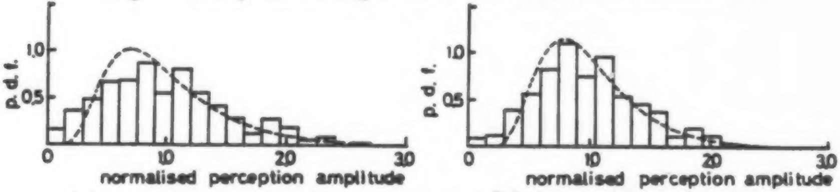

(a) increasing amplitude (b) decreasing amplitude

Fig. 8 Preception histogram for the side-to-side direction.

perception. Least squares fit lines are shown with ± one standard deviation in dotted lines. The gradient of perception limit against the frequency agrees well with the ISO curve [7]. The perception limit tends to be slightly more sensitive for the side-to-side direction than for the fore-and-aft direction and for the decreasing amplitude than for the increasing amplitude. This tendency is consistant with existing reports [6], although the difference is minor in comparison with the scatter or variation of data.

The statistics corresponding to Figs. 5 and 6 are shown in Table 2. The coefficient of variation (c.o.v.) is approximately 50 % for each frequency and similar for all cases. C.o.v. values are slightly greater for the increasing amplitude than for the decreasing. Frequency distributions are shown in Figs. 7(a)(b) and 8(a)(b) corresponding to Figs. 5(a)(b) and 6(a)(b). The abscissa of histograms is expressed in terms of the acceleration amplitude normalised by the mean value at each frequency. Smoothed curves show the log-normal probability density with the mean of unity and corresponding c.o.v. value. The log-normal probability distribution seems to be a reprentative model for the individual perception limit variation.

3.2 Effects of Age and Sex: In order to examine the effects of age and sex on the perception limit, plots for each age and sex group according to Table 1 are shown in Fig. 9 for the fore-and-aft direction. Probably because of the lack of sufficent numbers of data especially for groups of age 30's and 40's female, the gradient is rather unstable. Nevertheless the general tendency indicates that female subjects and younger subjects for the male have more sensitive limits as previously reported [6], but age differences for female subjects are not very clear.

Effects of such factors as the body orientation, increasing or decreasing, the age and the sex can be pointed out, however, differences due to those factors are not significant at least in comparison with the variation of individuals.

4. TENTATIVE PROPOSAL FOR PROBABILISTIC CRITEREA

Since the effects of direction, age and sex are not significant, one probabilistic criteria for human perception limit could be sufficient for practical applications. The body orientation can not be controlled in ordinary situations and seems to be at random, and so the average of means of both directions may be used. The range between 1 % and 99 % of cumulative probability in the frequency range examined is shown in Fig. 10 together with exsting guidelines and reports [1,5,7,8]. Some discrepancies among existing data fall in this range of the present test.

The human perception criteria for low-frequency horizontal vibration can be tentatively proposed as Fig. 11, where various percentile lines are shown. The 1 to 10 percentile lines approximately coincide with the ISO minimum line, (compared as $\sqrt{2}$ times r.m.s. value). This type of probabilistic expression fits to the serviceability limit state definition in the recent probability-based L.R.F.D. procedure rather than the deterministic perception and annoyance criteria [9]. Then, once the reliability index for non-perception of vibration for certain period, say one year, is determined, the design procedure can be developed in a fully probabilistic way.

5. CONCLUSIONS

Subjective human responses to the low-frequency horizontal vibration simulated by a newly constructed spring-pendulum-shaking simulater were obtained and

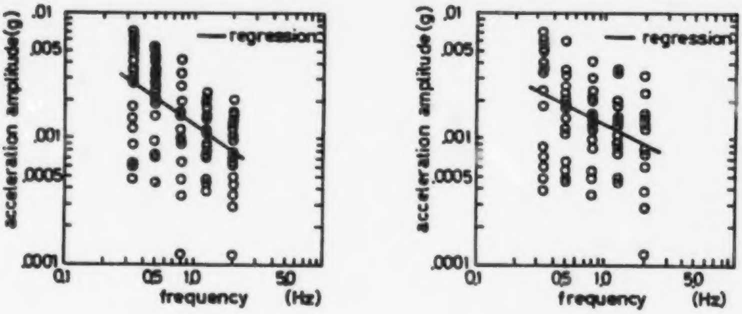

(a) male 20's

(b) female 20's

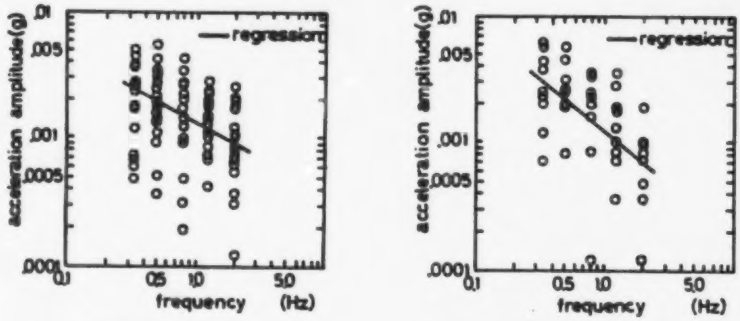

(c) male 30's

(d) female 30's

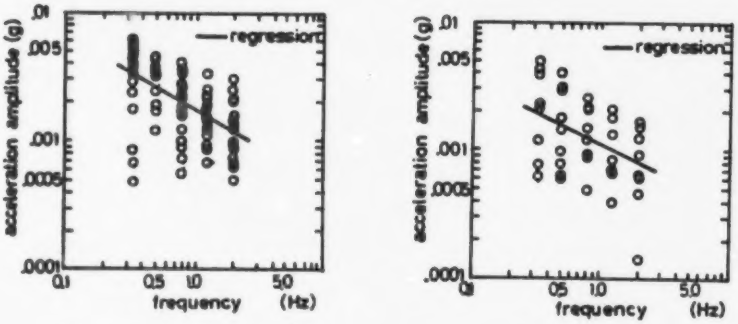

(e) male 40's and over

(f) female 40's and over

Fig. 9 Perception plots of sex and age categories for the fore-and-aft direction. (increasing amplitude)

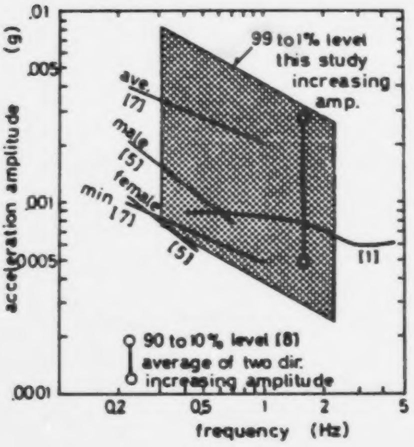

Fig. 10 Comparison of perception criteria for low-frequency horizontal vibration.

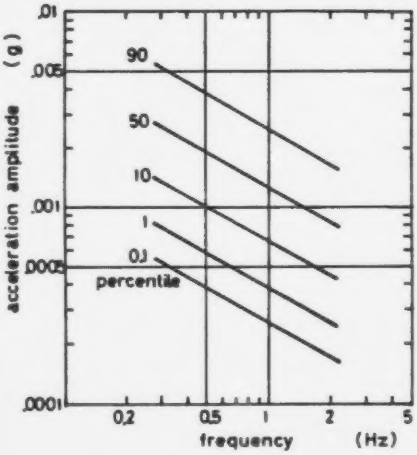

Fig. 11 Tentative proposal for perception criteria for low-frequency horizontal vibration.

statistically investigated. The probabilistic distribution of human perception limit may well be represented by a log-normal distribution with c.o.v. of approximately 50 % for each frequency between 0.33 Hz to 2.0 Hz. The gradient of perception limit v.s. frequency is similar to that of ISO guidelines. Probabilistic perception criteria for vibrations of tall residential buildings were tentatively proposed. Efects of body postures and random responses are to be examined in the next phase of this study and the application of proposed criteria to the serviceability limit state design against frequent strong winds will be provided.

ACKNOWLEDGEMENT

The assistance of Y. Sano, T. Ohtuki and H. Choi in operating experiments and analysing data is gratefully acknowledged. Modern Housing Reseach and Promotion Fund is also acknowledged for their financial support.

REFERENCES

1. Ishimoto, M. and Ootuka, M., Determination de la limite perceptible des secousses, Bull. Earthquake Res. Inst., Tokyo, No. 11-1, 1933.

2. Van Koten, H., The comparison of measured and calculated amplitudes of some buildings, and determination of the damping effects of the buildings, Proc. Wind Effects on Buildings and Structures, Tokyo, 1971, pp. 825-838.

3. Chen, P. W. and Robertson, L. E., Human perception thresholds of horizontal motion, J. Str. Div., Proc. ASCE, 1972, pp. 1681-1695.

4. Hansen, R. J., Reed, J. W. and Vanmarcke, E. H., Human response to wind-induced motion of buildings, J. Str Div., Proc. ASCE, 1973, pp. 1589–1605.

5. Fujimoto, M., Ohkuma, T., Amano, T. and Takano, M., Research on vibration perception of residents subjected to low-frequency horizontal moitons, Summaries of Tech. Papers of Ann. Meeting, Archit. Inst. Japan, 1979, pp. 677–678. (in Japanese)

6. Council on Tall Buildings and Urban Habitat, Tall building criteria and loading, PC-13, 1980, pp. 805–862.

7. ISO, Guidelines for the evaluation of the response of occupants of fixed structure, especially buildings and off-shore structures, to low-frequency horizontal motion (0.063 to 1 Hz), ISO 6897, 1984.

8. Jeary, A. P., Morris, R. G. and Tomlinson, R. W., Perception of vibration—tests in a tall building, Proc. 7th Int. Conf. Wind Engineering, Aachen, Vol. 2, 1987, pp. 253–262.

9. Tallin, A. and Ellingwood, B., Serviceability limit states : wind induced vibrations, J. Str. Eng. ASCE, Vol. 110, 1984, pp. 2424-2437.

HUMAN RESPONSE TO WIND-INDUCED VIBRATION OF TALL BUILDINGS

M. Fujimoto and T. Ohkuma
Department of Architecture and Building Engineering, Kanagawa University
Yokohama, Japan

T. Tamura
ORI, Shimizu Corporation
Tokyo, Japan

ABSTRACT: Human response to the low-frequency horizontal vibration, results of experiments using a model room mounted on shaking table, and an investigation of the response of an actual building in a typhoon are discussed.

1. INTRODUCTION

With increasing numbers of tall office and residential buildings, unfavorable effects on occupants from wind-induced vibrations of buildings have come to be widely recognized and specifications to prevent this effect would be expected. Although many investigations on human response to vibrations have been carried out in various fields, we have only little knowledge in regard to the low-frequency horizontal vibrations that occur in tall buildings, as was indicated by Tallin et al.[1]

In particular, investigations on vibration phenomena that occurred in real buildings are limited[2-4] and unfortunately, building vibrations are not measured in some observed cases. It seems that even human responses to the low-frequency vibration of simple harmonic motions are not well defined and that correlations between laboratory tests and actual phenomena are not clarified, either.

To address problems of the reduction of occupancy comfort from wind action, the authors have been conducting experiments using a model room mounted on a shaking table[5-7] and have investigated an actual building subjected to a typhoon.[3] This paper presents a summary of results of these studies. The laboratory results are compared with those from real buildings. Perception threshold, vibration sensitivity and effects of duration of vibrations are discussed.

2. LABORATORY TEST USING A MODEL ROOM MOUNTED ON SHAKING TABLE

In order to evaluate human comfort to vibrations of tall buildings under strong winds, laboratory tests were conducted using a model room mounted on a shaking table. The perception threshold, the vibration sensitivity to the low-frequency (below 1 Hz) horizontal vibrations, and the effects of duration of these actions were investigated.

2.1 Method:

The experimental installation consists of a room (2.7 m × 2.7 m × 2.3 m) mounted on a shaking table, which can be moved sinusoidally by a clank mechanism in each of two orthogonal directions in the horizontal plane. Accordingly, three types of orientation of vibration based on the human axes can be obtained: fore-and-aft, side-to-side, and circular motion. The duration of vibrations acting on test subjects is 30 seconds. The model room has a window and a door, but visual cues of the motion are eliminated by a screen. The vibration is given by changing the frequency for particular displacement amplitudes. Signal noise at a frequency of about 4-6 Hz was present in the accelerations, with a ratio of noise to required acceleration magnitude of about 5-15%. This decreases with increasing acceleration.

2.2 Perception Threshold:

Human perception threshold was investigated by the ascending series and the descending series based on the "Method of Minimal Changes."[8] Test subjects consist of 18 men and 22 women aged 20 to 30 years. Body posture is standing. A part of the experimental results is shown in Fig. 1, where α is the displacement amplitude (cm) and f stands for frequency (Hz).

The stimulus S, which represents the perception threshold, is given by:

$$S = \alpha \cdot \omega^m \qquad (\omega = 2\pi f,\ m = \text{const.})$$

The value m equals about 3 and the value of S at the 50% probability level (Fig. 2) is presented in Table 1.

The effect of the orientation of vibration is that the perception in the case of circular motion is the lowest, followed by the fore-and-aft motion and finally the side-to-side motion. Consequently the perception threshold (50% probability level) is presented as follows:

Men : $\alpha \cdot \omega^3 = 2.2 - 2.7$ (Ascending series)
$2.6 - 3.4$ (Descending series),

Women : $\alpha \cdot \omega^3 = 0.9 - 1.2$ (Ascending series)
$1.2 - 1.6$ (Descending series)

Thus the perception threshold for women is lower than that for men. The ascending series tend to be smaller compared to the descending series. This tendency stems from "Error of Habitation,"[8] which is the error due to an expected change of the sensitivity.

Fig. 3 shows the present results, along with the existing results and suggested values.[9-17] A typical investigation concerning the perception threshold was first carried out by Meister.[9] His experimental result indicated that the human sensitivity of vibration was represented as the power of frequency of vibrations. The perception threshold for low frequency vibrations below 2 Hz was given as:

$$\alpha \cdot f^3 = \text{Constant.}$$

That is, Jerk = constant. As mentioned above, the present experiments also show that Jerk = constant, the same as Meister's results. Vickery et al.[15] also made the suggestion similar to Jerk = constant. However, according to Chen et al.,[10] Irwin[13] and the standard regulations such as ISO[16] and ECCS,[17] the power index of the frequency becomes smaller than for the above cases. For the present results, the lowest threshold for acceleration is the case of circular motion for women; this is in agreement with the lower threshold proposed by ISO.

In general it can be stated that the perception threshold represented by acceleration decreases with an increase of the frequency of vibration. The threshold for men is higher than that for women. As indicated by Davenport,[14] the level of the perception threshold is approximately within the range of 1 to 10 gal (0.01 to 0.1 m/s^2).

2.3 Vibration Sensitivity:

Vibration sensitivity was investigated in the next experiment. The test subject was asked the question, "which category does the sensitivity imposed by the vibration belong to?" The content of categories is presented in Table 2. The various levels of vibrations of 30 seconds duration were imposed randomly on test subjects. The same vibration was imposed two times independently.

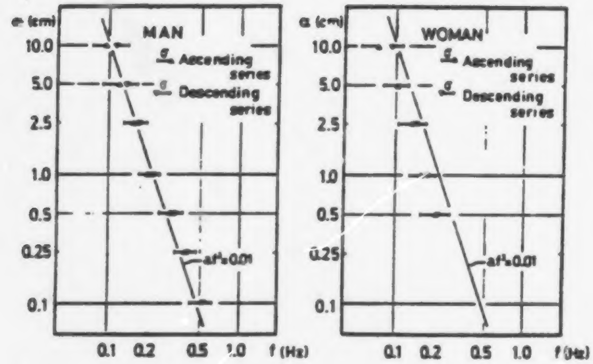

Fig. 1: Perception threshold (fore and aft)

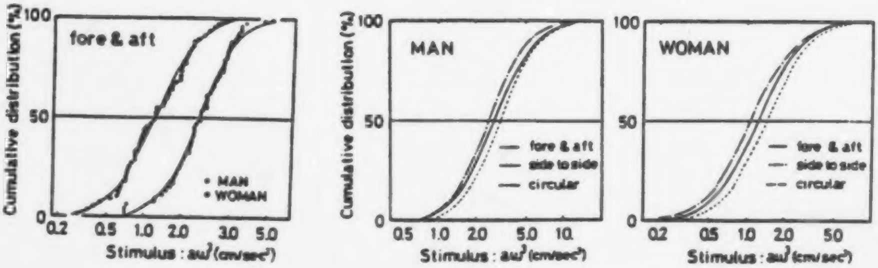

Fig. 2: Cumulative distribution of stimulus for perception threshold

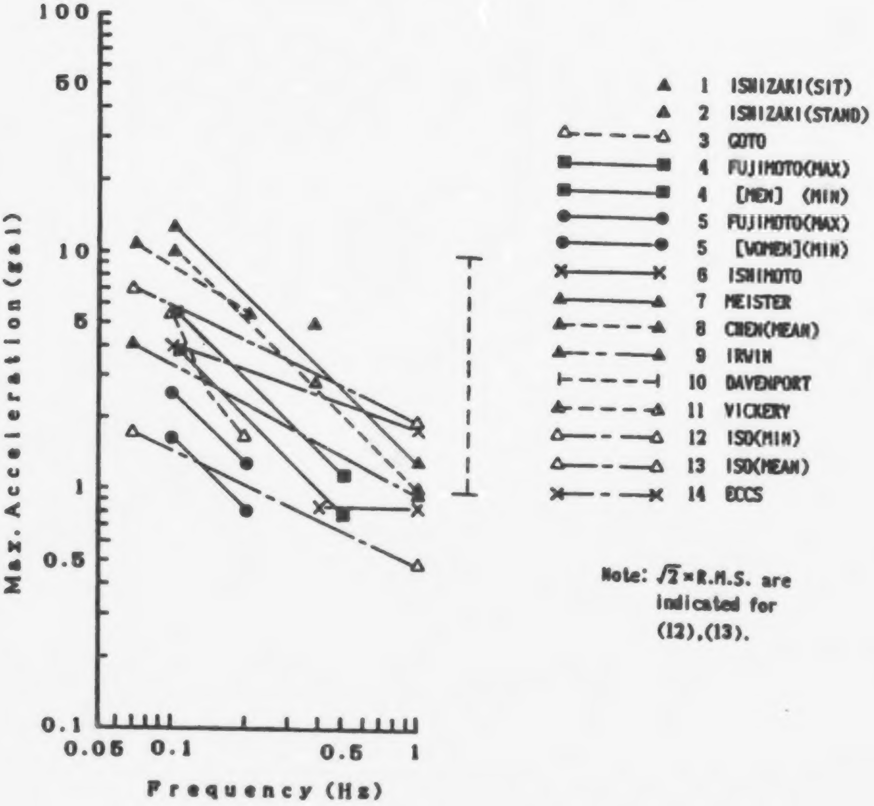

Fig. 3a: Perception threshold

No.	Researcher	Orientation of Vibration ① Fore-to-aft ② Side-to-side ③ Circular ④ Others				Test Subjects					Movement ① No ② Walking		Body Posture ① Sitting on floor ② Sitting on chair ③ Standing			Reference
						Age ① Childhood ② Youth ③ Middle age			Sex ① Men ② Women							
		①	②	③	④	①	②	③	①	②	①	②	①	②	③	
1	Ishizaki	○	○						○	○	○			○		Suspended room
2	Ishizaki	○	○						○	○	○				○	Suspended room
3	Goto	○	○			○	○	○	○	○	○		○	○	○	Averaged perception threshold
4	Fujimoto	○	○	○			○		○		○				○	Side-to-side≧ Fore-to-aft≧ Circular
5	Fujimoto	○	○	○			○			○	○				○	Side-to-side≧ Fore-to-aft≧ Circular
6	Ishimoto	○												○		Suspended Room
7	Meister															
8	Chen	○	○								○	○			○	HATS-I (50%)
9	Irwin				○											Suspended room & Room on a rail
10	Davenport															1~10mG Threshhold line
11	Vickery															60% perception threshold
12	ISO6897															Lower threshold of perception
13	ISO6897															Average threshold of perception
14	ECCS															

Fig. 3b: Experimental conditions for perception threshold

Table 1: Stimulus value(s) of perception threshhold (50%)

		Fore & aft	Side-to-side	Circular
Men	Ascending	2.34	2.73	2.21
	Descending	3.13	3.37	2.60
	Average	2.73	3.05	2.46
Women	Ascending	1.04	1.21	0.92
	Descending	1.36	1.62	1.20
	Average	1.22	1.43	1.07

Table 2: Categories of vibration sensitivity

Category No.	Content of Category
①	Not Perceptible
②	Lightly Perceptible
③	Distinctly Perceptible
④	Strongly Perceptible
⑤	Unpleasant

The experimental results are shown in Fig. 4. Accordingly, the vibration stimulus S describing the characteristic value of each category can be represented as follows:

$$S = \alpha \bullet \omega^{2.5}$$

Although there is a dependence on frequency, the power index of the frequency becomes smaller than for the perception threshold. The value of S of the 50% cumulative distribution (Fig. 5) is given in Table 3. The results show the effect of orientation of vibration. For perception threshold, people are less sensitive in the case of side-to-side motion than for the other orientations. There is little difference between the results for circular and the fore-and-aft motion.

Fig. 6 shows both the present results and the existing results concerning vibration sensitivity.[2-4,11,18] It follows that the acceleration in the range of several gal to a little larger than 10 gal generates the sensitivity level of the category "distinctly perceptible" or "strongly perceptible." The sensitivity level of the category "lightly perceptible" is close to the perception threshold. However, the power index is smaller than that for perception threshold.

2.4 Effect of Duration of Vibration:

The vibration of tall buildings in strong winds persists for several hours. The effect of the vibration on building occupants is not uniform nor constant. Therefore the effects of duration of low-frequency horizontal vibration on the occupants were investigated. The vibration imposed on test subjects is the circular motion at a period of 4 seconds. The levels of acceleration are 4, 8, 12, 16 and 20 gal. Test subjects are 14 men from 19 to 23 years old. Their posture during the experiments consists of sitting on a chair.

The experimental results are shown in Fig. 7. The maximum of "unpleasant" sensitivity is plotted against the time elapsed after the beginning of the vibrations. For each category the scaling is carried out by the "Method of Successive Categories."[8] Below 8 gal vibration, unpleasant sensitivity keeps increasing for only one hour duration. After one hour, that sensitivity becomes saturated and does not reach the level of "unpleasant." On the other hand, for more than 12 gal vibration the sensitivity exceeds the level of "unpleasant" and tends to increase successively for 2 hours at least. This tendency becomes more pronounced with an increase of acceleration level. The effect of duration of vibration for amplitudes of more than 12 gal is clearly stronger compared with the case of amplitudes under 8 gal.

3. FULL-SCALE INVESTIGATION OF HUMAN RESPONSE IN AN ACTUAL BUILDING UNDER TYPHOON

On the 19th of October 1979, typhoon 7920 hit mainland Japan and the strong wind continued blowing near Tokyo prefecture from noon until the evening. As a consequence, large vibrations occurred in the tall buildings in Tokyo and caused many building occupants to feel unpleasant or anxious. During the passing typhoon, the authors carried out full-scale measurements of wind velocity, wind-induced pressures and vibrations at Building N in Tokyo. Later, a questionnaire was distributed to occupants of Building N. This resulted in the vibration sensitivity for actual conditions.

3.1 Building N Under Typhoon 7920:

3.1.1 Building N: Building N, which was used for full-scale investigations, is a tall office building with a plan of 30 m × 36 m and a height of 115 m. This building is of steel construction and consists of 18 floors of working space above ground and 3 floors of antennas on the top. It has 3 floors below ground level. The dynamic characteristics of Building N are shown in Table 4, where X stands for the long direction, Y the short direction, and θ the torsional angle. Building N is located in a town with many low-rise buildings. There are no highrises except for one of about 70 m height at 200 m distance in the northeasterly direction of Building N.

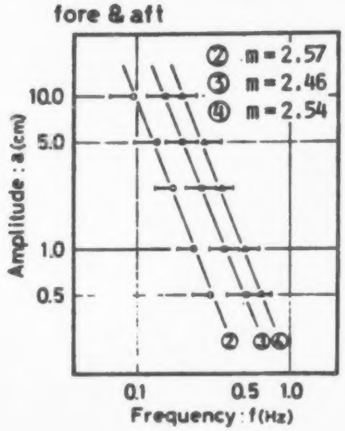

Fig. 4: Relation between amplitude and frequency for category 2, 3 and 4

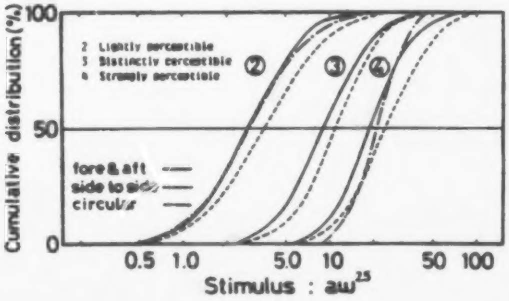

Fig. 5: Cumulative distribution of stimulus for vibration sensitivity

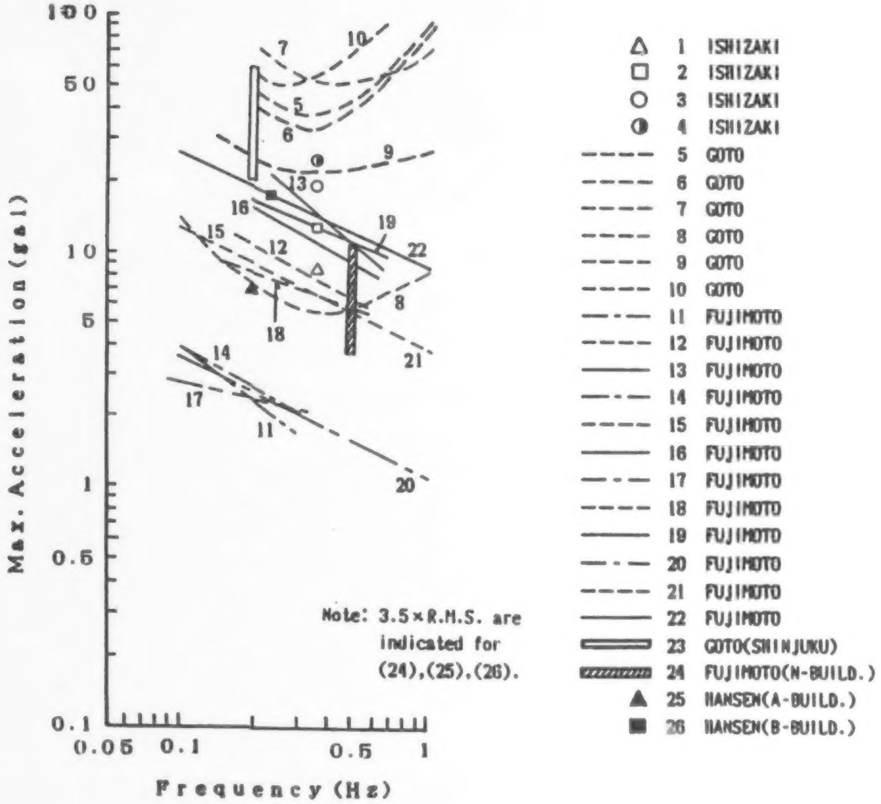

Note: 3.5×R.M.S. are indicated for (24),(25),(26).

Fig. 6a: Vibration sensitivity

No	Researcher	Orientation of Vibration ① Fore-to-aft ② Side-to-side ③ Circular ④ Others				Test Subjects					Movement ① No ② Walking		Body Posture ① Sitting on floor ② Sitting on chair ③ Standing			Sensitivity	Full-scale investigation
						Age ① Childhood ② Youth ③ Middle age			Sex ① Men ② Women								
		①	②	③	④	①	②	③	①	②	①	②	①	②	③		
1	Ishizaki	○	○						○	○	○				○	Sufficiently perceptible	
2	Ishizaki	○	○						○	○	○			○		Sufficiently perceptible	
3	Ishizaki	○	○						○	○	○				○	Strongly perceptible	
4	Ishizaki	○	○						○	○	○			○		Strongly perceptible	
5	Goto	○							○		○				○	Tolerance threshold	
6	Goto	○								○	○				○	Tolerance threshold	
7	Goto	○	○			○	○	○	○	○	○		○	○	○	Averaged tolerance threshold	
8	Goto	○	○									○			○	Limit of normal walking	
9	Goto	○	○									○			○	Limit of nearly normal-walking	
10	Goto	○	○									○			○	Limit of walking difficulty	
11	Fujimoto	○					○		○	○	○				○	Lightly perceptible	
12	Fujimoto	○					○		○	○	○				○	Distinctly perceptible	
13	Fujimoto	○					○		○	○	○				○	Strongly perceptible	
14	Fujimoto		○				○		○	○	○				○	Lightly perceptible	
15	Fujimoto		○				○		○	○	○				○	Distinctly perceptible	
16	Fujimoto		○				○		○	○	○				○	Strongly perceptible	
17	Fujimoto			○			○		○	○	○				○	Lightly perceptible	
18	Fujimoto			○			○		○	○	○				○	Distinctly perceptible	
19	Fujimoto			○			○		○	○	○				○	Strongly perceptible	
20	Fujimoto	○	○	○			○		○	○	○				○	Averaged lightly perceptible	
21	Fujimoto	○	○	○			○		○	○	○				○	Averaged distinctly perceptible	
22	Fujimoto	○	○	○			○		○	○	○				○	Averaged strongly perceptible	
23	Goto															70% physiological & psychological irregularity	Several tall buildings Estimated accel.
24	Fujimoto															54% unpleasant	Build. N Middle floor
25	Hansen															1.6%/year objection 36% motion sickness symptom	Build. A
26	Hansen															11.6%/year objection 47% motion sickness symptom	Build. B Estimated accel.

Fig. 6b: Experimental conditions for vibration sensitivity

Table 3: Central stimulus value of categories

Category	Fore & aft	Side-to-side	Circular
②Lightly Perceptible	2.79	3.52	2.82
③Distinctly Perceptible	9.09	10.93	9.18
④Strongly Perceptible	18.88	24.16	20.90

Table 4: Natural period (T)
and damping ratio (h) for Building N

Tx = 1.98 sec (2.15 sec)	Ty = 2.12 sec (2.14 sec)	Te = 1.43 sec (1.75 sec)
hx = 1.43 %	hy = 1.25 %	he = 1.57 %

( ) DESIGNED VALUE

Table 5: General survey of answerers

	Men		Women		Total
	Age under 40	Age 40 and over	Age under 40	Age 40 and over	
B1		1			1
1F		1			1
2F	6	4	1		11
8F	3				3
10F				9	9
11F	3				3
12F	1	2			3
13F	8	10			18
14F	2	2			4
Total	23	20	1	9	53

(Number of Persons)

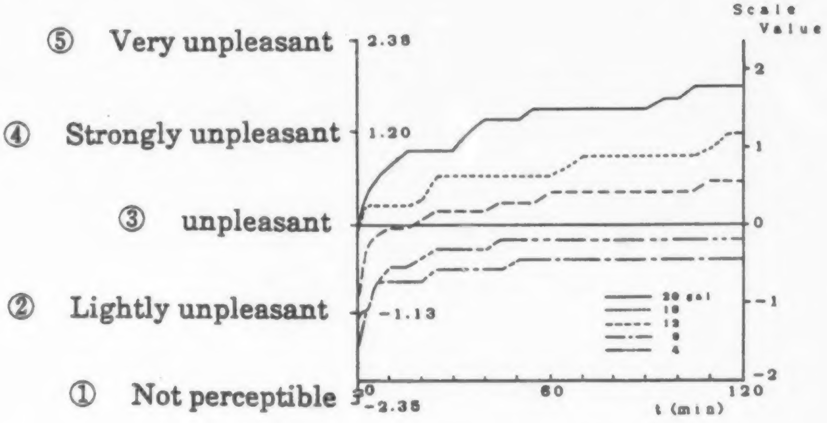

Fig. 7: Time variation of "unpleasantness"

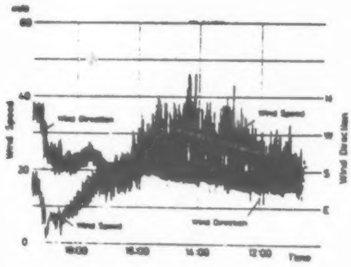

Fig. 8: Wind velocity record at the top of Building N

3.1.2 Typhoon 7920: The equivalent 10 m-height wind velocity at Tokyo Meteorological Observatory indicated 13.1 m/s of daily maximum 10 minute-averaged velocity and 28.7 m/s of the daily maximum instantaneous velocity. The return period of these velocities corresponds to about 1 year and 10 years, respectively. When this typhoon had passed the west of Tokyo, Building N was subjected to the wind-induced vibration for several hours. The wind velocity and direction recorded at the top of Building N is presented in Fig. 8. The time variation of the averaged wind velocity shows that the southerly wind became strong at 11:00 and continued blowing at about 30 m/s from 12:30 to 15:30. At about 14:00, the maximum instantaneous wind velocity exceeded 40 m/s.

3.1.3 Full-Scale Measurement of Building Vibration: The full-scale measurement of vibration was also carried out during the passing of typhoon 7920. Evaluation time of the response is 4 minutes, which is more than 100 times the fundamental natural period of Building N. The wind fluctuation can be taken to be steady. The simultaneous sample records of wind velocity and dynamic response are shown in Fig. 9. The envelope of the fluctuating amplitude of acceleration is similar to the variation of wind velocity. The orbit of the acceleration in the horizontal plane (without the torsional component) indicates that the vibrations in the X- and Y-direction are nearly the same. The maximum amplitude of vibration changes its direction rotationally, drawing an oval shape (Fig. 10). Fig. 11 shows the normalized spectra of the acceleration response. The along-wind, across-wind and torsional vibrations have a sharp peak in the region near the fundamental natural frequency.

Fig. 12 presents the relation between the averaged wind velocity and the standard deviations of the acceleration response in the X- and Y- direction at the 17th floor where the vibration sensors were set up. The r.m.s. value of acceleration response is about 1 to 3 gal in the range of 25 to 35 m/s of averaged wind velocity. This figure includes the records measured so far under the seasonal strong wind due to atmospheric depression. The translational responses in the X- and Y-direction are of the same extent. The equivalent response of torsional acceleration to the vibration at the edge of the building is almost equal to the translational response. The return period of the vibration is estimated at about 6 to 8 years based on past full-scale measurements mainly from seasonal strong winds.

3.2 Questionnaire Survey:

A survey about the sensitivity to vibrations was carried out in November 1979, about one month after the attack of typhoon 7920. Occupants of Building N were asked to respond to a questionnaire with the following contents:

1) General survey of respondent
2) General survey of occupant's perception of the vibration
3) Noticeability of motion cues
4) Duration of vibration sensitivity
5) Time variation of vibration sensitivity
6) Frequency distribution for maximum sensitivity
7) Type of building vibration

The results of the investigation are:

- The replies can be divided into the group at lower floors (B1 to 14F) and the group at higher floors (8F to 14F) (Table 5).
- All persons of the group at higher floors felt the vibration and almost all of them replied "strongly perceptible" (Table 6).
- Noticeability of motion cues consists of creaking sounds for the group at lower floors and feeling self-motion for the group at higher floors.
- Duration of vibration sensitivity is about 3 hours for men and 6 hours for women. As a whole, women are more sensitive to vibrations than men.
- One third of women at 10F reply "anxious" and none of them reply "unpleasant" (Table 7).

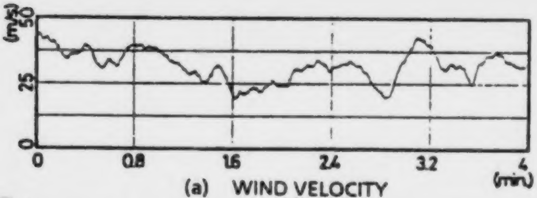

(a) WIND VELOCITY

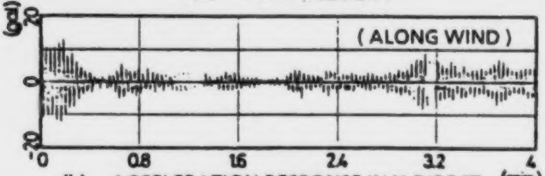

(b) ACCELERATION RESPONSE IN X-DIRECT.

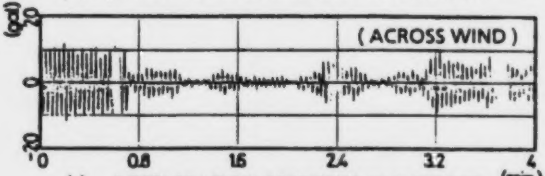

(c) ACCELERATION RESPONSE IN Y-DIRECT.

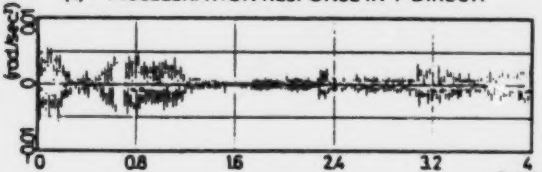

(d) ACCELERATION OF TORSIONAL VIBRATION

Fig. 9: Time history of wind velocity and building response

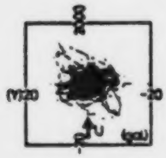

Fig. 10: Orbit of acceleration

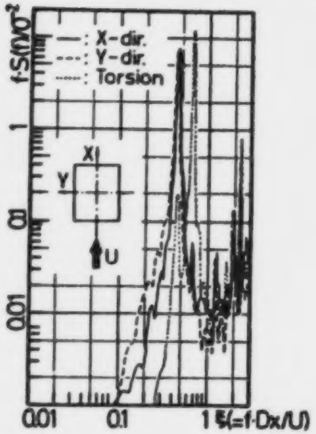

Fig. 11: Power spectra of acceleration response

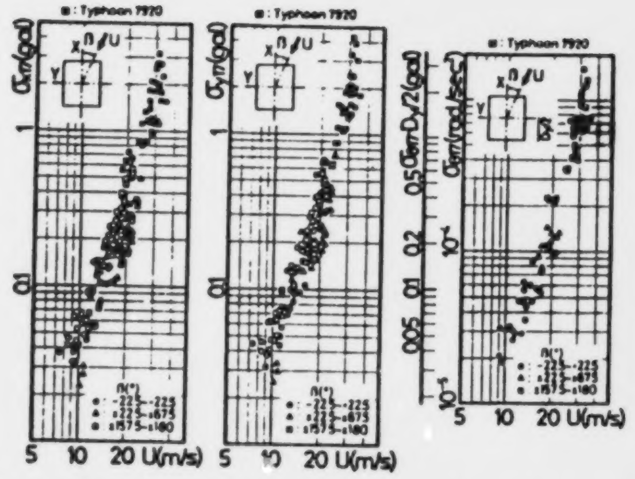

(a) X-DIRECT. (b) Y-DIRECT. (c) TORSION

Fig. 12: Relation between RMS acceleration response and wind velocity

Table 6: Time variation of vibration sensitivity

(a) Men (11F – 14F) (Number of Persons)

	Time	9		10		11		12		13		14		15		Total
Lightly Perceptible	Standing															
	Sitting			2					1	2						5
	Undecided					1	1									2
	Total			2		1	1		1	2						7
Distinctly Perceptible	Standing															
	Sitting							3		1	1	2	1	1		9
	Undecided					1		2	1	1		1				6
	Total					1		5	1	2	1	3	1	1		15
Strongly Perceptible	Standing							1		2		1				4
	Sitting							2				2			1	5
	Undecided							1				1		2		4
	Total							4		2		4		2	1	13
Unpleasant	Standing													2		2
	Sitting									1		1	1	2	1	6
	Undecided							1			1					2
	Total							1		1	1	1	1	4	1	10
Anxious	Standing									2				1		3
	Sitting													1		1
	Undecided										1			1		2
	Total									2	1			3		6

(b) Women (10F) (Number of Persons)

	Time	9		10		11		12		13		14		15		Total
Lightly Perceptible	Standing															
	Sitting	1	4													5
	Undecided															
	Total	1	4													5
Distinctly Perceptible	Standing							2								2
	Sitting			2												2
	Undecided			1				1								2
	Total			3				3								6
Strongly Perceptible	Standing															
	Sitting							1	3	3						7
	Undecided									1						1
	Total							1	3	4						8
Unpleasant	Standing															
	Sitting															
	Undecided															
	Total															
Anxious	Standing															
	Sitting											3				3
	Undecided															
	Total											3				3

Table 7: Cumulative frequency for maximum sensitivity

(a) Men (11F – 14F) (Number of Persons)

	Standing	Sitting	Undecided	Total	Cumulative freq.	%
Lightly Perceptible					28	100.0
Distinctly Perceptible		4	3	7	28	100.0
Strongly Perceptible	1	4	1	6	21	75.0
Unpleasant	5	8	2	15	15	53.6

(note) including the men who don't know the time of feeling "unpleasant".

(b) Women (10F) (Number of Persons)

	Standing	Sitting	Undecided	Total	Cumulative freq.	%
Lightly Perceptible					9	100.0
Distinctly Perceptible			1	1	9	100.0
Strongly Perceptible		7	1	8	8	88.9
Unpleasant					0	0.0

- About half the men at 11 to 14F reply "unpleasant" and very few of them reply "anxious" (Table 7).
- Concerning the direction of vibration in a horizontal plane, the number of persons replying "like drawing a circle," "straight" and "other" are nearly the same. Some reply "like being on ships." Concerning the rate of vibration, almost all men reply "slowly" and women reply "between slowly and trembling."

3.3 Vibration Sensitivity:

3.3.1 Time Variation of Vibration Sensitivity: As mentioned in 3.1, the r.m.s. acceleration response of about 1 to 3 gal was found at the 12th floor of Building N. This was estimated by means of the vibration mode and measurement data at the 17th floor from strong winds of about 30 m/s between 12:00 and 16:00, as the typhoon was passing the west of Tokyo. According to the questionnaire investigation, many persons felt the vibrations "perceptible," "distinctly," and "strongly" from 12:00 to 15:00. Many persons responded "unpleasant" at about 15:00 when the vibration had continued for a long time. This implies that the vibration sensitivity was affected by the duration of vibration.

3.3.2 Comparison With Laboratory Tests: The results of the questionnaire investigation are compared with that obtained in the laboratory test in 2.3. Fig. 13 shows the relation between the averaged wind velocity and the standard deviation of response acceleration in the across-wind direction.

Fig. 14 presents the cumulative distribution of vibration sensitivity to harmonic motions obtained from the laboratory tests. Based on Figs. 13 and 14, the virtual velocities corresponding to 50% and 90% for the laboratory stimulus value due to the circular motion, are plotted on the record of instantaneous wind velocity at Building N (Fig. 15). Compared with the actual wind velocity, the virtual velocities are higher, that is, the sensitivity of vibration for the laboratory tests is higher than that for the actual conditions. Here the virtual velocity was estimated without the component of torsional vibration.

4. SURVEY OF FULL-SCALE INVESTIGATION

Table 7 shows that 50% of the occupants at 10 to 14F felt "unpleasant." The result of the present field investigations and those of Hansen et al.[2] and Goto[4] are plotted in Fig. 6.

Hansen et al. studied the human response for two tall buildings which were buffeted by wind storms with peak wind velocities in a range of 18 to 27 m/s during the winter of 1971. Immediately after the storms, they conducted the interview concerning the vibration sensitivity of the workers in these two buildings. Building A was instrumented with four accelerometers and the wind-induced vibration was measured during the storms. However, Building B was not instrumented and the vibration level was estimated based on the result of wind tunnel tests carried out for the design of the building. Hansen et al. clarified the quantative relation between the building vibration and the objection to motion of the occupants. Also, based on the results of interviewing building owners/developers, Ref. 2 presented the allowable percentage of people objecting to the motion. 30 to 50% of the workers in the top one-third of the building claimed motion sickness symptoms. Taking account of the vibration level, this tendency is similar to the results for Building N where 50% of occupants felt "unpleasant."

Goto performed a questionnaire survey of the occupants of five tall buildings concerning the vibration sensitivity under typhoon 7920, the same typhoon as for the case of Building N. He obtained the statistical frequency of the acceptability to the vibration. Seventy percent of the occupants indicated some physiological and psychological irregularity. However, Goto did not measure the dynamic response of the building. His response acceleration was estimated based on the wind velocity record of Tokyo Meteorological Observatory and the response record of the other nearby buildings on other occasions.

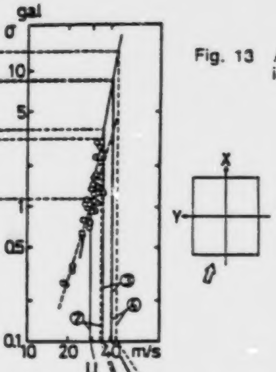

Fig. 13 Acceleration response in Y−direct.

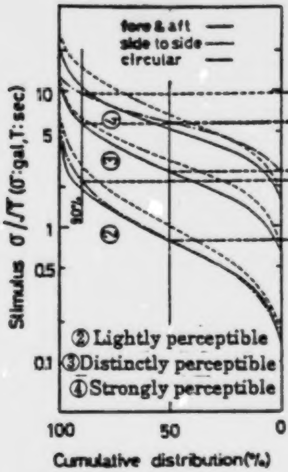

Fig. 14 Vibration sensitivity (Reduced from Fig. 5)

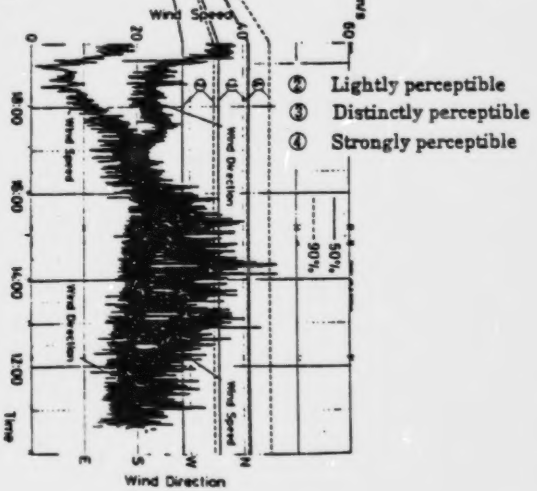

Fig. 15 Actual wind velocity and virtual wind velocity estimated by laboratory test results

4.2 Relation With Laboratory Tests:

As mentioned in 3.3, the comparison between the field investigation and the laboratory tests showed that the level of vibration sensitivity from both the present and Hansen's field investigations correspond to the level of "distinctly perceptible" or "strongly perceptible" of the laboratory tests. That is, greater sensitivity of people is indicated in actual field conditions. This may in part be due to the large vibration being the first experience or due to the effect of torsional vibrations. But it is mainly due to the strong effect that the duration of vibration has on the sensitivity. That is, the laboratory test in 2.4 shows that if the level of the vibration exceeds 8 gal, the ratio of persons feeling "unpleasant" increases as the duration becomes longer. For the present field investigation the peak acceleration reached a little more than 10 gal. Thus it seems that the vibration lasting for several hours produces such results. This is also indicated in the present questionnaire survey where the number of the persons feeling "unpleasant" increases with increasing exposure time.

5. CONCLUSION

Regarding unfavourable effects on building occupants by wind-induced vibrations, correlations of the vibration sensitivity between the laboratory test and the field investigation were studied. The major results obtained are as follows:

1) According to the laboratory tests, perception threshold and vibration sensitivity scaled by the acceleration of vibration depend on the period of vibration. That is, responses become dulled with an increase of the period. The effect of duration of vibration becomes pronounced at vibration levels of more than 10 gal.
2) According to the field investigation, vibration sensitivity is affected by the duration of vibration. Occupants' feelings of anxiety emerge.
3) Comparison of the field investigation with the laboratory tests indicates that the field results give greater sensitivity than the laboratory results. A major reason for this result could be differences in duration of the vibration.

Finally, guidelines for the limitation of vibration are expected for preventing the reduction of occupancy comfort in tall buildings caused by wind-induced vibrations. In fact, a number of proposals and regulations have been suggested. However, information available for assessing the suitability of these proposals seems to be inadequate. Thus it becomes increasingly necessary to study human response to vibrations, especially in actual buildings subjected to strong winds.

ACKNOWLEDGEMENT

The laboratory tests and the field investigation was carried out in cooperation with T. Amano (University of the Ryukyus), M. Takano (Shimizu Corp.), H. Akagi, K. Hiramatsu (N.T.T.), and R. Kato (IBM Japan). Grateful acknowledgements are given to them.

REFERENCES

1. Tallin, A. and Ellingwood, B. 1984. Serviceability limit states: Wind-induced vibration. J. of Structural Engineering, ASCE, 110(10), pp. 2424-2437.
2. Hansen, R.J. and Reed, J.W. et al. 1973. Human response to wind-induced motion of buildings. J. of Structural Division, ASCE, 99(7), pp. 1589-1605.
3. Fujimoto, M. and Ohkuma, T. et al. 1980. Full-scale measurement of pressure and vibration of a tall building due to typhoon 7920 (in Japanese). Proceedings, 6th Symposium on Wind Engineering, pp. 201-208.
4. Goto, T. 1983. Studies on wind-induced motion of tall buildings based on occupants' reaction. J. of Wind Engineering and Industrial Aerodynamics, 13, pp. 241-252.
5. Fujimoto, M. and Ohkuma, T. et al. 1979. Research on vibration perception of occupants subjected to low-frequency horizontal vibration (in Japanese). Summaries of Tech. Papers of Ann. Meeting, Archit. Inst. Japan, pp. 677-678.

6. Fujimoto, M. and Ohkuma, T. et al. 1979. Research on vibration sensitivity of occupants subjected to low-frequency horizontal vibration (in Japanese). Summaries of Tech. Papers of Ann. Meeting, Archit. Inst. Japan, pp. 679-680.
7. Fujimoto, M. and Ohkuma, T. et al. 1982. Research on effects of duration time of vibration on vibration sensitivity for low-frequency horizontal vibration (in Japanese). Summaries of Tech. Papers of Ann. Meeting, Archit. Inst. Japan, pp. 1171-1172.
8. Guilford, J.P. 1954. Psychometric Methods. McGraw-Hill.
9. Ohshima, M. 1969. Theory of somatological vibration (in Japanese). Univ. of Tokyo Press.
10. Chen, P.W. and Robertson, L.E. 1972. Human perception thresholds of horizontal motion. J. of Structural Division, ASCE, 98(8), pp. 1681-1695.
11. Ishizaki, H. and Mori, E. et al. 1976. Experimental studies on wind engineering problems of the high rise apartment houses (in Japanese). Takenaka Tech. Research Report, 15(3), pp. 74-87.
12. Ishimoto, K. and Ohtuka, M. 1933. Détermination de la limite perceptible des secousses. Bull. Earthquake Res. Inst., 11(3), pp. 113-121.
13. Irwin, A.W. 1975. Human reactions to oscillations of buildings - acceptable limits. Build. Int., 8, pp. 89-102.
14. Davenport, A.G. 1967. The treatment of wind loading on a tall building. Tall Building, Pergamon Press.
15. Vickery, B.J. et al. 1977. Architectural aerodynamics. Applied Science Publishers.
16. ISO. 1984. Guidelines for the evaluation of the response of occupants of fixed structure, especially buildings and off-shore structures, to low-frequency horizontal motion (0.063 to 1 Hz). ISO 6897.
17. European Convention for Constructional Steel Work. 1978. Recommendation for the calculation of wind effects on buildings and structures. Tech. Comm. T12.
18. Goto, T. 1975. The criteria to motions in tall building (in Japanese). Trans. of Archit. Inst. Japan, 237(11), pp. 109-119.

SESSION D/SÉANCE D

DIFFERENTIAL MOVEMENT/MOUVEMENT DIFFÉRENTIEL

STRUCTURAL SERVICEABILITY ASPECTS OF BUILDING ENVELOPES IN TALL BUILDINGS

Roland Bergmann, P. Eng., Dipl. Ing.
Partner, M. S. Yolles & Partners Limited,
Consulting Structural Engineers, Toronto, Canada

ABSTRACT

The paper provides an overview of serviceability aspects of the building envelope in highrise office buildings with particular respect to the interaction of the envelope and the supporting structure. The increased use of airtight building enclosures, of large prefabricated wall panels, of setbacks in the building face and other similar factors has increased the complexity of the design of both the enclosure and the interacting supporting structure.

Common defects in the building envelope are leaks through sealed joints or the air seal, corrosion of connection elements due to the presence of water and condensation or build up of ice within the envelope.

Most of the above problems can be traced back to excessive or unforeseen relative displacements of the various elements forming the building enclosure and the supporting structure.

The interfacing and interactive behaviour between the wall system and supporting structure must be fully understood by the designers of both systems in order to arrive at a successful design.

For a better understanding of the problems, common types of building enclosures are described together with their supports by the building frame. The interaction between the envelope and the building frame is examined as it may affect the proper functioning of the wall. Problem areas are identified and guidelines presented based on the experience with actual wall applications.

A. GENERAL

Several recent trends and conditions have had a profound effect on the design, detailing and construction of the enclosure of high rise office buildings.

Some of these are the following:

a) Todays' objective to create energy efficient buildings requiring airtightness and good insulation of the building with respect to the outside environment.

b) The increased use of totally prefabricated panels to take advantage of the better quality control of shop fabrication.

c) The construction of large panels, resulting in the reduction of the number of units to be installed and the lengths of the field joints, thus reducing erection time.

d) The use of high strength structural materials notably structural steel in the building frames and of longer spans between perimeter columns.

e) Increased building heights which lead to a much more complex pattern of relative displacements of the perimeter frame due to wind and column shortening.

f) The use of a great variety of exterior cladding materials, including stone masonry units with vulnerable joints within the individual panels.

g) The increased popularity with Architects to create setbacks in the faces of buildings, in particular at their top.

B. PERFORMANCE CRITERIA

The choice of the type of cladding and the layout of the joints in the cladding system is the responsibility of the Architect and the structural cladding consultant. To aid them in the proper choice of panels and the joint widths, it is imperative that the structural building consultant supplies estimated building displacements and deformations resulting from all applicable design loads together with appropriate construction tolerances.

One of the most difficult problems relating to the building envelope is the matter of who is responsible for its proper functioning. Ideally, there should be only one party who has this responsibility, namely, the enclosure sub-contractor. Under these circumstances, he designs, manufactures and erects the wall system, the design being based upon clearly stipulated performance criteria developed by the building's design team.

The building structural consultant must provide appropriate information to be included in the performance criteria (the specifications) but neither he nor the building architect are responsible for the design of the envelope system itself other than its architectonic component, which, of course, is shown by the Architect on his drawings. The following structural data should be included in the bidding documents:

a) Estimated deformations of the supporting frame.

b) Location, magnitude and direction of the cladding reactions assumed in the design of the structure.

c) A statement that the design of the structure may be affected should the reactions or the points of application be different for the finally adopted cladding system. In this case, a design review must be carried out by the structural consultant based upon reactions supplied by the enclosure sub-consultant.

C. THE WALL CLADDING AND ITS SUPPORTS

To better understand the interaction of the building enclosure and the structure, the more common types of enclosures are described first:

1. These are:

   a) Curtain wall with vertical mullions and wall panels and windows in between. Fig. 1 and 2.

   b) Full one storey prefabricated panels including windows. Fig. 3 and 4.

   c) Multi-unit wall cladding systems consisting of spandrel panels, column covers, windows, intermediate panels and the like interconnected in various ways. Fig. 5, 6, 7, 8 and 9.

   d) Systems with alternating curtain wall and cladding units. Fig. 10.

   e) Envelopes with the stone facing attached directly to a continuous backup structure. Fig. 11.

2. Common wall cladding compositions for tall buildings:

   a) Glazing panels supported between mullions in aluminum or steel.

   b) Precast concrete panels with glazing infills:

- Sandwich panels: Precast back-up with either precast or stone facing separated by air space and insulation.
- Exposed single wall precast panels with insulation behind either directly attached to panels or attached to exterior stud walls.

c) Steel framed panels with stone or metal facing and glazing infills.

d) Built in-situ block and brick walls with cavities and openings for windows.

e) Prefabricated masonry panels with window openings.

All solid panels are composed of four basic layers:

a) The outer exposed facing of stone or metal.

b) The insulation.

c) The vapour barrier.

d) The structural backup wall in concrete or steel framing.

3. Common support conditions of the cladding systems:

Vertical loads are generally transfered by brackets or seats to the floor slab, the spandrel beams or columns with lateral forces resisted by these brackets or seats augmented by tiebacks to the structure.

4. Design criteria for the cladding supports:

Supports and interconnections must sustain the following forces from the panels:

a) Gravity loads: Selfweight including temporary construction loads.

b) Wind pressures and suctions.

c) Internal pressures.

d) Temperature changes.

e) Lateral forces due to earthquake.

f) Forces created by the "racking" of the building due to lateral forces.

5. One of the most important decisions in the design of the cladding is the layout of the panels and with it the layout of the vertical and horizontal joints, the location of the horizontal expansion joint and the width of the various joints.

This width depends on factors including fabrication and construction tolerances, temperature changes, the effects of building displacements due to gravity, wind or earthquake, temperature changes, accessability for caulking and of course, the type of sealant used.

Three types of sealants are presently generally in use with different elastic properties, life expectancies and cost:

1. Polysulfides such as Thiocol and others with safe changes of 25% in closing and openings of joints.
2. Urethenes such as Tremco Dymeric with safe variations of +40% and -25%.
3. Silicones such as Dow 795 or GE SILPRUF with safe variations of +100% and -50%.

As joint layout is generally decided upon by the Architect (and his cladding consultant) they must make the appropriate economic study of the joint layout, taking into consideration factors such as, building frame displacements, movements due to temperature, construction tolerances of the frame and panels, joint sealants and fabrication and erection aspects.

D. THE PERIMETER STRUCTURAL SUPPORT FRAME

Considering only taller structures, the following are typical perimeter framing conditions:

1. Structural steel frames:
   a) Columns spaced 6 to 12 m apart connected by spandrel beams.
   b) Perimeter framing designed as a framed tube with closely spaced columns and deep spandrels or knee braces.
2. Concrete frames:
   a) Columns spaced 6 to 12 m apart connected by beams or thickened slab edge strips.
   b) A perimeter framing designed as a framed tube resulting

in closely spaced wide columns and deep spandrel beams.

Vertical and horizontal building displacements must be controlled for the following reasons:

a) To prevent any damage to non-structural elements of the building such as the building enclosure, interior walls, mechanical services, elevators, etc.

b) To control the magnitude of perceptible building vibrations.

c) In earthquake resistant construction, to reduce damage to non-structural elements under the effects of a moderate earthquake.

Deformations and tolerances of the supporting structure:

1. Deformations which may affect the cladding system:

    a) Spandrel beam deflections.

    b) Spandrel beam rotations.

    c) Column shortening or elongations.

    d) Lateral displacements due to wind or earthquakes.

    e) Length changes of the building parallel to the wall due to shrinkage and temperature changes during construction.

2. Normal building tolerances:

    Standard specifications generally outline the normal tolerances to which buildings should be constructed. For structural steel buildings, they are given in CSA Standard CAN3-S16.1-M78 and for concrete in CSA Standard CAN3-A23.1-M77.

Common limitations for building displacements as they relate to the wall cladding:

a) Maximum beam live loading deflections: A 360th of the span or 25 mm for a 9 m span. In the context of the cladding, vertical deflections of spandrel beams should be kept to considerably lower values unless the wall panels are not affected by such deflections.

b) Maximum lateral displacements (drift) between adjacent floors: A 500th of the floor to floor height due to a 10 year wind or about 8 mm.

From our past experience, we are of the opinion that limiting the floor drift to the 1/500 value is reasonable provided the drift calculations take into account torsional effects.

It should be noted that the critical zones for these maximum lateral displacements are the corners of the building near the top and in many cases, the area between the ground and 2nd floors in buildings where the wind resisting system consists of a rigid frame.

E. A REVIEW OF THE INTERACTION OF CLADDING AND THE SUPPORT FRAME

It is imperative that an appropriate cladding design includes the determination and analysis of the relative displacements between the adjacent panels and between panel support points and the supporting structure. Based on this analysis, the effects of these displacements on the changes in the widths of the joints and with it the sealants can be studied. Should this study reveal that the relative displacements are excessive, then one or more of the following modifications may have to be considered:

a) Widening of joints: The joint width is a very important detail from an architectural point of view. A wider joint also leads to an increase in the cost of the sealant.

b) Rearrange the supports for the panels to create a more favourable pattern of relative displacements.

c) To stiffen the spandrel beams to reduce their long term and live load deflections in cases where they provide the support.

d) To stiffen the wind resisting frame of the building to reduce the relative lateral displacements, the "racking" between floors.

A complete picture of the pattern and magnitude of the joint width must be obtained by combining critical relative displacements of the panels (after the installation and sealing of the joints) with the construction tolerances of the building and the panels.

It is recommended, that these studies be carried out by the building design team in consultation with an expert from the industry to verify feasibility of the proposed panel system.

Some typical displacement patterns are shown in fig. 12 to 16. For a better understanding of the changes in the joint widths, the geometry has been distorted.

There are several aspects of the interaction of the building enclosure with the frame which are worth highlighting and discussing:

a) In most cases, it should be possible to level out the wall panels by shimming to compensate for any sags of the spandrel beams or slabs at the time of the panel installations. In concrete structures, one could even consider super-elevating the various panels (if many smaller panels are being used) to compensate for part of the long term spandrel deflections due to creep.

b) If consecutive floors behave in a similar manner, the width of the horizontal expansion joints will be little affected. However, where there is an abrupt increase in the stiffness of a particular floor, the width of the horizontal joint immediately above the stiff floor must be increased accordingly. See fig. 17.

c) If one wishes to design a cladding system unaffected by spandrel beam deflections, the panels should be designed to span from column to column.

d) The building displacements create shear deformations along many of the panel joints. The forces created by the shear resistance of the sealant have a great effect not only on the forces within the wall panels, but also on the reactions of the panels on the supporting structure.

   The closing of joints during racking creates local direct pressure transfers which cause internal forces in the panels and a shift in the reactions of the panels onto the structure. See fig.13 .

   The magnitude of these forces depends to a large extent on the shear coefficient of the sealant, the flexibility of the panels in their own plane and on the amount of lateral displacement.

   Racking tests with full scale panels may be necessary to evaluate the actual forces and deformations of panels.

   Special attention needs to be paid to the lateral connections of the top and bottom panels as explained in fig.18 . These forces must be considered in the design of the supports of the panels.

e) In all types of enclosures, it is important to locate the horizontal joint above the finished floor or below the spandrel beams to allow easy access to the joint at the rear for caulking. For the same reasons, ample clearances should also be provided along the vertical joint in front of the columns. See fig. 4.

f) Wherever water may gain access to the structural connections, stainless steel material should be used to minimize corrosion.

g) The fit up of panels at corners often causes difficulties during their erection. Ample allowance for clearances should be made there.

h) During installation, upper panels are usually temporarily supported onto the panels below requiring their brackets and the like to be designed for the added loads.

i) Very generous excentricities should be assumed in the application point of the load onto brackets off steel columns to account for construction tolerances.

j) Where panels depend on the floor system to prevent torsional displacements, the flexibility of such a support should be checked. See fig. 15 and 16.

k) In concrete structures, it is much more difficult to estimate expected deflections and displacements, primarily due to the many variables involved such as creep. A conservative approach to determine the critical deflection is therefore recommended.

l) To control differential displacements between successive floors involving concrete cantilevers, it may be advantageous to consider a permanent vertical steel tie between floors at a critical location behind the wall cladding as shown on fig.17 .

m) Wall panel systems consisting of spandrel panels and infill window panels are much more affected by the end rotations of cantilevers as shown in fig. 15 as compared with cladding systems where individual mullions or panels span between floors. This problem is again more critical in concrete than in steel framed structures.

n) Horizontal forces from wind acting directly onto the panels can be transfered to the back up structure in several ways: Where clips or spacers to spandrel beams are used, vertical relative movements should be permitted to prevent loading the panels under the spandrel beam live load deflections.

m) Shop installed support brackets off columns or spandrel beams are a common solution to support large panels onto a steel structure. However, in setting the elevations of these supports, there should be an allowance made for shimming to avoid a situation where the brackets are found to be too high for a proper seating of the panels requiring costly remedial measures.

At building corners, large panels may project beyond adjacent returning panels due to wind induced racking as shown in detail ⓐ on fig. 14.

F. GRANITE FACED WALL PANELS SYSTEM AT BATTERY PARK WORLD FINANCIAL CENTRE IN NEW YORK CITY

After extensive cost comparisons and design evaluations between a variety of prefabricated wall panel systems including both precast concrete and structural steel concepts, a steel framed system using 30'-0 long by 12'-9 high shop-fabricated panels was adopted. The system was designed by FEI Limited of Hastings-on-Hudson, New York based on performance criteria prepared by the architects and our office. The design of the panels was based on the following principles:

i) Use large prefabricated elements for speedy erection and a minimum of field joints.

ii) Provide complete and easy access to all interior joints of panels for caulking.

iii) Provide complete independence of the panels' structural system from any deflections of the spandrel beams, thus allowing the floors to be concreted even after the panel installation, if this should become desirable.

iv) Transfer all gravity loads directly into the perimeter columns without loading the spandrel beams.

The system is described on fig. 19 and 20. The vertical channel elements of the panel frame were interconnected at their horizontal joints by moment connections to create vertical continuity while allowing vertical expansion. At the expansion joint at ceiling level, this moment connection allows for horizontal and small vertical relative displacements.

G. CLOSING REMARKS

There have been many instances of poor performances of cladding installations in tall buildings requiring excessive maintenance and often very expensive major remedial measures, although for obvious reasons these cases are not commonly publicized.

To design and construct a good and airtight building enclosure requires careful attention to many interrelated details by all parties involved, primarily concerning the interaction between the building enclosure and the supporting structure.

It is hoped that this paper will contribute to the better understanding of some of the more important aspects of this interaction.

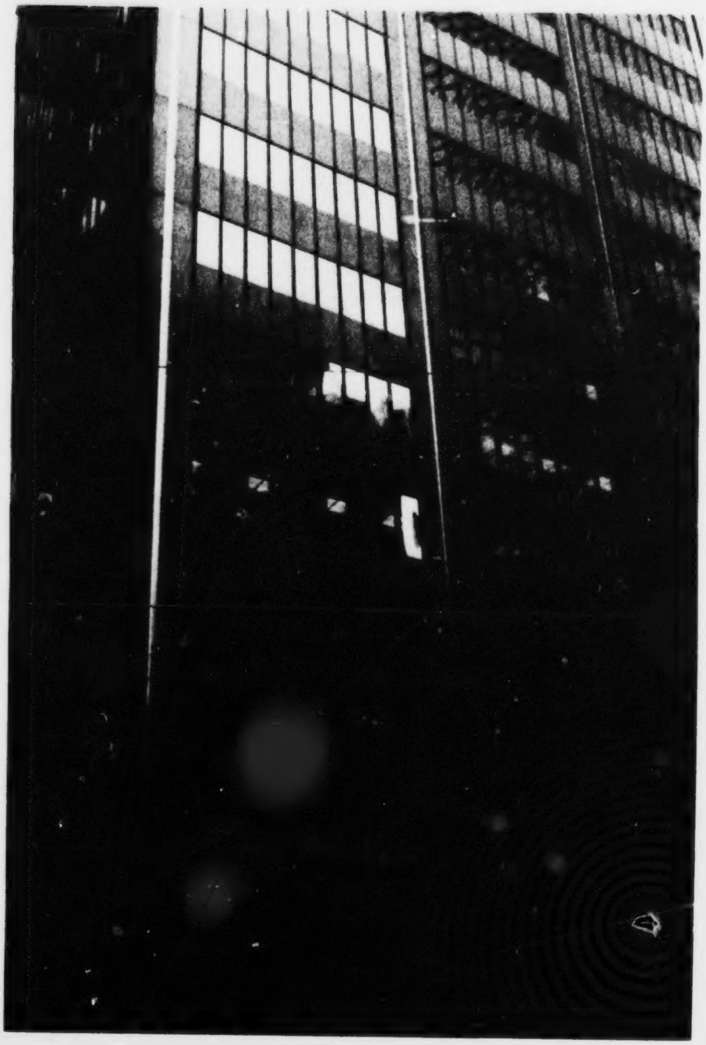

FIG. 1 TYPICAL CURTAIN WALL

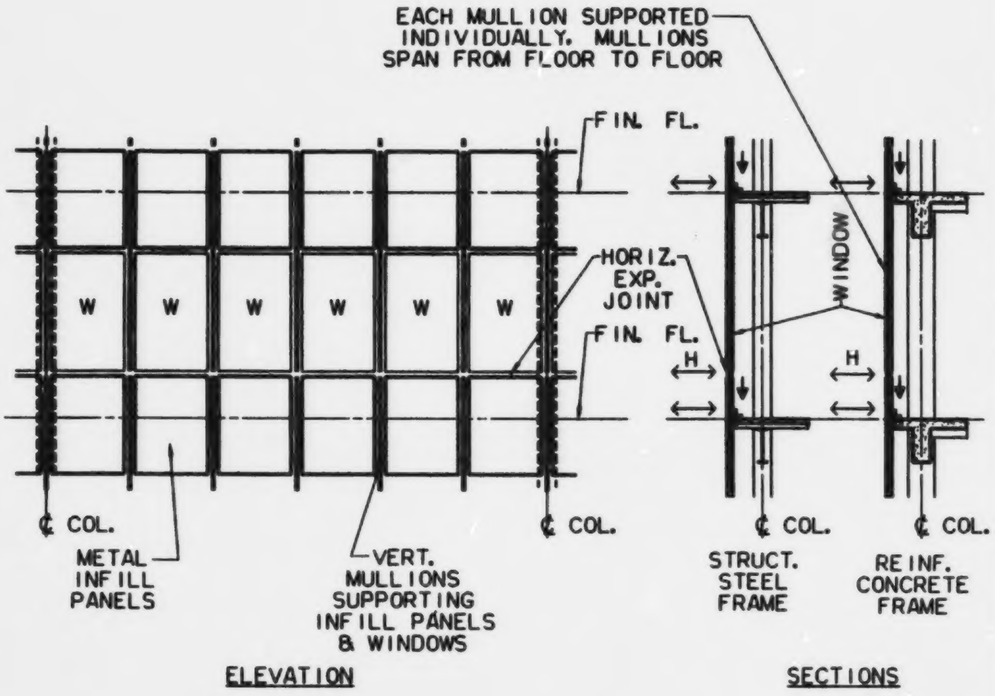

FIG. 2 CURTAIN WALL CLADDING SYSTEM

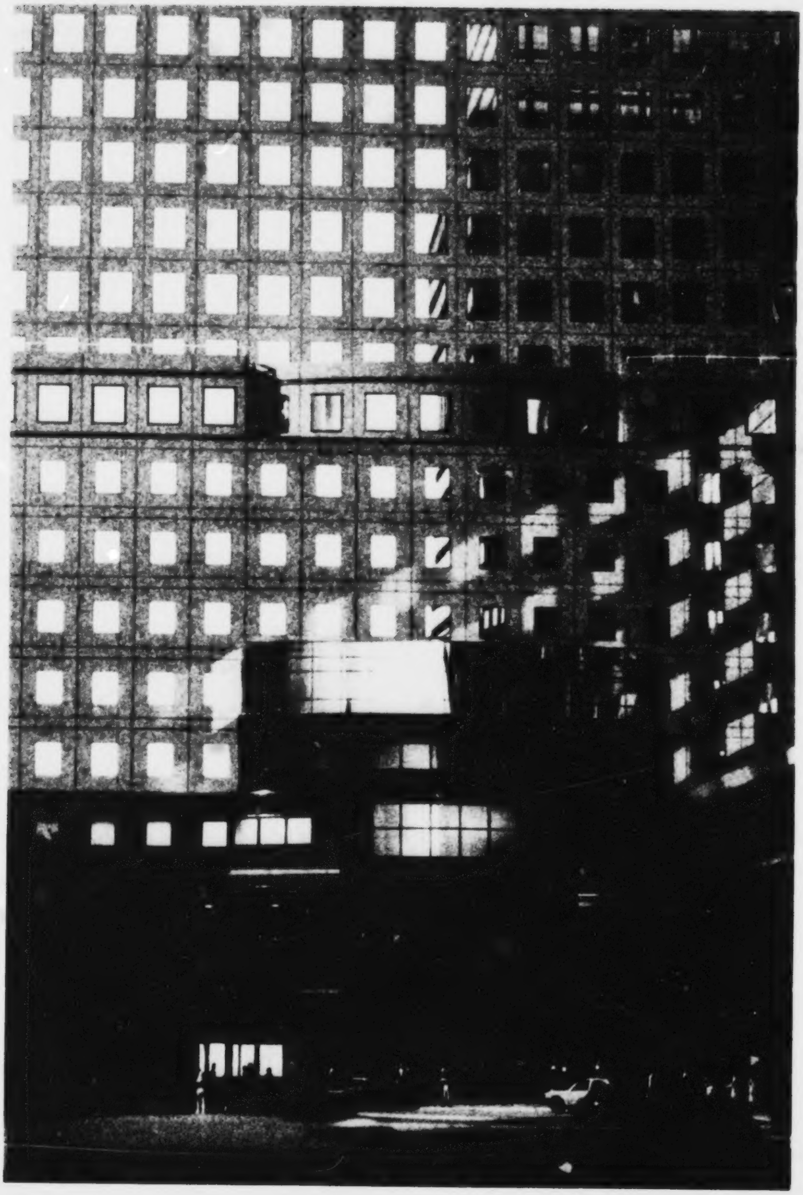

FIG. 3 ONE STOREY PREFABRICATED WALL PANELS

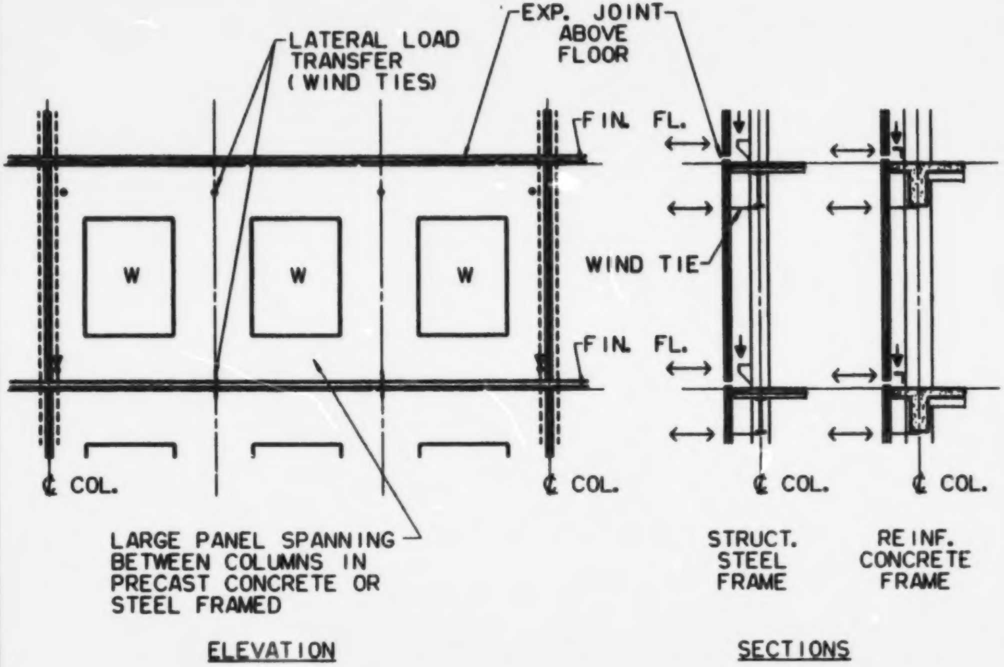

FIG. 4 LARGE PANEL CLADDING SYSTEM

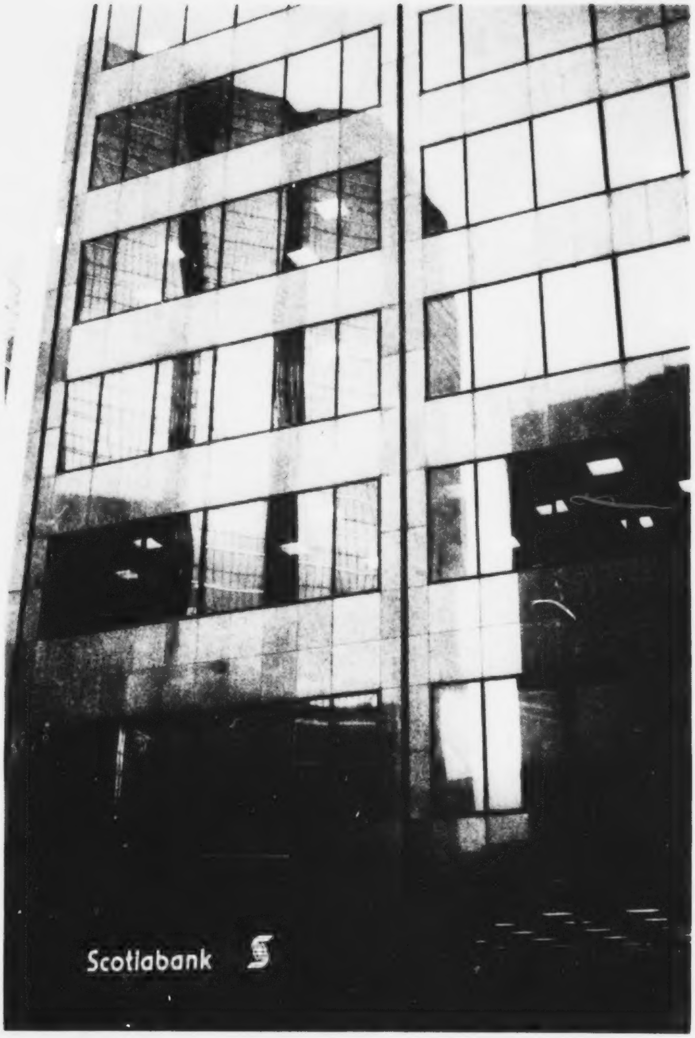

FIG. 5 MULTI UNIT WALL CLADDING WITH SPANDREL PANELS AND COLUMN COVER UNITS

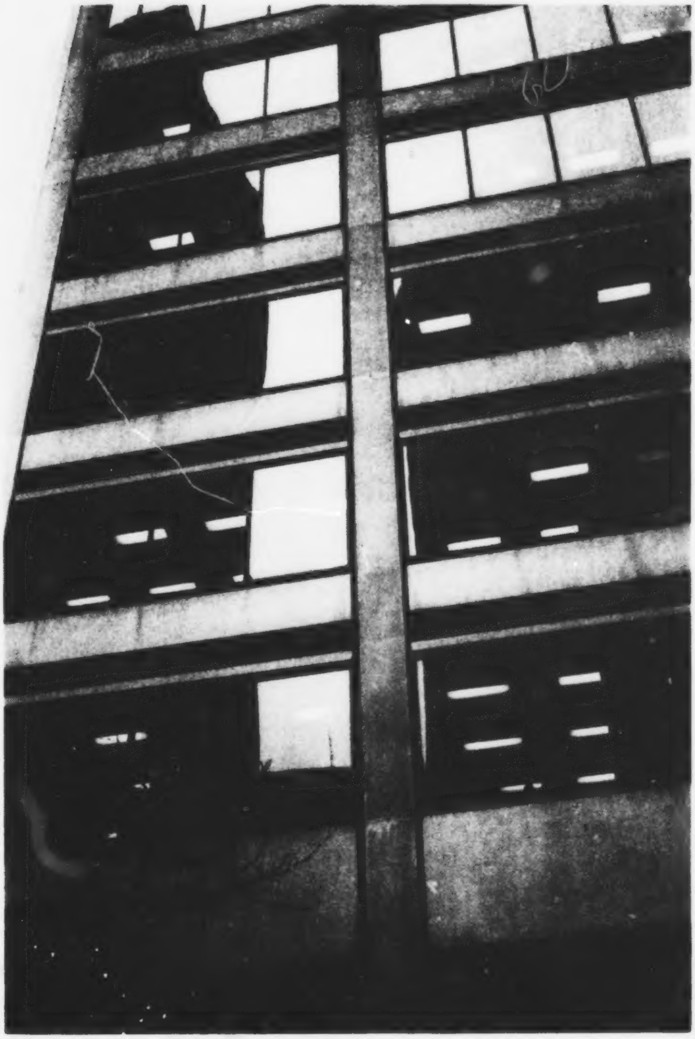

FIG. 6 PRECAST SPANDREL PANELS AND COLUMN COVERS

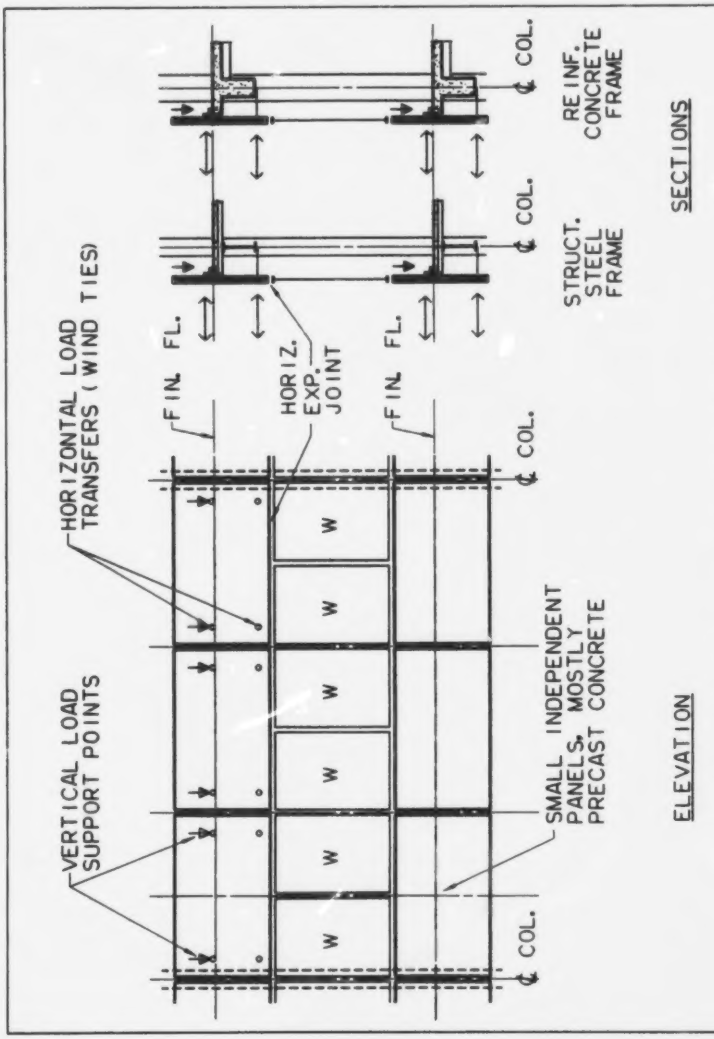

FIG. 7 **MULTI PANEL CLADDING SYSTEM**

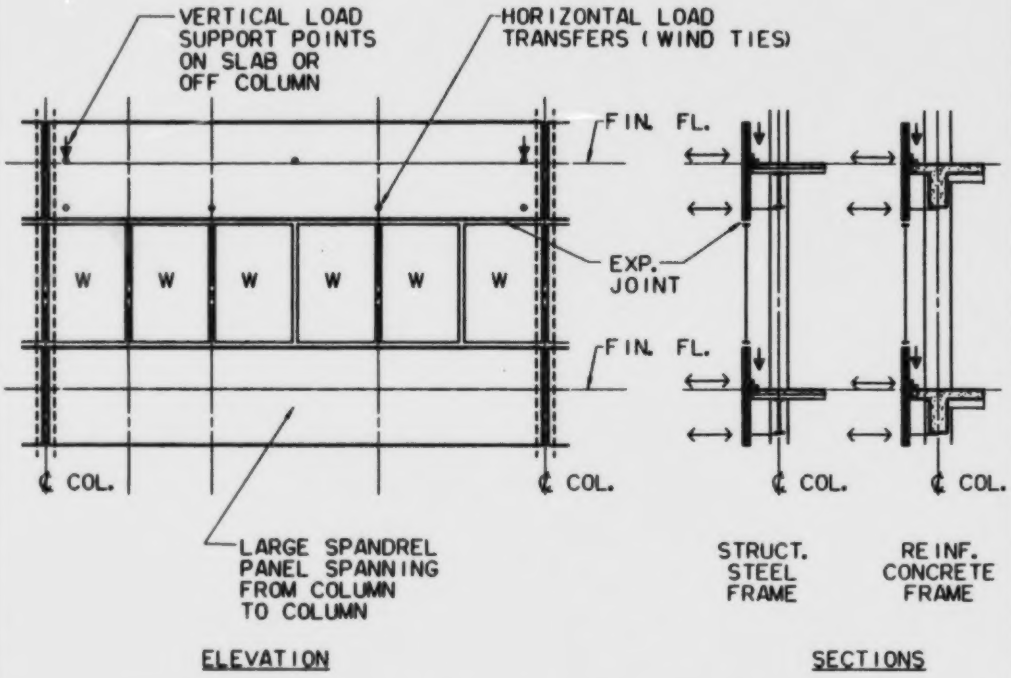
VERTICAL LOAD SUPPORT POINTS ON SLAB OR OFF COLUMN
HORIZONTAL LOAD TRANSFERS (WIND TIES)
FIN. FL.
EXP. JOINT
FIN. FL.
W
W
W
W
W
W
℄ COL.
℄ COL.
℄ COL.
℄ COL.
LARGE SPANDREL PANEL SPANNING FROM COLUMN TO COLUMN
STRUCT. STEEL FRAME
REINF. CONCRETE FRAME
ELEVATION
SECTIONS

FIG. 8 SPANDREL PANEL CLADDING SYSTEM

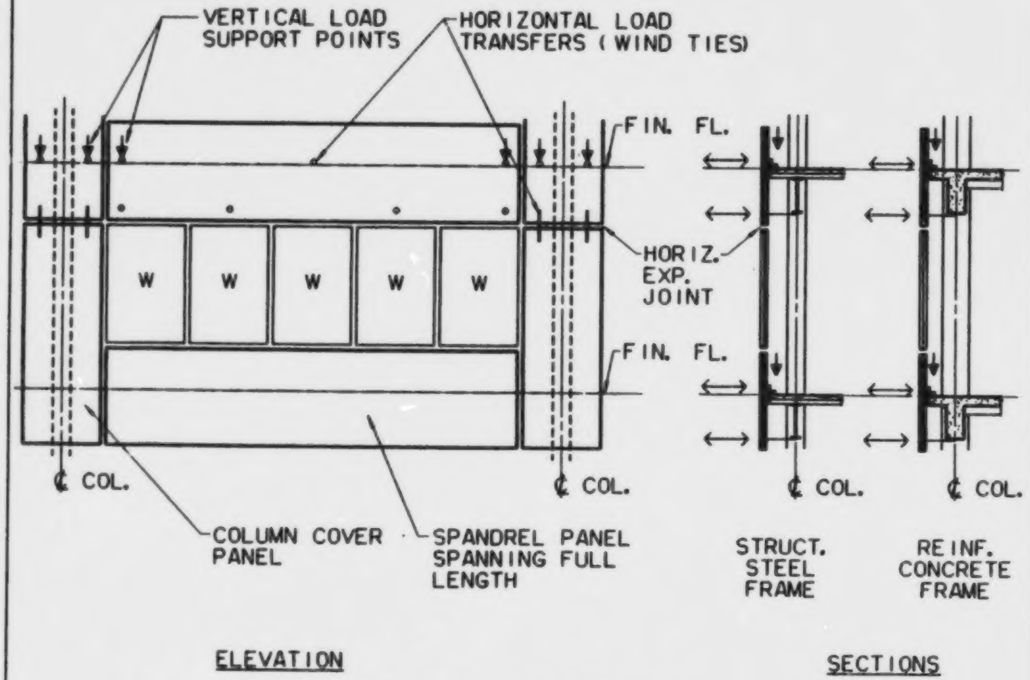

FIG. 9 CLADDING SYSTEM WITH SPANDREL PANELS AND COLUMN COVERS

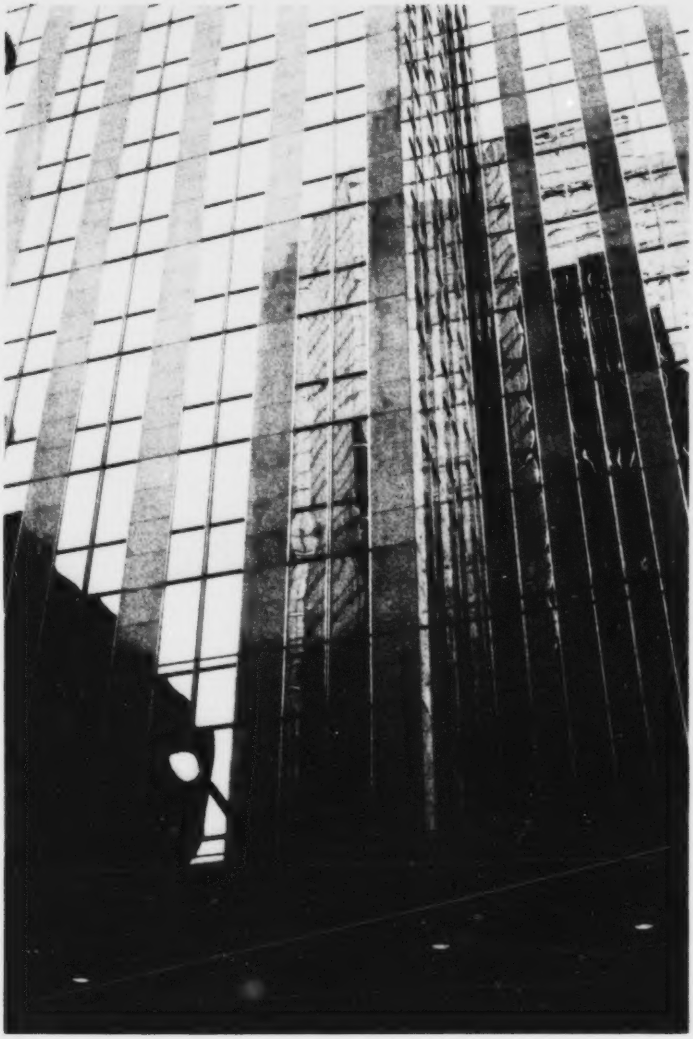

FIG. 10 WALL CLADDING WITH ALTERNATING CURTAIN WALL AND STONE FACED PANELS

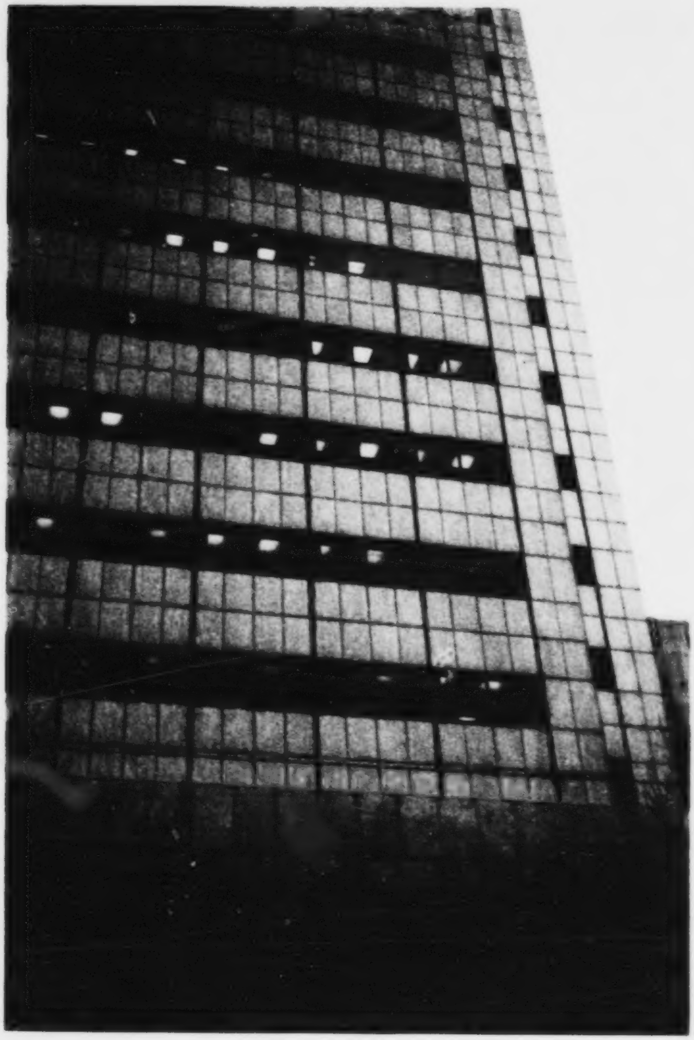

FIG. 11 STONE FACING DIRECTLY ATTACHED TO A
PLATE STEEL BACKUP

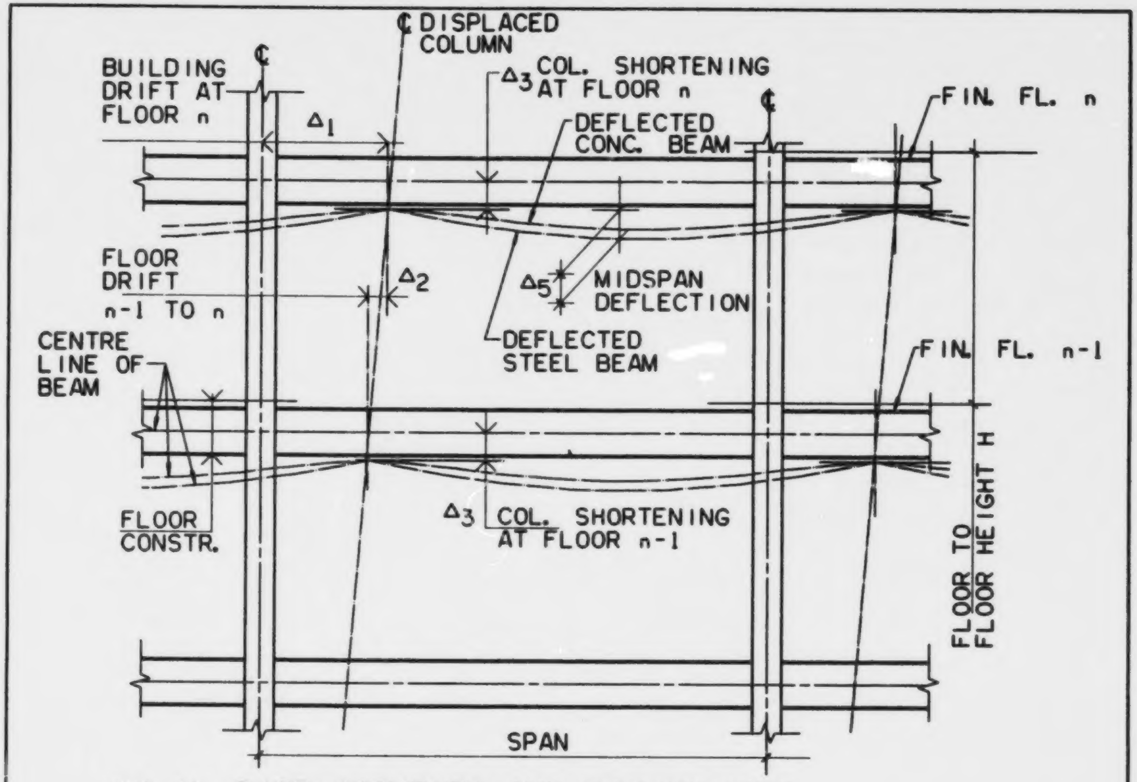

FIG. 12 **DISPLACEMENTS AND DEFLECTIONS OF THE BUILDING FRAME**

SHOWING DEFLECTIONS FOR A CONCRETE AND A STRUCTURAL STEEL EDGE BEAM

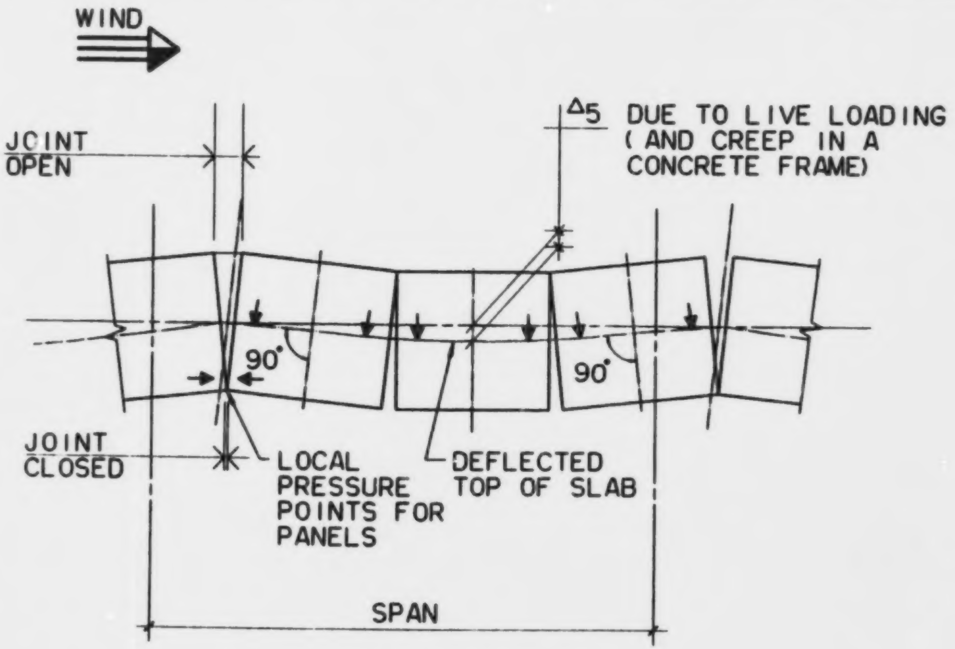
WIND
JOINT OPEN
Δ_5 DUE TO LIVE LOADING (AND CREEP IN A CONCRETE FRAME)
90°
90°
JOINT CLOSED
LOCAL PRESSURE POINTS FOR PANELS
DEFLECTED TOP OF SLAB
SPAN

FIG. 13 DISPLACEMENTS OF PANELS

DUE TO RACKING OF FRAME AND FLOOR DEFLECTIONS

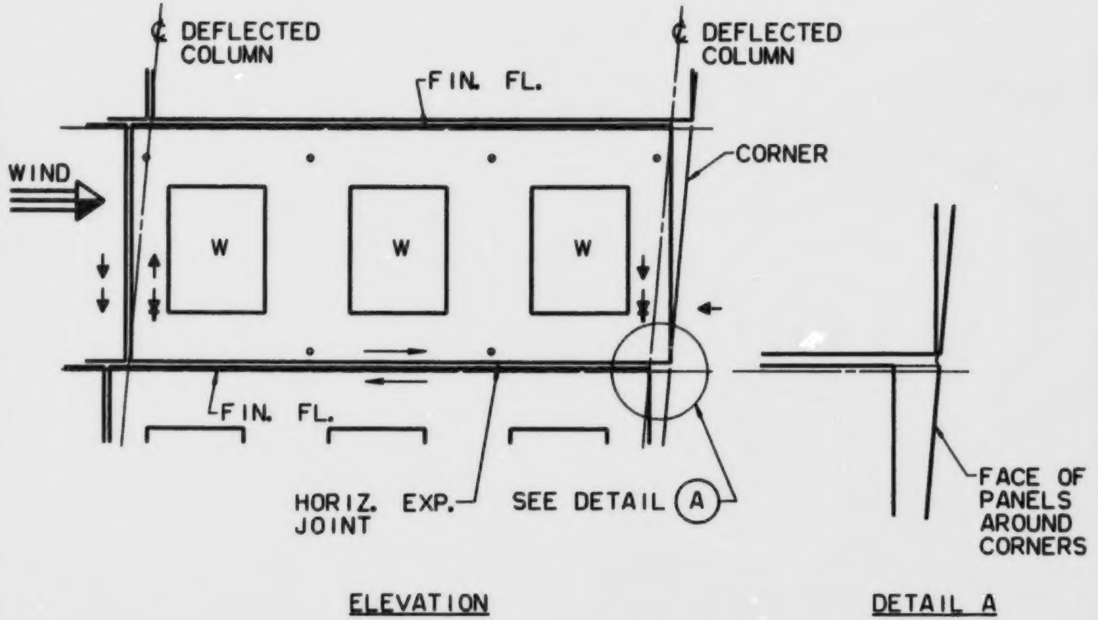

ELEVATION

DETAIL A

FIG. 14 DISPLACEMENT OF LARGE WALL PANELS

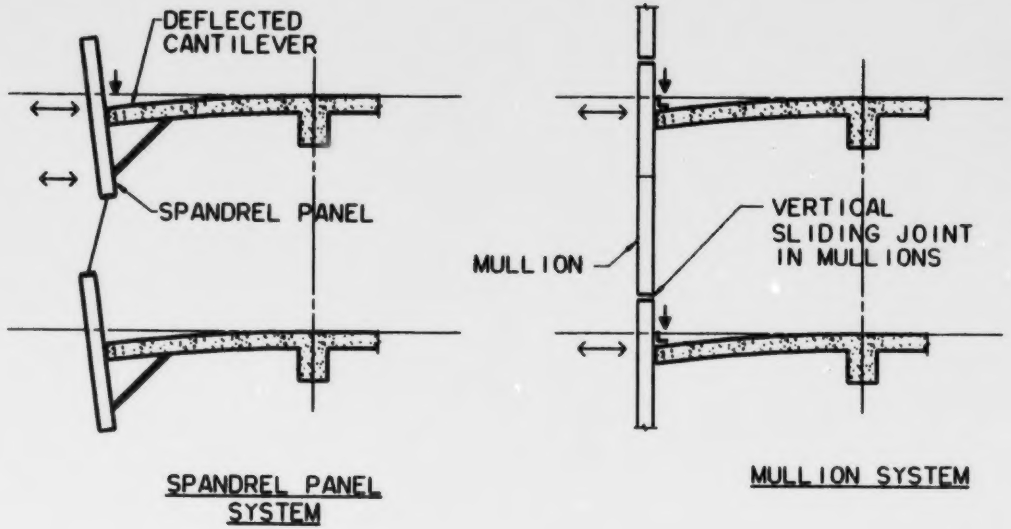

FIG. 15 **EFFECTS OF CANTILEVER DEFLECTIONS**

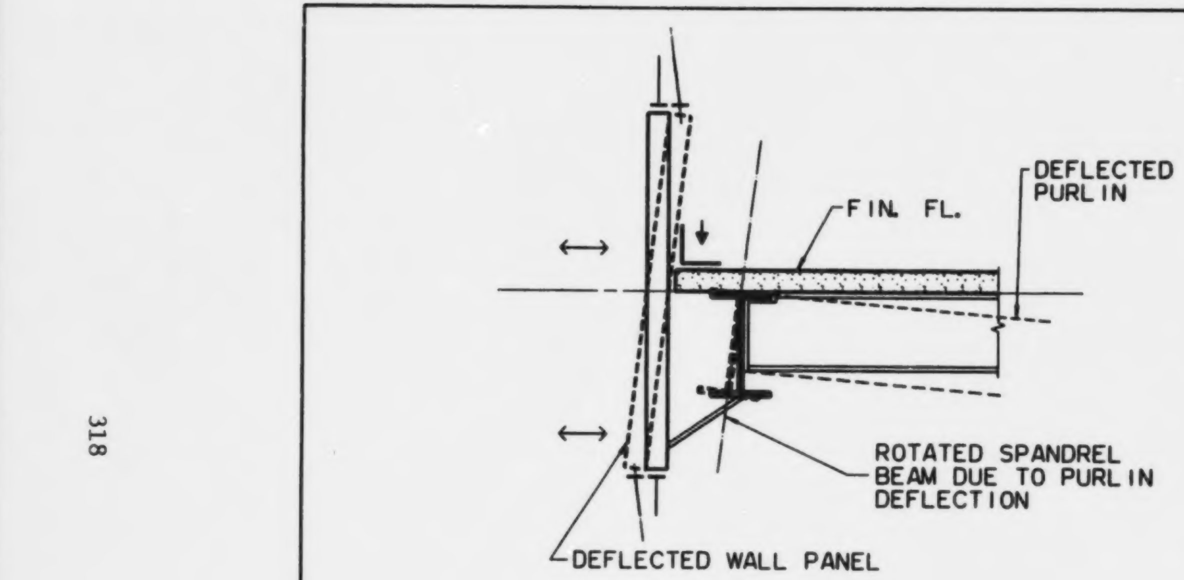

FIG. 16 EFFECTS OF SPANDREL BEAM ROTATIONS

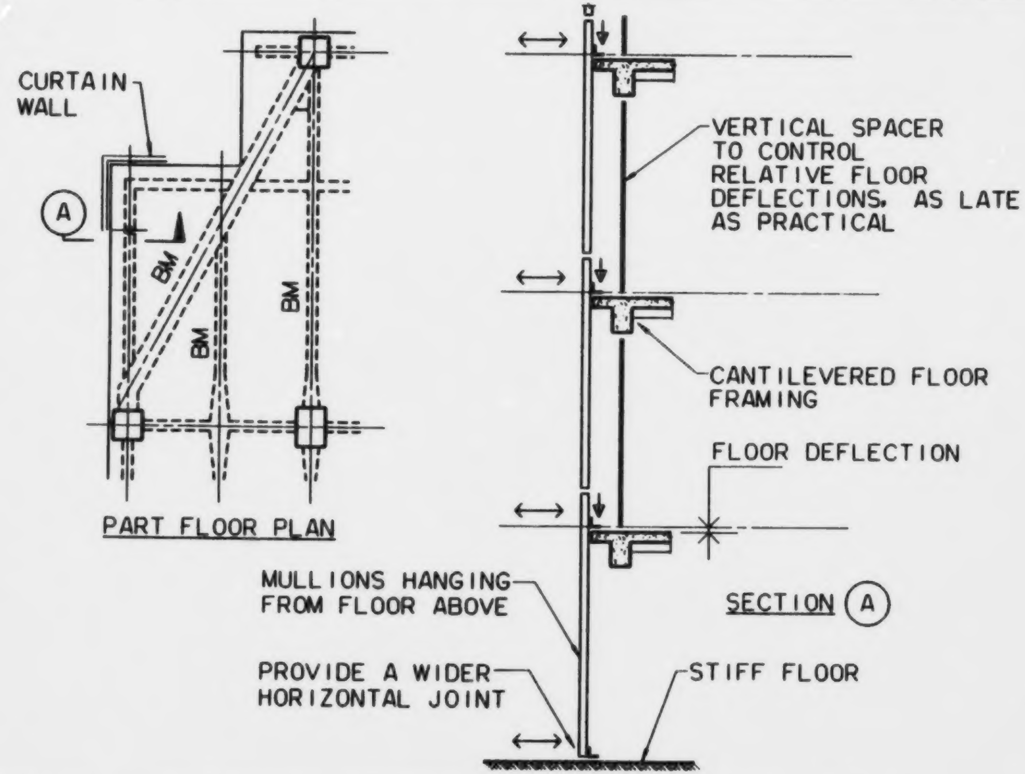
CURTAIN WALL
A
BM
BM
BM
PART FLOOR PLAN
VERTICAL SPACER TO CONTROL RELATIVE FLOOR DEFLECTIONS. AS LATE AS PRACTICAL
CANTILEVERED FLOOR FRAMING
FLOOR DEFLECTION
MULLIONS HANGING FROM FLOOR ABOVE
PROVIDE A WIDER HORIZONTAL JOINT
SECTION A
STIFF FLOOR

FIG. 17 DEFLECTION CONTROL IN CANTILEVERED AREAS AND FOR LONG SPAN SPANDRELS

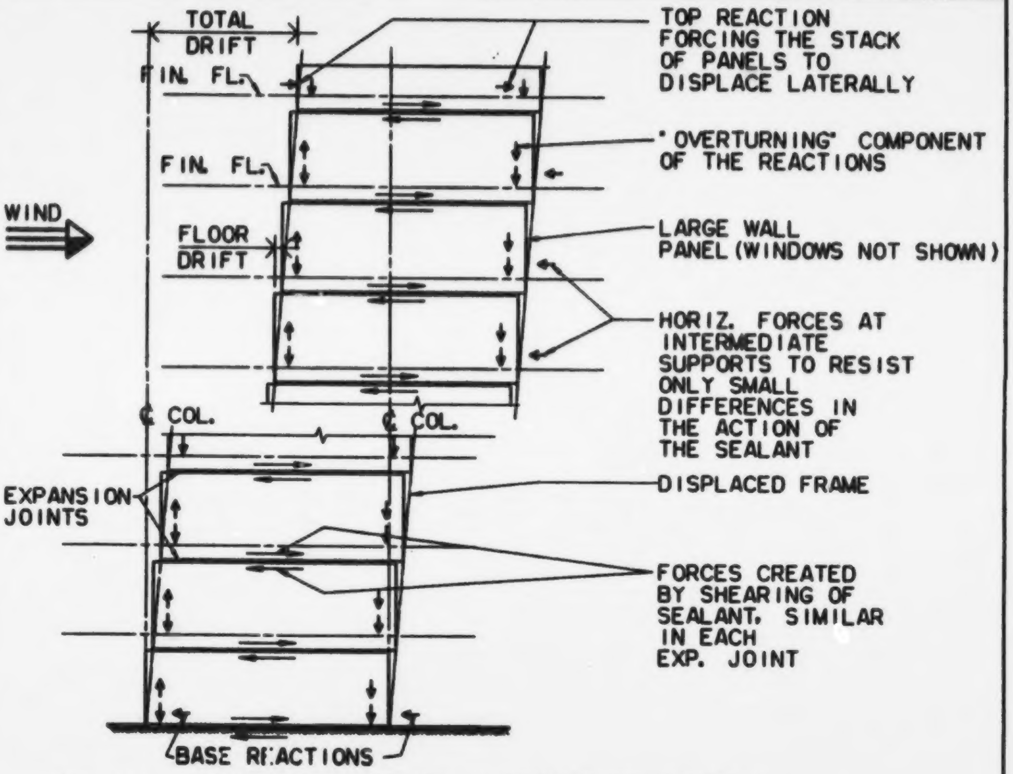
TOTAL DRIFT
FIN. FL.
FIN. FL.
FLOOR DRIFT
WIND
℄ COL.
℄ COL.
EXPANSION JOINTS
BASE REACTIONS
TOP REACTION FORCING THE STACK OF PANELS TO DISPLACE LATERALLY
"OVERTURNING" COMPONENT OF THE REACTIONS
LARGE WALL PANEL (WINDOWS NOT SHOWN)
HORIZ. FORCES AT INTERMEDIATE SUPPORTS TO RESIST ONLY SMALL DIFFERENCES IN THE ACTION OF THE SEALANT
DISPLACED FRAME
FORCES CREATED BY SHEARING OF SEALANT, SIMILAR IN EACH EXP. JOINT

FIG. 18 INTERACTION OF A STACK OF PANELS

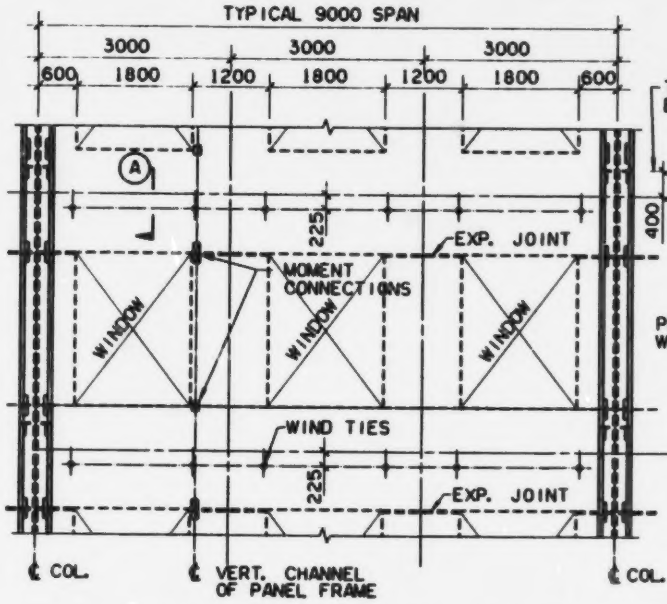

FIG.19 MID RISE PRE-FAB WALL PANELS SUPPORT AND CONNECTION LAYOUT

PANELS SHOWN DOTTED

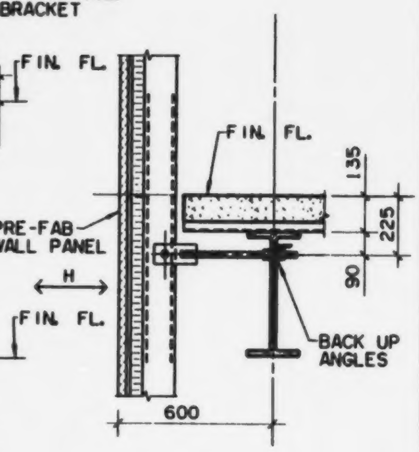

TYPICAL WIND TIE TO SPANDREL BEAMS

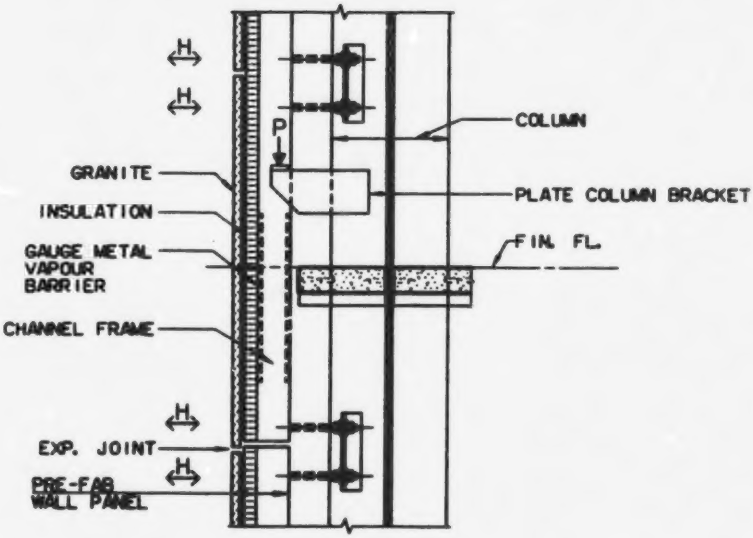

SECTION (A)

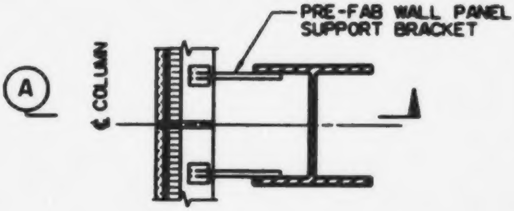

FIG. 20

TYPICAL COLUMN BRACKETS AND WIND TIES

THE DESIGN OF WALL CLADDING: NATIONAL AVIATION MUSEUM

M. Sommerstein
VicWest Steel Inc.
Rexdale, Ontario, Canada

ABSTRACT: A design and testing procedure based on acceptable engineering methods is presented as it was applied to the thermal and structural deformation of aluminum and porcelain cladding systems for the National Aviation Museum, Ottawa.

1. INTRODUCTION

The National Aviation Museum, located to the immediate south of Rockcliffe Airport, consists of a triangular exhibition building and a Spline building with approximately 16,000 sq. m. of usable space for exhibition, administration and support facilities.

The Spline building, situated on the west elevation of the triangular exhibition building, is a two-story structure housing the Museum's administration, storage, security and loading dock facilities. The exhibition building consists of a 4 m module triangular space frame structure on tubular steel columns while the Spline building is made up of floor slabs on reinforced concrete columns. The typical design of the wall assembly of the exhibition building (see Figs. 1 and 2) consists of:

a) 3.18 mm aluminum plate, acrylic enamelled exterior
b) 75 mm air space
c) 127 mm Fibreglas insulation AF530
d) .61 mm sheet metal air barrier, zinc coated c/w "S" cleats
e) 102 mm air space
f) .61 mm prepainted 5,000 series metal V-Rib liner.

The typical assembly design for walls on the Spline building consists of:

a) 1.20 mm porcelain enamel sheet c/w core and backup wpc metal sheet (total 15 mm thick)
b) 12 mm air space
c) 127 mm Fibreglas insulation AF530
d) .61 mm sheet metal air barrier, zinc coated c/w "S" cleats
e) 275 mm air space
f) 15 mm gypsum board or porcelain enamel sheet.

The design of aluminum and porcelain cladding of the National Aviation Museum project presented a specialized condition with regard to structural and thermal deformation for the following reasons:

- a roof design of a large scale space frame structure, with unknown exact deformations
- an unusual geometry of the outer skin, with very large aluminum panels
- very large door openings presenting irregular deformation patterns and vibration problems
- different deformation patterns between steel framing and aluminum
- large deformations of wall structural members
- the use of aluminum cladding for a sloping roof under high snow loads condition
- architectural requirement for a design free of any visual fasteners

2. PERFORMANCE CRITERIA

The basic design requirements were established by the architectural specifications and the 1980 National Building Code of Canada. The basic criteria for deformation consisted of the following:

a) Wind loads (N.B.C. 1980)

Framing	± 1.2 KN/m^2
Porcelain/Aluminum Subgirt	± 1.0 KN/m^2
Flat Liner (Air Barrier)	± 0.37 KN/m^2

b) Maximum Wall Deflection L/180

c) Temperature and Humidity

Winter condition:	Relative Humidity 40% Inside Temperature +20°C Outside Temperature -27°C
Summer condition:	Relative Humidity 60% Inside Temperature +24°C Outside Temperature +35°C

d) Fastener Criteria

No exposed fasteners were allowed - an architectural requirement.

e) Structure Movement Criteria - as shown in Fig. 3.

Design and testing to satisfy the performance criteria is described in the following.

3. DESIGN AND TESTING

3.1 Free Thermal Bow - Porcelain Panels

Temperature differentials between the interior and exterior skins produce differences in expansion or contraction, causing the panel to bow toward the high temperature side. If the bow exceeds architectural specifications (L/180) it can be reduced by adjusting the panel's length, colour, or thickness.

The effects of skin colour on thermal overstresses are dramatic and can be explained by the solar energy absorbed by skins of various colours. The temperature of the exterior skin of light coloured panels exposed to the sun was raised an average of 30°F above ambient air temperature, while medium coloured skins rose 55°F and dark colours, 80°F. Assuming that the interior skin remained at a constant temperature, the temperature differential between the skins of panels with a dark exterior colour is almost three times that of a panel with a light coloured exterior skin.

The free thermal bow due to temperature differential across the panel, as determined by calculation and checked by testing, is given by

$$D_t = .0000678 L^2 F/d \qquad (1)$$

where L is the panel length in feet, T the temperature difference of facing on °F (50°F light colours, 75°F medium colours and 100°F dark colours) and d is the panel thickness in inches (see Fig. 4).

For the panel dimensions and colours used on this job, application of Equation (1) showed that the free bow was less than the criterion, L/180.

3.2 Thermal Movement Of Porcelain Subgirts

Z bar subgirts deflect under the thermal movement of Porcelain panels. It is important to establish design equations and criteria for size and thickness of Z bar. Failure to do so may result in failure of the subgirts and of the Porcelain wall.

The design equations for the Z bar were determined on the basis of elastic restraint to thermal expansion/contraction of the panel indicated in Fig. 5, and a limiting stress of Fy/1.6. In addition, the fasteners were designed to resist the prying force (T in Fig. 5) developed by the restraint.

3.3 Thermal Movement - Aluminum Panel

Each panel within the boundary of the extrusions was made from four rectangular or six triangular smaller panels, as shown in Fig. 1. The smaller panels were rigidly connected to each other. To ensure panel flatness, each panel was stiffened with aluminum angles from behind.

An expansion joint at the end panel was provided to accommodate the thermal expansion and contraction. The effectiveness of the joint was confirmed by physical tests.

Extrusions were allowed to expand or contract longitudinally with the aluminum panel. Since the aluminum extrusions were fastened to steel subgirts, differential thermal movement had to be accommodated.

The aluminum panels were supported by vertical secondary structural tubing (see Fig. 2) which, by means of sliding connection, would not be subjected to any loading due to building movement.

A computer analysis of the restraint forces caused by thermal expansion/contraction of the panel, indicated in Fig. 6, showed that the maximum stress in the Z bar, 17.65 ksi, was less than the allowable.

3.4 Aluminum Panel Design

The aluminum reinforced plate design of the aluminum outer skin required modified design equations to establish stress and deformation in the flat portion of the plate.

When a plate is relatively thin and deflects appreciably under load, it will tend to act as a membrane; however, in most cases both bending and membrane stresses contribute to the strength. Aluminum, because of its low elastic modulus, lends itself to this type of design but care must be taken to provide adequate strength in the supporting framework.

The following design equations were used:

Load: $W = W_b$ (carried by bending stress) + W_M (carried by membrane stress).

Deflection: δ_b (bending deflection due to W_b) = δ_M (membrane deflection due to W_M).

where

$$\delta_b = 14\left(\frac{W_b\,b^3}{Lt^3}\right) \times 10^{-6}$$

$$\delta_M = .016\left(\frac{W_M\,b^3}{Lt}\right)^{1/3}$$

Tension Stress at Centre:

$$f_M = 8\left(\frac{W_M}{Lt}\right)^{2/3}$$

$$f_b = 0.75\left(\frac{W_b\,b}{Lt^2}\right)$$

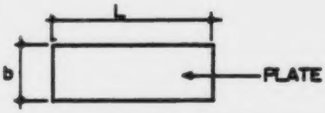

Plate supported all four sides (hinged cond.)

Uniform load over entire plate.

where dimensions are in inches, loads in kips and stresses in psi.

These design equations were verified by a pressure loading test carried out on an aluminum panel. A similar pressure test was carried out on the flat liner air barrier, with the following results:

1. At design load of 8 psf (.37 Kpa) maximum deflection = 0.264"
2. "S" cleats and seal (shown below) did not fail at 52 psf
3. Permanent deformation of flat sheet at zero load 0.23" after applying a load of 52 psf.

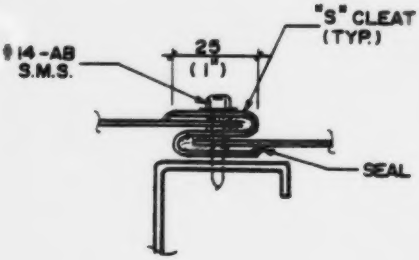

3.5 Studs And Fasteners Vibration Tests

The purpose of the tests was to establish a suitable method to permanently connect the aluminum extrusions to the 1/8" thick aluminum plate.

Under repeated wind loading, vibration and repeated deflection would develop in the exterior cladding. Since sheet metal screws cannot be used for this application, aluminum studs are welded to the 1/8" thick plate and a nut is used on each stud to connect the extrusions to the plate. It must be ensured that studs do not fail and nuts do not come loose when vibrated.

Vibration tests, shown in Fig. 7, were therefore carried out for different connection assemblies. The results are contained in Table I. The split-ring lock washer (Test No. 5) proved to be quite effective and was therefore adopted. To prevent breakage the aluminum stud cannot be torqued too tightly (manufacturer suggested maximum 32.5 in lbs); actual torque used was 24 in lbs maximum.

3.6 Window Supports

The large deformation at triangular windows (see Fig. 1) required a specialized sliding frame design. Sliding joints were achieved by the use of slotted holes in the support clips and neoprene bonded washers under the screws. Load tests were carried out to ensure that the sliding joints were effective and that the connections were fully effective and safe in supporting the lateral wind load.

4. SUMMARY AND CONCLUSIONS

The custom design of the aluminum and procelain wall panels on this structure presented several unusual and difficult deformation considerations, as follows:

a) The aluminum reinforced plate design of the aluminum outer skin required modified design equations to be evaluated accurately for various load criteria. The worst estimated conditions were tested in the laboratory and compared to calculated results.

b) The rain screen wall design and the use of flat liner as air and vapour seal required a careful evaluation as to the actual loads on liner and the liner deformation under maximum load to prevent failure at sealed joints.

c) Welded studs on the back of aluminum wall panels to which reinforced angles are attached were tested for strength and vibration adequacy and limits on the deformation of panels were established.

d) Design equation had to be developed for porcelain Z bar subgirts.

e) Large deformation at windows required design of a special sliding frame.

f) Many laboratory tests were performed to verify and prove the total design.

REFERENCES

1. American Society of Metals (1964). Metals Handbook, Vol. 1, 8 Ed.

2. Canadian Institute of Steel Construction (1982 Ed.). Handbook of Steel Construction.

3. Canadian Wind Engineering Association and Canadian Society of Civil Engineers (1981). Third Canadian Workshop on Wind Engineering, National Research Council Canada.

4. Eastman, R.W. (1976). Report on Screw Fastened Sheet Steel Connections, Vol. 1, Canadian Steel Industries Construction Council.

5. Leontovich, V. (1959). Frames and Arches - Condensed Solutions for Structural Analysis.

6. National Research Council Canada (1980). No. 17724, The Supplement of the National Building Code of Canada.

7. Salvadori, M. and Levy, M. (1967). Structural Design in Architecture, Prentice-Hall, Inc.

8. Schuster, R.M. and Lind, N.C. (1975). Cold Formed Steel Design Manual (Based on CSA STD S136-1974), Univ. of Waterloo Press.

9. Canadian Standards Association (1983). Strength Design in Aluminum - CAN3-S157-M83.

10. Tables for the Analysis of Plates, Slabs and Diaphragms--Based on the Elastic Theory - R. Bares.

TABLE I

VIBRATION TESTS OF STUDS AND FASTENERS

TEST NO	ASS'Y COMPONENTS	TORQUE IN LBS	MAXIMUM Δ F (IN)	NO. OF CYCLES PER(MIN)	TOTAL NO OF CYCLES	TEST RESULTS
1	#10-24NC alum. stud alum. washer SS nut	19	1.442	142	22,290	One stud broke at 2840 cycles, another at 22900 cycles two nuts loosening
2	#14-20NC alum. stud alum. washer SS nut end stud caulked silc.	24	1.479	142	20,700	4 nuts loose (4in-lbs torque)
3	#14-20NC alum. alum. washer locknut (nylon)	24	1.463	142	55,400	2 ctr. stud washers can be slipped sideways indication loosening of nuts
4	#14-20NC alum. stud alum. locknut with nylon insert - flat washer	25	1.463	142	124,500	3 centre nuts torque drop to 11 in. lbs.
5	#14-20NC alum. stud holes in angle 5/16" Ø hes. alum. nut on SS split lock washer	24	1.463	142	124,500	No change All studs tight at 24 in/lb torque. No broken studs.

Fig. 1 Aluminum Cladding - National Aviation Museum

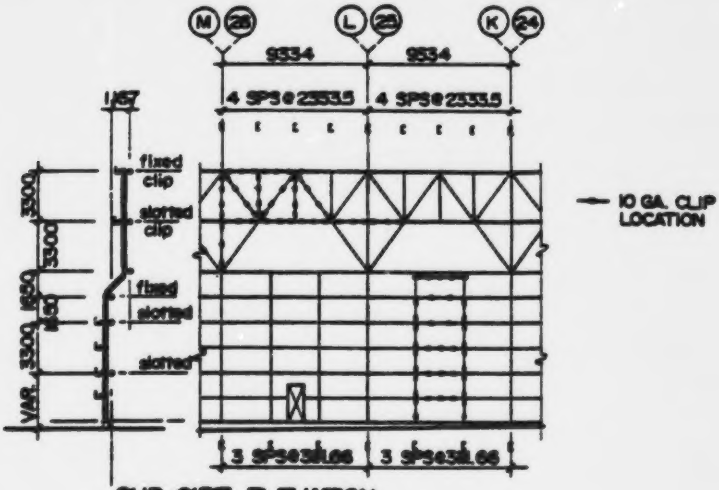

SUB-GIRT ELEVATION

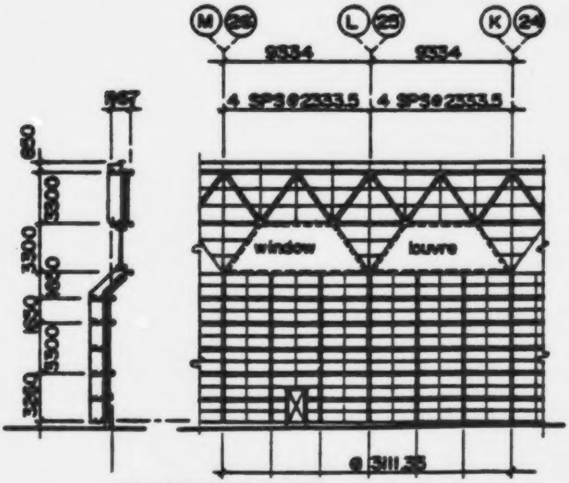

ALUMINUM PANEL ELEVATION

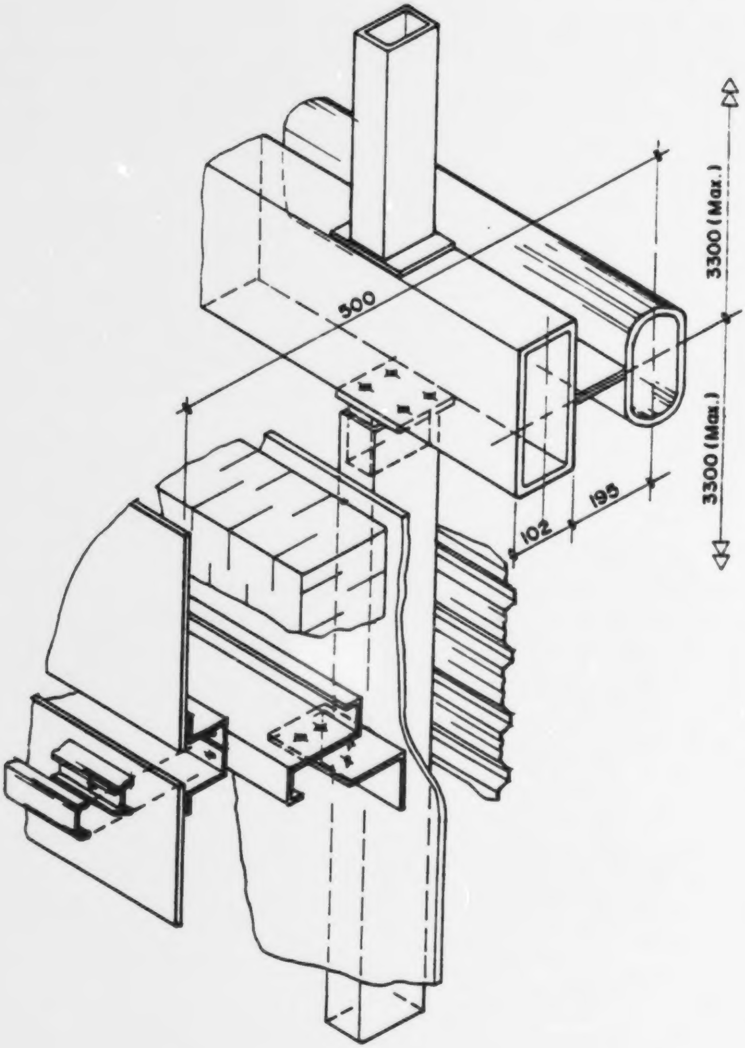

Fig. 2 Isometric View of Typical Aluminum Cladding System

Fig. 3 Performance Criteria - Structure Movement

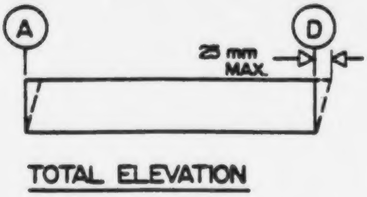

(a) LATERAL DIFFERENTIAL MOVEMENT 25mm MAX.

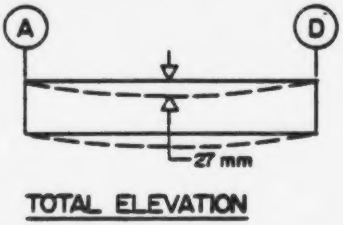

(b) DIFFERENTIAL SETTLEMENT 27 mm MAX.

(c) MAX. DEFLECTION OF STRUCTURE PURLIN 25 mm (9mm PROVIDED IN SPECIFICATIONS).

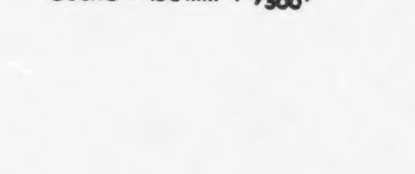

(d) MAX. DEFLECTION AT HANGER DOORS - 156 mm (L/300)

Fig. 4 Free Thermal Bow of Porcelain Panels

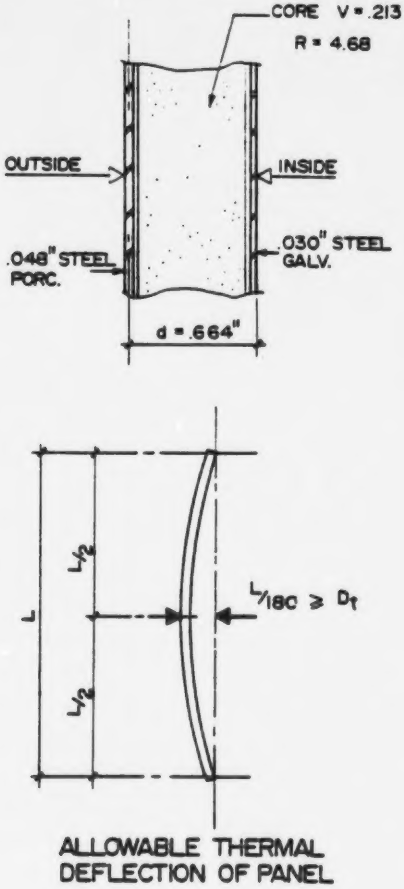

Fig. 5 Thermal Movement of Porcelain Subgirts

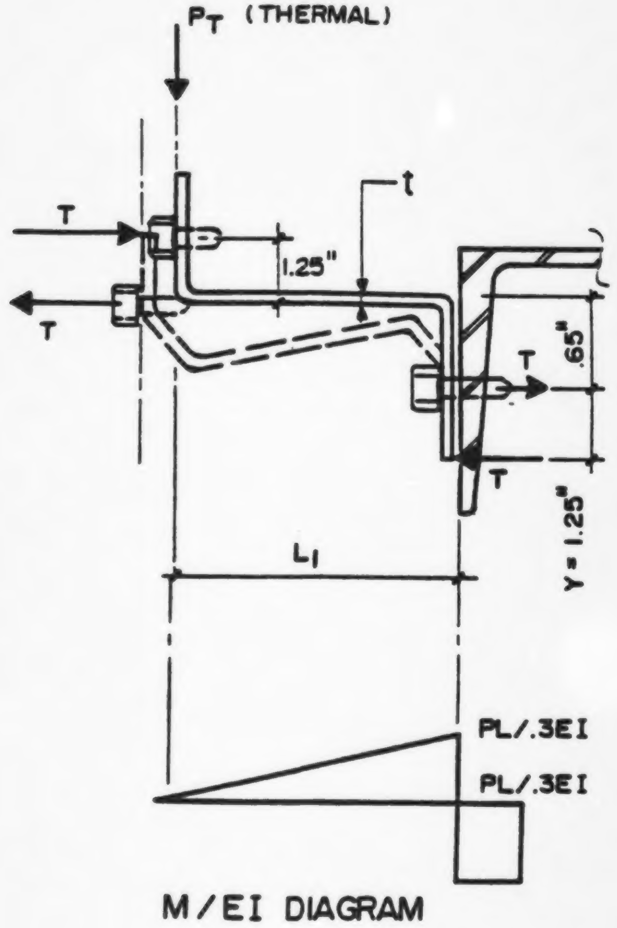

Fig. 6 Thermal Expansion and Contraction at Panel Edge Extrusion

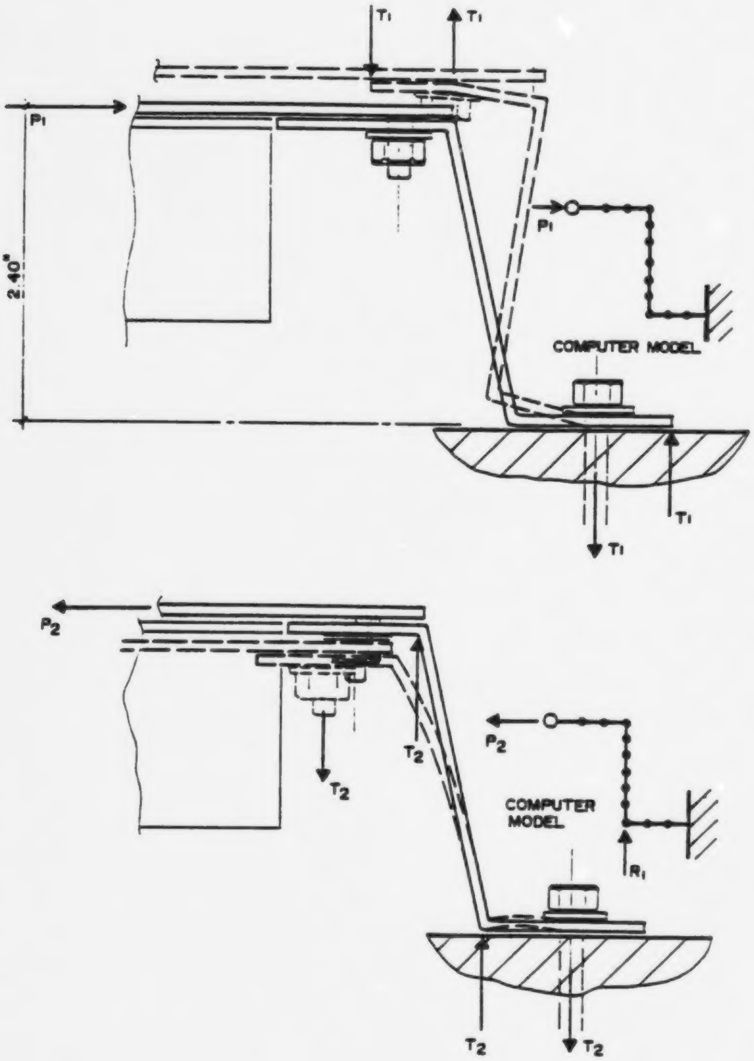

Fig. 7 Studs and Fasteners Vibration Test

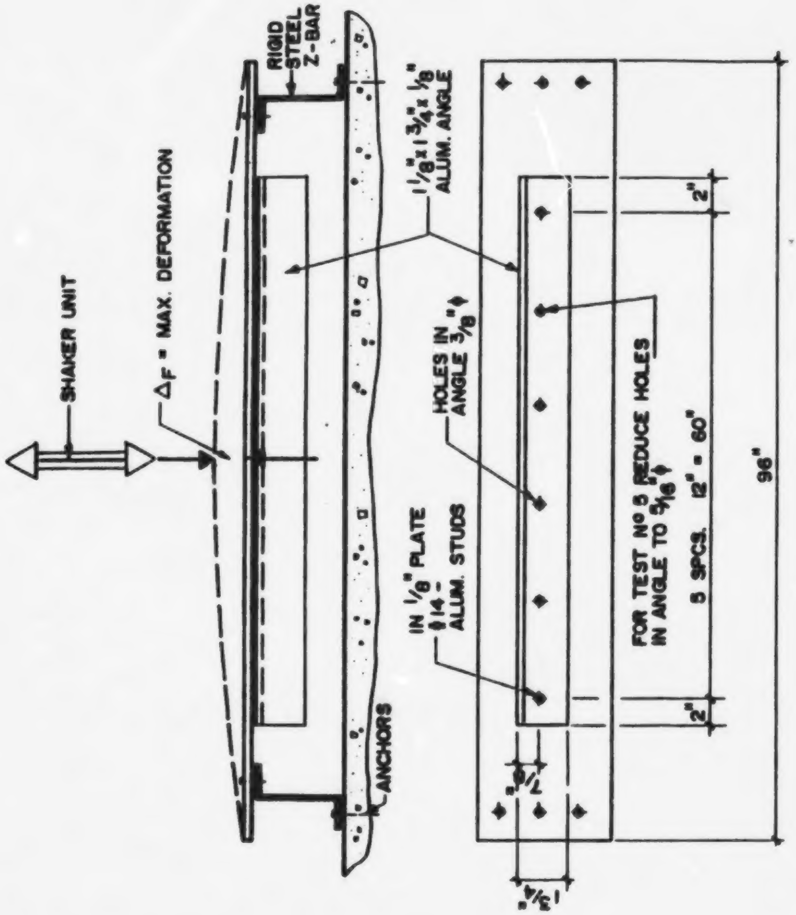
SHAKER UNIT
Δ_F = MAX. DEFORMATION
RIGID STEEL Z-BAR
1 1/8" x 1 3/4" x 1/8" ALUM. ANGLE
ANCHORS
HOLES IN ANGLE 3/8"φ
IN 1/8" PLATE φ14 - ALUM. STUDS
FOR TEST No 5 REDUCE HOLES IN ANGLE TO 5/16"φ
5 SPCS. 12" = 60"
96"
2"
2"
7/8"
1 3/4"

VÉRIFICATION DE L'ÉTAT D'UTILISATION DES COLONNES SOUS DÉFORMATIONS IMPOSÉES

Dusan B. Najdanovic, dr.sc.tech.
Faculté de Genie Civil
Belgrade, Yougoslavie

RESUME: Les colonnes et les pieux sont souvent capables de subir des rotations importantes dans leurs sections d'encastrement sans subir de dommage et sans diminution de la capacité portante. Tout calcul classique en théorie élastique ferait pourtant apparaître des moments de flexion plus ou moins importants qui, combinés à l'effort normal N, diminueraient la capacité portante et entraverait l'aptitude au service.

On propose dans cet article une méthode pratique de vérification de l'état d'utilisation des colonnes sous l'effet des charges et des déformations imposées aux extrémités, compte tenu de la fissurtation et des effets différés. Il s'agit de trouver les angles de rotations limites imposés aux colonnes qui soient acceptables en service. Grâce à la relaxation et à la fissuration du béton, les colonnes sont en effet plus ductiles qu'on pourrait l'imaginer de prime abord.

1. INTRODUCTION

Dans les structures où les efforts horizontaux sont repris par des éléments rigides (p.ex. noyaux ou refends d'un bâtiment), les colonnes sont sollicitées en premier lieu par des efforts normaux (figure 1). Cependant, par suite des liaisons rigides entre les colonnes et les porteurs horizontaux (dalles ou sommiers), des déformations imposées se produisent aux extrémités des colonnes. Elles sont provoquées par les déformations de ces porteurs horizontaux dues aux charges, au retrait, au fluage du béton, à la variation de température ou au tassement différentiel des appuis.

Le comportement réel d'une colonne sous déformations imposées est, en général, plus favorable que celui donné par les calculs habituels élastiques. Il est bien connu que, en se basant sur un calcul purement élastique, les colonnes ne peuvent supporter que des déformations faibles, ce qui ne correspond nullement à la réalité. D'autre part, des études basées sur la théorie de plasticité /3/ et /6/ confirmées par des recherches expérimentales effectuées ces dernières années

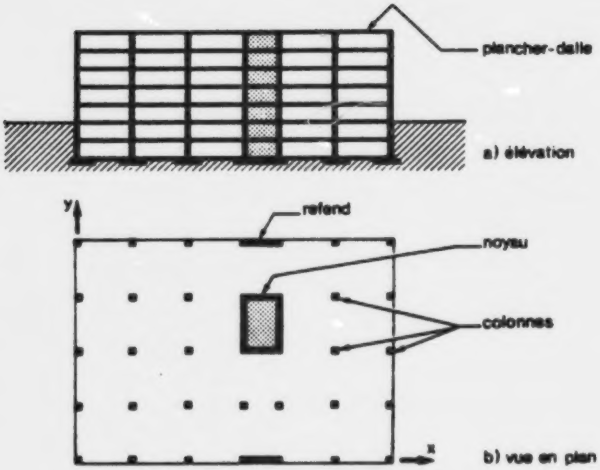

Figure 1: Exemple d'un bâtiment avec noyau et refend

/2/ et /4/, montrent que les colonnes, sollicitées par un effort normal et des déformations imposées aux extrémités, présentent une grande ductilité. Les colonnes peuvent transmettre à la rupture un effort normal élevé indépendamment des déformations qui leur sont imposées, pour autant qu'un certain angle limite de rotation ne soit pas dépassé. Par des raisonnements à la rupture, on n'est toutefois pas en mesure de porter un jugement sur le comportement réel de la colonne à l'état d'utilisation. De grandes ouvertures de fissures peuvent apparaître à la face tendue du béton. Il est également concevable qu'un éclatement de la zone d'enrobage du béton se produise.

Ces aspects montrent la nécessité d'adopter une approche différente dans l'analyse des colonnes de bâtiment /3/. Il est préférable de se contenter de contrôler que les colonnes ont une résistance suffisante à l'effort normal, mais de vérifier en plus qu'elles sont suffisamment ductiles pour supporter les déformations imposées à leurs extrémités.

Afin de vérifier certaines hypothèses émises on a fait une étude expérimentale avec des colonnes grandeur nature, dans le laboratoire climatisé de l'EPFL /1/.

2. COLONNE SOUMISE A DES DEFORMATIONS IMPOSEES DE LONGUE DUREE

Nous allons distinguer deux types de déformations imposées:

- dû au retrait du béton et à la variation de température, dont l'effet est représenté à la figure 2.a,
- dû aux charges, qui par suite des liaisons rigides entre les colonnes et les porteurs horizontaux, produisent des rotations imposées, voir figure 2.b.

Dans les cas courants de la pratique, ces deux types de déformations agissent simultanément et elles varient dans le temps; pour les charges quasipermanentes, cette variation provient du fluage, du retrait et de l'apparition successive des fissures.

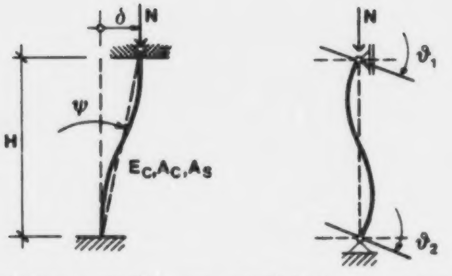

Figure 2: Déformations imposées aux extrémités des colonnes dues aux: a) raccourcissement des porteurs horizontaux, b) déformations des porteurs horizontaux sous l'action des charges

Analysons le compartement dans le temps d'une colonne sous déformations imposées aux extrémités, en négligeant dans un premier temps l'apparition des fissures dans la colonne.

2.1. Evolution des efforts dus aux déformations constantes imposées instantanément: Avec l'approche développée dans /5/ en utilisant la Méthode du module ajusté effectif (AAEM), nous pouvons calculer la diminution ΔM du moment fléchissant initial dans la colonne en béton symétriquement armée, dû aux déformations imposées au temps $t=t_o$ maintenues constantes:

$$\Delta M = \frac{M_{el}\,\phi}{(1+\alpha\frac{I_s}{I_c})\,(1+\chi\phi)} \tag{1}$$

où I_s - moment d'inertie de l'armature par rapport au centre de gravité de la section
I_c - moment d'inertie de la section du béton seul
M_{el} - moment fléchissant dans la colonne au temps $t=t_o$ dû aux déformations imposées
ϕ,χ - coefficent du fluage, respectivement de vieillissement
α - rapport E_s/E_c.

Or, si dans une colonne qui doit subir une déformation imposée au temps $t=t_o$ sous forme, p.ex., d'un déplacement horizontal d'appui δ, figure 2, le déplacement est instantané et constant dans le temps à partir de $t=t_o$, les moments engendrés sont maximum à t_o et ensuite décroissent selon une loi de relaxation d'après l'équation (1), voir figure 3.

2.2. Evolution des efforts dus aux déformations imposées lentes affines au fluage: Lorsque les déformations imposées croissent de manière lente et progressive à partir du temps $t=t_o$, nous obtenons que la variation du moment fléchissant est

$$\Delta M = \frac{M_{el}}{(1+\alpha\frac{I_s}{I_c})\,(1+\chi\cdot\phi)} \tag{2}$$

où M_{el}- moment fléchissant dans la colonne considérée comme purement élastique dû aux déformations imposées lentes qui au temps $t=t$ vaut $\Delta\theta = \theta_t - \theta$.

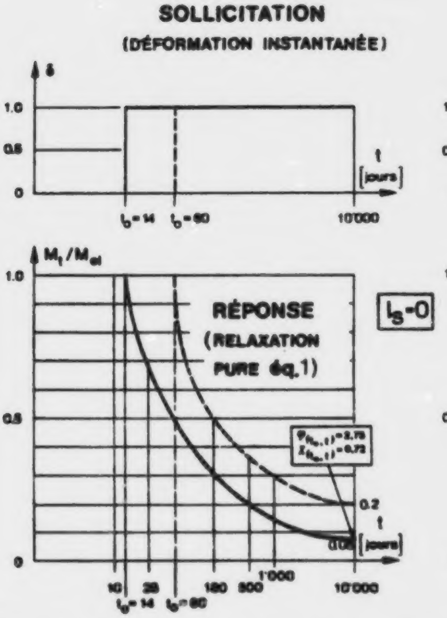

Figure 3: Effet de la relaxation du béton lors d'une déformation imposée instantanée ou lente

Or, si le déplacement n'est pas instantané (p.ex. dû au retrait) et dure de $t=t_0$ à $t=t$, les moments vont augmenter pendant cette période $(t-t_0)$ tout en réduits fortement par la relaxation selon l'équation (2), figure 3.

2.3. Passage du cas des colonnes sous déformations imposées lentes au cas des colonnes sollicitées par des efforts constants de longue durée: Lors de l'établissement du projet, il est vain de prétendre connaître ce qu'on peut appeler l'histoire de la construction, à savoir les conditions climatiques, l'âge au moment du décoffrage, des mises en charges, des surcharges temporaires, etc. De plus, dans une structure hyperstatique, sous l'effet du fluage du béton et de la présence de l'armature, une redistribution des efforts se produit dans le temps.

Si l'evolution des déformations imposées aux extrémités d'une colonne dans le temps est donc incertaine, nous pouvons tout de même estimer ses valeurs finales. Pour effecturer la vérification des colonnes à l'état d'utilisation en tenant compte des paramètres précédents, nous avons proposé certaines simplifications concernant l'évolution des angles imposés. Elles consistent à admettre que l'évolution de ces angles est affine au fluage et que ces angles peuvent être ramenés à ceux d'une colonne isolée et sollicitée à partir d'un âge moyen t_0, par $\bar{M}$ et $\bar{N}$ constants créant au temps $t \to \infty$, sous les effets différés et la fissuration, des angles de rotations identiques. Ainsi, le cas des colonnes sous déformations imposées est ramené à celui des colonnes isolées et sollicitées par des efforts constants. La question est de savoir quel sera le moment de remplacement $\bar{M}$ constant produisant au $t \to \infty$ des angles $\bar{\vartheta}_t$ égaux à ceux imposés $\Delta\theta$, figure 4.

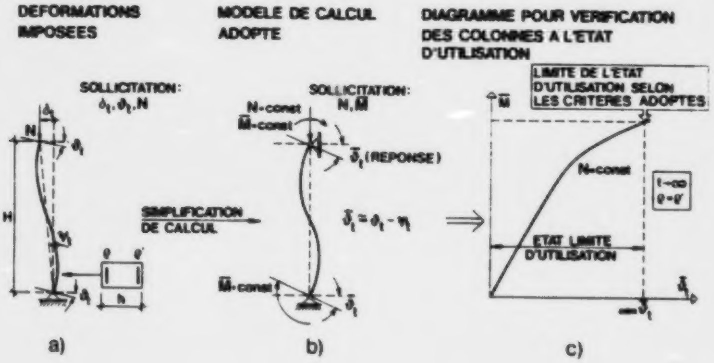
DEFORMATIONS IMPOSEES
MODELE DE CALCUL ADOPTE
DIAGRAMME POUR VERIFICATION DES COLONNES A L'ETAT D'UTILISATION
SOLLICITATION: $\vartheta_1, \vartheta_2, N$
N
ϑ_1
H
ψ_1
ϑ_2
ϱ
ϱ'
h
SIMPLIFICATION DE CALCUL
SOLLICITATION: N, $\bar{M}$
N=const
$\bar{M}$=const
$\bar{\vartheta}_t$ (REPONSE)
$\bar{\vartheta}_t = \vartheta_1 - \psi_1$
$\bar{M}$=const
$\bar{\vartheta}_t$
LIMITE DE L'ETAT D'UTILISATION SELON LES CRITERES ADOPTES
$\bar{M}$
N=const
$t \to \infty$
$\varrho = \varrho'$
ETAT LIMITE D'UTILISATION
$\bar{\vartheta}_t$
$\bar{\vartheta}_t$
a)
b)
c)

Figure 4: Démarche et modèle de calcul

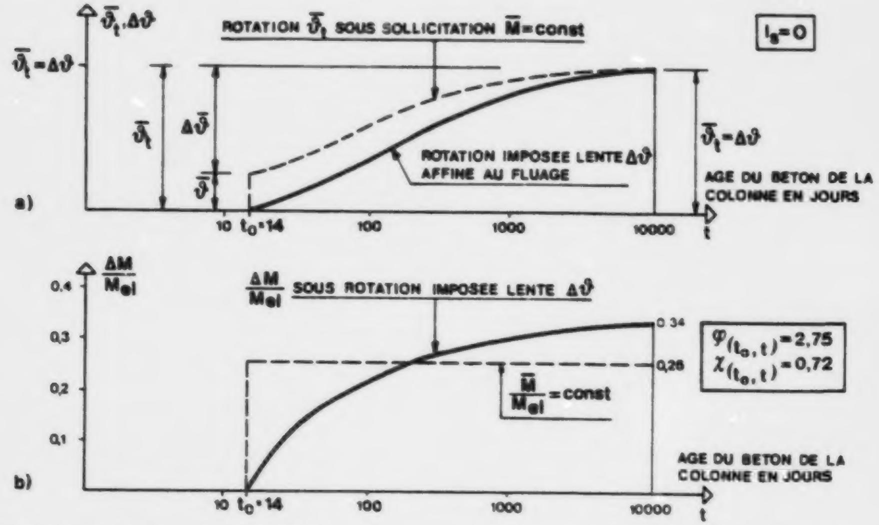

Figure 5a: Evolution des angles de rotation: sous sollicitation $\bar{M}$ = const (---
et sous rotation imposée lente (——)

b: Augmentation du moment ΔM en cas d'une rotation imposée croissante $\Delta\theta$ à partir de l'âge de la colonne $t_0 = 14$ jours (——) et moment de remplacement correspondant ($\bar{M}$ = const)

Ce moment, développé dans /5/, vaut:

$$\bar{M} = \frac{M_{el}}{1 + \dfrac{\phi}{1 + \alpha \dfrac{I_s}{I_c} (1 + X\phi)}} = \frac{M_{el}}{1 + \phi'} \qquad (3)$$

où M_{el} - moment fléchissant aux extrémités de la colonne considérée comme purement élastique dû à la rotation imposée $\Delta\theta$ au temps $t = t$

ϕ' - coefficient de fluage réduit (effet de l'armature dans la colonne).

A titre d'exemple, on peut voir à la figure 5 l'évolution du moment ΔM sous la rotation impose $\Delta\theta$ croissante à partir d'un âge de la colonne valant $t_o = 14$ jours. Le moment de remplacement correspondant $\bar{M}$, produisant l'angle de rotation θ_t au temps t=10000 jours égal au cas de rotation imposée $\Delta\theta$ est représenté à la même figure.

3. CRITERES POUR LA VERIFICATION DE L'ETAT D'UTILISATION DES COLONNES

Comme on a déjà mantionné, une colonne, qui a une sécurité à la rupture suffisante sous l'action combinée des charges et des déformations imposées aux extrémités, ne garantit pas forcément un comportement satisfaisant à l'état d'utilisation. A cet effet il faudra pouvoir estimer les valeur maximales des angles de rotation imposés à ses extrémités sans que l'état-l'imite d'utilisation soit dépassé. Nous proposons que les critères nous permettant de définir l'état-limite d'utilisation d'une telle colonne soit:

3.1. Limitation de l'allongement de l'armature tendue: L'acier d'armature au droit d'une fissure doit être capable de reprendre sans se plastifier l'effort de traction. Comme les contraintes dans l'armature tendue peuvent, dans certains cas, augmenter considérablement dans le temps à cause des effets différés, nous sommes d'avis qu'il faut limiter les contraintes dans l'armature tendue au temps infini (σ_{s2t}), par rapport à la resistance caractéristique de l'acier d'armature (f_{yk}), à une valeur

$$\sigma_{s2t} \leq f_{yk}/\gamma = 300 \text{ N/mm}^2 \qquad (\varepsilon_{s2t} \leq 1{,}5‰) \qquad (4)$$

où ε_{s2t}- allongement dans l'armature tendue au temps infini calculée en stade II-nu

γ - coefficient de minoration.

Le coefficient γ doit permetre de mentenir la fissuration à un niveau raisonable. On propose la valeur $\gamma = 1{,}6$ /5/.

3.2. Limitation du raccourcissement relatif de l'armature comprimée: Etant donné qu'une forte redistribution des contraintes entre l'armature et le béton se produit dans le temps (due au fluage et au retrait du béton), les contraintes dans l'armature comprimée peuvent atteindre des valeurs très élevées. Le raccourcissement relatif moyen, mesuré au niveau de l'armature comprimée de colonnes d'essais /1/, montre dans certains cas que la limite d'élasticité de l'acier d'armature était même dépassée, toutefois aucune altération de l'aspect des colonnes n'a pu être observée.

Nous jugeons prudent d'adopter une limitation du raccourcissement relatif de l'armature comprimée, au temps infini, valant

$$|\varepsilon'_{s2t}| \leq 2{,}3‰ \qquad (5)$$

3.3. Limitation de l'ouverture des fissures: A cause de la répartition du moment le long de la colonne sous déformations imposées, les sections dans lesquelles des fissures peuvent apparaître se trouvent à sa tête et à sa base. Il est bien évident que dans une colonne il ne peut apparaître qu'un petit nombre de larges fissures.

Dans des conditions d'ambiance peu ou modérément sévères, des ouvertures maximales de fissures de l'ordre de 0,4 mm peuvent être tolérées. Selon des publications récentes, une telle ouverture de fissure est sans effet significatif sur la corrosion de l'acier d'armature. De plus, en limitant les contraintes dans l'armature tendue au temps t=t selon le critère 3.a, on sait qu'on a des contraintes réduites au temps initial. De cette façon, la possibilité de l'apparition dans une colonne de fissures dont l'ouverture est plus grande que 0,4 mm est fortement diminuée.

Dans des colonnes se trouvant dans des conditions d'ambiance sévères, ainsi que lorsque les exigeances relatives à l'aspect sont élévées, il faut fixer la limite de l'ouverture maximale des fissures à environ 0,25 mm. Une limitation beaucoup plus sévère de la fissuration poura être requise dans le cas d'ouvrages spéciaux.

4. COURBURE MOYENNE

La courbure moyenne varie entre les deux cas limites: la courbure calculée en stade I (limite inférieure) et la courbure calculée en stade II-nu (limite supérieure). Pour le cas de la flexion composée, la courbure moyenne au temps t=t peut être définie par la relation suivante:

$$1/r_{mt} = (1 - \zeta_t)\, 1/r_{1t} + \zeta_t\, 1/r_{2t} \qquad (6)$$

avec:

$1/r_{1t}$ - courbure dans le stade I calculée au temps t=t

$1/r_{2t}$ - courbure dans le stade II-nu calculée au temps t=t

ζ_t - coefficient de répartition.

Ce coefficient est déterminé en se basant sur les valeurs mesurées au cours des essais en laboratoire /1/:

$$\zeta_t = 1 - \left(\frac{\sigma_{sr}}{\sigma_{s2t}}\right)^{n_t} \qquad (7)$$

où $n_t = 0{,}5$ pour $0 < e/d \leqslant 1{,}5$

avec

e - excentricité de l'effort normal par rapport au centre de gravité de la section

d - hauteur statique.

Une analyse comparative des resultats expérimentaux et théoriques a cependant montré que, dans le cas des colonnes, nous avons le droit d'approcher la courbure moyenne par celle calculée en stade II-nu, donc

$$1/r_{mt} \simeq 1/r_{2t} \qquad (8)$$

5. CALCUL DE L'OUVERTURE DES FISSURES

L'analyse des resultats obtenus au cours des essais, a mis en évidence que l'ouverture moyenne des fissures (W_m) dépend principalement de deux facteurs: l'allongement de l'armature tendue et la hauteur de la zone tendue du béton. Par conséquent, dans le cas de la flexion composée, nous proposons l'expression suivente:

$$W_m = \lambda \cdot (h - x) \cdot \varepsilon_{sm} \tag{9}$$

où λ - coefficient dont la valeur moyenne vaut 1,4 /5/
   h - hauteur de la section de la colonne
   x - position de l'axe neutre au temps $t=t_o$
   ε_{sm}-déformation moyenne de l'armature au temps $t=t_o$.

Pour l'augmentation de cette ouverture moyenne par suite des effets différés, nous proposons que celle-ci soit fonction de l'augmentation de la courbure moyenne au cours du temps:

$$W_{mt} = \frac{d - x_t}{d - x} \, \frac{1/r_{mt}}{1/r_m} \cdot W_m \tag{10}$$

où le terme $(d-x_t)/(d-x)$ présente le rapport des zones tendus calculées dans une section au droit d'une fissure (stade II-mu) au temps $t=t$ et $t=t_o$. Pour les caractéristiques rhéologiques habituelles, nous avons toujours

$$\frac{d - x_t}{d - x} < 1 \tag{11}$$

d'où on conclut que l'accroissement du rapport entre l'ouverture des fissures au temps $t=t$ et au temps $t=t_o$ est plus petit que celui entre les courbures. Les résultats des essais confirment que c'est bien le cas /5/.

L'état de déformations relatives et l'état de contraintes d'une section au temps $t=t$ sont calculés en utilisant la méthode AEMM et en tenant compte du fait que la zone comprimée du béton varie dans le temps par suite des effets différés, et cela dans les stades I et II-mu.

6. APPLICATION PRATIQUE

La vérification d'une colonne à l'état d'utilisation consiste à limiter au temps $t=t$ les déformations imposées (θ_t) aux extrémités de la colonne à des valeurs admissibles. Il faut donc que la relation suivante soit satisfaite:

$$\theta_t < \bar{\theta}_{t\ adm} \tag{12}$$

où $\bar{\theta}_{t\ adm}$ dépend des trois critères sousmentionnes. Dans le cas général en utilisant ces critères nous pouvons exprimer l'angles $\bar{\theta}_{t\ adm}$ en fonction de l'ouverture caractéristique des fissures W_{kt}, pour les différents paramètres suivents: effort normal (N), caractéristique géométrique de la colonne (b,d,H), cas de déformation de la colonne, pourcentage d'armature (ρ et ρ'), fluage (ϕ), retrait (ε_{cs}) du béton.

Pour faciliter la vérification pratique selon (12) on a développé /5/ un programme d'ordinateur permettant la construction des différents abaques d'interaction. A titre d'exemple, un tel abaque est représenté à la figure 6 pour le cas de la déformation de la colonne en "S".

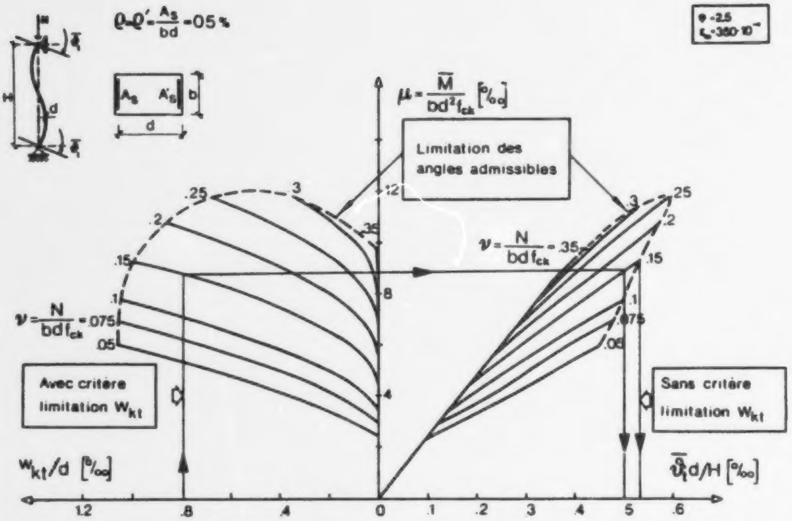

Figure 6: Représentation sans dimension des relations entre l'angle de rotation et l'ouverture caractéristique des fissures pour les différentes valeurs de l'effort normal

L'effort relatif ν représenté dans cette figure est fonction de la résistance caractéristique du béton à la compression f_{ck}, selon le Code-Modele CEB-FIP.

Les angles admissibles maximum limités selon les critères 3.1 et 3.2 sont représentés en traitillé à la figure 6. Les angles de rotation admissibles en fonction de l'ouverture caractéristique des fissures peuvent être estimés au moyen de la partie gauche du diagramme.

Pour la plupart des colonnes de bâtiments le critère explicite de l'ouverture des fissures peut être négligé. En effet, le critère 3.1 contrôle déjà en grande partie l'ouverture des fissures. Par conséquent, pour l'application pratique, les abaques peuvent être présentés sous forme de diagrammes d'interaction N/N_u-$\bar{\theta}_t$ d/H dont un exemple est représenté à la figure 7.

L'avantage de cette représentation des abaques est telle que les angles de rotation $\bar{\theta}_t$.d/H sont donnés en fonction du rapport N/N_u, où N signifie l'effort normal dû aux charges de longue durée à l'état d'utilisation et N_u l'effort normal de rupture centré, où la résistance du béton à la compression est donnée selon la norme SIA 162 (projet mars 1987).

Etant donné qu'à chaque valeur de la déformation relative de l'armature tendue (ou comprimée) correspondent des angles différents de rotation $\bar{\theta}_t$.d/H et des rapports différents N/N_u, nous pouvons établir les deux familles de courbes (voir figure 7). Une famille représente les déformations relatives de l'armature tendue et l'autre celles de l'armature comprimée. Les courbes sont limitées par les déformations relatives correspondant aux critères: ε_{s2t}=1,5‰, respectivement ε'_{s2t}=-2.3‰.

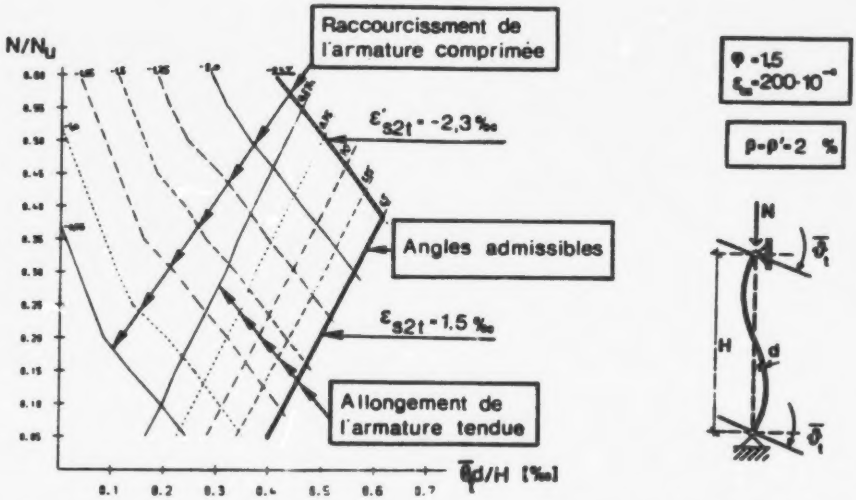

Figure 7: Angles de rotation des extrémités de la colonne en fonction de N/N_u pour les différentes valeurs de déformations relatives de l'armature tendue et comprimée (ε_{s2t} et ε'_{s2t}).

On peut voir dans ces abaques que les valeurs des angles de rotation admissibles dépendent fortement du rapport N/N_u, des dimensions de la colonne, du pourcentage d'armature et des caractéristiques rhéologiques du béton. La plus grande valeur de $\bar{\theta}_t\, d/H$ s'obtient lorsque les deux critères, à savoir $\varepsilon'_{s2t} = -2.3‰$ et $\varepsilon_{s2t} = 1{,}5‰$, sont remplis en même temps. Le rapport N/N_u correspondant à cette valeur se trouve entre 0,25 (pour $\rho = \rho' = 3\%$ et $\phi = 2{,}5$) et 0,55 environ (pour $\rho = \rho' = 0{,}5\%$ et $\phi = 0{,}5$).

7. CONSLUSIONS

La vérification de l'état d'utilisation des colonnes est basée sur les critères suivants:

- l'armature comprimée ne doit pas être plastifiée,
- l'allongement relatif de l'armature tendue ne doit pas dépasser certaines valeurs-limites choisies,
- l'ouverture maximale des fissures est limitée.

Pour faciliter la vérification pratique des colonnes des bâtiments à l'état d'utilisation, nous avons établi des abaques d'interaction entre N et $\bar{\theta}_t$, valables pour les colonnes à sections rectangulaires armées symétriquement. Des abaques similaires pourraient être établis selon la même procédure pour n'importe quels critères d'utilisation choisis de toute autre manière que celle que nous avons adoptée, ainsi que pour des colonnes ayant des sections de formes différentes (p.ex. circulaires, évidées, etc.).

Les analyses que nous avons faites ont montré qu'une colonne peut supporter à l'état d'utilisation des déformations imposées lentes relativement importantes, grâce à une forte relaxation. Les valeurs des déformations imposées admissibles dépendent du rapport N/N_u, des dimensions de la colonne, du pourcentage d'armature et des caractéristiques rhéologiques du béton. Pour un effort normal N donné, une augmentation du pourcentage d'armature accroît, en général, les déformations admissibles.

En raison de la forte augmentation due aux effets différés des contraintes dans l'armature comprimée, le critère du raccourcissement relatif de l'armature comprimée est souvent le critère déterminant pour la vérification des colonnes à l'état d'utilisation.

REFERENCES

/1/ Dal Busco S., Najdanovic D., Suter R. 1986. Dimensionnement des colonnes de bâtiment - Essais de longue durée - Série expérimentale A et B, Rapport d'essais, Publication IBAP N° 116, EPF Lausanne.

/2/ Dal Busco S., Suter R. 1986. Dimensionnement des colonnes de bâtiment - Série expérimentale C, Rapport d'essais, Publication IBAP N° 112, EPF Lausanne.

/3/ Favre R., Najdanovic D., Suter R., Thürlimann Ch. 1984. New design concept for reinforced concrete columns in buildings, Final Raport, 12th Congres IABSE, Vancouver.

/4/ Ford J.S., Chang D.C., Breen J.E. 1981. Behaviour concrete columns under controlled lateral deformation, ACI Journal, Proceedings V.78, N° 1, N° 2.

/5/ Najdanovic D. 1987. Contribution à la vérification de l'état d'utilisation des colonnes sous déformations imposées, Thèse N° 680, EPF Lausanne.

/6/ Thürlimann Ch. 1984. Design of reinforced concrete columns subjected to imposed and deformations, IABSE Periodica.

EXPERIMENTAL ANALYSIS OF THE DEFORMABILITY OF PARTITION WALLS AND BRITTLE COVERINGS

É. Nemestothy, Gy. Visnovitz

Department of Strength of Materials and Structures
Technical University, Budapest H-1521

ABSTRACT: Tests were carried out to determine the ultimate deformations of different types of partition walls and brittle ceramic coverings. Based on the test results simple methods of calculation were developed to give approximate information on the deformability of these non load-bearing structures.

1. PURPOSE OF TEST

Damage to non load-bearing elements is one of the most frequent consequences of excessive deformations of the load-bearing structures. To avoid these types of damages we have to know, first of all, the value of deformation constraints these adjacent elements can bear.

In this test series we investigated the deformability of partition walls and brittle coverings as the two largest groups of damage-prone elements. The test series were made in the Laboratory of T.U.B.

2. DEFORMABILITY OF PARTITION WALLS

2.1 Test-program: In the development of the test program two approaches were followed:

- investigation of basic deformation cases;
- investigation of typical partition walls regarding their structure and statical behaviour.

The test equipment shown in Fig. 1 was used to investigate the following deformation constraints:

a/ vertical in-plane bending of partition walls;
b/ in-plane distortion of partition walls;
c/ vertical in-plane compression of partition walls.

The deformation constraint was transferred to the partitions by a steel frame representing the surrounding load-bearing structure. Because the partitions are room-sized the actual number of the tests amounted to 2-3 pieces.

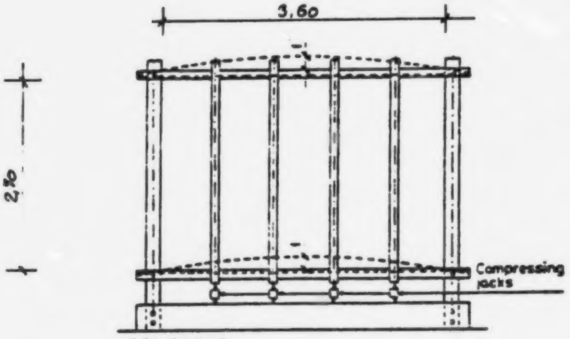

a) Bending test

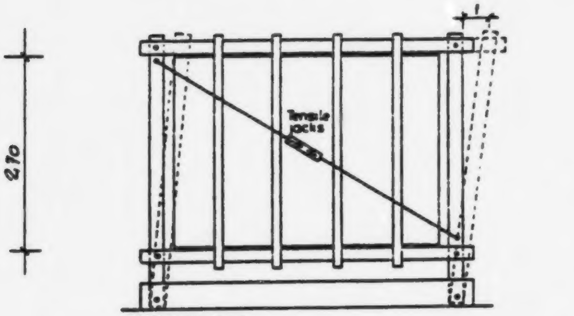

b) Distortion test

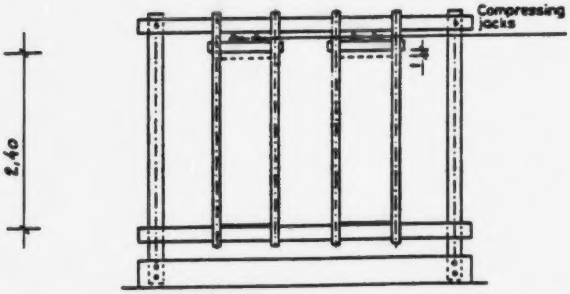

c) Compression test

Fig. 1. **Layout of the testing equipment**

In practice the partition walls differ in material, structure and in their connection to each other and to the load-bearing structures. As to their statical behaviour these partitions can be divided into five groups:

1. partition wall systems of room-sized units (precast r.c. partition walls);
2. partition walls composed of units (special bricks, gypsum perlite etc.) smaller both horizonally and vertically than room-size, built in-situ with mortar joints;
3. partition walls built of narrow vertical boards with mortar joints;
4. partition walls of thin, 10 to 15 mm sheets (plasterboard, chipboard, etc.) either nailed or screwed to the frame members;
5. partition walls of similar units as in group 4 but with the sheets sliding freely in their grooves rather than fixed to frame units.

The last group was not tested because the deformabilities of such types can be calculated simply from geometrical data (slab size, groove size), the deformation of the sheets being negligible due to their slenderness. For test purposes a type most commonly used in Hungary was chosen for each of the other four groups.

2.2 Test results: Failure of the partition walls belonging to groups 1, 2 and 3 was very similar, so we can consider all of them as solid, "brittle" partition walls. Their behaviour was absolutely different from group 4, which type has been named "assembled partition walls" in this paper (illustrated by Fig. 2-Fig. 5 in case of bending).

Failure of solid partitions can be characterized as follows:

- The failure-pattern and load-bearing capacity of the walls first of all depends on their side ratio H/L (see Fig. 2, and 4);
- The first cracks in the short partitions (ratio 1:1,3) appear as a consequence of the principal tensile stresses limiting the compression zones; the load-bearing capacity of the wall doesn't decrease because of these cracks. The total failure of these walls follows crushing in the compression zone when the load-bearing capacity diminishes quickly;
- The first cracks of longer walls (side ratio 1:2) appear in the middle of the panel and divide it into shorter parts; the behaviour of these parts after cracking is independent from each other.
- The load-bearing capacity of solid partitions is large (Fig. 3);
- The deformatibility of the solid partition walls is small (6-10 mm), but the deformation of the sheet itself is much smaller; nearly 70-80% of the total deformation is due to plastic compression of the mortar joints at the edge of compression zones (Fig. 5).

The deformability of a partition wall can be estimated using simple formulae. The formula in the case of bending is:

$$f_{max} = \Delta H + \epsilon_f [H + \frac{L^2}{4H}]$$

where

ΔH plastic compression of the edge joints

ϵ_f average strain of the compressed wall-strip

H height of the wall-panel

L Length of the wall-panel

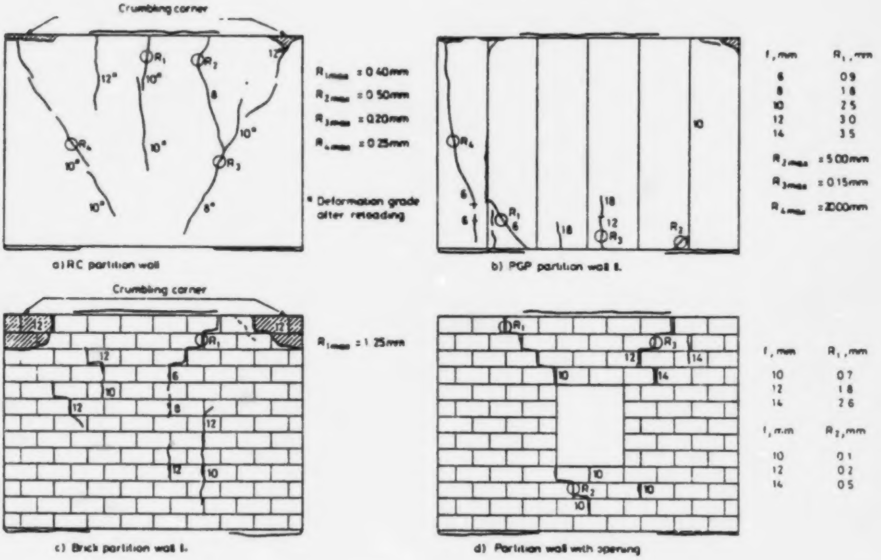

Fig. 2. Failure of partition walls 1 : 1.3 in bending (load and support as in Fig. 1a)

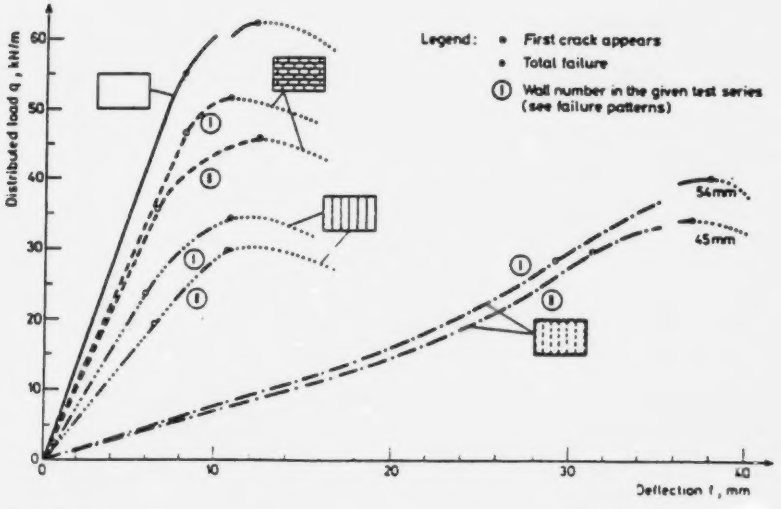

Fig. 3. Force-deflection diagram of partition walls 1 : 1.3 in bending

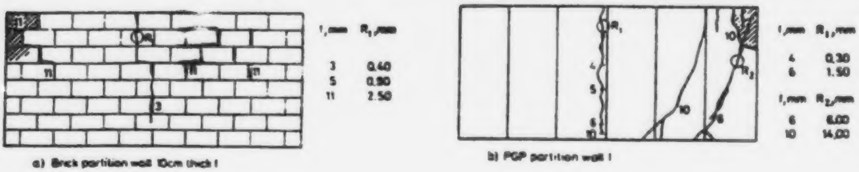

a) Brick partition wall 10cm thick !

b) PGP partition wall !

Fig. 4. **Failure** of partition walls 1 : 2 in bending (**load and support as in Fig. 4a**)

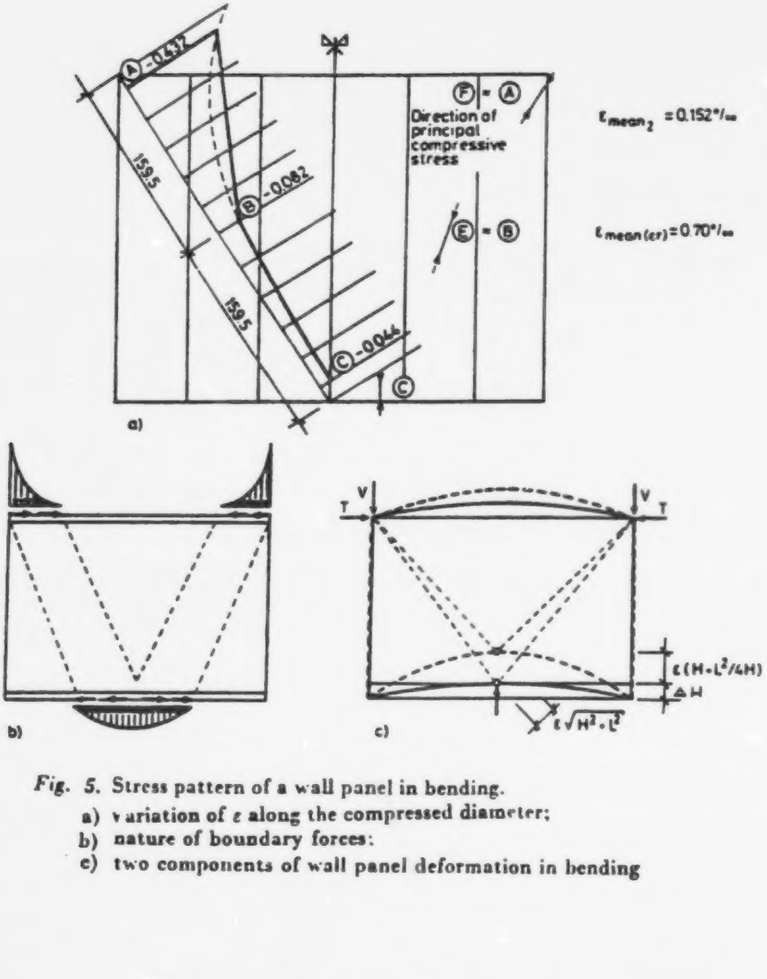

Fig. **5. Stress pattern of a wall panel in bending.**

a) variation of ε along the compressed diameter;

b) nature of boundary forces;

c) two components of wall panel deformation in bending

Hence for brick walls with L/H = 1.5, using the experimental data the relationship simplifies to:

$$f_{max} = 5 + \frac{L}{2000} \text{ [mm]}$$

This relationship holds as long as the horizontal forces can be balanced by adhesion and friction on the wall edge. This requirement is satisfied as long as the side ratio is less than 2:1. At higher ratios the corners of longer walls slip, consequently the deformability of these walls decreases to nearly zero.

Similar relationships can be written for other cases of deformation constraints.

Failure of assembled partition walls differs as follows:

- the load-bearing capacity was much smaller and the deformability was determined by the edge joints only
- the total failure occurred by failure of the inner joints: the sheets were torn off the skeleton.

2.3 Conclusions, suggestions: Based on these test results it can be concluded that

- solid, brittle partition walls connected to the load-bearing structures by mortar joints possess very small deformability but large load-bearing capacity. Failure of these partition walls occurs if the surrounding load-bearing structure produces deformation constraints and loads greater than their capacity. As long as the load is less than its bearing capacity, the partition wall can limit the deformation of the load-bearing structure, rearranging its stress pattern;
- assembled partition walls have significant deformability but only small load-bearing capacity, therefore they do not participate in the stress pattern of structures;
- the deformability of partition walls is due first of all to the edge joints between the partition and structure; the span has no sigificant influence on the deformability of the partition wall, only its L/H ratio.

To determine the limiting values of deformations we suggest the following directives:

- absolute values are more justified than limits depending on the span; for solid partitions this limit is rather small, 8-10 mm; for assembled partitions it has a wide range depending on the joints;
- this is acceptable if the span is such that the value of L/H is 2:1 or less. If the span is longer, we suggest that the partition wall be divided by mobile joints into shorter components.

3. ULTIMATE DEFORMATIONS OF BRITTLE CERAMIC COVERINGS

3.1 Tests: The purpose of the tests was to determine ultimate deformation values for the most common covering types, and to obtain a deeper knowledge of the behaviour of the coverings by measuring deformations and displacements.

In conformity with building practice, the structure was modelled by concrete compression and flexural reinforced concrete members amounting to 10×3 specimens.

From large brittle ceramic covering tiles with high modulus of elasticity the following were tested:

Wall tile 150×150×5.5 mm
Stoneware tile 150×150×7.5 mm

A selection aspect was the rather different rigidities while the identical sizes and bonding technologies ensured the comparability of results. Bonding was made either with an improved lime mortar 15 mm thick complying with the former Hungarian Building Code, or with an up-to-date single-component silicate based adhesive.

From among the possible deformations of the structure, the following were investigated:

a/ contraction without bending (e.g. walls);
b/ contraction with concave bending (e.g. floor covering at midspan);
c/ strain concentrated in cracks with convex bending (e.g. ceiling finishes, floor coverings over a support).

The effect of repeated loads on bonding was simulated by 70 repetitions of the deformation corresponding to the load at the serviceability limit state of the r.c. slab.

By applying edge tiles which allowed practically no displacement (using a resin mortar), the case was specially considered where, in addition to bonding, there was interaction with the edge tile (phenomenon of arching). A typical example of test layout, with measurement locations, is shown in Fig. 6.

3.2 Results of tests:

3.2.1 Coverings on the compressed surface of the structure: The more important test parameters and the measured ultimate deformation values for the various covering types are compiled in Table 1.

Nearly identical failure deformations on compressed and flexural specimens showed that, contrary to hypotheses in the literature, imposed strain (unit deformation) rather than bending was significant for covering damage. The curvature is only significant for the specific strain values in the plane of a covering.

It is noted that "compressed" coverings with edges free to displace relative to the based, behave differently than those with both ends fixed.

A free-edge covering fails in shear along the free edge. The failure is due to the edge displacement (S_R) relative to the base exceeding the value provided by the bond (see Table 1).

The ultimate deformation of the base (structure) can be calculated as follows:

$$\epsilon_a = \frac{2\cdot\tau_R\cdot S_R}{E_f\cdot t_f}$$

where

ϵ_a specific strain of base;

E_f average modulus of elasticity of the covering (with joints);

t_f covering thickness;

τ_R plastic adhesive-shear strength of the bond.

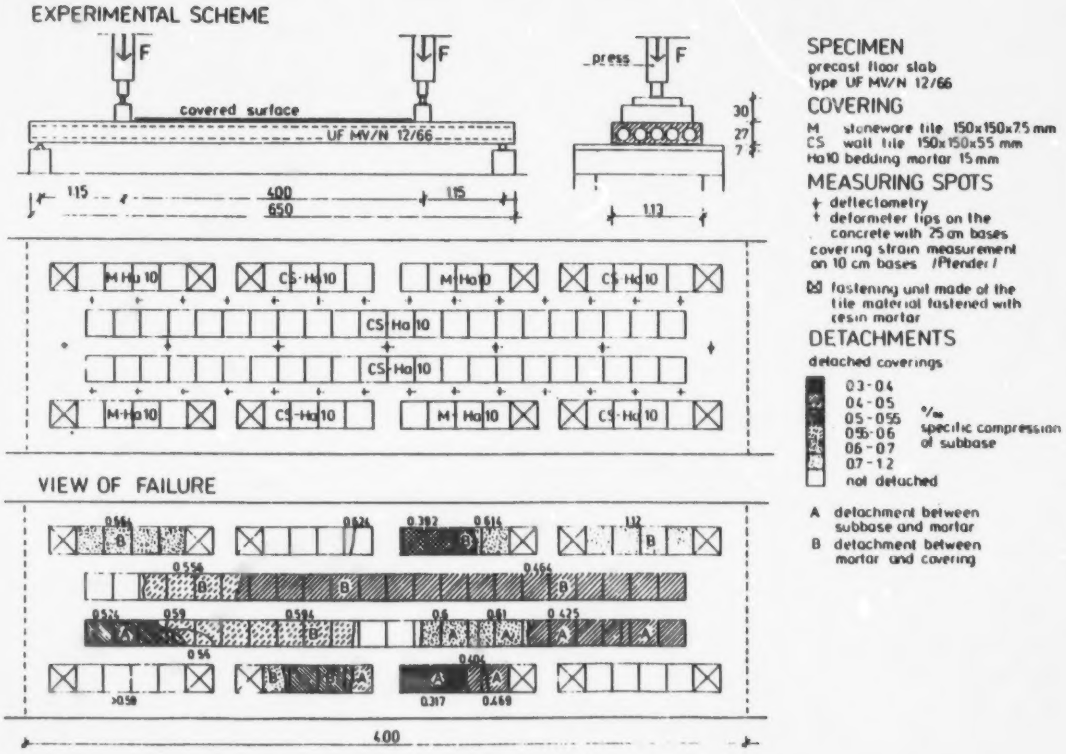

Figure 6: Test of coverings on a precast floor slab

The basic types of failure of fix-edge (arching) coverings are:

a/ vertical bond detachment followed by abrupt blow-up;
b/ joint crushing or breaking of ceramic tiles.

Both failure types may be produced experimentally. Models made with mortar failed according to the first type. The surface detachment was local, spreading gradually, then rising some mm and, finally, the covering blew-up (buckling). Obviously, the specified ultimate deformation relates to the rising.

As opposed to shear stress redistribution, no plastic redistribution of the normal adhesive forces can be observed.

The formula for the calculation of the ultimate deformation is in this case:

$$\epsilon_a = \frac{\sigma_{tR} \cdot L_f}{\alpha \cdot E_f \cdot t_f}$$

where, in addition to the previous symbols
σ_{tR} tensile strength of the bond connection
L_f length of a covering tile:
α bedding slope ($\Delta t_h / L_f$); inaccuracy of setting
Δt_h mortar thickness difference over a length L_f.

From this relationship it is clear that less () rigid coverings are more prone to rising.

The bond strength of up-to-date adhesives is much higher than that of mortars (0.10 to 1.00 N/m^2). So coverings fixed by adhesive failed only beyond the serviceability limit state according to failure type b. From analysis of the measured displacements, deformations of 0.3 to 0.4‰ were measured on stoneware, and 0.7 to 0.8‰ on tiles, corresponding to 20 to 25 N/mm^2 of normal stresses. This fact shows that in certain cases the covering may itself rupture. On the other hand, the covering may absorb much of the loads on the structure reducing thereby its deformation. In certain cases this favourable effect may be taken into consideration.

3.2.2 Coverings on tensile surface of structure: No tested coverings subjected to tension were found to be damaged on a crack-free concrete base (up to a 0.2‰ strain). Structural cracks beyond 0.03 mm appear also in brittle coverings with practically the same width. The crack extends in the covering causing either local detachments, step-wise along the joints, or, depending on the crack location, cracking the tile.

3.3 Conclusions and suggestions: Numerical values of the test results showed that the possibility of deformation damage of the covering cannot be ignored. The relevant structural deformation damage of 0.3 to 1.0‰ may also occur due to creep of concrete or brick structures. An important consequence of the plastic behaviour of adhesives is the sensitivity of bond coverings to repeated loads. Under repeated loads the forms of failure are exactly the same as under static loads but failure may also be induced by repeating 20 to 60 times a lower deformation value depending on the covering type and the load level.

The test results may indirectly be applied to prevent damage due to other than structural deformations. Humidity, temperature changes and shrinkage may subject coverings to further deformation constraints, and the structural soundness is only safeguarded if the total deformation due to simultaneous loads and other causes does not exceed the ultimate value.

The different effects may be converted to structural (base) deformations:

- covering elongations (swelling, thermal expansion) correspond to base deformations of the same size but with opposite sign;
- the value of the elongation relative to the mortar bedding layer ($\Delta\epsilon_m$) is given by

$$\Delta\epsilon_a = \Delta\epsilon_m \cdot \frac{t_m E_m}{t_f \cdot E_f + t_m \cdot E_m}$$

Thus the resultant of different, simultaneous effects may be obtained by simple addition!

Based on the test results and theoretical research the role of the joints and dilatations of ceramic coverings became clearer.

- Joints are primarily required by utility aspects, but they also affect the stress pattern of the covering. Because of a lower modulus of elasticity, joints absorb covering deformations in a proportion exceeding their share by width, thereby indirectly reducing the stresses in the covering. Thus, an increased width improves the deformability of covering, this is why recent building codes recommend wider joints.
- Dilatation of large surfaces has secondary importance. The role of these dilatations becomes more significant only after the commencement of detachment. In this state the behaviour of the detached covering will be similar to a covering originally independent of the structure. The rules of dilatation must be developed accordingly.

Comparison of deformabilities of covering types points to the extreme dependence of deformability limits on construction and on materials (Fig. 7). No general ultimate deformation values for coverings can therefore be specified. At the same time, empirically founded theoretical relationships offer a possibility to forecast the behaviour of a covering in knowledge of its sizes and material properties.

4. SUMMARY

The deformability of adjacent, non-load-bearing structures is relatively small as shown in these tests. To prevent these types of damages does not mean that we have to design stiffer structures. The solution of these problems requires more complex structural design: the selection of compatible load-bearing and non load-bearing structures, the design of the most suitable joints between them, the most advantageous technological specifications, etc.

DINAMIC TYPE	COVERING TYPE	MORTAR	EDGE MOTION 10^{-3} mm	ε_H ‰	MODE OF FAILURE DESCRIPTION	MODE OF FAILURE CONFIGURATION
A 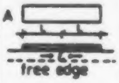 free edge	stoneware tile.	mortar 15 mm	60-70	0.3-0.4	shear, concrete-mortar detachment	
	wall tile		70-80	0.4-0.6	shear, covering-mortar detachment	
B 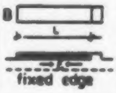 fixed edge	stoneware tile	adhesive 2-3 mm	70-80	0.6-0.8	shear, cover-adhesive detachment	
	wall tile		65-75	0.9-1.1	shear, concr.-adhesive detachment	
C 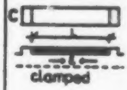 clamped	stoneware tile	mortar 15 mm	—	0.6-0.7	raising blowing_ up	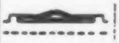
	wall tile		—	0.9-1.2	raising blowing up	
	stoneware tile.	adhesive 2-3 mm	—	> 1.0	1. joint material crushing 2. tile break	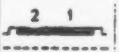
	wall tile		—	> 1.0		

Table 1: Ultimate deformations of coverings

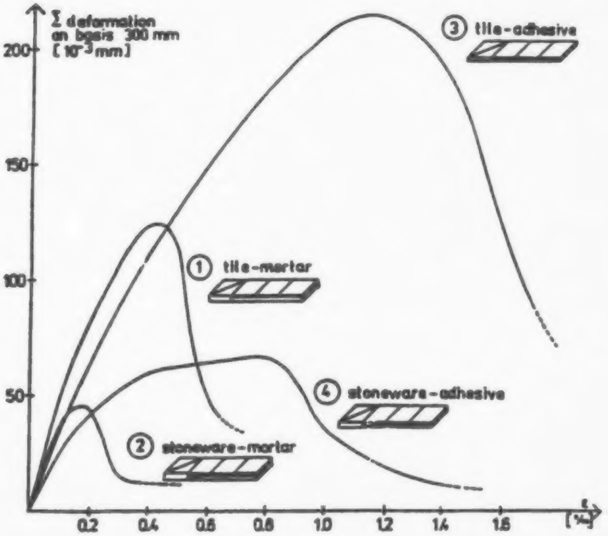

Figure 7: Behaviour of different covering types

5. REFERENCES

Gy. Deak, É. Nemestothy, Gy. Visnovitz: Limitation of the deformation of structures at the serviceability limit state. (1980 É.T.I. Research report in Hungarian and Russian language.)

É. Nemestothy: Experimental analysis of the deformability of partition walls. (1982 T.U.B. Dissertation in Hungarian.)

Gy. Visnovitz: Experimental analysis of the deformability of brittle coverings. (1984 T.U.B. Dissertation in Hungarian.)

FOUNDATION PROBLEMS AND THEIR EFFECT ON THE SERVICEABILITY OF BUILDINGS

J.R. Schuring, D. Raghu, and E.G. Dauenheimer

Department of Civil and Environmental Engineering
New Jersey Institute of Technology
Newark, New Jersey, U.S.A.

ABSTRACT: This paper examines the effects of differential foundation movements on the structural serviceability of buildings. Existing criteria for building settlement from various sources are reviewed. Some common situations of structural distress in buildings are analyzed including loss of beam bearing, wall tilting, wall buckling, and development of secondary stresses. The analyses indicate the tolerance of buildings for structural damage resulting from foundation movements. Several case studies involving buildings with foundation problems are described.

1. INTRODUCTION

Unsatisfactory foundation performance is a frequent cause of unserviceability in buildings. When designing the above-ground structure, the professional selects from a variety of components and systems whose behavior is well known. In contrast, the designer has no choice in the geologic materials which underlie the building. Failure to thoroughly analyze the natural formations and man-placed fill which occur at the site can lead to foundation problems and distress to the building structure.

Most foundation problems in buildings fall into one of the following three categories:

a. Differential movements resulting from settlement or heave of the foundations
b. Differential movements resulting from lateral thrust of soil and/or water on the foundations.
c. Water infiltration into occupied spaces below grade.

Whether or not a foundation problem will render the building unserviceable is determined by the severity of damage to the structure. Minor damage such as cosmetic cracking of the walls and ceilings is usually classified as "architectural damage." This level of damage generally does not affect the serviceability of the building unless, for example, there happens to be a valuable fresco painted on the affected wall. Nevertheless, buildings should be designed to avoid even architectural damage for obvious esthetic reasons.

"Functional damage" occurs when the use of the building is seriously impaired by the foundation problem. A classic example is sensitive machinery which fails to operate as a result of differential building movements. Occupant discomfort resulting from uneven floors and ill-fitting doors could also be considered to be a functional failure.

In extreme cases, foundation problems may cause "structural damage" to the building making it unsafe. Sometimes there is considerable economic pressure to continue occupancy and use of structures with foundation problems. The question which then must be answered is: How much differential movement can the structure tolerate?

In response to this difficult question, the focus of the paper will be foundation problems which cause a building to become structurally unserviceable. The paper will begin with a review of existing criteria for evaluating differentially settled structures. Some common situations of structural distress in buildings will then be analyzed using static methods. Several case studies will be described to illustrate the behavior of various construction materials subjected to foundation movements. It should be noted that for the purposes of this paper, average workmanship and material quality were assumed, and structural distress was the result of foundation movements only.

2. EXISTING CRITERIA FOR DIFFERENTIAL MOVEMENT OF BUILDINGS

A number of investigators have posed criteria for the tolerable differential movement of various structures. A majority of these criteria have been developed empirically based on past performance data. Figure 1 provides a definition of the most common parameters used to measure differential movements in buildings. The terminology used in this paper conforms with the standard

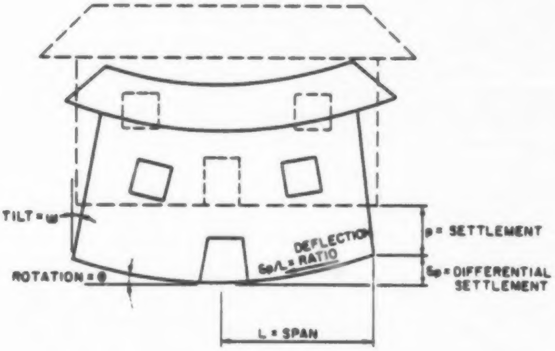

FIGURE 1: DEFINITIONS OF DIFFERENTIAL MOVEMENT

definitions adopted at the British Geotechnical Society Conference on the Settlement of Structures (1974). It is noted that the term "deflection ratio," which is also referred to as "angular distortion" and "settlement slope," will be used consistently.

The study by Skempton and MacDonald (1956) is generally regarded to be the first comprehensive study on the subject of building settlements and continues to be a major reference source. These investigators collected settlement data from 98 buildings, 40 of which had exhibited settlement damage. Based on the results of their study, they estimated damage limits of settlement and deflection ratio for traditional frame buildings. They also recommended values for use in design. These criteria are summarized in Table 1.

Table 1

Settlement Damage Limits and Design Recommendations for Frame Buildings *

Criterion	Isolated Foundations	Rafts
Deflection Ratio (Angular Distortion)	1/300	
Greatest Differential Settlement	Clays: 1 3/4 (1½) in. Sands: 1¼ (1) in.	
Maximum Settlement	Clays: 3 (2½) in. Sands: 2 (1½) in.	3-5 (2½-4) in. 2-3 (1½-2½) in.

Note: Values recommended for design given in parentheses. 1 in.-25.4mm

* From Skempton and Mac Donald (1956)

Polshin and Tokar (1957) published values of maximum allowable non-uniform settlement of structures based on field observations at 100 sites. This information was included in the USSR Code of 1955. Their study also correlated the threshold of visible cracking with the critical tensile strain in the material. They estimated these values at 0.05-0.1% and 0.03-0.05% for brick and reinforced concrete, respectively.

A chart of limiting deflection ratios compiled by Bjerrum (1963) is shown in Figure 2. It provides a graduated scale of damage limits ranging from difficulties with sensitive machinery (1/750) to structural damage for general buildings (1/150).

Feld (1965) reviewed a number of case histories and cited the difficulty of establishing a general set of criteria for all structures. He emphasized the ability of structures to adjust to localized overstresses caused by differential settlement, especially when the rate of movement was slow.

Grant, et al., (1974) investigated the effect of settlement on 95 buildings with the purpose of updating and examining the earlier classic study by Skempton and MacDonald (1956). They basically affirmed the 1/300 deflection ratio beyond which structures will probably suffer damage. However, they disputed the popular assertion that settlement rate has a significant effect on the degree of damage.

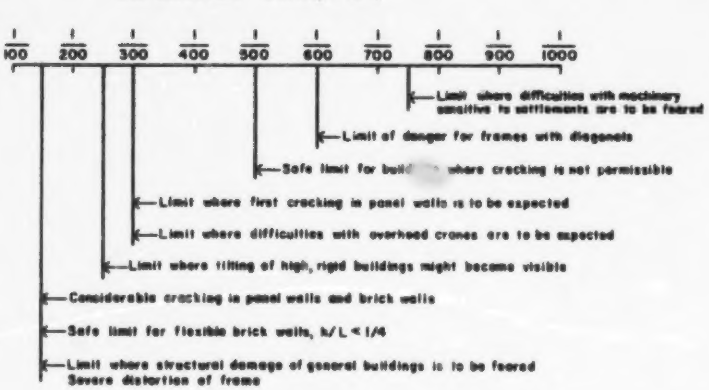

FIGURE 2: LIMITING DEFLECTION RATIOS FOR BUILDINGS (BJERRUM, 1963)

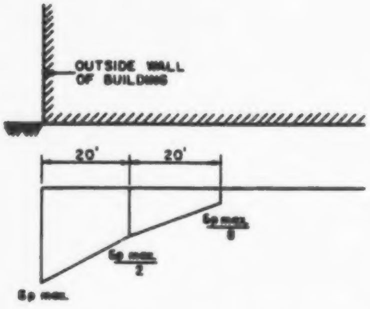

STRUCTURE	δp max.
BRICK	2 inches
CONCRETE OR CINDER BLOCK	3/4 inches
MONUMENTAL STONE	1 inch
STEEL OR CONCRETE FRAME	2 inches

FIGURE 3: MAXIMUM TOLERABLE SETTLEMENT TO PREVENT ARCHITECTURAL DAMAGE (D'APPOLONIA, 1971)

They stated that rate is only important in extreme situations, i.e. very slow or very fast.

Some countries have incorporated allowable settlement criteria into their building codes. One such example from Czechoslovakia is shown in Table 2 (Myslivec and Kysela, 1978). These criteria indicate the significance of structure type, rigidity, and rate of movement in determining tolerable movement.

Foundation problems may also be caused by excavation or other adjacent construction activities. D'Appolonia (1971) provides an excellent review of this subject and gives differential settlement criteria for buildings which become damaged as a result of adjacent construction. The criteria are shown in Figure 3, and represent the settlement limit beyond which architectural damage may be anticipated for various construction types.

Table 2

Ultimate values of the settlement of foundations (according to CSN 73 1001)*

Type of building	The foundation soil consolidates			
	very quickly (for example, sands)		slowly (for example, clays)	
	difference of settlement	total settlement	difference of settlement	total settlement
	δp/L	p[cm]	δp/L	p[cm]
1. Buildings:	0.0005	6	0.0007	8
bricks and blocks	0.0007	6	0.001	8
bricks, block reinforced with concrete strips	0.001	8	0.0013	10
reinforced concrete skeleton	0.0007	6	0.001	8
2. Structures:				
statically determinate	0.003	10	0.003	10
statically indeterminate steel	0.0015	6	0.002	8
statically indeterminate reinforced concrete	0.001	4	0.0015	6
rigid and massive				
massive foundation to a height of 20 m	0.005	20	0.005	20
higher than 20 m (chimneys)	0.002	10	0.002	10
3. Crane tracks with bridge crane longitudinally and laterally	0.0015	--	0.0015	--

*from Myslivec and Kysela (1978)

3. ANALYSIS OF COMMON DISTRESS SITUATIONS

Although the criteria presented in the previous section indicate some differences of opinion among the various investigators, there is one point on which they were essentially unanimous: No criteria is absolute and each situation must be analyzed individually. It is also noted that most of the criteria address either architectural or functional damage. Buildings can generally tolerate greater differential movements before they pose a structural hazard.

In the authors' experience, the most common distress situations which may affect the structural integrity of a building are:

a. loss of beam bearing
b. tilting and/or buckling of walls
c. development of secondary stresses in members

Although the analysis of any distress situation will depend on the particular materials involved, it is useful to examine these situations generically. In the remainder of this section the above distress situations will be analyzed with the goal of understanding the ultimate behavior of building structures subjected to differential movements. The analyses will be restricted to two-dimensional movements, even though actual building movements are three-dimensional.

3.1 Distress Situation: Loss of Beam Bearing

The first distress situation to be analyzed is the loss of bearing of a simple beam caused by differential movement. Figure 4 depicts the situation schematically and defines the pertinent variables. In this analysis it will be assumed that only vertical movements of the supports occur and the beam behaves as if it is pinned at one end. The analysis would also be applicable to tilting supports as long as the supports remain parallel.

The table in Figure 4 summarizes the results for several assumed values of span, L, and bearing distance, b. The differential settlement, δp, required for the beam to slip off the support ranges from 1 to 2 meters (3 to 6 ft.). Since failure would probably occur before the beam actually slips due to local overstress and crushing, a smaller value of differential settlement, δp_{30}, was also calculated. This corresponds to the differential movement when the bearing distance at the left support has diminished to 30% of the full value.

The differential settlements computed above for loss of beam bearing are surprisingly large. It may be concluded that a structural failure arising from purely vertical or parallel differential movements is highly unlikely. It is interesting to note that a deflection ratio of 1/150 indicated by Bjerrum as the threshold for structural damage corresponds to a beam bearing of over 99%.

The preceeding analysis does suggest a related and potentially dangerous distress situation: horizontal spreading of the beam supports. In contrast to the rather large vertical movements required for loss of beam bearing, small horizontal movements on the order of the bearing distance of one support can cause failure. Buildings with severe differential settlements must be inspected carefully for this mode of movement.

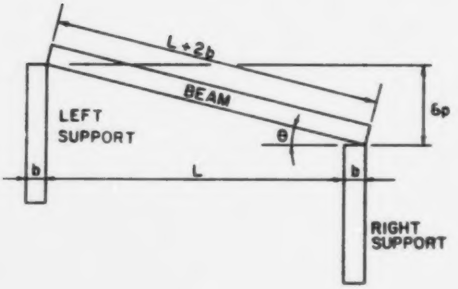

SUMMARY OF ANALYSIS					
L m (FT)	b m (FT)	δp m (FT)	$\delta p/L$	θ DEG	δp_{30} m (FT)
4.6 (15)	0.1 (0.33)	0.94 (3.1)	0.21	12.0	0.79 (2.6)
4.6 (15)	0.15 (0.5)	1.2 (3.8)	0.26	14.8	0.98 (3.2)
7.6 (25)	0.15 (0.5)	1.5 (5.0)	0.20	11.5	1.3 (4.2)
10.7 (35)	0.15 (0.5)	1.8 (5.9)	0.17	9.7	1.5 (4.9)

NOTE:

δp_{30} IS THE DIFFERENTIAL SETTLEMENT CORRESPONDING TO 30% BEARING AT LEFT SUPPORT.

FIGURE 4: ANALYSIS OF BEAM BEARING LOSS

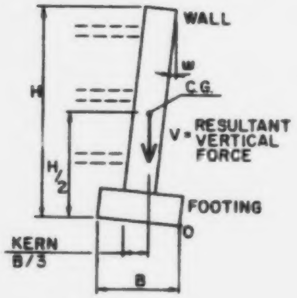

SUMMARY OF ANALYSIS					
H	B	V THROUGH EDGE OF KERN		V THROUGH POINT O	
m (FT)	m (FT)	ω DEG	TILT %	ω DEG	TILT %
3 (10)	0.5 (1.5)	2.9	5	8.5	15
6.1 (20)	0.6 (2)	1.9	3.3	5.7	10
9.1 (30)	0.9 (3)	1.9	3.3	5.7	10
12.2 (40)	1.2 (4)	1.9	3.3	5.7	10

FIGURE 5: ANALYSIS OF TILTED WALL

3.2 Distress Situation: Tilting and Buckling Walls

The two main considerations in the analysis of tilted and buckled walls are overturning stability and secondary stress. This section will address the issue of wall stability. The effect of secondary stresses will be treated in the next section.

A schematic diagram for a tilted wall which rests on a spread footing is shown in Figure 5. The center of gravity of the wall is located at mid-height and the wall is assumed to be free-standing. This is an idealized situation since building walls are connected to the floors, roof and other walls which afford some degree of support. The assumed condition is useful, however, in defining limits of tilt which would be cause for structural concern, i.e. the tilt at which the wall needs to be supported.

A criterion used in standard design practice of eccentrically loaded footings requires that the vertical resultant force remains within the kern, since in this condition, the contact pressures remain entirely compressive. Therefore, the wall was analyzed for overturning stability by determining the amount of tilt when the center of gravity of the wall would begin to violate the kern criterion. For the subject wall, the kern may be defined as the middle third of the footing, and the corresponding wall tilts for various wall geometries are summarized in the table in Figure 5.

The other stability condition of interest is the one referred to in solid physics as "unstable equilibrium." This occurs when the center of gravity of the wall passes through the outside edge of the footing. The calculated values of tilt for unstable equilibrium are summarized in Figure 5 for the various wall geometries.

The results of the analysis suggest that a very small degree of tilt (3 to 5%) will violate kern criteria of the wall system. This probably represents the amount of tilt where concern for the structural integrity of the building should commence. In this condition, the contact pressure at the outer edge of the footing is twice the uniformly distributed condition.

The tilt corresponding to unstable equilibrium is three times greater (10 - 15%) and is an absolute upper limit for overturning stability, since beyond this point the wall is supported solely by the members which frame into it. Analysis of this condition yields the disturbing result that the contact pressure at the outer edge of the footing approaches infinity.

It is important to note that failure may occur long before overturning stability becomes critical due to secondary stresses induced in the structure. The issue of secondary stresses will be addressed in the next section.

Wall buckling is often encountered in basement walls which have been subjected to lateral thrust by soil and/or water, especially those constructed of unreinforced masonry. The schematic for a buckled wall is shown in Figure 6. The wall is assumed to buckle symmetrically at mid-height, which is reasonable in the authors' experiences.

The results of the buckled wall analysis are shown in Figure 6. Stability of the wall was checked using the kern criterion in a manner similar to the tilted wall. Two locations for the resultant force were assumed: 1) at the

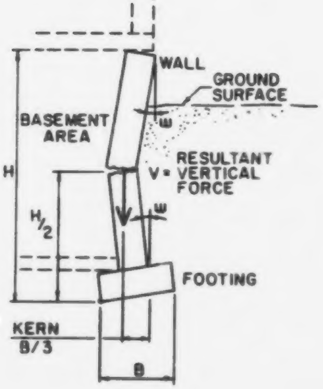

SUMMARY OF ANALYSIS					
H	B	V ASSUMED AT WALL CENTER		V ASSUMED AT WIDTH/3*	
m (FT)	m (FT)	ω DEG	TILT %	ω DEG	TILT %
3.0 (10)	0.5 (1.5)	2.9	5	4.8	8.4
3.0 (10)	0.6 (2)	3.8	6.7	5.7	10.1
4.6 (15)	0.6 (2)	2.5	4.4	3.8	6.7
4.6 (15)	0.8 (2.5)	3.2	5.6	4.5	7.8

* WALL WIDTH ASSUMED TO BE 0.3m (1 ft)

FIGURE 6: ANALYSIS OF BUCKLED WALL

vertical centerline, and 2) at a point one-third from the outside face of the wall. This latter location was chosen in recognition of the shift in the centroid of compressive stress as the wall bends inward.

In this analysis the wall should be assumed unsafe when the resultant reaches the structural kern since, unlike the tilted wall, there are no intermediate framing members which provide support. There is an additional hazard for buckled walls located below grade: the potential for sudden heavy rainfalls which saturate the soil backfill causing a sudden increase in lateral thrust. In view of this, buckled walls should conservatively be shored or repaired at the first sign of distress.

3.3 Distress Situation: Secondary Stresses

When a building undergoes differential movements, the stress regime assumed by the designer is no longer valid. As the geometry of the building changes and the members deform, new stresses are created known as "secondary stresses." The development of secondary stresses are critical for two reasons: 1) They may exceed the original primary design stresses, and; 2) They may occur in members which were not designed to resist that particular kind of stress.

A classic example of the effect of secondary stresses on horizontal members is a multi-span continuous beam with supports that settle unequally. Analysis of this condition is straightforward using standard structural methods, e.g. moment distribution, slope deflection. Such analyses illustrate the advantages of using statically determinate structures where substantial differential settlement is anticipated.

Secondary stresses in vertical load bearing members are usually the result of load eccentricities introduced by tilting or bending. Analysis of these members involves consideration of moment magnification also known as the "P - Δ" effect. Provisions exist in current U.S. design codes for making adjustments to the basic allowable stress to consider the effects of slenderness and load eccentricity. Implicit in this approach is the assumption of lateral elastic buckling.

Figure 7 demonstrates the influence of secondary effects on the ability of a wall to carry vertical forces. The table summarizes the percent of the original concentric load capacity of the wall for a practical range of slenderness values (H/t) and end eccentricities (e_1/e_2). For large e/t ratios the carrying capacity of the wall is reduced dramatically to only 13% of its concentric load capacity.

The results in Figure 7 are based on the assumption that elastic buckling governs. However, for wall systems with negligible tensile strength and low compressive strength, e.g. unreinforced masonry, local inelastic distress may cause failure by crushing and cracking. This failure mode may occur with little warning, and further confirms the seriousness of buckling walls discussed from a stability perspective in the previous section.

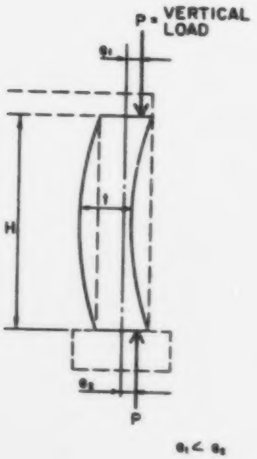

SUMMARY OF ANALYSIS

H/t	e_1/e_2	PERCENT OF ORIGINAL CONCENTRIC LOAD		
		$e/t = 0.0$	$e/t = 0.16$	$e/t = 0.33$
5	0.0	100	72	47
5	1.0	100	66	33
10	0.0	93	67	44
10	1.0	93	61	31
20	0.0	67	44	22
20	1.0	40	26	13
30	0.0	40	29	19

FIGURE 7: ANALYSIS OF SECONDARY EFFECTS IN WALLS

4. CASE STUDIES OF BUILDINGS WITH FOUNDATION PROBLEMS

Several case studies will now be described to show the effect that foundation problems can have on building serviceability. The cases comprise a variety of construction types and materials.

4.1 Case Study: Failing Basement Walls in Condominium Complex

This case study involves a condominium complex containing 9 buildings in Northern New Jersey. The three story structures consisted of wood-frame construction with brick veneer. The buildings were founded on basements which extended below grade. The typical composition of the basement walls was 305 mm (12 inch) unreinforced hollow concrete blocks supported by 305 x 610 mm (1 x 2 ft) wide reinforced concrete footings.

Approximately one year after completion of construction and occupancy of the complex, the residents reported cracks in the brick veneer and water infiltration into the basements. An engineering inspection revealed that some of the foundation walls in the buildings were bulging and/or tilting inward. Vertical profiles of some of the distressed walls are shown in Figure 8.

Analysis of the buckled walls indicated that the vertical resultant force at some locations was already outside the structural kern of the footing. This created a dangerous condition and immediate corrective action was recommended. The probable reason why collapse had not yet occurred was the lateral stiffness afforded by the corners and projections in the wall. Also, some temporary wood shoring had been installed to support the wall at some locations by the contractor during construction and had never been removed.

As shown in Figure 8b, some of the basement walls tilted rather than buckled. These walls were non-bearing and thus were not supported at the top like the bearing walls.

The distress was caused by the thrust from the soil backfill which had exceeded the structural capacity of the wall. A major contributing factor to the wall failures was their height. Some had unbalanced backfills that ranged up to 3.4 m (11 ft), which is excessive for unreinforced masonry. The prevailing building code limited the height of unbalanced fill for unreinforced walls to 2.1 m (7 ft). Beyond this height, the code required that the masonry be engineered and reinforced. This obvious code violation of wall height was the result of unauthorized deviations from the design drawings due to the encountered field conditions. An old industrial complex had previously occupied the site and the contractor extended his foundations deeper at many locations than had been indicated on the design drawings. An additional factor was an apparent shortage of fill material at the site. It is also possible that some of the observed distress to the basement walls was the result of improper backfilling procedures.

4.2 Case Study: Differentially Settled Wood Frame Residences

Wood-frame residential structures represent a substantial percentage of the total construction in the United States. Due to their lower unit cost relative to commercial and industrial facilities, soil investigations are typically not undertaken. As a result foundation problems are not uncommon, especially in developed areas where it becomes economically attractive to develop land of marginal quality.

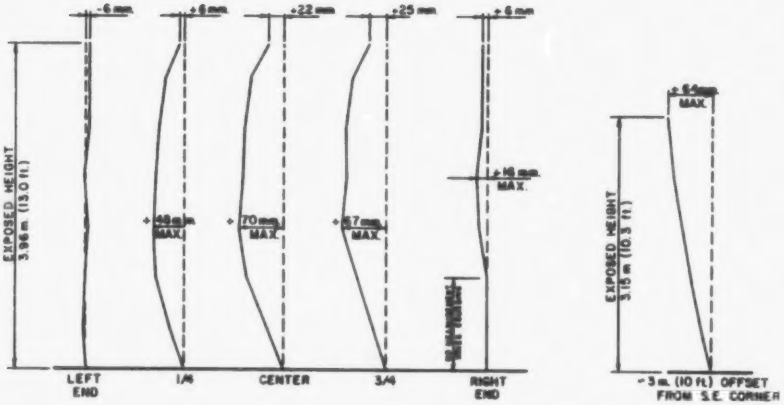

BUCKLED WALL
(a)

TILTED WALL
(b.)

FIGURE 8: VERTICAL PROFILES FOR BASEMENT WALLS - CONDOMINIUM COMPLEX

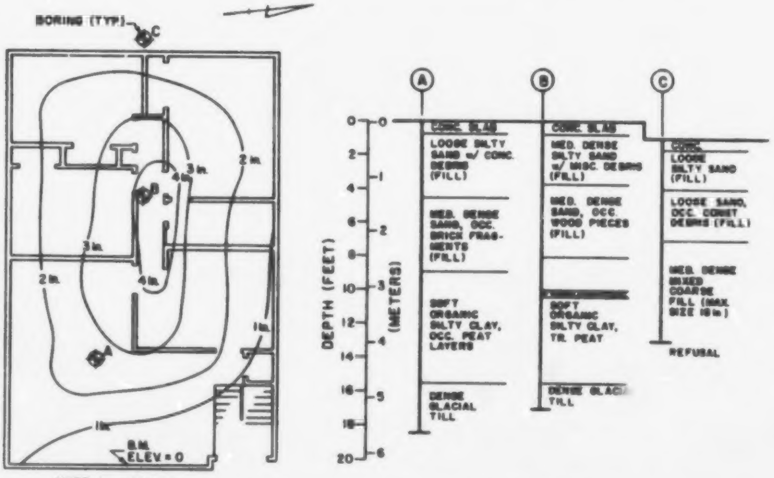
BORING (TYP.)
C
B
A
4 in.
3 in.
2 in.
1 in.
B.M.
ELEV. = 0
DEPTH (FEET)
(METERS)
0
2
4
6
8
10
12
14
16
18
20
0
1
2
3
4
5
6
CONC. SLAB
LOOSE SILTY SAND w/ CONC. DEBRIS (FILL)
MED. DENSE SAND, OCC. BRICK FRAGMENTS (FILL)
SOFT ORGANIC SILTY CLAY, OCC. PEAT LAYERS
DENSE GLACIAL TILL
MED. DENSE SILTY SAND w/ MISC. DEBRIS (FILL)
MED. DENSE SAND, OCC. WOOD PIECES (FILL)
SOFT ORGANIC SILTY CLAY, TR. PEAT
DENSE GLACIAL TILL
LOOSE SILTY SAND (FILL)
LOOSE SAND, OCC. CONST DEBRIS (FILL)
MED. DENSE MIXED COARSE FILL (MAX. SIZE 18 in.)
REFUSAL

NOTE: 1 in. = 25.4 mm

SETTLEMENT CONTOURS
(2nd FLOOR PLAN)

BORING LOGS

FIGURE 9: SETTLED & SUBSURFACE DATA WOOD-FRAMED RESIDENCE #1

This case study will focus on two separate wood-frame residences which sustained large differential settlements. They are both located in Northern New Jersey.

The first case involves a residence built adjacent to a tidal marsh. When the residence was approximately eight years old, it was purchased by a new owner who reported that the structure appeared to be in good condition as verified by a home inspection consultant. Such inspections have become standard practice during real estate transactions in many areas of the United States. It is noted that the home's interior had been completely redecorated prior to placing it on the market.

After approximately one year, the new owners began to notice unevenness in the floors, cracks in the walls, and ill-fitting doors. Subsequently they engaged a consultant to investigate the cause of the problems.

An elevation survey made of the floors and perimeter foundation walls 18 months after the sale revealed that over 200 mm (4 in) of differential settlement was present in the building. This data is presented in the form of elevation contours in Figure 9. The level data showed that the greatest amount of settlement had occured along the central bearing wall and internal lolly columns. The perimeter wall footings had settled less but had still caused an overall tilt of the structure towards the southwest.

Soil borings were subsequently performed in and around the residence and the logs are also shown in Figure 9. The borings revealed that approximately 7 feet of soft organic silty clay and peat were present beneath the interior foundations of the house. The borings also showed that the perimeter foundations were founded on a coarse, non-engineered rubble fill, which explains why they had settled less than the interior foundations.

Consultation with old topographic maps confirmed that the house was just within the limit of the tidal marsh. The records at the Municipal Building Department indicated that the contractor had been aware of the soft soils and had agreed to remove and replace them with fill. Unfortunately, the fill was not extended underneath the interior foundations and was of generally poor quality.

An additional aspect of this case is worth noting. The reason why the settlement problem appeared suddenly after the new owner occupied the 8 year-old residence was that the house had been pressure grouted or "slab-jacked" level prior to sale. The interior redecoration had concealed the distress from earlier settlements which had occurred. The "slab-jacking" procedure provided only temporary relief, however, since the high surface pressure caused by the process only initiated new cycles of primary and secondary consolidation of the underlying organic soil.

In spite of a deflection ratio (0.03 or 1/33) which far exceeds architectural damage criteria, the residence was determined to be safe from a structural point of view. No detectable loss of beam bearing was observed, since differential movements had been essentially vertical. The greatest concern was the effect that the settlement had on the utilities in the residence, especially the natural gas service. These were checked by a mechanical contractor and flexible connectors were installed at potential strain points.

A second wood frame residence was investigated which had experienced over 250 mm (10 in.) of differential settlement over its 15 year life. The two-story home had been built on a vacant lot in a neighborhood of much older homes. Prior to construction, the lot had been a depository for fill. As a result, the true nature of the soil conditions was apparently obscured and forgotten.

Soil borings were conducted to determine the cause of the large differential settlement, and they revealed the residence was founded on miscellaneous fill underlain by a layer of peat which varied in thickness from 2 to 5 feet. The subsurface conditions are shown in section on Figure 10.

Figure 10 also depicts the distorted condition of the wood structural frame which had a maximum deflection ratio of 0.04 or 1/25. It is interesting to note that a gap was observed between the bottom plate of the central bearing partition and the top of the central wall footing. Apparently the building had acted like a structural diaphram and "bridged" the interior loads to the front and rear of the residence. This demonstrates the ability of wood structures to redistribute loads and is proof of their superior redundancy and resiliency. Even in this distorted state, the residence still did not pose an immediate structural hazard, but modification to the utility services was again necessary. Occupant discomfort was acute, however, and the residence was eventually vacated and is awaiting repair.

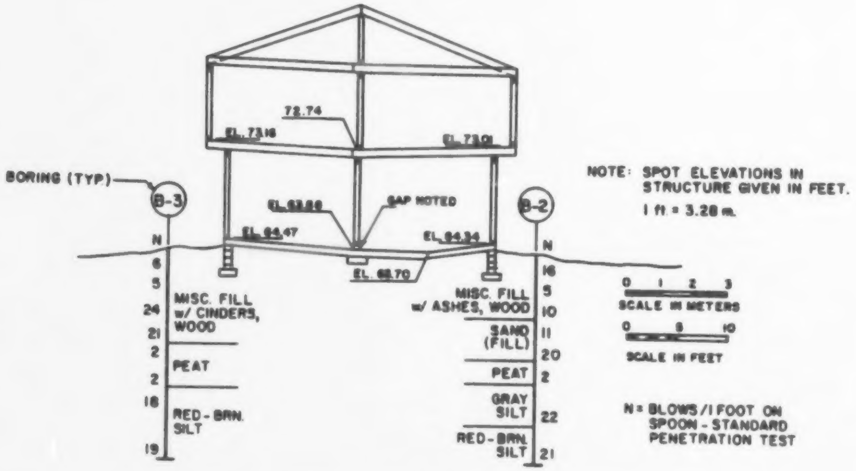

FIGURE 10: SECTION OF WOOD FRAME RESIDENCE #2

4.3 Case Study: Secondary Stresses In Masonry Structures

Two examples will now be described involving masonry structures which were subjected to secondary stresses resulting from differential movements. It will be shown that one of the structures was able to accommodate the movements, while the other responded with a devastating effect.

The first example involves a five-story brick bearing wall structure which had experienced significant differential settlement during its 60 year life. A subsurface investigation confirmed that the cause of the severe differential movements was the presence of a layer of soft organic soil beneath portions of the building. Work had been performed on the structure through the years to repair architectural damage and to provide structural reinforcement.

Considering the amount of settlement which had been sustained by the building, the structural frame of the building had accommodated the movements reasonably well. This was due in part to the composition of construction, i.e. wood joists on brick bearing walls, which is relatively flexible. In addition, the building consisted of five towers connected by a common public corridor which allowed each tower to settle independently.

Evidence of the ability of this building to accept high levels of secondary stress is shown in Figure 11. This is a line drawing of a lintel over a doorway located near the juncture of two of the towers. A differential settlement of 50 mm (2 in) had occurred in a lateral distance of 0.79 m (2.6 ft), which corresponds to a local deflection ratio of 0.063 or 1/16. In spite of the

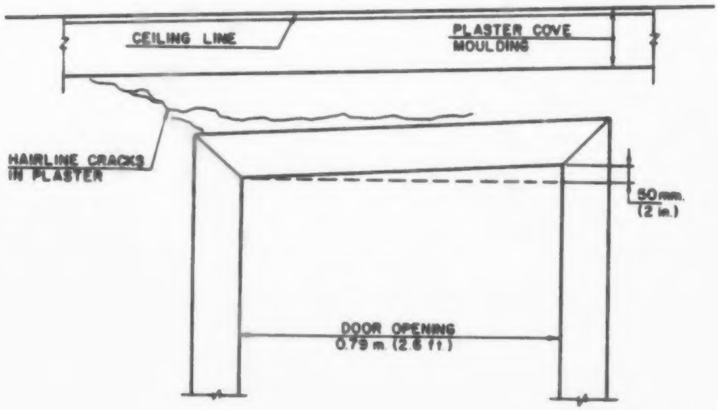

FIGURE 11: SETTLED DOOR LINTEL IN BRICK BUILDING

obvious high stress levels, cracking of the plaster coated brick wall was minimal. The only possible explanation for the plastic behavior of an otherwise brittle materials is that the movement occurred very slowly and allowed the masonry to creep rather than fracture. The relative flexibility of brick masonry and its ability to sustain larger differential movements than many other construction materials is reflected in the various criteria presented earlier in the paper.

The second example of the effect of secondary stresses on building structures is taken from Tschebotarioff (1973). He describes the conditions surrounding the catastrophic collapse of a bell tower located in the city of Venice. (Note: It seems that Italy has their difficulties with bell towers, another example being the Leaning (bell) Tower of Pisa which probably represents the most famous foundation failure in history.)

The Venice tower was constructed of stone masonry and measured 330 feet high. The foundation was supported on timber piles and like the Tower of Pisa, it began to lean after completion but at a much slower rate. By the year 1902 it had reached 0.8% out of plumb, at which time it suddenly collapsed. The collapse is attributed to the secondary stresses present in the structure due to the tilt and also to some structural modifications performed on the tower which weakened it. This rather brittle behavior of the stone masonry tower provides a sharp contrast with the very flexible behavior of the brick structure in the previous example.

4.4 Case Study: Collapse of a Brick Building During Foundation Renovation Work

When renovating the foundations of a building, there is a great potential for differential movement. For example, when buildings are underpinned, i.e. the foundations are extended to a lower level, it is almost impossible to avoid some damage to the structure. The question during underpinning is usually not whether movements will occur, but whether the movements will be tolerable.

A tragic example of the effect that foundation renovation can have on buildings occurred recently in New York City when a five story brick bearing wall structure collapsed killing one person. While the cause of the collapse is still under investigation, it appears that a contractor had excavated a trench along one side of the building which measured approximately 3 feet wide by 7 feet deep exposing the foundation wall. The construction workers reported that the brick wall just above basement level suddenly started shaking and then buckled outward. This caused the wall to slide down leaving the floor joists unsupported.

Based on these reports, it appears that the failure was precipitated by the loss of lateral earth support along the basement wall. This incident emphasizes the extreme care which must be exercised when exposing and renovating foundations.

5.0 CONCLUSIONS

This paper has examined the effects of differential foundation movements on the structural serviceability of buildings. A review of existing settlement criteria revealed that criteria usually address either architectual or functional damage. Buildings can often tolerate greater differential movements before structural damage renders them unsafe.

In order to investigate the ultimate behavior of buildings subjected to differential movements, several common situations of structural distress were analyzed. It was shown that the risk of bearing loss by a simple beam is minimal when differential movements of the supports are purely vertical. Horizontal spreading of the supports is much more serious and buildings should be checked carefully for this form of distress.

A stability analysis of tilted walls indicated that minimal tilt (3 to 5%) will begin to violate the kern criterion. The stability of buckling walls was also analyzed using the kern criterion, and it was concluded that buckling walls below grade are particularly hazardous due to the potential for sudden increases in lateral thrust resulting from saturated backfill.

The development of secondary stresses in buildings subjected to differential movement were discussed. Analysis of a wall system with eccentric loading demonstrated that substantial reductions in load capacity were experienced compared with the concentric load capacity. Structural damage resulting from secondary effects probably represents the greatest danger to buildings with foundation problems.

The case studies and the reviewed criteria illustrated the response of various structural systems and materials to differential movements. Wood frame structures proved to be highly tolerant of large movements on account of their high degree of redundancy and resiliency. Large unit unreinforced masonry structures (block and stone) were found to have a very low tolerance for movement, and were very susceptible to damage by secondary stresses. Brick masonry was shown to be more flexibile than other forms of masonry, especially when the rate of movement was very slow. The potential for differential movement and structural damage during foundation renovation was emphasized.

ACKNOWLEDGEMENTS

The assistance of Mr. John Kwok in this project is gratefully acknowledged. Special thanks are extended to Mrs. Marsha Terwilleger and Mr. Leonard Mitchell for the preparation of this manuscript.

REFERENCES

Bjerrum, L. 1963. Discussion in Section VI, Proceedings European Conference on Soil Mechanics and Foundation Engineering, Weisbaden, Vol. 2, Pg. 135.

British Geotechnical Society 1974. Settlement of Structures, John Wiley, New York.

D'Appolonia, D.J. 1971. "Effects of Foundation Construction on Nearby Structures," Proceedings 4th Panamerican Conference on Soil Mechanics, Puerto Rico, Vol. 1, pp. 189-236.

Feld, J. 1965. "Tolerance of Structures to Settlement," ASCE Journal of the Soil Mechanics and Foundation Division, Vol. 91, SM3, May 1965, pp. 63-77.

Grant, R., Christian, J. and Vanmarcke, E. 1974. "Differential Settlement of Buildings," ASCE Journal of the Geotechnical Engineering Division, Vol. 100, GT9, pp. 973-991.

Myslivec, A. and Kysela, E. 1978. Bearing Capacity of Building Foundations, Elsevier, New York, Pg. 154.

Polshin, D. and Tokar, R. 1957. "Maximum Allowable Non-Uniform Settlement of Structures," 4th International Conference on Soil Mechanics and Foundation Engineering, Vol. 1, pp. 402-405.

Skempton, A. and Mac Donald, D. 1956. "The Allowable Settlement of Buildings," Proceedings, Institute of Civil Engineers, Vol. 5, Part III, pp. 727-784.

Tschebotarioff, G.P. 1973. Foundations, Retaining and Earth Structures, 2nd Edition, McGraw-Hill, New York, Pg. 159.

A SIMPLE DESIGN AID FOR PREDICTING SHRINKAGE AND CREEP STRAINS IN BUILDINGS

P. Arumugasaamy
Dept. of Ocean Engineering
Florida Atlantic University
Boca Raton, Florida 33431

and R. N. Swamy
Dept. of Mechanical Engineering
University of Sheffield
England S 1 3JD

Synopsis: This paper presents a simple design aid for predicting long-term movements up to 25 years in reinforced concrete columns made of normal and lightweight aggregate concrete. The method is based on the principle of super position using a creep factor chart, which takes into account varying sizes of members, age at loading, exposure conditions and the percentage of reinforcement, and it requires only a knowledge of the concrete strength and the loading history of the member. The method is developed from the study of in-situ movements in two reinforced concrete structures subjected to increment loading.

The shrinkage strains in columns are predicted using a shrinkage chart which takes into account all the variables considered for creep and the amount of cement content per cubic metre of concrete. This requires only a knowledge of elastic modulus of concrete at 28 days.

The predicted load-induced (i.e. elastic + creep) and basic (i.e. elastic + creep + shrinkage) strains show excellent agreement with measured strains in the two structures with an acceptable error coefficient. The method is shown to give good agreement with the measured strains on normal weight and lightweight concrete columns from the Portland Cement Association.

Keywords: Reinforced concrete; Lightweight concrete; creep factor; shrinkage strains; Prediction; columns; Buildings; Elastic Modulus Design Charts;

Introduction:

The problem of axial creep and shrinkage of concrete has place increasing demands on structural engineers to take account of such long-term deformations in the design of concrete building structures. The problem becomes even more severe when the temperature effects in the exterior columns and the differential creep and shrinkage shortening are combined.

It is possible to design a structure such that the above conditions are either minimized or controlled within acceptable limits. Engineers must then attempt to make a realistic prediction of the long-term movements in structural elements. Therefore, it has become necessary to predict accurately the movements in individual members at the design stage. The practising engineers prefer a relatively simple aid of prediction of creep and shrinkage of concrete to mathematically lengthy and complex problems, which can be easily used in the design office.

In this paper, a relatively simple method is presented to predict long-term movements occurring in service up to 50 years. The method is related to two reinforced concrete structures built using ready-mixed and site-produced concrete. Further evidence of the validity of the method is derived from reinforced concrete columns reported from Portland Cement Association.

Method of Creep Prediction:

In many structures, the columns are loaded in as many increments as there are storeys above the level under consideration. With this type of loading history, the amount of total creep that occurs can be computed by the principle of superposition (1,2). Although this principle has certain limitations, it is simple and, in practice, predicts behaviour close to the actual behaviour of the concrete, provided that suitable specific creep curves are available (3).

Creep strain can generally be expressed as a function of elastic strain in terms of a creep coefficient or creep factor ϕ:

$$\varepsilon'_{cc} = \frac{f_{ci}}{E_{cti}} \phi_i \qquad \ldots(1)$$

where

ε'_{cc} is the creep strain corresponding to a stress f_{ci}

E_{cti} is the elastic modulus of concrete at the time of application of stress

f_{ci} is the applied stress (or stress increment)

ϕ_i is the creep factor

The total creep strain ε_{cc} of an incrementally loaded column with N storeys above the column will then be

$$\varepsilon_{cc} = \sum_{i=1}^{n} \frac{f_{ci}}{E_{cti}} \phi_i \qquad \ldots(2)$$

where f_{ci} is the stress increment corresponding to the load caused by each floor above the column under consideration. Thus the total load-induced strain ε_{ec} (creep + elastic) can be expressed as

$$\varepsilon_{ec} = \sum_{i=1}^{n} \frac{f_{ci}}{E_{cti}} (1 + \phi_i) \qquad \ldots(3)$$

Individual values of the creep factor ϕ_i are easily obtained from the chart described below.

Determination of Creep Factor:

In determining the creep factor, the exposure condition, age at loading, the size and shape of the member, and the amount of reinforcement have to be considered. The size and shape of a structural member is usually expressed in terms of an 'effective' or 'theoretical' thickness which is twice the volume-surface area ratio of the member. The chart in Fig. 1 was prepared on the basis of CEP-FIP recommendations (4) and other data (4-11), gives the creep factor for various environmental conditions for plain and reinforced concrete loaded at any time from 3 days to 365 days and having an 'effective' thickness of 50mm to 500 mm.

For plain concrete either of the creep factor scales at the top or on the right-hand side can be used. The top scale is used when the percentage reinforcement lines are ignored (as shown by the dashed lines). When the zero percentage reinforcement line is used, the scale on the right-hand side gives the creep factor, again as shown by the dashed lines. Thus for a plain concrete member having an effective thickness of 100 mm, loaded at 28 days and subjected to an exposure condition of 74% r.h., the creep factor is 2.2. The ultimate creep strain is then 2.2 x the elastic strain developed on loading, or the loaded induced strain = 3.2 x elastic strain.

The creep factor of concrete is influenced by the amount of reinforcement. Fig. 1 also gives the creep factor for symmetrically reinforced concrete members, the scale on the right-hand side being used.

In deriving the creep factors, it was assumed that

(a) the slump of concrete lies between 50 mm and 100 mm; and

(b) the air content of the concrete is less that 6%.

To apply Fig 1 to concrete having slump and air content outside the above limits, corrections have to be applied to the creep factor. Based on data published by ACI Committee 209 (7), the equations 4 and 5 provide correction factors for both slump and air content.

$$\text{C. F. for slump } \alpha_{sc} = 0.8 + 0.003S \quad \ldots(4)$$

$$\text{C. F. for Air content } \alpha_a = 1 + 0.092\,A \quad \ldots(5)$$

where S = slump in mm

A = Air content in percent

Thus if the concrete had a slump of 25 mm and air content 8%, the correction factors from equations 4 and 5 are:

Correction factor for slump α_{sc} = 0.875

Correction factor for air content α_a = 1.18

Thus, creep factor = 2.2 x 1.18 x 0.875

= 2.271

Hence, load induced strain = 3.271 x elastic strain

The effect of a lower slump is thus counterbalanced by the air content above 6%. Although test results (7) show that the effect of member thickness tends to offset the effects due to variation in slump and air content, it is better to incorporate these effects in determining the creep factor.

Prediction of shrinkage of concrete:

a) Simplified Method:

The drying shrinkage depends on the exposure condition (relative humidity) and size and shape of the member in addition to composition of the concrete mix. In the case of reinforced concrete, drying shrinkage is influenced by the inclusion of reinforcement, since the stiffness of the member increases with increase in percentage of reinforcement. In the prediction of shrinkage, the elastic modulus of concrete at 28 days subjected to the same curing condition is considered as the basis. Fig. 2 gives the ultimate shrinkage of concrete for various environmental conditions for normal, plain and reinforced concrete with various elastic modulus and effective thickness, whereas Fig. 3 give the same shrinkage strains of lightweight concrete. The shrinkage of plain concrete is given by top scale while the vertical scale gives the shrinkage of reinforced concrete as noted for the creep factor.

The shrinkage values obtained by this method (Fig 2 & 3) correspond to a concrete having a slump of about 50 mm. The shrinkage of concrete having different slumps can be computed using the following correction factor. This correction factor is based on the ACI Committee 209/II recommendation (7).

$$(C.F)_{slump} = 0.90 + 0.0017\,S \qquad \ldots(6)$$

The shrinkage of concrete of various ages may be obtained using hyperbolic equation as suggested by Meyers et al (9,10). Hence the following equation may be used

$$\epsilon_s = \frac{\epsilon_{sh}\ t}{t + 35} \qquad \ldots(7)$$

where ϵ_{sh} = ultimate shrinkage value obtained from Fig 3.

ϵ_s = shrinkage of concrete at time t-days of age

Thus for a plain concrete with cement content of 300 kg/m^3, having an effective thickness of 150 mm and an elastic modulus E_c = 33 kN/mm^2, and subjected to an exposure condition of 70% r.h, the shrinkage strain is 330 microstrains (as indicated by the dashed lines). If this concrete is produced with 100 mm slump and used for member with about 1% steel, then the shrinkage of r.c. member is 270 x 1.07 = 289 microstrains. Further, if the same concrete is produced using a cement content of 360 kg/m^3 and other conditions considered to remain the same, although the value of E_c will change), then the shrinkage of the r.c. member is 350 x 1.07 = 375 microstrains.

b) Estimation of shrinkage in reinforced concrete columns:

In addition to the above approach, the shrinkage of insitu columns is also estimated from values obtained on control specimens (100x100x500 mm) made at site with the same concrete used for the members and subjected to the same environmental conditions. The shrinkage of control specimens is then adjusted for member thickness and reinforcement according to CEB-FIP recommendations (4).

Presentation of Results:

It is shown now how the simplified method can be used to predict long-term movements occurring in concrete structures. The predicted movements are then compared with measured movements of in situ structures as reported by the authors and various other investigators.

The creep strains are predicted through Fig 1 and the shrinkage strains from both simplified approach and from control specimens with appropriate correction factors for size and inclusion of reinforcement as discussed above. The elastic strain is predicted from the known stress history of the in-situ members, and the elastic modulus, either measured or predicted from the known compressive strength.

The predicted strains are compared initially with the measured in-situ movements in several columns of two reinforced concrete structures, A and B (12-14). The prediction and the comparison are then extended to data reported from the PCA Laboratory on several laboratory columns of normal weight and lightweight concrete.

The prediction method is thus shown to be valid for a wide range of data reported by other investigators for different types of structural columns.

Applications of proposed prediction method to UK data on in-situ columns

Structures A and B:

The columns in which movements were measured are in two structures, A and B, situated in Sheffield. Structure A is a six-storey reinforced concrete building (12,14) in which the movements of 11 columns were studied. Structure B is an eight-storey structure with the columns continuous through all the floors. The details of the two structures are reported elsewhere (12,13,14).

Prediction of load induced strains:

The simplified method of superposition is used here to predict the load induced strains in the several columns of structures A and B. Tables 1 and 2 show typical calculations of elastic and creep strains for column C5 of structure A and for an internal column I3 of structure B, respectively. The elastic strains in the columns for the design load are calculated from the elastic properties of the reinforcement and concrete. The modulus of elasticity of concrete used in structure A was calculated from cube strength and that of the concrete in structure B from static loading tests on control specimens at various ages.

In predicting creep strains, the creep factor ϕ was obtained from Fig 1. The exposure condition for the Sheffield area was found to be an average r.h. of 75% (18).

The calculations in Tables 1 and 2 are based on the design loads; the loads carried by the columns in service may, however, be different. In general, the actual loads carried by columns in buildings are not precisely known, limited data only being available concerning these loads (14-16). From observed and measured loading data in the two structures, the following basis is used in arriving at the proportion of the design load carried by the columns. It was assumed that, in structure A (a university building, consisting of lecture rooms and laboratories), the internal columns carry 100% of their design loads, and the perimeter columns, about 80% of their design loads. Structure B is an office building; on the basis of the study of loads in this and other similar buildings, the columns were assumed to carry about 60-80% of their design loads (14-16). Table 3 shows the load induced strains based on the service loads in the columns of structure B.

Measured Movements at 10, 25, and 50 years:

The strains in all the columns of structure A and B have been measured over a period of up to 10 years. These strains were plotted on a semi-logarithmic scale from construction up to 10 years; the trend of the basic strains (i.e. elastic + shrinkage + creep) was seen to be linear with logarithm of time (Fig 4). These curves thus allow extrapolation to be carried out to estimate the measured strains at 25 and 50 years. The linear strain-log-time relationships do not involve any complex assumptions and have been shown to be valid for all practical purposes (17,18).

The linear strain log-time relationship is confirmed by tests carried out by the US Bureau of Reclamation (19) which show that the rate of specific creep is inversely proportional to time, i.e.

$$\varepsilon_{sp} = F(k)\ln(t+1) \qquad \ldots(8)$$

where

ε_{sp} is the specific creep

F(k) is the parameter obtained experimentally representing the rate of specific creep with logarithm of time

t is the time (in days or years)

Since the shape of the shrinkage curve has the same trend as creep, the assumption that shrinkage is proportional to the logarithm of time gives a fair agreement with measured values on control specimens. Thus the relationship that shrinkage and creep movements of concrete are proportional to the logarithm of time may be used to estimate movements at various ages.

Comparison of Predicted and Measured Strains:

The predicted load-induced ultimate strains are compared with the measured load-induced strains at 10, 25 and 50 years in Table 4 for structures A and B. The measured load-induced strains are estimated by deducting the shrinkage strains of the column from the measured basic strains. The ratio of the predicted to measured load-induced strains for structure A varies between 95% (column C8) and 122% (column C11) at 10 years; at 25 years, the same ratio varies between 94% and 116%, while for structure B, the same ratio varied between 87% (column I5) and 108% (column I3), with an average of 100.6% when both structures are considered. It is considered at the age of 25 years, almost all the time-dependent movements had taken place.

The accuracy of the prediction can be evaluated by an error coefficient M defined as

$$M = \frac{1}{\varepsilon_{ep}} \sqrt{\frac{\sum (\varepsilon_{ep} - \varepsilon_{em})}{N}} \qquad \ldots(9)$$

where

ε_{ea} is the measured load-induced strain at time t

ε_{ep} is the predicted load-induced strain at time t

N is the number of test made

The value of M is expressed as a percentage and is analogous to the coefficient of variation. A value of 15% is considered acceptable (20); the error coefficients shown in Table 4 vary between 7.5% (at 25 years) and 11.03% (at 10 years) and may be considered very reasonable. It appears that the predicted values are in slightly better agreement with the measured values at later ages in both structures.

Comparison of Basic Strains:

The serviceability of structures is often governed by the total deformation that takes place during their service life. Thus it is appropriate to consider the basic strains (i.e. elastic + shrinkage + creep strains) to assess performance.

The predicted and measured basic strains in service in the columns of structures A and B are shown in Table 5. The predicted values were obtained by adding the appropriate shrinkage strain to the load induced ultimated strains. The shrinkage strains were estimated by both approach as discussed earlier: a) using the elastic modulus, exposure conditions, effective thickness of the member, percentage of reinforcement and the slump of the concrete mix; and b) using the data from control specimens of the same concrete exposed to same environmental conditions. The measured values were obtained by extrapolciting strain - log time curves as explained before. The agreement between the predicted and measured values is very good, and the error coefficients for prediction vary between 4.0% and 8.6%. It appears that the predicted values using the shrinkage of control specimens is in better agreement as the error coefficients are lower than the others. The predicted load-induced strains, and hence, the basic strains by the proposed method in this paper gave good agreement with measured values even at 50 years of age (18).

Application of the proposed method to Laboratory columns

This method of predicting the creep and basic strains outlined above has been applied to some laboratory data on normal and lightweight concrete columns. Pfeiffer (21) has reported data on the time dependent movements of model reinforced concrete columns, with 75 mm effective thickness, observed for 2 1/2 years in laboratory environment (50% r.h. at 73°F). The reinforcement in the columns varied between 0% and 8.38%. In the laboratory, of course, the environmental conditions are controlled, unlike those outside where there are variable factors.

Pfeiffer reported the elastic modulus of concrete Ec used as the product of concrete area and the elastic modulus. From the reported modulus of concrete and steel, the elastic strains developed on loading at 28 days was computed. The creep factors were obtained from Fig 1 from the known details of the columns and exposure conditions. As the creep factors give the ultimate values, the predicted creep factors are corrected for 2 1/2 years of age by a factor of 0.8 (22,23). Similarly the predicted shrinkage values are corrected for 2 1/2 years of age by a factor of 0.9 (22,23). The predicted load induced and basic strains are compared with measured values as reported by Pfeiffer in Table 6. The prediction of shrinkage strains for lightweight concrete is carried out using Fig. 3.

Table 6 also shows the results of Laboratory columns observed at Sheffield University under indoor variable environmental conditions: the relative humidity varied between 58% and 78% with an average of 65% while the temperature varied between 7 and 16 degree c with an average of 12.7 degree c. The reinforcement in the columns varied between 0% and 6.48%. The concrete mix had about 200 mm slump (almost collapse slump).

The predicted creep factors are corrected for 1000 days of age by a factor of 0.85 while the shrinkage values are corrected for the same age by a factor of 0.9.

It is again seen that the agreement between predicted and measured values is very good, since the error coefficients for both load-induced strains and basic strains are within acceptable limit. It is interesting to note that the method proposed in this paper to predict creep factors gives good approximation to lightweight aggregate concrete columns as well.

CONCLUSIONS:

Simple method of predicting long-term movements in buildings and bridges using design charts for creep factors and shrinkage strains is presented. The method is shown to give good agreement with field and laboratory test data obtained on normal and lightweight aggregate concrete made from ordinary Portland cement.

REFERENCES

1. McHenry, D., "A New Aspect of Creep in Concrete and its Applications to Design", Proceedings, American Society for Testing and Materials, 43, 1943, p. 1069.

2. Swamy, R.N., and Arumugasaamy, P., "Flow Hardening Method of Creep Analysis of In-situ Reinforced Concrete Columns", Journal of the American Concrete Institute, May to June 1980.

3. Kamshiu, K., and Russell, H.G., "Knowledge Gained from Instrumentation of the Kishwaukee River Bridge", Journal of Prestressed Concrete Institute, Proceedings Sept.-Oct. 1983, pp. 33-53.

4. CEB-FIP International Recommendations for the Design and Construction of Concrete Structures, Principles and Recommendations, Cement and Concrete Association, London, June 1970, p. 80.

5. Hansen, T.C., and Mattock, A.H., "Influence of Size and Shape of Member on the Shrinkage and Creep of Concrete", Journal of the American Concrete Institute, Proceedings, 63, No. 2, February 1966, p. 267.

6. Neville, A.M., "Creep of Concrete: Plain, Reinforced and Prestressed", North-Holland Publishing Co., Amsterdam, 1970, p. 622.

7. ACI Committee 209, "Prediction of Creep, Shrinkage and Temperature Effects in Concrete Structures", Publication SP-27, American Concrete Institute, 1971, p. 51.

8. Leonhardt, F., "Prestressed Concrete: Design and Construction", 2nd ed., W. Ernst and Son, Berlin, 1964.

9. Myers, B.L., and Branson, D.E., "Design Aid for Predicting Creep and Shrinkage Properties of Concrete", Journal of the American Concrete Institute, Proceedings, 69, No. 9, September 1972, p. 551.

10. Myers, B.L., Branson, D.E., and Schuman, C.G., "Prediction of Creep and Shrinkage Behavior from 28-day Data", Report No. 70-8, XIV South American Conference of Structural Engineering and the IV Pan-American Symposium of Structures, Buenos Aires, Argentina, October 1970.

11. Wu, H., and Huggin, M.W., "Size and Sustained Load Effects in Concrete Columns", Journal, Structural Division, Proceedings, American Society of Civil Engineers, 103, No. ST3, March 1977, p. 493.

12. Swamy, R.N., and Arumugasaamy, P., "Long-term Behavior of In-situ Reinforced Concrete Columns", Joint I. Struct. E/BRE., Seminar on Structural Assessment Based on Full and Large Scale Testing, BRE, Garston, England, April 1987.

13. Swamy, R.N., and Potter, M.M.A., "Long-term Movements in an Eight-story Reinforced Concrete Structure", Proceedings, International Conference on Performance of Building Structures, Glasgow, Pentech Press, London, 1, April 1976, p. 413.

14. Swamy, R.N., and Arumugasaamy, P., "Deformations in Service of Reinforced Concrete Columns", Douglas McHenry International Symposium on Concrete and Concrete Structures, Mexico, Publications SP-55, American Concrete Institute, 1978, p. 375.

15. Swamy, R.N., and Potter, M.M.A., "Measurements of In-situ Stresses in Reinforced concrete Columns", The Structural Engineer, 55, No. 4, April 1977, p. 165.

16. Mitchell, G.R., and Woodgate, R.W., "Floor Loading in Office Buildings-the Results of a Survey", BRS Current Paper CP3/71, January 1971.

17. Tyler, R.G., "Creep, Shrinkage and Elastic Strain in Concrete Bridges in United Kingdom", 1963-1971, Magazine of Concrete Research, 28, No. 95, June 1976, p. 55.

18. Swamy, R.N., and Arumugasaamy, P., "A Simple Aid for Predicting Shrinkage and Creep Strains in Buildings and Bridges", The Structural Engineer, 59, No. 3, March 1981, p. 93.

19. US Bureau of Reclamation, "A 10-year Study of Creep Properties of Concrete", Concrete Laboratory Report No. SP-38, Denver, Colorado, July 1953.

20. Neville, A.M., and Myers, B.L., "Creep of Concrete Influencing Factors and Prediction", Symposium on Creep of Concrete, Publication SP-9, American Concrete Institute, 1964, p. 1.

21. Pfeiffer, D.W., "Reinforced Lightweight Concrete Columns", Journal, Structural Division, Proceedings, American Society of Civil Engineers, 95, No. ST1, January 1969, p. 57.

22. Evans, R.H. and Kong, F.K., "Estimation of Creep of Concrete in RC and PC Design", Civil Engineering Public Works Review, 61, May 1966, p. 593.

23. Troxel, G.E., Raphael, J.M. and Davis, R.E., "Long-time Creep and Shrinkage Tests of Plain and Reinforced Concrete", Proceedings, American Society for Testing and Materials, 58, 1958, p. 1101.

Table 1 - Typical calculation of load induced strain in column C5, structure A

Age at loading	$E_c \times A_c$ $\times 10^{-6}$	$E_sA_{sc} + E_cA_c$ $\times 10^{-6}$	Design load (kN)	Elastic strain $\times 10^6$	Creep factor	Creep strain $\times 10^6$
30	1771	2285	86	38	1.15	44
110	2067	2581	86	33	0.85	28
156	2138	2652	87	33	0.80	26
195	2175	2689	86	32	0.75	24
235	2175	2689	86	32	0.72	23
295	2175	2689	86	32	0.72	22
				200×10^{-6}		167×10^{-6}

Total load-induced strain (creep + elastic) $= 367 \times 10^{-6}$

Table 2 - Typical calculation of load induced strain in column I3, structure B

Age at loading days	$E_c \times A_c$ $\times 10^{-6}$	$E_sA_{sc} + E_cA_c$ $\times 10^{-6}$	Load* from	Design load (kN)	Elastic strain $\times 10^6$	Creep factor	Creep strain $\times 10^6$
60	9871	11090	S(3)+CL(4)	676	61	1.1	67
110	10180	11399	S(4)+CL(5)	616	54	0.95	51
130	10242	11461	S(5)+CL(6)	634	55	0.95	52
180	10398	11617	S(6)+CL(7)	663	57	0.78	44
210	10462	11681	S(7)+CL(8)	660	57	0.73	42
240	10510	11729	S(8)+screed	707	60	0.70	42
					344×10^{-6}		298×10^{-6}

In actual practice only 75% of the design load had been experienced by the column. Hence correcting for 75% of the design load.

Load induced strain $= 482 \times 10^{-6}$

*S(3) = Slab 3 immediately above column 3.
CL(4) = column 4.

Table 3 - Load induced strain (long-term, i.e. at ultimate) in columns, structure B

Column no.	Calculated according to design load			Approximate* percentage of design load carried by column	Predicted load-induced strain $\times 10^6$
	Elastic $\times 10^6$	Creep $\times 10^6$	Load induced $\times 10^6$		
I1	413	327	740	60	444
I2	390	341	731	60	438
I3	344	298	642	75	482
I4	301	318	619	70	433
I5	248	300	548	70	384
I6	197	232	429	70	300
I7	130	165	295	75	221

*Values based on Carlson stress meter readings (ref. 14)

Table 4 - Comparison of load induced strains (structure A and B)

Column no.	Predicted* load induced strain $\times 10^6$	Measured load-induced strain $\times 10^6$			Predicted/measured (estimated) (%)		
		At 10 yrs	25 yrs	50 yrs	At 10 yrs	25 yrs	50 yrs
			structure A				
C1	245**	203	235	254	121	104	97
C2	300	305	312	320	98	96	94
C3	300	305	312	320	98	96	94
C4	246**	245	259	271	100	95	91
C5X	294**	274	294	319	107	100	92
C6	284**	269	279	286	106	102	99
C7	284**	256	290	318	111	98	89
C8	430	455	459	468	95	94	92
C9	430	401	401	401	107	107	107
C10	430	396	401	405	109	107	106
C11	430	350	371	386	122	116	111
			structure B				
I1	444	486	460	500	102	96	89
I2	438	413	412	441	106	106	99
I3	482	416	447	483	116	108	100
I4	433	390	418	427	111	104	101
I5	384	401	444	437	96	87	88
I6	300	325	345	381	92	87	79
I7	221	(184)	204	230	120	108	96
				Average	106.5	100.6	95.8

* Ultimate values.

** Assumed 80% of the design load carried by the column.

Error coefficient at 10 years: 11.03%
Error coefficient at 25 years: 7.5%
Error coefficient at 50 years: 8.6%

Table 5 - Comparison of basic strains in the columns of structure A and B

Column no.	Age in years	Estimated from measured strain x 10^6	Predicted* basic strain x 10^6	Predicted / measured (%)	Predicted** basic strain x 10^6	Predicted / measured (%)
			Structure A			
C1	10	540	504	93	582	108
	25	584	518	89	595	102
C2	10	555	550	99	550	99
	25	579	563	97	567	98
C3	10	555	550	99	550	99
	25	579	563	97	567	98
C4	10	543	496	91	544	100
	25	575	509	89	562	98
C5	10	543	504	93	563	104
	25	576	515	89	576	100
C6	10	555	494	89	570	103
	25	576	505	88	581	101
C7	10	510	494	97	538	105
	25	560	505	90	554	99
C8	10	635	633	100	610	96
	25	651	651	100	622	96
C9	10	601	633	105	630	105
	25	618	651	105	647	105
C10	10	619	633	102	653	106
	25	640	651	102	669	105
C11	10	537	633	118	617	115
	25	575	651	113	634	110
			Structure B			
I1	10	608	672	111	644	106
	25	690	684	99	674	98
I2	10	610	695	114	658	108
	25	666	708	106	692	104
I3	10	625	672	108	713	114
	25	710	682	96	755	106
I4	10	630	652	103	673	107
	25	700	663	95	715	102
I5	10	660	603	91	670	102
	25	730	614	84	713	98
I6	10	540	519	96	554	103
	25	595	530	89	590	100
I7	10	424	440	104	492	116
	25	492	452	92	522	106
	10	Error coefficient		8.1%		7.6%
	25			8.6%		4.0%

* Shrinkage strains were computed using proposed method.

** Shrinkage strains were estimated from control specimen data.

Table 6 - Comparison of load induced and basic strain in laboratory columns.

	Load induced strain x 10^6			Basic strain x 10^6 elastic + creep + shrink		
	Predicted	Measured	Predicted / measured %	Predicted*	Measured	Predicted / measured %
PCA laboratory - 2 1/2 year results: Normal weight concrete						
8A	579	673	86	1137	1153	99
8B	601	698	86	1024	1078	95
8C	642	658	96	858	847	101
8D	626	695	90	722	775	93
Lightweight concrete						
14A	849	823	103	1389	1383	100
14B	847	820	103	1225	1220	100
14C	835	745	112	1042	910	115
14D	752	682	113	842	772	109
Author's results - 1000 day - Normal weight concrete						
C02	954	830	115	1411	1347	105
C12	941	1024	92	1293	1405	92
C22	927	1088	85	1206	1289	94
C32	941	943	100	1131	1072	106
C42	833	825	101	945	929	102
		Average	98.6			100.6

* Shrinkage strain calculated as 90% of the ultimate value.

Error coefficient - Load induced strain = 10.2%

Error coefficient - Basic strain = 6.5%

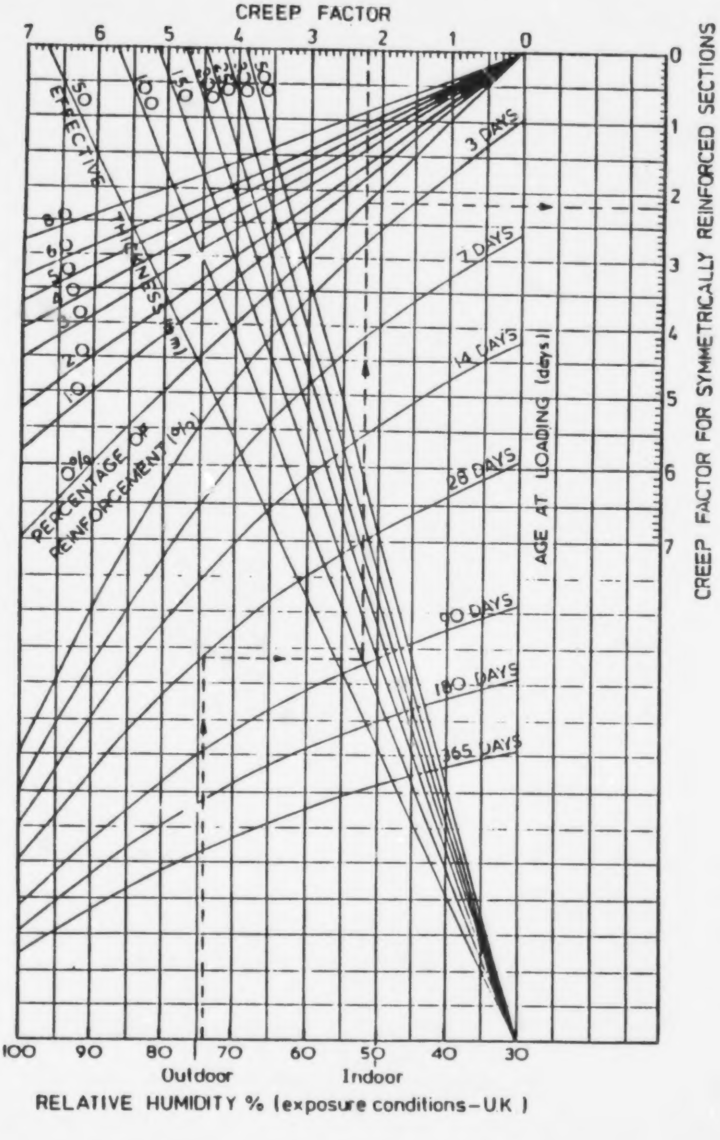

Fig. 1 Creep factor chart for plain and reinforced concrete

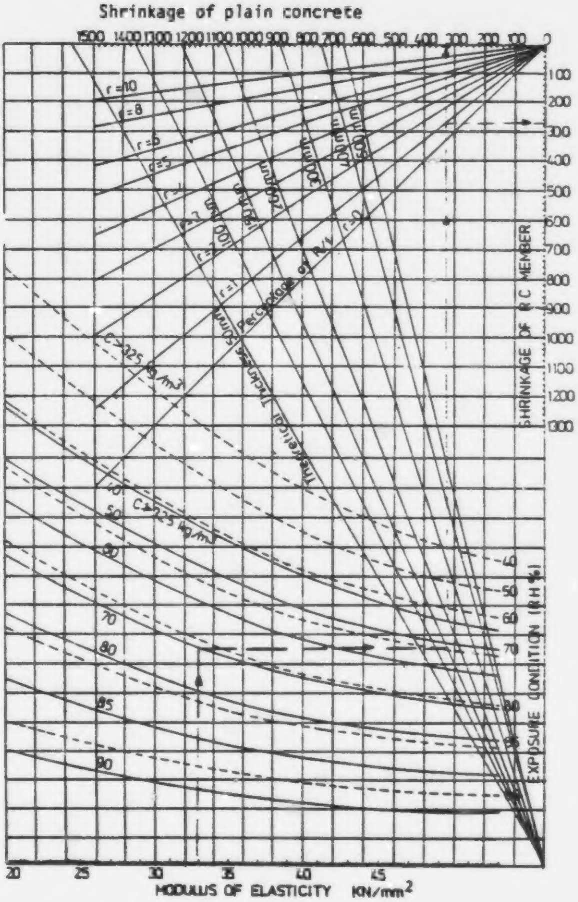

FIG. 2 SHRINKAGE OF REINFORCED NORMAL WEIGHT CONCRETE.

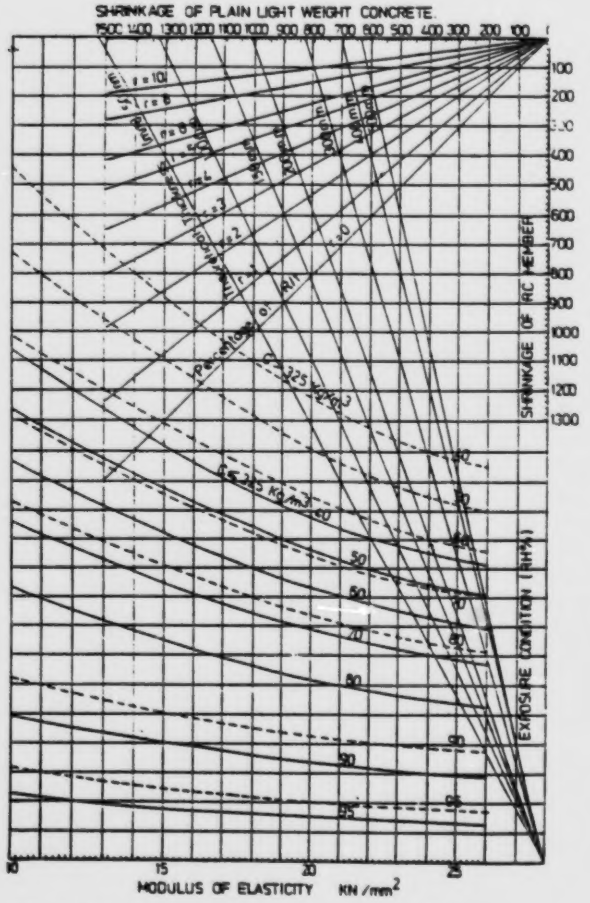

FIG. 3 SHRINKAGE OF REINFORCED LIGHTWEIGHT CONCRETE.

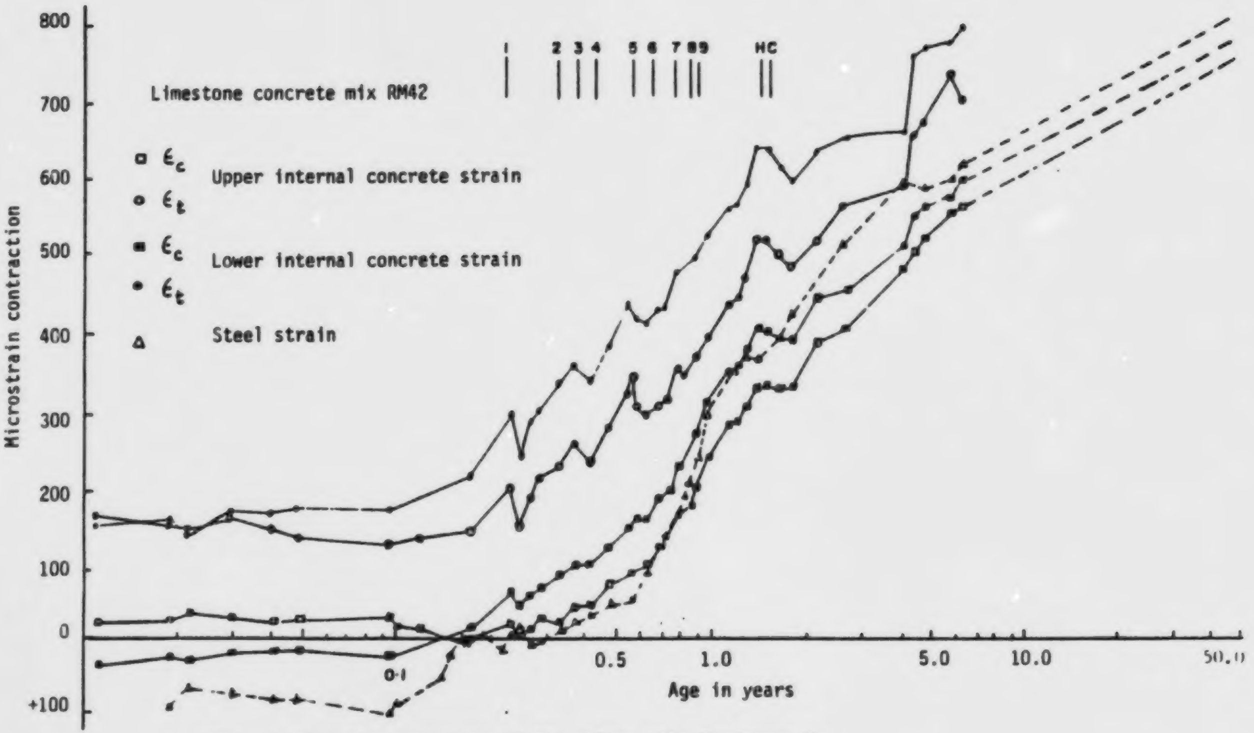

Fig. 4 Long-term movements of the column I1: Structure B

RELAXATION OF RESTRAINT EFFECT CAUSED BY TEMPERATURE DIFFERENCE OR SETTLEMENT OF A SUPPORT IN LONG TERM TESTS

Jukka Jokela
Technical Research Centre of Finland
Concrete and Silicate Laboratory
Espoo, Finland

ABSTRACT: The creep of concrete has considerable influence on the relaxation of the restraint effects and restraint stresses; particularly if the temperature of concrete is higher than normally. Risk of cracking e.g., caused by the settlement of supports, is also diminished owing to creep; particularly if the rate of restrained displacement (settlement of a support) is slower than the rate of creep. It is difficult to consider the effect of relaxation from a calculational point of view, because the time dependencies of several factors cannot be reliably modelled. In this research, the relaxation of the restraint effects, due to both sudden and slow settlement of a support, was examined as a function of time; the relaxation of the restraint effect due to a thermal gradient was also investigated. It was observed the relaxation was fairly rapid in a heated beam in particular. Also the relaxation of restraint effects caused by the settlement of supports was considerable.

1. INTRODUCTION

Concrete has characteristic properties such as a tendency to deformations at the changes of temperature or humidity as well as a tendency to creep, which refers to the continued increase with time in deformation of concrete under stress. Creep occurs both in compressed and tensioned concrete. Mechanisms affecting the time-dependent behaviour of concrete are, as well known, fairly complicated and as far as practical calculations are concerned they are not yet under complete control. In most cases, it is also nearly impossible to tell the difference between the mechanical and non-mechanical deformations. Practical calculations are mainly based on the constitutive material models, which do not pay enough attention to the changes of temperature and humidity. Neither can the development of cracking be taken into account by means of these models. So far the problem of the combined effect of cracking, temperature and humidity, let alone the effect of time, has not been solved.

A solution to the problem should take into account both mechanical and other deformations, due to e.g. the conditions of exposure: they include both fast and time-dependent parts, which again can be either reversible or irreversible. Further, deformation processes may be interdependent. The mentioned factors should, in addition, be examined in relation to cracking and the possible dependency on it.

It is known that the effect of temperature is two-way. On the one hand, the rising temperature accelerates the rate of deformation and on the other hand, it acclerates the rate of hydration reactions i.e. the hardening rate of concrete.

If deformations or displacements have been induced or restrained onto a structure, one must instead of creep speak about a relaxation phenomenon which means the continuing reduction of stress with time. An induced or restrained displacement in a structure can, in principle, be of short or long duration. When the time period of formation and effect is short, relaxation cannot take place in concrete and it cracks if the restrained strain is greater than the strain at failure.

Restrained displacements with long-term effects consist of both rapidly and slowly developing displacements. If no cracking occurs in connection with a rapidly forming restrained displacement, the corresponding restraint effect grows in relation to the stiffness of a structure. At the formation phase of cracks, the restraint effect grows clearly more slowly than the restrained displacement since every new crack reduces the stiffness of a structure. The restraint effect cannot be assumed to grow at the rate of the restrained displacement before the crack formation has stabilized. After having reached its greatest value the action effect due to restrained displacement starts to relax owing to creep. Since the rate of creep decreases with time the relaxation of the action effect is the greater the earlier the restrained displacement takes place.

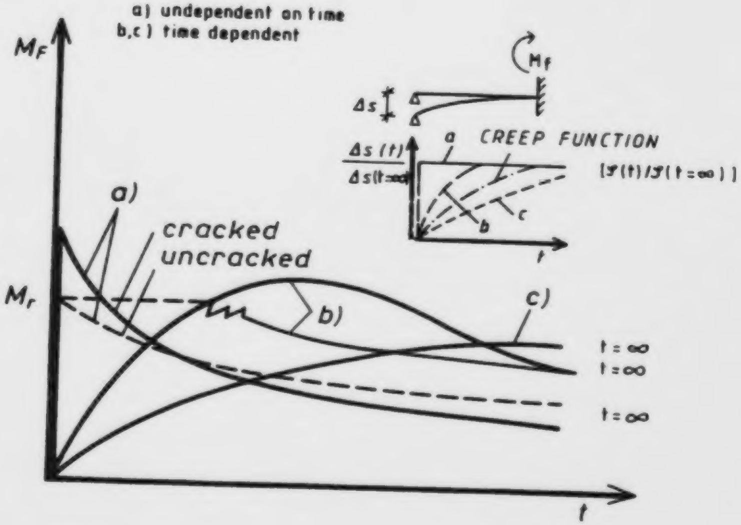

Figure 1: Influence of the rate of restraint stress development on creep /8/.

As the rate of the displacement formation slows down a partial relaxation of the restraint effect takes place. If the restrained displacement, which only increases at the formation phase of cracks, grows quicker than the deformation induced by creep, the structure will crack, but the restraint effect does not grow greater than the crack action effect. If, on the other hand, the restrained displacement grows more slowly than the creep, the structure will not crack at all (Fig. 1).

In order to estimate relaxation by calculational means the time dependency of restrained displacement and that ot creep as well as the changes taking place in the structural properties, above all in stiffness, during the displacement formation must be known. If the temperature deviates from the normal the temperature dependency of creep must also be known. The problem has been examined from the calculational point of view by e.g. in references /1, 3, 8/.

In this article, results from tests with four reinforced concrete beams relating to the relaxation of the restraint effect due to displacement of supports in different situations are presented.

2. EXPERIMENTAL STUDY OF CONCRETE RELAXATION

2.1 Structural Model: The statical structural system of the test beams corresponded to a double support beam stiffened at one end, whose free end was subjected to various restrained displacement. A heat gradient of about 50 °C was directed to one beam: a restraint moment was induced at the fixed support.

2.3 Test Beams: Two double beams were manufactured for the tests and they were marked with the following symbols: 1a, 1b, 2a and 2b. The amount of tension and compression reinforcement in beams 1a and 1b was 0.43 % and 1.29 % in beams 2a and 2b. The dimensions and structures of the beams set out in Fig. 2 and material properties in Table 1.

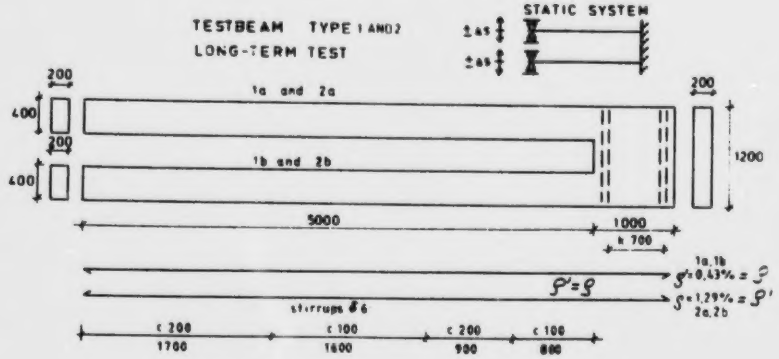

Figure 2: Dimensions and structure of the test beams.

Table 1: Material properties of the test beams based on samples.

Beam	Concrete	Reinforcement (A400H)						
	Compressive strength MN/m^2	Yield stress MN/m^2	Ultimate strength MN/m^2	Diameter mm	Rib angles α	β	Rip spacing mm	Relative rib area α_{sb}
1a, 1b	52	458	690	10	48	61	6.5	6.7 %
2a, 2b	52	434	630	20	53	69	13.6	8.0 %

2.3 Long-term Tests: In long-term tests (total duration 8 months) a thermal gradient of about 0.1 °C/mm (temperature difference of 40 - 50 °C) was directed to beam 1a in such a way that the temperature of the upper surface remained at about 35 - 40 °C and that of the lower surface at about 80 - 85 °C. A thermal gradient was produced by heating the lower surface of a beam using electrical resistance mats. In order to direct heat flow mainly in one direction and to ensure a maximum thermal gradient, the sides of the beams were provided with approximately 50-mm thick mineral wool isolation. The upper surface was not isolated. The measuring plugs were installed for deformation measurements along the upper and lower edges of the entire length of the beam. For displacement and rotation measurements inductive displacement transducers were intalled. The support reactions of the free end of beams were measured by menas of a load cell. The measurement results, along with output, were registered throughout the test using a microcomputer. The loading arrangements of the beam are shown in Fig. 3.

A displacement of about 20 mm, which was kept constant, was instantaneously forced onto the free support of beams 1b (upwards) and 2a (downwards). The temperature of these beams was kept at about 20 °C during the entire test.

Displacement of the support corresponding in size to that of beam 1b and 2a was gradually forced onto the free support of beam 2b over a period of about 2 weeks. Displacement was increased daily in approximately equal amounts; subsequently it was kept constant (Table 2). The temperature of the beam was kept at about 20 °C throughout the test. The final displacement of supports produced a calculational steel stress of about 200 N/mm^2 at the fixed support, when the stiffness of the beams was chosen as the average value of the uncracked and cracked stiffness.

Table 2: Displacements at the free ends and at the centre of beams in long-term tests.

Beam	Restrained displacements (mm) 1)							
	1a		1b		2a		2b	
Date	end	centre	end	centre	end	centre	end	centre
28.8.-85	-1.55	-0.84	19.10	7.02	-18.50	-7.56	0.05	-0.23
2) 29.8.-85	-1.56	-0.75	19.10	6.99	-18.54	-7.51	3.97	1.07
30.8.-85	-1.86	-3.10	18.92	6.73	-18.54	-7.57	6.09	1.70
3) 10.9.-85	-1.79	-2.68	18.97	6.95	-18.52	-7.37	19.73	6.60
7.1 -86	-1.80	-3.04	18.99	6.69	-18.55	-7.39	19.82	6.50
5.5.-86	-1.78	-3.23	19.00	6.54	-18.59	-7.47	19.84	6.43

1) direction of displacements positive upwards
2) heating of beam 1a starts
3) increase in the settlement of beam 2b was discontinued.

During the tests, measurements were made relating to

- crack widths
- crack spacings
- displacements
  - deflections
  - rotations
- deformations at the upper and lower edges of a beam
  - strains in steel
  - compressive strains and elongations
- support reactions
- temperature of a beam at different heights.

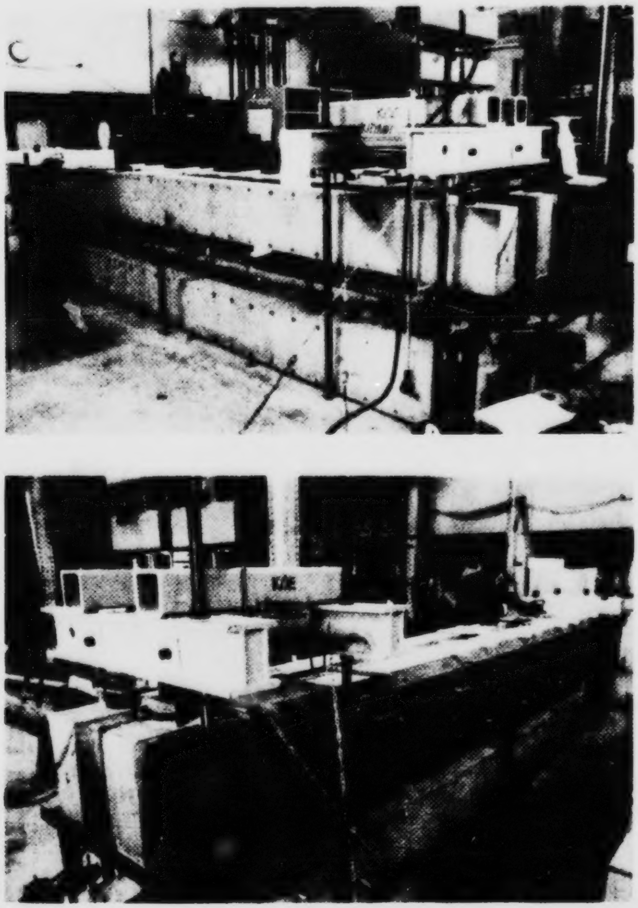

Figure 3: Test arrangements in long-term tests.

2.4 Results: The main results of relaxation tests are presented in the following figures:

- the temperature gradient of the beam 1a measured at different times during the test in Fig. 4
- the deflection in the mid-span of the beam 1a in Fig. 5
- the support reactions of the free end of the test beams measured during the test in Fig. 6
- the development of average crack widths measured from the test beams during the test in Fig. 7.

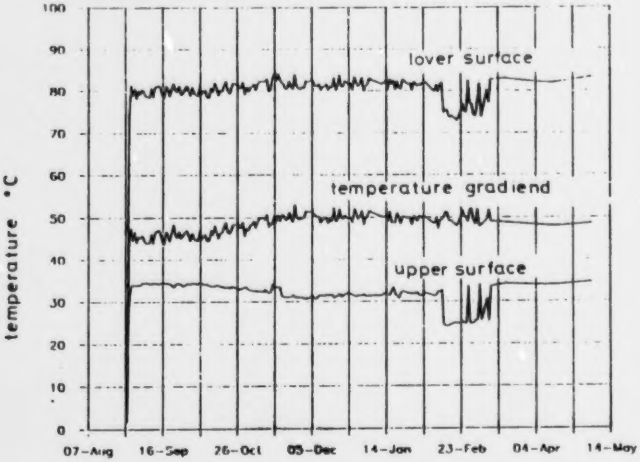

Figure 4: Temperature of upper and lower surface and temperature gradient of the heated beam during the test.

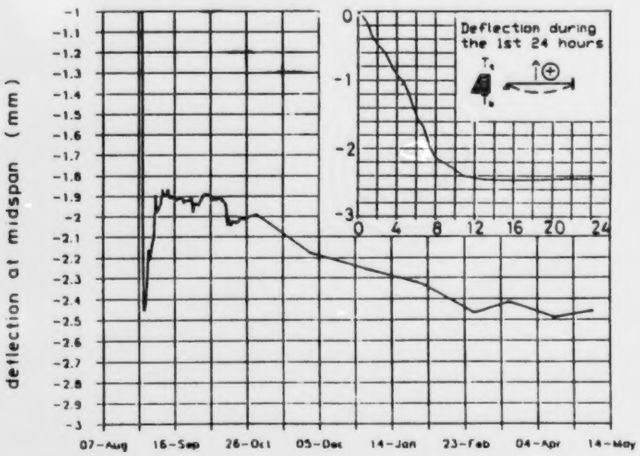

Figure 5: Deflection at the mid-span of the heated beam 1a.

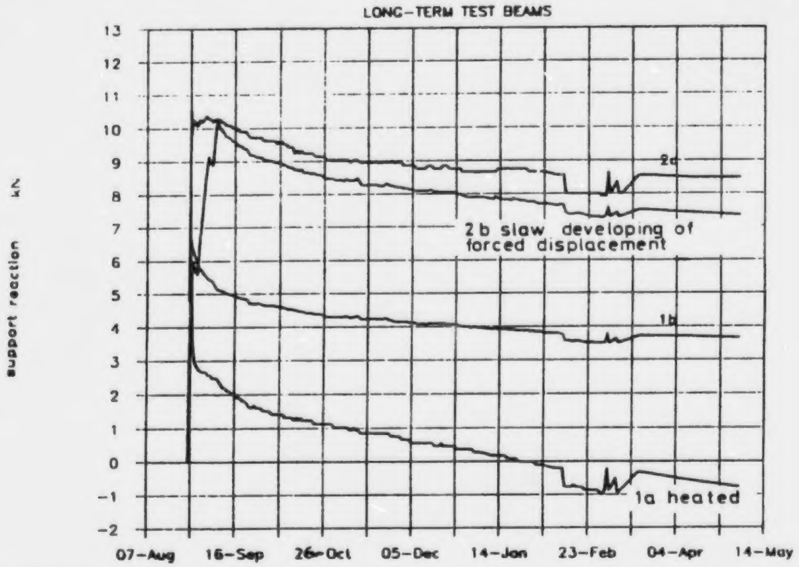

Figure 6: Support reaction values (including own weight) in the free end of all beam during the first eight months.

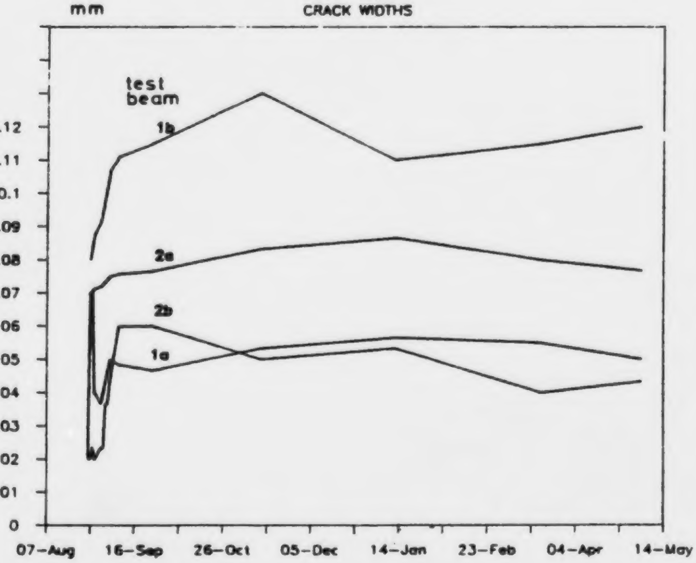

Figure 7: Development of crack widths during tests.

3. EXAMINATION OF RESULTS

In the heated beam, 1a, a linear thermal gradient of about 0.1 °C/mm was produced about 8 hours from the onset of heating; subsequently it remained nearly the same during the entire test.

The effect of temperature on the creep of concrete and its relaxing influence on the restraint effects is surprisingly powerful. Short-term tests carried out earlier, lasting about 12 h /5/, had yielded similar results.

In the now reported tests, as well as in earlier ones, the temperature of the heated, creeping part of concrete was about 80 °C. The maximum value of the restraint moment in beam 1a, due to thermal gradient, was 27.5 kNm and it was reached about 5 h from the onset of heating. Due to the accelerated rate of creep, over 10 % of the restraint moment had relaxed as soon as 7 h from the onset of heating and about one third (1/3) during the first 24 hours. The relaxation of the restraint moment continued so that after about one month one third of the maximum original value was left and after 6 months the entire restraint moment due to heating had relaxed. The final measured support reaction of the free end of the beam is greater than the original because the stiffened support had cracked and the weight of the loading equipment had been ignored.

In the beams, the ends of which were subjected to a restrained displacement corresponding to a steel stress of 200 N/mm^2, the relaxation of a support reaction took place quite rapidly even at normal temperature. A decrease in the support reaction with different beams is set out in Table 3, assuming that in all cases the proportion of the beams' own weight is 5 kN of the support reaction.

The proportion of the shrinkage during the tests was not measured. Its influence is estimated approximately from 5 - 10 %, because the tests beams were at the beginning of long-term tests 1,5 years old and stored in test hall conditions.

Table 3: Decrease in restraint effect owing to creep.

Beam	Proportion of the relative value of the restraint effect to its greatest value during different testing periods, %						
	14 days	1 month	2 months	3 months	4 months	6 months	8 months
1a 1)	42	31	22	18	10	0	-3 3)
1b	71	67	61	58	55	53	52
2a	97	94	88	85	84	84	82
2b 2)	90	84	78	76	74	71	68

1) heated

2) displacement of a support carried out step by step during the course of 2 weeks

3) due to cracking of the support and the measuring equipment's own weight.

Relative relaxation of the support reaction due to the creep and shrinkage of more heavily reinforced beams 2 (ρ = 1.29 %) was distinctly slower than in the case of more lightly reinforced beams (ρ = 0.43 %).

The relative relaxation of the restraint moment in beam 2b, the restrained displacement of which took place in 2 weeks, was faster than in beam 2a, the restrained displacement of which took place momentarilly. Also the degree of relaxation of beam 2b, corresponding to the end of the test, was greater. The difference in the degree of relaxation was considerable already at the beginning of the test.

The deflection downwards of the mid-span of the heated beam increased nearly linearly in relation to the thermal gradient; subsequently its value remained constant at 2.45 mm for about 12 hours. As the heated and compressed lower surface of the beam started to creep, the deflection decreased rapidly i.e. about 25 % in a few days. As it has been stated, the restraint effect also relaxed down to half of its maximum value in the equivalent course of time. Subsequently, the value of the deflection remained nearly unchanged for about 2 months, after which the deflection started to grow again. This is due to the fact that after 2 months about 20 % of the maximum value of the restraint effect remained and owing to the moment caused by its own weight, the upper surface of the beam gradually became compressed and thus creep could begin. Since also the temperature of the upper surface was above the normal (about 35 °C) the rate of creep, even in this phase, was greater than normally. The increase in the deflection was slowed down about 6 months after the start of the test when the value of the deflection was approximately the same (about 2.5 mm) as the maximum deflection due to a short-term thermal load (about 0.1 °C/mm).

The average carck widths did not change essentially during the long-term test.

4. CONCLUSIONS

1. The effect of temperature (+80 °C in the test) on the rate of the creep in concrete and thus on relaxation is considerable. With the thermal gradient used in the test, the restraint effect was reduced to 30 % of its original value during one month when the corresponding reduction without heating was only to 65 % of the original value. After six months the restraint effect was totally reduced in the heated beam.
2. The relaxation of the restraint effect in a stiff, heavily reinforced beam is relatively slower than in a lightly reinforced beam, and the degree of relaxation is not as great.
3. The slower development of the restraint effect causes a faster relaxation and a greater degree of relaxation.
4. If a structure is subjected to a thermal gradient and some other mechanical load (e.g. own weight) the statical system of a structure and the relaxation of the restraint effects must be taken into account when estimating structural long-term deformations in order to find out the direction of curvature that is caused by creep. The direction of change of the deflection may vary according to which side of a structure is compressed or heated and according to the degree of relaxation of the restraint effects and the redistribution of the external load effects due to cracking.
5. The average width of cracks is not essentially changed at the relaxation of the restraint effects, but instead keep approximately the same width they had at formation.

REFERENCES

/1/ Chali, A. et al. Time dependent forces induced by stllement of supports in continuous reinforced concrete beams. Journal of the American Concrete Institute 66(1969)11, pp. 907 - 915.

/2/ Dilger, W. et al. Time-dependent forces induced by settlement in continous prestressed concrete structures. IABSE Symp. Design of Concrete Structures for Creep, Shrinkage and Temperature Changes. Madrid, 17 - 18 Sept. 1970. Zürich 1970, International Association for Bridge and Structural Engineering, Reports of the Working Commissions, Vol. 5. Pp. 89 - 98.

/3/ Dimel, E. Einfluss des Betonkriechens auf Setzungzwängungen. Beton- und Stahlbetonbau 60(1956)6, pp. 140 - 150.

/4/ Jokela, J. Dimensioning of strain or deformation-controlled reinforced concrete beams. Espoo 1986, Technical Research Centre, Publications 33. 118 pp. + app. 33 pp.

/5/ Jokela, J. Restrained concrete beam under thermal and mechanical load. RILEM-ACI Int. Symp. on Long-Term Observation of Concrete Structures. Budapest, 17 - 20 Sept. 1984. Budapest 1984, Institute for Quality Control of Building. Vol. 1. Pp. 89 - 101.

/6/ Kordina, K. et al. Tragfähigkeit und Verformung von Stahlbetonbalken unter Biegung und gleichzeitigen Zwang infolge Auflagerverschiebung. Berlin 1982, Deutscher Ausschuss für Stahlbeton, Heft 336. 66 pp.

/7/ Pajuhesh, J. Thermal relaxation in concrete structures. Journal of Am. Concr. Inst. 73(1976)9, pp. 522 - 525.

/8/ Schaper, G. Stahlbetonplatten unter Last- und Zwangbeanspruchung - Berechnung des zeitabhängigen Verhaltens bei Berücksichtigung der Rissbildung. Dissertation. Braunschweig 1978, Technische Universität Carolo-Wilhelmina zu Braunschweig. 204 pp.

/9/ Sidhu, H. & Limaye, R. G. Creep of concrete at elevated temperatures. Indian Concrete Journal 57(1983)10, pp. 269 - 273.

EFFECT OF DIFFERENTIAL SETTLEMENT ON THE PERFORMANCE OF A CONTINUOUS TRUSS

H. P. Niu

Associate Professor of Civil Engineering
University of Missouri-Columbia/Kansas City
Independence, Missouri 64050

ABSTRACT: This paper concerns the case study of an industrial plant which encountered excessive settlement of its spread footings. This settlement was creating added stresses in the members of the six spans indeterminate truss roof support structure.

Excessive settlement appeared to be due to scouring from ruptured subsurface liquid carrying pipes. Methods of preventing further settlement and repair of existing support damage were hindered by the machinery, piping and electrical conduit at the columns.

The study involved reviewing the original design, site inspection and determination of possible damages. A subsequent computer analysis of the truss was made using settlement information not previously included in the initial design. It was then found that the truss was originally designed to resist vertical loads, as a simple truss with the bottom chord connections to the columns eliminated. The bottom chord connection is necessary, however to resist lateral wind load without overstressing the columns. But it is through this connected bottom chord that the truss becomes indeterminate and overstressed from excessive settlement.

A number of remedial steps was recommended to prevent further settlement.

INTRODUCTION

This study was undertaken to determine the probable causes of a differential settlement of supporting columns in a continuous truss and its effect on the performance of its members. As shown in Fig. 1 the structure involved consists of a six span continuous truss. Each truss is approximately 15 m long and is composed of A 36 steel with double angle members and riveted connections. The columns are composed of four angles connected by lacing bars and supported on reinforced concrete slabs and footings. Design loads are approximately equal within each truss and each column settlement was estimated less than 10 mm. Periodical records showed that the settlement was progressively worsened, causing serious concern, and at one time measured settlements were recorded from 10 mm - 250 mm under different columns. The relatively large degree of variation observed between some of the settlements can be attributed mainly to poor soil condition and scouring due to ruptured pipes.

In carrying out the investigation, an analysis of stresses due to settlement was performed. Subsequent site inspection was made to determine if any physical evidence of overstressing occurred at the connection.

The main purpose of this paper is to illustrate that actual and predicted performance are sometimes so widely different that in spite of our present analytical capabilities, our present ability to predict actual field conditions is still woefully inadequate.

LOAD AND STRESS ANALYSIS

To evaluate load settlement behavior, a computer analysis of stresses was performed for the following load combinations of dead load D, live load L, wind load W, and settlement load S: D + L + W; D + L + S; and D + L + W + S.

Using the given load data, a summary of members stress under different load combinations is listed in Table 1 and 2. Space limitations preclude inclusion of all the members herein; however, members connected to the columns with the largest or smallest settlement are included for comparison.

Comparison of data indicates stress reversals in the upper chord members (member 24 and 25) and several bottom chord members stress are exceeding its allowable stress (140 MPa). In order to determine the degree to which the results of the analysis reflected the behavior of the truss, a site inspection was conducted. Visual inspection of the top chord members has not proven that the connection angles have yielded. However, the bottom chord connection did show signs of yielding, but the amount of stress relieving is difficult to predict. Although predicted and observed conditions are not all in agreement, the calculated stresses are reasonable considering that the design loads are probably higher than the actual loads.

In order to predict the effect of continual settlement, a hypothetical condition of 130 mm increment in settlement is assumed for the column with the largest settlement. The result shown in Table 3 is a two hundred percent increase in stresses in some members. These high stresses will certainly lead to the failure of the structure.

Based on the data obtained, it can be seen that the truss was originally designed to resist vertical loads as a simple truss with the bottom chord connections to the column eliminated. The bottom chord connection is necessary, however, to resist lateral wind loading without overstressing the columns. But it is through this connected bottom chord that the truss becomes indeterminate and overstressed from excessive settlement.

TABLE 1 - Stresses (MPa) of Members Connected to the Column with Largest Settlement (250 mm)

Members designation	Loading Combinations		
	D + L + S	D + L + W	D + L + W + S
9	14.48	92.50	117.20
10	18.40	78.70	107.20
36	-177.10	4.68	-180.00
37	-166.40	-0.84	-175.80
38	1.57	96.59	3.14
39	-20.90	89.20	-25.80
40	165.80	-73.80	155.06
41	169.30	-59.70	172.64

TABLE 2 - Stresses (MPa) of Members Connected to the Column with Smallest Settlement (10 mm)

Members designation	Loading Combinations		
	D + L + S	D + L + W	D + L + W + S
3	-1.83	101.90	109.83
4	-4.66	88.60	91.96
18	57.42	-3.48	46.50
19	72.25	-3.22	56.55
20	135.76	110.59	138.85
21	108.59	91.02	101.85
22	-133.86	-87.52	-151.57
23	-132.70	-71.76	-135.07
24	90.88	0.24	82.92
25	89.04	6.66	74.67

TABLE 3 - Results of Computer Analysis of Members Stress under a hypothetical settlement Condition (380 mm)

Members designation	Loading Combinations		
	D + L + S	D + L + W	D + L + W + S
36	-424,73	4.68	-427.49
37	-414.59	-0.84	-423.69
38	-174.45	96.64	-172.85
39	-196.50	89.20	-201.33
40	508.29	-73.81	497.61
41	511.60	-59.71	515.05

REMEDIAL STEPS

To minimize further damage due to settlements the following remedial steps were recommended:

1) Repair subsurface leaks in pipes.

2) Approximate volume of grout required to fill soil void under scoured footings. Calculate pressure at the toe due to superimposed dead load, live load, and wind load from the column, existing footing, and the dead load due to the added grout.

3) If the maximum soil stress is within the allowable limits, inject grout under the footings to fill the voids created by scouring.

4) Work on one truss at a time to avoid column overstressing due to wind during construction.
   - a) Remove the rivets connecting the bottom chord to the column.
   - b) Prepare a galvanized channel C8 × 13.75 with 6 longitudinal slots 13/16"x 1 7/8" long. Roughen area of contact with bottom chord.
   - c) Clean off the paint and wire brush contact surface of the bottom chord of the truss. Weld the channel and the stiffeners to the column as shown in Fig. 2. Field drill the bottom chord in the center of the slots of the channel. Bolt the channel to the bottom chord with 6 A325-F bolts.
   - d) Weld a seat to resist the shear force from the chord connection to the column directly under the top chord connection and shim with flat plates under the connection to provide bearing against the new seat as shown in Fig. 2.

CONCLUSION

The failure to include settlement estimation in the analysis can lead to serious error in determine the stresses in the members and its connections.

In lieu of any further leaks and excessive settlement the repaired structure should adequately resist the original design live and wind loads. The connection should slip prior to overstressing the truss members if there are further relative small settlements. However, the loads induced by the wind will be resisted by the friction developed in the connection.

The grouting of the footing should not induce loading beyond the allowable stress limits of the supporting soil, and grouting will facilitate replacement of footing bearing material with a minimum of interference to existing machinery, pipes and plant operations.

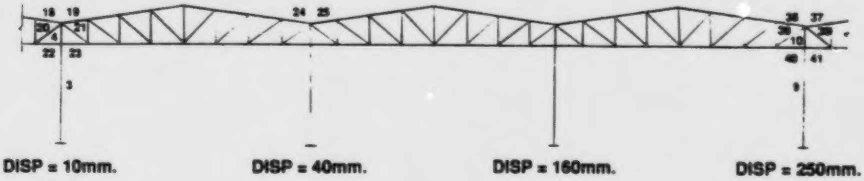

Fig. 1. Multi-bay Continuous Truss

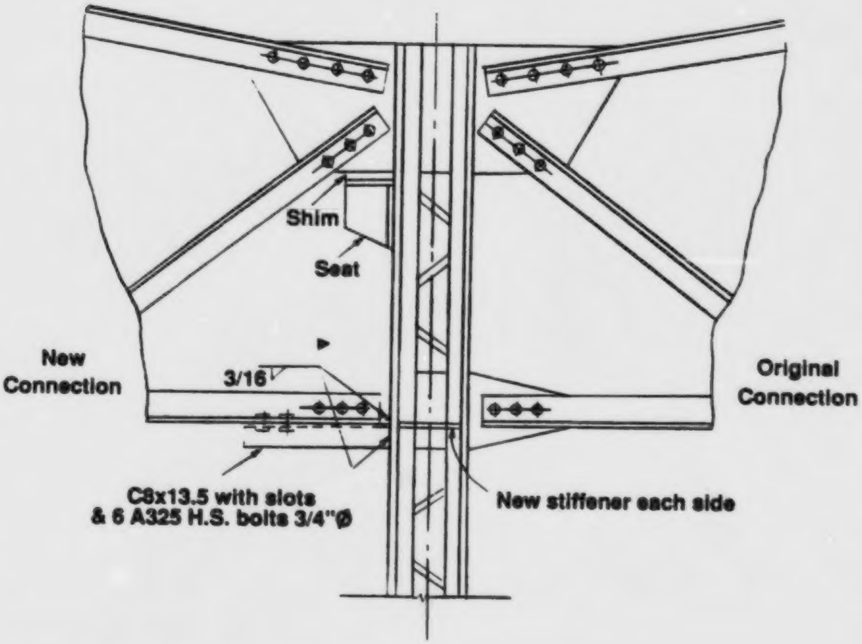

Fig. 2. Revised Connection Design

INVESTIGATION OF THE SERVICE TOWER MOVEMENTS AT THE JOCK HARDY ARENA

Stephen Robins, P. Eng.
McNeely Engineering and Structures Limited
Kingston, Ontario

ABSTRACT: This case study consists of the results of an investigation made into the movements of the service towers located on the perimeter of Jock Hardy Arena at Queen's University, Kingston.

The service towers have been pushed away from the main building structure resulting in significant cracking of the masonry in the towers. The forces causing the movement have arisen from frost action in the concrete roof slab and at the perimeter of the slab.

Arresting the movement will involve sealing the roof to prevent further penetration of water or alternatively, the construction of a new roof over the existing.

1. INTRODUCTION

The Jock Hardy Arena is part of the Physical Education Building complex at Queen's University, Kingston. The arena is approximately 71 metres (m) in length by 42 m in width (see Figure 1). The overall height is approximately 16 m. Tennis courts are located on the roof.

The roof is comprised of triangular steel trusses supported on steel beams and columns. The steel roof deck over the trusses supports a roofing membrane, insulation, a 100 millimetre (mm) thick concrete slab and two asphalt topping courses. The overlay was replaced approximately 5 years ago.

On the north, east and south sides of the building, stair and service towers are located on the perimeters. These towers are essentially of block masonry construction with a face stone veneer.

Since the arena's construction in 1969, there have been ongoing problems with the building in the form of cracking of block and stonework in the towers, cracking of interior floor slabs and leakage of water through the roof.

This paper examines the movements which have occurred in the towers and the problems of water leakage through the roof

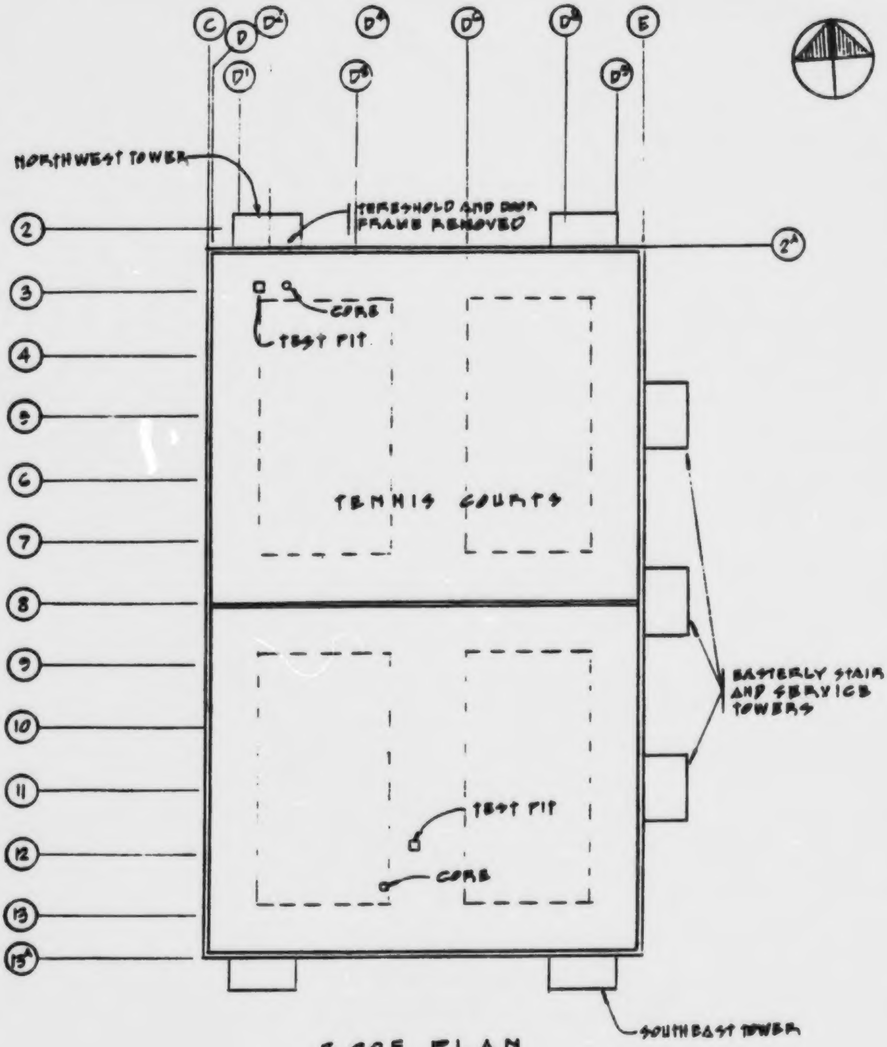

ROOF PLAN
SCALE 1" = 40'-0"

QUEENS UNIVERSITY
PHYSICAL EDUCATION BLDG.

FIGURE No 1

2. FIELD INSPECTIONS

Significant movements have occurred in the building stair and service towers. The northwest tower has moved significantly to the north with a maximum movement the order of 28 mm. It appears that this has been an ongoing movement since the shifted stonework on the exterior has been repointed, reportedly the order of 10 years ago and the repointing is now loosened with further movements. The nature of the movement indicates that the top of the tower has been pushed outward at roof level causing it to rotate about a line on the exterior wall at the mid second floor level. This rotation has been so great that the resultant stresses in the masonry at the line of rotation at the northeast corner of the tower have reached the crushing strength of the masonry and the tower has shifted laterally outwards at this corner. This behaviour is shown diagrammatically in Figure 2. The tower, at the northeast corner of the building, has rotated about a similar line through the exterior tower wall, but failure of the masonry along this line has not yet occurred. The tipping out of the top of the tower at this location is the order of 60 mm.

Horizontal measurements taken on the southerly towers indicated that the towers have translated laterally as opposed to a rotation about the base as observed for the northerly towers. Measurements, using the exterior fabric of the main building as a reference line, to indicate that these towers have translated laterally the order of 12 mm.

The stairwell and service towers on the east side of the building exhibit cracking in the masonry walls, but it is not as severe as noted in the north and south towers.

Where the stairwells exit onto the main roof, a depression in the perimeter parapet wall was made to eliminate stepping over the parapet to get to the tennis courts. The flashings in this depression have been repaired frequently with not much success and water is readily entering the block walls at these locations. Besides resulting in paint peeling and efflourescence of the blockwork below the landing, freeze-thaw cycling has occurred in the top one to two courses of blockwork in which the stair landing is supported and this, in turn, has loosened the landing and pushed it toward the interior of the stairwell by as much as 12 mm.

3. DISCUSSION

Movements of the perimeter towers are considered to be a result of imposed thrusts at roof level. Foundations are founded on bedrock and movements due to foundation settlement are therefore most improbable.

The tower movements infer that thrusts are being imparted to the towers through some action in the roof slab. Three phenomena are possible; thermal movements, expansive aggregate in the roof slab concrete, or frost action.

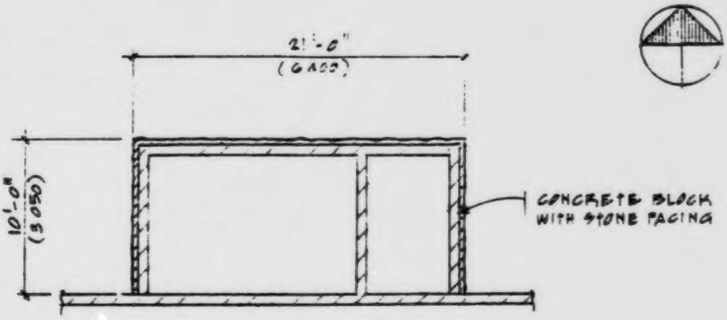

SECTIONAL PLAN (TOWER)
SCALE 1/8"=1'-0"

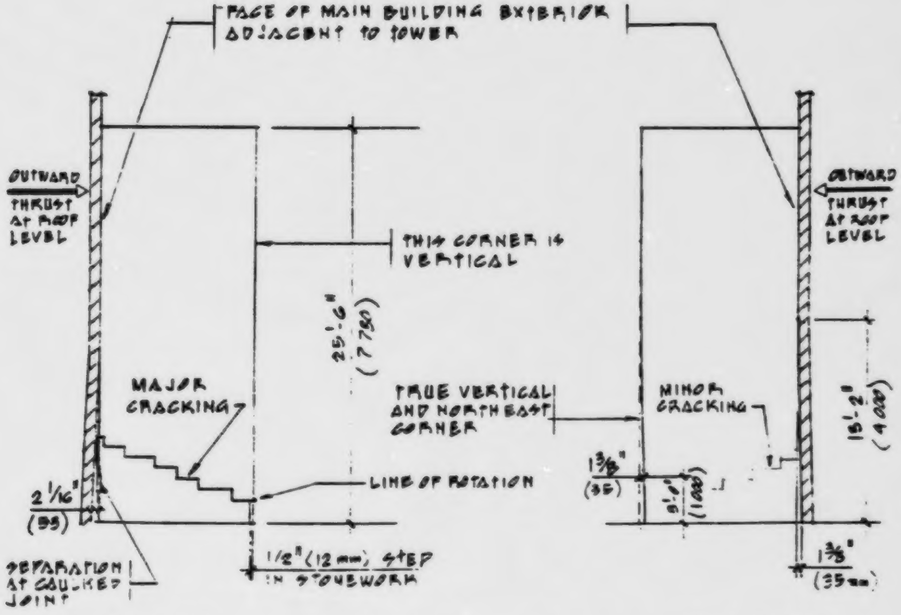
FACE OF MAIN BUILDING EXTERIOR ADJACENT TO TOWER
OUTWARD THRUST AT ROOF LEVEL
OUTWARD THRUST AT ROOF LEVEL
THIS CORNER IS VERTICAL
25'-6"
(7750)
MAJOR CRACKING
TRUE VERTICAL AND NORTH EAST CORNER
MINOR CRACKING
15'-2"
(4000)
LINE OF ROTATION
2 1/16"
(55)
1 3/8"
(35)
3'-0"
(1000)
1/2" (12 mm) STEP IN STONEWORK
1 3/8"
(35 mm)
SEPARATION AT CAULKED JOINT

EAST FACE ELEVATION WEST FACE
SCALE 1/8"=1'-0"

QUEENS UNIVERSITY
PHYSICAL EDUCATION BLDG
MEASURED DEFORMATIONS
AT NORTHWEST TOWERS

FIGURE No 2

3. DISCUSSION (Continued)

Theoretical thermal movements are of the order of 9 mm for the long (north-south) direction of the roof and approximately a third of this for the short (east-west) direction. Observed movements are of the order of 28 to 60 mm at the north end of the building and 12 mm at the south end of the building. Certainly these are much greater movements than could be produced by thermal effects and, in addition, one would expect to see a form of "mirror image" cracking which would result from the cyclic nature of thermal effects. This was not observed and it is probable that the movements have not occurred as a result of temperature expansion.

Test pits through the asphalt overlay and cores through the concrete slab were taken to check the integrity of the slab as well as the possibility of the presence of reactive aggregates.

The concrete core specimens do not exhibit any crazing, rimming of aggregates or disruption indicative of an aggregate reactive problem.

At each test pit location, which was selected to coincide with cracks in the asphalt overlay, the crack in the asphalt overlay is a reflection of the crack in the underlying concrete slab. Of particular significance is the condition of the concrete adjacent to the crack. Freeze-thaw action has resulted in significant deterioration of the concrete for approximately 100 millimetres on either side of the crack. This concrete could be removed easily and little or no bond remained between the aggregates. The fact that freeze-thaw action is occurring in the cracks, suggests that the imposed thrusts to the towers may be in part, or wholly, due to a cumulative effect of freez-thaw action at the cracks. There are presently a large number of visible reflection cracks in the asphalt overlay, and probably many others in the slab not visible due to the application of the relatively new overlay, and the summation of these crack widths can easily approach a value of 25 to 50 mm, the magnitude of movements observed at the towers.

In combination with freeze-thaw action at cracks in the roof slab, water penetration through the roof at the exterior walls which in turn freezes could result in thrusts to the towers. At the perimeter curb of the roof slab, the roofing membrane is turned up between the outside face of the curb and the inside face of the exterior block wall. Water leaking in from the parapet above would be trapped in the pocket formed by the membrane turning up. Since there is no thermal protection at this level, the water would freeze and expand. With alternate freeze-thaw cycles and further ingress of moisture, the expansion outwards would be cumulative.

4. CONCLUSIONS

The absence of aggregate reactivity in the concrete roof slab, and the fact that computed thermal movements are much less than the tower movements observed, means that the thrusts to the towers in the roof slab are a result of freeze-thaw action in the roof slab at the perimeter of the slab and in cracks throughout the slab.

Repairs to the building should therefore be directed primarily at sealing the roof structure to prevent further ingress of moisture. Alternatively, a new roof could be placed over the tennis courts and moisture penetration would again be eliminated.

SESSION E/SÉANCE E

VIBRATIONS FROM HUMAN ACTIVITY/ VIBRATIONS CAUSÉES PAR L'ACTIVITÉ HUMAINE

PRACTICAL CASES OF STRUCTURES WITH MAN-INDUCED VIBRATIONS

Hugo Bachmann
Institute of Structural Engineering (IBK)
Swiss Federal Institute of Technology (ETH) Zürich
Switzerland

ABSTRACT: Man-induced vibrations in structures can lead to serious problems to the extent to render a structure unserviceable. At the beginning of this paper, the following points, important for the objective of avoiding excessive vibrations, are considered: major parameters, possible countermeasures, classification of structures with man-induced vibrations, representative types of motion and dynamic loads, and frequency tuning. Then, case reports of footbridges, gymnasia and sports halls, dance halls and concert halls without fixed seating, concert halls with fixed seating and high-diving platforms are presented. In some cases, existing buildings had to be upgraded. In other cases, where structures were still in the planning stage, significant modifications to the design were necessary.

1. PRELIMINARIES

Lately, man-induced vibrations in structures have caused serious problems. Only recently has it become possible to establish guidelines on how to avoid problems of man-induced vibrations [1,2]. While some theoretical considerations did play a role, experience and understanding of the phenomena were gained, however, through practical case studies. Most important were tests, carried out in situ before and after rehabilitation of a structure.

Before describing such practical cases, attention is drawn to some general characteristics.

1.1 Major parameters: In the case of vibrating structures the following parameters dominate the dynamic behaviour

- dynamic loads
- dynamic system
- dynamic bending stiffness
- damping

These four parameters govern the structural response. In existing structures, response can mostly be measured. For structures in the planning stage, the structural response can only be predicted and this represents a much more difficult task.

Sufficient knowledge of these four major parameters is vital for conceiving anti-vibration measures.

1.2 Possible measures: Three classes of measures can be distinguished with reference to the forementioned major parameters:

- Frequency tuning of the structure, based on the loading frequency, i.e. the spectrum of Fourier amplitudes of the dynamic load. For frequency tuning beside of the load-time function the dynamic system and the dynamic bending stiffness are also important, whereas damping is less important.
- Calculating the forced vibration of the structure and comparing the amplitudes to certain acceptance criteria. For the calculation of a forced vibration, the load-time function, the dynamic system, the dynamic bending stiffness and especially the damping are important.
- Taking special measures such as, for instance, general stiffening of the structure, increasing the damping, installing tuned vibration absorbers, or, instead, restricting the use of the building or facilities.

Depending on circumstances, these measures can differ greatly in potential, their feasibility and expenditure.

1.3 Classification of structures with man-induced vibrations: Based on the various dynamic loads and the countermeasures applicable, structures affected by man-induced vibrations can be grouped as follows:

- pedestrian structures
- office buildings
- gymnasia and sports halls
- dance halls and concert halls without fixed seating
- concert halls with fixed seating
- high-diving platforms in swimming pools

Man-induced vibrations are primarely a problem of serviceability, in terms of annoying or disturbing the respective users. On pedestrian structures and high-diving platforms the causative person himself may feel disturbed, whereas in other buildings only users not directly involved in creating vibrations are affected. In rare cases, a safety problem may arise, i.e. the stability of the structure is at risk. A detailed description of serviceability and safety problems of man-induced vibrations in structures is given in the book [1].

1.4 Representative types of motion and dynamic loads: Knowing the dynamic loads is the basis to the understanding of the vibration phenomena. This understanding allows measures to be taken to reduce vibrations. The innumerate variances of rhythmical human body motions constitute a large variety of possible dynamic loads. Of those, rhythmical motions often performed to music by several people at the same time synchronising their movements have to be especially considered. When lasting up to 20 seconds or more, they lead to almost periodic loads resulting in more or less steady-state structural vibrations. Although the loads differ in their dominant frequencies and their load-time function, they can be grouped into the following representative types of motion and the corresponding dynamic loads:

- walking
- running
- jumping
- dancing
- clapping

One can say that until recently the understanding of the dynamic loads induced by man was very limited. Calculations were based on a single harmonic function of the basic loading frequency (e.g. the pacing rate). Over the last few years, however, incidences of structural inadequacies shed light on the contribution of upper harmonics (as part of the Fourier decomposition of the loading function), which may become critical for the dynamic design of a structure [1,2,3].

1.5 Frequency tuning: The simplest countermeasure, which proved efficient in numerous practical cases, is frequency tuning of the structure. The structural frequency, mostly the fundamental natural frequency, has to be established with regard to the most critical frequencies of the load-time function. This is quite often not the nominal loading frequency itself, but the frequency of an upper or lower harmonic in the spectrum of the load-time function.

The following criteria can be used for frequency tuning in the forementioned structural classes:

- Pedestrian structures:
  Avoidance of the 1st and 2nd harmonic of the dynamic load due to "walking".

- Office buildings:
  High-frequency tuning with respect to the 3rd harmonic of the dynamic load due to "walking".

- Gymnasia and sports halls:
  High-frequency tuning with respect to the 2nd harmonic of the dynamic load due to "jumping" (see [1]).

- Dance halls and concert halls without fixed seating:
  High-frequency tuning with respect to the 2nd harmonic of the dynamic load due to "dancing" (see[1]).

- Concert halls with fixed seating:
  High-frequency tuning with respect to the 1st harmonic due to "clapping" [4]. In structures with low damping, the frequency of the 2nd harmonic of the same load should be considered (avoidance or high tuning).

- High-diving platforms in swimming pools:
  Consideration of special frequency and stiffness criteria (see [1]).

On determining the frequency bounds for different structural types, the accurate stiffness, mass and damping have to be taken into account.

The above mentioned criteria together with a general consideration of the properties of the different structural types lead to the recommendations for eigenfrequencies given in Table 1 (fundamental and higher frequencies). Observing these frequency bounds should in most cases result in adequate dynamic performance.

Table 1: Recommendations for the eigenfrequencies [Hz] of structures with man-induced vibrations

Structural type / Structural class	Reinforced concrete	Prestressed concrete	Composite steel-concrete	Steel
Pedestrian structures	Avoidance of 1.6 to 2.4 Hz and 3.5 to 4.5 Hz			
Office buildings	> 7.5	> 8.0	> 8.5	> 9.0
Gymnasia and sports halls	> 7.5	> 8.0	> 8.5	> 9.0
Dance halls and concert halls without fixed seating	> 6.5	> 7.0	> 7.5	> 8.0
Concert halls with fixed seating	> 3.4			

In the following, several practical cases are described. Some cases deal with existing structures most of which had to be upgraded. The other cases are projects, the design of which had to be substantially modified. In most cases, the above frequency criteria became relevant.

2. FOOTBRIDGES

2.1 Footbridge of ~ 2 Hz: A 4 m wide footbridge was planned to cross a canal over a total length of ca. 91 m, divided into three spans of 25.7 m - 40 m - 25.7 m, Figure 1a. The U-shaped cross-section is made up from a ~ 20 cm thick slab and two 40 cm thick parapet walls of 1 m inner height, topped by a 30 cm high metal non-loadbearing metal railing. Above the intermediate supports, the slab is

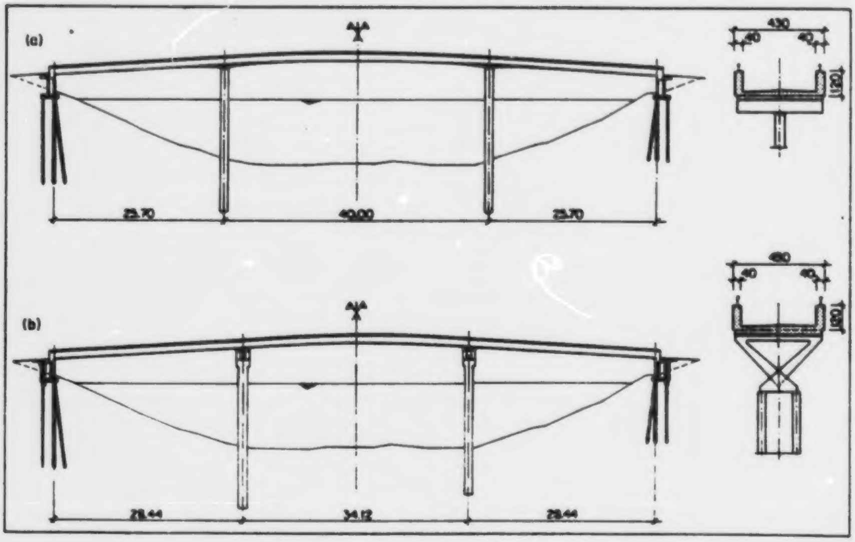

Figure 1: Project of a footbridge before and after dynamic calculations

haunched to 40 cm. The girder will be prefabricated in 3.5 m segments and assembled on the site with resin joints and post-tensioned by means of longitudinal prestressing cables.

During the design, the dynamic behaviour was calculated, and the fundamental frequency was found to be ~ 2.0 Hz. A forced vibration was calculated, estimating the damping ratio to 0.5% of critical, a value which was found in similar structures. For a mean flow rate of 20 pedestrians per minute an acceleration of ~ 8% g was obtained (after [1]). As the acceleration in footbridges should not much exceed 5% g and peak flow rate could well be higher, design modifications were envisaged to reduce the proneness to vibration.

The following measures were examined:

- increasing the height of the parapet walls
- making a much heavier railing part of the load-bearing structure
- further haunching of the slab over the intermediate supports
- changing the ratio of spans.

Heightening the parapets or thickening the slab seemed aesthetically undesirable. Stiffening of the bridge by the railing was kept as a last resort for post-constructional upgrading. Hence the lengths of the spans were altered from 25.7 m - 40 m - 25.7 m to 28.44 m - 34.12 m - 28.44 m, Figure 1b. This raised the calculated fundamental frequency to ~ 2.4 Hz and reduced the acceleration at 20 persons/minute to ~ 4% g. In addition, the structural detailing provided for a certain encastrement of the girder in the piers.

The bridge is going to be built in the spring of 1988. After completion, dynamic tests will be carried out and the results compared with the design calculations.

2.2 Footbridge of ~ 4 Hz: When a steel footbridge showed noticeable vertical vibration, its frequency and amplitude were measured during normal evening peak traffic [1]. The number of people crossing varied between 30 and 55 per minute. It became obvious that the bridge vibrated predominantly in its fundamental frequency of about 4 Hz. This was excited by the second harmonic of the load-time function with a pacing rate frequency of about 2 Hz.

2.3 Footbridge of ~ 1.1 Hz lateral: During the opening ceremony, about 300 to 400 persons moved across a new steel footbridge which was excited to strong lateral vibration [5]. Figure 2a shows the structural system of an S-shaped continuous girder over several spans, of which the main of 110 m is suspended from an angular arch. The intermediate supports of the girder are centric pivot joints.

Figure 2b gives the first mode shapes for lateral vibration, Figure 2c is a double-logarithmic plot of the transfer function for the lateral displacement amplitude in the center of the main span, calculated for stationary excitation over the length of the main span and a damping ratio of 0.5%.

The frequency of the lowest lateral mode is in the range of ~ 1.1 Hz and thus very close to half the mean pacing rate at ~ 2 Hz, producing an almost resonating vibration. Moreover, it could be supposed that in this case the pedestrians synchronized their step with the bridge vibration, thereby enhancing the vibration considerably (as described in Section 2.2.1 in [1]).

Upgrading was achieved by tuned vibration absorbers to be effective in the lateral direction.

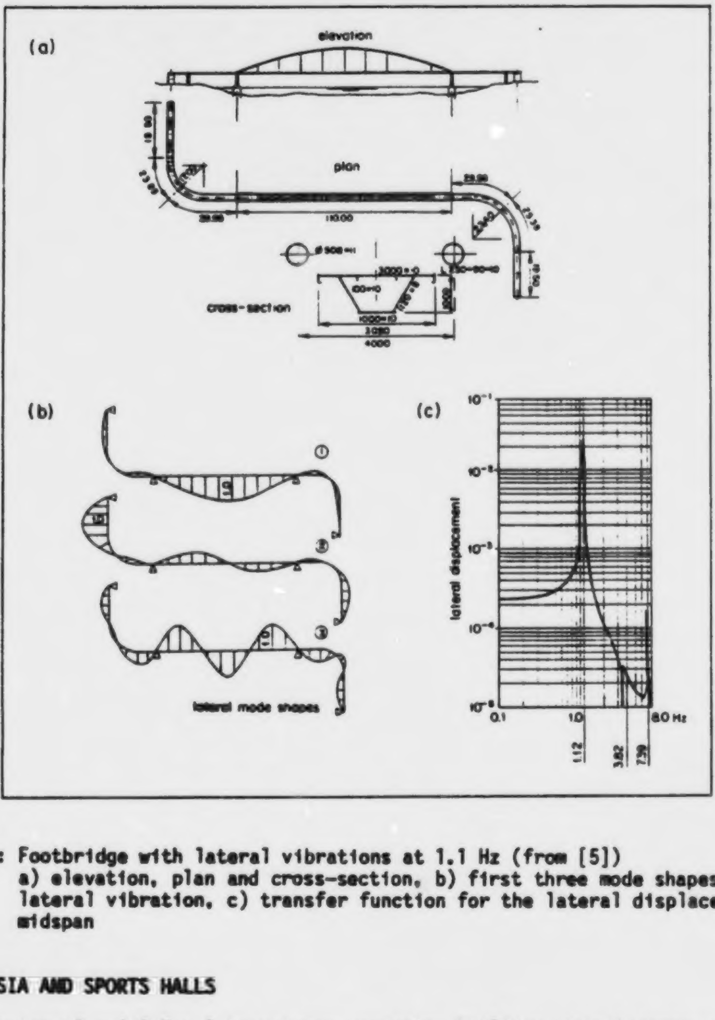

Figure 2: Footbridge with lateral vibrations at 1.1 Hz (from [5])
a) elevation, plan and cross-section, b) first three mode shapes of lateral vibration, c) transfer function for the lateral displacement at midspan

3. GYMNASIA AND SPORTS HALLS

3.1 Gymnasium of ~ 4.9 Hz: A two-storey gymnasium building showed severe vibrations soon after its opening [6]. They occurred regularly whenever the upper hull was used by modern-style fitness classes, performing jumping and running exercises to strongly rhythmic music. They became manifest mainly in the lower hall, where the vertical swinging of the intermediate floor under the direct loading due to the fitness class was clearly noticed and where the glazed exterior walls vibrated horizontally. The secondary effects were also rather dramatic: rattling of the entrance doors and the shutters to the apparatus store-room, clattering of equipment attached to floor and walls, and a strong, alternating draught due to compression and decompression of the air volume in the lower hall, which one could feel when standing near the open entrance door. Several times these combined phenomena caused people to leave the lower hall hastily during fitness classes going on above.

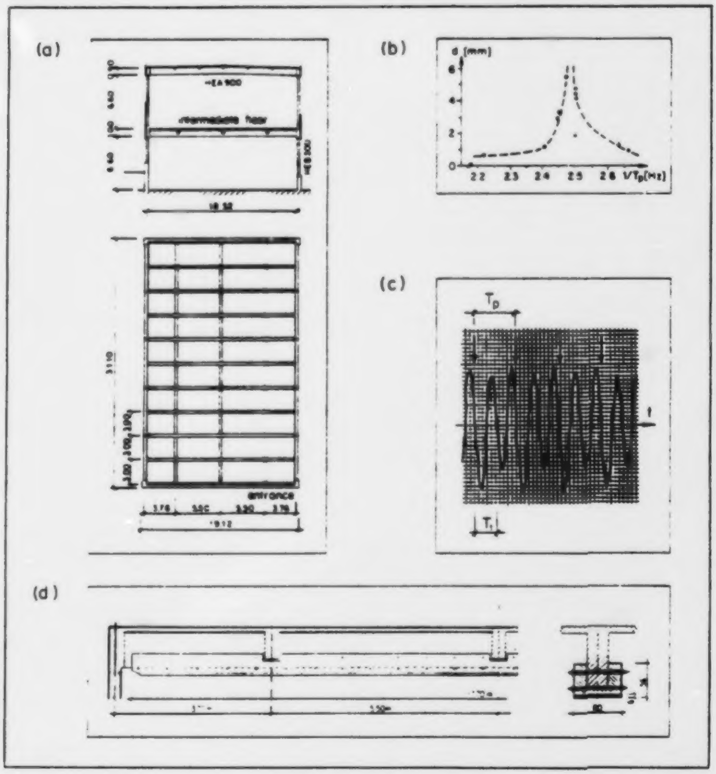

Figure 3: Two-storey gymnasium hall (from [6]:)
a) cross-section of building and plan of the intermediate floor
b) resonance curve of displacements
c) detail of the displacement plot with the supposed incidents of loading with period T_p and structural period $T_1 = T_p/2$

d) elevation and cross-section of the upgrading carried out

Figure 3a shows the building in plan and section. The intermediate floor is constructed as reinforced concrete beams of 1 m height, 18.5 m span, and at 3 m spacing. They rest on edge beams supported by steel columns at 6 m intervals.

The dynamic properties of the floor and the magnitude of loading were measured during controlled tests in which fitness classes of up to 130 participants were instructed to perform various exercises at specified frequencies, synchronized by the loadspeaker amplified beat of a metronome.

Resonance curves were evaluated for approximately 20 seconds from jumping exercises with frequencies varied from 2.0 to 3.2 Hz (Figure 3b). The strongest vibration occurred at ~2.48 Hz. Since the fundamental frequency of the floor was ~ 4.9 Hz, resonance was excited by the 2nd harmonic of the load-time function as though the gymnasts were loading the floor on every other downward swing (with a certain phase shift) (Figure 3c). The peak amplitudes were measured to ± 5.5 mm vertical displacement, ± 167 mm/s corresponding velocity, and 5.15 m/s^2 acceleration, i.e. 52% g (!).

The damping ratio was determined as 2.4% of critical damping by measuring the vibration decay after a commanded sudden standstill of the group. (The damping ratio would have been smaller without people on the floor.)

Upgrading of the structure was imperative because the high stress level entailed the risk of fatigue deterioration of the reinforcing steel and of other damage; moreover, the serviceability was much reduced as in the upper hall fitness classes with the usual number of participants would have to be discontinued.

In order to avoid resonance with the 2nd harmonic of all possible load-time functions, the fundamental floor frequency had to be brought to some 7.5 Hz. The beams were stiffened by adding a bottom flange made of a steel plate 800 mm x 60 mm and two side plates and filled with concrete. For a good bond the surface of the concrete beam was chipped ans the flange with the concrete infill pressed against the beam by means of prestressed cross-bolting (Figure 3d).

New excitation tests with fitness classes as before yielded a much reduced vertical displacement amplitude of ± 0.3 mm, i.e. only 5% of the value prior to upgrading, and did not produce resonance. The new fundamental frequency was measured to 7.3 ± 0.1 Hz and the damping ratio to 2%. As this was done in a drop-test with a 100 kg sandbag from a height of 1.8 m, this damping value cannot directly be compared to the previous one, in which many more people were on the floor. Further details, discussion of theory and upgrading variants can be found in [6].

3.2 Gymnasium of ~ 5.2 Hz: A two-storey gymnasium showed severe vibrations of the intermediate floor caused through normal gymnastics, especially rhythmical exercises. These vibrations were disturbing and raised doubts about the safety of the floor.

The floor is a ribbed slab of reinforced in-situ concrete, spanning an area of ca. 15 m x 27 m. The load is carried across the short span by 0.15 m thick and 0.46 m high ribs spaced about 0.65 m apart. On one side, along the glazed front of the building, the ribs are indirectly supported via an edge beam by slender columns, which provides virtually no rotational restraint; on the opposite side, the ribs are fixed rigid in the concrete walls and adjacent floor slabs.

In order to determine the dynamic behaviour of the floor, drop tests were performed as well as resonance excitation by jumping and running of schoolchildren from two classes. A total of 34 pupils, aged about 14 years, carried out a standard test of jumping on the spot synchronized by a metronome with frequencies

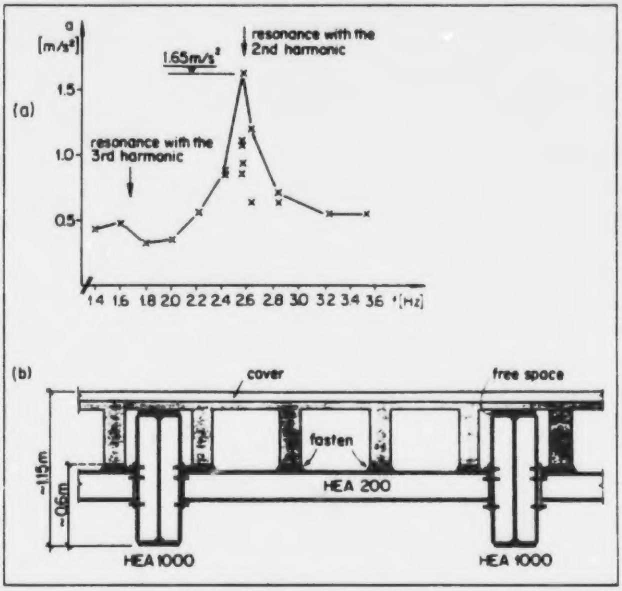

Figure 4: Gymnasium floor; a) resonance curve from jumping exercises
b) section of the upgraded structure

between 1.4 and 3.5 Hz. This way, the frequency response curve of Figure 4a was obtained. The strongest vibration resulted from jumping at 2.58 Hz. The fundamental frequency of the floor was 5.15 Hz. Thus resonance was excited by the 2nd harmonic of the load-time function or - figuratively speaking - pupils exerted a thrust in (shifted) phase with every second downward swing of the floor. However, Figure 4a shows another resonance with the 3rd harmonic, which time did not permit to explore further. The peak amplitudes obtained were ± 50 mm/s velocity and ± 1.65 m/s² acceleration.

The damping ratio was determined to 3% of critical, which is fairly high for gymnasium floors. It was derived from a sudden stand-still of the jumping pupils, so that the decaying vibration could be monitored. Because the pupils standing on the vibrating floor provided extra energy dissipation, the damping ratio of the unloaded floor must be expected to be smaller than the 3% measured.

Serviceability of floors in gymnasia limits acceleration to 5% g, at most 10% g. Since the respective gymnasium is used by adults as well, and may host a larger number of participants than in the tests, the owner of the facility decided to upgrade the structure. The fundamental frequency of the floor was to be raised to about 7.5 Hz [1]. Out of six alternatives, two seemed equally cost-effective: (a) to demolish the existing floor and to replace it with a prestressed concrete joist floor, and (b) to install a steel girder grid as supporting structure underneath the existing floor. It was decided to use option (b) for its shorter construction time, although it reduces significantly the clear height of the lower hall. Figure 4b gives a cross-section of the upgraded floor.

Post-rehabilitation tests were carried out again with jumping on the spot, this time by a group of 51 pupils, aged about 15 years, who were lined up in the relevant central area of the floor at a high density of one person per 2 m^2 [1]. The fundamental frequency of the upgraded floor was measured to ~ 7.47 Hz, the damping ratio from decay measurements was 3.2%. The fundamental frequency could be excited to resonance by both the 3rd and 4th harmonic of the load-time function, i.e. with jumping frequencies of ~ 2.5 Hz and ~ 1.9 Hz. Associated peak accelerations were 0.74 m/m^2 and 0.60 m/s^2, respectively. Thus they do not exceed the upper bound of 5 to 10% g. The calculated displacement and acceleration (according to [1]) overestimate the experimental results by about 10%.

3.3 Sports hall adjacent to grandstand of ~ 2.4 Hz: The design project of a large two-storey sports hall involved 3 m high and 42 m spanning prestressed concrete beams [1]. On one side, the columns had also to support a grandstand (Figure 5a). For a first assessment of the vibrational performance under rhythmic excitation as during fitness classes, dynamic calculations were applied to a simplified but conservative model structure (Figure 5b) and yielded a fundamental frequency of ~ 2.4 Hz. The low value was mainly due to a very adverse contribution of the horizontally swinging grandstand mass. For the resonance case of the excitation frequency being equal to the structural frequency, a forced vibration computation (according to [1]) with 1% damping and a user density of one person jumping per 4 m^2 indicated amplitudes of ± 34 mm displacement, ± 560 mm/s velocity, and 8.6 m/s^2 (!) acceleration. The high stress level was expected to lead to damage or even structural collapse. Therefore, one had to consider substantial design modifications and strengthening with the goal of reaching a fundamental frequency of the floor of about 8 Hz.

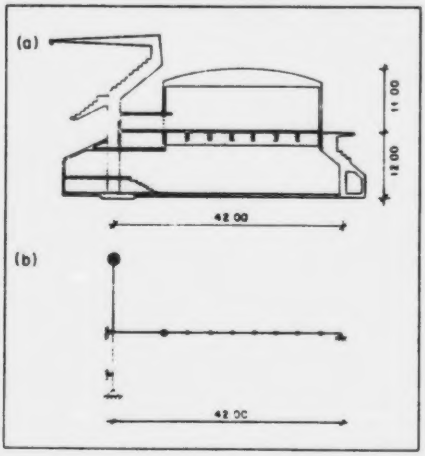

Figure 5: Sports hall connected to grandstand:
a) cross-section, b) simple dynamic model

4. DANCE HALLS AND CONCERT HALLS WITHOUT FIXED SEATING

4.1 Concert hall without fixed seating of ~ 6.2 Hz: A medium-size hall of 32.8 m x 55 m area exhibited strong floor vibration during pop concerts [1]. These events were attended by up to 4000 people, a part of the audience was always enthused to activities such as clapping of hands, body rocking or light bouncing up and down to the music. Several hall areas without fixed seats brought about differences in density of the audience with a particular grouping (estimated up to a maximum of 6 persons per m^2) towards the stage whenever the musicians were on show.

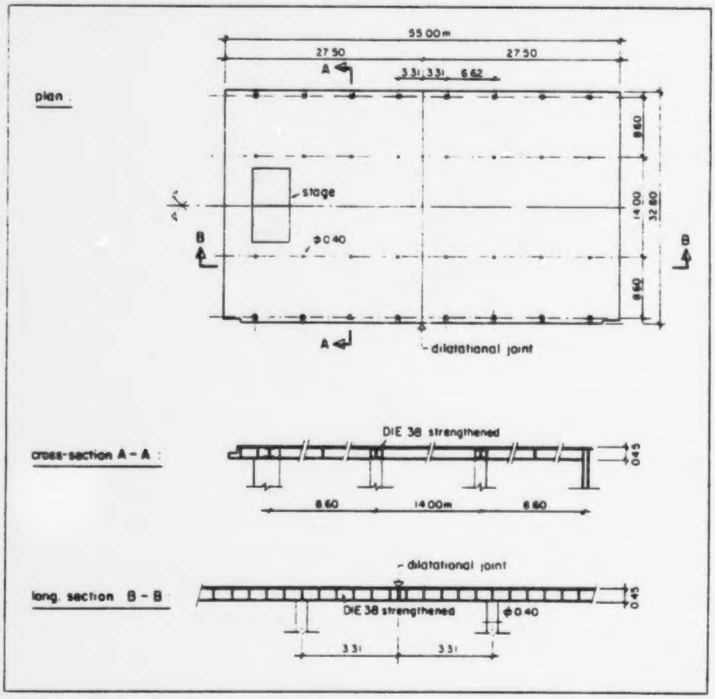

Figure 6: Concert hall with hallow-cast floor structure (from [1])

The plan and the sections of the floor structure in Figure 6 reveal a hollow-block slab of 0.45 m thickness and about 450 kg/m^2 mass. The floor is supported by two rows of columns spaced 6.62 m apart, across which runs in longitudinal direction an internal joist (a cast-in strengthened steel section DIE 38). The structural action can thus be described as a predominantly crosswise-spanning continuous plate over three openings of 8.6 m/14 m/8.6 m. The floor is bisected by a dilatational joint. Designated originally as an exhibition hall, the building had merely been designed for static loads, so that the new problems are to be attributed to the unanticipated utilization for concerts.

Measurements were made at several concerts, showing that the vibration intensity depended more or less on the kine of music influencing the activities of the audience, and on its beat frequency. For example, soft pop music (Band "Simple Minds") with a beat frequency ≈ 2.0 Hz ÷ 2.5 Hz and 3500 relatively quiet spectators yielded at a beat frequency of ≈ 2 Hz ÷ 3 Hz a peak vibration amplitude of ± 4.6 mm vertical displacement and ± 1.66 m/s^2 acceleration. During hard rock music (Band "Status Quo"), however, with a beat frequency of ≈ 2.1 Hz ÷ 3 Hz and an audiance of about 200C (of which about one third was quit electrified), the displacement at a beat frequency of ≈ 2.1 Hz reached ± 9.5 mm, the peak velocity ± 177 mm/s and the maximum acceleration 2.7 m/s^2.

When excited by a local impulse, the unloaded floor showed a fundamental frequency of ~ 6.2 Hz. Dynamic loadings on a larger area would probably bring out the inherent structural action in the crosswise direction of the building and - with the additional mass of the audience - a fundamental frequency in the range of double the beat frequency of the music (~ 4.0 Hz ÷ 4.5 Hz). This indicates a resonance-like excitation of the fundamental frequency of the structure, as found for the gymnasium floor described under 3.1, by the 2nd harmonic of the audience's bouncing-time function.

The measured vibration magnitudes and concluded stressing of the floor exceeded the admissible values by far so that the hall had to be closed for pop concerts. For upgrading, the floor would have to be supported by additional beams in the cross-direction, or temporary props would have to be fitted and removed before and after every concert if the use of the lower storey was not to be greatly restricted. Finally, the discussion became inconsequential as another location for such concerts was found with a much higher floor frequency of about 12 Hz (unloaded).

5. CONCERT HALLS WITH FIXED SEATING

5.1 Concert hall with fixed seating of ~ 2.5 Hz: The floor of a concert hall with approximately 2000 seats span on an area of about 40 m x 40 m. The floor vibrated considerably whenever the audience clapped their hands rhythmically (seated or standing up). This phenomenon is quite common in pop-concerts while clapping in rhythm to the music or demanding encors. It may also occur in classical concerts when clapping to a piece like the Radetzky March by Strauss. The floor in question had a measured fundamental frequency of ~ 2.5 Hz (unloaded), which dropped to ~ 2.4 Hz due to the audience present; this corresponds to a usual rhythm or clapping frequency. Dynamic loads due to clapping are usually of minor importance [4]. In this case, however, the audience was able to excite the floor to near-resonance by clapping with the natural frequency of the structure (1st harmonic of the load ≈ 1st structural frequency).

As no plausible magnitudes for the dynamic load were available, special experiments had to be carried out. Figure 7 shows the load-time function and the Fourier amplitude spectrum of the dynamic load exerted by a seated person clapping hands. Figure 8 shows the Fourier amplitudes of the different harmonics created through various ways of rhythmical clapping (after [4]).

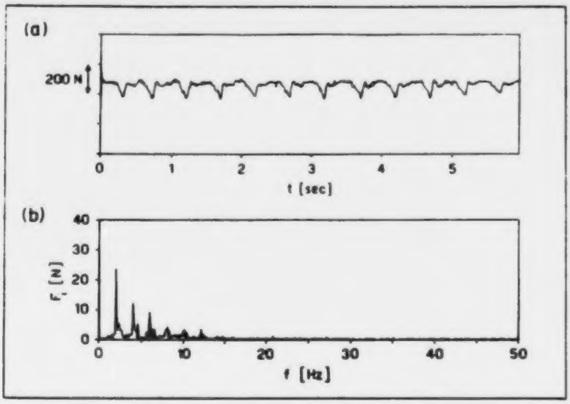

Figure 7: Load-time function of the dynamic load (a) and Fourier-amplitude spectrum (b) created through rhythmical hand clapping (2 Hz) by a person being seated (from [4])

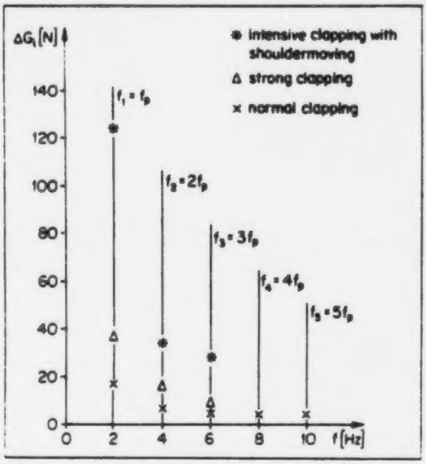

Figure 8: Amplitudes of harmonics created through various types of hand clapping (2 Hz) (from [4])

6. HIGH-DIVING PLATFORMS

6.1 Diving platform with torsional vibrations: The shaft of a 3 m and a 5 m platform showed intolerably large twisting vibration soon after completion [1]. The two reinforced-concrete platforms are each supported by two steel columns with cantilever beams, resulting in an excentric layout of the facility with the four columns forming the corners of an open rectangular shaft. The columns were braced horizontally only near the foundation. The design engineer, although he had calculated the fundamental bending frequency and had found it uncritical, must have overlooked the low torsional rigidity of his design. Subsequently, two concrete wall members were erected between the foundation and each platform parallel to the flights of stairs, combining an architecturally satisfying solution with a much improved dynamic behaviour.

6.2 Diving platform of ~ 2.8 Hz: A reinforced concrete diving platform has two slabs at 3 m and 5 m elevation, supported by a Y-shaped shaft (Figure 9).

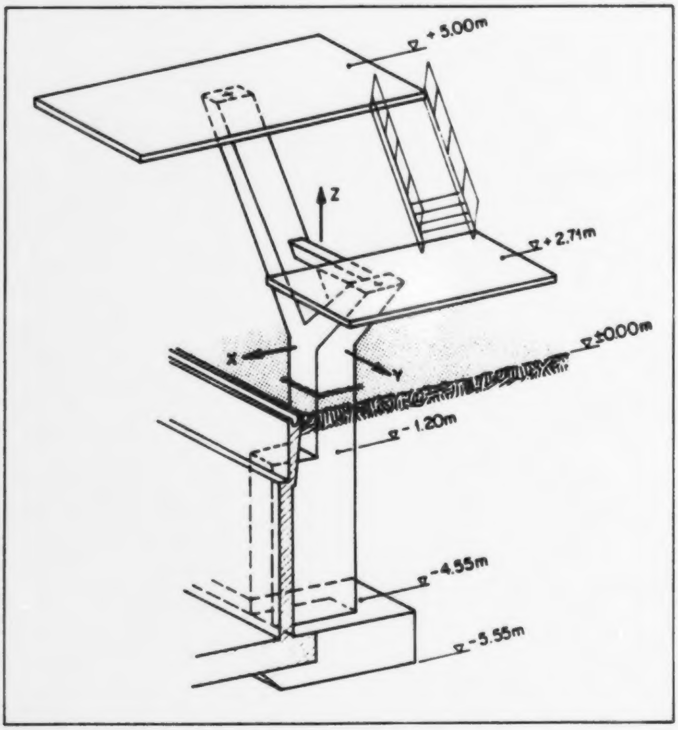

Figure 9: Diving platform

The shaft arms are connected by a tie-beam at the height of the lower slab. Below the ground the shaft is joined to the wall of the pool from the foundation base upwards to 1.20 m below surface. The lower slab is equipped with a soft springboard.

During normal use, irritating vibrations were felt when diving off the springboard. Moreover, the entire platform could deliberately be excited by jumping on the upper slab or rhythmical pushing and pulling on its railing ("vandal loading" by youngsters). Because of the frightening amplitudes thereby obtained, the owner of the facility became concerned about long-term deterioration of the structure. The Swiss Federal Laboratory for Testing Materials and Research (EMPA) was called in to investigate. For an experimental modal analysis, the platform was excited with a hammer (including a contact-force sensor) and the resulting accelerations were measured at 50 points in all three orthogonal axes, in groups of 6 points.

By a phase-separation technique, the following basic modes were identified:

- Mode 1 (lateral sway about the x-axis): $f_1 \approx 2.8$ Hz, $\xi = 1.64\%$.
- Mode 2 (shaft nodding about the y-axis): $f_2 \approx 4.2$ Hz, $\xi = 1.18\%$.
- Mode 3 (Torsion of the upper slab about the z-axis): $f_3 \approx 4.8$ Hz, $\xi = 0.88\%$.

Higher modes at $f_4 \approx 10.8$ Hz, $f_5 \approx 11.8$ Hz, $f_6 \approx 14.6$ Hz, etc. show a combination of these spatial components.

Additional resonance excitations were performed through test persons. Rhythmical jumping of a person on the upper slab caused vertical displacements at the slab center of max. 5.7 mm and accelerations of max. 2.8 m/s² at the rear edge of the slab. The fundamental frequency decreased by about 5% because larger sway amplitudes decreased the flexural rigidity about the x-axis (opening of cracks). From single-jump tests with amplitudes of a few mm (especially in mode 1), the damping ratio was derived to ~ 2% of critical. A high-diver jumping off the spring board on the lower slab caused accelerations at the rear end of this slab of max. 4.6 m/s² lateral (y-direction) and max. 2.6 m/s² vertical.

The acceptance criteria in [1] require the following lower bounds on shaft vibrations:

- slab without springboard: $f \geq 3.5$ Hz
- slab with springboard: $f \geq 5.0$ Hz

The platform in case does not meet the frequency criteria, although in this particular case the most critical vibration is not in take-off direction. Stiffening the structure without gross changes in its appearance will be difficult. No decision on upgrading has been made to date.

7. CONCLUSIONS

In practical cases frequency tuning of the structure is a useful countermeasure to curb excessive vibrations. The structural frequency, mostly the fundamental frequency, has to be established in view of the most critical frequency of the spectrum of the load-time function. This is quite often not the nominal loading frequency itself, but the frequency of an upper or lower harmonic of the dynamic load.

REFERENCES

[1] Bachmann H., Ammann W., Vibrations in Structures Induced by Man and Machines, Structural Engineering Document No. 3e, International Association for Bridge and Structural Engineering (IABSE), Zürich, 1987.

[2] Allen D.E., Rainer J.H. and Pernica G., Building Vibrations due to Human Activities, Proceedings of the Structures Congress of the American Society of Civil Engineers (ASCE), Orlando, FL, USA, 1987.

[3] Baumann K., Bachmann H., Durch Menschen verursachte dynamische Lasten und deren Auswirkungen auf Balkentragwerke (Man-induced dynamic loads and their influence on beam structures), Institute of Structural Engineering (IBK), Swiss Federal Institute of Technology (ETH) Zürich, Report No. 7501-3, December 1987, Editor Birkhäuser, Basel.

[4] Vogt R., Bachmann H., Dynamische Lasten durch rhythmisches Klatschen, Fussstampfen und Wippen (Dynamic loads from rhythmic hand clapping, footstamping and moving up and down), Institute of Structural Engineering (IBK), Swiss Federal Institute of Technology (ETH) Zürich, Report No.7501-4, September 1987, Editor Birkhäuser, Basel.

[5] Peterson C., Theorie der Zufallsschwingungen und Anwendungen (Theory of random vibrations and applications), work report No. 2/72, Structural Engineering Laboratory, Technical University Munich, FRG, 1972.

[6] Bachmann H., Vibrations of building structures caused by human activities, case study of a gymnasium, National Research Council of Canada, Ottawa, Ontario, Technical Translation 2077, 1984.

TEN YEARS OF FLOOR VIBRATION RESEARCH
- A Review of Aspects and some Results

Sven V. Ohlsson

Chalmers University of Technology
Dep. of Structural Engineering
Div. of Steel & Timber Structures
Gothenburg, Sweden

ABSTRACT: Several research projects mainly related to vibration problems for short and medium span floors are summarized. Dynamic footfall loading, human perception of floor vibration, modal analysis, floor properties, design criteria and a design method currently in use in Sweden are reviewed. The different topics are discussed based on research of both theoretical and experimental nature. The laboratory experiments include dynamic and static tests on numerous timber, steel and composite floor specimens, studies of footstep loads and the influence of design improvements such as transverse stiffening and added artificial damping. Dynamic field tests at a large number of sites have been conducted as well.

1. BACKGROUND AND FLOOR VIBRATION RESEARCH AT CHALMERS' DIVISION OF STEEL & TIMBER STRUCTURES

For many design engineers the concept serviceability of floors means meeting design criteria related to *static* stiffness under uniformly distributed load. Human footfall loading has been shown to be a major source of annoyance as it induces disturbing floor vibrational response. In fact, this continuous *dynamic* load with impulsive components often forms the most serious loading case for a floor structure in the sense that it may govern the structural design and dimensions. This fact is not easily accepted, because it means that serviceability requirements result in higher demands than safety and structural integrity in some cases.

in 1976 a research project was started at Chalmers' Division of Steel & Timber Structures. The origin of this project was frequent customer complaints about "springy" timber joist floors in one-family prefabricated timber framed houses. Prefabricated wood houses dominate the Swedish market and an informal questionnaire survey among manufacturers of such houses showed that some producers designed the floors with respect to the static deflection criterion in the Swedish building code of that time and then increased the dimension of the joists one or two "steps" but still got complaints now and then.

The research that followed included both static and rather primitive dynamic laboratory tests. Three facts became obvious after a rather short time:

- The dynamic effects are most important.
- The low ability to distribute the action from concentrated dynamic and static loads for "one-way" joist floors is a bad property.

- The problem is not unique for timber floors, but is rather independent of construction material.

Most light-weight floors are strongly orthotropic, which leads to dynamic properties characterized by *closely spaced modes* of vibration. This means for instance that the second eigenfrequency often is only 15-20 % higher than the first one. Furthermore, this means that in contrast to many other civil engineering dynamic problems it is *not sufficient* to consider the fundamental mode only. When this became obvious, a Fourier transform based equipment for dynamic testing and modal analysis was purchased.

The research now went on more systematically with separate theoretical and experimental studies of dynamic footstep loading, floor structural and modal properties and improved design of various kinds. Parallel literature studies of material related to human tolerance of vibration were made. Subjective tests, where people were asked to rate different floor test specimens were carried out as well.

The essential parts of the research carried out so far were presented in |1|. Some general guidelines for design methods and criteria were included as well. The research within the area of floor vibration went on and requests from design engineers and owners of houses with troublesome floors concerning some practical design methods were put forward more frequently. As a result a design guide for springiness and floor vibration properties was published in 1984 |2|. This guide includes a proposed design method relevant for short and medium span floors which have a fundamental frequency f_1 higher than 8 Hz. It has been in use among practising engineers in Sweden and occasionally in Norway and Finland since then and the feed-back so far indicates a good ability to avoid the design of problem floors.

The present research is directed to two specific areas; 1) Long-span floor vibration problems and 2) possible design improvements such as artificially added damping and the use of separate secondary structural elements for serviceability requirements only. The spectral low-frequency loading from people in supermarkets etc. is one main part of the first area. Ref. |3| contains a presentation of some results here.

The following part of this paper is intended to point out important aspects and to present some essential results.

2. DYNAMIC FOOTFALL LOADING

As in many dynamic problems the characterization of the expected *load* is a major difficulty. Several sources of dynamic loading may be present in different building types, i.e. installed machinery etc. Forces due to human motion are especially difficult to model appropriately. The relevant "loading case" including the number of active persons, the type of motion and the correlation between the motion of different persons is not easily foreseen.

As footstep forces from walking and running persons seemed to be the most common source to disturbing floor vibrations, a laboratory test series was carried out in 1980 and later reported in |1|. The results established by Galbraith and Barton |7| were confirmed as far as force time histories are concerned. Examples of single footstep force time histories measured against a rigid ground are shown in fig. 1.

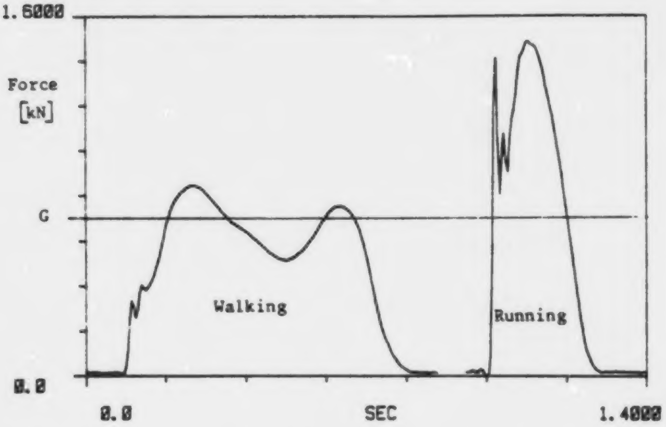

Figure 1: Footfall forces measured between foot and rigid ground for single steps. G is the weight of one person. After |1|.

Force pulses related to walking, like the left-hand one in fig. 1, were then used to form a pulse train in order to represent normal walking stationary force. Such a stationary force could then be Fourier transformed. The spectral density of this force is illustrated by the right-hand part of fig. 2.

The footfall load from walking can be characterized as a stationary dynamic force of the broadband type provided that the horizontal walking velocity is assumed to be small. However, the time history also contains impulsive parts of a more transient kind as well. The impulsive parts of common footstep force time history as well as forces from occasional jumps are to be considered as impacts.

According to the spectral representation in fig. 2 the footstep forces are dominated by their low-frequency components (0-6 Hz), but they also include high-frequency components (6-50 Hz) with an intensity which is approximately inversely proportional to the frequency. As a consequence two very different cases can occur:

1. At least one eigenfrequency for the floor is located in the low-frequency region, say $f_1 < 8$ Hz. This case is common for long-span floors and the response will be dominated by resonant vibrations for the mode(-s) with eigenfrequency below this limit.

2. The fundamental frequency is well above the low-frequency region, $f_1 > 8$ Hz. This is normal for short and medium spans. The response is here composed by two different types of vibration of the same order of significance: Low-frequency forced vibration which can be considered as semi-static (Large force multiplied by low flexibility) and high-frequency resonant vibration for a number of modes (Small force multiplied by high flexibility).

The distinction between these two separate cases is fundamental and *both cases can certainly cause very severe disturbance although of a very different nature.* For convenience, the first case is referred to as "long-span floor vibration" and the second one as "short and medium span floor vibration" although the latter case may comprise spans up to 7-8 meters for different light-weight designs.

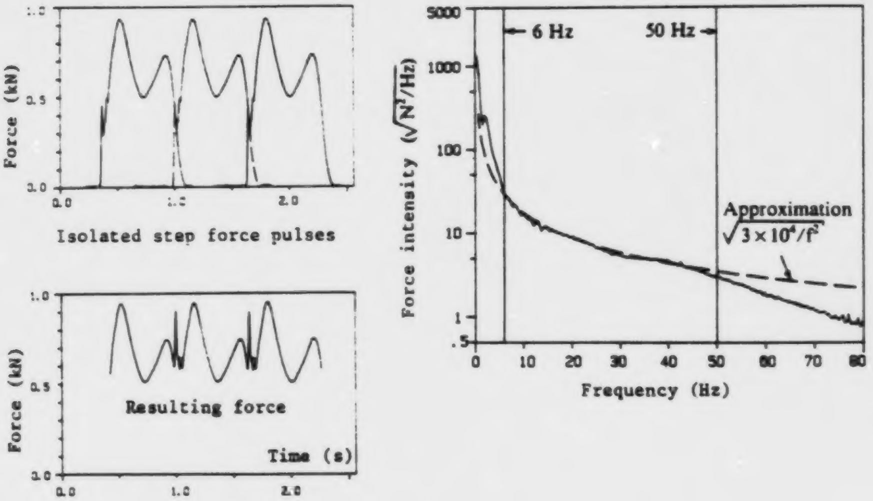

Figure 2: Footstep force from walking person. Three overlapping steps. Superimposed step forces and stationary force intensity (= square root of force power spectral density). After |1|. The simplifications introduced in calculating the spectral density implies an uncertainty related to absolute values, although the relative values within the frequency band 6-50 Hz are reasonably accurate.

3. HUMAN PERCEPTION OF FLOOR VIBRATION

The acceptable floor vibration level is usually determined by human sensitivity to vibration, but sometimes also by sensitive equipment like computers etc. Human sensitivity to vibration depends on a large number of parameters. The dependence of time is very strong, which means that short-term, strongly damped vibrations may have many times higher amplitudes than stationary, continuous vibrations and still be rated as being less disturbing. The activity of a disturbed person is also crucial. A walking person accepts much larger vibrations than a person who is reading a paper.

For floor vibrations induced by persons it is suitable to distinguish between two different situations with respect to the source and the sensor:

- *Springiness* of a floor is associated with the sensation of self-generated floor deflection and vibration from a single footstep during the time of contact between foot and floor surface.
- *Vibrational disturbances* caused by foot-fall on a floor are characterized by perception of floor vibration induced by other persons then the one that is disturbed.

There are many examples of floors where only one of these two cases has been the origin of complaints. In fact, springiness is usually restricted to light-weight floors and floors with a low local rigidity with respect to concentrated loading.

The degree of experienced *springiness* is governed by the low-frequency semi-static, forced motion together with resonant high frequency decaying vibration. The low-frequency response is more or less independent of mass and damping and can consequently be treated as a problem of static stiffness under concentrated force. The high frequency decaying vibration part is induced primarily by the very initial part of each footfall pulse. Here a very high rate of force increase occurs and this part can be considered as an almost ideal impulse. The human response to impulsive vibration is a complicated matter. In the case of vibration with frequency components above 8 Hz, most researchers agree that vibration *velocity* is the most appropriate representation. This was for instance concluded by Wiss & Parmelee |8| and also used in an ISO draft addendum, ISO 2631 DAD1, |9|. The strong influence of decay rate has been stated by various researchers, see for instance |8|. A relatively certain conclusion is that the disturbance from transient impulsive vibration is in some sense proportional to vibration velocity and inversely proportional to the decay rate. The decay rate with respect to *time* seems most relevant.

The degree of floor *vibrational disturbance* is mainly governed by the stationary resonant floor vibration although the more impulsive events previously discussed do contribute as well. For the case of stationary vibration with frequency components above 8 Hz most researchers seem to agree that the RMS-value for vibration *velocity* is a good measure of the expected human disturbance. As shown in the previous section, the footfall force power spectral density is approximately inversely proportional to the frequency squared in the frequency band above 8 Hz. This means that the force is inversely proportional to the frequency which in turn leads to a situation where the lower modes of vibration will dominate the disturbance for short and medium spans.

For long span floors with resonances in the low-frequency region below say 8 Hz corresponding modes of vibration will be excited by much higher force levels and this low-frequency resonant vibration will totally dominate the response. In the frequency band below 8 Hz most researchers seem to agree that the RMS-value for vibration *acceleration* is a good measure of the disturbing effect.

Apart from these more widely spread results indicating that human disturbance is related to floor vibration velocity or acceleration there was another approach presented in |10|. It is the author's opinion that these ideas might have certain qualities. Farah |10| quite simply stated that the discomfort was proportional to the *vibration power absorbed* by the human body. If this approach should be applied, some reliable dynamic models of the human body must be developed. Although it might be a good idea not to use this approach in designing floors (since it will be rather difficult), there is another aspect of the matter worth explaining. It is well known that the presence of human beings on a floor increases the system damping. Considering Farah's proposal it is, however, not reasonable to count on this extra damping in design calculations, as this damping is nothing else than a sign of vibration absorption in the human body - the absorbed power!

So far, only the different parameters which are believed to represent the human annoyance from vibration have been discussed. Most human senses are believed to be of a logarithmic rather than a linear character and the perception of vibration is probably not an exception from this. The absolute values for vibrational tolerance are very uncertain. Many factors as duration, activity and health influence these limits. It is, however, surprising how good repeatability people show when they are asked to select the better one of two sample floors. This holds even if the floors are covered with dark plastic film. The good ability to detect small *relative* differences is valid also for floor vibrational properties.

4. PROPERTIES OF SHORT AND MEDIUM SPAN FLOORS

In order to simplify the presentation here the floors are supposed to be rectangular in plan and with all four edges simply supported if nothing else is explicitely stated. It is obviously not possible to describe all specific types of light-weight floors here. Timber joist floors are for instance treated in |1| and |6| and "dry" steel floors are commented upon in |4|. This section is rather meant to describe important properties which are relatively common for short and medium span floors.

4.1 Static flexibility: The static flexibility related to a concentrated vertical force at the weakest location somewhere at midspan is an important property for the degree of springiness. Since most floor designs have developed over the years, mainly to fulfil code criteria related to strength and stiffness under uniformly *distributed* loads, the stiffness for concentrated load is often low. A concrete slab typically shows stiffness values for concentrated force of the order of 100 times the corresponding value for a light-weight joist floor at equal spans, say 4 m. The low local rigidity of joist type floors is usually depending on the low bending rigidity in the direction perpendicular to the joists. This matter as well as suggested improvements are further discussed in |6|. Figure 3 illustrates the modelling of a joist floor as a grillage and resulting deformation shape. Static stiffness is more deeply studied in |4| and |6|.

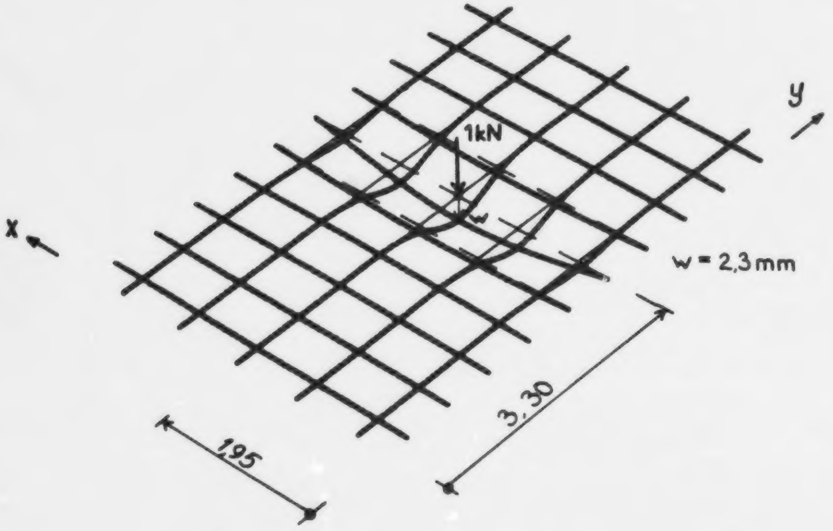

Figure 3: Grillage-type computer model of a flexible timber joist floor under concentrated static force.

4.2 Modal parameters: Modal analysis is a classic way to interprete the dynamic behaviour of linear mechanical systems. The idea is to represent the real dynamic behaviour as a sum of modal contributions. Continuous mechanical structures have an infinite number of eigenmodes. Each eigenmode n is characterized by the following four modal parameters:

- Eigenfrequency (or resonance frequency) f_n
- Modal damping c_n
- Mode shape function $\Phi_n(x,y)$
- Modal mass m_n

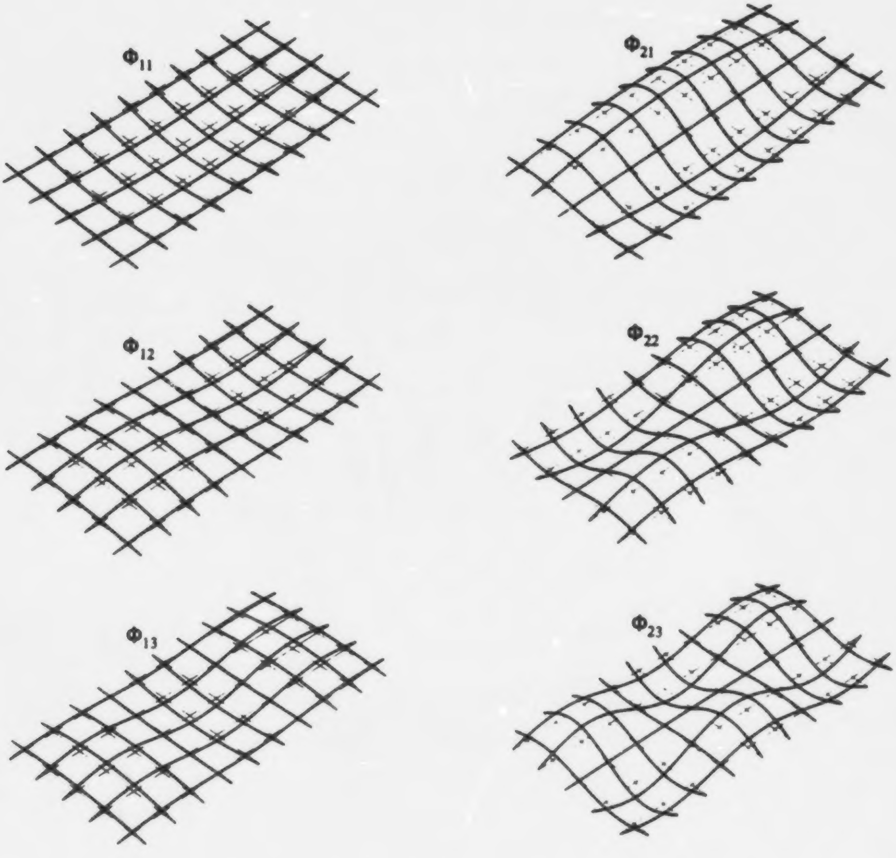

Figure 4: Low-order mode shapes $\Phi_{mn}(x,y)$ for orthotropic plates. First order modes to the left.

Since these modal parameters are the basis for the calculation of the dynamic response under a specified load, simple ways to calculate them are very useful.

The mode shape functions $\Phi_{mn}(x,y)$ for orthotropic plates are illustrated in fig. 4. In practice, only the first order modes ($m = 1$) are of interest here so we denote Φ_{1n} as Φ_n which now means the n:th mode of the first order. Φ_n is characterized by one half-wave along the joists and n half-waves perpendicular to the joists.

The modal mass m_n can be interpreted as a shape-weighted sum of the mass of the different parts of a floor. The modal mass is by definition:

$$m_n = \int_0^L \int_0^B g(x,y) \cdot \Phi_n^2(x,y)\, dxdy \qquad \text{(kg)} \qquad (1)$$

where $g(x,y)$ is the mass per m^2. Provided that the mode shapes are normalized such that the maximum value equals 1.0 in each mode, the modal mass m_n can be shown to be one quarter of the floor mass for simply supported, rectangular floors with uniform mass distribution.

The eigenfrequencies f_n for an orthotropic plate can approximately be calculated as

$$f_n = \frac{\pi}{2}\sqrt{\frac{D_x}{gL^2}}\sqrt{1 + (2n^2(L/B)^2 + n^4(L/B)^4)\frac{D_y}{D_x}} \qquad \text{(Hz)} \qquad (2)$$

where D_x and D_y are plate bending rigidities ($D_x > D_y$), g = mass per m^2, L/B is the aspect ratio and n the mode number. In order to facilitate the calculation of different eigenfrequencies for orthotropic, simply supported plates, different diagrams like the one in fig. 5 have been worked out and are included in |2|. The fact that orthotropic plates with small D_y/D_x-values have closely spaced resonances is clearly visualized by this diagram.

The modal absolute damping c_n is usually assumed to be viscous and then has the dimension (N/(m/s)). It is common practice to use the nondimensional relative modal damping (c/c_{cr}) instead. This parameter is sometimes also referred to as the damping ratio. The relative modal damping is a structural property which typically shows different values for different modes of vibration.

Damping is probably the most misunderstood dynamic parameter. There are many possible explanations for this; The origin of damping mechanisms is not fully understood, damping is expressed in several different ways, e.g. loss factor, logarithmic decrement, quality factor etc. and damping is usually explained as applied to a free *harmonic* vibration for a single degree of freedom system. Furthermore, damping parameter values are now and then presented without reference to any specific damping parameter. Such information is obviously useless and causes confusion. The word damping is sometimes used for amplitude decreasing phenomena in general, for instance "geometrical damping". It would be beneficial if the word damping could be reserved for phenomena related to energy absorption.

High modal damping ratios have two beneficial effects on floor vibration. They limit the resonant vibration amplitudes for stationary forced vibration and they govern the decay rate for impulse excited free vibration. Since damping is such an important property for good floor serviceability, it is essential to gain knowledge about damping parameters for different floor types and especially about the *scatter* involved. Some damping values found in the literature are based on

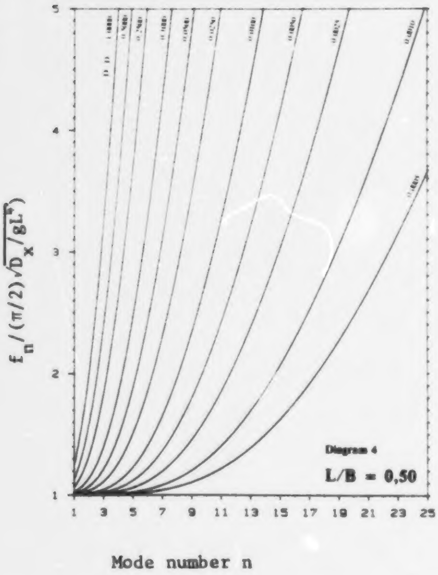

Aspect ratio L/B = 0.5
Different curves represent different degrees of orthotropy D_y/D_x.

The left-hand curve represents an isotropic plate, $D_y/D_x = 1$.

The right-hand curve represents a strongly orthotropic case where $D_y/D_x = 0.0005$.

Figure 5: Normalized first order eigenfrequencies for simply supported orthotropic plate. Typical example from a set of diagrams in |2|.

free vibration tests and evaluation of logarithmic decrement from multi-frequency decaying vibration. This methodology is not in agreement with the theory of dynamics and usually results in severe overestimation of the floor damping capacity. This is due to the fact that even for a case with equal damping ratio for all modes of vibration, the higher mode components will be damped out more quickly with respect to *time*.

4.3 Dynamic flexibility: The dynamic flexibility related to *stationary vibration* is a complex function of frequency. It is usually called *compliance* and denoted $\alpha_{ij}(f)$, where j is the loading point and i the point of resulting displacement. The compliance is calculated based on the modal parameters as:

$$\alpha_{ij}^{\text{mode } n}(f) = \frac{\Phi_n(\text{point } i)\ \Phi_n(\text{point } j)}{4\pi^2(f_n^2 m_n - m_n f^2 + (i/2\pi)c_n f)} \qquad (\text{m/N}) \qquad (3)$$

$$\alpha_{ij}(f) = \sum_{n=1}^{\infty} \alpha_{ij}^{\text{mode } n}(f) \qquad (\text{m/N}) \qquad (4)$$

where "i" denotes the complex constant and "f" denotes frequency in Hz. The summation in Eq. (4) must be truncated in practice. The transfer compliance related to two points i and j near midspan for a laboratory wooden joist floor is shown in fig. 6. The more irregular function is based on measurements. This and other compliance functions have then been curve-fitted and corresponding modal parameters estimated. The smoother function is a synthetized version based on

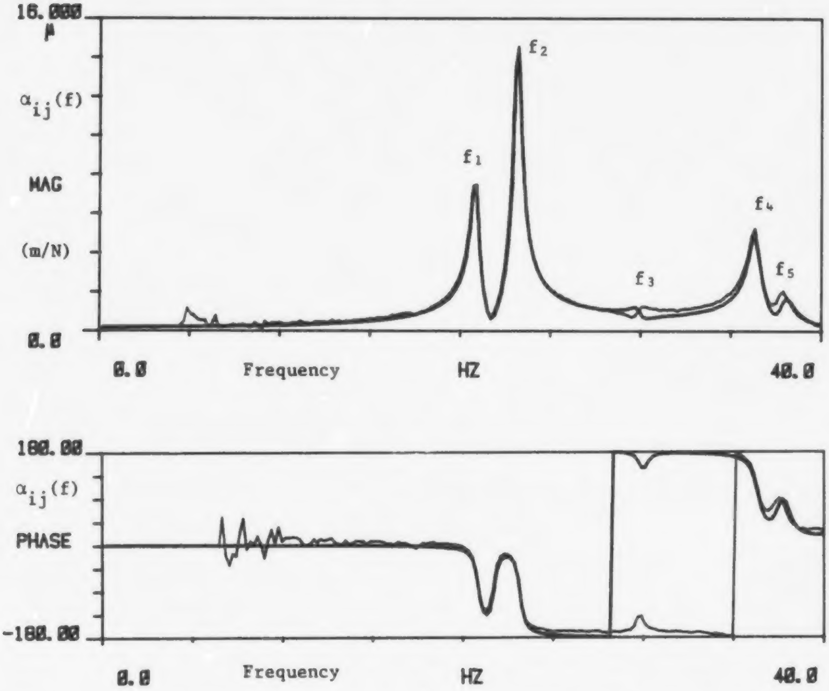

Figure 6: Measured and synthetized transfer compliance for a wood joist floor element.

the modal parameters. The compliance function has the dimension (m/N). Corresponding functions for velocity and acceleration are called *mobility* ((m/s)/N) and *accelerance* ($(m/s^2)/N$) respectively. The mobility M(f) is directly related to the compliance as:

$$M(f) = 2\pi f i \alpha(f) \qquad ((m/s)/N) \qquad (5)$$

Reference |11| is a monography on modal testing and related topics.

The dynamic flexibility for *transient loading* is usually described via the "Duhamel integral", which is applicable to various force-time histories. The basis for this integral is the *unit impulse response function* h(t). It can be shown that this real function of time in fact is equal to the inverse Fourier transform of the complex compliance function α of frequency. The impulse response h(t) describes the displacement caused by an ideal impulse with unit magnitude (1 Ns) at the time t = 0, cf. fig. 7. The corresponding function for vibration velocity is called the *unit impulse velocity response* h'(t) and is accordingly the first time derivative of h(t). As shown by fig. 9, the different modes contribute to form a multi-frequency time history, which includes time intervals with co-action between components with different frequencies. It can further be shown that the

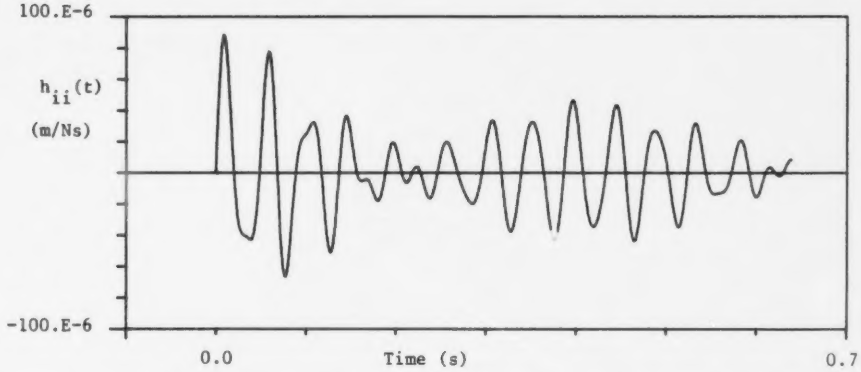

Figure 7: Unit impulse response function h(t) for a wood joist floor element corresponding to a compliance function like the one in fig. 6.

very initial value h'max can be calculated as:

$$h'\max = \sum_{n=1}^{n\,\max} \frac{\Phi(\text{point } i)\ \Phi(\text{point } i)}{m_n} \qquad ((m/s)/Ns) \qquad (6)$$

It is worth noting that this expression is strongly depending on the different modal masses m_n. So far the response at one location i has been discussed. The effect on floor deformation shape from different modal contributions is illustrated by fig. 8.

The different flexibility type functions (α, h, h', etc) have been etablished by theoretical as well as experimental modal analysis for a variety of short, medium and some long span floors |1|. This experience is one part of the basis for the design method proposed in Ref. |2|.

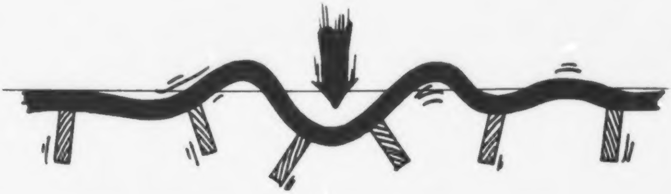

Figure 8: An artist's expression of modal co-action at impact loading.

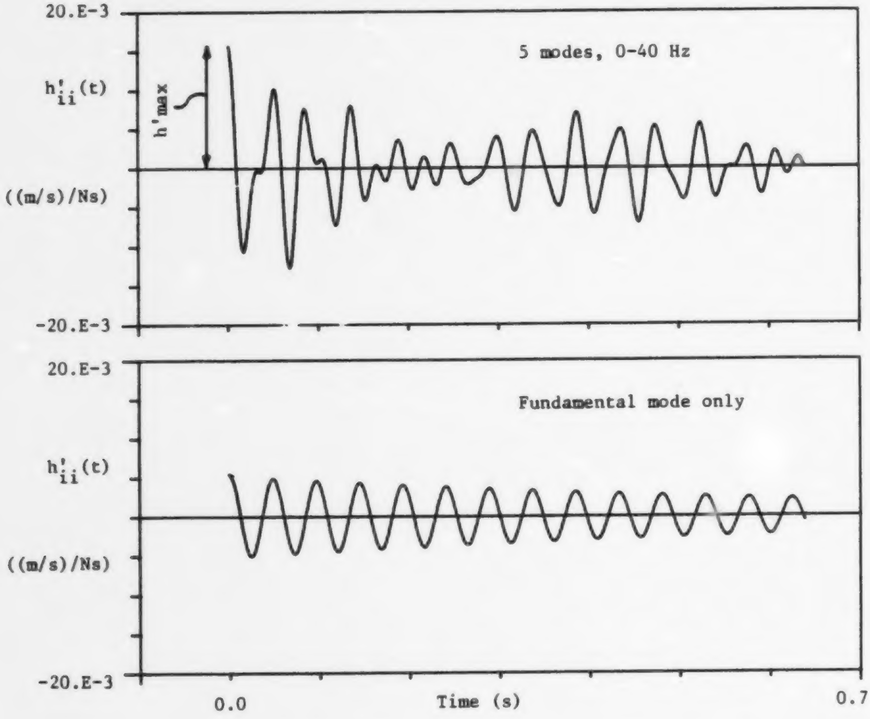

Figure 9: Unit impulse velocity response function estimates for a wood joist floor element at midspan. The upper function is based on all 5 modes below 40 Hz and the lower on the fundamental mode alone. Damping ratio values, $(c/c_{cr})_n$ for mode nos. 1-5 vary between 0.8 % and 1.1 %.

5. DIFFICULTIES RELATED TO DESIGN AND DESIGN REGULATIONS

Structural design with respect to potentially unacceptable floor vibrations must usually be carried out based on incomplete knowledge in various fields. The following points are essential examples of that:

- The real dynamic loading is only vaguely known both with respect to amplitude and frequency content.
- The "static" system relevant to low-amplitude vibration is often unknown. Partitions and other "non load-bearing" components may or may not change the static model established for heavy static loading.
- The modal relative *damping* c/c_{cr} - *a most important parameter* - is *not controlled* by the design engineer, but will usually have to be guessed (embarrassing!). As damping is not ensured by designed structural components it occurs with very large scatter in finished buildings. Neither can the durability of

damping level be ensured.

- The human tolerance level is individual and depends on various circumstances. The overall design philosophy is seldom discussed, namely the question: To what extent and with what reliability shall disturbances be avoided?

With these limitations in mind it is natural to be humble when discussing different proposed vibrational design criteria. It is, however, also natural to aim at the use of relevant parameters, although the corresponding design limit values must be chosen with regard to the relatively low overall design accuracy.

Another intricate matter is the one related to the question of *which* building *components* should be taken into account when designing for vibrational serviceability. For the case of ultimate limit state design it is well established practice only to incorporate "structural" members. In the case of serviceability limit state vibrational design the situation can often be characterized as follows; The existing partitions and other "non load-bearing" components make the difference between acceptable and unacceptable vibrational response. This is especially true for light floors. These components, on the other hand, may be removed any day by the user. It is the author's opinion that the serviceability limit state design should not rely upon "non load-bearing" components. If, however, such components are classified as structural members only with respect to serviceability aspects, there is a need for some relatively liberal rules to regulate the engineering use of such members.

6. SWEDISH DESIGN GUIDELINES (PROPOSAL)

6.1 Background and approach: In 1984 the author published some guidelines for the design of short and medium span floor vibrational serviceability, |2|. These guidelines have been in use among Swedish practising engineers and occasionally in Norway and Finland since then. The design method included in |2| has so far proven to be capable of reflecting the serviceability changes due to structural modifications in a proper manner. The ability to prevent the design of floors with unacceptable vibrational response seems quite good as well. The design method and its background will be outlined in the following. A more detailed description is given in |5|.

The following points reflect the intentions when the work was started in 1983:

A design method with respect to floor vibrations should

- Reflect the degree of vibrational serviceability.
- Be neutral with regard to the construction material and structural configuration.
- Only include such well defined quantities, that are possible both to calculate and to measure.
- Be clearly understandable and enable the engineer to predict the effects of structural modifications.

Within the limits of these demands the overall aim has been to develop a design procedure which is relatively easy to carry out and is based only on structural parameters available at the design stage.

The design procedure is limited to floors with *fundamental frequency above 8 Hz*. The design is related to the prevention of two different phenomena:

- Springiness (static flexibility & impulse velocity response)
- Vibrational disturbance (impulse velocity response & stationary RMS velocity response)

Three primary design parameters (in parenthesis) are suggested. Each of them will be commented upon in the following sections.

6.2 Static flexibility: The static flexibility related to a concentrated vertical force at the most compliant location of the floor is suggested to take account of the low-frequency response related to springiness. This parameter includes the local flexibility contribution from flooring boards etc. Since it is common practice to calculate stiffness related only to the primary structural joists or beams, such values are used until better knowledge is achieved. A static flexibility limit value of 1.5 mm/kN is for instance suggested in the present Swedish building code. This is a calculated value for maximum deflection under a concentrated force applied over a joist at midspan relevant for simply supported timber joist floors.

6.3 Impulse velocity response: The initial maximum value h'max for the unit impulse velocity response with modal contributions from resonances below 40 Hz is suggested to take account of the high-frequency resonant response related to springiness as well as to vibrational disturbance. The influence of damping is taken via a diagram (fig. 10), where higher values for h'max are accepted for strongly damped floors. The damping *coefficient* σ_0 for the fundamental mode is chosen as the appropriate parameter:

$$\sigma_0 = f_1 \cdot (c/c_{cr})_1 \qquad (s^{-1}) \tag{7}$$

The value for c/c_{cr} is to be taken between 0.8 % and 1.0 % for ordinary cases. The value for h'max is rather difficult to calculate from Eq. (6). The author found, however, a very simple and accurate approximation |2|, which reads:

$$h'max = \frac{4(0.4 + 0.6\,N_{40})}{gBL + 200} \qquad ((m/s)/Ns) \tag{8}$$

where N_{40} is the number of modes with eigenfrequencies below 40 Hz and gBL is total floor mass. The approximation is valid for rectangular simply supported floors. An additional mass of 50 kg (200/4) is included, representing a part of a person. The value of N_{40} is easily calculated via diagrams of the type shown in fig. 5.

6.4 Stationary RMS velocity response: The calculated RMS vibration velocity response w'_{RMS} caused by a concentrated force with the power spectral density $30\,000/f^2$ (N^2/Hz) is taken as the design parameter to represent stationary resonant vibrational disturbance, cf. fig. 2. The calculation is limited to the frequency band 8-40 Hz. The components below 8 Hz is taken into account via the static flexibility. w'_{RMS} is calculated as:

$$w'_{RMS} = \sqrt{\int_8^{40} (30\,000/f^2)\,|M(f)|^2 df} \qquad (m/s)_{RMS} \tag{9}$$

where M(f) is the point mobility for the "weakest" location. This expression is not easily used for design purposes. There is, however, also in this case an approximate formula that may be used for rectangular, simply supported floors:

$$w'_{RMS} = \frac{100}{gBL\sqrt{(c/c_{cr})_1}} \sqrt{\frac{N_{1.2}^2 + 1}{2\ f_1^3}} \qquad (m/s)_{RMS} \tag{10}$$

where $N_{1.2}$ represents the number of resonances with eigenfrequencies below 1.2 f_1. No fixed limit values for w'_{RMS} have been suggested so far. Such values must take into account the number of active persons as well as the type of building (workshop, office etc.). The stationary vibration velocity is seldom critical for short span floors in residential houses with closely spaced partitions.

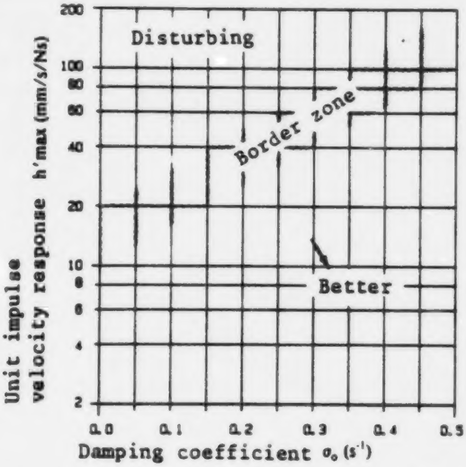

Figure 10: Diagram for rating of impulse velocity response after |2|.

REFERENCES

The literature list is rather limited. Ref. |1|-|11| are referred to in the text and ref. |12|-|17| are a few examples of relatively early papers on floor vibration while ref. |18|-|20| are examples of recent papers. The literature list in Ref. |1| is more extensive and it also includes papers on some related topics such as human perception and structural properties.

|1| Ohlsson, Sven: Floor Vibrations and Human Discomfort. Chalmers Univ. of Technology, Div. of Steel and Timber Struct., Ph.D.thesis, Gothenburg 1982.

|2| Ohlsson, Sven: Svikt, svängningar & styvhet hos bjälklag - Dimensioneringsmetoder (Springiness, Vibrations and Stiffness Properties of Floors - Design Methods). The Swedish Council for Building Research, Publication T20:1984, Stockholm 1984, Sweden. (An English translation is under preparation 1987.)

|3| Eriksson, Per-Erik & Ohlsson, Sven: Dynamic Footfall Loading from Groups of People. To be submitted to the Symposium on Serviceability of Buildings to be held at University of Ottawa, May 1988.

|4| Ohlsson, Sven: Stiffness Criteria and Dynamic Serviceability of Light-Weight Steel Floors. Proc. of IABSE Coll. in Stockholm 1986, IABSE Rep. Vol. 49, pp. 427-433, Zürich 1986.

|5| Ohlsson, Sven: A Design Approach to Footstep-induced Floor Vibration. To be submitted to the Timber Engineering Conference, Seattle in September 1988.

|6| Ohlsson, Sven: Stiffness Characteristics of Wood-Joist Floors. To be submitted to the Timber Engineering Conference, Seattle in September 1988.

|7| Galbraith, F.W. & Barton, M.V.: Ground Loading from Footsteps, J.Acoust., Soc. of America, vol.48,1970, part 2, pp. 1268-1292.

|8| Wiss, J.F. & Parmelee, A.: Human Perception of Transient Vibrations, Journal of the Structural Division, ASCE 1974, pp. 773-787.

|9| ISO 2631, DAD1: Guide for the Evaluation of Human Exposure to Vibration and Shock in Buildings, Addendum 1; Acceptable Magnitudes of Vibration, 1980, Note: Draft proposal!

|10| Farah, A.: Human Response; A Criterion for the Assessment of Structural Serviceability, Ph.D. Thesis, Univ. of Waterloo, Dep. of Civ.Eng., Ontario, Canada 1977.

|11| Ewins, D.J.: Modal Testing; Theory and Practice. Research Studies Press, Letchworth, Great Britain 1984.

|12| Allen, D.E. & Rainer, J.H.: Vibration Criteria for long-span Floors, Canadian Journal of Civil Engineering, pp. 165-172, 1976.

|13| Atherton, G., Polensek, A. & Corder, S.: Human Response to Walking and Impact Vibration of Wood Floors, Forest Products Journal, vol. 26, no.10, Oct. 1976, pp. 41-47.

|14| Lenzen, K.H.: Vibration of Steel Joist-Concrete Slab Floors, AISC Eng. Journal, No.2, July 1966, pp. 133-136.

|15| Murray, T.M.: Design to Prevent Floor Vibrations, AISC Eng. Journal, No.3, 1975, pp. 82-87.

|16| Onysko, D.: Performance of Wood-Joist Floors; A Questionnaire Survey, Eastern Forest Prod. Lab., Rep. no. OPX 120 E, Ottawa 1975.

|17| Polensek, A.: Human Response to Vibration of Wood-Joist Floor Systems, Wood Science, vol.3, No.2, Oct. 1970, pp. 111-119.

|18| Chui, Y.H.: Evaluation of Vibrational Performance of Light-Weight Wooden Floors. Research report no.2/86, Timber Research and Development Association, High Wycombe, England 1986.

|19| Ellingwood, B. & Tallin, A.: Structural Serviceability; Floor Vibrations. Journ. of Struct. Eng., ASCE, Structural Division Vol 110, No.2, 1984, pp. 401-417.

|20| Allen, D.E., Rainer, J.H. & Pernica, G.: Vibration Criteria for Assembly Occupancies. Can. Journ. of Civ. Eng. Vol 12, 1985, pp. 617-623.

CROWD-INDUCED DYNAMIC LOADS

A. Ebrahimpour, and R. L. Sack

Department of Civil Engineering
University of Idaho
Moscow, Idaho 83843
U.S.A.

ABSTRACT: Dynamic loads created by crowds can impose severe structural vibrations and displacements. Using a combination of experimental data and statistical methods we characterized load-time histories for individuals and small groups performing a myriad of transient and periodic maneuvers. Comparison of peak loads generated by individuals performing alone and in small groups indicates there is a group synergism. That is, the time between peak loads generated by individuals is minimized when performing together. Group loads for periodic jumping are modeled using measured distributions of critical parameters in conjunction with Monte Carlo simulation. Design values for periodic jumping at 2 Hz and 3 Hz asymptotically approach 70 psf (3.4 kPa) as the number of participants exceeds ten.

1. INTRODUCTION

Crowds impose significant live loads on stadiums, grandstands, theaters, and other assembly structures. Although static occupant loads can be predicted accurately, the dynamic components of these forces are difficult to determine and are typically influenced by the nature of the crowd activity.

Many assembly structures have fundamental natural frequencies in the range of the coherent rhythmic movements of the crowd (e.g., periodic jumping to music); the loads may produce resonant or near-resonant structural vibrations (12,19,22). These vibrations can wreak structural damage and produce uncomfortable, sometimes intolerable, oscillations for members of the crowd. With reduced structural damping, other troublesome vibrations are developed by a single coherent movement of the crowd. For example, a crowd standing or jumping once in unison can produce a transient long-duration structural oscillation of the structure. Studies on human induced vibrations in various structural floor systems and temporary grandstands produced threshold perception levels for steady state and transient motions (1, 2, 8, 17, 24).

When designing a structure, both strength and serviceability requirements must be satisfied. Strength criteria ensure material integrity, while the serviceability requirements restrict the deflections and vibrations to a tolerable level. Many structural design values are specified as quasi-static equivalent load intensities, and require no dynamic analysis. This is the case for human live loads prescribed by most U.S. building codes and standards (4, 7, 18, 23); the provisions are based on studies dating back several decades (3, 5, 6, 13, 21). Therefore, designers are unable to check serviceability for dynamic loads and excessive vibrations.

Ellingwood, et al (10) have proposed probability-based load criteria that are independent of the structural materials. These provisions, based solely on strength criteria, provide uniform levels of safety for preselected combinations of structural loads. To obtain the same confidence levels for vibration thresholds, a probability-based design procedure based on serviceability criteria must be developed. Before such methods are established, the loads causing structural vibrations should be accurately modeled and the parameters statistically analyzed.

The objective of our research is to define the dynamic loads generated by insitu movements of individuals and groups of people, and in particular, the parameters influencing crowd coherency. A force platform was used to measure input forces produced by individuals and groups of two and four people performing predefined movements. Analytical models are proposed for periodic and transient human loads, along with a temporal summation technique to create coherent crowd loads. Design criteria are suggested for periodic loads.

2. DATA MEASUREMENTS

A force platform is a device used in biomechanics to measure forces developed by various athletic maneuvers (11, 14, 16). This same instrument can also be used to measure force-time histories imposed by human movements. Tuan used a small piezoelectric force platform to study loads generated by movements of individuals (22).

We designed a 4 by 8 ft (1.2 by 2.4 m) suspended-type force platform similar to McLeish and Arnold (15) to assess forces imposed by individuals and small groups. The platform has a high stiffness-to-mass ratio so that its transfer function is unity in the frequency range of human movements (i.e., 0 to 6 Hz). Therefore, it transmits the exact input loads. The platform deck is supported vertically and in two orthogonal horizontal directions by eleven pretensioned rods attached to thin steel strip strain gage transducers, which register the data for the vertical and horizontal components of the imposed loads. See references (9) and (20) for construction and calibration details of the platform.

The data acquisition system consists of a signal conditioner, an analog-to-digital converter, and a microcomputer functioning as the system controller. An audible prompter simulated music tempos for the participants; it was recorded, along with the load data, to provide a time reference.

3. LOAD MODELING

The human body is a complex mechanism capable of various movements. The body can be envisioned as a multidegree-of-freedom system in which the bones, joints, and muscles act as springs and dampers. This idealized system is controlled by physiological and psychological factors. Thus it is difficult for an individual to duplicate a prescribed load-time history, and we must treat human loads as random functions of time.

For this study, we defined seven unique movements: periodic jumping; periodic jouncing (i.e., jumping without leaving the ground); periodic swaying; random jumping; a single jump; sitting down suddenly; and standing up suddenly. The term periodic refers to the general pattern of the load-time history, but the movements are considered as random functions. The first four specified maneuvers are steady state, and the last three are transients. Individual and group periodic loads were conducted at 2, 3, and 4 Hz. Our testing involved 20 males and 15 females ranging from 103 to 234 lb (458 to 1041 N), with an average weight of 158 lb (703 N) and a standard deviation of 33 lbs (147 N). Figures 1 and 2 show typical load-time histories for an individual and a group of four performing two predefined maneuvers.

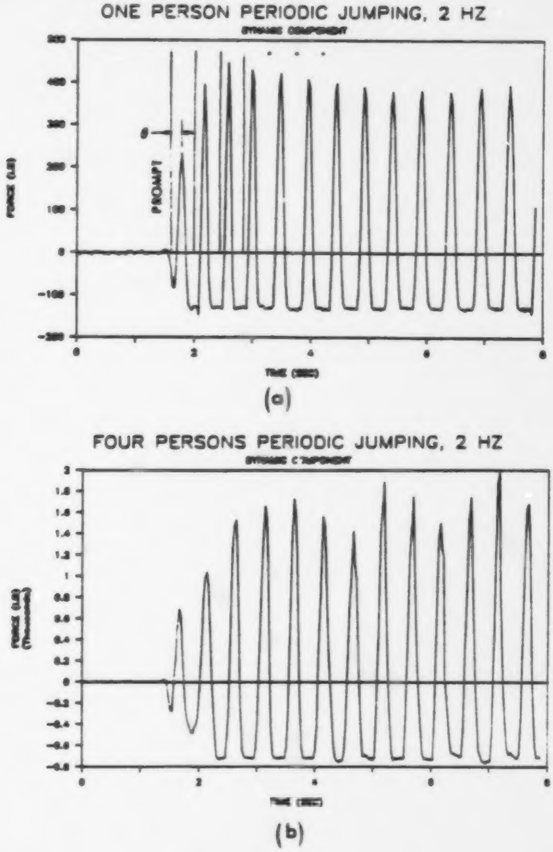

Fig. 1 Vertical force components due to periodic jumping: (a) one person; (b) four persons (1 lb = 4.45 N)

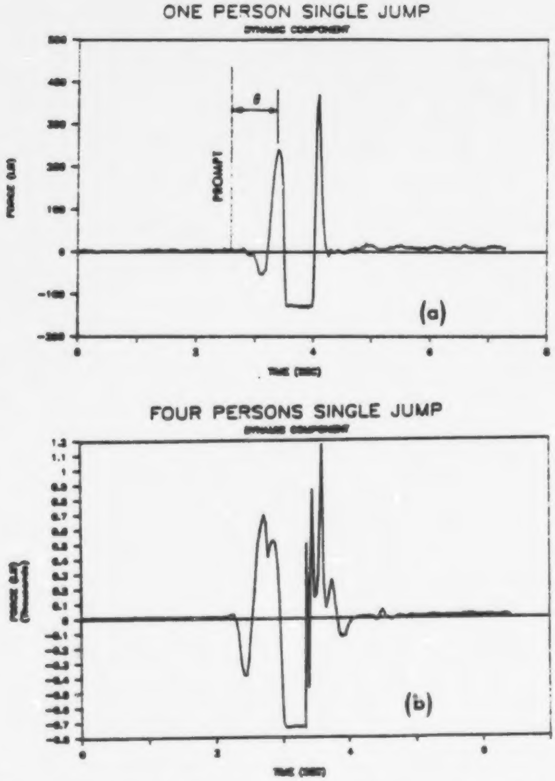

Fig. 2 Vertical force components due to a single jump:
(a) one person; (b) four persons (1 lb = 4.45 N)

3.1 Individual Load Models: The parameters describing a certain load-time history can be obtained using curve fitting techniques; wherein, the descriptive parameters may be treated as random variables amenable to statistical analysis. We modeled periodic jumping of individuals using a Fourier Series (F.S.) fit of the measured data as follows:

$$y(t) = \sum_{n=1}^{N} [a_n \cos(2n\pi t/T) + b_n \sin(2n\pi t/T)] \qquad (1)$$

where $y(t)$ = the load-time history, a_n, and b_n = the F.S. coefficients, and T = the period. We treated the dominant F.S. coefficients and the period as the load descriptive parameters.

Transient loads can be modeled using one or more decaying functions and other arbitrarily defined parameters. In particular a segment of a transient load can be fit with an exponentially decaying function in the form:

$$y(t) = A_1 \sin(2\pi t/T) \exp(-A_2 t) \qquad (2)$$

where A_1, A_2, and T are the descriptive parameters.

Using relations similar to Eqs. (1) and (2), we modeled individual periodic jumping and single jumps. The corresponding descriptive parameters were then used in a general multivariate regression model as functions of several independent variables (e.g., sex, and weight of individuals). References (9) and (20) show details of the individual load curve fitting and the multivariate regression models.

3.2 Group Effect: Temporal summation of individual load histories yields the load-time history for a group. The prompt signals were recorded and are shown on the load-time histories in Figs. 1a and 2a. For the periodic events these audible prompts served as the beat of the music. For transient maneuvers, the participants were instructed to react as soon as they heard the signal; this is indicative of a crowd reacting to a particular event. The prompt signal also served as a time reference; the arbitrarily defined parameter θ (see Figs. 1a and 2a) is the time difference between the prompt and the subsequent peak force. We assumed that θ values do not control the shape of the load history but indicate: if a person is in rhythm with the music (periodic movements); and the reaction time (transient events).

If an individual has the same load pattern acting alone and when performing in a group, the only variable that must be further considered is the time phase lag between the participants. Therefore, either: a) the θ values are unchanged in a group situation; or b) the phase values are changed due to the group effect. By aligning the prompt signals and summing the loads over time, we superimposed the load-time histories of two individuals performing at different times on the platform. Superposition was done for both transient and periodic loads. The general shapes of superposed load-time histories do not resemble measured plots (see Figs. 3 and 4), and peak loads are smaller than measured values. Thus, the group effect alters the phase values.

Although group coherency can be envisioned for long-duration rhythmic movements, our data show that the group effect occurs even for transient loading (e.g., a prompted single jump). That is, individuals in a group performing either transient or steady state movements synchronize their motions to a prompt and movements of the neighboring people. Hence, crowd coherency is strongly influenced by auditory and visual effects.

The force platform yields the response of the group as a whole; the individual loads can not be distinguished. Thus the time phase between two individual peak loads (used here as a measure of group coherency) can not be experimentally measured. We wrote a FORTRAN computer program (PHASE.FOR) to produce a set of randomly simulated phase lags. For simplicity, the program was designed to perform the simulation using data for only two people. The definitions of the phase lag value (ϕ) for both periodic and single jumps of two people are illustrated in Fig. 5.

For periodic loading, ϕ is the difference in time values for the nearest peaks of two load histories. For single jumps the first of the two peaks was arbitrarily chosen to serve as the time reference. The programming strategy underlying PHASE.FOR is as follows:

1. Two individual load descriptive parameters (e.g., weight and sex) were randomly simulated using a random number generator subroutine and the appropriate regression model and its statistics.
2. A peak force value was randomly determined using the data from two people measured on the force platform.
3. Using the two random descriptive parameter vectors in step 1, the program simulated the corresponding load-time histories. One load history was shifted relative to the other until the difference between the resulting temporal peak value matched the peak value in step 2. The criterion for this match was chosen to be the minimization of the square of the differences in load magnitudes. This gave the corresponding optimum simulated phase lag, ϕ_{opt}.
4. Finally the program repeated steps 1 to 3 multiple times, generating a set of optimum phase lag values.

Reference (9) contains a program source listing for PHASE.FOR.

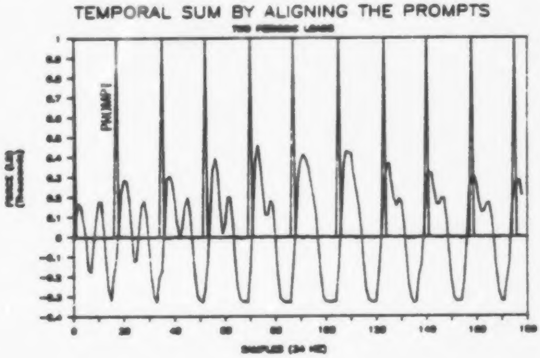
TEMPORAL SUM BY ALIGNING THE PROMPTS

(a)

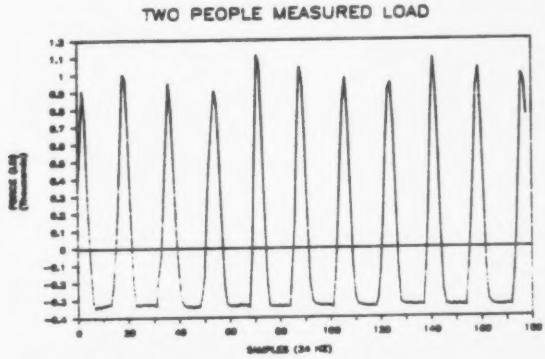
TWO PEOPLE MEASURED LOAD

(b)

Fig. 3 (a) Temporal summation by aligning the prompts; and (b) measured periodic load. (1 lb = 4.45 N)

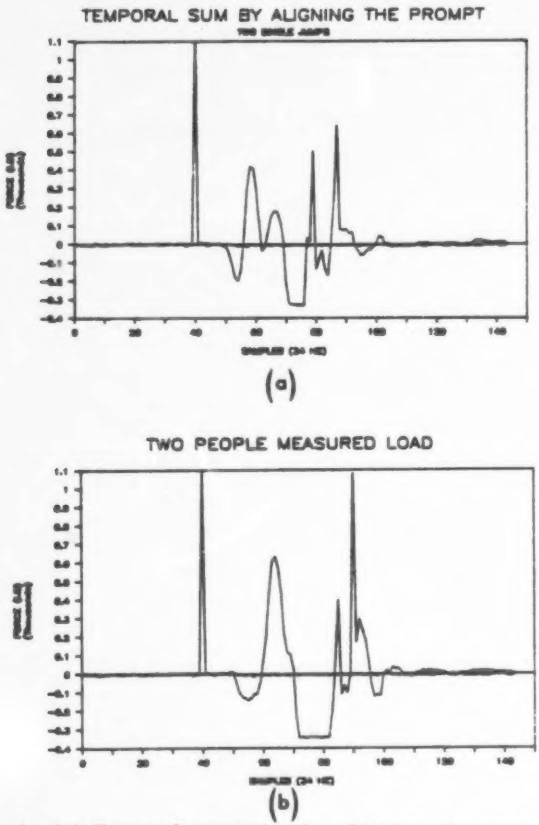

Fig. 4 (a) Temporal summation by aligning the prompts; and (b) measured single jump load

Optimum phase lags were measured in terms of the number of digitized samples (1 sec = 34 samples). Figure 6 shows the histograms for 100 simulated phase lag values for three load cases. The histograms have higher densities around zero (i.e., the ordinate decreases with increasing number of samples). Because of this, we used an exponential distribution to represent the theoretical distribution of these random variables. Exponentially distributed phase lags indicate that people in a crowd tend to be in phase. The phase lag probability density function (pdf) is

$$f(\phi) = \mu \exp(-\mu\phi) \qquad (3)$$

where $f(\phi)$ = the density function; ϕ = the optimum phase lag random variable (the subscript is dropped for simplicity); and μ = the distribution parameter.

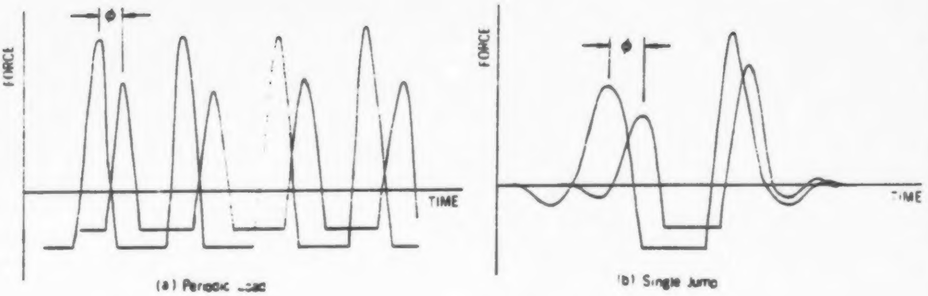

(a) Periodic Load

(b) Single Jump

Fig. 5 Phase lag between two people

PHASE LAG HISTOGRAM FOR 2 HZ LOADING

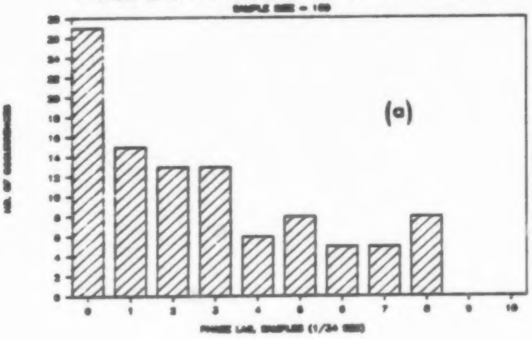

PHASE LAG HISTOGRAM FOR SINGLE JUMPS

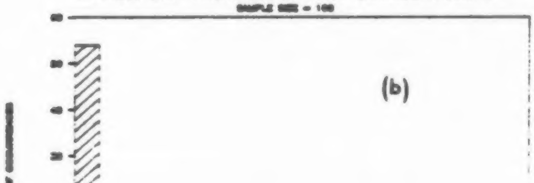

Fig. 6 Phase lag histograms

Using the method of maximum likelihood we estimated μ to be 0.37 and 0.76 for periodic movements (2 and 3 Hz, respectively) and 0.5 for single jumps. Figure 7 shows the sample cumulative distribution functions (cdf) and the theoretical distribution functions for phase lag random variables based on the estimated parameters.

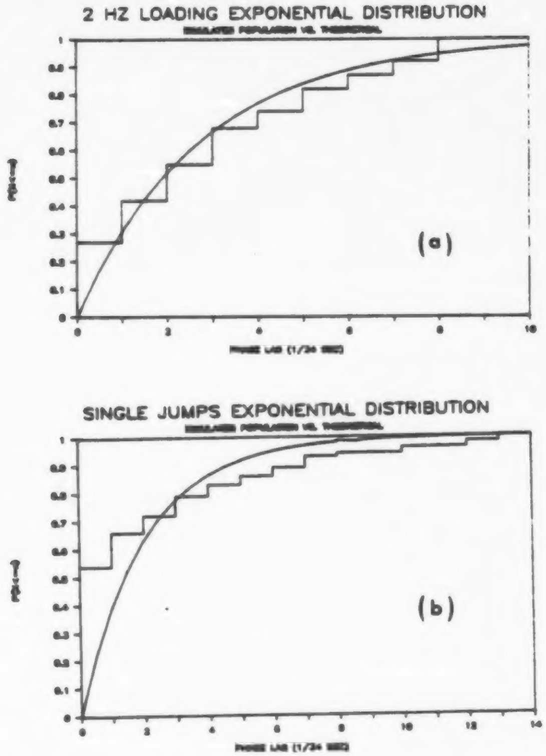

Fig. 7. Phase lag cumulative distribution functions

3.3 Group load Simulation: We wrote the FORTRAN computer program, Group Load Simulation (GLSIM.FOR), to generate loads created by different crowd movements for small groups of varying size. The program uses data from the individual load models and the group coherency parameters described above. Reference (9) contains program details and the source listing.

Using GLSIM.FOR we generated the load-time histories for groups of four and compared the loads with the values measured on the force platform. Thus the experimental data for groups of four people were used only as a check for the temporal summation method. The simulated results compared very well with the corresponding laboratory-measured data in both time and frequency domains (see reference (9) and (20).

4. DESIGN IMPLICATIONS

In general, crowd movements can be idealized as time-varying point loads. The response of the structure can be obtained by randomly simulating the load histories, shifting them on the time axis by random time phase lags, and placing the loads at critical locations on the structure. This procedure seems cumbersome and requires large amounts of computing time. Alternatively, we propose to define an equivalent dynamic load per person in a crowd and divide it by the area occupied by each person to yield a distributed design load.

Using the results of the multivariate regression and temporal summation, we can obtain an expression for the periodic load-time history intensity per person in the crowd as:

$$q(t,M) = \frac{1}{AM} \sum_{m} \sum_{n} \{a_n \cos[2\pi nf(t-\phi_m)] + b_n \sin[2\pi nf(t-\phi_m)]\} \qquad (5)$$

where $q(t,M)$ = dynamic load intensity (psf) per person in a group of M individuals; A = seating area; M = total number of individuals; m = index for number of people ($m=1,2....M$); n = index for dominant F.S. coefficients; f = load fundamental frequency (Hz); and ϕ_m = the mth random time phase lag (sec).

Figure 9 shows the amplitude of load intensity per person as a function of the number of active people in the crowd, M, for 2 Hz periodic loading. The values were obtained using the GLSIM computer program and 3.5 ft^2 (0.325 m^2) of seating area per person (22). The mean and standard deviations are based on fifty randomly simulated cases for each group size. Note that as the size of the crowd increases, the mean becomes asymptotic to 70 psf (3.4 kPa) for both 2 and 3 Hz periodic loadings; the standard deviation for 2 Hz is 9 psf (430 Pa), and for 3 Hz it is 6 psf (290 Pa).

The force magnitudes in Fig. 8 are peak values of the simulated crowd periodic loads; therefore more information about the shape of the curve is required to determine the response of the structure. If the loadings were approximately harmonic, these values could have been used as the amplitude of the harmonic forcing function and placed on the structure to find the corresponding response deflection.

5. LARGE GROUP COHERENCE

We are currently investigating crowd coherency by measuring the response of a light-weight floor system loaded with 10, 20, 30, 40, and 50 people performing transient and periodic vertical loadings. The 12 by 15 ft (3.7 by 4.6 m) cold formed steel floor system has a 3/4 in. (19 mm) plywood deck. The deck is attached to seven simply supported 8-in. C (203 mm) steel joists that are bolted to two end beams made from two back-to-back 10-in. C (254 mm) sections. The entire floor assembly is supported by four short columns resting on 3/8 in. (9.5 mm) thick steel plates. An isometric view of the floor system is shown in Fig. 9. The steel joists and the base plates are instrumented with strain gages. The stain data are recorded by the same data acquisition system used for the force platform.

Using a 3-lb impulse hammer and a spectrum analyzer, we found the first two natural frequencies to be 19 Hz and 25 Hz. The half-power method in the first mode indicated platform damping of 1.1%. We plan to compare finite element results with measured response to determine general crowd coherency and suggest design values.

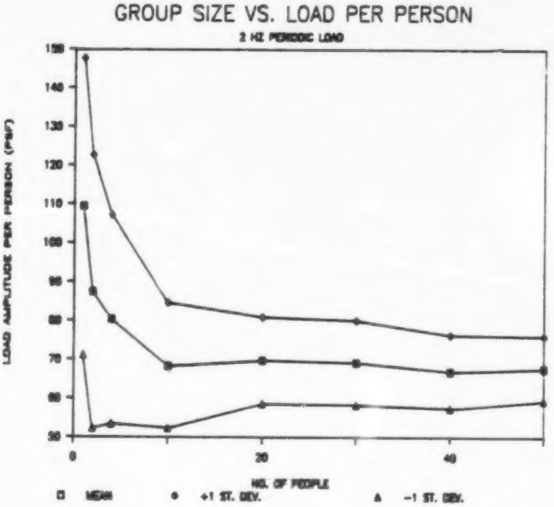

Fig. 8 2 Hz load intensity amplitude per person versus the number of people in the crowd

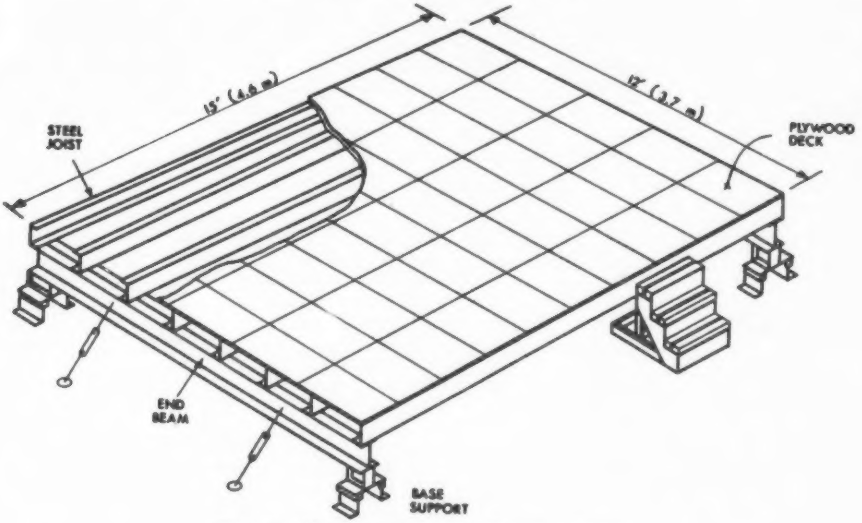

Fig. 9 Floor system for large groups

6. SUMMARY AND CONCLUSIONS

Thirty-five subjects, alone and in small groups, performed seven preselected maneuvers on a force platform. Data were collected using a microcomputer-based acquisition system. Transient activities were analytically modeled with exponential functions, and periodic maneuvers were described using Fourier Series; in both cases the descriptive parameters were regarded as random variables. Temporal summation of individual load histories revealed that persons performing in a group tend to synchronize their movements and produce large loads. By comparing simulated load histories for individuals and aligning these to duplicate group synergism, we generated a set of optimum phase lags that were exponentially distributed. Using the randomly distributed descriptive parameters for periodic jumping, together with the phase lag distribution, loads for crowds were generated.

Results of this research indicate that:

1. Individuals performing maneuvers in a group are cued by auditory and visual stimuli so that the total group load generated is greater than the temporal sum of load histories produced while performing alone.
2. The phase lags of individuals performing single jumps and periodic jumping at 2 Hz and 3 Hz are exponentially distributed and are clustered about zero.
3. Simulated group loads for periodic jumping at 2 Hz and 3 Hz approach 70 psf (3.4 kPa) for groups of ten or greater.
4. Dynamic occupant live load statistics as described herein are suitable for use in a probability-based design code that addresses serviceability.

7. ACKNOWLEDGEMENT

This material is based upon work supported by the National Science Foundation under Grants CEE-8213966 and ECE-8609575. Any opinions, findings, and conclusions or recommendations expressed in this publication are those of the authors and do not necessarily reflect the views of the National Science Foundation.

8. REFERENCES

1. Allen, D. E., and Rainer, J. H., "Vibration Criteria for Long-Span Floors," Canadian Journal of Civil Engineering, Vol. 3, No. 2, June 1976, pp. 165-173.

2. Allen, D. E., Rainer, J. H., and Pernica, G., "Vibration Criteria for Assembly Occupancies," Canadian Journal of Civil Engineering, Vol. 12, 1985, pp. 617-623.

3. The American Architect and the Architectural Review, "The Dynamic Effect of Moving Floor Loads - Stresses Measured in the Floor Balcony of a College Gymnasium," Vol. 126, Oct. 5, 1924, pp. 455-456.

4. American National Standard, "Building Code Requirements for Minimum Design Loads in Buildings and Other Structures," ANSI A58.1-1982, New York, 1982.

5. American Standards Association Bulletin, "Horizontal Forces Produced by Movements of The Occupants of a Grandstand," Vol. 3 No. 4, Apr. 1932, pp. 123-126.

6. American Standards Building Requirements, "American Standard Specifications for Portable Steel and Wood Grandstands," ASA, Z20.1-1941, May 1941.

7. The BOCA Basic National Building Code, Sec. 906, "Uniformly Distributed Live Loads," Building Officials and Code Administrators, International, Inc., Chicago, Illinois, 1984.

8. Dickie, J.F., "Demountable Grandstands," The Structural Engineer, Vol. 61A, No. 3, 1983, pp. 81-86.

9. Ebrahimpour, A., "Modeling Spectator Induced Dynamic Loads," thesis presented to the University of Idaho, Moscow, Idaho, in 1987, in partial fulfillment of the requirements of Doctor of Philosophy, 1987.

10. Ellingwood, B., et. al., "Development of a Probability Based Load Criterion for American National Standards A58," National Bureau of Standards Special Publication 577, Washington, 1980.

11. Gola, M. M., "Mechanical Design, Construction Details, and Calibration of a New Force Platform," Journal of Biomechanics, Vol. 104, No. ST2, Feb. 1978, pp. 348-351.

12. Greimann, L. F., and F. W. Klaiber, "Dynamic Forces Induced by Spectators," Journal of the Structural Division, ASCE, Vol. 104, No. ST2, Feb. 1978, pp. 348-351.

13. Johnston, L. J., "New Data on the Weight of a crowd of People," Association of Engineering Societies, Vol. 34, No. 1, Jan. 1905, pp. 1-5.

14. Lees, A. "Methods of Impact Analysis When Landing from a Jump," Engineering in Medicine, Vol. 10, No. 4, Oct. 1981, pp. 207-211.

15. McLeish, R. D., and Arnold, D. A., "Foot-Ground Reaction Force Plate," J.B.C.S.A. Conference, 1972.

16. Mizrahi, J. and Z. Susak, "Analysis of Parameters Affecting Impact Force Attenuation During Landing in Human Vertical Free Fall," Journal of Engineering in Medicine, Vol. 11, No. 3, July 1982, pp. 141-147.

17. Murray, T. M., "Acceptability Criterion for Occupant-Induced Floor Vibrations," Sound and Vibration, Nov. 1979, pp. 24-30.

18. National Fire Codes 1982, "Standard for Assembly Seating, Tents and Air-Supported Structures, NFPA, 102-1978," Vol. 9, Section 102, National Fire Protection Association, Mass., pp. 102.26-102.27.

19. Pernica, G., "Dynamic Live Loads at a Rock Concert," Canadian Journal of Civil Engineering, Vol. 10, No. 2, June 1983, pp. 185-191.

20. Sack, R. L., and A. Ebrahimpour, "Simulating Dynamic Spectator Loads," Proceeding Third International Conference on Civil and Structural Engineering Computing, Vol. 1, Civil-Comp Press, Edinburgh, 1987, pp. 215-222.

21. Tilden, C. J., "Kinetic Effects of Crowds," Proceedings, ASCE, Vol. 34. No. 3, Mar. 1913, pp. 325-340.

22. Tuan, C. Y., and W. E. Saul, "Loads Due to Spectator Movements," Journal of the Structural Division, ASCE, Vol. 111, No. 2, Feb. 1985, pp. 418-434.

23. Uniform Building Code, 1985 Edition, Section 2304(a), pp. 108 and 124-127.

24. Wiss, J. F., and R. A. Parmelee, "Human Perception of Transient Vibrations," Journal of the Structural Division, ASCE, Vol. 100, No. ST4, Apr. 1974, pp. 773-787.

DYNAMIC STUDY OF A STUB GIRDER FLOOR SYSTEM

C. M. Matthews(1) and C.J. Montgomery(2)

(1)Centre for Frontier Engineering Research
(2)Lamb McManus Associates Ltd.
Edmonton, Alberta, Canada

ABSTRACT: Results are presented from an experimental investigation to determine the dynamic response of a stub girder floor system when subjected to heel impacts. The authors believe that this is the first study undertaken to determine the dynamic characteristics of a stub girder floor.

The natural frequencies of vibration, the peak acceleration response, the mode shapes, and the modal damping ratios have been derived by monitoring the response of a floor to a series of heel impact tests. From consideration of the test results, a procedure is suggested for evaluating the dynamic characteristics of stub girder floor systems at the design stage.

1.0 INTRODUCTION

In the early seventies, J.P. Colaco introduced the "stub girder" floor system (Colaco, 1972). Because this novel system allows the integration of mechanical and electrical building components within the structural framework of the floor, the stub girder framing system has become popular. Numerous office towers have been constructed using the floor system.

In Canada, the stub girder floor system was used for the first time in the Nova Corporation head office tower in Calgary, Alberta. Since little was known at the time about the dynamic characteristics of a stub girder floor, the opportunity was taken to study the dynamic response of the floor system in the Nova Building. This paper presents the results of the study and describes how to extend current design procedures for assessing floor vibrations to the stub girder system.

2.0 FLOOR DESCRIPTION

The dynamic tests took place on the sixth floor of the Nova Building. Figure 1 shows the irregularly shaped floor plan of the building. Semi-lightweight concrete slabs, cast on top of metal decking, span between a steel cantilever floor framing system. These floor beams are, in turn, supported by stub girders. The stub girders span between exterior columns and interior concrete walls along two sides of the building core.

An elevation of a typical stub girder is shown in Figure 2. To ensure composite action between the steel sections and the concrete slabs, shear connectors were attached to the top flanges of both the floor beams and the girder stubs.

The area in which the dynamic tests were conducted is shaded in Figure 1. At the time of testing, the concrete floor slabs were bare, and no partitions or ceilings had been installed.

3.0 EXPERIMENTAL INVESTIGATION

Four series of dynamic tests were conducted to determine the natural frequencies and mode shapes of the floor. In three of the test series, the response of the floor parallel to the stub girders was monitored. In the fourth series, the floor response perpendicular to the girders was monitored. In each test series, the floor was excited at three or more positions by standard heel impacts (Canadian Standards Association, 1984). The impact locations were selected to excite different modes of vibration of the floor system.

Piezoelectric accelerometers were used to measure the acceleration response of the floor system. Figure 3 shows the placement of the accelerometers in the test area. In the first three test series, an additional accelerometer was located at position 6B. The accelerometer signals were recorded by two four-channel FM tape recorders for subsequent analysis. A more detailed description of the monitoring equipment, test procedures, and analysis techniques is provided by Matthews et. al. (1982).

4.0 NATURAL FREQUENCIES AND MODE SHAPES

Magnitude spectra derived through a Fourier analysis of the transient acceleration-time response records were used to determine the natural frequencies and corresponding mode shapes of the stub girder floor system. Figure 4 shows magnitude spectra representative of the dynamic response at three different positions in the test area for the impact locations indicated. Overall, the results of the study revealed that the floor system had a complex dynamic response with two groups of closely spaced natural frequencies below 13 Hz. The seven natural frequencies which contributed significantly to the response of the floor have been tabulated in Table 1. Each frequency has been assigned a mode number which will be used in the following discussion.

Table 1: Natural frequencies of stub girder floor

Mode No.	Frequency (Hz)
1	5.4
2	6.2
3	6.6
4	7.4
5	11.3
6	11.6
7	12.2

Within the two distinct groups of natural frequencies, Modes 3 and 7 (6.6 and 12.2 Hz, respectively) dominated the response of the floor bay centred by line 3 (see Figure 3). Similarily, modes 2 and 5 (6.2 and 11.3 Hz, respectively) were generally the most prominent for the floor bay centred by line 7. Along the stub girder (line 5), the prominent modal response was related to that of the floor bay in which the impact was delivered. Impacts over the stub girder (position 5D) excited the prominent modes of both floor bays to a similar degree.

Figure 5 shows the vibrational pattern of the test area for dominant modes 2 and 3. The mode shapes shown in this figure were obtained by relating records of modal amplitudes measured along lines 3, 5, 7, and D (see Matthews et. al., 1982). Because of the high relative stiffness, the response along the stub girder (line 5) was smaller than the response in the middle of the floor bays (positions 3D and 7D). Note that the floor at positions 3D and 7D, respectively, moved in phase for mode 2 and out of phase for mode 3. Apparently, the discontinuity of stiffness of the floor beams in the bay centred by line 7 (see Figure 3) influenced the dynamic response.

The shapes corresponding to the dominant modes of the second group of natural frequencies are shown in Figure 6. These mode shapes were measured for impacts at the third-points of respective lines. The results indicate that a full sine wave pattern developed in modes 5 and 7 along lines 3 and 7, which centred the two floor bays of the test area. A one-half sine wave shape was retained along the stub girder (line 5). Note that the modal amplitudes at the stub girder position were much lower than those at the middle of both floor bays.

Figure 7 shows the vibrational pattern for mode 5 perpendicular to the stub girder along line D associated with an impact at position 5D. The nodes which developed near the midspan of lines 3 and 7 in mode 5 (see Figure 6a) are quite evident in Figure 7 and, as expected, the amplitude of the response at position 5D was greater for the 5D impact (Figure 7) than for the third-point impact (Figure 6a).

5.0 MODAL DAMPING RATIOS

Modal damping ratios were determined from magnitude spectra by the one-half power bandwidth method and from filtered time response records by the logarithmic amplitude decay method (Matthews et. al., 1982). Because filter limitations prevented the separation of the modal response associated with the closely spaced natural frequencies, the latter method was used to determine an average damping value for the two mode groups (ie. modes 1 to 4 and modes 5 to 7, respectively). Acceleration-time records lowpass filtered at 8.5 Hz and bandpass filtered between 9.0 and 14.5 Hz, respectively, were used in calculating the average damping ratios of the two mode groups.

The damping ratios determined by the two methods are summarized in Table 2.

Table 2: Modal damping ratios (%critical)

Mode No.	Half-power Bandwidth Method	Logrithmic Decay Curve Method
1	4.3	(average for modes 1 - 4) 2.6
2	2.9	
3	2.5	
4	1.8	
5	2.2	(average for modes 5 - 7) 3.0
6	1.3	
7	1.9	

The individual modal damping ratios of the two mode groups determined by the half-power bandwidth method compare reasonably well with the averaged group values obtained by the decay method. With 2.0 to 3.0 % critical damping in the lower modes, the damping of the stub girder floor was was found to be typical of other bare concrete floors supported on steel beams and girders.

6.0 PEAK ACCELERATION RESPONSE

Filtered acceleration-time records of the type shown in Figure 8 were used to determine the peak response of the floor for the two mode groups discussed in the previous section. Table 3 provides a summary of the peak acceleration response at the positions in the test area where heel impacts were delivered.

Table 3: Peak acceleration response of stub girder floor

Impact Location	Peak Acceleration (%g) 0.0 - 8.5 Hz	Peak Acceleration (%g) 9.0 - 14.5 Hz
3D	1.5	0.3
between 3B & 3C	1.3	1.6
5D	0.6	0.7
between 5B & 5C	0.4	0.4
7D	1.9	0.3
between 7D & 7C	1.4	1.1

The response did not exceed 2.0% g at any position for either modal combination. The low acceleration response at positions 3D and 7D in the 9.0 to 13.5 Hz frequency range provides further evidence of the nodes which form close to those positions in the second mode group. The peak accelerations at the two positions on line 5 reflect the low response of the floor along the stub girder.

The peak accelerations of the lower modal combination were used to assess the adequacy of the stub girder floor system for a quiet occupancy. When plotted on the annoyance criteria for floor vibration chart presented by the Canadian Standards Association (1984) at an average frequency of 6.4 Hz, all acceleration values were below the annoyance threshold for a quiet occupancy floor with 3.0 % damping with the one exception of the 1.9 %g acceleration at position 7D which fell slightly above that threshold. Since the peak acceleration values used in assessing the floor represent the combined response of several modes, and not the uncoupled response in the fundamental mode for which the chart was intended, the floor would be acceptable for a quiet occupancy. Furthermore, the damping of the floor system would be much higher in its completed state and the annoyance threshold would rise accordingly.

Observers present during the dynamic tests were not annoyed by the vibration levels generated by the heel impacts.

7.0 DESIGN PROCEDURE

In this section, a method is outlined which extends the application of the design procedure presented by the Canadian Standards Association (1984) for assessing floor vibrations to stub girder floor systems. The results of the dynamic study were used to verify the validity of the proposed method.

In the proposed method, the stub girder floor is considered to be a two-way system in which the stub girders are treated as flexible supports for the floor beams. The floor bays between stub girders are assumed to act independently of adjacent floor bays. With the following modifications, the normal procedure is used to determine a system frequency for the floor :

1) In calculating the moment of inertia of the composite T-beams, the average spacing of the floor beams is used as the effective concrete flange width and the reduced stiffness of the drop-in beams is ignored. The fundamental frequency of the T-beams is calculated using the standard equation.

2) The provisions of clause 17.3.2.1 of CAN3-S16.1-M84 (Canadian Standards Association, 1984) are used to estimate the concrete flange width which contributes to the composite stiffness of the stub girder supports. The "stubs" should be included when the composite moment of inertia is calculated. All structural and non-structural components supported by the stub girder are assumed to contribute to its mass. The fundamental frequency for the girders is calculated using the same equation as for the floor beams.

To assess the dynamic serviceability of a stub girder floor at the design stage, an estimate of the peak acceleration resulting from a heel impact is required. The peak acceleration is calculated by the equation given in Appendix G of Canadian Standards Association (1984), using the length of the stub girders for the width of the effective beam.

The acceptability of the stub girder floor for a quiet occupancy is then determined by plotting the calculated peak acceleration on the annoyance criteria for floor vibration chart at the system frequency of the floor and noting whether the annoyance threshold for an appropriate level of damping has been exceeded.

8.0 SUMMARY AND CONCLUSIONS

The dynamic response of a stub girder floor system was determined experimentally. The floor was found to have seven prominent natural frequencies in two distinct groups below 13 Hz. In the first mode group (5.4, 6.2, 6.6, and 7.4 Hz), both of the adjacent floor bays and the stub girder were characterized by a one-half sine wave pattern parallel to the stub girder. A full sine wave shape developed at the middle of the floor bays in the second mode group (11.3, 11.6, and 12.2 hz), while the one-half sine wave pattern was retained along the stub girder. Differences in the mode shapes perpendicular to the stub girder were responsible for the variation in frequency of the modes within the two groups.

Modal damping ratios were determined by two methods with good agreement between the results. The modal damping ratios were typically 2.0 to 3.0% of critical. Although the floor system was in an unfinished state, the measured dynamic response was found to be acceptable for a quiet occupancy.

ACKNOWLEDGEMENTS

The authors wish to thank Mr. G. Culham for his permission to monitor floor vibrations at the Nova Corporation head office tower, and H.J. Rainer for his advice and assistance during the experimental phase of the study.

REFERENCES

Canadian Standards Association (1984), Steel structures for buildings (limit states design), CSA, Rexdale, Ontario, CAN3-S16.1-M84.

Colaco, J.P., A Stub girder system for high rise buildings, Engineering Journal, AISC, July, 1972.

Matthews, C.M., Montgomery, C.J., Murray, D.W., "Designing floor systems for dynamic response", Structural Engineering Report No. 106, Department of Civil Engineering, University of Alberta, October, 1982.

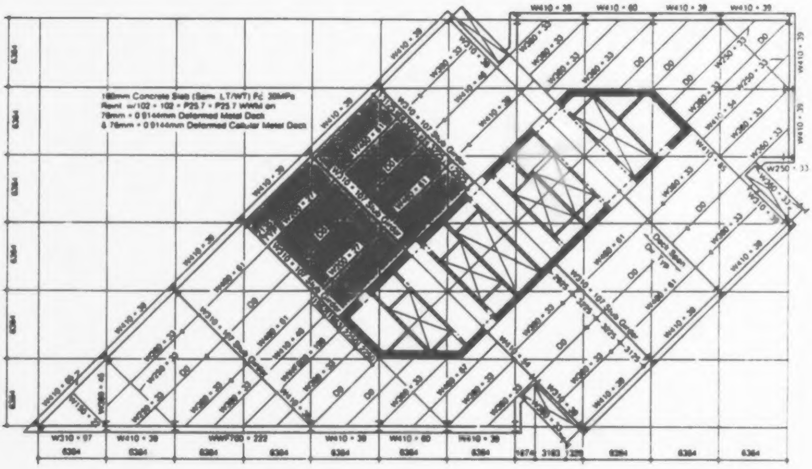
160mm Concrete Slab (Semi LT/WT) Fc 30MPa
Reinf. w/102 × 102 – P25.7 × P25.7 WWM on
76mm × 0.9144mm Deformed Metal Deck
& 76mm × 0.9144mm Deformed Cellular Metal Deck
W410 × 39
W410 × 60
W310 × 107 Stub Girder
W360 × 33
W250 × 33
W460 × 61
W410 × 54
W410 × 85
DD
Deck Span Typ
W310 × 97
WWF700 × 222
6384
1674
3183
1220

Figure 1: Sixth floor plan of Nova Building

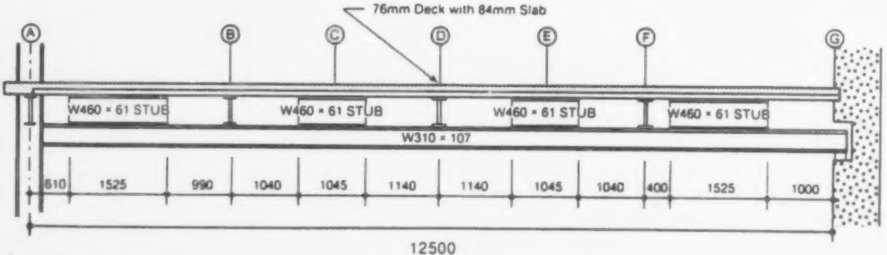

Figure 2: Elevation of typical stub girder

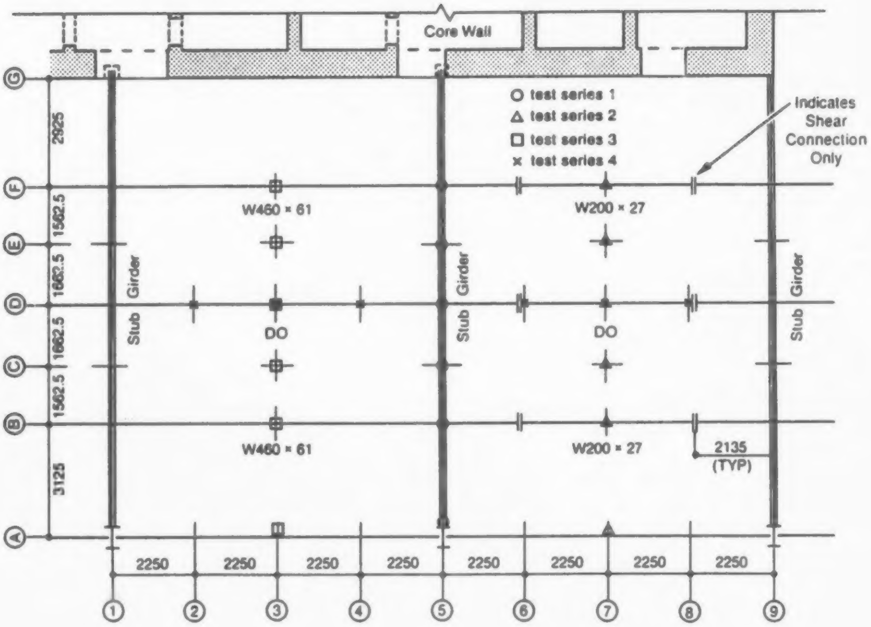

Figure 3: Test area indicating accelerometer positions

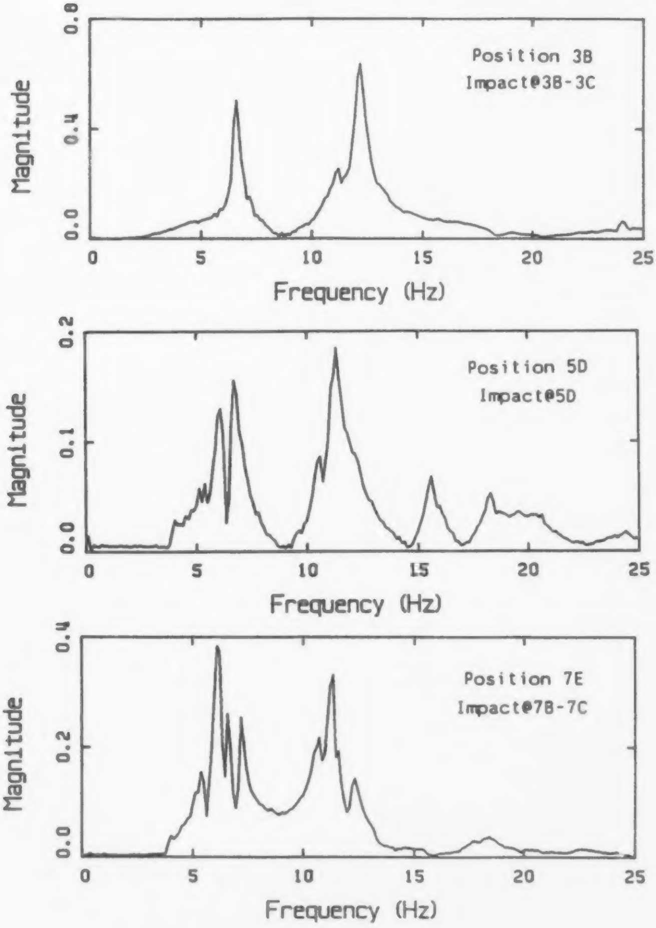

Figure 4: Magnitude spectra

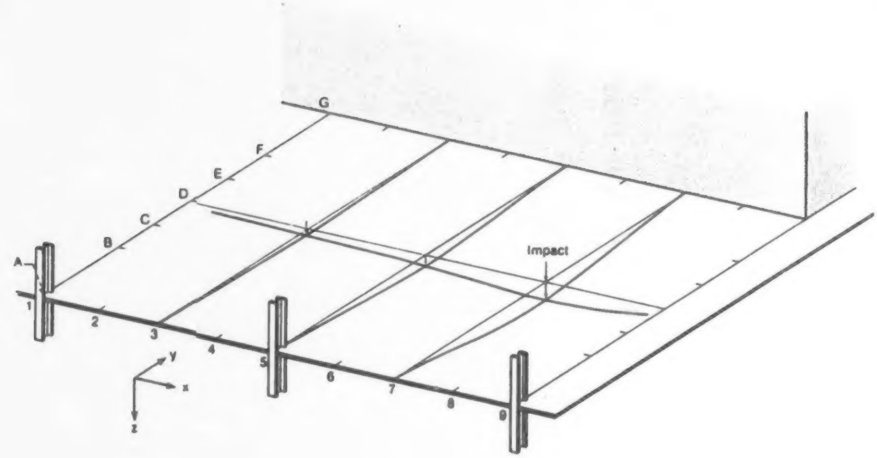

(a) Mode 2

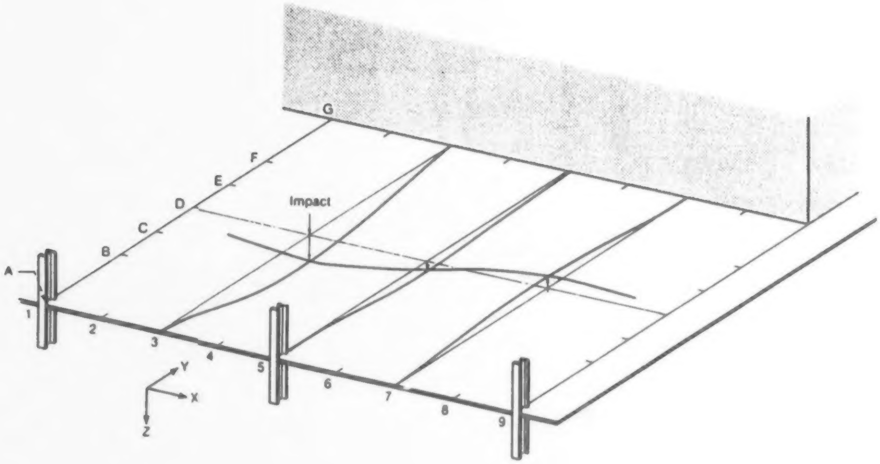

(b) Mode 3

Figure 5: Mode shapes

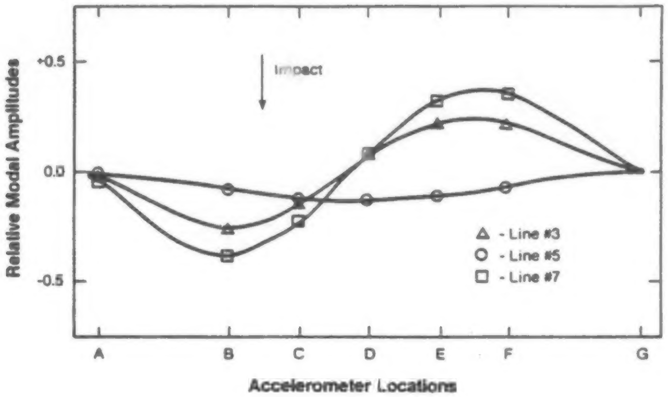

(a) Mode 5

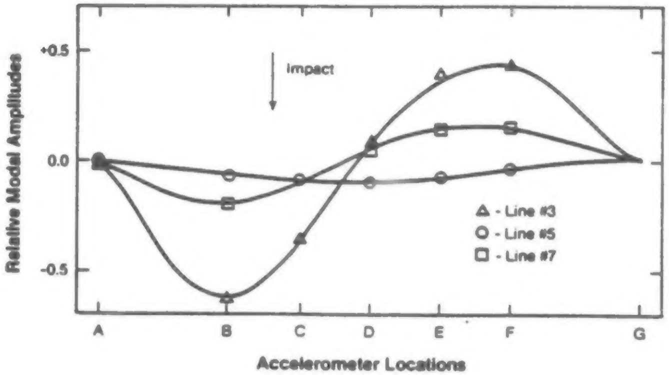

(b) Mode 7

Figure 6: Mode shapes

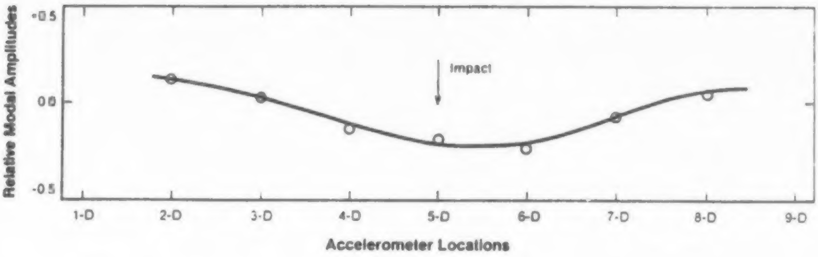

Figure 7: Shape of mode 5 along line D

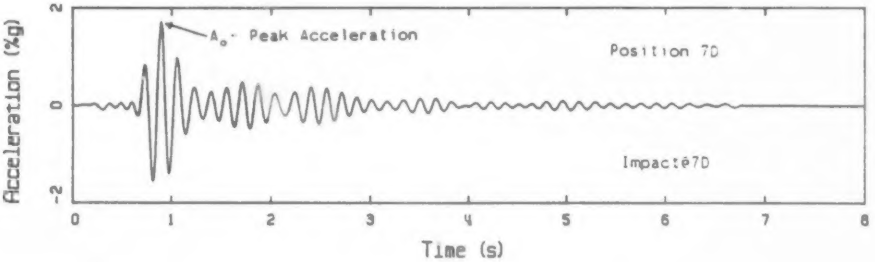

Figure 8: Peak acceleration from typical heel impact

PERFORMANCE AND ACCEPTABILITY OF WOOD FLOORS-FORINTEK STUDIES

D.M. Onysko
FORINTEK CANADA CORP.,
OTTAWA, ONTARIO.

ABSTRACT: The results of floor research at Forintek are summarized. Included are investigations on the contribution of bridging, the effect of its placement and the effect of drying out of floors on its effectiveness. Other studies concern the contribution to floor stiffness made by parquet flooring and multiple layer flooring, field gluing, continuous joists, and the placement and attachment of partitions. The analytical techniques used were extensions of work by others. Field studies provided data for correlation of floor performance with acceptability by occupants and the formulation of a performance criterion based on the deflection of floor systems under the action of a concentrated point load.

1.0 INTRODUCTION

Floors must be designed to meet both strength and stiffness requirements. The long standing stiffness requirement in general use is based on the concept that maximum deflection of a floor under a uniform load should be limited to a certain proportion of the span. In Canada, the ratio commonly used has been 1/360 for a uniform load of 1.9 kN/m^2 in residential construction. Ostensibly, while this ratio has been required to limit the potential for cracking of plaster ceilings, it has also been thought to result in floor designs that are stiff enough to prevent excessive deflections or vibrations.

Overall, that simple criterion has served both designers and regulatory agencies moderately well. But, there are situations where vibrations or excessive deflections occur and unacceptable performance results. In the past, traditional floors usually consisted of at least two layers of structural and semi structural flooring, e.g., diagonal board subflooring with hardwood strip flooring as the finished floor surface. When panel materials came into general use, plywood subflooring became the working platform and other panel materials were often added later as a base for vinyl tiles or for parquet flooring. In more recent years, single-layer subflooring/underlayment has been used to reduce costs. In this evolution of construction practice, the transverse flooring stiffness provided has declined. Since the design criterion used for deflection only influenced the stiffness of joists provided, the criterion fails to deal with other factors that also influence the acceptability of a floor resulting in a decline in the quality of performance provided.

This paper is a summary of the results of a research program that was initiated at the Eastern Forest Products Laboratory of the Canadian Forestry Service in the early 1970's (now the Eastern Laboratory of Forintek Canada Corp.) (Onysko, 1970). Feedback on poor floor performance came to us from home owners, builders and from Canada Mortgage and Housing Corporation (CMHC) whose inspectors found a larger than usual number of complaints at that time in certain regions of the country. Some classes of conventionally built floors were too "bouncy" from the occupant's point of view. Preliminary work suggested the reasons why the simple deflection criterion based on uniform loading was inadequate, and laboratory and field studies were begun to address the problem by acquiring data upon which a new criterion might be based.

Broadly speaking, this program consisted of experimental work to obtain an understanding of the influence of construction techniques on floor performance, analytical studies to determine the performance of floors based on the properties of their individual parts, and studies in which physical performance was correlated with the opinions of occupants about the acceptability of floors in their residences.

2.0 FLOOR PERFORMANCE STUDIES

Both field and laboratory testing was done to better understand how floors perform in practice and to provide test data for comparison with the results from analytical techniques. The following sections provide brief summaries of the findings of some of these studies.

Before doing so, a brief description will be provided of the test methods used. Concentrated loads were usually applied using the mass of a person supplemented by additional dead mass to bring the total to 100 kg. In the laboratory we have preferred to use a small loaded trolley. In either case, the load is applied through a relatively small area. Deflections of joists were measured from below to obtain transverse deflection profiles for each position of load.

Dynamic impact tests involved dropping a steel ball onto a neoprene rubber slab, or by use of a cone-drop tester that was developed to apply an impulsive load to the floor. The resulting transient vibration was monitored with accelerometers, or velocity or displacement transducers, and the resulting signals were recorded on magnetic tape for subsequent analysis.

2.1 Contribution of Bridging

Minimum performance floors are very much affected by the presence of bridging. It was important for us to assess that contribution and to have some way of including it in the structural analysis.

Bridging can act primarily as a bending element or as a shear element depending on its type. Some of the types studied are shown in Figure 1. A wooden strap nailed to the underside of the floor joists is forced to conform to the transverse deflection profile of the floor when it is loaded by a concentrated load. The strap bends and the resisting forces help to distribute load to the other joists in the vicinity of the load. On the other hand, solid wooden blocking or cross bridging act primarily as shear elements that attempt to prevent distortion of the space between joists. In either case, bridging acts to assist floor sheathing in distributing the effect of concentrated static loads or dynamic loads to adjacent floor areas. This is demonstrated in Figure 2 where the effect of low and high load sharing is drawn pictorially. The fact that the deflection and dynamic response of a floor are reduced by the presence of bridging suggests that it will have an effect on floor acceptability.

2.1.1 Relative Importance of Various Bridging Types

Our initial bridging study (Onysko and Jessome, 1973) on a full-sized floor with the minimum plywood thickness allowed showed that deflection under a concentrated load could be reduced by up to 49 percent depending on the bridging type. The contribution to reduction of deflections and peak dynamic responses of this specific test floor was found to vary from zero, for a 25 by 3-mm steel strap nailed across the bottom of the joists at midspan, to 49 percent for the combination consisting of a bottom wood strap and solid skewed blocking. The reduction in response made possible by the bridging depends on the stiffness of the flooring and the floor joists, as well as on how the bridging is attached. Floors that are substantially stiffer to begin with will not benefit to the same degree.

2.1.2 Effectiveness of Bridging in Floors That Dry Out

Seven full-size floors were built from joists having a relatively high moisture content which were then allowed to dry out (Onysko and Garrant, 1981). There were seven 28 by 184-mm Spruce-Pine-Fir (SPF) joists in each floor, and 12.5-mm Douglas-fir plywood was used for the subflooring. Each was built with a clear span of about 3.5 m and with joists at 406 mm on centres. Eight bridging combinations were investigated.

Floor joists experienced an increase in stiffness about as predicted based on average shrinkage properties of SPF species and known relationships between the modulus of elasticity and moisture content of wood. There was a 0.5 percent increase in stiffness for each one percent decrease in moisture content. Despite this, the nailed floors decreased in stiffness apparently because the nail connections loosened. A rigidly glued floor, on the other hand, increased in stiffness.

Some bridging types lost more of their effectiveness than others. For example, a bottom wood strap lost very little of its effectiveness, but it was the least effective to begin with. Wooden cross bridging and skewed blocking had a 5 percent loss in effectiveness. Where a bottom strap was combined with shear-type bridging, especially skewed blocking, the largest improvement in stiffness resulted. When only nailed, the largest percentage reduction also occurred on drying. The effectiveness was only maintained when effective nailing was supplemented with elastomeric adhesive. On the other hand, if relatively poor nailed connection was used with gluing, the largest percentage loss in effectiveness resulted because the adhesive failed to take the stresses caused by differential shrinkage.

2.1.3 Effect of Bridging Location

Bridging is most often placed at the middle of the floor span. When the span exceeds 4.2 m, two lines of bridging are required, usually placed at the third points of the span. The effect of bridging placement was studied in two unreported test series.

In the first study, the bottom wood straps (38 by 89 mm) were placed symmetrically about the centre of the span at different locations. When the straps are placed at the third point of the span, their combined effect is about 0.75 of the effect if both had been at the midspan position. One strap placed at midspan was about equivalent to having straps placed at 0.3 of the span from each support.

In the second study, tests were conducted on 305-mm-deep wooden floor trusses spaced at 488 mm on a span of 5.92 m, and with 14-mm Douglas-fir plywood. The effect of one piece of lumber placed on its edge (sometimes called a strongback) and attached to the trusses at the centre of the span was about equivalent to the effect of strongbacks at the third point of the span, as already noted. The deflected profile of the trusses was also measured and it was found that if only one strongback was used in the centre of the floor, the maximum deflection under a point load no longer occurred when the load was at the centre of the floor. This is shown in Figure 3 where the deflection envelopes are shown for the floor with and without strongbacks at various locations. It would appear that if more than one line of bridging is to be used, the distance between them should be somewhat less than one-third of the span to maximize the benefit of the bridging on the total deflection envelope of the floor.

The effect of positioning shear-type bridging was similar to that for bending element bridging.

2.1.4 Effect of Distributed Strapping and Ceilings

In another unreported study, the effect of distributed strapping was examined. It was found that the stiffness of the strapping could be assumed uniformly distributed (or smeared) along the joist length. This equivalent stiffness could also be added directly to that of the flooring in the floor analysis. When a ceiling was added to the floor and the joints were not taped or plastered, the gypsum board stiffness could also be added to that of the flooring for the analysis of deflections under concentrated loads.

2.2 Contribution of Composite Action Between Components

Composite action between the various components in a floor can occur intentionally and sometimes inadvertently. When parquet flooring is bonded to plywood or waferboard subflooring, as it must to stay in position, an increase in stiffness is imparted to the subflooring which is not recognized in the building standards. Composite action also results when layers are well nailed to each other, or when subflooring is glued to floor joists. Several of these cases have been investigated to a limited degree at the Eastern Laboratory.

2.2.1 Composite Action of Parquet Flooring With Subflooring

A limited study was undertaken to assess whether parquet flooring provided significant composite action with subflooring to which it is bonded (Onysko, 1981a). It was found that an important contribution was made by parquet flooring despite the fact that it is made of small blocks with joints in between. The bending stiffness that most affects floor system deflection (when the face grain of the plywood is laid across the joists) increased by a factor of from 2.04 to 1.25. Stiffness in both principal directions are involved for local flooring deflections under the action of point loads. It was found that a 66 to 36 percent reduction in local plate deflection could be attributed to the composite action provided by the bond of parquet flooring to the plywood. In fact, for the panels tested, the average deflection of the 12.5-mm plywood with parquet flooring was slightly less than that found for the 15.5-mm plywood without parquet flooring.

The study concluded that, as a rough estimate, parquet flooring could be thought of as a layer of plywood-like material equal in thickness to half the parquet thickness. The coating used to finish the flooring surface was also found to be a factor.

In a second unreported study involving field tests in two houses in which continuous steel joists were used, with 15.5-mm plywood nailed or nail-glued to the joists, static and dynamic tests were done before and after parquet flooring was installed. It was found that floor system deflections were reduced by the installation of parquet flooring in amounts ranging from 9.1 to 20.4 percent for the nailed floors and 9.1 to 23.7 percent for the nail-glued floors (average reduction of 17.2 and 18.1 percent respectively).

2.2.2 Multilayer Flooring

Because so many floors inspected in the field had two or more layers, a limited study (also unreported) was done to see what contribution might be counted on when multilayer flooring panels were used.

The floor tested consisted of 38 by 184-mm SPF joists spaced at 406 mm and tested on a 3.49-m span. Three layers were used: 12.5-mm plywood, 9.5-mm particleboard and, finally, a 6-mm Douglas-fir sanded plywood. Tests were performed at intermediate stages of the construction of the floor to assess the static and dynamic performance of the floor when each layer was added. The layers were nominally nailed together, and nailing into the joists was avoided. Overlap of layers at joints was only about 100 mm.

It was found that nominal nailing of layers to each other did not result in composite action between them. The effect of adding layers could be accounted for almost entirely by the additional transverse stiffness provided. The small overlaps provided did not seem to add to composite action with the joists (by providing continuity over butt joists). It was only when more nails were finally added directly into the joists that additional composite action with the joists resulted. It was concluded that, unless care was taken to assure continuity at butt joints in the subflooring by having sufficient overlap of the overlying materials, multilayer flooring using panels could probably be treated as the summation of stiffness of all the layers without composite action between them.

2.2.3 Field-Glued Floors

The theoretical and practical work done at the USDA Forest Products Laboratory has provided an adequate means for estimating the stiffness of field-nailed and field-glued floors (McCutcheon, 1977). Together with simplified analysis techniques developed at the Eastern Laboratory, a reasonable estimate of maximum deflection performance under concentrated loads of field-glued floors can be obtained. Two field studies will be mentioned here to highlight the degree of contribution that is possible.

The first study in which field gluing was involved has already been noted in section 2.2.1. These were tests on nailed and nail-glued steel joist floors in which we studied the contribution of parquet flooring. Field gluing of the subflooring to joists was found to result in a 20 to 30 percent decrease in deflection on average.

The second field study was done at the HUDAC MARK XI Energy Research Houses in Orleans (Onysko, Demers and Garrant, 1981). Comparisons of floor performance in these houses showed that nail gluing caused differences in deflection under concentrated load of 32 percent and 38 percent on average before installation of bridging, and 31 percent and 44 percent on average after the installation of bridging. Even the simply supported nailed-only floors showed composite action because the plywood had been installed so tightly that compression stress transfer was possible at the tongue and groove edges.
Another study involved the re-testing of floors in two of the HUDAC MARK XI houses more than two years after the first tests mentioned above (van Rijn, 1982). These showed that deflections of both the nailed floors and the nail-glued floors were greater than before. Small changes in the properties of the materials caused by further drying and loosening up of connections probably served to allow greater deflections to occur, even of the nail-glued floors.

2.3 Continuous Joists

Continuity of joists over a central support beam has sometimes been considered to provide a benefit to performance. While some increase in stiffness is provided, there are other characteristics of behaviour that should be considered. In our field studies, we have found instances where continuity of joists permitted transfer of vibrations into other rooms causing disturbances that were considered annoying.

Designers often assume idealized support conditions. Tests of continuous joist floors at the HUDAC MARK XI houses showed that reality can cancel benefits thought to be real on paper (Onysko, Demers and Garrant, 1981).

It was found that about a 10 percent reduction in deflection under point loads could be attributed to joist continuity compared with simply supported spans when there was no bridging. This difference was reduced to about 4 percent once bridging had been added. Continuity is thus considered to provide only a minor benefit to this aspect of performance.

When the floors were loaded by a 1.85 kN/m^2 uniform load, one span at a time, we found deflections of the supporting central beam to have a large effect on the overall deflection profile. Support beam deflection was large in comparison with the negative deflection of the adjacent non-loaded span. The negative deflection and resulting moment that might be expected to develop was substantially less than assumed. Consequently, the maximum positive moment in the loaded span was larger than when unyielding supports are assumed. This effect is normally ignored in the preparation of span tables for continuous joists. The support beam itself deflected only 1/1200 of the span under this partial load (on a 3.55-m span). It would appear that present design practice should be modified to account for these effects. On the basis of serviceability, little seems to be gained by joist continuity; in respect to strength requirements, the design may be unconservative because of support settlement.

2.4 Effect of Partitions on Floor Performance

The influence of non-load-bearing partitions on the performance of floors is not normally accounted for in design for a very good reason. The designer cannot always depend on the partitions remaining there nor that they will be built where the drawings indicate. Secondly, they introduce a complexity in the design that is not welcomed and there is little information that can be used to guide a designer should he wish to take them into account.

In our field studies of floor performance, it was necessary to be able to approximate the influence of partitions for computational purposes. For this reason, one limited study (unreported) was undertaken in the laboratory. These tests involved a wooden truss floor which has already been described in section 2.1.3.

A full-size partition was positioned across the floor at different locations and attached to the floor in various ways. A summary of the results of the static and dynamic results are given in Figure 4. This figure shows the ratio between the actual measured response and the response of the floor without a partition as a function of the position of the partition on the span.

The partition was found to affect the floor performance without even being attached to the floor simply by preloading the floor. Nailing of the bottom wall plate only to the subflooring had no effect on the floor response. Only when the bottom wall plate was nailed directly to the floor trusses were the deflections substantially ameliorated. In the absence of any other data, we have used the relationship shown in Figure 4 for predicting the influence of partitions in floors encountered in our acceptability studies.

3.0 COMPUTATION OF FLOOR PERFORMANCE

Only a very brief summary can be given of our work in this area. We have been concerned with being able to compute the deflection of floors encountered in our field survey work.

For uniformly loaded simple spans, with or without partial composite action, the procedures are quite straightforward. In the case of concentrated point loadings or point loadings distributed over a small area, the problem is more complex but it is relatively easy to handle by computers. We have extended the simplified theory initially set forth by Vermeyden (1968). His solution was for a 7-joist floor with unsymmetrical properties. This approach was modified to include the effects of bending and shear bridging, individually or in combination (Onysko, 1981b). The method was then expanded to provide a deflection solution for floors having up to 13 joists, with free or with supported edges, and taking symmetry into account.

A general purpose computer program was also prepared to handle the analysis of floors based on internal assumed properties for various flooring and subflooring materials and joists, and many combinations of bridging types. This program has been used for our field survey work in which an estimate of performance was required for correlation with occupant acceptability ratings.

As a comparison of the efficacy of the method, based entirely on assumed properties, a plot of computed versus measured maximum deflection under a concentrated load is given in Figure 5 for 74 floors tested in the field. This plot shows that quite good agreement was attained.

Computation of the peak response of a floor to an impulsive load requires a further degree of complexity. The floor is assumed to be a single-degree-of-freedom system and an estimate of the effective mass is required. A procedure outlined by Lenzen and Dorsett (1968) was used. This procedure requires that the effective width of the floor participating in the vibration be calculated. The effective width depends on the transverse deflection profile of the floor. In our laboratory testing where the transverse deflection profile from static point loading was measured, this procedure produced good agreement between the measured values and the computed frequency and peak displacement response.

In the field, not only the properties of the floor elements in the floors must be estimated, but the mass and the damping ratio are required as well. Agreement with measured test results was not as satisfactory. For example, the poor comparison between computed and measured frequency of vibration for 30 floors is given in Figure 6. In part this is disagreement is caused by the relatively poor estimate of the overall shape of the deflection profile produced by the program used. An analysis program that has greater accuracy in predicting the transverse deflection profile of floors without bridging was developed by Foschi (1982). However, additional development would be required on this program to incorporate the effect of bridging.

It should be noted that dynamic tests are more subject to problems with instrumentation and analysis than are concentrated load tests. It is not normally possible to apply the same impact loading each time to each and every floor because of the cushioning provided by carpets and underpadding. Multiple-layer floors also tended to absorb the impulse differently because of separation between layers. This was partially accommodated for recently when we reanalyzed all of our static and dynamic field test data (Onysko and Bellosillo, 1985).

Before passing on to the next section, it is worth noting that typical light-framed floors do not behave in the same way as relatively heavy longer span floors when subject to human impact. The reason for this is that the human body represents a relatively larger portion of the vibrational mass involved and is heavily damped in relation to that of the typical light-framed floor. The presence of even one person in the middle of a floor greatly modifies its performance. In the case of human impact, such as the heel drop test which some investigators have used in their testing, the impulse imparted to the floor and the maximum response are greatly influenced by the human floor interaction. This interaction has been modeled recently (Foschi and Gupta, 1987). However, in our correlation studies we have only attempted to compute the response of floors under the action of a short fixed impulse and assuming no person was on the floor.

4.3 ACCEPTABILITY STUDIES

The most direct way to find out if a product is acceptable to a population is to conduct a properly designed survey. While this is relatively straightforward for a product that is of uniform consistency and to which consumers have equal access, it is not as simple for assessing floor performance where each consumer experiences a different quality of performance and where the performance may be different within the same residence. Further, the consumer's reaction to his or her floors is affected by expectations, lifestyle, the placement of furnishings, the demands put on the structure, conditioning, and other factors. None the less, a survey approach can be an effective way to obtain consumer acceptability of floor performance versus studies based solely on human perception of vibration.

The Eastern Laboratory conducted two pilot surveys in preparation for what was to be a national survey of floor performance. The first study involved 20 houses in Ottawa. The occupants were screened by a questionnaire survey from the population of the laboratory. This work helped identify effects that respondents took into account in formulating their opinions about floors.

This was followed by an extensive pilot survey in Hamilton in which various survey techniques were investigated. Here, 365 occupants were interviewed, 185 houses were inspected in detail, and testing was performed in 25 houses. This preliminary work helped refine a survey questionnaire, and the most useful approach to use in selecting houses for the survey. It also provided additional backup test data for the development of the floor analysis program. The test experience also showed that testing was expensive and that, if possible, performance should be calculated in order that the number of floors included could be as large as possible for the research budget available.
The final acceptability study was carried out in Ottawa, Hull, Toronto, Montreal, Saskatoon and Regina. Detailed interviews and inspections were held in 107 houses providing data and opinions for 646 floors, while informal interviews and inspections for a further 186 floors were also obtained. A report on the initial analysis of the survey included tentative performance criteria (Onysko and Bellosillo, 1978). The final report, with a reanalysis of the data, was completed in 1985 (Onysko, 1985).

5.0 DEVELOPMENT OF PERFORMANCE CRITERIA

The process of developing a performance criterion depends on the quality of the data and on the number and nature of the factors that are controllable in design. It would not be appropriate, for example, to include the occupant's weight or sex into account even though, as it turns out, these factors do have an effect. If only one variable or combination of variables can be determined that best identifies good and poor floors, as shown in Figure 7, then a performance criterion might be set part way between the two groups of floors with a minimum of floors from either group on the wrong side of the boundary. The aim of the analysis to establish a criterion is to assess the coefficients and variables that would cause the acceptable and unacceptable classes of floors to be identified so that the least number of misclassifications result. The statistical technique used is called discriminant analysis.

The most important variables were found to be deflection under concentrated load (y), peak dynamic response to an impulse loading (Δ), the damping ratio which is a measure of the decay of a transient vibration (α), the frequency of vibration (F), and the floor span (L). It was found that the deflection of floors under a uniform load was a relatively poor discriminator between good and poor floors.

The design criterion could be cast on the basis of either static point load response or on the basis of dynamic response to impulsive loading. In our initial formulations (Onysko and Bellosillo, 1978) a criterion based on dynamic impulse response was ventured. This criterion was tempered by examination and inclusion of data for long spans floors evaluated by others (Allen and Rainer, 1976). The damping ratio appropriate for different classes of wood floor construction can not yet be confidently assigned despite the data base that we have accumulated (Onysko and Bellosillo, 1987). This value is required for computation of peak dynamic response. Since much better correlation was found between measured and computed deflections under point loading, it was decided to recommend a design criterion based on this approach.

The criterion boundary which resulted in the minimum number of misclassifications in the field survey is shown in Figure 8 and is based on acceptability ratings which were based on the occupant's opinion with an override provided by the inspectors when the difference in acceptability rating was by more than one category. An upper deflection limit of 1.75 mm was chosen because insufficient data was available to allow higher deflections for spans under 3 meters. It must be noted that this criterion is based on the best estimate of actual average performance which in turn is based on mean in-grade data for floor joists and other material properties, including assumed partial composite action of the flooring materials with the floor joists.

More recently, this tentative criterion was reassessed using the most recent in-grade data to be recommended for joist and panel materials (Onysko, 1988). It was decided to calibrate the criterion against a class of floor that was considered to have been satisfactory in the past. This floor type consists of 15.9-mm Canadian Softwood Plywood, nailed at an average spacing of 200 mm to No. 2 grade 38 by 185-mm SPF joists spaced at 400 mm, and with a 19 by 89-mm bridging strap nailed to the joists at midspan. The permissible span for this floor under a 1.9 kN/m^2 uniform design live load using the present design criterion and pre 1980 bare joist properties was 3.450 meters. The design equation which just allows this floor to pass is given by the following equation:

$$y = \frac{8.0}{L^{1.3}}$$

where y is the maximum deflection of the floor system in millimeters under a concentrated mass load of 100 kg, and L is the clear joist span in meters. The deflection limit was shifted to 2.0 mm and this equation has been plotted on Figure 8 together with the measured field data for which acceptability ratings were available.

It is felt that this boundary provides an acceptable compromise for minimum performance floors, the quality of which can be easily increased by various simple construction practices. The impact of a performance criterion of this nature is that it accounts for the floor system performance as opposed to that of only the floor joists. Thus, it can permit the manufacture of products, such as waferboard, to achieve the highest possible transverse stiffness consistent with the need for an optimum cross-sectional area for composite action with the floor joists (Lau, 1982).

6.0 CONCLUSIONS

Field and laboratory studies on floor performance by the Eastern Laboratory have been summarized. Many factors were found that affect floor performance that are not now accounted for in design. The work has shown that deflection of floors under uniformly distributed loading is not well related to acceptability of floors in occupied houses. It has also led to the formulation of a performance criterion based on the deflection of floors under a concentrated load. When this criterion has been confirmed, it is hoped that its availability will permit the building industry to more properly design floors and to take best advantage of construction methods leading to better all round performance and consumer satisfaction.

REFERENCES

Allen, D.E. and J.H. Rainer. 1976. Vibration criteria for long-span floors. DBR Paper No. 668. Div. of Bldg. Res., National Research Council, Ottawa, Canada. (Reprint from Can. J. Civil Eng. 3 (2): 165-173).

Foschi, R.O. 1982. Structural analysis of wood floor systems. Journal of the Structural Division, ASCE. 111(11), pp. 1557-1574.

_______. and A. Gupta. 1987. Reliability of floors under impact vibration. Canadian Journal of Civil Engineering (in press).

Lau, P.W.C. 1982. Performance of residential floors with oriented waferboard. Presented at the second Canadian Waferboard Symposium, June 1982. Ottawa, Canada.

Lenzen, K.H. and L.P. Dorsett. 1968. Effect of the variation of structural parameters on the vibrational characteristics of steel joist-concrete slab floor systems and suggested designs. Studies in Engineering Mechanics, Rep. No. 32. Univ. of Kansas, Lawrence, KS.

McCutcheon, W.J. 1977. Method for predicting the stiffness of wood-joist floor systems with partial composite action. USDA Forest Service. Research Paper FPL 289. Forest Products Laboratory, Madison, Wis.

Onysko, D.M. 1970. Performance of wood-joist floor systems: A literature review. Info. Rep OP-X-24. Forintek Canada Corp., Ottawa, Canada.

______. 1981a. Contribution of parquet flooring to the stiffness of plywood subfloors. Rep. to Can. For. Ser. Project 12. Eastern Lab., Forintek Canada Corp., Ottawa, Canada.

______. 1981b. Deflection of floors under concentrated loads. Rep. to Can. For. Ser. Project 12. Eastern Lab., Forintek Canada Corp., Ottawa, Canada.

______. 1985. Serviceability criteria for residential floors based on a field study of consumer response. Project 03-50-10-008. Forintek Canada Corp., Ottawa, Canada.

______. 1988. Deflection serviceability criteria for residential floors. Project 03-43-10C-024. (in preparation). Forintek Canada Corp., Ottawa, Canada.

______. and S.B. Bellosillo. 1978. Performance criteria for residential floors. Final report to CMHC. Grant No. 120-74. Forintek Canada Corp., Ottawa, Canada.

______________________________. 1987. Static and dynamic field tests of residential floors. Project 03-43-10-019. Forintek Canada Corp., Ottawa, Canada.

______, R. Demers and J.C. Garant. 1981. performance testing at the HUDAC Mark XI project. Rep. to Can. For. Ser. Project 9. Eastern Laboratory, Forintek Canada Corp., Ottawa, Canada.

______, and J.C. Garant. 1981. Effectiveness of bridging in floors that dry after construction. Rep. to Can. For. Ser. Project 8. Eastern Laboratory, Forintek Canada Corp., Ottawa, Canada.

______ and A.P. Jessome. 1973. Effectiveness of various bridging methods. Info. Rep. OP-X-51. Forintek Canada Corp., Ottawa, Canada.

van Rijn, G.J. 1982. A comparison of the performance under concentrated load of floors at the Mark XI project. Report to Can. For. Ser. Project 7. Eastern Laboratory, Forintek Canada Corp., Ottawa, Canada.

Vermeyden, P. 1968. Research into the load sharing action of the decking of a wooden floor with concentrated load. Department of Fisheries and Forestry translation no. 41 (from Dutch). Ottawa, Canada.

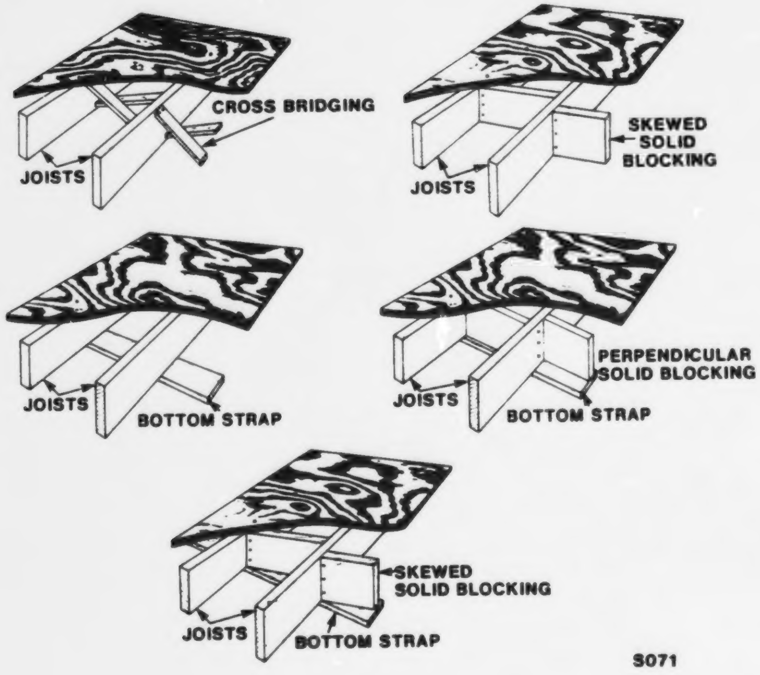

FIGURE 1: Representation of some of the bridging types tested.

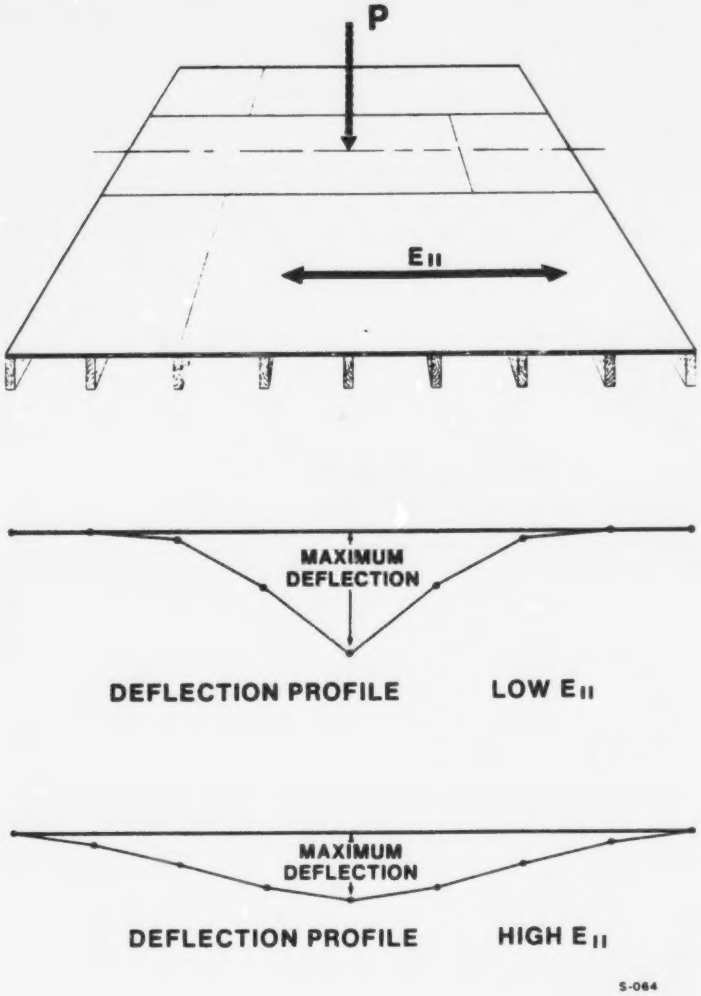

FIGURE 2: The effect of low and high flooring stiffness on the deflection of a floor when loaded by a concentrated load

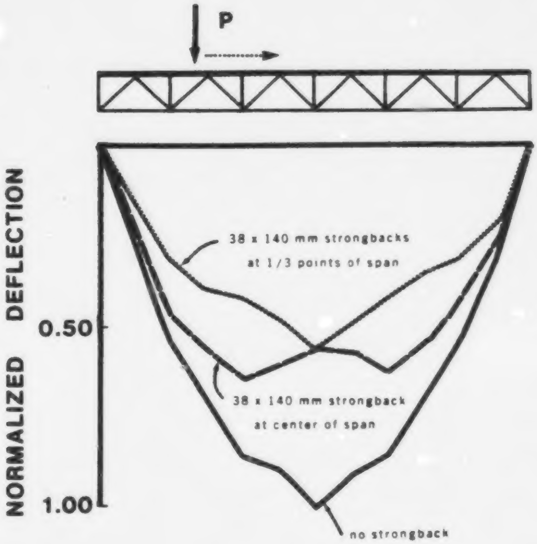

FIGURE 3: Envelope of maximum deflections of a truss floor under the action of a concentration load, shown as a function of placement of strongbacks.

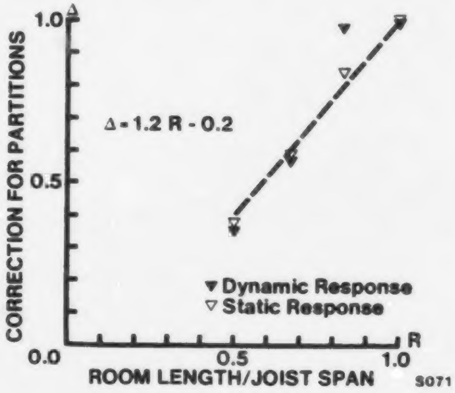

FIGURE 4: Influence of partitions on static and dynamic response.

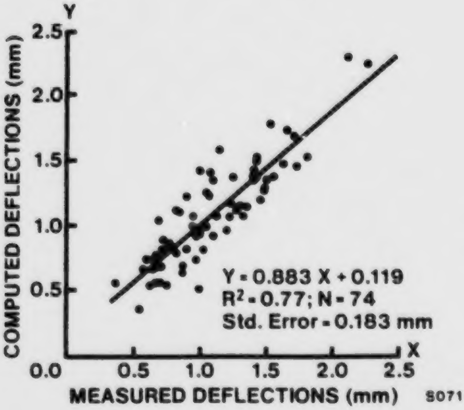

FIGURE 5: Comparison of measured and computed deflections under a concentrated load of 100 kg for 74 field tests.

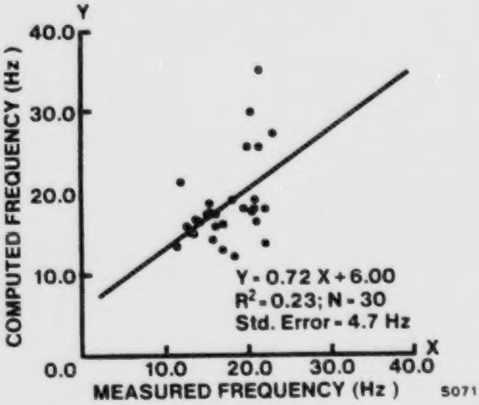

FIGURE 6: Comparison of measured and computed natural frequencies for 30 field tests.

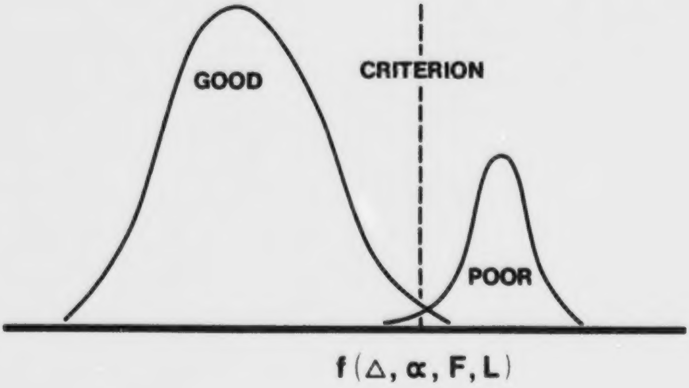

FIGURE 7: Distribution of "good" and "poor" floors based on a single variable or combination of variables with placement of a performance criterion to minimize misclassification.

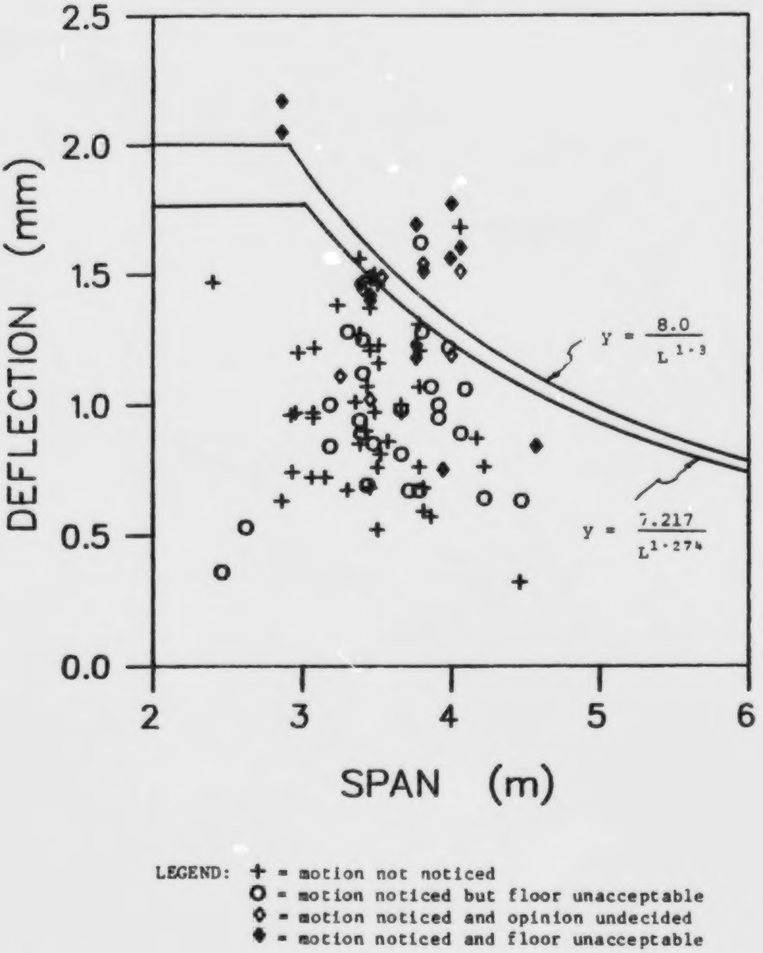

FIGURE 8: Plot of serviceability criterion with maximum delections for 98 floors tested in the field for which acceptability ratings are available.

PRACTICAL ASPECTS OF FLOOR SERVICEABILITY DESIGN

Thomas M. Murray

Department of Civil Engineering
Virginia Polytechnic Institute and State University
Blacksburg, Virginia, USA

ABSTRACT: Practical aspects of controlling user induced floor vibrations are discussed. Methods for improving floor serviceability by controlling each of the three fundamental floor motion parameters, damping, frequency and amplitude (or acceleration) are suggested.

1. INTRODUCTION

Annoying floor motion induced by building occupants is probably the most persistent floor serviceability problem encountered by designers. A number of criteria which allow a designer to ascertain the probable acceptance of a floor system at the time of design are available [Murray 1981]. Although it has been shown that the various criteria differ substantially in the evaluation of a particular floor system, they are useful tools for the designer. Most of the criteria require an estimate of system damping, calculation of first natural frequency, and calculation of maximum deflection or acceleration due to a specified impact.

If a floor system is found to be unsatisfactory at the time of design, usually the system can be improved by adding mass in the form of a thicker concrete slab which, of course, increases the cost of the entire framing and foundation systems. If the system is judged to be unsatisfactory after construction is complete, correction is very difficult and can be expensive. Only a very few successful retrofits are known to the author.

The purpose of this paper is to discuss concepts which can be used to improve the performance of floor systems subject to occupant induced motion from either walking, dancing or exercising. Control of any of the three fundamental floor motion parameters, damping, frequency and amplitude (or acceleration) can improve the performance of a floor system. The following sections describe methods for improving the performance of a floor system thru modification of its fundamental characteristics.

2. DAMPING

For floor systems supporting residential or office environments, the most important parameter affecting the response of occupants to floor motion is damping. Even a very light flexible floor system will be acceptable if sufficient damping exists.

A typical office building floor system, hung ceiling and minimal mechanical ductwork exhibits 3-4% of critical damping. Additional damping may be provided by office furniture, partitions, equipment and the occupants themselves. However, if the required damping from a criterion such as the above is much greater than 4%, the designer must be able to identify an exact source of damping or artificially provide additional damping to be sure the floor system will be satisfactory. Framed in-place partitions (sheetrock on wood or metal studs) are very effective sources of additional damping if (1) each partition is attached to the floor system in at least three locations and (2) their spacing does not exceed the number of effective beams or the effective floor width that are part of the various acceptability criteria to calculate system amplitude. The direction of the partitions with respect to supporting member span does not affect the damping provided. Also, partitions are equally effective if they are attached below the slab as compared to directly on the floor slab.

Although methods to artificially increase damping have been proposed in the literature (dashpots, viscoelastic materials, second mass systems), the author is unaware of any real successes.

3. FREQUENCY

In office/residential environments, the frequency of the floor system must be kept above about 3 hertz to avoid resonance with walking. In dancing/exercising environments, it has been suggested [Allen et al 1985] that the frequency be above 8-9 hertz, again to avoid resonance. Further, floor systems having a natural frequency in the 6-8 hertz, without adequate damping, seem to be particularly annoying (possibly because of resonance with body organs).

The most effective methods to change the frequency of a floor system is to increase or decrease mass or supporting member stiffness. The performance of floor systems can also be improved by using non-regular framing, e.g. other than equal beam spacing, or by periodically introducing significantly stiffer members. Both methods tend to break up harmonics in the floor systems.

4. AMPLITUDE

Although amplitude (or acceleration) is an important floor motion parameter, control by modifying characteristics of the floor system is difficult without also changing frequency. However, changing beam or joist spacing can affect the number of effective beams or the effective floor width, which in turn affects the magnitude of the amplitude.

REFERENCES

Murray, T. M., Acceptability criterion for occupant-induced floor vibrations. Engineering Journal, American Institute of Steel Construction, 18(2), 1981, pp. 62-70.

Allen, D. E., Rainer, J. H. and Pernica, G., Vibration criteria for assembly occupancies, Canadian Journal of Civil Engineering, 12(3), 1985, pp. 617-623.

DYNAMIC FOOTFALL LOADING FROM GROUPS OF WALKING PEOPLE

Per-Erik Eriksson and Sven V. Ohlsson

Chalmers University of Technology
Dep. of Structural Engineering
Div. of Steel & Timber Structures
Gothenburg, Sweden

ABSTRACT: The main objective of this study is to establish an estimate of the resulting force spectrum as a function of the number of walking persons. The study is based on laboratory measurements of the response of a test floor to prescribed motions of a varying number of persons. The force spectrum is then determined indirectly via the laws for spectral response. Typical features of the loads in general caused by walking people are discussed. Such features are e.g. the distribution in time and space as well as the influence of walking rate. The interest is focused on long-span floors and a "model" of the load to be used in the design of such floors is proposed.

1. INTRODUCTION

Over the last fifteen years a lot of research has been done in the field of floor vibrations and various design methods have been suggested. However, although a lot of these methods deal with the load induced by persons walking on the floor, to the authors' knowledge, no one of them is based on a proper determination of the low-frequency (0-10 Hz) force spectrum caused by continuous walking. Furthermore, little has been written about the influence on the floor response of more than one walking person and in [1] it is even stated that "dynamic forces from groups of people walking about the floor at random would seldom cause serviceability problems". While this may be true for some types of residence buildings, it appears not to be the case for shopping areas and offices with crowds of walking people.

The aim of the present study is to estimate the force spectral density related to one walking person as well as to express the additive effects on the dynamic load when several persons are walking on the floor simultaneously. This is achieved by laboratory tests, fig. 1, as well as computer analyses. The paper also gives a general description of the loads from walking as a basis for the simplifications introduced when proposing a design procedure. The study is focused on frequencies below 8 Hz, which is relevant for long-span floor vibrations. It is assumed that the root mean square (rms) value of the vibration acceleration is the governing quantity for human discomfort within this frequency range in accordance with the proposed ISO standards [2].

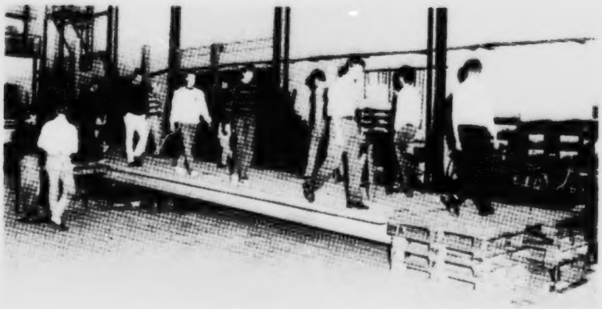

Figure 1: Laboratory test for estimating the forces from groups of walking people.

2. FOOTFALL FORCES AND WALKING

2.1 Single step force pulses: Forces from footsteps have been studied for various reasons ranging from ergonomic considerations to the detection of intruders |3| as well as to prediction of floor and footbridge vibrations |4, 5, 6|. Different researchers agree as to the time functions of footfall loads from walking and running. It is also generally concluded that the type of footwear has a minor influence on the low-frequency part of the load. A typical footfall force pulse at normal walk is shown in fig.2, where the first peak corresponds to the heel strike and the second to the toe liftoff contact.

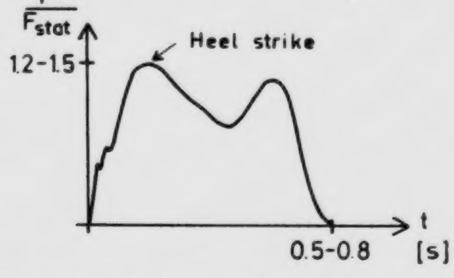

Figure 2: Typical force pulse from single step, after .

The duration of the pulse is directly dependent on the rate of walking and as successive footsteps overlap by approx. 15% a duration of 0.5 to 0.8 s would correspond to 1.4 - 2.5 steps per second. One can find even lower step frequencies (e.g. uninterested husband with supermarket trolley) but that is hardly of interest as the dynamic load is then much lower.

At the upper end of the range 2.5 or, possibly, 2.6 steps/s seems to be a reasonable limit. It is very difficult to maintain an ordinary walking pattern above that. The ratio F/F_{stat}, i.e. the ratio between the heel strike peak force and the weight of the walker, is also strongly dependent on the rate of walking and increases with increasing walking rate. This is confirmed by the experimental results described later.

One phenomenon that might distort the shape of the force pulse is the interaction between the floor and the human body. The presence of a floor resonance will cause the force to drop at the resonance frequency and if the floor is very springy the drop can be quite severe. However, for long-span floors, the main interest here, this effect can probably be ignored as the weight of the floor system is large compared to the weight of the walkers.

2.2 Continuous walking: The continuous load from walking could be described as a series of footfall force pulses, over-lapping in the manner described above. The force intensity of such a series, as a function of frequency, together with an approximation to be used for frequencies between 6 and 50 Hz, is given in |7|. Some mathematical models of this idealised pulse-train have also been suggested, e.g. in |8|, but they are difficult to use in a design situation. Different rates of walking are also difficult to take into account when using a time-domain forcing function. Therefore it seems appropriate to establish force spectra in the frequency domain for different step frequencies or, possibly, an envelope to these spectra. The latter could be a "worst case" curve or a "mean" curve or a combination of the two.

A matter that is not very easily dealt with is the horizontal motion of the load source. If the fundamental mode of vibration of the floor was assumed to dominate the response totally, the prediction would be fairly easy as the floor could then be treated as a single degree of freedom system. The response would only have to be "scaled down" by the spatial average of the mode shape function in the case of a random walking pattern assumed to cover the whole floor. However, as floors are often mainly one way structural systems with relatively low flexural rigidity in the transverse direction, there will be a number of first order modes (half a sine wave along the primary beams) with closely spaced natural frequencies. Also, the damping ratios (modal damping) might differ quite significantly between the different modes. For such reasons, the assumption mentioned above may be erroneous. For one person walking on a long span, open plan floor, it seems reasonable to idealise this as "treading in place" at the weakest point of the floor in the "governing mode". The governing mode means, here, the mode that has the highest ratio between excitation level and the product of modal damping and modal mass. By the "weakest" point in this mode is understood the point having the maximum mode shape value.

2.3 The effects of several walkers: If a number of persons, say n_p, would be walking in step and in the same manner (producing identical footfall forces), then the magnification factor for the load would be n_p (n_p^2 for the spectral density of the load). Although small groups of people walking together are often seen walking in step, the assumption above has experimentally been found true only for the first harmonic of the step frequency. In larger groups, the influence of other people is even weaker.

The "treading in place" idealisation still holds when dealing with the load from groups of people, but it is no longer correct to apply the total load at the weakest point. The load is, however, usually restricted to certain areas (e.g. walking paths in a shopping centre). Given this and the mode shapes of the floor, an equivalent load can be estimated. Suggested values of the maximum number of persons per square meter are referred to in |8|.

3. FORCE SPECTRAL REPRESENTATION

As was mentioned earlier it is preferable to represent the load as a spectrum in the frequency domain. This is due to the fact that the simplest way of describing the dynamic behaviour of a complex structure is in terms of its modal properties (eigenfrequencies, mode shapes, modal masses and modal damping). If these properties are known, a transfer function between force and response (a frequency response function, or FRF) can be established and, given the force spectrum, the response can be calculated.

3.1 Random vibrations of linear systems: In a normal situation with a number of persons walking on a floor, the load input to the structure is probably best described as a random process. The response to such excitation (the vibrations) is also a random process and, provided that the structure behaves like a linear mechanical system, can be estimated in much the same manner as when dealing with deterministic loads. However, it is no longer relevant to talk about peak response, but instead the root mean square (rms) value over a certain frequency bandwidth is used.

3.2 Spectral density: A random process cannot be represented by a discrete Fourier series because it is not periodic. It is therefore necessary to use some other means of describing the frequency content of the process. This is achieved through use of spectral densities which are Fourier transforms of the autocorrelation function of the process (as opposed to the process itself). Only a brief description of the theory will be given here. For further informations see, for instance |9|. For a measured acceleration time history, a(t), which can be treated as a random process, the autocorrelation function is defined as

$$R_a(\tau) = E\left[a(t)a(t+\tau)\right] \tag{1}$$

i.e. the expected value of the acceleration at time t multiplied by the acceleration at a time τ later (note that single subscripts are used for autocorrelations and power spectral densities). For a stationary process this quantity will be independent of absolute time, t. The *single-sided* power spectral density of the acceleration, $S_a(f)$ is the Fourier transform of $R_a(\tau)$ so we have

$$S_a(f) = 2\int_{-\infty}^{\infty} R_a(\tau)\, e^{-i2\pi f\tau} d\tau \tag{2}$$

and

$$R_a(\tau) = \int_{0}^{\infty} S_a(f)\, e^{i2\pi f\tau} df \tag{3}$$

Setting $\tau = 0$ and combining (1) and (3) it is clear that

$$\int_{0}^{\infty} S_a(f)\,df = E\left[a^2(t)\right] \tag{4}$$

i.e. the mean square value of the process.

If the measured acceleration is the result of a load F(t), which is also a random process, then the relation between their spectral densities is

$$S_a(f) = |A(f)|^2\, S_f(f). \tag{5}$$

$A(f)$ is the complex transfer function between force and acceleration and is called the accelerance. When two or more random loads $(F_1(t), F_2(t), \ldots . F_N(t))$ are applied to a linear mechanical system, the resulting spectral density of the acceleration is

$$S_a(f) = \sum_{r=1}^{N} \sum_{s=1}^{N} A_r^*(f)\, A_s(f)\, S_{F_r F_s}(f) \tag{6}$$

where $A_r^*(f)$ is the complex conjugate of the transfer function between F_r and the acceleration. $S_{F_r F_s}(f)$, for $r \neq s$, is the cross-spectral density of the pair $F_r(t)$ and $F_s(t)$ defined as the power spectral density but using the cross-correlation instead of the autocorrelation. Also, $S_{F_r F_r} = S_{F_r}$. If the loads are uncorrelated, all cross-spectral densities are zero and eq.(6) gives

$$S_a(f) = \sum_{r=1}^{N} |A_r(f)|^2\, S_{F_r}(f) \tag{7}$$

a $A^*(f)A(f) = |A(f)|^2$. This means that the spectral density of the resulting acceleration is simply the sum of the spectral densities of the accelerations caused by each load separately. If, on the other hand, all the loads are identical $(=F(t))$ and fluctuate in phase with each other (this might be the case for several persons walking "in step") and are also applied at the same point (more difficult!), then we have

$$S_a(f) = N^2 |A(f)|^2\, S_F(f) \tag{8}$$

These calculations, however, require *complete* knowledge of the modal properties of the structure. In order to adjust to the design situation where this is generally not the case, some simplifications have to be made.

3.3 The design situation (Narrow band processes): When a broad band excitation is applied to a structure this functions as a mechanical filter. Provided that the damping is low for one or more excited modes, the response will be totally dominated by its resonant parts. We then get what is usually called a narrow band process or a sum of such processes. The calculation of the spectral density of the response can be carried out in an approximate way outlined in figure 3. Instead of the accelerance $A(f)$, the dynamic flexibility, $\alpha(f)$ (displacement/force $= w/F$), is used. The excitation is white noise with the spectral density S_o and the structure is a single degree of freedom (SDOF) system with the static stiffness k, the natural frequency f_1 and the damping ratio $\zeta = c/c_{cr}$, i.e.

$$\underbrace{w_{rms} = \sqrt{S_o \frac{\pi f_1}{4\zeta k^2}}}_{\text{L.H.S. of fig. 3}} = \underbrace{\sqrt{\frac{S_o}{(2\zeta k)^2}\, \pi f_1 \zeta} = w_{1,rms}^{est}}_{\text{R.H.S.}} \tag{9}$$

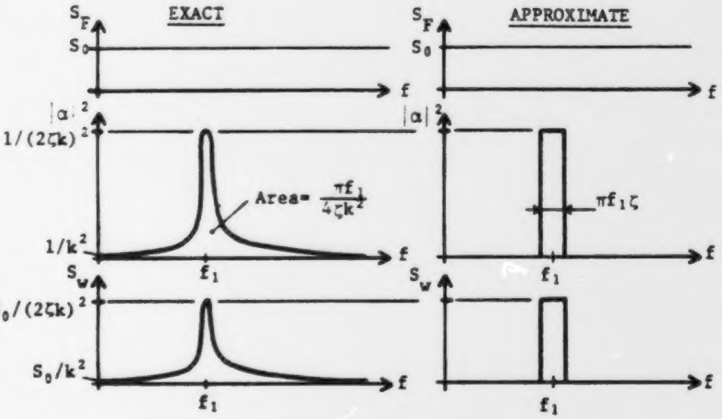

Figure 3: Response of single degree of freedom system to white noise excitation and simplified solution for lightly damped system. The parameters are described in the text.

This means that for the situation outlined above, the approximate method gives the true rms value of the displacements. However, after converting this into an acceleration rms value and considering that the force spectral density varies with the frequency, we arrive at the approximation

$$a_{rms} \approx a^{est}_{1,rms} = (2\pi f_1)^2 \, w^{est}_{1,rms} = \sqrt{S_F(f_1)\,\frac{(2\pi f_1)^4 \pi f_1}{4\zeta k^2}}$$

$$= \sqrt{S_F(f_1)\,\frac{\pi f_1}{4\zeta m^2}} \qquad (10)$$

where m is the mass of the SDOF system ($=k/(2\pi f_1)^2$). *This approximation should be reasonable for* $\zeta < 3\%$.

For a multidegree of freedom (MDOF) system the "governing mode" mentioned in section 2.2 is the one with the highest "estimated modal rms acceleration" which is expressed by

$$a^{est}_{n,rms} = \frac{\sqrt{S_F(f_n)\pi f_n \zeta_n}}{2\zeta_n m_n} \qquad (11)$$

i.e. the ratio between the approximate rms force over the equivalent frequency interval ($\pi f_n \zeta_n$) and the double product of the modal damping and the modal mass n denotes the mode number and m_n is the modal mass defined for a two-dimensional structure as

$$m_n = \iint_A g(x,y) \, [\phi_n(x,y)]^2 dA, \qquad (12)$$

where g(x,y) is the mass per square meter and $\phi_n(x,y)$ is the mode shape function of the n:th mode. A discussion on how to estimate the modal properties is given in |7|.

Finally, for a system with more than one resonance frequency in the considered frequency interval we may write the approximate acceleration rms value as

$$a_{rms}^{est} = \left[\sum_{n=1}^{N} (a_{n,rms})^2\right]^{1/2} = \left[\sum_{n=1} S_F(f_n) \frac{\pi f_n}{4\zeta_n m_n^2}\right]^{1/2} \qquad (13)$$

provided that the natural frequencies are reasonably well separated. f_N is less than the upper limit of the considered frequency interval.

4. EXPERIMENTAL DESIGN AND SET-UP

4.1 Idea and outline: In order to measure the dynamic load from groups of people walking in an ordinary manner it is necessary to use a fairly large test floor. The technique used for measuring the load from a single step, i.e. using a "stiff, massless" platform with one force transducer is apparently not applicable here. The method chosen for this study is to determine the dynamic load *indirectly* from measurements of the response of a well-known floor structure to excitation from walking. The "semi-static" part of the response (i.e. the frequency range below the first natural frequency) will mainly be used and the measurement point is selected so that contribution to the response from all modes except the fundamental mode can be neglected. The measured quantity is the vertical acceleration at midspan.

4.2 Test floor properties: The test floor is a precast concrete element of a type frequently used in floor construction in Sweden. The element, called TT/F 240/40, is 2.4 m wide and 0.4 m deep. It is 10 m long and simply supported at both ends, which gives a lowest natural frequency of approx. 8 Hz. The weight of the element is 6.5 tons, which means that the presence of people on the floor will not change the dynamic properties of the system dramatically. Figure 4 shows the geometry of the test floor arrangements.

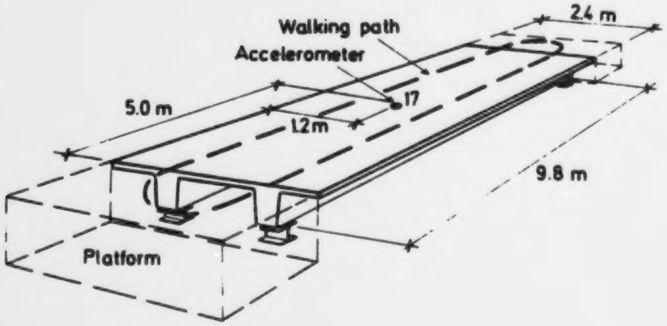

Figure 4: The test floor geometry and walking path.

Experimental as well as theoretical modal analysis of the structure was performed. The eigenfrequency of the first mode was experimentally found to be 7.9 Hz and the mode shape very nearly that of half a sine wave along the length of the element. Point no. 17, the midpoint of the floor, was chosen for the response measurements as the mode shape values for all modes of interest except the fundamental mode were close to zero (as expected) at this point. The point accelerance function for point no. 17, denoted $A_{17-17}(f)$, was then synthesized from the modal test data and is shown in figure 5.

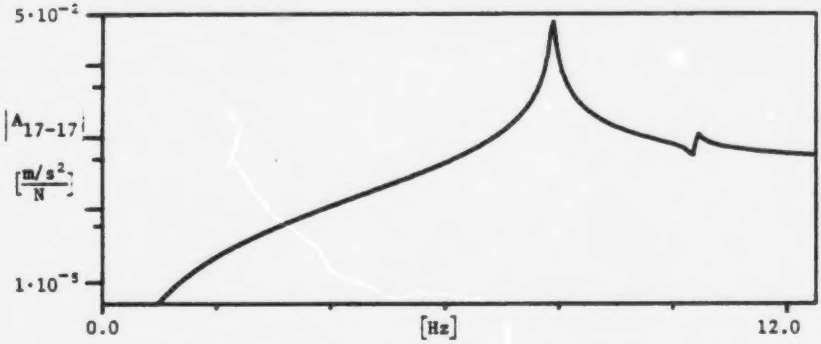

Figure 5: Magnitude of the point accelerance for the response measurement point (no. 17). Vertical axis is in logarithmic scale.

4.3 Test floor response measurements: Experiments were carried out with different rates of walking and with a varying number of participants. The walking path is shown in figure 4. It goes along the webs of the floor element and in order not to disturb the walk, the turning areas are located on separate platforms at each end of the element.

The acceleration signals were recorded continuously during walking and later analysed in a frequency analyser to produce acceleration spectral densities. Each recordning was taken to be about 100 seconds in order to allow for averaging over a number of time intervals. For the experiments with one walker the main objective was to study the effect of various walking rates. The rate was kept constant by means of a metronome and the rate was changed from 1.3 to 2.6 steps per second in increments of 0.1 steps/s. For tests with several walkers the response was measured when walking in step (1.7 or 2.0 steps/s) as well as for irregular walking rates (i.e. each walker used his/her own rate although all moved with the same speed).

4.4 Force estimation and generalizations: From eq.(5) in ch.3 it is clear that if we know the spectral density of the response and the transfer function between force and response, the force spectral density can be obtained as

$$S_F(f) = S_a(f)/|A(f)|^2 \tag{14}$$

In this case the acceleration spectral density at point no. 17 as well as the point accelerance for this point are known. The spectral density of an equivalent force applied at point no. 17 can therefore be obtained from eq.(14). If the mode shape of the fundamental mode is normalized with respect to this particular point (say $\emptyset_1(17) = 1$, where $\emptyset_1(i)$ is the mode shape value at point i), then this force is what is usually called the first mode generalized force, denoted F_1. The real load in this case is assumed to be uniformly distributed along the walking path, i.e. along the webs of the element. Using the notations in figure 6 the relationship between the u.d.l., q(x), and F_1 is given by

$$F_1 = 2\int_0^{\ell} q(x)\,\emptyset(x)\,dx \qquad (15)$$

In this case the mode shape values are given at discrete points as estimated from the modal testing and hence eq.(15) will become a summation:

$$F_1 = q\sum_{i=1}^{10} \emptyset_1(i)\Delta\ell_i \qquad (16)$$

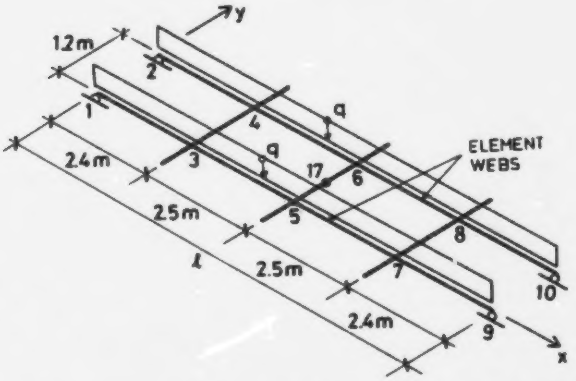

Figure 6: Measurement grid at modal test and idealisation of load

The mode shape values from the modal testing and the legnth increments related to each point in figure 6 are given in table 1. If the load q is replaced by the resultant, F, of the load from the walkers and if it is also taken into account that only 85% of the walking path is on the element (the rest being on the end platforms), the relationship between F and F_1 is given by

$$F = 2q\ell/0.85 = 2F_1\ell/\left[0.85\sum_{i=1}^{10} \emptyset_1(i)\Delta\ell_i\right]$$

$$F = 2.20\,F_1 \qquad (17)$$

Table 1: Mode shape values for the fundamental mode, $\emptyset_1(i)$, and length increments $\Delta\ell_i$ for points 1-10 & 17.

i	1	2	3	4	5	6	7	8	9	10	17
Ø (i)	0.02	0.02	0.64	0.65	0.90	0.87	0.55	0.61	0.00	0.01	1.00
$\Delta\ell_i$ |m|	1.20	1.20	2.45	2.45	2.50	2.50	2.45	2.45	1.20	1.20	-

In order to convert this into a relationship between the spectral densities of the forces the proportionality factor should be squared. Thus from eqs.(14) and (17) we have the sought spectral density of the load from walking as

$$S_F = (2.20)^2 \frac{S_{a,17}}{|A_{17-17}|^2} \tag{18}$$

A typical force spectral density calculated in this manner is shown in figure 7. The calculation involves a division by the squared magnitude of the point accelerance for point no. 17 (eq.(18)). This quantity is very low at low frequencies (equal to zero at 0 Hz) and the effect of the noise present in the acceleration signals will therefore be greatly enlarged in the low frequency region of the load spectral density. Furthermore, the transducers involved have a lower frequency limit at 0.4 Hz. Also, as was said earlier, the study is focused on frequencies below 8 Hz. For these reasons, mainly the frequency range 1.2 - 8 Hz will be included in the further discussion.

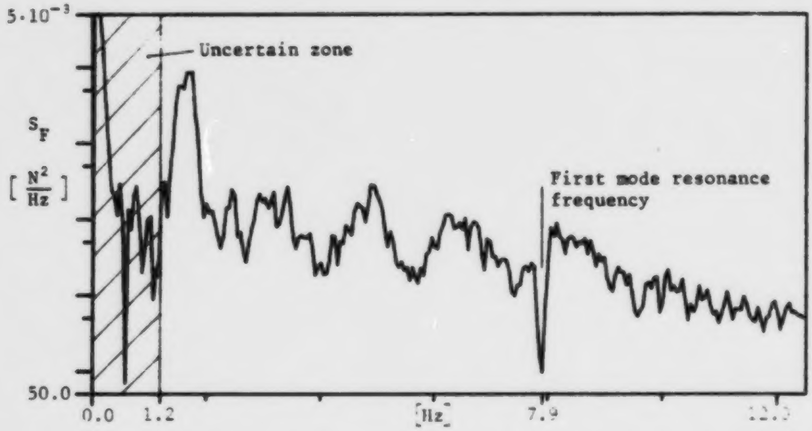

Figure 7: Estimated spectral density of the load from 11 persons walking at irregular rates ("normal walk"). Note that the vertical axis has a logarithmic scale.

It is worth commenting here upon the dip in the load spectral density at the first natural frequency. This is partly explained by the high flexibility of the floor element at that frequency (which causes the load to drop). It is, however, quite likely that it is also caused by the slight change of the natural frequency that occurs with the presence of people on the floor.

5. EXPERIMENTAL RESULTS

5.1 One person walking at different walking rates. The rate of walking was varied from 1.3 up to 2.6 per second. The results discussed in this section refer to a male person weighing 75 kg. In figure 8 the spectral densities of the load from walking at four different rates are given. This figure shows very clearly the peaks at ecah harmonic of the step frequency, f_s. Also, when comparing the amplitudes of the peaks of the first harmonic, the strong dependence upon the rate of walking is evident. The peaks of the higher harmonics are all of the same order of magnitude but sloping off somewhat towards higher frequencies. When this information is compiled to obtain an envelope of the peaks of the spectral densities it is clear that the curve will have to be divided into two parts:

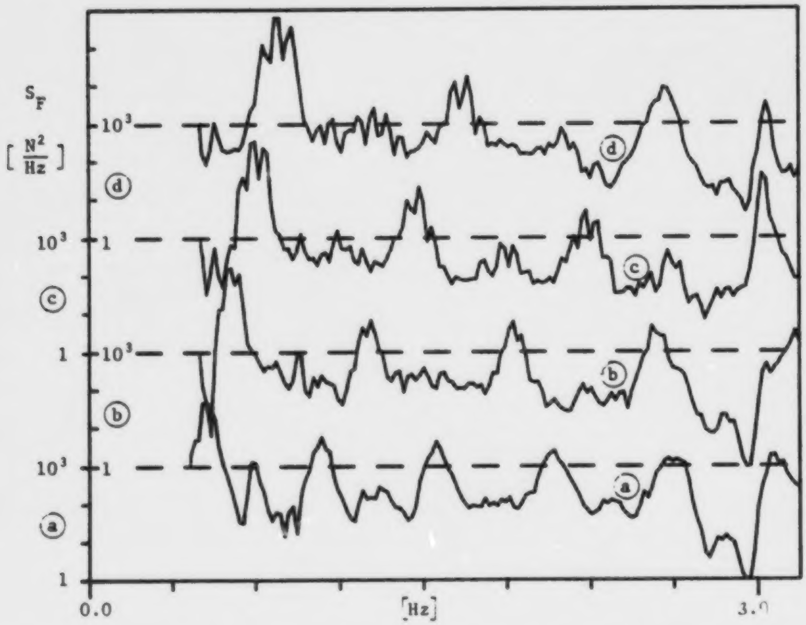

Figure 8: Spectral densities of the load from a 75 kg male person walking at rates: ⓐ 1.4, ⓑ 1.7, ⓒ 2.0 and ⓓ 2.3 steps/second.

one for the first harmonic (1.3 < f < 2.7 Hz) with a positive slope and one for the higher harmonics with a negative slope. A proposed estimate of this envelope is shown in figure 9 together with the spectral density of the load for the case $f_s = 2.0$ Hz. The idea is to apply this to the "governing mode" of the floor (see sections 2.2 and 3.3). If there is more than one mode present in the frequency range below 8 Hz, the use of the envelope function for all of these would probably give an overestimation of the resulting response. Therefore a "mean curve" is also given in figure 9, which is meant to be used for the rest of the excited modes. This latter function is a curve fit of the mean square values of the force in each harmonic divided by the bandwidth, i.e.

$$1/f_s \int_{nf_s-f_s/2}^{nf_s+f_s/2} S_F(f)df \qquad (19)$$

where n is now the number of the harmonic. The square of the stationary force intensity suggested in |7| proved to be a good approximation for frequencies above 2.7 Hz and is therefore used.

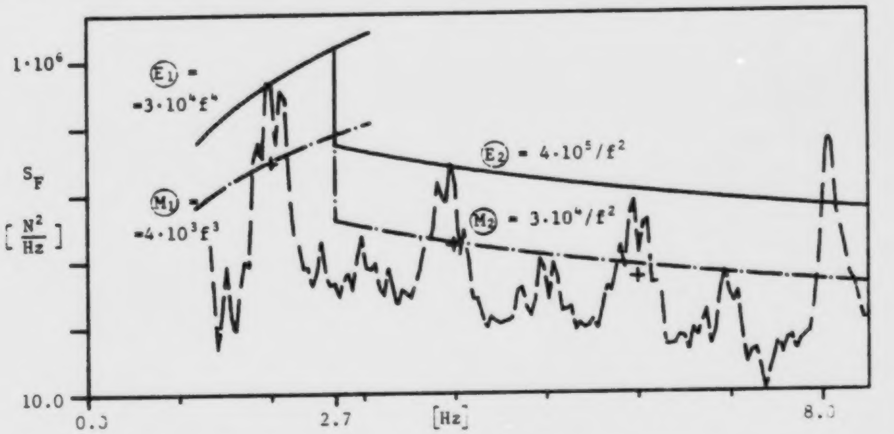

Figure 9: Proposed envelope Ⓔ (-) and "mean" Ⓜ (-·-) functions for the spectral density of the load from one person (weighing 75 kg/ walking continuously. For comparison the spectral density (---) as well as the values obtained from (19) (+) for f_s = 2.0 Hz are shown .

In |8| is given the Fourier amplitudes of the first five harmonics of the load from a person weighing 60 kg walking with f_s = 2.0 Hz. These are compared in figure 10 with the square root of the values obtained from (19) multiplied by f_s (from curve ⓒ , fig.8) and also with the corresponding values from curves (M1) and (M2) in figure 9.

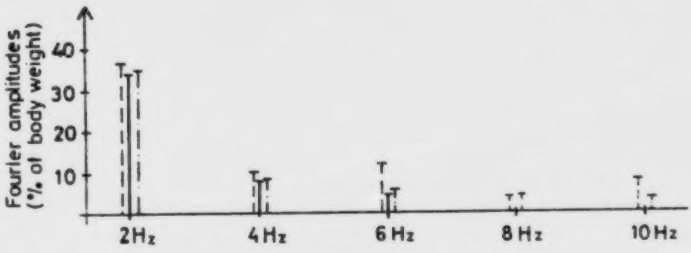

Figure 10: Fourier amplitudes of the harmonics of the load from a pedestrian as given in |8| (---) in comparison with corresponding experimental results (-) and a curve-fit of the latter (-·-).

5.2 Several persons walking in step: The peaks of the spectral densities of the load *at the first harmonic* of the step frequency have been found to be $(n_p)^2$ times higher than the corresponding peaks for one person (n_p is the number of persons). This is in agreement with eq.(8). However, at the higher harmonics the magnification factor for the peaks is instead n_p, i.e. the same as the theoretical value for uncorrelated random processes (eq.(7)). This is somewhat surprising but the explanation is probably that the footfall forces from different persons are not identical. It might also be due to the fact that the whole group does not walk *exactly* in step but probably as close to that as one would find in a real situation (apart from marching troups). The magnification factors apply to the peak envelope Ⓔ as well as to the "mean curve" Ⓜ in fig.9.

The load spectral densities established at the tests with groups of people are not as distorted above the fundamental eigenfrequency of the test floor (7.9 Hz) as those for one person. They suggest that the proposed design functions can be used up to at least 12 Hz.

5.3 Several persons walking at individual walking rates: The groups were asked to walk like they do in a normal situation as well as when in a hurry. The different walking rates thereby occuring within the groups have the effect of smoothing out the peaks of the load spectral densities. The magnification factors to be used for the peak envelope are therefore less than $(n_p)^2$ and n_p for Ⓔ$_1$ and Ⓔ$_2$ respectively. These factors still apply to the curves Ⓜ$_1$ and Ⓜ$_2$ though, and for very large groups of people the "mean curve" and the peak envelope take the same values.

5.4 Summary of the experimental results:

- The proposed peak envelope and "mean" function in fig.9 can be used for frequencies below 12 Hz. For other static weights than 75 kg per person, the functions should be multiplied by the squared ratio between the weight in question and 75 kg.
- The vertical line connecting the functions Ⓔ$_1$ to Ⓔ$_2$ and Ⓜ$_1$ to Ⓜ$_2$ should be placed at approx. 2.7 Hz to incorporate a certain width of the spectral density peak at step frequencies 2.5 - 2.6 Hz (see fig.8). Some safety factor seems appropriate in order to take account of the uncertainties in the calculation of the eigenfrequencies of the floor.
- Groups of five persons or less are quite likely to walk in step and therefore the magnification factors given in section 5.2 are to be used for such groups. For larger groups the magnification factors for the peak envelope function are lower. The values obtained during the experiments are compiled in figure 11. Test data was obtained for groups of up to 11 persons but the graphs in figure 11 are extended further. The magnification factors obtained from this figure for the curves Ⓔ$_2$ and Ⓜ$_2$ should be squared when applied to the curves Ⓔ$_1$ and Ⓜ$_1$ respectively.

The proposed design loads according to figures 9 and 11 for 11 persons are given in fig.12 together with the load spectral density measured during the experiments at "hurried walk". For this specific case the design loads give overestimations of the load below 2.7 Hz.

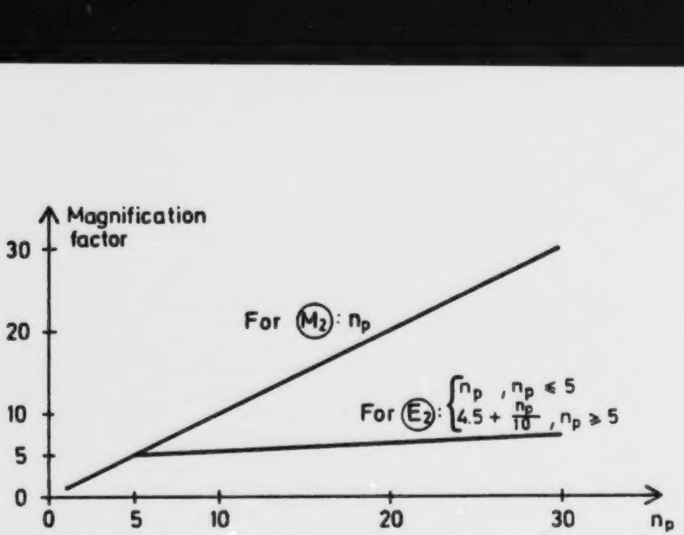

Figure 11: Magnification factors for the functions E_2 and M_2 in fig.9 as function of the number of persons, n_p. For functions E_1 and M_1 use the factors squared instead.

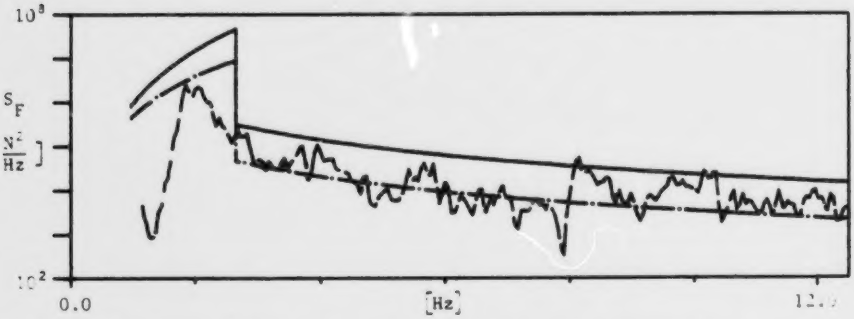

Figure 12: Proposed design loads and experimentally established load spectral density for 11 persons.

6. DISCUSSION AND DESIGN PROCEDURE

A "model" of the load from walking people has been proposed and a design procedure for long-span floors has been indicated. This procedure is outlined and discussed below.

1. **Estimate the modal parameters (eigenfrequency, mode shape, modal mass and modal damping ratio) of the floor for modes with an eigenfrequency below 8 Hz.**

That is the frequency region where the human being is most sensitive to vibration acceleration according to |2| (a higher frequency limit has recently been suggested in |10|). The modal parameters, apart from damping, can be estimated by means of computer analyses but it would be preferable to establish design charts for different floor systems. More knowledge about the modal damping is also required.

2. For groups of people the laods given by figures 9 and 11 should be converted into load per square meter. Critical loaded areas (walking paths etc.) should be selected and an equivalent modal load calculated in the same manner as described in section 4.4. For small groups (up to, say, 5 persons) the load should be treated as a point load (treading in place).

Values for the number of persons per square meter for different occupancies have still to be suggested

3. Establish which eigenmode is the "governing" for the response, using eq.(11) where $S_F(f)$ is either function $\textcircled{E_1}$ or $\textcircled{E_2}$ (fig.9) multiplied by the values given in fig.11.
4. Calculate $a^{est}_{n,rms}$ for each mode according to eq.(11), where $S_F(f)$ is now the adjusted values from curve $\textcircled{E_1}$ or $\textcircled{E_2}$ for the governing mode and from curve $\textcircled{M_1}$ or $\textcircled{M_2}$ for all other modes of interest.

The reason for this procedure is given in section 5.1.

5. Calculate the total acceleration rms value, a^{est}_{rms}, according to eq.(13) and compare this to some acceptability limit curve, for instance those given in the proposed ISO standards |8|.

Further simplifications are probably necessary in order to facilitate the use of the procedure among practising engineers. The method also needs to be validated by means of comparisons to measurements in existing buildings. Furthermore, load "models" for other activities (e.g. jumping and dancing) have to be established. Results from |11| can probably be used for this.

ACKNOWLEDGEMENTS

This study forms part of a project sponsored by the Swedish Council for Building Research (BFR), the Swedish Precast Concrete Federation and the Development Fund of the Swedish Construction Industry (SBUF). We would like to express our thanks to these organizations for their support.

REFERENCES

|1| Ellingwood, B. & Tallin, A.: Structural Serviceability; Floor Vibrations. Journ. of the Struct. Div., Proc. of ASCE. Vol. 110, No.2, 1984. 401-417.

|2| ISO 2631, DAD1: Guide for the Evaluation of Human Exposure to Vibration and Shock in Buildings, Addendum 1; Acceptable Magnitudes of Vibration. 1980. Note: Draft proposal!

|3| Galbraith, F.W. & Barton, M.V.: Ground Loading from Footsteps. J. Acost.Soc. of America, Vol. 48, 1970, Part 2, pp. 1268-1292.

|4| Ohlsson, Sven: Floor Vibration and Human Discomfort. Chalmers Univ. of Techn. Div. of Steel and Timber Struct., PhD thesis, Gothenburg 1982.

|5| Wheeler, B.: Prediction and Control of Pedestrian-Induced Vibrations in Footbridges. Journ. of the Struct. Div., ASCE, Vol.108, No.ST9,1982,pp.2045-2965

|6| Becker, R.: Simplified Investigations of Floors under Foot Traffic. Journ. of the Struct. Div., ASCE, Vol.106, No.ST11, 1980, pp.2221-2234.

|7| Ohlsson, Sven: Ten Years of Floor Vibration Research - A review of Aspects and some Results. Submitted to the Symposim on Serviceability of Buildings to be held at Univ. of Ottawa, May 1988.

|8| Bachmann, H. & Ammann, W.: Schwingungsprobleme bei Bauwerken - Durch Menschen und Maschinen Induzierte Schwingungen. IABSE-AIPC-IVBH, Zürich 1987.

|9| Newland, D.E.: An Introduction to Random Vibration and Spectral Analysis. Longman, London 1975.

|10| Corbridge, C. & Griffin, M.J.: Vibration and Comfort: Vertical and Lateral Motion in the Range 0.5 to 5.0 Hz. Ergonomics, Vol.29, No.2,1986,pp.249-272.

|11| Allen, D.E., Rainer, J.H. & Pernicia, G.: Vibration Criteria for Assembly Occupancies. Can. Journ. of Civ. Eng., Vol. 12, 1985, pp.617-623.

A SERVICEABILITY CRITERION TO AVOID HUMAN DISCOMFORT FOR LIGHT-WEIGHT WOODEN FLOORS

Ying Hei Chui and Ian Smith

Department of Forest Engineering
University of New Brunswick, P. O. Box 4400
Fredericton, New Brunswick, Canada E3B 5A3

ABSTRACT

An appraisal is given of previous studies on vibrational performance of light-weight wooden floors with respect to associated human discomfort criteria. It is argued that any specific design criterion for motion must be sensitive to the amplitude, rate of decay and frequency components of the "design vibration". Frequency-weighted root-mean-square acceleration experienced by a human observer is proposed to be such a criterion. A programme of tests on both laboratory-built and in-situ floors is described. From the results, a suitable acceptance threshold for r.m.s. acceleration experienced by an observer at the centre of a wooden floor under a defined impact is derived. Finally, a 'designer usable' method for predicting the acceptability of a projected design based on the threshold identified is introduced.

1. INTRODUCTION

In comparison with other common building materials, wood has a relatively high stiffness to weight ratio, and as a result wooden floors tend to be relatively light-weight. The self-weight of a floor usually has only a minor effect upon its static performance. Studies of dynamical behaviour of structures reveal that the response of any structure to an excitation is inversely proportional to the mass of that structure. Hence light-weight structures such as wooden floors tend to produce a high level vibrational response when excited, for example, by the building's occupants, machinery or street traffic. As human bodies are sensitive to vibrations, this high level response can cause discomfort and undue disturbances to the occupants under normal working conditions.

The traditional working stress methods of design generally produce wooden floors with acceptable vibrational performances. However, due to the use of more refined analysis and design methods, the use of higher moduli of elasticity and the adoption of new construction techniques, floor systems produced in recent times are relatively light and flexible. Consequently, the number of complaints about excessive floor vibration has been increasing. Whilst some of these cases can be attributed to poor workmanship or improper material quality control on site during construction, the majority occur in 'properly' designed and constructed wooden floors.

Current design practices, which treat wooden floor systems as one-dimensional beam structures, do not directly include the checking of vibrational serviceability, although the static deflection limit does provide some indirect control over the problem. In some cases static deflection limits have been found to be inadequate. This is mainly because vibrational performance of a wooden floor depends very much upon the properties (both stiffness and mass) of the floor in the two orthogonal directions rather than the stiffness alone in the joist span direction.

Lack of design guidelines is at least a primary cause of the problem. A proper design method which incorporates means of checking the vibrational serviceability must be devised for ensuring consistent acceptable floor performance.

The research described in this paper was initiated because of performance problems with light-weight wooden floors in the United Kingdom, but the results are equally valid in Canada and elsewhere. Previous research activities on vibrational performance of floors dealing with human discomfort criteria are reviewed. A brief description is given of new tests conducted on both laboratory built and in-situ floors. Finally the paper discusses the proposed human discomfort threshold level and a design method which is based on the threshold identified.

2. PREVIOUS RESEARCH

A very comprehensive literature survey has been conducted by Onysko and Bellosillo (12). They also reported the results of a field study of vibrational characteristics in domestic dwellings in Canada. Questionnaires were sent out to house occupants in a number of cities. They discovered that one of the most influential factors affecting human reaction to floor vibration was whether sound was produced as a result of either the vibration itself or motion induced in furniture and china cabinets. They also concluded that a static deflection limit did not adequately ensure satisfactory vibrational performance. Onysko and Bellosillo classified all relevant research studies up to then into two categories; acceptability-based and perception-based studies. Acceptability-based studies correlate acceptability of a floor with its engineering performance characteristics (e.g. static deflection under a given load). Perception-based studies relate one aspect of performance (e.g. an observer's perception of whole body motion) with acceptability or satisfaction.

Studies by Russell (16) and Hansen (7) come under the first category. Russell tested six floors in the laboratory. During the test, the participants were asked to walk and jump on the floors and also to feel the vibration created by other people walking on and impacting the floors. They were then asked to rate the vibrations. The floors were statically loaded by a concentrated load and by a uniformly distributed load , and the deflections produced related to the ratings given by the participants. He concluded that deflection under a concentrated load is a better predictor of human tolerance than deflection under a uniformly distributed load. Hansen evaluated human response to floor vibration in a laboratory and in occupied dwellings. People were asked to rate the vibration and their responses were related to static deflections. In both studies vibrational characteristics were not measured.

Perception-based studies reported in the literature relate amplitude and frequency of vibration to human perception. Polensek (14) carried out impact tests on wooden floors with plywood sheathing. Frequencies and amplitudes were measured and these were correlated with human ratings of the test floors. Lenzen

(9) tested forty-six concrete-and-steel floors in fourteen buildings. The types of dynamic loading used included steady-state impulses induced by shakers and transient impulses induced by dropping an iron ball or by a person jumping. Participants were then asked to rate the floors on a scale similar to the one devised by Reiher and Meister (15). A later study by Lenzen (10) revealed that damping strongly influenced an observer's perception of transient vibration. Shaver (17) carried out an impact test on an in-situ floor. He measured the accelerations and displacements resulting from impact and from walking. His objective was to verify the procedure for analysing perceptibility of floor vibrations. Parks (13) subjected seated occupants to various levels of transient vibration in a laboratory. The occupants were asked to rate the vibration on the basis of a four-point scale. Wiss and Parmalee (19) conducted similar tests, in which the standing occupants were asked to rate the vibration on a five-point scale. The objective of the studies by Parks and Wiss et al was to develop relevant rating scales.

Ohlsson (11) conducted rating tests on eight floors. Each floor was tested by the same fifteen people. Each participant was asked to walk on a floor, and to feel the vibration created by another person walking and heel-impacting on it. A heel-impact is applied by a person standing on his toes, then rapidly dropping his heels through a distance of about 65 mm to impact the floor surface. The same test procedure was repeated on a reference floor, typical of those in a one-family house in Sweden. The participants were then asked to rate the test floors relative to the reference floor. Ohlsson's study could not be directly classified as belonging to either of Onysko's categories as the rating was related to the performance of a reference floor rather than to the characteristics of the test floors.

Various rating scales have been developed by diffferent workers. Apart from those developed by Parks, Wiss and Parmalee and Polensek, the most well known is perhaps the one developed by Allen and Rainer (1), which gives equal human sensitivity curves for vibration with certain frequency, peak acceleration and damping ratio.

The British Standard BS6472: "Evaluation of human exposure to vibration in buildings (1 Hz to 80 Hz)": 1984 (2) provides general guidance on human exposure to building vibration in the low frequency range. Equal human sensitivity curves for root-mean-square (r.m.s.) acceleration and peak velocity in each of the three orthogonal directions in relation to the human body are given. Similar curves are also given in the international standard ISO 2631: 'Guide for the evaluation of human exposure to vibration': 1978 (8) which deals with human response to vibrations in general rather than to building vibration only. It is shown later that the human discomfort threshold developed in this study is based on the curves and recommendations given in the British Standard, (2).

3. VIBRATION TESTS ON LABORATORY-BUILT FLOORS

The objective of those tests with which the authors were associated was to determine the effects of changes in construction variables on vibrational characteristics of wooden floors. Six wooden floors of different forms of construction were built and tested in the laboratory to determine their vibrational characteristics, such as natural frequencies, and the associated damping ratios and mode shapes. The response of each floor to human impact loading was also measured.

Dynamic impact tests were performed on the test floors. These were carried out by impacting the floor at one point by a hammer or by a heel-drop and measuring the response of the floor at various locations. The principal method of exciting the floors was the hammer impact. Heel-drop impact excitation was conducted when the influence of human presence was assessed. The impact force and response were measured with a load cell and an accelerometer respectively. A micro-computer based acquisition system was used to record the test data via an analogue-to-digital convertor. The data was then analysed using a modal analysis computer program to determine the natural frequencies and the associated damping ratios and mode shapes of the floor under test.

The construction details of each floor are listed in Table 1. The joists were Canadian hem-fir with nominal size 50 mm x 200 mm. They were supported at the ends only on a test base by means of an adjustable clamping device. In order to maximize the number of variables that could be studied in the test programme, most floors were retested after the addition of a construction variable. The test programme enabled the effect of the following to be investigated:

1. Floor size
2. Joist spacing
3. Between-joists strutting (bridging)
4. Concentrated dead load
5. Joist to sheathing connection detail
6. Addition of plasterboard to undersides of joists
7. Flooring material (sheathing)
8. Joist end fixity
9. Additional supports to edge and interior joists

The full set of test results have been reported by Chui (3, 6). Table 2 presents the natural frequencies and viscous damping ratios of the first five modes of vibration of each floor when it was unloaded and with its edge joists unsupported. Although it is not possible to present all the results in this paper, the findings which arose from the test results are briefly discussed in the following paragraphs.

The effect of reducing joist spacing from 600mm to 400mm was to raise the fundamental natural frequency and reduce the spacing between adjacent modes of vibration.

Significant improvement in floor performance was obtained when a floor was stiffened in the across-joists direction by inserting solid wooden blockings between joists . Although this had little effect on the fundamental mode of vibration, it greatly increased the spacing between adjacent modes and reduced the amplitude of vibration.

The effect of adding dead weights on a floor was to lower its natural frequencies and increase the damping ratios. The increase in damping ratios was found to be significant.

It can be noticed from Table 2 that the difference in vibrational characteristics between the glued (floor 3) and the nailed (floor 2) floors was very small. It, therefore, leads to the conclusion that there is no significant advantage in gluing flooring to joists as far as improving vibrational performance is concerned. The value of elastomeric adhesives in this context is thought to be in reduction in the squeak-level for floors.

The fixing of plasterboard to the underside of the joists had two effects on the test floor. It increased the self-weight and the stiffness of the floor. The former lowered the natural frequencies and affected the lower order vibration modes more whilst the latter raised the natural frequencies and had greater effects on the higher order modes.

Three types of flooring material were tried in the test programme. The test results suggested that, other parameters being equal, floors built with plywood flooring behave better than those built with particleboard flooring. This is because plywood generally has a higher stiffness to mass ratio than particleboard.

In the United Kingdom wooden floors are normally constructed with their two edge joists unsupported. One of the test floors was retested after its edge joists were supported (which is common practice in Canada). This led to stiffening of the floor. Although the fundamental natural frequency was virtually unaffected, the higher natural frequencies were increased significantly. The amplitude of the response resulting from human impact was found to be lowered. Thus the Canadian practice of supporting rectangular floors on all four edges is well founded.

The influence of a human body was studied by carrying out, in addition to the hammer impact test, the heel-drop impact test. It was found that human presence enhanced the damping capacities of the test floors but it also resulted in a slight drop in natural frequencies.

4. PROPOSED HUMAN DISCOMFORT CRITERIA FOR CONTROLLING VIBRATION IN LIGHT-WEIGHT WOODEN FLOORS.

Apart from indirect static displacement controls, criteria given by most design codes for controlling vibrations in structures are frequency limits. Research studies of human reaction to vibration have revealed that humans are very sensitive to vibrations having frequencies within the range of 4 Hz to 8 Hz. The frequency limits (if imposed) in design codes relate to this range.

The use of a frequency limit is sufficient for relatively heavy structures such as those built with concrete. For light-weight structures like wooden floors, it can be shown that their natural frequencies are not likely to be below 10 Hz unless their spans are large. The fact that troublesome wooden floors are being designed implies that for wooden floors the use of frequency limits alone does not necessarily ensure consistent acceptable floor performance. A limitation must also be placed upon the magnitude of the vibrational response.

It has been proposed by both the British (2) and ISO (8) standards that the frequency-weighted root-mean-square (r.m.s.) acceleration of a vibration is a good indicator of the human response to mechanical vibration. The root-mean-square acceleration Ar of a vibration signal is given by:

$$Ar = \left[\frac{1}{T}\int_{o}^{T} a^{2}(t)\,dt\right]^{\frac{1}{2}} \qquad [1]$$

where: T is the total duration in seconds
a(t) is the acceleration at time t seconds.

The frequency-weighting procedure is described in the ISO standard (8). Its objective is to emphasize the frequencies to which humans are more sensitive.

A study by Chui (4) has already shown that the frequency-weighted acceleration of the vibration produced by a heel-drop impact applied at the centre of a floor may be used to assess the vibrational serviceability of that floor. A series of field tests was then conducted. Six floors of varying performances were selected. Twenty heel-drop impacts were applied near to the centres of each floor and the responses measured at the centre. The response data were anlaysed to find the r.m.s. acceleration of the vibration. Table 3 presents the mean value for each floor. It can be observed that the human threshold level is about 0.37 m/s^2. This compares favourably with that given in British Standard BS 6472 (2) which recommends a value between 0.3 m/s^2 and 0.45 m/s^2 for transient vibration in domestic dwellings. As the test data were obtained under the most critical condition with the impacts applied at the floor centres, it is proposed that the human threshold level is set at the higher limit of 0.45 m/s^2.

In addition to this response limit, a frequency limit should also be imposed to ensure that all natural frequencies of any floor are above the sensitive frequency band of 4 Hz to 8 Hz. Therefore, logically, natural frequencies of wooden floors should be above 8 Hz. It is recommended that, to ensure acceptable vibrational performances of a wooden floor, both the response and frequency criteria should be satisfied.

5. METHOD OF DESIGN AGAINST VIBRATION

Having established the criteria needed to ensure acceptable vibrational serviceability of wooden floors, this section presents methods for calculating the fundamental natural frequency of a floor and the frequency-weighted r.m.s. acceleration experienced by an observer under a heel-drop impact at the centre of the floor.

The authors have previously presented the derivation of the expression for predicting fundamental natural frequency (18). Applying the well-known Rayleigh method it is possible to show that the fundamental natural frequency f_o of a wooden floor with equally-spaced joists and wood-based sheathing semi-rigidly attached to the upper surfaces of the joists, can be determined from:

$$f_o = \frac{\pi}{2a^2} \sqrt{\frac{EI\,(n-1)}{\rho_s\, hb + \rho_J\, A\,(n-1)}}\ \text{Hz.} \qquad [2]$$

where: E = joist modulus of elasticity
I = second moment of area per joist
n = number of joists
a = floor span
ρ_s = sheathing density
h = sheathing thickness
b = floor width
ρ_J = joist density
A = cross sectional area per joist

Equation [2] assumes that the strain energy of the sheathing and the composite action between sheathing and joists are negligible. These are justifiable assumptions as common sheathing materials are wood-based panels with relatively low stiffness, and the connections between the sheathing and the joists have a low rigidity, e.g. low density nailing. If stiff sheathing or a glued sheathing-to-joists connection is used, advantage can be taken of the stiffening effect due to these. Guidance is given by the authors (18) on the calculation of the fundamental natural frequencies in such cases.

The derivation of the expression for estimating the frequency-weighted r.m.s. acceleration is rather more complicated than for the fundamental natural frequency. Certain assumptions have to be made to simplify the final expression. These are:

1. the response is dominated by the fundamental mode and there are negligible contributions from the higher modes.

2. The impact causing the vibration is applied at the centre of the floor.

3. The mass of the person applying the impact is 70 kg.

4. The total duration of the response caused by one impact is one second.

From the first assumption, a wooden floor can be regarded as a one degree-of-freedom system analogous to a simple mass connected to a fixed point via a spring and a dashpot.

Using the well-known Duhamel integral, Chui (5) has derived a simple expression for estimating the frequency-weighted r.m.s. acceleration Ar of a wooden floor under a heel-drop impact:

$$Ar = \frac{2000\ K}{m\ \pi (f_o')^2}\ \mathrm{m/s^2} \qquad [3]$$

where: $$f_o' = \frac{\pi}{2a^2}\sqrt{\frac{EI\ (n-1)}{\rho_s hb + \rho_J\ A\ (n-1) + \frac{280}{a}}}\ \mathrm{Hz} \qquad [4]$$

$$m = \frac{a}{2}\left(\rho_s hb + \rho_J\ A(n-1) + \frac{280}{a}\right)\ \mathrm{kg} \qquad [5]$$

$$K = \sqrt{\frac{\omega_n[1-e^{-2\delta\omega_n t_1} + (1-e^{-2\delta\omega_n(1-t_1)})\ (1-2e^{-\delta\omega_n t_1}\cos \omega_n t_1 + e^{-2\delta\omega_n t_1}))]}{4\delta}} \qquad [6]$$

where: f_o' = fundamental natural frequency of the floor with a 70 kg observer at the centre
ω_n = $2\pi\ f_o'$
δ = viscous damping ratio
t_1 = duration of the impulse producing the vibration

Experimental data obtained in this and another study (11) indicate that t_1 is normally between 0.05 s and 0.07 s, whilst for normal domestic dwellings δ can be taken as 0.03. Assuming δ to be constant K is, therefore, a function of f'_o and t_1. A Table of K against f'_o has been worked out for $8 \text{ Hz} \leq f'_o \leq 40 \text{ Hz}$. Table 4 presents the maximum value of K at any f'_o for $0.05 \text{ s} \leq t_1 \leq 0.07 \text{ s}$.

To predict whether a floor design is likely to have an unsatisfactory vibrational behaviour both the f_o and Ar should be calculated using equations [2] and [3] respectively. The calculated values are then compared with the criteria given in the last section. It is recommended here that design of light-weight wooden floors should follow the procedure illustrated in Figure 1. The initial stage is identical to present static design, which is retained to ensure that the floor is structurally safe. The remaining stages involve the checking of both f_o and Ar.

6. CONCLUSIONS

The main conclusion that emerged from the literature study was that there was no proper design criteria or guidelines given in current design codes for ensuring vibrational serviceability of light-weight wooden floors. The present static deflection limits for controlling vibrations do not necessarily achieve this objective. The nature of light-weight wooden floors necessitates the limiting of not only the frequency of the vibration but also the mean magnitude of the response if satisfactory performance is to be attained. Controlling the magnitude of the response requires account to be taken of amplitude, rate of decay and frequency components of the "design vibration".

The fundamental natural frequency and the frequency-weighted root-mean-square acceleration together give a control over the frequency range and the magnitude of vibrations caused by a human foot-fall. The critical values have been determined as 8 Hz and 0.45 m/s^2 respectively.

Simple measures such as supporting edge joists and installation of adequate bridging improve vibrational performance of wooden floors. It is recommended that these practices should be incorporated whenever possible in floor constructions.

The design method described in this paper is a suitable method for predicting vibrational serviceability of light-weight wooden floors. The introduction of this approach into current design practices will lead to the production of wooden floors that are consistently acceptable.

ACKNOWLEDGEMENT

Much of the work, on which this paper draws, was undertaken by the first author for the Timber Research and Development Association (TRADA), United Kingdom. Financial support from TRADA and the British Government Department of the Environment is gratefully acknowledged.

REFERENCES

1. **ALLEN, D.E. and RAINER, J.H.** Vibration criteria for long-span floors. Canadian Journal of Civil Engineering, June 1976, 3(2) 165-173.

2. **BRITISH STANDARDS INSTITUTION.** Evaluation of human exposure to vibration in buildings (1 Hz to 80 Hz). British Standard BS 6472. London, BSI. 1984.

3. **CHUI, Y.H.** Evaluation of vibrational performance of light-weight wooden floors: Determination of effects of changes in construction variables on vibrational characteristics. TRADA Research Report 2/86. Hughenden Valley, TRADA. 1986.

4. **CHUI, Y.H.** Evaluation of vibrational performance of light-weight wooden floors: Method of assessment of floor vibration due to human footsteps. TRADA Research Report 3/86. Hughenden Valley, TRADA. 1986.

5. **CHUI, Y.H.** Evaluation of vibrational performance of light-weight wooden floors: Design to avoid annoying vibrations. TRADA Research Report 15/86. Hughenden Valley, TRADA. 1986.

6. **CHUI, Y.H.** Design aspects of floor vibration. Final Report to the Department of the Environment. (Unpublished report). Hughenden Valley, TRADA. 1986.

7. **HANSEN, H.** Deflection characteristics of wood-joist floors. National Research Council of Canada, Translation NRC-TT883. Ottawa, Canada, NRCC. 1960.

8. **INTERNATIONAL ORGANIZATION FOR STANDARDIZATION.** Guide for the evaluation of human exposure to vibration. International Standard ISO 2631. Geneva, ISO. 1978.

9. **LENZEN, K.H.** Final Report: Vibration of steel joist-concrete slab floor system. University of Kansas, Studies in Engineering Mechanics, Rep. 16. Lawrence, Kansas, 1962.

10. **LENZEN, K.H.** Vibration of steel-joist-concrete slab floors. Jnl. Eng. (AISC), 1966, 3(3) 133-136.

11. **OHLSSON, S.** Floor vibrations and human discomfort. Ph.D. Thesis, Dept. of Structural Engineering, Chalmers University of Technology, Gothenburg, Sweden, 1982.

12. **ONYSKO, D.M. and BELLOSILLO, S.B.** Performance criteria for residential floors. Final report to Central Mortgage and Housing Corporation, Grant no. 120-74. Ottawa, Canada, Eastern Forest Products Laboratory, Wood Structures Group. March 1978.

13. **PARKS, D.L.** Defining human reaction to whole-body vibration. Human Factors, October 1962, 305-313.

14. **POLENSEK, A.** Human response to vibration of wood-joist floor systems. Wood Science, 1970, 3(2) 111-119.

15. REIHER, H. and MEISTER, F.J. The effect of vibration on people. Translated from German, Rep.F-TS-616-REH, 1931, by Air Material Command. Wright Field, Ohio, AMC. 1946.

16. RUSSELL, W.A. Deflection characteristics of residential wood-joist floor systems. U.S. Housing and Home Finance Agency, Housing Research Paper 30. Washington, D.C., HHFA. 1954.

17. SHAVER, J.R. Correlation of floor vibration to human response. U.S. National Bureau of Standards, Technical Note 904. Washington, D.C., NBS. 1976.

18. SMITH, I. and CHUI, Y.H. Predicting the natural frequencies of light-weight wooden floors. Proceedings of Joint Meeting of IUFRO Wood Engineering Group and CIB-Working Commission W18, Florence, September 1986. p. 19.

19. WISS, J.F. and PARMALEE, R.A. Human perceptions of transient vibrations. Jnl. of Structural Division, ASCE, April 1974, 100(ST4) 773-787.

Table 1: Construction Details of Test Floors

Floor	Span (m)	Width (m)	Joist Spacing(mm)	Flooring	Fastener	Comments
1	3.6	4.8	600	T & G 22mm flooring grade chipboard (particleboard)	3.35 x 65mm ring shank nails at 200mm c/c	Test with no bridging and then retest with two rows of bridging.
2	3.6	4.8	400	"	"	Retest with plasterboard.
3	3.6	4.8	400	"	Elastomeric adhesive	Test with bridging.
4	3.6	4.8	400	15mm T & G plywood sheathing	3.0 x 50mm ring shank nails at 250mm c/c	Test with bridging. Retest with denser nailing.
5	3.6	4.8	400	19mm T & G softwood board	3.0 x 50mm Bright wire nails - two on each board	Test with bridging. Retest with 4 edges supported, and with middle joist supported.
6	3.92	2.4	600	15mm T & G plywood sheathing	3.0 x 50mm ring shank nails at 300mm c/c	Test with no bridging.

Table 2: Natural Frequencies and Viscous Damping Ratios of Test Floors

Floor	Mode Number				
	1	2	3	4	5
1	17.2 Hz 1.54%	20.6 Hz 0.86%	25.1 Hz 0.76%	31.5 Hz 1.18%	39.2 Hz 2.27%
2	18.7 Hz 1.48%	21.5 Hz 1.18%	25.2 Hz 1.09%	30.3 Hz 2.50%	39.5 Hz 1.81%
3	18.9 Hz 1.51%	21.4 Hz 1.16%	25.2 Hz 1.17%	30.9 Hz 1.58%	39.6 Hz 1.74%
4	23.3 Hz 1.61%	27.1 Hz 0.96%	30.4 Hz 0.96%	34.6 Hz 1.11%	42.1 Hz 1.05%
5	18.5 Hz 1.55%	21.6 Hz 0.73%	25.4 Hz 0.95%	31.8 Hz 1.31%	40.9 Hz 1.34%
6	21.1 Hz 1.25%	23.8 Hz 1.25%	30.8 Hz 1.40%	38.7 Hz 1.15%	48.7 Hz 1.05%

Table 3: Root-Mean-Square Accelerations Of In-situ Floors

Floor	Performance Class	r.m.s. acceleration (m/s^2)
1	Threshold	0.368
2	Threshold	0.376
3	Good	0.160
4	Bad	0.753
5	Bad	0.714
6	Bad	0.534

Table 4: K Values

f'_o (Hz)	K
8	38.8
9	41.4
10	44.0
11	45.5
12	45.6
13	44.5
14	42.2
15	38.7
16	34.4
17	35.9
18	45.1
19	52.9
20	58.7
21	62.0
22	62.7
23	61.9
24	65.8
25	67.7
26	67.4
27	65.1
28	69.5
29	72.6
30	74.1
31	74.0
32	72.4
33	69.3
34	72.8
35	76.8
36	77.9
37	76.1
38	71.8
39	74.8
40	80.2

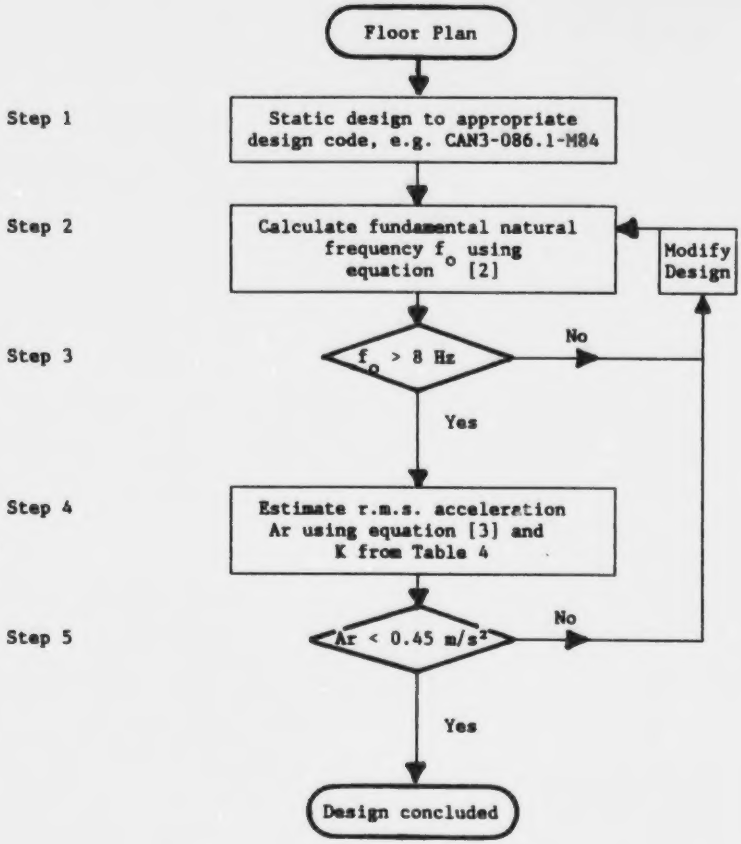
Floor Plan
Step 1
Static design to appropriate design code, e.g. CAN3-086.1-M84
Step 2
Calculate fundamental natural frequency f_o using equation [2]
Modify Design
Step 3
f_o > 8 Hz
No
Yes
Step 4
Estimate r.m.s. acceleration Ar using equation [3] and K from Table 4
Step 5
Ar < 0.45 m/s²
No
Yes
Design concluded

Figure 1. Flow Chart For Proposed Design Method

VIBRATION RESPONSE OF A RIBBED SLAB FLOOR TO DANCING

I. Rosenthal, M. Itskovitch

Building Research Station
Faculty of Civil Engineering
Technion - Israel Institute of Technology
Haifa, Israel

ABSTRACT: Large deflections in a hall used for dances, with a reinforced concrete ribbed slab floor, felt both by the dancers and by the occupants of the lower storey, caused the owners to carry out vibration measurements in order to obtain the dynamic capacity of the floor. Measured results exceeded the allowable limit values for floor vibrations, and clearly indicated a case of resonance.

The minimum fundamental frequency of the floor, calculated according to serviceability criteria, was higher than the actual one.

Remedial structural measures were suggested for improving the dynamic properties of the floor in order to eliminate the attendant cumulative damage in the future.

INTRODUCTION

A large hall with a reinforced concrete floor, the second storey of a student union building originally designed as a cafeteria, was converted after several years for dances. This conversion, apparently undertaken without checking the dynamic capacity of the slab, resulted in visible cracks and in noticeable vibration, felt both by the dancers and by the occupants of the ground storey space below, serving as a recreation hall.

As a result, vibration measurements were ordered and carried out during a folk dance evening, with more than three hundred participants.

DESCRIPTION OF FLOOR

The floor consisted of a 350mm deep reinforced concrete ribbed slab, with in-filled hollow concrete blocks, and having dimensions of 10.5mx23.1m. Actually, there were 32 main ribs, 700mm apart, each one having a cross-section of 120x300mm with 2φ1" deformed bar - as reinforcement. The top slab was 50mm thick and included 6mm bar reinforcement in both directions, 300mm apart. Two longitudinal ribs, located at 3.0m from each slab edge, were part of the floor.

EXPERIMENTAL PROCEDURE

Vertical displacements were directly measured on the underside of the floor, at midspan of the central rib, using a B&K Vibration Meter. The dynamic loading, which was of random forcing frequency, consisted of folk dances only.

There were eleven series of dances, as follows:

- Series 1 to 4 - rondo type dances, which affected mainly the floor edges, and less its central portion.
- Series 5 to 11 - dancing couples, including jumps, which affected the whole area of the floor. In these cases, the number of participants exceeded three hundred.

All measurements were recorded both in chart form and on magnetic tape, and later analysed by means of a B&K Tunable Band Pass Filter and a Level Recorder.

RESULTS

Records of the dynamic displacements of the floor central point are shown in Fig. 1, with maximum values (Table 1), ranging between 0.16mm (dances 3 and 4) and 2.20mm (dance 6). The displacement spectrum of dance 6, carried out with a 3% Bandwidth Filter, is shown in Fig. 2. The dominating frequency found was 2.9 Hz, which is very close to the fundamental frequency of the floor, namely 2.7 Hz, determined by decay curves obtained through sudden stops. Using these curves, the critical damping ratio was calculated and found to be 4%.

Table 1 - Midspan floor dynamic displacement, in mm

Dance	Maximum	Peak to Peak
1	0.26	0.44
2	0.51	0.64
3	0.16	0.28
4	0.16	0.28
5	0.70	1.32
6	2.20	2.80
7	1.50	2.40
8	1.05	1.40
9	0.75	1.28
10	1.25	2.24
11	1.20	1.76

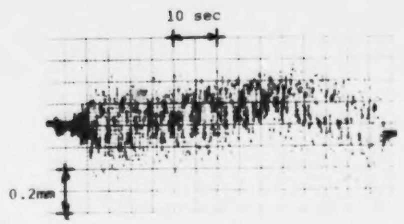

Dance 1

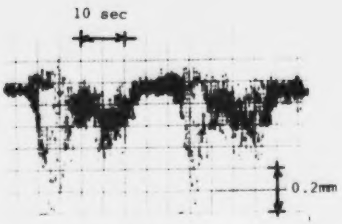

Dance 2

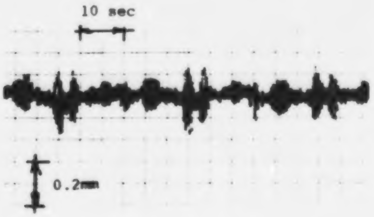

Dance 3

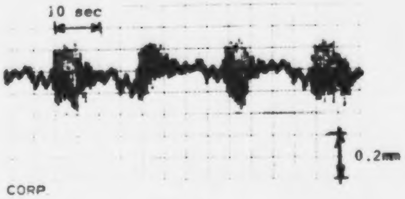

Dance 4

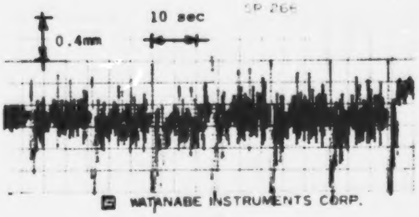

Dance 5

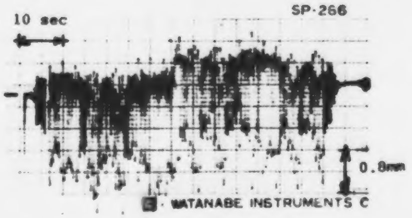

Dance 6

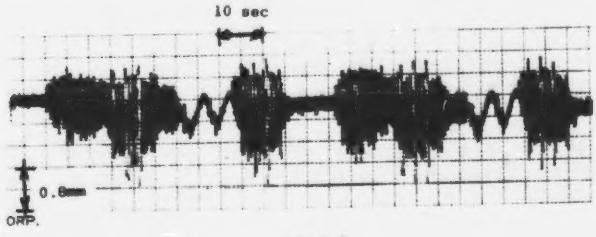

Dance 7

Fig. 1a - Dynamic Deflections of the Floor Central Point, Due to Dances 1 to 7

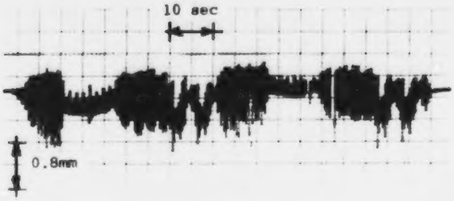

Dance 8

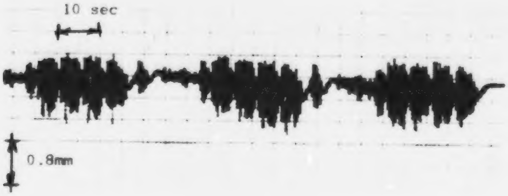

Dance 9

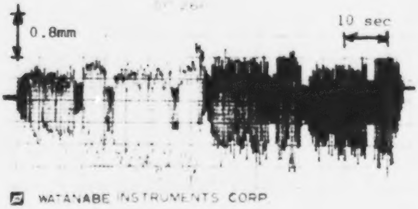

Dance 10

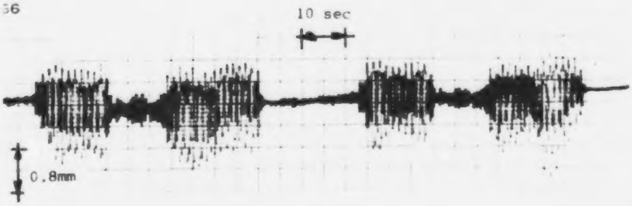

Dance 11

Fig. 1b - Dynamic Deflections of the Floor Central Point, Due to Dances 8 to 11

The computed natural frequency of the floor was 2.9 Hz (Appendix A) - again very close to the one obtained from the measurements.

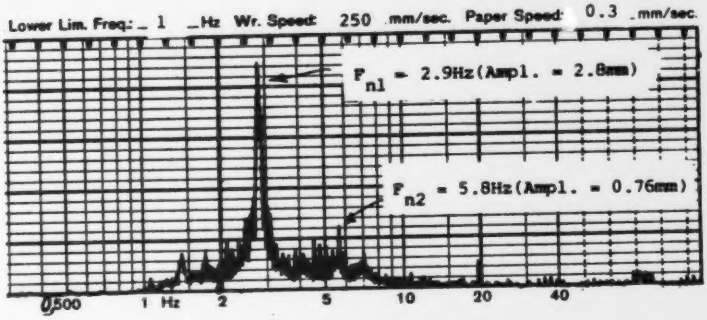

Fig. 2 - Displacement spectrum of dance 6 (Bandwidth Filter 3%)

DISCUSSION

Analysis of the vibration records of dance 6 has shown that the floor was in a state of resonance with the acting forces. The maximum measured displacement was 2.2mm, with a peak to peak value of 2.8mm. The corresponding maximum velocity and acceleration were 37.4 mm/sec and 6.5%g respectively.

The results obtained considerably exceeded the accepted vibration limits for floors, based on both annoyance and structural criteria. In general, these limits are in the frequency range 1 to 10 Hz, as follows: 0.2 to 2mm for displacements, 5 to 10mm/sec for velocity, and 0.5% g to 5% g for acceleration, with the lower limits corresponding to human response and the upper - to likely damage in the structure [1-6].

As can be seen from comparing the measured results with the prescribed standard limits, the present floor has, besides the discomfort aspect - a much more serious structural problem, in view of the fact that the upper vibration limits coincide with a state of cracking and damage.

It is of interest to mention that the natural frequency of a concrete slab designed for dining and dancing activities, according to serviceability criteria, with an acceleration limit of 2% g should be at least 6.4 Hz, [4],[7], and if designed for "lively concerts", with an acceleration limit of 5% g - 4.8 Hz. The corresponding maximum deflections caused by the dynamic loading of the participants are 0.43mm and 0.85mm respectively (Appendix B).

CONCLUSIONS

1. Vibration measurements indicate the serious state of the floor, when used for dances - an activity for which it has not been designed.

2. It was recommended accordingly, that the floor be strengthened by in-situ casting of reinforced-concrete flanges to its ribs, after a pair of suitable steel angles has been attached to each of them.

REFERENCES

1. Draft International Standard: "Measurement and Evaluation of Vibration Effects on Buildings", ISO/DIS 4866, 1986.

2. International Standard Organization, "Guide for the Evaluation of Human Exposure to Whole Body Vibration", ISO 2631, for 1978.

3. DIN 4150, Part 3: "Vibrations in Building: Effects on Structures", Table 1 and Fig. 1, May 1986.

4. Supplement to the National Building Code of Canada, 1985 Edition, Commentary A, "Serviceability Criteria for Deflections and Vibrations", pp. 146-152.

5. Harris, C.M. and Crede, C.E., "Shock and Vibration Handbook", 2nd ed., Chapter 19, "Vibration Standards", McGraw Hill, 1976.

6. Allen, D.E. and Rainer, J.H., "Floor Vibration", Canadian Building Digest, No. 173, Sept. 1975.

7. Allen, D.E., Rainer, J.H. and Pernica, G., "Vibration Criteria for Assembly Occupancies", Canadian Journal of Civil Engineering, Vol.12, No.3, September 1985, pp. 617-623.

8. Timoshenko, S., Young, D.H. and Weaver, W., "Vibration Problems in Engineering", 4th ed., Wiley, New York, 1974.

APPENDIX A: FUNDAMENTAL FREQUENCY OF FLOOR IN QUESTION

For a simply supported one way floor, the fundamental frequency is calculated [8], according to:

$$F = \frac{\pi}{2\ell^2}\sqrt{\frac{EI}{m}} = 2.88 \text{ Hz}$$

where: $l = 10.5\text{m}$

$E = 25000 \text{ MPa} = 25\text{x}10^6 \text{ kPa}$

$I = 8.2\text{x}10^{-4}\text{m}^4$ (per rib)

$m = \frac{W_t}{g} = \frac{D.L.+W_p}{g} = \frac{5 \text{ kN/m}}{10\text{m/sec}^2} = 0.5 \text{ kPa/sec}^2$ (per rib)

APPENDIX B: FREQUENCY AND DEFLECTION OF R.C. FLOOR

The minimum frequency of the floor (D.L. = 5kPa) and maximum deflection under dynamic loading of the participants, calculated according to structural criteria [4],[7], are:

$$f_o \geq f\sqrt{1 + \frac{1.3}{a_{o/g}}\left(\frac{\alpha W_p}{W_t}\right)}$$

$$\Delta_s \leq \frac{a_o}{(2\pi f)^2}\left[\frac{1}{1 + \frac{a_{o/g}}{1.3}\left(\frac{W_t}{\alpha w_p}\right)}\right]$$

Activity	Dancing and Dining	Lively Concert
Acceleration limit (a_O/g)	2%	5%
Forcing frequency (f)	3 Hz	3 Hz
Weight of participants (W_p)	0.6 kPa	1.5 kPa
Dynamic load (αW_p)	0.3 kPa	0.4 kPa
Total weight (W_t)	5.6 kPa	6.5 kPa
Minimum frequency (f_o)	6.4 Hz	4.8 Hz
Maximum deflection (Δ_s) under (αW_p)	0.43mm	0.85mm

A DANCE FLOOR WITH UNSATISFACTORY DYNAMIC RESPONSE

C. M. Matthews (1) and C.J. Montgomery (2)
(1)Centre for Frontier Engineering Research
(2)Lamb McManus Associates Ltd.
Edmonton, Alberta, Canada

ABSTRACT: This paper presents results from an experimental investigation undertaken to determine the dynamic response of a steel-joist concrete-slab dance floor in a combined dining-dancing occupancy. The opportunity to study the dynamic response of the floor came as a result of patron complaints of bothersome vibrations during dances.

The study consisted of measuring the floor response to a series of heel impact tests and monitoring the response of the floor during an evening dance. Dynamic properties reflecting the free vibration of the floor system were derived from the heel impact records. Analysis of the dance records indicated that the floor response was a forced vibration at the rhythmic frequency of the various dance activities. These results were used in making recommendations to improve the dynamic performance of the floor system.

Also presented is a procedure to evaluate the serviceability of a dance floor at the design stage. The results of the dance floor study were used to establish a set of annoyance criteria to be used in conjunction with the proposed method. The method is compared to the procedure outlined in Commentary A, Chapter 4 of the Supplement to the National Building Code of Canada (Associate Committee on the National Building Code, 1985) for the design of floor systems subjected to rhythmic activities.

1.0 INTRODUCTION

Until recently, there have been few guidelines for design engineers to follow when they have had to contend with a dance floor situated on or adjacent to the same joist span as a dining area. Consequently, there have been several cases where the dynamic response of such floor systems has been unacceptable for the dual purpose intended (Matthews et. al. 1982, Rainer and Allen 1973).

To prevent resonance from occurring with respect to the first or second harmonic of floor response, the National Building Code of Canada since 1975 has recommended a minimum fundamental frequency of 10 Hz for floor systems subjected to repetitive activities. This requirement was introduced to prevent floors from vibrating in resonance with the periodic forces generated in the 1 to 4 Hz frequency range by human activities such as dancing or jumping. However, structural designers have faced difficulties in economically meeting this criteria and the need for better design guidelines became evident as the number of floors exhibiting unacceptable dynamic response increased.

This paper presents the results from an investigation into the dynamic response of a dance floor. These results have been used in developing a procedure to assess the dynamic serviceability of floor systems for certain types of assembly occupancies.

2.0 DESCRIPTION OF FLOOR SYSTEM

The dance floor in question is located on a dropped section of the second floor of a three storey building. The structural layout of the dance floor and surrounding area is illustrated in Figure 1. The structural system consists of a non-composite concrete slab supported by open-web steel joists, which are in turn simply supported on steel beams. The beams spanning beneath the sunken floor area are arranged in a cantilever system that is supported by columns below the second floor. Other floor beams are simply-supported on columns which extend the full building height.

The 100 mm thick concrete floor slab consists of normal weight concrete cast on 38 mm corrugated steel decking which spans 940 mm between 600 mm deep open-web steel joists in the test area. The 13 m by 18 m sunken floor area is 400 mm below the general elevation of the second floor.

When the dynamic tests took place, the building had been occupied for several months. With the exception of a 7 m by 9.8 m hardwood dance floor, the sunken floor area was carpeted. Tables and chairs used for dining surrounded the dance floor on three sides while a stage was located on the fourth side. A low partition divided the tables located on the sunken floor from those on the main floor level.

3.0 EXPERIMENTAL INVESTIGATION

The experimental investigation of the dance floor consisted of taking two sets of vibration measurements. The first set of measurements recorded the floor response to a series of heel impacts. In the second set of measurements, the vibration response was monitored during an evening dance.

Up to four piezoelectric accelerometers were used simultaneously to measure the response of the floor system during the various tests. Figure 1 shows the positions on the sunken floor at which the floor response was monitored during two series of heel impact tests and throughout the evening dance. All signals were recorded on a four channel FM tape recorder for subsequent analysis. A more detailed description of monitoring equipment, test procedures, and analysis techniques is provided by Matthews et. al. (1982).

4.0 FREE VIBRATION CHARACTERISTICS

The heel impact tests were conducted to determine parameters associated with the free vibration response of the floor system including its natural frequencies, mode shapes, and modal damping ratios.

Magnitude spectra derived through a Fourier analysis of the transient acceleration-time records resulting from the heel drop impacts on the floor revealed that the floor system had several natural frequencies of vibration below 10 Hz. The fundamental frequency of the floor system was 5.0 Hz, with higher natural frequencies occurring at 6.8, 7.3, 9.4, and 9.8 Hz. A typical magnitude spectra for position E5 (see Figure 1) corresponding to a heel impact at position E6 is illustrated in Figure 2.

As illustrated in Figure 3, the mode shape of the floor system along lines C, E, and 6 (see Figure 1) for the fundamental frequency of 5 Hz was found to approximate a one-half sine wave. In the first mode, the entire sunken floor area vibrated in phase as a single panel. Because of the close frequency spacing, the corresponding uncoupled response of the floor in the higher modes of vibration could not be established from the recorded data.

The fundamental mode was found to be the most highly damped with a ratio of approximately 5.0 % of critical, while the other four modes were more lightly damped with values in the 2.5 to 3.5 % range.

4.1 Discussion: The results derived in the heel impact study were used to assess the adequacy of the floor system for a quiet occupancy. Filtered acceleration-time records from position E6 (see Figure 1) for an adjacent heel impact revealed a peak acceleration response of 1.4 %g in the fundamental mode of vibration. When plotted on the annoyance criteria for floor vibration chart presented by the Canadian Standards Association (1984) at a frequency of 5.0 Hz, the measured acceleration was below the annoyance threshold for a quiet occupancy floor with 3 % damping. Since the floor had a damping ratio of 5 % of critical in the fundamental mode, the floor would be acceptable for such occupancies.

This assessment agreed with observations made during the tests that vibration levels generated by the heel impacts or by normal walking activities were not bothersome to patrons seated or standing within the sunken floor area.

5.0 DANCE VIBRATION STUDY

Since the heel impact study did not reveal the cause of the bothersome vibrations reported on many occasions by patrons, a second investigation was undertaken to assess the response of the floor system to coordinated dance activities. For this study, two accelerometers were mounted near the edge of the dance floor (see Figure 1) in the general vicinity where the most annoying vibration levels had been reported by seated patrons, as well as those taking part in the dances. The response of the floor system to a variety of dance activities was then recorded throughout an evening dining-dance reception. The evening's dance selection included waltzes, polkas, and various modern and rock and roll dances which resulted in the floor being subjected to a wide variation of dynamic loads.

5.1 Test Results: The recorded accelerometer signals were processed to obtain filtered acceleration-time records and the corresponding frequency domain representations of the floor response in the form of magnitude spectra. A typical filtered acceleration-time trace is shown in Figure 4, while magnitude spectra representative of the floor response for a waltz, a polka, and a rock and roll dance are presented in Figure 5.

The spectra of Figure 5 clearly show the floor system responded to each dance activity at the rhythmic frequency of the dance, and not at the floor's fundamental frequency of 5.0 Hz. These results demonstrate that the excessive vibration levels which had been causing concern among patrons were not due to resonance, but rather the result of forced vibrations at frequencies well below the fundamental floor frequency.

Table 1 presents a summary of the results derived in the dance vibration study.

The results reveal that the predominant excitation frequency of the various dance activities ranged from 1.9 Hz for a waltz to 3.3 Hz for a fast rock and roll dance. In several cases, a significant response at the second harmonic frequency was observed in the results. Considering the wide assortment of dances that took place, forcing frequencies exceeding 4.0 Hz seem unlikely for dance activities, although harmonics up to 8.0 Hz may contribute significantly to the response.

For a particular dance, the excitation frequency was found to be directly related to the musical beat and dance step and not to the number of participants. This is understandable, since the majority of participants were able to keep time with the music during the dances. However, the number of participants did have a direct bearing on the vibration amplitudes associated with a particular type of dance activity. This was clearly evident during individual dances when the amplitude of the floor response increased in proportion to the number of people dancing. A simple explanation for the increased dynamic response is that the entire dance floor area responded in phase to the dance activities in a pattern similar to the fundamental mode shape (see Figure 3) and therefore coordinated impacts at any position on the floor contributed directly to the vibration amplitude.

The relative spectral magnitudes listed in Table 1 indicate the contribution of the respective frequency components to the overall response during each dance. The individual values were determined by normalizing the spectral magnitudes of the components associated with each dance record to the component with the overall maximum spectral magnitude. This accounts for the one rock and roll component in Table 1 having a value of 1.0.

The average and maximum peak acceleration values presented in Table 1 for each of the dances were obtained from acceleration-time records which were lowpass filtered at first 25.0 and then 6.5 Hz. The significance of the respective values for a segment of a typical dance record is illustrated in Figure 4. A comparison of the two average acceleration values given for each dance clearly shows that frequency components above 6.5 Hz contributed little to the overall response in all cases.

The maximum peak acceleration values provide an indication of the response which occurred periodically for short periods during the various dances. Since these intermittent peak accelerations were generally much higher than the average accelerations, they could be readily perceived by the patrons seated near the dance floor. These peaks likely contributed significantly to the annoyance of those patrons. The remarks included in Table 1 reflect comments made during the various dances by people dining on the sunken floor section in the general vicinity of the accelerometers. The floor vibration levels outside the sunken floor area did not appear to bother diners during any of the dances.

5.2 Discussion: When the dance vibration study took place, there were no explicit guidelines available to evaluate human response to the forced vibration of the dance floor under the dynamic loads generated by the dancing activities. The authors felt that a reasonable assessment could be made by comparing the measured average peak acceleration values for the various dances (see Table 1) with the continuous vibration curve shown on the annoyance criteria for floor vibrations chart presented by the Canadian Standards Association (1984) for quiet occupancies, since the dining areas surrounding the dance floor could be considered as such. The chart indicates that continuous vibrations with average peak accelerations above 0.5 %g will be annoying for floors with natural frequencies below 8 Hz These comparisons did yield excellent results. For every dance where the average peak acceleration response exceeded the 0.5 %g level, the diners seated near the accelerometers had expressed annoyance with respect to the vibration levels. The average accelerations exceeding 0.5 %g have been underlined in Table 1.

The results of the dance vibration study confirmed that the dynamic response of the floor system was unacceptable for the combined dining-dancing occupancy that existed. The results showed that the excessive vibration amplitudes were from forced vibrations and not from a resonance condition. The stiffness of the floor system was inadequate to restrict the dynamic response to an acceptable level. This does not suggest that the strength of the floor system was in any way inadequate. Rather, the stiffness resulting from the standard span-related live-load deflection criteria used in designing the floor system was inappropriate for dynamic load situations. The patrons perceive the actual vibratory amplitudes, and not the span related deflections. As a result of this study, recommendations were made to substantially increase the stiffness of the floor system so that its dynamic response would be acceptable for the dual dining-dancing occupancy.

6.0 DESIGN PROCEDURE

In this section, a design procedure is developed to assess the the dynamic serviceability of simple beam and open-web steel joist floors subjected to dancing activities. The procedure must be considered in addition to strength requirements at the design stage. The procedure can be used to assess the dynamic response of seating or dining areas located adjacent to or on the same span as a dance floor.

The design procedure presented herein is meant to augment a similar method recently introduced by the Associated Committee of the National Building Code (1985).

6.1 Model of Floor System: In the procedure, the floor system is divided into a series of T-beams with a top flange width equal to the spacing of the joists or beams. The concrete slab is assumed to act compositely with the joists or beams, whether or not shear connection has been provided. Figure 6 shows the T-beam model of the floor system.

The T-beams are assumed to be simply supported and to have uniform flexural rigidity of EI, width of b, and mass per unit length of $\bar{m}$. In Figure 6, a(x,t) is the floor acceleration as a function of position x and time t, p(x,t) is the dynamic dance load which has a maximum value of P_o, and $\bar{f}$ is the forcing frequency for the dance load. Note the dance load only acts over a portion of the T-beam.

6.2 Design Procedure Development: By using the floor model described above, it can be shown (Clough and Penzien 1975) that the peak acceleration, A_o, of a dance floor in the fundamental mode of vibration is given by the expression

$$A_o = \frac{2\, P_o\, \beta_1^2\, D_1}{\pi\, \bar{m}} \sin \frac{\pi x}{L} \left[\cos \frac{\pi c}{L} - \cos \frac{\pi d}{L} \right] \tag{1}$$

In Equation (1), the symbols β_1 and D_1 are the ratio of the forcing frequency of the dance load to the fundamental frequency of the floor system and the dynamic magnification factor in the fundamental mode, respectively, and c, d, and L are as shown in Figure 6. The dynamic magnification factor is calculated from the expression

$$D_1 = \left[\left[1 - B_1^2 \right]^2 + \left[2 \xi_1 B_1 \right]^2 \right]^{-0.5} \qquad (2)$$

in which ξ_1, is the damping ratio in the fundamental mode.

Equation (1) was used in conjunction with the observed peak acceleration values (from records lowpass filtered at 6.5 Hz) and estimates of the weight of people on the dance floor during the various dances to derive a dynamic dance load. The resulting dynamic load of 0.25 KN/m^2 is representative of the loading conditions associated with a full dance floor and a lively dance activity.

For Equation (1) to be used in assessing the servicability of a floor system subjected to dynamic loads, guidelines on acceptable vibration levels must be available. The proposed guidelines presented below were established on the basis of the results from the dance vibration study and they apply to seating areas located on the same joist span as a dance floor. Significantly higher levels of acceleration may be tolerated if no dining areas are situated on or adjacent to the joists or beams supporting a dance floor.

ACCEPTABLE ACCELERATION GUIDELINES

Peak Acceleration Ao (%g)	Serviceability Criteria
0.00 - 1.25	acceptable
over 1.25	unacceptable

6.3 Summary of Design Procedure: The following steps illustrate the procedure to follow in assessing the serviceability of a floor system for a dual dining and dancing occupancy.

1) Calculate the uniform mass per unit length of the assumed T-beam, including structural and non-structural components which contribute to the dead load.

2) Determine the flexural rigidity of the T-beam. Where ribbed decking is used, the effective flange thickness is determined by averaging the weight of the concrete over a unit area.

3) Calculate the fundamental natural frequency, f_j, of the T-beam in Hz from the expression

$$f_j = \frac{\pi}{2} \sqrt{\frac{E\,I}{\bar{m}\,L^4}} \qquad (3)$$

If the floor joists are supported on flexible beams (or floor beams on flexible girders), a system frequency (f_f) should be calculated using the formula

$$\frac{1}{f_f^2} = \frac{1}{f_j^2} + \frac{1}{f_g^2} \qquad (4)$$

where f_g is the fundamental frequency of the supporting beams or girders calculated assuming they are loaded with the floor weight they support but neglecting any contribution of the slab to the stiffness unless the beams or girders were designed compositely.

4) Using the fundamental floor frequency, f_o, determined by either (3) or (4), calculate the frequency ratio from the expression

$$\beta_1 = 3.5/f_o \qquad (5)$$

In this equation, the forcing frequency of the dance load is assumed to be 3.5 Hz.

5) Determine the dynamic magnification factor, D_1, from Equation (2), with the critical damping ratio estimated from values suggested by Canadian Standards Association (1984) or Wilson and Heidebrecht (1976), with regard to the floor construction and finish.

6) Evaluate the peak acceleration of the floor according to Equation (1) at the position where the seating or dining area is closest to the dance floor. The maximum value of the dynamic dance load, P_o, in Equation (1), is obtained by multiplying 0.25 KN/m² by the width of the T-beam, b.

7) Compare the calculated peak acceleration to the recommended limits stated above. Note that the acceleration calculated from Equation (1) will have units consistent with those for the problem at hand. The acceleration must be converted to a percentage of gravity for comparison with the suggested limits. The floor system should be redesigned if the acceptable level is exceeded. In most cases, the floor stiffness will need to be raised through an increase in the size and number of joists or beams, or by decreasing the joist or beam span.

7.0 COMPARISON WITH NBC PROCEDURE

The dynamic analysis procedure for dance floors outlined by the Associate Committee to the National Building Code (1985) uses the following criteria:

maximum acceleration - 2.0 %g
(dining/dancing occupancy)
forcing frequency - 3.0 Hz
dynamic load (P_o) - 0.3 KN/m²

For the dance floor considered in this study, these design criteria and the the code procedure result in a minimum recommended floor system frequency of 8.1 Hz.

By comparison, the corresponding criteria applicable to the design procedure presented in this paper are as follows:

maximum acceleration - 1.25 %g
forcing frequency - 3.5 Hz
dynamic dance load - 0.25 KN/m²

Substitution of the suggested acceleration limit (1.25 %g) into design Equation (1) gives a minimum recommended natural frequency of 7.7 Hz. Thus, the results of the two procedures compare extremely well.

The procedure presented herein can be extended to the design of floor systems for other types of assembly occupancies by appropriately adjusting the dynamic load, P_o, to suit the activity and by using peak acceleration criteria which reflect the type of occupancy. A minimum forcing frequency of 3.5 Hz should be used to calculate the frequency ratio, with higher values substituted for cases such as exercise room floors where jumping activities may be common.

8.0 SUMMARY AND CONCLUSIONS

Results were presented from a study of the dynamic response of a steel-joist concrete-slab floor system in a combined dining-dancing occupancy. The study was undertaken to investigate patron complaints of bothersome floor vibration levels during dances.

The dynamic study consisted of measuring the floor response to both heel impacts and a variety of dance activities. The results of the heel impact tests showed the floor system had a fundamental natural frequency of 5.0 Hz with a corresponding modal damping ratio of 5.0% of critical. In the fundamental mode, the entire sunken floor area vibrated in phase with a typical one-half sine wave shape in both directions. The heel impact test results were used to show the floor system would be acceptable for a quiet occupancy.

The results of the dance vibration study showed that the bothersome vibration levels during dances were not due to resonance, but were the result of a forced response at frequencies well below the fundamental floor frequency. The unacceptable dynamic response was attributed to an inadequate floor stiffness.

A procedure to assess the dynamic serviceability of dance floors at the design stage was presented. Results obtained by the procedure agreed favorably with those determined by a similar method outlined in the National Building code of Canada.

ACKNOWLEDGEMENTS

The cooperation of G. Culham of J.H. Cook Architects and Engineers of Calgary in arranging permission to conduct the dynamic tests is gratefully acknowledged. The authors wish to express their gratitude to J.H. Rainer of the Division of Building Research (NRC) for his assistance in the experimental work.

9.0 REFERENCES

Associate Committee on the National Building Code. 1985. The supplement to the national building code of Canada. National Research Council of Canada, Ottawa, Ontario, Commentary A, pp.146 to 152.

Canadian Standards Association. 1984. Guide for floor vibrations, Appendix G. In-Steel structures for buildings - limit states design. Canadian Standards Association, Rexdale, Ontario, CSA Standard CAN3-516.1-M84.

Clough, R.W. and Penzien, J. 1975. Dynamics of structures. McGraw-Hill Inc., New York, N.Y., 634 p.

Matthews, C.M., Montgomery, C.J. and Murray, D.W. Designing floor systems for dynamic response. Structural Engineering Report No. 106. Department of Civil Engineering, University of Alberta, Edmonton, Alberta. 253 p.

Rainer, J.H. and Allen, D.E. 1973. Vibration characteristics of a dance floor. National Research Council of Canada, Division of Building Research, Ottawa, Ontario, TN576.

Wilson, J. and Heidebrecht, A. 1976. Vibration characteristics of long span floor systems. Report for the Canadian Steel Industries Council, McMaster University, Hamilton, Ontario, 97 p.

Table 1: Summary of dance test results

Type of Dance	Prominent Forcing Frequency of Dance Activity	Relative Spectral Magnitudes *		Average Continuous Accelerations (%g)		Maximum Peak Accelerations (%g)		Approx. Number of Couples Dancing	Remarks **
		Forced Response Component	5.0 Hz Component	Components below 25 Hz	Components below 6.5 Hz	Components below 25 Hz	Components below 6.5 Hz		
Fast Rock and Roll	3.3 6.6	1.00 0.22	0.34	2.0	1.6	4.4	3.0	30 - 35	vb
Fast Rock and Roll	2.9 5.8	0.80 0.45	0.15	1.8	1.6	3.4	2.7	25 - 30	vb
Moderate Rock and Roll	2.8 5.6	0.57 0.21	0.14	1.5	1.3	2.3	2.1	25	vb
Polka	2.2 4.4	0.36 0.22	0.04	0.9	0.7	1.6	1.3	20 - 25	b
Modern	3.1 4.7	0.29 0.18	0.07	1.0	0.7	1.8	1.4	25 - 30	b
Modern	2.6 5.2	0.26 0.18	0.11	0.6	0.5	1.0	0.8	30 - 35	a
Waltz	1.9 3.8 5.4	0.02 0.03 0.03	0.01	0.2	0.1	0.3	0.2	20	a
Waltz	none	----	0.04	0.3	0.2	0.4	0.3	25	a

* Provides an indication of the relative dynamic response at the predominant frequencies associated with the various rhythmic dance activities. The spectral magnitude of each component listed was normalized to the overall maximum value. (ie: one rock and roll component has a value of 1.0)

** vb - very bothersome, b - bothersome to some, a - acceptable

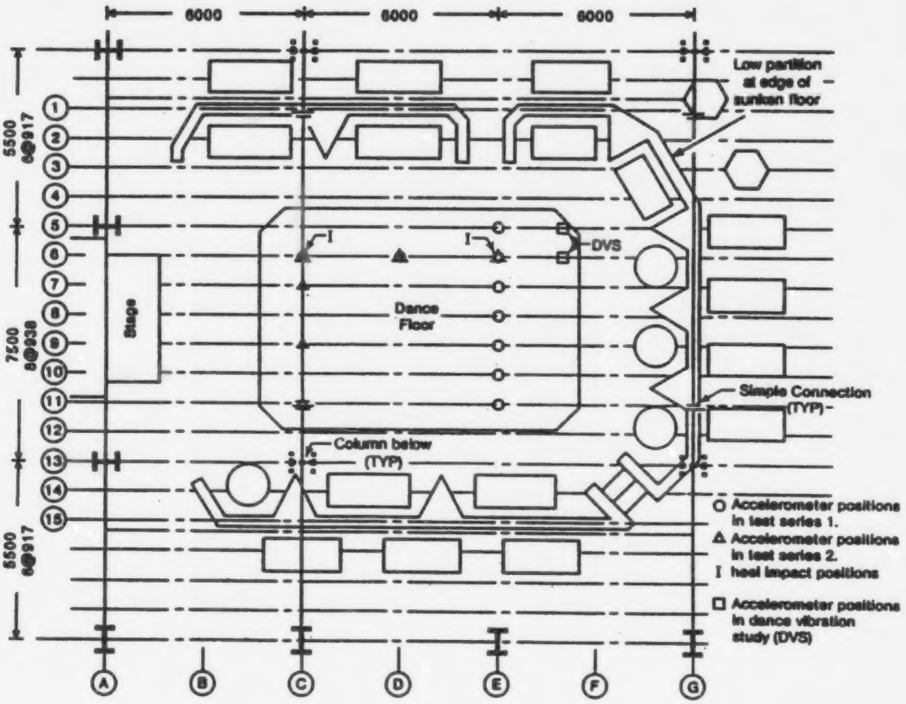
6000
6000
6000
Low partition at edge of sunken floor
5500
6@917
7500
8@938
5500
6@917
1
2
3
4
5
6
7
8
9
10
11
12
13
14
15
Stage
Dance Floor
I
I
DVS
Simple Connection (TYP)
Column below (TYP)
○ Accelerometer positions in test series 1.
△ Accelerometer positions in test series 2.
I heel impact positions
□ Accelerometer positions in dance vibration study (DVS)
A
B
C
D
E
F
G

Figure 1: Plan of sunken dance floor

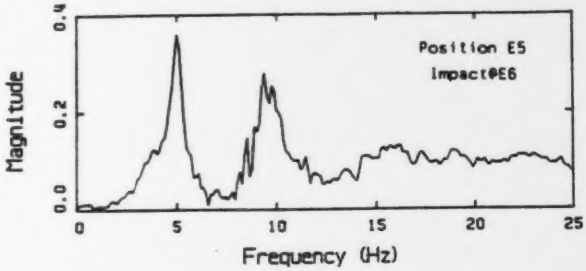

Figure 2: Frequency-magnitude spectra for heel impact

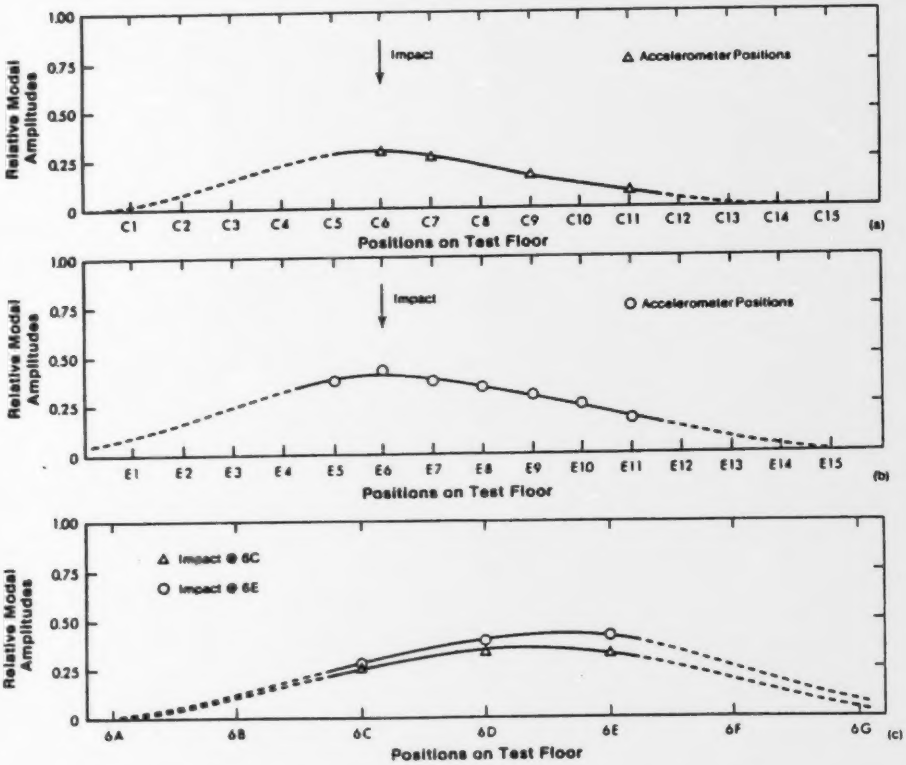

Figure 3: Response of floor in fundamental mode of vibration
(a) along line C, (b) along line E, (c) along line 6

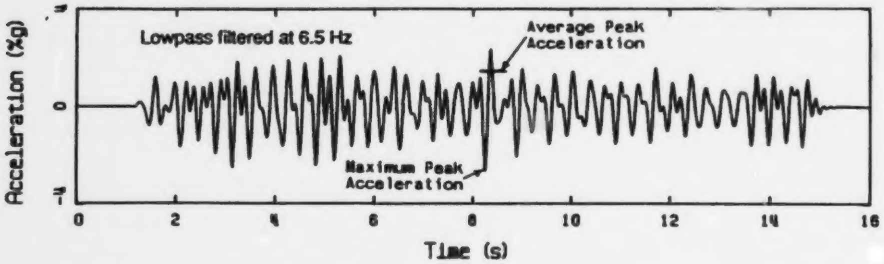

Figure 4: Typical filtered acceleration-time trace for a polka

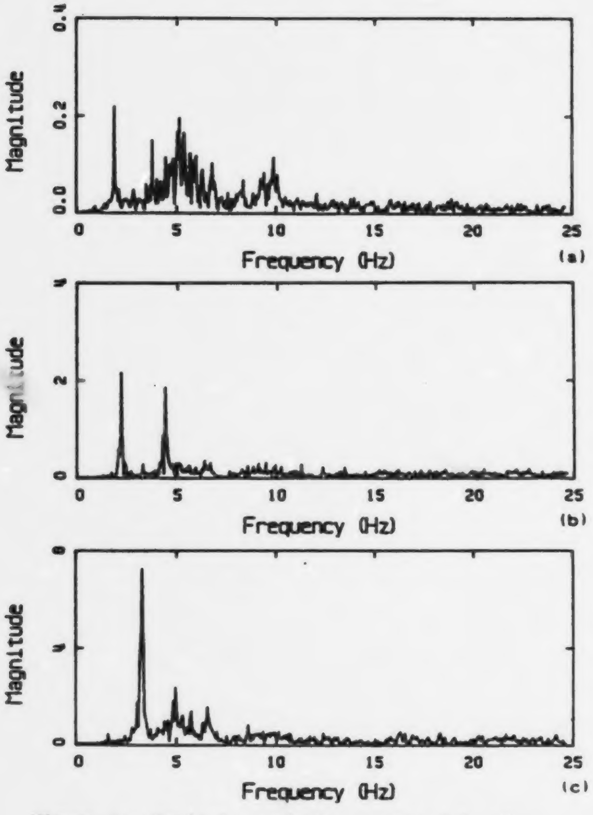

Figure 5: Typical magnitude spectra (a) waltz, (b) polka, (c) rock and roll

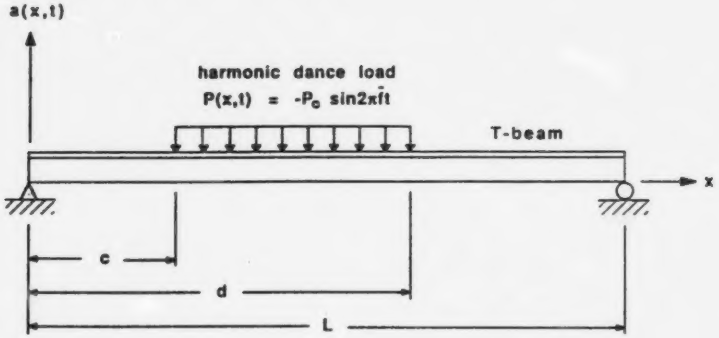

Figure 6: Dynamic model of floor system

SERVICEABILITY CALCULATIONS FOR TIMBER BUILDING COMPONENTS WITH MECHANICAL CONNECTIONS

Ian Smith and Ying Hei Chui

Department of Forest Engineering
University of New Brunswick, P. O. Box 4400
Fredericton, New Brunswick, Canada E3B 5A3

ABSTRACT

Timber buildings have traditionally been designed on an element by element basis to ensure that certain allowable stresses are not exceeded. In relatively recent times this has been replaced with element by element design to satisfy a range of limit states selected by the designer with guidance from an appropriate code or standard. For a majority of timber building components such an approach is inappropriate as several elements act together to form a load supporting system. Interaction between elements, e.g. between floor joists and attached sheathings, is normally achieved through mechanical (semi-rigid) connections. A rational ultimate or serviceability limit state design check requires focus on the system and account to be taken of interactions and complex support conditions. Analytical models capable of accounting for semi-rigid connections exist for common timber components such as walls, floors, and trusses. Unfortunately these models require information on load-deformation responses of connections which is not always well defined.

This paper examines the influence of inaccuracy in the specification of load-slip properties of fasteners such as nails, staples or bolts on serviceability calculations for timber components. Consideration extends to response under short-term "static" loadings, transient dynamic loadings and longer-term sustained loadings, but is restricted to connections producing lateral loads on fasteners. It is shown that distribution of loads on components, in time, and in space, can be critical with respect to attainable precision in serviceability calculations.

1. INTRODUCTION

It is traditional to design timber (wood) buildings on an element by element basis to ensure that certain allowable stresses are not exceeded. This neglects, for example, interactions between elements such as floor joists to support concentrated loads. 'Serviceability' is presumed for an element when it is loaded below its allowable stress level. In certain cases deflection limitations are superimposed on working stress checks, giving a rudimentary limit states design approach. Design calculations are confined to static or pseudo-static loading situations.

In relatively recent times there has been the introduction of partial coefficient limit states design codes for timber structures, (e.g. 2, 7). Calculations, at this stage, are on an element by element approach. For the heavier framed structures this provides a sound basis, which is in line with that for steel and reinforced concrete framed systems. Light-weight timber buildings are often of a constructional form which relies on interaction of elements and complex support conditions to provide 'resistance' to applied loadings, at the normal (working) level and at collapse, (5, 6). Semi-rigid mechanical joints are most often the means of making structural connections. This includes joints with nails, staples, punched metal truss plates, bolts and screws. An eventual aim in Canada and elsewhere (mid 1990's?) is to develop codes which specify distinct limit states appropriate to integral systems (components), such as a joisted floor or a trussed roof, as well as limit states appropriate to frame type arrangements.

If reliable checks are to be made to avoid designs which infringe a prescribed set of limit states (design criteria), there is need for reliable structural models, and for reliable materials properties data. This paper examines how sensitive serviceability calculations for light-weight wood systems are to variations in the load-slip characteristics of mechanical connections between elements of those systems. Knowing this gives a guide to code writers, who have to decide the degree of information that needs to be collected and specified, (13), and to designers who want to know the level of precision they are likely to attain in their design calculations.

2. LOAD-SLIP CHARACTERISTICS OF JOINTS

Load-slip characteristics are usually measured using joint specimens such as that shown in Figure 1 which apply lateral load only to the fastener(s). Slip is taken to be relative displacement of the outer and inner members, at the centroid of the fastener, or fastener group. Most often tests involve direct loading to failure, occasionally following some low level mono-directional load cycling, with times to failure in the order of 5 to 10 minutes, Figure 2a). This yields response characteristics applicable to fasteners in components not subject to load reversals. When load reversals occur, response characteristics such as those that can be found from Figure 2b) are more appropriate.

In serviceability calculations for wood systems it is normal to adopt a linear-elastic analysis technique, which is usually acceptable because non-linearity occurs at high load levels. Thus there has arisen the concept of an elastic slip modulus of a connection, k. (k = load per fastener per unit slip, N/mm). If fasteners are equally spaced at s, e.g. nails at 150 mm centres, we can further rationalize the connection parameter to; connection modulus = k/s (N/mm²). Figures 2a) and 2b) show slip moduli that might sensibly be used based on the observed load-slip responses in those diagrams. Numerically, $k_{initial}$ and k_{cyclic} are of the same order of magnitude. In this paper it is assumed, for simplicity, that $k_{initial} = k_{cyclic} = k$ when derived from tests of ten minutes duration or less.

Sustained load tests are used to find load-slip responses of connections under "long term" loads. The normal approach is to modify the "short term" slip by a factor, to convert to "long term" slip. Data defining a suitable factor is scarce, but Burgess (1) suggests that long term slip can be assumed to = 4.25 x short term slip for nailed joints. Long term here is vaguely defined, and means several months or years. A number of researchers are currently trying to characterise more precisely the rheological behaviour of mechanical wood joints.

Continuing on the theme of vibrational serviceability of the ply-web beam discussed above, a second serviceability criterion for vertical vibrations is also applied. As discussed in the paper by Chui and Smith (4) human response to floor vibrations is dependent upon the amplitude, rate of decay and frequency components of the vibration. Frequency weighted root-mean-square (r.m.s.) acceleration experience by a human observer is a parameter which can reliably account for all the factors influencing his perception. Using the calculation method developed by Smith and Chui (12) frequency weighted root-mean-square acceleration Ar is given in Figure 6 as a function of connection modulus. Estimation of Ar is associated with a heel-drop impact supplied by the man while standing at the mid-span position. The design impact has an amplitude of 500 N (for a 70 kg man) and a duration within the range 0.05 to 0.07s. The actual design impact duration used is the value which maximizes Ar. Examination of Figure 6 reveals first, that there is an impossible region corresponding to $f_o < 8$ Hz. Second, predictions of Ar are sensitive to connection modulus, in the vicinity of the reference value 18 N/mm². Apart from a calculation method for root-mean-square acceleration there is need for a scale against which to judge the serviceability of the structural system for which a prediction is being made. The work of Chui (3) suggests that for transient vibrations, of which the heel-drop impact is representative, root-mean-square accelerations in excess of 0.5 m/s² are unacceptable in the domestic environment to all observers. Clearly the nailed ply-web beam, which would satisfy other serviceability criteria addressed above, would not be acceptable according to this final measure.

Suppose the ply-web beam is retained as a component of a larger system which will, or so it is hoped, provide an acceptable level of root-mean-square acceleration under a heel-drop impact. Figure 7 shows the two new alternative systems investigated. Referring now to Figure 8, it is seen that a system with more than three ply-web beams is required to reduce Ar to an "acceptable" level. An important point to note is that for the largest (3 beam) system Ar is not particularly sensitive to variations in connection modulus in the region of $k/s = 18$ N/mm². Which is in stark contrast with observations for the smallest (1 beam) system.

To this point, emphasis here has been on serviceability of wood systems under live loadings. As an illustration, of sensitivity of serviceability calculations to connection moduli associated with long-term loadings, the single beam construction of Figure 3 is again used. For demonstration, consider a 4.2 m span and a permanently applied load of 1.0 kN/m. Table 1 compares mid-span displacement under a short term loading connection modulus $k/s = 18$ N/mm² with

Table 1
Comparison of mid-span displacements

Connection modulus (N/mm²)	long term loading			short term loading		
	3.36 (-20%)	4.2	5.04 (+20%)	14.4 (-20%)	18.0	21.6 (+20%)
Mid-span displacement (mm)	9.11	8.45	7.91	5.32	4.92	4.63
(relative value)	1.85	1.72	1.61	1.08	1.00	0.94

3. SENSITIVITY STUDIES

Examples based on the typical nailed ply-web beam construction shown in Figure 3 are used to illustrate the sensitivity of different measures of a wood system's serviceability to changes in connection modulus (k/s). The reference value k/s = 18 N/mm^2 used is typical for short term tests of the types represented in Figure 2. The relatively simple beam system possesses all of the essential attributes of more complex systems, such as two-way floors, trussed roof systems and diaphragm walls, in which fasteners are also subjected to lateral loads. The further reading list, referred to in the discussion section of this paper, broadens consideration to more complex systems.

Taking a 4.2 m span simply supported beam with a 70 kg man in the middle and using the theory by Smith (11), the static displacement under 'live' load varies as shown in Figure 4, as a function of connection modulus. Displacement due to the presence of the man is approximately 4 mm if there is no composite action between the wood flanges and the plywood webs, and approximately 0.75 mm if there is full composite action. Using the reference base k/s = 18 N/mm^2, connection modulus would have to change by an order of magnitude to significantly alter the predicted static displacement. The static displacement range for live load is from

$$\frac{1}{5660} \text{ to } \frac{1}{1060} \text{ x span.}$$

Mid-span displacement under the beam's dead weight is in the range

$$\frac{1}{22440} \text{ to } \frac{1}{4200} \text{ x span.}$$

Static displacements are clearly of an acceptable magnitude for human occupancy of buildings.

The fundamental natural frequency of a structural system is often estimated at the design stage when the dynamical response is likely to be a crucial factor. For example, a serviceability criterion in domestic environments for vertical vibrations is that the fundamental natural frequencies of floors are greater than 8 Hz. This avoids the 4 to 8 Hz. frequency band to which humans are sensitive, (8, 10). Figure 5 shows the relationship between fundamental frequency f_o and connection modulus for the ply-web beam used before*. The most obvious influence on f_o is not connection characteristics, but is the presence of the 70 kg man. His presence reduces the fundamental natural frequency by about 60%. Taking the case of the beam with a man as the governing design situation, the partial composite action generated by, for example, a nailing pattern with k/s = 18 N/mm^2 has shifted the beam response from an unacceptable f_o = 7.2 Hz. (no composite action) to an acceptable f_o = 12.6 Hz. Also, it is observed from Figure 5 that natural frequency predictions are only sensitive to fairly large variations in connection modulus.

---

* Calculations of f_o values are in accordance with the method described by Lenczner, (9).

that for a long term loading value k/s = 18/4.25 = 4.2 N/mm², (1). Also shown in Table 1 is the influence of ± 20% variations in k/s for each loading duration. Even with the neglect in calculations of factors such as stress redistribution and non-linearity of creep functions, this crude example enables a broad conclusion to be drawn. More reliable definitions of modification factors adjusting from short term slip to slip at other durations is a more pressing need than further refinement of the existing relatively good knowledge of short term response.

4. DISCUSSION

A number of sensitivity studies have been undertaken in recent years by the authors and co-workers to answer the same kind of questions addressed here, but for a broader range of, generally more complex, structural wood systems. The list of further reading at the end of this paper covers static and dynamic response of two-way floor systems and static response of diaphragm wall systems. This represents the two dominant classes of light-weight timber building components, those with out-of-plane displacements and those with in-plane displacements. Work on floors involved both experimental and numerical (finite element) investigations, while that on diaphragm walls was dominantly numerical (finite element) with a small amount of experimental validation of model predictions. From all of the work, some broad trends and conclusions have emerged.

Sensitivity to connection characteristics depends upon the size and complexity of structural system involved. As size and complexity increase the sensitivity reduces. The work by Devonport and Whale (FR4) on diaphragm walls indicates that displacement calculations for complex systems are relatively insensitive to connection characteristics both at low load levels, and at high load levels when some of the fasteners have begun to deform plastically. This presumes predominantly short term loads on diaphragm walls.

Especially for smaller less complex systems, such as the ply-web beam used in examples in this paper, serviceability can be sensitive to changes in connection characteristics. The important factor here is the distribution of loads on components, in time, and in space, with respect to attainable precision in serviceability calculations. As was shown here, a designer's choice of the range of serviceability criteria to be considered may well decide whether he realises that he is in fact dealing with a system (component) for which connection detailing is important.

5. CONCLUSIONS

From a designer's perspective, provided he has reliable analytical models and connection modulus data accurate to ±20%, or so, he can with confidence make predictions for the serviceability of timber building components. This extends across a range of static and dynamic serviceability criteria. From the perspective of code writers, there is adequate information to satisfy the needs of designers for checks associated with short term or transient loadings. There is a need for new information on connection behaviour under longer term loadings, so that code writers can provide the same quality of guidance in this instance as for other cases.

Overriding all of this is the need to provide a design code framework which provides designers with design criteria for light-weight integral systems, as well as those appropriate to frame type arrangements.

REFERENCES

1. BURGESS, H.J. 1980. Nail deformation data for design. International Council for Building Research Studies and Documentation Working Commission W18 - Timber Structures. Paper No. 13-7-6.

2. CANADIAN STANDARDS ASSOCIATION (CSA). 1984. Engineering design in wood (limit states design). CSA, Rexdale, Ontario, CAN 3-086.1-M84.

3. CHUI, Y.H. 1986. Vibrational performance of timber floors and the related human discomfort criteria. Journal of the Institute of Wood Science, 10, 5 (issue 59), pp. 183-188.

4. CHUI, Y.H. and SMITH, I. 1988. A serviceability criterion to avoid human discomfort for light-weight wooden floors. NRCC Symposium/Workshop on Serviceability of Buildings, University of Ottawa.

5. FOREST PRODUCTS RESEARCH SOCIETY (FPRS). 1979. Metal plate wood truss conference, 1979. FPRS, Madison, Wis, Proceedings P-79-28.

6. FPRS. 1983. Wall and floor systems: Design & performance of light-frame structures. FPRS, Madison, Wis, Proceedings 7317.

7. INTERNATIONAL COUNCIL FOR BUILDING RESEARCH STUDIES AND DOCUMENTATION (CIB). 1983. Structural timber design code. 6th Edition. CIB, Rotterdam, Publication 66.

8. INTERNATIONAL ORGANIZATION FOR STANDARDIZATION (ISO). 1978. Guide for the evaluation of human exposure to whole-body vibration. ISO, Geneva, Switzerland, Standard 2631.

9. LENCZNER, D. 1981. Movements in buildings. Pergamon Press, Oxford.

10. OHLSSON, S. 1982. Floor vibrations and human discomfort. Ph.D. Thesis, Chalmers University of Technology, Göteborg, pp. 6.11-6.19.

11. SMITH, I. 1980. Series type solutions for built-up timber beams with semi-rigid connections. Proceedings, Institution of Civil Engineers Part 2. 69, pp. 707-719.

12. SMITH, I. and CHUI, Y.H. Design of light-weight wooden floors to avoid human discomfort. Paper accepted for publication in the Canadian Journal of Civil Engineering, (In press).

13. WHALE, L.R.J., SMITH, I. and LARSEN, H.J. 1987. Design of nailed and bolted joints - proposal for the revision of existing formulae in draft Eurocode 5 and the CIB Code. CIB-W18-Timber Structures. Paper No. 20-7-1.

FURTHER READING

FR1. CHUI, Y.H. 1985. Sensitivity of statically loaded light-weight wooden floors to changes in construction variables. Timber Research and Development Association, United Kingdom (TRADA), Hughenden Valley, Research Report 7/85.

FR2. CHUI, Y.H. 1986. Evaluation of vibrational performance of light-weight wooden floors: Determination of effects of changes in construction variables on vibrational characteristics. TRADA, Hughenden Valley, Research Report 2/86.

FR3. CHUI, Y.H. 1986. Design aspects of floor vibration. TRADA, Hughenden Valley, Final Project Report PIF No. TRADA3.

FR4. DEVONPORT, I. and WHALE, L.R.J. 1984. Sensitivity studies on the influence of joint characteristics on load deformation relationships in timber shear walls. Paper presented to International Union of Forestry Research Organizations Timber Engineering Group, Xalapa, Mexico, December.

FR5. SMITH, I., METTEM, C.J. and DEVONPORT, I. 1984. Towards a rational design of timber structures with mechanical joints. Proceedings of 12th Congress of International Association for Bridge and Structural Engineering, Vancouver, pp. 985-990.

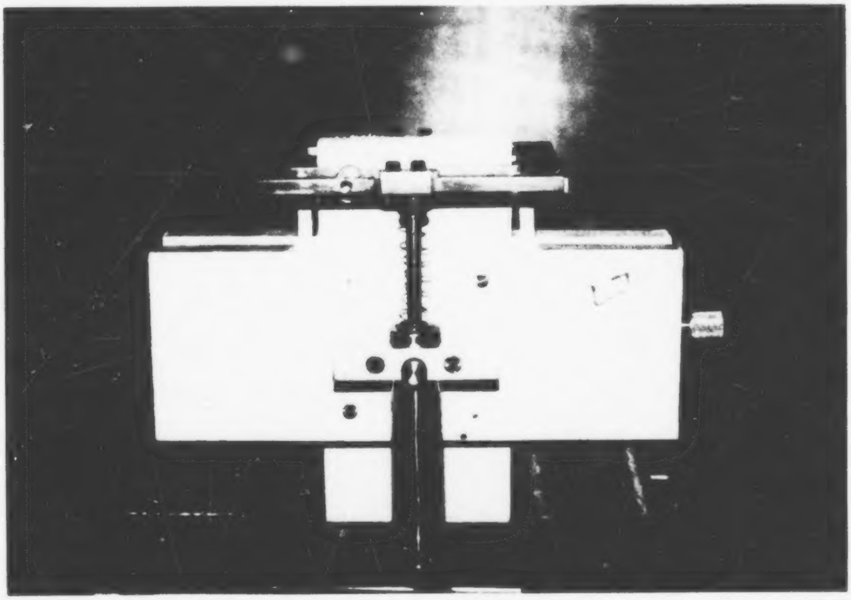

Figure 1. Typical nailed joint specimen

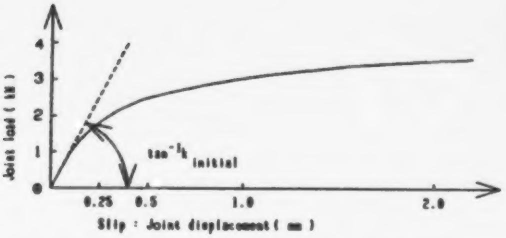

a) Typical response for direct loading to failure at displacement-rate of 2.5 mm/min.

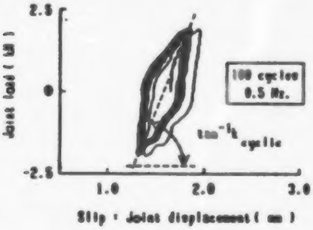

b) Typical response for cyclic loading at the working load level

Figure 2. Shapes of load-slip relationships

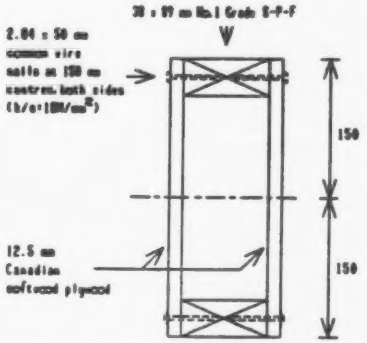

Figure 3. Nailed ply-web beam used in examples

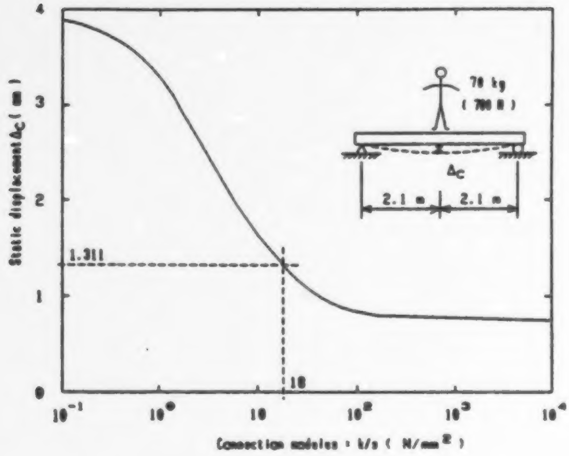

Figure 4. Static displacement - Nailed ply-web beam

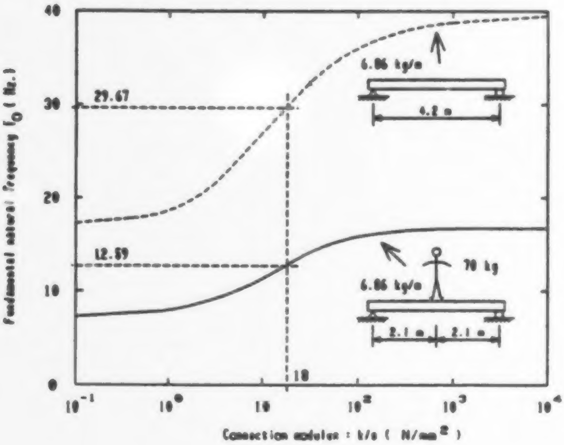

Figure 5. Fundamental natural frequency - Nailed ply-web beam

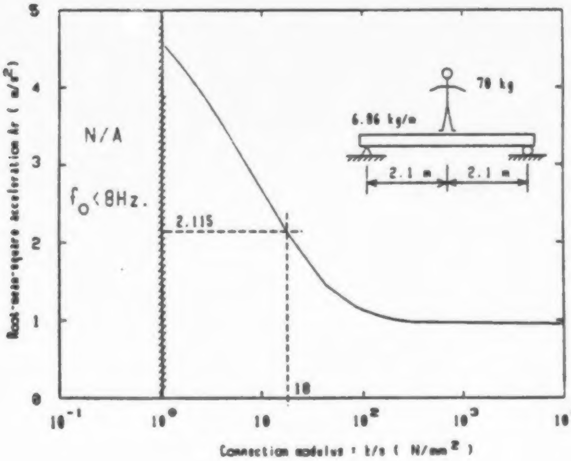

Figure 6. Root-mean-square acceleration - Nailed ply-web beam

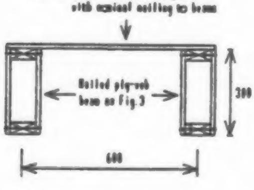
10.5 mm Canadian softwood plywood
with nominal nailing to beams
Nailed ply-web
beam as Fig.3
300
600

a) Two beam detail

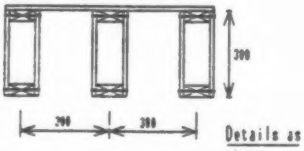

b) Three beam detail

Figure 7. Multi beam nailed ply-web systems

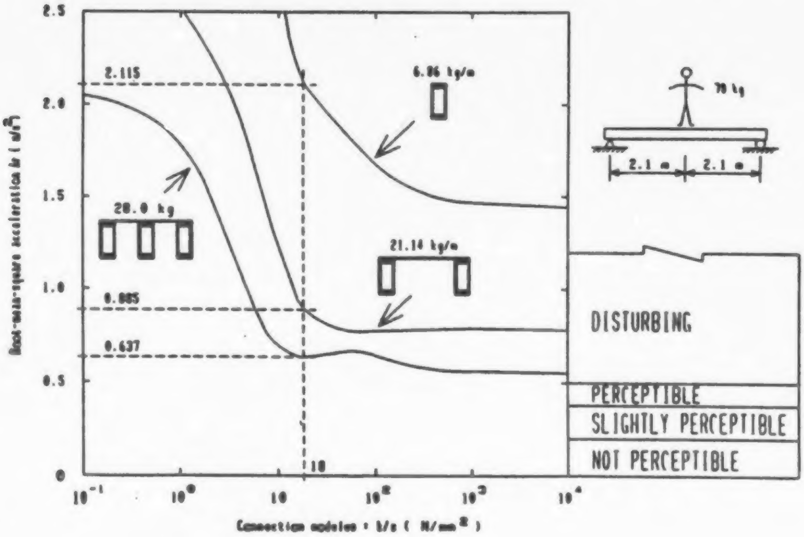

Figure 8. Root-mean-square acceleration - Multi beam nailed ply-web systems

AN AUTOMATED APPROACH TO FLOOR VIBRATION ANALYSIS

Raed A. Tolaymat

LeMessurier Consultants
Cambridge, Massachusetts, USA

ABSTRACT: A computer program is developed to calculate the response history of a floor system excited by any time-dependent force. Behavior under forces other than the standard heel-drop impact can be studied. The new program is used to analyze the behavior of 96 already-built floor systems. Based on the analysis results, a new acceptability requirement is established.

1. INTRODUCTION

Available vibration analysis methods deal with floor system's response under either transient or steady-state impulse loading independently. The results obtained from three such methods (Wiss-Parmelee R Rating factor, Reiher-Miester Scale and Murray's Acceptability Criterion) have a great deal of variation and are frequently in direct contradiction with field results of constructed floor systems.

A major cause of this variation and unreliability is the way these methods were developed, namely, statistical best-fitting of accumulated data. The methods are also limited in that none of them consider the effect of multiple heel-drops applied at certain intervals to a floor system, which is a more accurate representation of a person walking across a floor.

2. DEVELOPMENT OF NEW ANALYSIS PROCEDURE

A computer program is developed to calculate the dynamic response of a damped single-degree-of-freedom oscillator, using Duhamel integral[4]. The integral is calculated numerically.

The program calculates the response of the simple damped system excited by any time-dependent piecewise-linear external force. By using this program to study floor system's behavior, it was possible to:

1) Apply the exact heel-drop impact as was measured by Omhart instead of the approximate forcing function which has been used to date[2], (see Figure 1(a)).

2) Study the response history of a floor system due to consecutive heel-drops applied at equal time intervals, see figure 1(b).

3) Study floor systems behavior under exciting forces other than the standard heel-drop impact. For example, the response of a floor system in a health club or a ballroom can be evaluated under the impact of a person jogging, doing aerobics, or dancing.

3.TEST RESULTS

A summary of test results made on 96 already-built steel joist- and steel beam-concrete slab floor systems is reported in Reference [3]. A rating was assigned ,by Murray, to each system, acceptable=A or unacceptable=U, based on reported subjective evaluation by owners, occupants and researchers.
Tolaymat, based on the reported frequency and initial amplitude, calculated stiffness and mass of each system. Then, using mass, stiffness, available damping and heel-drop impact similar to that shown in Fig.1(b), re-analyzed all 96 tests using the program described above. The analysis results are listed in Table 1(a).

4.DISCUSSION

45 of the 49 tests that were rated acceptable, by subjective evaluation, satisfy either one or both of the following conditions:

1) $\frac{A_2}{A_1} \leq 1.15$ with $A_{max} \leq 0.05$ in.

2) Rieher-Meister scale rating for F and Amax falls within the slightly perceptible range (Amax.F < 0.05).

On the other hand, 43 of the 47 tests that were rated unacceptable do not satisfy either one of the two conditions mentioned above.

This leads to the conclusion that there are three different vibration categories under which any floor system behavior can be classified:

1) A system with adequate damping to reduce the initial impact amplitude by 85% or more before the second heel-drop is applied. Because the amplitude decays rapidly, only the initial impact will be felt. Such a system will always be acceptable regardless of the value of Amax.F.

2) A system with insufficient damping to reduce the initial impact amplitude by 85% before the second heel-drop is applied, but Amax.F < 0.050. In this system, vibration will be felt but it will be within the slightly perceptible range. Hence, the floor will still be acceptable.

3) A system with insufficient damping to reduce the initial impact amplitude by 85% before the second heel drop is applied, with Amax.F > 0.050. In this system, vibration will be felt and it will be within the distinctly or strongly perceptible ranges. Hence, the floor will be unacceptable.

Ratings using the three methods mentioned above as well as ratings using the new categories discussed above are compared to the available subjective ratings for all 96 floor systems. A (*) is assigned to each method when its rating does not agree with the field subjective rating. This comparison is shown in Table 1(b).

5. CONCLUSIONS AND RECOMMENDATIONS

Based on lowest natural frequency and available damping, floor systems are clasified under 3 different categories:

1) Systems that dissipate 85% or more of the heel-drop impact energy within (0.6-0.75) second. Humans do not perceive motion in such systems as annoying vibration regardless of the magnitude, because such motions decay rapidly.

2) Systems that do not dissipate impact energy quickly. But the magnitude and frequency of the motion are such that humans perceive it as slight acceptable vibration.

3) Systems that do not dissipate impact energy quickly. Also, the magnitude and frequency of the motion are such that humans perceive it as distinct annoying vibration.

On the other hand, the computer program developed is somewhat simple, and can be installed on a small personal computer when available. This program provides the designer with the flexibility to study a system's behavior, when desired, under exciting forces other than the standard heel-drop impact. In such cases,The exciting force frequency and magnitude as well as perceptibility threshold would be different.

Table 1(a). Test data and new method results.

		FREQUENCY (cps)		AMPLITUDE (in)			EVALUATION		
No.	DAMP	F	f	A1	A2	Amax	A2/A1	Amax.F	Rating
1a	2.0	4.0	1.38	0.007	0.011	0.014	1.593	0.054	U
2a	1.4	4.7	1.66	0.029	0.051	0.105	1.760	0.492	U
3a	10.4	10.6	1.52	0.040	0.040	0.040	1.010	0.424	A
4a	12.3	8.3	1.38	0.004	0.004	0.004	1.003	0.032	A
5a	4.1	12.5	1.39	0.005	0.005	0.005	1.092	0.064	A
1	9.4	5.6	1.40	0.015	0.016	0.016	1.093	0.092	A
2	10.9	5.9	1.47	0.016	0.016	0.016	1.060	0.097	A
3	9.2	6.0	1.50	0.010	0.011	0.011	1.095	0.067	A
4	8.0	9.0	1.50	0.015	0.016	0.016	1.048	0.141	A
5	10.2	10.0	1.43	0.012	0.012	0.012	1.010	0.118	A
6	10.0	10.0	1.43	0.012	0.012	0.012	1.000	0.120	A
7	8.7	9.3	1.55	0.013	0.014	0.014	1.028	0.127	A
8	7.1	9.8	1.40	0.012	0.013	0.013	1.043	0.123	A
9	9.2	9.1	1.52	0.005	0.005	0.005	1.031	0.046	A
10	10.9	11.1	1.59	0.019	0.019	0.019	1.000	0.212	A
11	8.3	5.9	1.47	0.015	0.017	0.017	1.116	0.100	A
12	10.5	5.6	1.40	0.014	0.015	0.015	1.070	0.083	A
13	9.4	5.6	1.40	0.016	0.017	0.017	1.093	0.097	A
14	7.3	9.1	1.52	0.011	0.011	0.011	1.063	0.101	A
15	10.2	8.3	1.38	0.011	0.011	0.011	1.021	0.089	A
16	13.0	3.6	1.67	0.008	0.009	0.009	1.134	0.034	A
17	5.0	4.9	1.64	0.020	0.028	0.033	1.385	0.160	U
18	3.0	7.5	1.50	0.009	0.012	0.014	1.387	0.105	U
19	8.0	7.5	1.50	0.012	0.013	0.013	1.079	0.099	A
20	3.0	8.8	1.47	0.018	0.023	0.026	1.319	0.226	U
21	6.0	6.0	1.50	0.014	0.016	0.017	1.211	0.104	U
22	5.0	9.0	1.50	0.015	0.017	0.017	1.152	0.153	U
23	6.0	5.5	1.38	0.018	0.022	0.023	1.217	0.129	U
24	2.5	2.7	1.38	0.017	0.029	0.048	1.707	0.130	A
25	7.0	8.0	1.60	0.011	0.012	0.012	1.104	0.098	U
26	9.4	7.7	1.54	0.007	0.007	0.007	1.052	0.056	A
27	11.7	6.3	1.57	0.007	0.008	0.008	1.051	0.048	A
28	8.0	4.6	1.54	0.006	0.007	0.007	1.219	0.034	A
29	7.9	9.9	1.65	0.005	0.005	0.005	1.048	0.053	A
30	8.2	7.5	1.50	0.005	0.006	0.006	1.074	0.042	A
31	8.9	7.1	1.42	0.004	0.004	0.004	1.060	0.030	A
32	11.1	7.5	1.50	0.005	0.006	0.006	1.029	0.042	A
33	4.1	12.5	1.39	0.006	0.007	0.007	1.092	0.083	A
34	9.0	7.5	1.50	0.009	0.010	0.009	1.057	0.071	A
35	8.0	10.8	1.54	0.006	0.006	0.006	1.029	0.069	A
36	14.0	13.4	1.49	0.005	0.005	0.005	1.000	0.066	A
37	7.1	12.5	1.39	0.007	0.007	0.007	1.016	0.086	A
38	7.6	15.2	1.38	0.009	0.009	0.009	1.000	0.134	A
39	4.1	8.0	1.60	0.004	0.006	0.006	1.276	0.048	A
40	12.8	8.3	1.38	0.004	0.004	0.004	1.000	0.032	A
41	6.8	9.0	1.40	0.005	0.005	0.005	1.049	0.047	A
42	10.1	7.2	1.44	0.004	0.004	0.004	1.041	0.028	A
43	6.4	6.9	1.38	0.004	0.004	0.004	1.129	0.028	A
44	2.0	6.7	1.67	0.020	0.032	0.048	1.605	0.324	U
45	2.0	5.0	1.67	0.009	0.015	0.027	1.686	0.134	U
46	13.0	4.2	1.40	0.002	0.002	0.002	1.079	0.010	A
47	2.0	5.1	1.67	0.004	0.007	0.010	1.657	0.051	U

cont'd.

Table 1(a). Cont'd.

48	8.0	6.0	1.50	0.014	0.015	0.016	1.127	0.094	U
49	3.9	5.5	1.38	0.010	0.014	0.016	1.370	0.090	A
50	3.9	6.0	1.50	0.012	0.017	0.019	1.375	0.116	A
51	4.0	5.0	1.67	0.018	0.026	0.033	1.470	0.165	U
52	1.7	5.3	1.38	0.006	0.008	0.008	1.461	0.045	U
53	11.6	6.0	1.50	0.002	0.002	0.002	1.059	0.012	A
54	8.0	7.5	1.50	0.002	0.002	0.002	1.079	0.013	A
55	5.0	6.0	1.50	0.004	0.006	0.006	1.285	0.036	A
56	3.0	4.5	1.50	0.002	0.004	0.005	1.565	0.023	A
57	3.0	5.0	1.67	0.004	0.006	0.009	1.568	0.044	U
58	0.0	5.6	1.40	0.009	0.018	0.053	1.995	0.297	U
59	0.7	5.2	1.67	0.006	0.011	0.014	1.746	0.072	U
60	2.1	4.1	1.38	0.007	0.011	0.018	1.668	0.075	U
61	1.7	4.0	1.38	0.007	0.012	0.015	1.628	0.060	U
62	0.4	4.1	1.38	0.009	0.016	0.041	1.919	0.168	U
63	0.9	4.1	1.38	0.006	0.011	0.024	1.837	0.100	U
64	4.0	4.2	1.40	0.008	0.011	0.014	1.470	0.061	U
65	0.4	7.9	1.57	0.010	0.019	0.049	1.859	0.308	U
66	1.6	10.4	1.48	0.007	0.010	0.013	1.489	0.137	U
67	0.0	11.9	1.49	0.008	0.015	0.044	1.959	0.520	U
68	0.0	8.5	1.42	0.009	0.017	0.053	1.985	0.448	U
69	0.5	7.9	1.57	0.006	0.011	0.027	1.832	0.213	U
70	2.7	7.6	1.52	0.010	0.014	0.016	1.426	0.124	U
71	0.0	7.8	1.56	0.009	0.016	0.033	1.778	0.260	U
72	1.5	5.7	1.43	0.004	0.007	0.012	1.682	0.066	U
73	1.2	5.6	1.40	0.005	0.009	0.016	1.741	0.092	U
74	5.3	7.4	1.48	0.006	0.008	0.008	1.188	0.058	A
75	0.8	7.4	1.48	0.007	0.012	0.024	1.776	0.181	U
76	0.0	7.3	1.46	0.005	0.010	0.031	1.993	0.229	U
77	2.6	8.1	1.63	0.008	0.011	0.014	1.444	0.111	U
78	2.3	5.5	1.38	0.022	0.034	0.049	1.583	0.267	U
79	2.9	5.4	1.38	0.027	0.039	0.044	1.426	0.236	U
80	3.5	5.9	1.47	0.021	0.029	0.036	1.400	0.210	U
81	4.2	9.7	1.61	0.023	0.028	0.029	1.284	0.278	U
82	6.0	7.9	1.57	0.055	0.061	0.062	1.108	0.487	U
83	5.5	9.1	1.52	0.059	0.066	0.067	1.125	0.612	U
84	2.7	6.6	1.65	0.025	0.030	0.050	1.506	0.328	U
85	0.0	6.8	1.38	0.025	0.049	0.111	1.952	0.754	U
86	2.3	6.8	1.38	0.018	0.026	0.030	1.446	0.207	U
87	2.4	6.9	1.38	0.013	0.019	0.024	1.457	0.166	U
88	1.4	4.7	1.56	0.029	0.051	0.105	1.768	0.493	U
89	5.2	6.3	1.57	0.025	0.032	0.034	1.270	0.214	U
90	4.5	10.6	1.52	0.018	0.020	0.021	1.135	0.220	A
91	4.6	10.6	1.52	0.009	0.010	0.010	1.129	0.110	A

Damp = System available damping (% of critical damping)
F = System frequency (cps)
f = Heel drop frequency applied (cps)
A1 = First heel drop maximum amplitude (in.)
A2 = Second heel drop maximum amplitude (in.)
Amax = Absolute maximum heel drop amplitude (in.)
Rating = Owner/User subjective evaluation of floor system
(A = acceptable , U = unacceptable)
(c) - As reported in Reference [3], table 1.
- All other systems reported in Reference [3], table 2.

Table 1(b).Comparison of available and new method results to field ratings.

No.	R	R-M	MUR	NEW
1a		•		
2a				
3a	•	•	•	
4a				
5a	•	•	•	
1	•	•		
2	•	•		
3	•	•		
4	•	•		
5	•	•		
6	•	•		
7	•	•		
8	•	•		
9	•	•		
10	•	•	•	
11	•	•		
12	•	•		
13	•	•		
14	•	•		
15	•	•		
16				
17				
18				
19	•	•		
20				
21			•	
22				
23				
24	•	•	•	•
25			•	•
26	•	•		
27	•	•		
28				
29	•	•		
30	•			
31				
32	•			
33	•	•	•	
34	•	•		
35	•	•		
36	•	•		
37	•	•		
38	•	•		
39	•			
40				
41	•			
42				
43				
44				
45		•		
46				
47	•	•		
48			•	•
49	•	•	•	•
50	•	•	•	•
51				
52		•		•
53				
54				
55				
56				
57	•	•		•
58				
59		•		
60		•		
61		•		
62		•		
63		•		
64		•	•	
65				
66				
67				
68				
69		•		
70				
71				
72	•	•		
73		•		
74	•	•		•
75				
76		•		
77				
78				
79				
80				
81				
82				
83				
84				
85				
86				
87				
88				
89				
90	•	•	•	
91	•	•	•	

(R) = Wiss-Parmelee Rating Factor.
(R-M) = Modified Reiher-Meister Scale.
(MUR) = Murray Acceptability Criterion.
(NEW) = New Evaluation Method.
(•) - Indicates method does not agree with field rating.
(a) - As reported in Ref.[3], Table 1.
- All other systems reported in Ref.[illegible], Table 2.

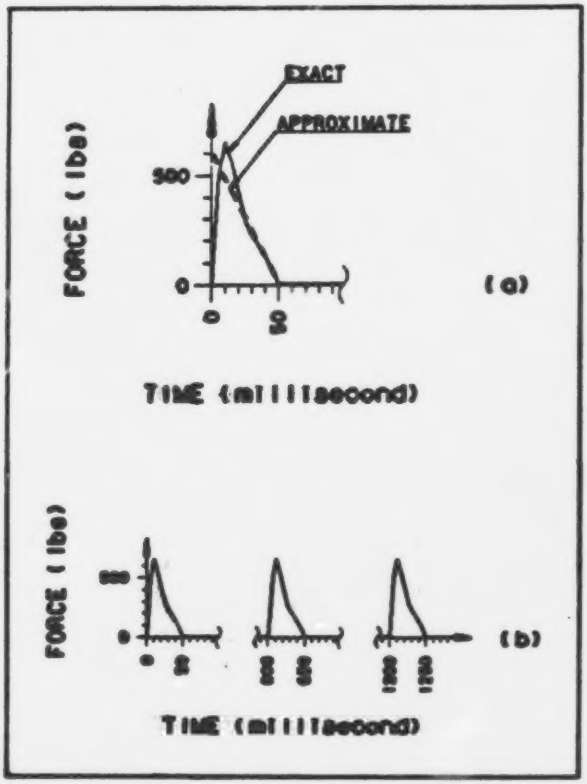

Fig. 1 Comparison of exact and approximate heel-drop impact histories of available and new methods.

REFERENCES

1. Galambos, Theodore V., Vibration of Steel-Joist-Concrete Slab Floors, Technical Digest No. 5, Steel Joist Institute, Arlington, Virginia, p. 20-21.

2. Murray, Thomas M., Design to Prevent Floor Vibrations, Engineering Journal, American Institute of Steel Construction, Vol. 12, No. 3, 1975.

3. Murray, Thomas M., Acceptability Criterion for Occupant-Induced Floor Vibrations, Engineering Journal, American Institute of Steel Construction, Vol. 18, No. 2, 1981.

4. Paz, Mario, Structural Dynamics-Theory and Computation, Van Nostrand Reinhold Book Company, New York, 1980, p. 28, 378-380.

5. Wright, Richard N. and Walker, William H., Vibration and Deflection of Steel Bridges, Engineering Journal, American Institute of Steel Construction, Vol. 9, No. 1, 1972.

DYNAMIC RESPONSE OF FLOORS DUE TO PEOPLE IN MOTION

J.H. Rainer, D.E. Allen, and G. Pernica
Institute for Research in Construction
National Research Council of Canada, Ottawa, Ontario

ABSTRACT: The interaction between the supporting structure and the dynamic forces generated by people in motion is presented. The dynamic loading from people activities such as walking, running, jumping, etc. is described by means of dynamic load factors at harmonics of the step frequency. Dynamic load factors are presented for a range of activity rates. The dynamic response of floor structures to such loading is briefly discussed and design guidelines for floors are given.

1. INTRODUCTION

When people walk, run, jump, dance or move about in other ways, they exert vertical as well as horizontal forces on supporting elements. Occasionally these supporting elements, such as floors or walkways, will vibrate at amplitudes unacceptable either to the occupants or for the intended use of the building. To avoid these types of problems or to alleviate existing ones, it is important to understand the dynamic loading and the resulting structural response.

This paper describes the vertical dynamic loading arising from typical human activities in the low frequency range (up to 10 Hz) and gives design guidance based on dynamic structural response.

2. DYNAMIC LOADING

The dynamic forces generated by human activities can be measured by means of instrumented force platforms. While some investigators have used small platforms that measure the force from one or two steps, at the Institute for Research in Construction (IRC) a 17 m long floor strip shown in Figure 1 was employed so that the entire force history of a walker or runner could be determined (Rainer and Pernica 1986). This avoided the difficulties and errors that arise in sequencing isolated pulses from individual steps.

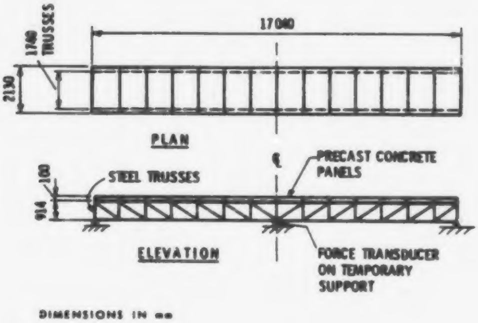

Figure 1: Instrumented floor strip

Figure 2 shows the dynamic reaction at the mid-support of the floor strip due to a person walking along it. The reaction is represented by both its time record and its Fourier spectrum determined by Fourier analysis of the time record. Note that the Fourier spectrum contains large spikes at multiples of the step frequency.

A person walking, running or jumping imparts a sequence of step forces to the floor. Each step force for an activity is nearly the same in magnitude and shape and for a given step rate recurs at equal time intervals. The forcing functions for the activities are therefore essentially periodic and can be represented by a Fourier series of the following type:

$$F(t) = P[1 + \Sigma\alpha_n \sin(2\pi nft + \phi_n)] \qquad (1)$$

where P = weight of the person;
α_n = amplitude of the n-th harmonic as a ratio of the person's weight, called "dynamic load factor";
f = activity rate, steps per second;
ϕ_n = phase angle of n-th harmonic.

This representation separates the load into static and dynamic components. The dynamic component is represented by the summation term and consists of sinusoids having amplitudes $\alpha_n P$ at frequencies f, 2f, 3f... These harmonic components can be seen in the spectra of the force-time record shown in Figure 2.

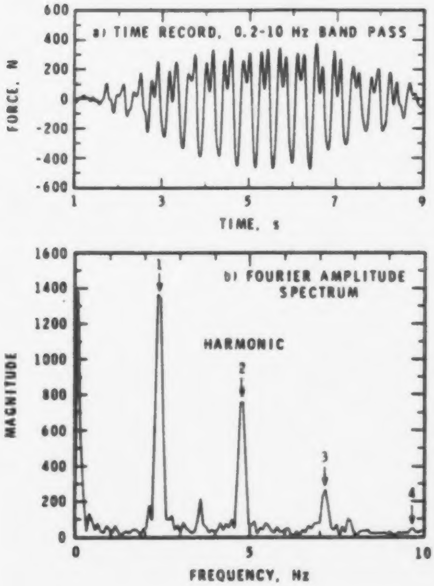

Figure 2: Dynamic forces from walking at 2.4 steps per second

A number of walking, running and jumping tests were carried out on the floor strip to determine the dynamic load factors of the harmonic components as functions of activity rate. Averaged factors for several participants performing each activity individually are shown in Figs. 3, 4 and 5 for walking, running and jumping, respectively (Rainer et al. 1986). Figures 3 to 5 show that the dynamic load factors of the three activities vary substantially with activity rate. For walking, the dynamic component of the first harmonic, α_1, reaches 0.5 times the person's weight while for jumping it reaches a value of 1.7.

The dynamic load factors in Figs. 3 to 5 are for one person. Groups of people walking, running or jumping in unison also create dynamic loading functions described by Equation (1). Because of lack of perfect coherence between individual step forces, the dynamic load factors (applied to the weight of the group) decrease in relation to those for one person as the harmonic, n, increases. Some information on dynamic load factors for a small group of people is given by Allen et al. (1985), but more information based on tests of large groups of people is required.

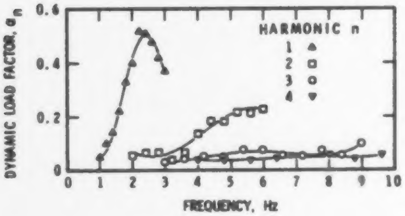

Figure 3: Averaged dynamic load factors for walking

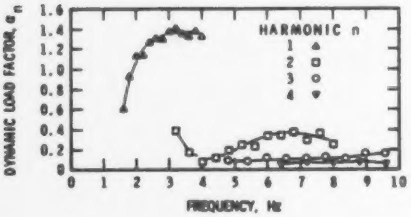

Figure 4: Averaged dynamic load factors for running

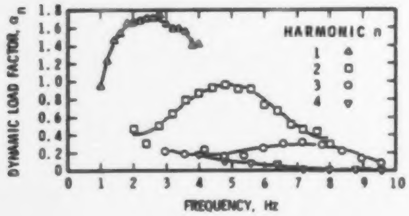

Figure 5: Averaged dynamic load factors for jumping

2.1 Common Ranges of Activity Rates: As dynamic load factors vary with activity rate, it is important to know the range over which activity rates commonly occur. These ranges are presented in Table 1 for five activities. Activity rates outside these ranges may occur, but are generally infrequent.

Table 1: Common ranges of activity rates

Activity	Common Activity Rate f, Steps per second
Walking	1.7 - 2.3
Running	2.0 - 3.5
Jumping	1.8 - 3.0
Exercising	2.0 - 3.0
Dancing	1.9 - 3.3

Figures 3 to 5 show that the common ranges for running and jumping coincide with the frequency range of maximum dynamic load factors. For walking, the frequency range of maximum dynamic load factors, 2.0 - 2.8 Hz, encompasses only the faster rates in the common range, i.e. 2.0 - 2.3 Hz.

3. DYNAMIC RESPONSE OF FLOOR STRUCTURES

Floors support people engaged in a variety of activities: ordinary floors are subject to walking, gymnasium floors to jumping, running and exercising, and dance floors to jumping and dancing.

Floor structures possess natural modes of vibration, characterized by mode shapes, modal frequencies and modal damping ratios. When one of the modal frequencies coincides with a step frequency or its second or third harmonic, excessive vibration amplitudes can result (Pernica 1983, Bachmann 1984). When an activity is performed by a large number of people, the floor can also be set in motion by simple repetitive forcing even when the natural frequency of the structure differs from the forcing frequency. Both the resonant and non-resonant conditions are encompassed by the design recommendations presented by Allen, Rainer and Pernica (1985, 1987) and Commentary A of the National Building Code of Canada (NBCC 1985). The following summarizes the main principles.

Consider a person jumping at mid-span of a simply-supported platform or floor. Assume that resonance occurs at a harmonic of the step frequency, i.e. $nf = f_0$, where f_0 is a modal frequency of the floor. The acceleration response of the floor at resonance is determined from the steady-state solution (Allen et al. 1987):

$$a_{peak}/g = \frac{1}{2\beta} \cdot \frac{\alpha_n P}{W/2} \qquad (2)$$

where W is the weight of the floor platform and β is the damping ratio. Response to other harmonic loading components also occurs but the magnitude is much less.

For walking or running the step forces change location; so, a simple steady-state solution is not achieved as it is for jumping (see Rainer et al. 1986 for the solution for walking). A partial build-up towards steady-state resonance, however, does occur and this can be approximated by replacing the numerator 1 in Eq. 2 by a reduction factor R (Allen et al. 1987). Figure 6 shows the resonant effect at the second harmonic for a person walking at different step frequencies on the floor strip in Fig. 1 with the mid-support removed (Rainer et al. 1986).

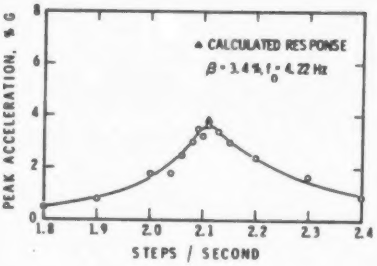

Figure 6: Dynamic response of a floor strip to walking at various rates

Harmonic resonance is a primary cause of annoying vibration (Allen et al. 1987) in long-span floors because long-span floors often have natural frequencies corresponding to the second, third or fourth harmonic of common walking step frequencies. It might be possible to avoid resonance by designing the floor so that the natural frequencies lie between or above the significant force harmonics, but in practice this is difficult to do. One is left with providing sufficient damping or mass to keep the resonant accelerations within limits that are acceptable to the use and occupancy of the building. Design criteria contained in Appendix G of CSA Standard S16.1 embody this requirement in a semi-empirical fashion based on heel impact response.

For a group of people jumping, the dynamic loading can be several orders of magnitude greater than for a person walking, particularly for the first and second harmonics. It is generally not possible to provide sufficient mass or damping to keep resonant vibrations within acceptable limits. One must therefore avoid resonance; the following restriction on natural frequency is recommended for design (Allen et al. 1985):

$$f_0 \geq nf\sqrt{1 + \frac{1.3}{a_0/g}\,\frac{\alpha_n w_p}{w_t}} \tag{3}$$

where w_p is the equivalent uniformly distributed weight of people, w_t is the total weight of the floor system including people and a_0/g is a criterion for limiting acceleration as a fraction of gravity. In the past problems associated with people jumping on floors were caused by the first or second harmonic. Recently, however, a problem involving the third harmonic of jumping arose on a floor of mixed occupancy.

Rhythmic activities such as people foot stamping in assembly halls, stadia and arenas, are similar to jumping exercises. Although the force generated per person is considerably less than for jumping, the people are closer together and can therefore induce large resonant vibrations, particularly at the first harmonic (Pernica 1983). However, more information is needed on the dynamic load factors for foot stamping by large groups of people.

4. SUMMARY

Dynamic loading caused by people walking, running and jumping can be adequately described by dynamic load factors at harmonics of the step frequency. Such factors are presented for a wide range of activity rates. The dynamic response of floors to such loading is described in terms of resonance, the main cause of annoying vibrations in long-span floors. Design criteria either recommend the reduction of resonant vibration by increasing the damping or mass, as for walking, or the avoidance of resonant vibration, as for jumping or foot stamping by a large group of people.

ACKNOWLEDGEMENT

This paper is a contribution from the Institute for Research in Construction, National Research Council of Canada.

REFERENCES

Allen, D.E., Rainer, J.H., and Pernica, G. 1985. Vibration criteria for assembly occupancies. Canadian Journal of Civil Engineering 12(3), p. 617-623.

Allen, D.E., Rainer, J.H., and Pernica, G. 1987. Building vibrations due to human activities. Proceedings, ASCE Structures Congress, Orlando, Florida, p. 438-447.

Bachmann, H. 1984. Vibrations of building structures caused by human activities, case study of a gymnasium. National Research Council of Canada, Ottawa, Ontario, Technical Translation 2077.

Canadian Standards Association. 1984. Steel structures for buildings - limit states design, Appendix G: Guide on floor vibrations. CSA S16.1-1984, Rexdale, Ontario.

National Building Code of Canada 1985. Supplement 1, Commentary A: Serviceability criteria for deflections and vibrations. National Research Council of Canada, Ottawa, Ontario, p. 146-152.

Pernica, G. 1983. Dynamic live loads at a rock concert. Canadian Journal of Civil Engineering 10(2), p. 185-191.

Rainer, J.H. and Pernica, G. 1986. Vertical dynamic forces from footsteps. Canadian Acoustics 14(2), p. 12-21.

Rainer, J.H., Pernica, G., and Allen, D.E. 1986. Dynamic loading and response of footbridges. Proceedings, CSCE Second International Conference on Short and Medium Span Bridges, Ottawa, Ontario, August 12-21, 1986, Vol. 2, p. 335-347.

SESSION F/SÉANCE F

GROUND-TRANSMITTED AND MACHINERY-INDUCED VIBRATIONS/ / VIBRATIONS CAUSÉES PAR LES MACHINES ET LES TRANSPORTS

CONTROL OF BUILDING VIBRATION FROM GROUND-BORNE EXCITATION

D.L. Allen, B. Howe
Vibron Limited
Mississauga, Canada

ABSTRACT: Control of building and structural element vibration from train and subway induced ground-borne excitation requires carefully conceived vibration control strategies. Ground vibration measurements at the building site will define the need for implementation of vibration control strategies.

Building foundation support design, vibration isolators, the design of the foundation walls/soil interface and the detailed design of building structural elements and their connections are all strategies which, when appropriately combined, can control building vibration within human response levels.

The paper will outline the conceptual design process for building vibration diagnosis and control and then discuss case histories and field observations, supported with data.

1. INTRODUCTION

Buildings founded near or over subways and/or train tracks are vulnerable to ground borne vibration which can be transmitted to the building structure. Such a structural vibration can create a perceivable vibration or a radiated noise which can be disturbing to occupants.

The successful control of building vibration and structurally radiated noise requires specific design of the foundation and building structural elements for adequate vibration mitigation. When building foundations alone cannot be designed to control ground borne vibration to an acceptable degree, vibration isolation may be necessary.

This presentation addresses the design concepts needed to control vibration transmission into the foundation and structure of multi-storey buildings with specific emphasis placed on building location, environmental factors, structural/foundation design and the possible necessity for vibration isolation.

2. ENVIRONMENTAL FACTORS

The degree to which ground borne vibration is transmitted to a structure is related to:

i) Rail type or subway tunnel, rail bed, train type, speed, number of cars.

ii) Height separation between the rail bed and the building foundation. Substructures can be beside or below building foundation. Train tracks can be on the same level or above the foundation.

iii) Soil type and its ability to transmit vibration from the point of excitation to the building foundation.

iv) Physical orientation of the building involving factors such as distance from the point of excitation, whether the building is founded on a subway structure, and the foundation geometric orientation with respect to the vibration excitation source.

Combinations of the above factors define the level of soil or subway structure vibration excitation input to the proposed building foundation. The strength of the source at the soil/foundation interface defines the need for vibration control measures and the degree to which vibration control is required. The building foundation type, wall and structural elements can often be conceived for adequate vibration control. Building vibration isolation may be necessary where structural design concepts cannot be chosen to provide adequate vibration reduction.

3. STRUCTURAL VIBRATION MITIGATION USING CONVENTIONAL FOUNDATION DESIGN CONCEPTS

Ground borne vibration from rail or subway tunnel excitation can have an impact upon a foundation through side walls or on the bottom of the foundation to a varying degree, depending upon whether the excitation is beside or below the foundation. Each source location has implications on the choice of building foundation types.

3.1 Foundation Transmission

When the ground borne excitation source is at or below the foundation supports, emphasis must be placed on the specific design of caissons, spread footings or possibly vibration isolation. Spread footings or caissons interfacing with and loaded on the soil can become springs which provide building isolation with respect to soil vibration. However, it is not the load on the column that provides vibration attenuation but it is the mass of the footing above the interface (i.e. blocking mass) which can provide optimum attenuation.

Often adequate vibration mitigation from an excitation at or below the foundation supports can be achieved by proper design of the caissons or spread footings alone.

3.2 Walls

A vibration excitation source beside or below a foundation can also transmit vibration into the foundation walls and structure to possibly propagate several storeys upward and cause an annoying structural vibration or radiated noise. Foundation wall vibration can also excite floor vibration modes which often fall within the frequency region of train/subway vibration excitation. As a result resonant modes can be amplified.

Foundation design for vibration mitigation requires thick walls facing the ground excitation, connected to thin floor slabs, creating an interface vibration impedance mismatch between the floor/wall elements. A better solution often dictates that the foundation wall adjacent to the ground excitation be disconnected from the structure by having independent interior columns near the wall to support the floor slabs. Vibration isolation between these columns and the disconnected foundation wall can support horizontal ground thrust loading while maintaining a superior structural impedance mismatch between the wall and the columns.

Interior shear walls close to a ground borne excitation from below can often transmit vibration upward unless similar floor/shear wall connections are designed with a structural impedance mismatch.

3.3 Interior Structural Design & Environmental Factors

Structural vibration diminishes with height above the excitation source. Often, the placement of noise insensitive occupancies such as parking and retail space closest to the foundation can be a good design strategy, provided the vibration/radiated noise levels are sufficiently low. Since structural vibration reduces with height, the design goal is then to reduce the vibration levels to an acceptable region at the first occupied office or residential floor.

Care must be taken to ensure that resonances are not excited to cause a floor to vibrate at a sufficiently high level to radiate an unacceptable noise on occupied floors. Structurally radiated sound, depending upon the building use, can be absorded in acoustically soft rooms whereas the same vibration level may be bothersome for acoustically hard rooms such as bathrooms and kitchens in residential buildings. Light drywall panels tend to amplify vibration levels compared to the base building structure and become a source of radiated noise. Drywall panels near high vibration levels on the structure, must be designed to minimize amplification.

4. VIBRATION ISOLATION

If environmental factors, foundation types and structural elements cannot be conceived and designed to reduce building vibration to an acceptable level then vibration isolation may need to be considered. Alternatively, it may be more cost effective to install vibration isolation rather than specific and sometimes extensive foundation design for vibration mitigation. If it is not feasible to have buffer zones of parking and retail space in a building then possibly vibration isolation might be required.

Even though a building may be isolated, structural elements must still be designed to minimize vibration amplification. Column footings require blocking masses. Even with vibration isolation, the foundation wall/floor interface requires structural element impedance mismatches as does shear wall/floor connections.

Vibration isolation pad design requires that each load point has the correct stiffness and deflection for sufficient vibration isolation. The isolator material must be designed to have adequate longevity.

5. OVERVIEW

There are many factors involved in building foundation design for ground borne vibration mitigation. Environmental factors, foundation structural element design and possibly vibration isolation are all strategies which can be applied toward providing a cost effective approach to the reduction of building vibration.

SWD CRITERIA FOR BUILDING DAMAGE FROM GROUND VIBRATIONS

R. Ciesielski, J. Kawecki, E. Maciag
Institute of Structural Mechanics, Technical University of Cracow
Cracow, Poland

ABSTRACT: This paper deals with admissible vibration levels of residential structures built of brick, blocks of light concrete, stone and slag concrete. Vibrations transmitted to the buildings from the ground originate from blasting in quarries, vehicle traffic (trucks, trains), driving of piles, etc. Admissible vibration levels for two categories of buildings were expressed by scales SWD-I and SWD-II. The scales were verified by means of vibration measurements on buildings.

1. INTRODUCTION

A number of countries have established standards or recommendations concerning estimation of action of paraseismic vibrations on buildings (4, 5, 6, 8, 11, 15, 17, 18, 20). Some of these standards have already been modified. The major part of these standards concerns vibrations from sources such as blasting in open coal mines, quarries, and construction blasting in the vicinity of buildings. Another group consists of scales applied for estimation of earthquake effects, e.g. MCS, MM, MSK. These are, however, not the subject of our present considerations.

Estimation of the damaging effect of paraseismic vibrations on residential structures is performed in an approximate way on the basis of advisory scales or recommendations. Safe vibration levels in particular standards differ substantially. The standards in question apply to small residential and commercial structures which, as a rule, were not designed for dynamic loads resulting from ground motion. Noticeable discrepancies exist between actual effects of vibration influence on buildings and admissible vibration level adopted in standards. This concerns the admissible vibration level before appearance of the first architectural damages to structures. Investigations show (see e.g. (9, 19)) that already at vibration velocity 0.1 to 0.5 cm/s first damages may appear, whereas the vibration level adopted in certain standards is 10 cm/s (see e.g. (4)). In (5, 15) still higher values of vibration velocity are admissible. Paper (15) gives a review concerning the problem of vibration effects as well as the results of many years' studies carried out in the USA in the Bureau of Mines. Studies carried out by the Bureau of Mines, described in (15) concern mainly wooden buildings (wood frames). In our opinion, wooden buildings respond to dynamic loads in quite a different way than buildings built of brick, structural ceramic tiles, blocks of light concrete, gravel and slag concrete.

The most frequently applied estimation criterion for vibration damage is maximum vibration velocity. The place where measurements of vibrations are performed is of great importance: vibrations measured on the ground surface in the vicinity of the building and in its lower part can differ greatly in the amplitude and frequency range. This problem is often neglected, though not correctly so. As a rule the vibration level of the ground is higher than that of the building at the level of the surrounding ground. This results from interaction of the foundation soil and the building (soil structure interaction).

2. ASSUMPTIONS ADOPTED FOR FORMULATION OF SWD SCALES

In 1961 estimation of damaging vibrations of buildings by means of new scales, formulated in a different way as in other countries, was proposed in Poland for the first time. The scales were assumed to concern only some types of buildings that are mostly used in residential structures of traditional type. By limiting the class of buildings it is easier to formulate appropriate estimation criteria since dynamic characteristics of such buildings are similar. Buildings of brick, concrete, lightweight concrete, and slag concrete were taken into consideration. Roofs and floors of these buildings can be stiff in their plane (e.g. of reinforced concrete) or less stiffening (e.g. of wooden beams). Examples of these types of buildings are presented in Fig. 1. For these buildings simple computational models were adopted. They were subjected to forced vibrations transmitted from the foundation soil; the influence of ground flexibility was also considered. On the basis of calculated dynamic responses of these buildings (the forces and displacements), stresses in the walls were determined. Long duration of vibration application was assumed; thus, in calculations, fatigue of materials was taken into consideration, which in turn will lead to decrease of admissible stress. Consideration of these results and possibility of appearance of first architectural damage for these kind of buildings led to theoretical calculation of curves. These determined the expected response of buildings to a known measured vibration level characterized by the following parameters: maximum amplitude of displacement (velocity or acceleration) and respective frequencies. Not only were strength conditions checked but stiffness conditions as well. Material damping was also considered.

Two main building classes were distinguished. It was assumed that the character of vibration traces of the building is similar to a stationary one. Scale SWD-I is intended for compact structures of small dimensions in plan and of one or two storeys. Scale SWD-II is designed for multi-storey buildings up to 5 storeys in which the condition $h/b \leq 2$ is satisfied, where h is the building height above the ground level, b is the smaller plan dimension.

3. APPLICATION OF SWD SCALES

Horizontal components of vibrations, measured in directions parallel to the longitudinal and transverse axes of the building, have been adopted as reliable kinematic loads on the above-mentioned buildings. The direction in which the higher vibration level occurs is taken for damage estimation. Fig. 2 shows the two scales expressed in terms of displacements, velocities and accelerations. Vibrations measured on buildings at the ground level or below (basement walls, foundations) are taken for estimation purposes.

Fig. 3 presents propagation of vibrations on the ground surface excited by driving Franki piles for various heights of ram blows H. Vibrations were measured on the ground in front of the building and on the bearing wall (a bit above the ground level). Fig. 3 shows a measurement example of the reduction of maximum amplitudes of displacements at the contact between ground and building. Although Fig. 3 concerns vertical vibration components, similar relations occur for the horizontal ones. In general, a change in vibration frequencies occurs at the ground-building contact, e.g. in the case of vibrations excited by pile driving. Vibrations measured on the building are usually of lower frequencies than those recorded on the ground. A building behaves then like a filter; vibrations of frequencies equal to or approximately equal to frequencies of building natural vibrations are transmitted to the building. Thus, in the case of a vibration source from pile driving, vibrations measured on buildings must be considered in estimation of damage vibration. On the other hand, in the case of explosive of big charges in quarries, a change in the character in vibration traces and their transmission from the ground to the building is almost not noticeable. In the case of great energies emitted from the vibration source, practically no reduction of vibrations at the ground-to-building contact takes place. Then almost identical results both for vibrations of the ground and building are obtained in estimating vibration damage for the building.

SWD Scales have five zones (I to V). The following criteria of classification into particular zones of damages have been adopted:

Zone I - vibrations not felt by the building.
Zone II - vibrations felt by the building, but not damaging to the structure. At vibrations of long duration, first cracks may occur in plaster and mortar.
Zone III - damaging vibrations for the building, local cracks may appear in structural elements of the building; this in turn leads to weakening of the structure and decreases its capacity to further dynamic effects; falling off of plaster and mortar may occur.
Zone IV - vibrations of great damage to the building; numerous cracks appear, local damage of walls and other individual elements of the building; there is a possibility of falling down of objects hung on the walls, falling off of sheets of ceiling plaster, of wooden joists slipping out of walls. It is necessary to remove the vibration source or to reduce the vibration effect.
Zone V - vibrations cause serious damage in the building by collapse of walls and floors - dangerous conditions for people. When such vibration levels are expected, the building cannot be used by people.

Limits between these zones are given in Fig. 2 in two variants: as a function of the technical state of the building depending on, among other factors, its age and type of the foundation soil. Classification into a particular variant is made according to the prevailing number of respective characteristics listed as a guiding principle in Table I. The zone limit may be raised by one for the case of vibrations of short duration and for the case when all conditions mentioned in Table I, column 3, are satisfied in estimating building vibration damage. For example, effects classified in Zone I can be attributed to vibrations of parameters corresponding to Zone II in Fig. 2.

Vibrations caused by blasting in quarries are, according to certain standards, e.g. (15), treated as rather sporadic ones; this results in adoption of a high admissible vibration level. If in the vicinity of the building a quarry has existed for several years and blasting occurs twice a week or more often, such vibrations cannot, in our opinion, be treated as vibrations of short duration. Hence the effect of low-cycle fatigue cannot be neglected. A very limited amount of work has been done on fatigue or damage from long-term repeated blasting. It is known that for engineered materials fatigue strengths are typically a fraction of the ultimate strengths - e.g. 50 percent.

4. EXPERIMENTAL VERIFICATION OF SCALES

Investigations of building vibrations and comparison between the results of observations of the state of buildings subjected to vibrations and the estimation resulting from various scales have been carried out at the Institute of Structural Mechanics of the Technical University of Cracow since 1960. For vibration measurements, seismographs WEGIG and S5S of USSR production and occasionally, accelerometers of Bruel-Kjaer production were used. The vibrasources were: passages of vehicles (trucks, trains), machines and other equipment located in the vicinity of the buildings, blasting in quarries, driving of Franki and vibro-L piles. In total, about 250 buildings were studied. The agreement between the degree of vibration damage determined according to the SWD scales and the existing state is good in about 80% of the cases. For over 20 years the SWD scales were applied experimentally in the project of the standard. Since the beginning of 1986 the SWD scales have been included into the new Polish standards (11).

Measured vibrations of buildings are, as a rule, of irregular nonstationary character. In analysing vibration traces, their most unfavourable parameters must be taken into consideration in the estimation procedure. As a rule, the biggest displacements and corresponding frequencies are considered. If the vibration traces of the building components are of smaller amplitudes but of higher frequencies than those corresponding to maximum amplitude of displacements, then vibration accelerations are calculated as for a harmonic motion. These acceleration parameters are then also considered in the estimates.

5. COMPARISON WITH OTHER STANDARDS

In other standards the admissible vibration level is usually higher. In some of them no distinction is made between materials of construction. Investigations show, however, that the admissible vibration level until the moment of first appearance of damage is different for brick and gravel-concrete and for blocks of lightweight concrete. The latter is of low resistance to vibrations since cracks easily occur in joints. In paper (3), masonry cracking induced by blasts in a block and a poured concrete box filled with sand was studied. It was found that poured concrete walls were much stronger than block walls and required high levels of both strain and particle velocity to induce cracking. The mortar joints of the concrete block wall failed at considerably lower strains, but the blocks themselves had the same ratio of strain to velocity as the concrete walls. The walls of concrete block and mortar did not act as monolithic bodies but as concentrated strains at the mortar joints. Crawford and Ward (3, 15) measured strain levels across the mortar joints that were 10 times those on the adjacent blocks. Similar relations were obtained in (10). A good review of standards and publications on estimation of damage of paraseismic vibrations to the building is given in (15, 20). Lowest admissible levels of vibrations are adopted in (6, 18).

The weak side of a number of standards is lack of differentiation in the duration of vibration. From the known standards, (18) is an exception. It takes into account the time factor in an indirect way. For such vibration sources as machines and road traffic, lower levels than for blasting are admitted for the same category of buildings. The frequency range for admitted vibration velocities depends on the vibration source and lies within the limits 10 - 90 Hz and hence includes rather high frequencies. Four types of buildings and other objects were distinguished. Depending on the type of object, vibration velocities from 18 to 3 mm/s are admitted. In known standards the progression of damages is not distinguished, although in papers concerning the question of damage vibration estimation, a distinction is made between architectural and structural damages, e.g. (7, 9).

Differentiation of zones in SWD scales is of some importance in the evaluation of paying damages. In the case of low vibration levels, only architectural damages occur and damages paid are not high; they concern costs of painting renovation, wall paper and possibly repair of cracks in mortar and plaster. When a high vibration level occurred in buildings and damages are structural, the costs are different. Differentiation of zones of vibration damage will simplify the estimation of paying damages in proportion to the degree of their advancement.

6. CONCLUSIONS

It follows from the considerations presented that estimation of the degree of vibration influence on buildings is a complex problem. It depends on a number of objective factors and moreover on elements of random character or subjective approach in classification.

It is also clearly seen that it is impossible to apply completely unified, approximate methods to all types of buildings. Therefore an approach seems right in which a chosen class of most frequently encountered buildings is identified with regard to common features. A scale of dynamic influences such as SWD could then be elaborated for them. Experimental verification carried out over many years confirmed the correctness of diagnostics by use of the SWD scales, provided they are properly applied; it proved simultaneously how useful these scales are in application. Therefore adoption of the SWD scales as a simple means of dynamic diagnostics of buildings is proposed.

Results of other basic studies concerning dynamics of structures, e.g. damping of structure vibrations, wave traces in structures, and possibility of occurrence of low-frequency fatigue may contribute to further improvement of the SWD scales.

REFERENCES

1. Ciesielski, R., The Evaluation of Dynamic Damages in Buildings, in Polish, Arkady, 1973.

2. Ciesielski, R., Calculations and Evaluation of Vibrations from Exterior Sources on Some Types of Buildings, Technical University of Cracow, The Report 1, 1961.

3. Crawford, R., Ward, H.S., Dynamic Strains in Concrete and Masonry Walls, Div. Bldg. Res., National Research Council Canada, Ottawa, Bldg. Res. Note 54, December 1965, pp. 1-13.

4. Czechoslovak Standard, Seismic Load of Structures, CSN 730036, 1973.

5. Damage Levels from Blasting (after Langefors and Kihlstrom), 1963.

6. German Vibration Standards, DIN 4150

7. Jackson, M.W., Thresholds of Damage Due to Ground Motion, Proc. Int. Symp. on Wave Propag. and Dynamic Properties of Earth Materials, University of New Mexico Press, New Mexico, 1967, pp. 961-969.

8. Limiting Safe Vibration Values of Pseudo Vector Sum Peak Particle Velocities (after Esteves), 1978.

9. Nadolski, M.E., Architectural Damage to Residential Structures from Seismic Disturbances, Bull. Seism. Soc. Adm., vol. 59, No. 2, 1969, pp. 407-502.

10. Northwood, T.C., Crawford, R., Edwards, A.T., Blasting Vibrations and Building Damage, The Engineer, vol. 215, No. 5601, May 31, 1963, pp. 973-978.

11. Polish Standard, Evaluation of the Damage Building Vibrations Due to Ground Motion, 1985.

12. Power, D.V., A Survey of Complaints of Seismic-related Damage to Surface Structures Following the Salmon Underground Nuclear Detonation, Bull. Seis. Soc. Am., vol. 56, No. 6, 1966, pp. 1413-1428.

13. Scholl, R.E., Farhoomand, I., Statistical Correlation of Observed Ground Motion with Low-rise Building Damage, Bull. Seism. Soc. Am., vol. 63, No. 5, 1973, pp. 1515-1537.

14. Scholl, R.E., Low-rise Damage from Low-amplitude Ground Motions, Bull. Seism. Soc. Am., vol. 64, No. 6, 1974, pp. 1743-1755.

15. Siskind, D.E., Stagg, M.S., Kopp, J.W., Dowding, C.H., Structure Response and Damage Produced by Ground Vibration from Surface Mine Blasting, Bureau of Mines, Report of Investigations 8507, 1985, pp. 1-74.

16. Stagg, M.S., Engler, A.J., Measurement of Blast-induced Ground Vibrations and Seismograph Calibration, Bureau of Mines, Report of Investigation 8506, 1985, pp. 1-27.

17. Studer, J., Suesstrunk, A., Swiss Standard for Vibrational Damage to Buildings, Proc. X Int. Conf. Soil Mech. and Found. Eng., Stockholm, vol. 3, 1981, pp. 307-312.

18. Swiss Standard 690312, Effects of Vibration on Structures, Swiss Association of Standardization, Zurich, Switzerland.

19. Wall, J.F., Jr., Seismic - Induced Architectural Damage to Masonry Structures at Mercury Nevada, Bull. Seism. Soc. Am., vol. 57, No. 5, 1967, pp. 991-1007.

20. Wiss, J.F., Construction Vibrations: State-of-the-art, Journ. Geot. Eng. Div., ASCE GT.2, 1981, pp. 167-181.

TABLE 1

Estimation According To:	Characteristics Permitting Application of the Limit Lower Continuous Line in Fig. 2	 Higher Broken Line in Fig. 2
1	2	3
state of the building	old buildings, with damages; reconstructed or strengthened buildings	undamaged buildings, without structural changes
material and structure of building	buildings of masonry elements, slag concrete or stone, not well built; lack of foundation, lack of tie beams, arching floors, big openings in walls or irregular openings	brick walls properly built, reinforced, concrete foundations, stiffness floors joining walls with tie beams
type of foundation soil and foundation type	foundation soil of low stiffness (e.g. dusty sands, loose) non-continuous (various heights or intermediate) foundations	stiff soil, e.g. firm silt, plane foundations
type of vibrations	vibrations of long duration or permanent	vibrations of short duration

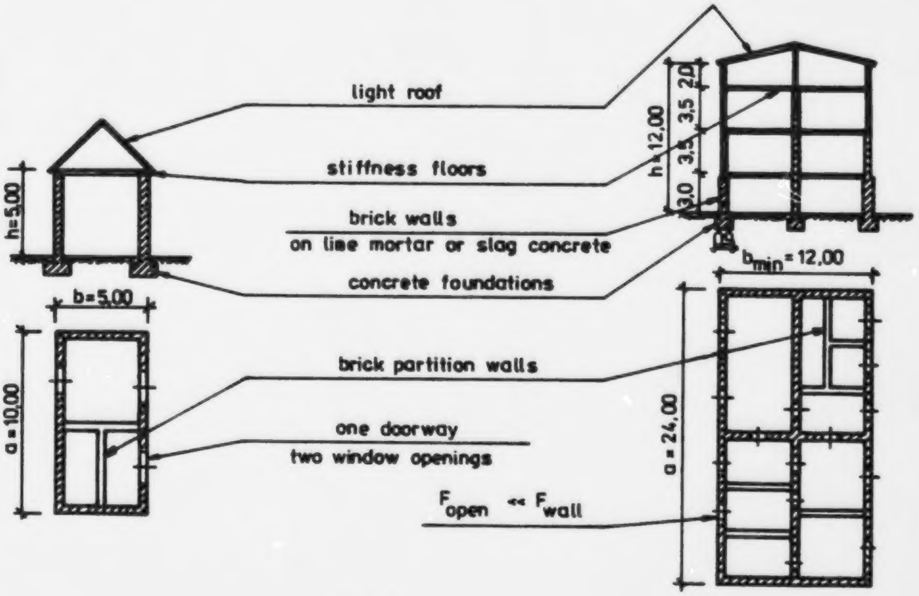

Fig. 1

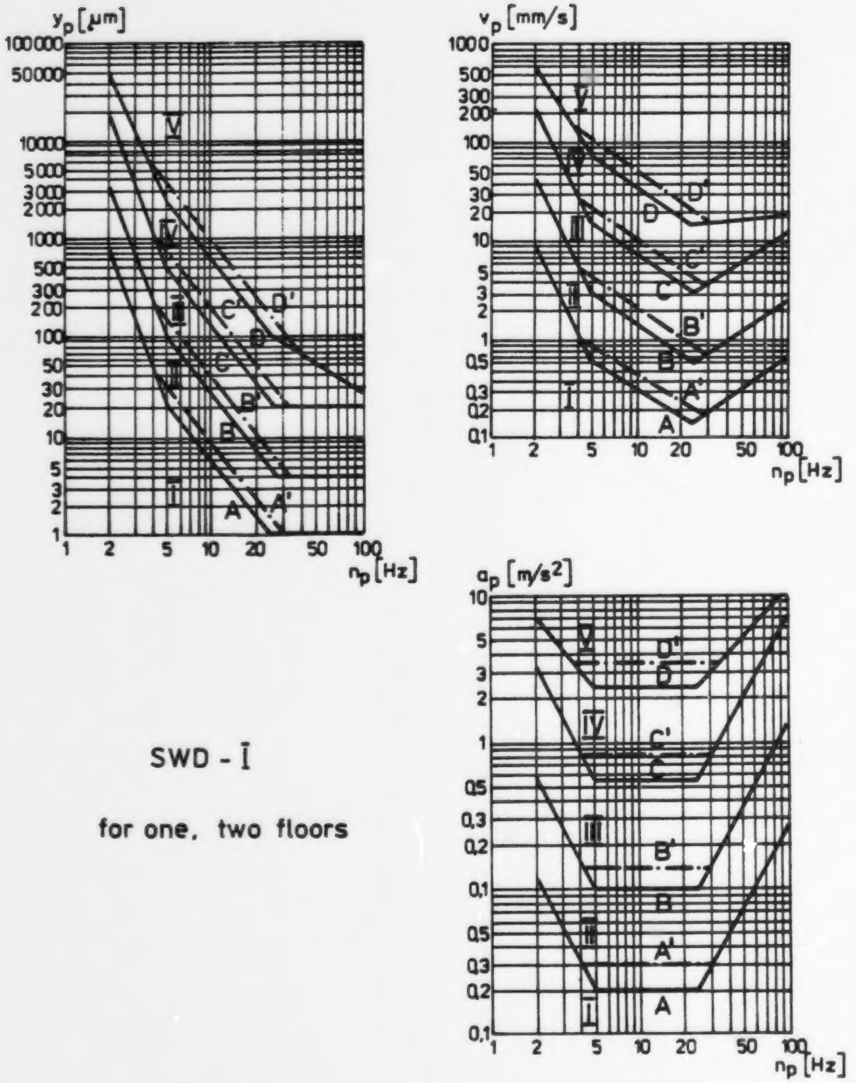

SWD - I

for one, two floors

Fig. 2a

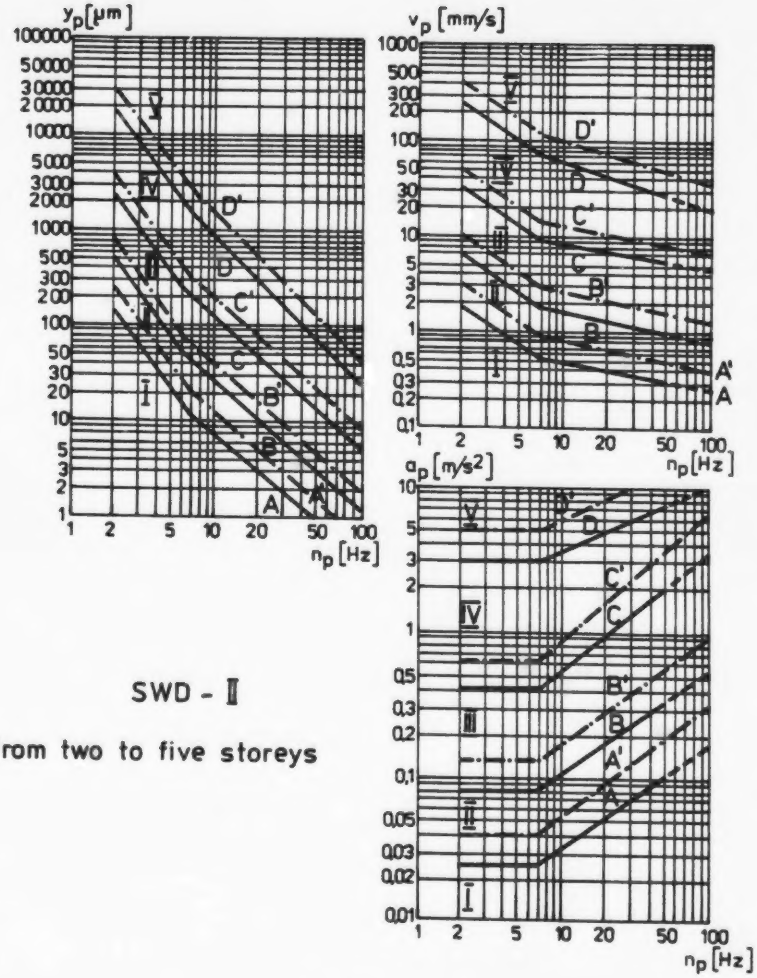

SWD - II

from two to five storeys

Fig. 2b

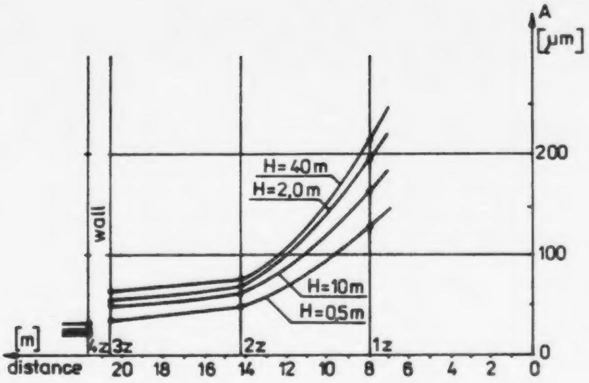
A
[μm]
200
100
0
H=4,0m
H=2,0m
H=1,0m
H=0,5m
wall
[m]
4z
3z
2z
1z
distance
20
18
16
14
12
10
8
6
4
2
0

Fig. 3

MICRO-VIBRATION CONTROL PROCEDURE FOR HIGH-TECH FACILITIES

Kiyoto Shioya and Kazuhiko Maebayashi

Shimizu Corporation
Tokyo, Japan

ABSTRACT : In high-tech facilities, floor vibration even of the order of a micrometer can be a problem as elaborate pieces of equipment for precision fabrication and inspection are installed. To resolve this problem a measurement and analysis procedure estimating vibration level from the planning stage of selection of the facility site to the stage of actual structural design was established. The present paper describes a design procedure based on dynamic response analyses of structures and a case study of an existing research institute building.

1. INTRODUCTION

In semiconductor fabrication facilities and research institutes, there have been growing demands for stricter vibration-free environments. Vibrations, if uncontrolled, can affect production of large-scale integrated circuits (LSIs) and accuracy of inspection. Aligners, steppers, and lithography equipment are sensitive to vibrations in semiconductor fabrication facilities. Since circuit line widths are commonly no more than a few submicrons, vibration levels of this order at plant floors can be a problem.

At research institutes, electron microscopes and other measurement equipment are sensitive to vibrations. Blurs and distorted images can be generated. When building a facility which needs to satisfy such strict vibration requirements, careful investigation is necessary from the planning stage of selection of the facility site to the stage of actual structural design. Therefore, an effective vibration measurement and analysis system for estimation of floor vibrations is needed.

The effectiveness of a micro-vibration isolation procedure was verified in the design and construction of a research institute for fine ceramics. Severe allowable vibration levels were mandated as 1,200,000-magnification scanning electron microscopes (SEMs) and various kinds of inspection equipment were to be installed in the institute. Furthermore, the construction site was adjacent to a highway, while there were also railroad lines close by, and these made vibration isolation even more important.

Before starting work on the design, an ambient vibration survey of the site was carried out to examine the vibration level distribution, vibration attenuation according to the distance, and frequency characteristics. A fundamental plan of the building was selected on the basis of the data obtained. Dynamic response analyses of the structure and isolation equipment were performed using observed data, and calculation results were compared with allowable vibration levels. A vibration survey (ambient vibration measurements, forced vibration tests using an actuator, and human footfall tests) was carried out after completion of the building, and the appropriateness of the procedure employed was confirmed.

2. DESIGN PROCEDURE FOR MICRO-VIBRATION CONTROL

A basic design procedure for vibration-free facilities is outlined on the flow chart shown in Figure 1. The first step in designing is to understand and to define the allowable floor vibration level for precision instruments. The second step is to grasp the characteristics of vibration sources such as vehicular traffic, railroads, building equipment, and human footfalls. After defining the allowable vibration level and examining vibration sources, the planning stage of design starts with both architectural and structural designs such as the locations of instruments and the types of main structural members studied. Vibration isolation systems such as air-supported bases or rigid massive slabs are then examined. In the next stage, detailed design planning, dynamic response analyses of structures and spectral analyses of response time histories are performed to evaluate whether the response values are below the allowable vibration levels. If the response values exceed allowances, the design is reviewed and revised.

2.1 Allowable Vibration Level :

Excessive floor vibrations seriously affect the performances of instruments. Therefore, it is essential to carefully examine the allowable floor vibration level. As there are many types of expressions for allowable vibrations, it is very important to clarify on what kind of definition the specification is based. Allowable vibration levels have been specified in the past by magnitude of acceleration, velocity, or displacement. However, specifications of spectrum forms are preferred in detailed vibration analysis because the frequency characteristics of instrument responses are important. As for the specifications in spectrum form, the power spectral density function, the Fourier spectrum, and the one-third octave band spectrum are chiefly mentioned. The power spectral density function describes the general frequency composition of the data in terms of the spectral density of its mean square value. The Fourier spectrum is obtained from a Fourier integral and describes the root mean square of harmonics. The one-third octave band spectrum describes the root mean square value of a sample time history record in a frequency range of a one-third octave band pass filter. The one-third octave band spectrum is the best expression for vibration allowance of these spectrum forms because the definition is unique and there is wide-spread use by engineers.

2.2 Vibration Sources :

To design a satisfactory vibration-free facility, vibration sources within the facility itself and external sources must be taken into consideration. As examples of the former, fans, pumps, compressors, and ducts in air-handling units produce vibrations. Furthermore, operating personnel are sources of vibration since footfalls can produce troublesome vibrations in the vicinities of sensitive pieces of equipment. As examples of the latter, vibrations resulting from vehicular traffic and railroads will have influences on the facility. Additionally, every site has an ambient vibration level caused by tidal rises and falls and by man-made sources. Characteristics of ambient vibration depend on geological formations, and soil types and depths at the site. Therefore, ambient vibrations are important in selection of the facility site.

2.3 Analysis Method :
Vibration analyses are closely related with each step of design. Wave propagation analyses for traffic and other vibration sources are performed in investigation of the facility layout. The vibration level distribution at the site is estimated from the analyses, and calculation results are applied in examination of the building location. Measured data may be used for analysis when a vibration survey at the site is possible.

After deciding on the layout of the facility, analyses of structural responses to ground motions and inside vibration sources need to be carried out. Ground motion is attenuated in the process of propagation from ground surface to building foundation by the effect of rigid foundation restraint. This effect is a kind of soil-structure interaction and is called filtering effect of foundation. Yamahara proposed the following low-pass filter as the analysis model for this effect.

$$H(f)=(L/l)\sin(l/L) \qquad (1)$$

where, $H(f)$ is the gain factor of the frequency response function, l is foundation length, and L is wave length.

In structural response analyses, major structural members such as columns, beams, walls, and slabs are modeled by lumped mass models or frame models. Structural response is calculated for the input motion estimated in the previous stage. In regard to vertical responses of slabs, the finite element method is applied and eigenvalue analyses are performed. Eigen-frequencies are then examined for coincidence with predominant frequencies of vibration sources and response analyses of slabs are carried out.

In the end, spectral analyses are performed to evaluate the calculation results. As mentioned previously, one-third octave band analyses are recommended for providing criteria.

3. CASE STUDY ON EXISTING BUILDING

The building as proposed was a five-story reinforced concrete structure (as shown in Figure 2) and the bases of SEMs were to be supported by air suspension. Dynamic response analyses of the structure and isolation equipment were performed using observed data and calculation results were compared with allowable vibration levels. After completion of the building, a vibration survey (ambient vibration measurement, forced vibration test using an actuator, and human footfall test) was carried out and the appropriateness of the present procedure was confirmed.

3.1 Vibration Survey at Construction Site :
The construction site of the building was close to a highway and railroad lines. Accordingly, there was concern that the traffic of vehicles and trains would affect the precision instruments in the laboratory. A vibration survey was carried out at the site to grasp the vibration characteristics of vehicles and to obtain data for analyses.

Ground surface vibrations caused by vehicles passing by were measured to obtain the vibration attenuation curve with distance from the highway. The measurement locations for vehicular vibrations were arranged as shown in Figure 3. Six measurement point were provided and three sensors for radial, transverse, and vertical directions were set at each point. Time histories of 18 components were recorded simultaneously. Sample attenuation curves obtained from traffic vibration data are shown in Figure 4. Ambient vibrations in the vertical direction were measured simultaneously at 20 points for one hour to evaluate the vibration distribution at the site. The distributions of maximum accelerations and locations of measurement points are shown in Figure 5.

Power spectra were calculated and predominant frequencies of ambient vibrations were estimated using these records. Figure 6 shows an example of power spectra of displacement at measurement point #5, in Figure 3. The predominant frequency and other characteristics of the site were grasped with these results, and the building was designed to be located at the northeast part of the site with the SEMs installed on the first floor. Table 1 shows the predominant frequency of the ground at the site.

3.2 Estimation of SEM base :
Dynamic response analyses of the SEM bases, was carried out using the results of the vibration survey. Vibration levels of response were compared with the allowances of the SEM. The allowable vibration levels of the SEMs were under 0.05 cm/sec^2 in the horizontal direction and under 0.07 cm/sec^2 in the vertical direction. A high-performance base isolation system was needed to satisfy these specifications. Therefore, massive concrete bases supported by means of air suspension as shown in Figure 7 were used. The isolation system was designed to have an eigen-frequency of 1.5 Hz in every direction, in consideration of the predominant frequency of the ambient vibration.

Firstly, the response of the building foundation was calculated using the numerical filter for the model of filtering effect of the foundation slab. The accelerogram obtained at point #4 from vehicular traffic was used as the input ground motion of this model. Secondly, the response of the isolated base was calculated by numerical integration of a single-degree-of-freedom lumped mass model. Maximum values of input ground motion and of calculation results for the building foundation and isolated base are given in Table 2. The calculated responses of the isolated base were lower than the allowable vibration levels of the SEMs in all directions. Therefore, the design of this of isolated system was adopted for the building.

A vibration survey to confirm the appropriateness of the estimation in design was conducted after installation of the SEMs had been completed. The locations for making measurements is shown in Figure 7. The frequency response functions of the isolated system were calculated using the records of the building foundation and the isolated bases. Eigen-frequencies and damping ratios of the system were obtained from the frequency response function. The eigen-frequencies of the system were 1.4 and 1.5 Hz in horizontal directions and 1.2 Hz in the vertical direction.

These values were nearly equal to the values in design. Table 3 shows the maximum accelerations of the individual measurement points. According to these values, the response accelerations of the isolated bases were 0.03 and 0.04 cm/sec^2 in horizontal directions and 0.04 cm/sec^2 in the vertical direction. These values are lower than specified for SEMs. Therefore, the appropriateness of the present method had been confirmed.

3.3 Examination of Effects of Human Footfalls :

The vibration source within the building having the greatest effect is the human footfall. Many kinds of equipment can of course be sources of vibration, but they can be dealt with by isolation. To examine the effects of human footfalls, it is indispensable to understand the dynamic characteristics of slabs. Accordingly, eigenvalue analyses and response analyses were performed by the finite element method (FEM) at the design stage. Figure 8 shows the finite element model of the slab. Table 4 shows eigen-frequencies and Figure 9 the eigen-mode shape of the slab. In dynamic response analysis, the dynamic force record of footfalls obtained in walking tests of a male person was used as the input force to the FEM model. The input time history was forced in the vertical direction at the center point of the slab and the response displacement at the forced point was obtained. Time histories of input forces and response are shown in Figure 10. The one-third octave band spectrum of response was calculated and is shown in Figure 11.

After completion of the building, forced vibration tests using an actuator and footfall tests were carried out on a typical slab of the third floor. The electro-magnetic type actuator was placed at the center of the slab surrounded by girders. A sweep forced vibration test in the vertical direction was conducted. The maximum acceleration of actuator was set at 400 cm/sec^2 and sweeping frequency range from 5 to 40 Hz. Measurement locations of 35 points were set in an area of 10.5 m * 6 m and accelerometers were placed at these points. The frequency response functions at all measurement points were calculated from response records. The eigen-frequencies and damping ratios were calculated by regression analysis of the frequency response function at the center of the slab. The mode shapes were calculated from magnification factors and phases of all frequency response functions. The eigen-frequencies and damping factors of the slab are given in Table 4.

Next, response displacements were measured when a male person was walking along the center line of the slab to grasp the vibration level of slab caused by human footfall. Maximum response and one-third octave band spectrum were obtained from the response time history. An example of the one-third octave band spectrum is shown in Figure 11 with calcuation result. These results agree well with the values predicted at the design stage.

3.4 Study on Vertical Response of Structure for External Vibration :

A pre-study on vertical response analysis of the structure for external vibration was not performed in the present case because the influence of human footfalls was critical. However, dynamic response analysis of the proposed building was carried out using the measured record to examine the vertical response analysis procedure.

A response analysis by numerical integration in the time domain was conducted on the structural response caused by the influence of vehicular traffic. The frame and slabs of the building were modeled as a lumped mass system having freedom in the vertical direction as shown in Figure 12. The stiffness of the frame was calculated from the data of columns and shear walls. Slab stiffness was calculated from the FEM model. The effective mass of a slab was calculated from the stiffness and eigen-frequency of the fundamental mode. Input acceleration for the lumped mass model was obtained from the measurement record of the ground surface passing a low-pass filter modeled as the effect of foundation restraint. The frequency response function of the foundation in relation to the ground is shown in Figure 13. The time histories of measurement records and filtration records are shown in Figure 14. The time histories of structural responses were calculated using the filtration records. Figure 15 shows the comparison of measurement records and calculation result. Figure 16 shows comparisons of maximum accelerations at all of the floors. According to these results, the calculated values at the centers of slabs are slightly different from the measured values. The reason for this tendency may be that the measurement records include the influences of higher modes of the slab. However, calculated values of floor vibration levels coincided with measured values.

Mean square response analysis in the frequency domain was performed regarding structural response caused by ambient vibration of the ground. The random vibration theory could be applied in this case as ambient vibration is regarded as a stationary random process. If the input were to be a stationary random process, the output of the linear system will be a stationary random process. The relationship between input and output power spectra is given by

$$Sy(f)=|H(f)|^2 Sx(f) \tag{2}$$

Where, Sx(f) is the input power spectrum, Sy(f) is the output spectrum and H(f) is the gain factor of the frequency response function.

The power spectrum of ambient vibration was computed from the measurement record of the ground surface. As before, the frequency response function of the fifth floor to the ground motion was calculated for the lumped mass model. The power spectrum of response was calculated by the product of the power spectrum of ambient vibration and the square of gain factor of the building.

The power spectra at the slab of the fifth floor obtained from the measurement record and analyses are shown in Figure 17. The peak occurring at 3 Hz is the predominant frequency of the ground and the peaks at 15 Hz and 22 Hz are the eigen-frequencies of the slab. The analytical result differs from the measurement result particularly at the peak at 22 Hz. This difference arises from the fact that the model of the slab is idealized by an SDOF system and that the eigen-modes of the slab are excited by inside vibration sources when measuring. The overall tendency of the power spectrum obtained from analysis agrees with that of the power spectrum from the measurement record.

4. Summary and Conclusions

The outline of a micro-vibration control procedure and a case study on an existing research institute building have been presented in this paper. In this case, as the allowable vibration level for SEMs was the severest in the building, a vibration survey and analytical investigation were conducted concentrating on this problem. According to the vibration survey after completion of construction, the vibration levels of the SEM bases were sufficiently below the allowable value. It was verified that the analytical model for base isolation was appropriate. The responses of slabs to human footfalls were examined by the FEM model and the analysis results agreed with measurement results. Vertical response analyses of the structure were performed in the time and frequency domains for the measurement records. It was found that a lumped mass model gives good agreement with the measured value.

After the various examinations, it was concluded that the micro-vibration control procedure described in this paper is effective in practical design of high-tech facilities. The accuracy of the present procedure should be improved through accumulation of data from further case studies.

REFERENCES

Shioya, K.,and Yamahara, H. 1980. Study on Filtering Effect of Foundation Slab. Proceedings of 7th world Confrernce on Earthquake Engineering, Istanbul, 5, pp. 181-188

Shioya, K., and Maebayashi, K. 1987. Study on Micro-vibration Isolation for High-tech Facilities. (Part 1) Estimation of Foot-fall Impulse. (Part 2) Response Analysis by External Vibration Source. Summaries of Technical Papers of Annual Meeting, Architectural Institute of Japan. pp. 957-960 (in Japanese)

Ellingwood, B., and Tallin, A. 1984. Structural Serviceability: Floor Vibrations. Journal of Structural Engineering, ASCE, vol.110, No. 2, pp.401-418

Table 1 : Predominant frequency of ambient vibration

Direction	Predominant frequency (Hz)
Radial	3.1
Transverse	3.8, 2.7
Vertical	2.9, 5.7, 7.2

Table 2 : Calcuration results of maximum response of SEM base

Direction	Observed	Calculation	
	Ground	Bldg. Foundation	Isolated Base
Radial	0.698	0.250	0.041
Transverse	0.834	0.279	0.046
Vertical	1.198	0.419	0.059

(Unit:cm/sec^2)

Table 3 : Observed results of maximum response of SEM base

Direction	Ground	Bldg. Foundation	Isolated Base
Radial	0.356	0.144	0.034
Transverse	0.467	0.153	0.035
Vertical	2.30	0.207	0.042

(Unit:cm/sec^2)

Table 4 : Eigen-frequency and damping ratio of the slab

Mode	Eigen-frequency (Hz)		Damping ratio
	Calculation	Observed	Observed
1	17.0	18.7	0.023
2	25.7	22.7	0.021
3	37.3	38.7	0.018
4	49.7	49.8	0.018

Figure 1 :
Basic design procedure

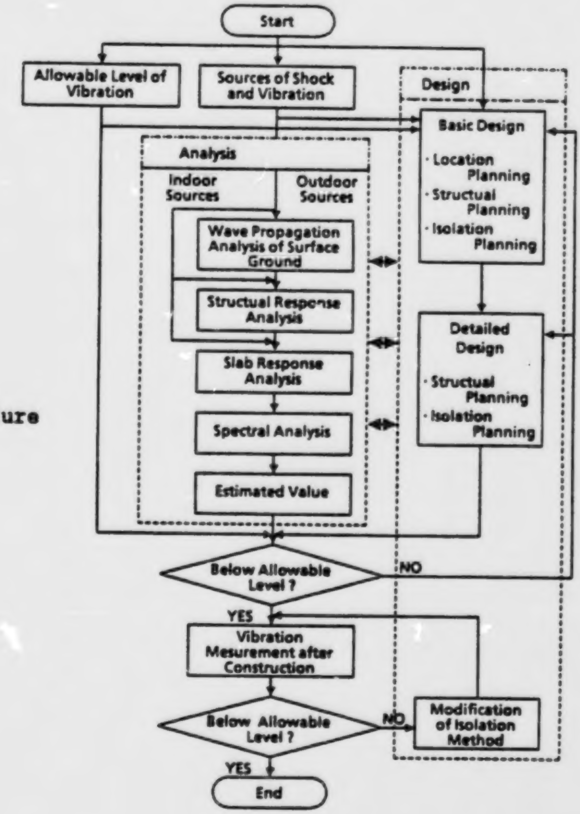

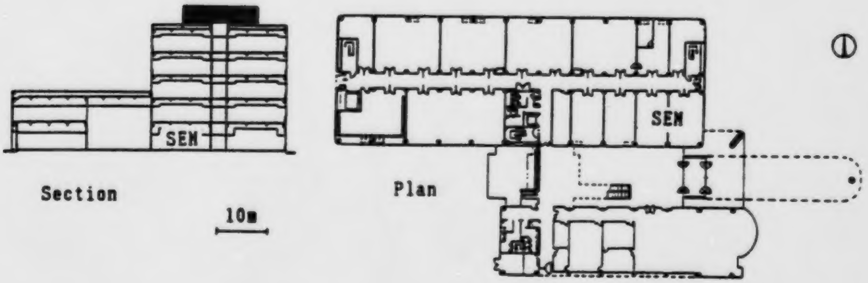

Section

Plan

Figure 2 : Outline of proposed building

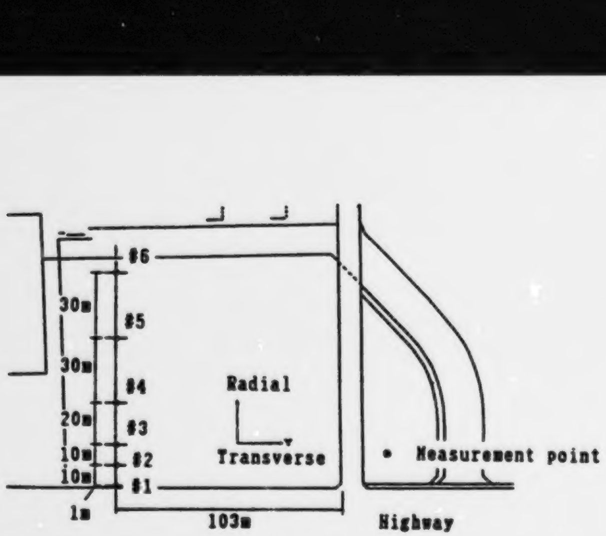

Figure 3 : Measurement location for vehicular traffics

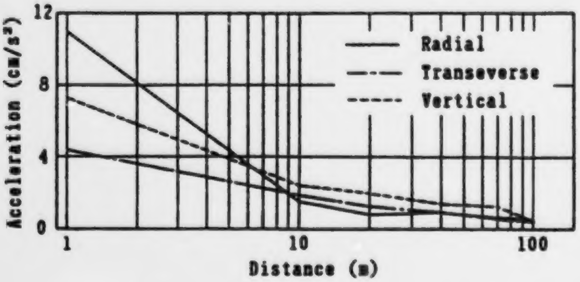

Figure 4 : Attenuation curve with distance

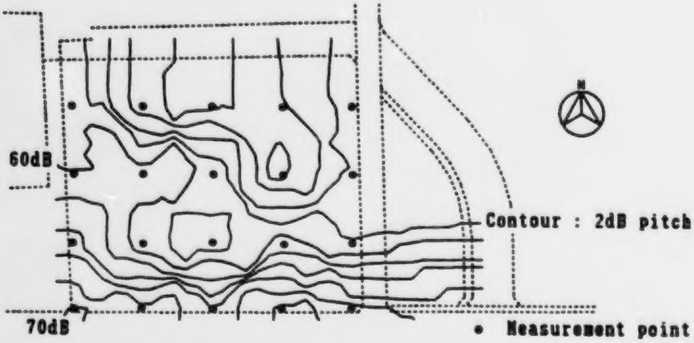

Figure 5 : Maximum acceleration distribution of the site

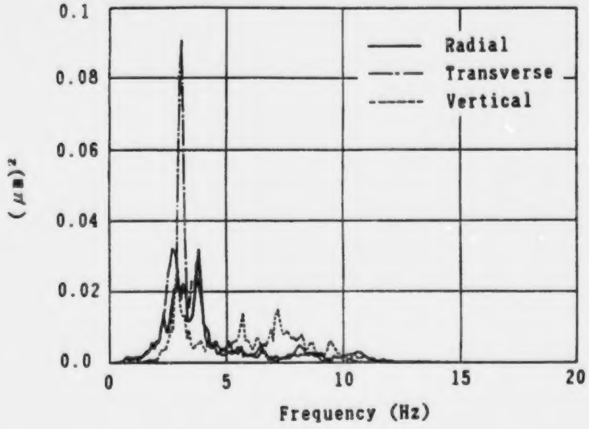

Figure 6 : Power spectra of ambient vib ation

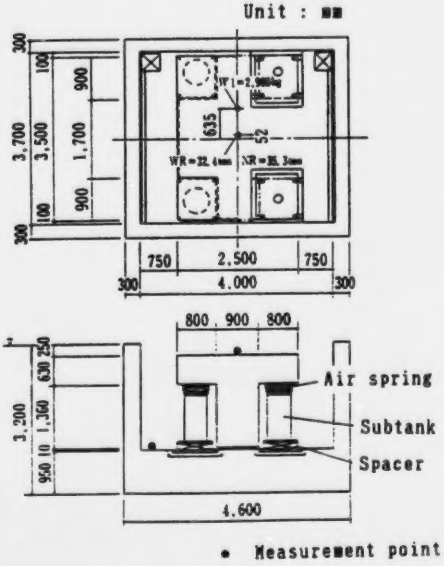

Figure 7 : Base isolation system of the SEM

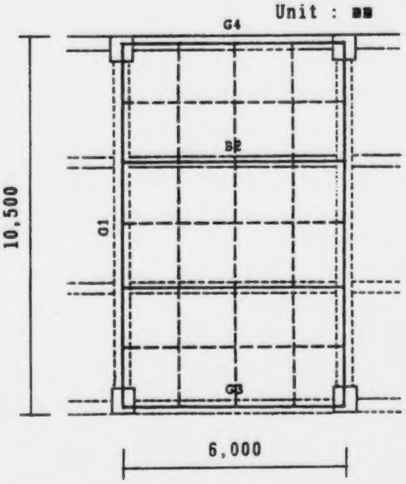

Figure 8 : Finite element model of the typical slab

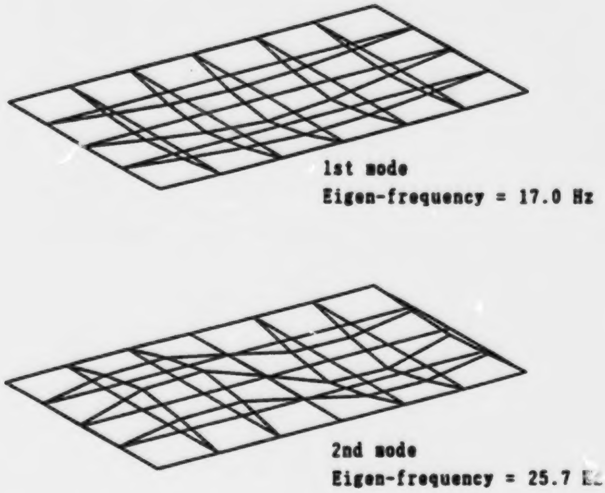

1st mode
Eigen-frequency = 17.0 Hz

2nd mode
Eigen-frequency = 25.7 Hz

Figure 9 : Eigen mode shapes of the slab obtained by FEM

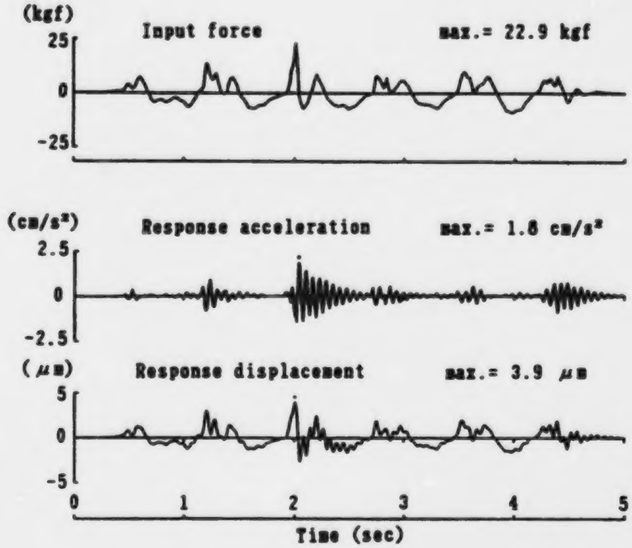

Figure 10 : Time histories of human footfall and response of the slab

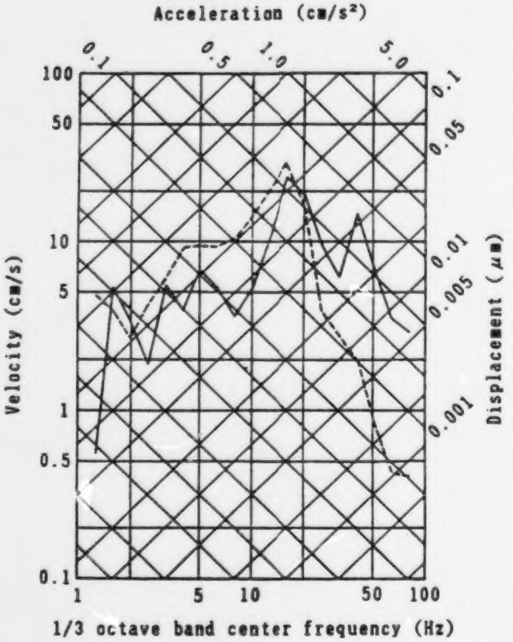

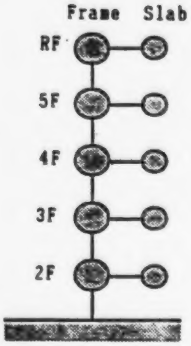

Figure 11 : One third octave band spectrum of response by human footfall

Figure 12 : Lumped mass model

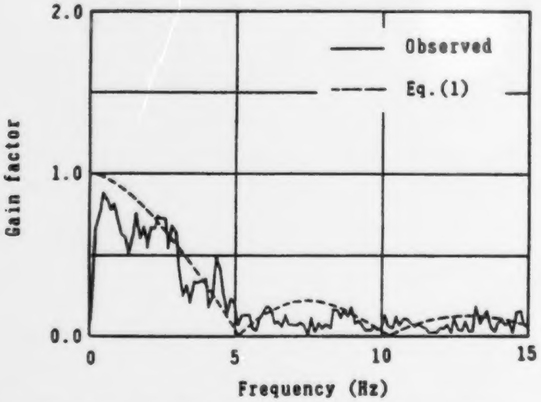

Figure 13 : Frequency response function of the foundation to the ground

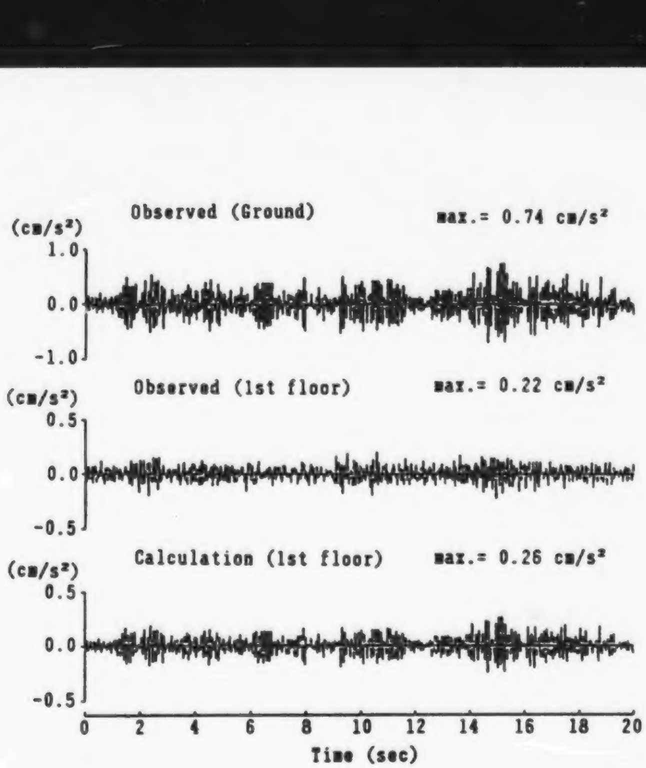

Figure 14 : Time histories of the ground surface and the first floor

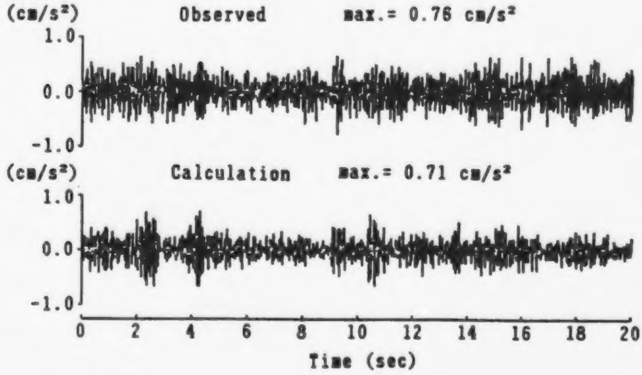

Figure 15 : Time histories of 5th floor slab

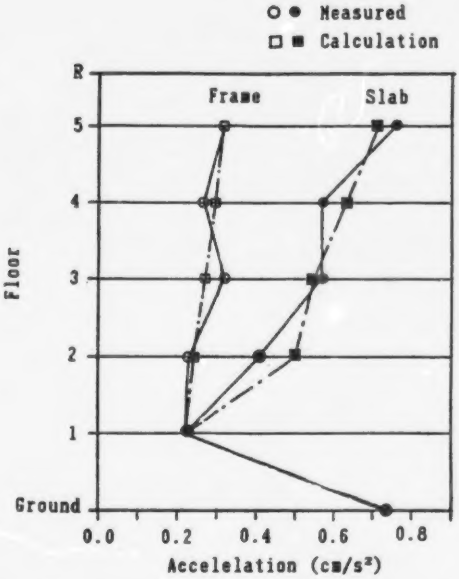

Figure 16 : Comparison of maximum acceleration

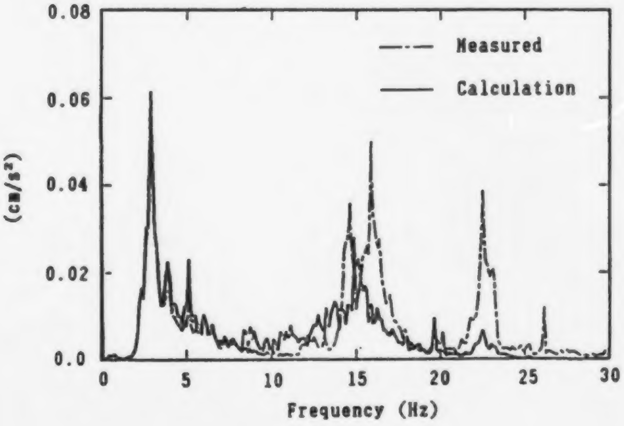

Figure 17 : Power spectra at the 5th floor slab

EFFECT OF TRAIN-INDUCED VIBRATIONS ON HOUSES - A CASE STUDY

J.H. Rainer, G. Pernica, A.H.P. Maurenbrecher, K.T. Law, and D.E. Allen

Institute for Research in Construction
National Research Council of Canada
Ottawa, Canada K1A 0R6

ABSTRACT: Train-induced vibrations of houses and mobile homes in Kamloops, British Columbia, were investigated to determine whether the vibrations could have resulted in damage to residences near the tracks. A detailed investigation showed that building resonance could result in architectural damage up to 250 m from the tracks and that vibration-induced settlement could occur for certain mobile home foundations located on loose wet fill. The criterion for possible architectural damage to stucco and brittle interior finishes was taken as 5 mm/s peak velocity, measured at the ceiling level of the one-storey houses. As a result of this study, general recommendations are presented regarding the methods employed in investigating similar train vibration problems.

1. THE PROBLEM

The Canadian National Railways (CN) main line has passed through the Brocklehurst and Rayleigh areas of the city of Kamloops, British Columbia since the early part of this century. In the fall of 1984, a second track was added adjoining the existing one. Immediately complaints were registered by homeowners regarding excessive vibrations in houses nearby as a result of trains travelling on the new track.

The complaints precipitated two investigations in the residential areas abutting the railway tracks. These studies concluded that although the vibrations exceeded acceptable perception levels, they would not be high enough to cause damage to the houses. The findings were rejected by the Citizen's Committee of homeowners. A subsequent investigation by the Institute for Research in Construction (IRC) of the National Research Council of Canada (NRC), requested by Transport Canada, determined that the rejection of damage claims was premature, since two possible damage mechanisms, horizontal house resonance and vibration-induced soil settlement, had not been sufficiently investigated. Although these mechanisms are not part of most traffic vibration studies, they were considered to play a major part in this particular case.

This paper briefly describes the investigations carried out by IRC and the resulting conclusions reached; it also contains recommendations on the methods that are used to study similar train-induced vibration problems.

2. THE INVESTIGATION

The purpose of the investigation was to establish whether vibrations from trains in Kamloops, B.C. are a valid cause of damage to nearby buildings, notably those for which damage claims had been submitted to CN. Two possible damage mechanisms - horizontal house resonance and vibration-induced soil settlement - were to be investigated. The following measurements were undertaken:

2.1 Dynamic Properties of Houses: The lowest horizontal natural frequencies and damping ratios were determined for six one-storey wood frame houses with basements in the Brocklehurst area. See Figure 1 for locations. Excitations employed for these measurements were impacts from door closures and ambient vibrations. The following results were obtained:

(a) fundamental frequencies of six typical houses in the Brocklehurst area of Kamloops, B.C. ranged from 7.0 to 8.9 Hz, with an average of 7.8 Hz;
(b) damping ratios for the fundamental mode of the six houses range from 3.5 to 7.5% of critical, with an average of 4.8%.

2.2 Ground Vibrations From Trains: Ground vibrations produced by passing trains were measured at three locations along the track at 1160 Bentley Place, and at various distances from the track along Lines 1 and 2 as shown in Fig. 1. Vibrations were measured in both horizontal and vertical directions. Train speeds were measured by "radar guns" located near Line 1 and Line 2.

Ground vibrations from a number of trains were monitored on Line 1 under the then current operating conditions, namely 50 mph (80 km/h) speed limit on the old track and 20 mph (32 km/h) speed limit on the new track. The speed limit on the latter had been reduced from 50 mph (80 km/h) as a result of the homeowners' complaints. To provide a range of train speeds for purposes of this study the speed limit on the new track was raised in stages from 20 to 50 mph over a two-day period.

The measurements of ground vibrations from train passages showed the following:

(a) The ground vibrations emanating from trains on the new track consisted of 1 or more predominant sinusoidal waves (Fig. 2).
(b) The frequencies of the dominant ground vibration components generated from loaded freight trains travelling on the new track increased linearly with train speed, with a dominant frequency ranging from 6 Hz at 42 km/h train speed to 10 Hz at 70 km/h (Fig. 3).
(c) The maximum ground vibration amplitudes varied along the track and with distance from the track, depending on train speed and train load (Fig. 4).
(d) The vibration amplitudes produced by trains on the old track were approximately one-third those produced from the new track; this agrees with the results from previous investigations.

2.3 House Response to Train-Induced Ground Vibrations: The horizontal vibration response of a single-storey house with basement, 1160 Bentley Place (Fig. 2), was monitored on the basement slab, at the first floor level, and at ceiling level at the same time as the ground vibrations were measured during train passage as described in 2.2. Typical results of the measurements are presented in Fig. 5 in the form of envelopes of peak accelerations.

The results demonstrated that large resonant response in a house as a result of trains travelling on the new track produced amplifications of 9 to 10 times between the ground and the first floor ceiling of the house under investigation. The maximum response recorded at the first floor ceiling level in the house tested was 4.0% g acceleration or 8.0 mm/s velocity.

2.4 Evaluation of Soil Behaviour: To determine the effect of ground vibration on foundation settlement the following investigations were carried out on soil in the Brocklehurst area, Kamloops, B.C. (Fig. 1):

(a) A comprehensive picture of the type and geological history of the soil was obtained from borehole information, air photo interpretation, soil analyses for grain size distribution and other relevant data supplied by CN and the City of Kamloops.
(b) Vertical ground shaker tests were carried out in the field under both dry and wet soil conditions to determine the effect of vertical cyclic loading on settlement.
(c) Laboratory tests were carried out to determine the compression of the soil, under dry or wet conditions, due to static and cyclic loading. Most tests were on undisturbed natural soil samples obtained by means of a new double tube sampler, whereas some samples were reconstituted to represent loosely compacted fill that may be found in the area.

The results of these investigations are as follows:

(a) Previous studies have shown that the silty soil present in the area under investigation has high strength and low compressibility while dry, but its strength becomes reduced when the soil is wet, whereupon the grain structure collapses. No information on behaviour of this type of soil under vibrations could be found in the literature.
(b) Air photo interpretation and borehole information showed that the surficial deposits are composed of floodplain sediments of loose silt and sand. The soil samples obtained from the top two metre surface layer are composed mainly of angular silt size particles with 20 to 75% mica and the rest quartz. No appreciable amount of calcium carbonate, a possible cementing agent, was found.
(c) Tests on naturally-deposited soil showed that the soil at its natural moisture content does not undergo appreciable settlement for static loading intensity associated with one- to two-storey residential buildings and trailer homes, or for dynamic loading of an amplitude induced by the passage of trains at houses 40 m from the tracks. The tests showed that wetting the soil produces an additional settlement of about 5 mm per metre of soil under the same static loading and that this settlement is further increased slightly under cyclic loading. This increase, however, is not sufficient to give rise to appreciable settlement under footings of one- to two-storey houses.
(d) Tests on reconstituted soil samples showed that loosely compacted fill consisting of the silty material present in Brocklehurst will, when wetted, settle substantially more than the naturally-deposited wetted soil (Fig. 6). Vibrations of amplitudes as stated above will cause little additional settlement when the void ratio of the soil is less than 1.25.
(e) Foundations supporting trailer homes may rock under train-induced ground vibrations (Fig. 7). This rocking motion can cause a high concentration of dynamic stresses under small footings. If such footings rest on loose and wetted fill, at a void ratio 1.25 or higher, some appreciable settlements may occur (Fig. 8).

3. DAMAGE SUSCEPTIBILITY OF HOUSES

3.1 Damage Criteria: Damage criteria for continuous vibrations for the types of houses considered in this investigation are scarce. Previous investigations reported in the literature have shown that damage to interior and exterior finishes such as plaster and stucco can occur at low vibration amplitudes of 2 to 3 mm/s, since locked-in stresses may already be present. The vibrations then provide the small additional loading needed to cause cracking or extensions of existing cracks. It was felt that for the frequency range and the brittle finishes under consideration, 5 mm/s represented a realistic criterion, below which architectural damage was unlikely to occur. While failure strain would provide for a more direct criterion, this is not usually done in practice due to numerous complexities and uncertainties. Rather, an upper limit of velocity as a damage criterion is chosen based on empirical data. For some special circumstances, however, a strain calculation is possible and this was carried out for basement walls for which the strains induced by travelling ground waves were found to be well below the cracking strength of concrete.

It has been common practice in previous damage investigations to measure vibration levels at or near the foundation level and to relate criteria to these measurements. This location is satisfactory for short-term excitations and non-resonant conditions for which the amplification from foundation to upper storey is close to 1.0. At resonance, however, the amplification may be 10 or more, resulting in much greater deformations between the footing and the top of the building than those referred to the ground measurements. The criterion of possible damage of 5 mm/s therefore should be applied over the full height of a one-storey building. This is also the position taken in the German vibration standard for buildings, DIN 4150 (1983).

Since it was predominantly ground motion measurements that were carried out here, the ground motion amplitudes that correspond to the criterion for possible damage of 5 mm/s vibration velocity of the superstructure have to be divided by the resonant amplification factor of up to 10. Thus the horizontal ground motion that corresponds to the resonant damage criterion of 5 mm/s is 0.5 mm/s.

3.2 Operative Mechanisms Causing Possible Damage: For a damage mechanism to be considered operative or valid, the response of the structure has to meet or exceed the applicable damage criterion. On the basis of theoretical and experimental investigations conducted here, the following emerged as possible damage mechanisms from train-induced vibrations in the Brocklehurst area:

(a) Horizontal resonance amplifications in houses from ground motion due to trains travelling on the new track at more than 30 mph (50 km/h);
(b) Settlement of mobile home foundations of narrow configuration set on loose wet fill, as a result of train-induced rocking of the footings.

3.3 Distance From Track for Possible Vibration Damage: The ground vibration measurements indicated local variations in ground motion. Attenuation of ground vibration amplitudes with distance from the track takes place due to material damping in the soil. A mathematical model which incorporates this reduction is described in Richart, Hall and Woods, 1970. With this attenuation relationship, the distance was calculated at which the maximum ground velocity observed at 1160 Bentley Place (0.6 mm/s rms - see Figure 4) decreases to the 0.5 mm/s peak ground vibration amplitude. This calculation and an evaluation of area-wide measurements from a previous investigation (Barron and Associates, 1985) showed that, based on the 0.5 mm/s ground velocity criterion, the affected area can be divided into three zones:

- Zone 1: up to 100 m from the track, where exceedance of the 0.5 mm/s ground velocity criterion is likely and relatively widespread;
- Zone 2: from 100 to 250 m from the track, where exceedance of the 0.5 mm/s ground velocity criterion is possible in isolated pockets;
- Zone 3: more than 250 m from the track, where exceedance of the 0.5 mm/s ground velocity criterion is unlikely.

Within Zones 1 and 2, however, damage due to train vibrations need not necessarily have occurred because of variations of material strengths and local attenuations observed along the track and at various distances from the track. Furthermore, not all houses have the same dynamic properties as those measured in this investigation and therefore may not reach the same response level. An on-site inspection and evaluation of each damage claim was therefore required.

4. APPLICABILITY OF RESULTS TO ADJACENT AREAS

This investigation centred mainly on the ground and house responses to train-induced vibrations south of the CN tracks in the Brocklehurst area of Kamloops, B.C. The phenomena of house resonance and soil settlement also apply to the adjacent areas of Rayleigh where excitation and house and soil properties are similar.

4.1 Rayleigh Area of Kamloops, B.C.: It was decided not to take any new measurements of vibrations or soil properties in Rayleigh until the underlying phenomena were better understood. The findings at Brocklehurst were transferred to Rayleigh for the following reasons.

From previous measurements, the vibration intensities generated at Rayleigh by trains on the new track were similar to those on the new track at Brocklehurst. Soil conditions are similar to those at Brocklehurst, both in geologic origin, and type and depth of layering; and the type of wooden houses are comparable, so that the anticipated range of dynamic properties would be similar.

4.2 Other Geographic Locations: The findings of this investigation are applicable only to the Brocklehurst area, and by extension, the Rayleigh area of Kamloops, B.C. since the ground properties, characteristics of track and trains, and building properties can vary from one site to another. However, the methods employed and the mechanisms identified may be applicable elsewhere.

5. RECOMMENDATIONS FOR FUTURE INVESTIGATIONS

This case study demonstrates that commonly used procedures and assumptions employed in investigations of ground-induced vibrations are not always adequate for the following reasons:

- It is common practice to measure only vertical vibrations in the ground and in houses and to virtually ignore the presence of horizontal components. Both can be significant since either can cause resonance; thus both should be measured.
- It is often assumed for attenuation, that ground vibrations originate from a point source. While this may be justified for blasting and other localized sources, for long freight trains a line source is more appropriate. In a perfectly elastic medium a line source does not attenuate with distance from the source, whereas those from a point source attenuate with the square root of the distance.
- Damage criteria for traffic vibrations are often selected from dissimilar types of excitation, e.g. blasting. These do not apply to train-induced vibrations since the frequency ranges and the durations are different, both of which affect the likelihood of achieving resonance.
- Resonance of buildings or their components is rarely considered explicitly. The planning of a program of investigation should deal with the possibility of resonance response.
- The properties of the subsoil are seldom studied. Such a study can produce deformational and damping characteristics which are useful in analysis of the results.

In addition, certain analysis procedures and criteria, which are employed routinely for traffic-induced vibrations, are not always adequate. These include:

- One-third octave band analyses of measured ground and house vibrations should be supplemented by narrow-band spectra. The latter can provide important information about signal characteristics such as frequency shifts.
- Peak vibration amplitudes rather than broadband or third-octave band r.m.s. amplitudes should be used for assessing damage; cracking is a result of exceedance of material strength which is more closely represented by peak vibration amplitudes than r.m.s. or mean value.
- Operative damage mechanisms should be identified in order to understand the problem better and develop strategies about how to avoid it.

These considerations should be taken into account in the assumptions and procedures contained in guidelines or standards for assessing the effects of traffic-induced vibrations in buildings.

6. CONCLUSIONS

Investigations of train-induced vibrations in buildings should consider the following:

(1) Unexpectedly large house response can result from train-induced vibrations due to resonance effects.
(2) Horizontal and vertical vibrations of ground motion and building response need to be considered in investigating traffic-induced vibrations.
(3) Commonly used criteria for vibration damage need to be examined for applicability and suitability. Consideration should be given to frequency range, and duration of excitation, type of structure and materials, and signal description (r.m.s., peak).
(4) One-third octave band analysis should be supplemented by narrow-band spectra for additional information on signal characteristics.

In addition, there is a need for development of improved damage criteria.

7. ACKNOWLEDGEMENT

This investigation was carried out under a contract from Transport Canada and the results are published with their permission.

The cooperation and assistance of the following individuals and organizations is gratefully acknowledged: Railway Freight Policy Branch of Transport Canada; the many home owners and residents in the Brocklehurst area of Kamloops, B.C., who provided access to their properties; CN Rail in Kamloops and Edmonton, who cooperated fully with coordination and scheduling requirements; the City of Kamloops for information on soil conditions; the Agriculture Research Station of Kamloops for providing a "staging area" for the investigating team; and Dr. P.E. Grattan-Bellew of the Institute for Research in Construction (IRC) for mineralogical examination of soil samples. The geological history of the Kamloops area was analyzed by Mr. Roy van Ryswyk, geotechnical engineer, of Delta B.C. The technical assistance by R. Glazer, E.C. Luctkar, T.J. Hoogeveen, A. Laberge, J. Turcotte, and R. Laplante is gratefully acknowledged.

8. REFERENCES

Barron and Associates. 1985. Private communication.

DIN 4150-1983, Part 3: Vibrations in buildings - influence on constructions. German standard, Berlin.

Richart, F.E., Hall, J.R. and Woods, R.D. 1970. Vibrations of soils and foundations. Prentice-Hall Inc., Englewood Cliffs, New Jersey.

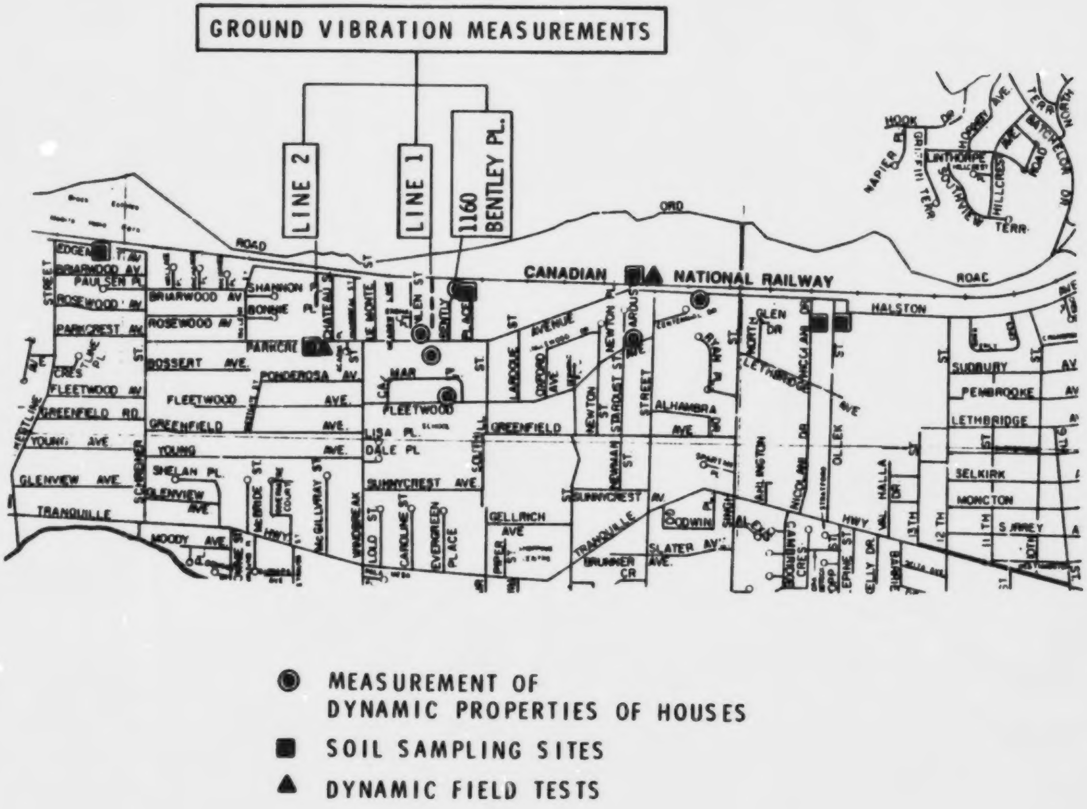

Figure 1: Measurement locations and soil sampling sites, Brocklehurst, Kamloops, B.C., October 1986.

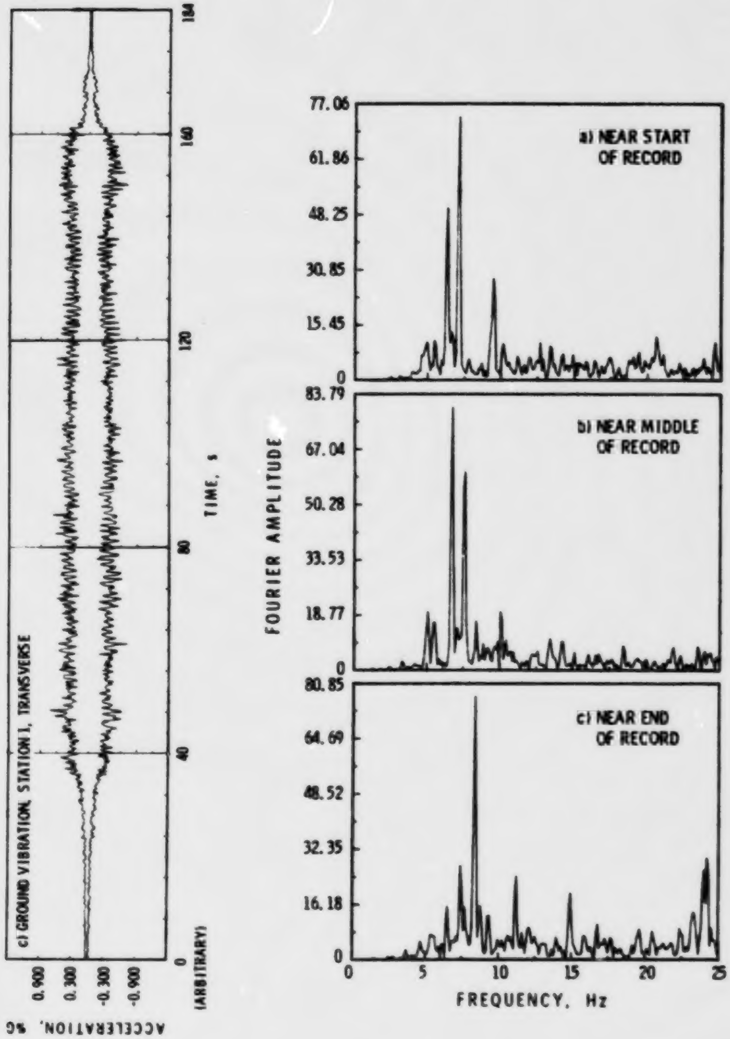

a) Time Envelope

b) Fourier Amplitude Spectra

Figure 2: Transverse ground vibrations at Station 2, Line 1, from Train 5248.

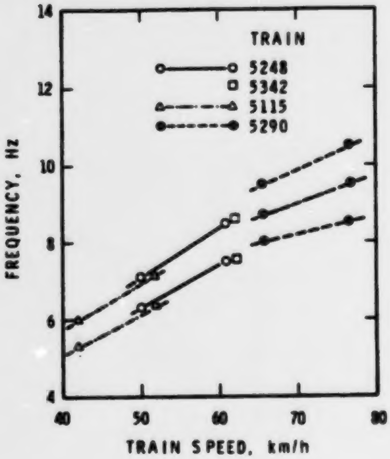

Figure 3: Variation of dominant frequency components in ground motion with train speed.

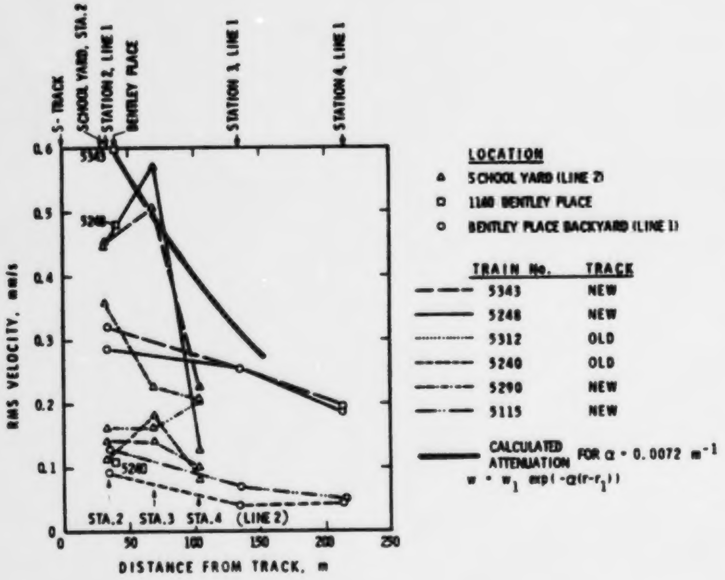

Figure 4: Maximum rms transverse velocities in the 8 Hz one-third octave band for selected train passes.

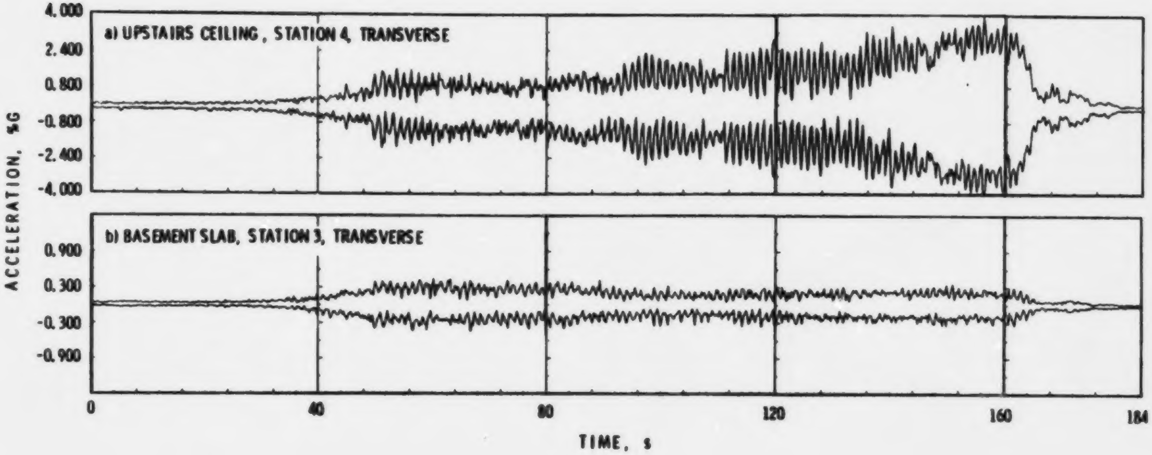

Figure 5: Envelopes of house response from train 5248.

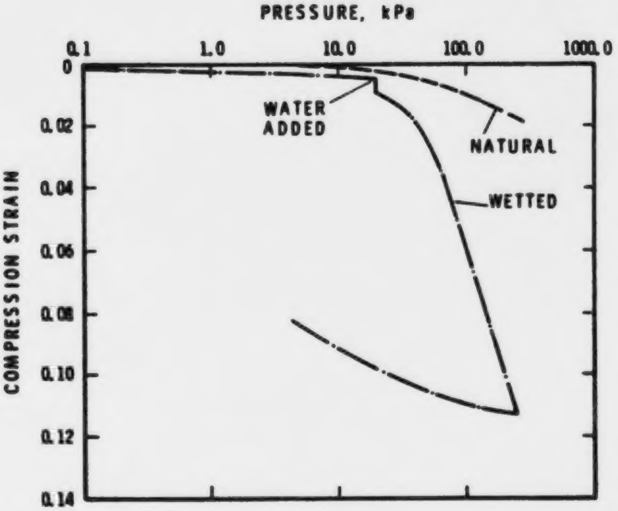

Figure 6: Static pressure-compression curves for soil sample from Bentley Place.

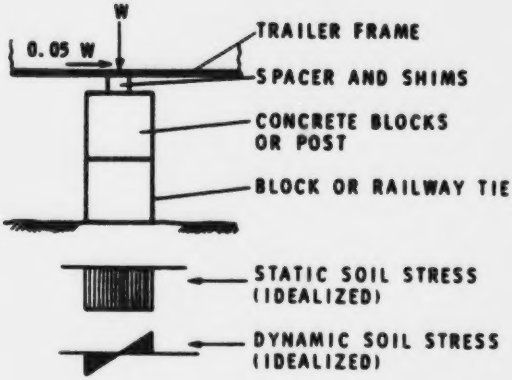

Figure 7: Static and dynamic soil pressure under mobile home footing.

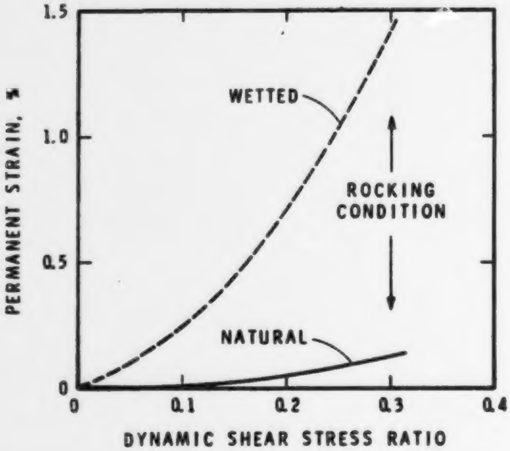

Figure 8: Permanent deformations measured in triaxial test on soil sample from Orchard Trailer Park reconstituted to initial void ratio of 1.25.

CASE STUDY: EFFECT OF RAIL TRAFFIC VIBRATIONS ON JAIL STRUCTURE

Thomas B. Morris

Morris Engineering Company
Dallas, Texas

1. INTRODUCTION

The Jefferson County Jail, Beaumont, Texas, is a four story, steel and concrete structure with plan dimensions of 100 feet (30.5 m) by 172 feet (52.4 m). The structural framing consists of steel columns and beams supporting concrete floors. The exterior curtain wall and interior partitions are made of concrete masonry units (cmu). Granite panels are attached to the exterior cmu walls to provide the exterior facade. Since the jail was completed 6 years ago, numerous items of distress have occurred throughout the building. The most notable items are cracks in the cmu walls.

Located approximately 30 feet (9.1 m) north of the jail are two mainline railroad tracks used by 10 to 15 trains per day. At the time of the investigation, the section of track adjacent to the jail was in a state of disrepair. The ties were rotted, the spikes and joints were loose, abutting rail sections were uneven, and the ballast appeared deteriorated.

2. INVESTIGATION

Three possible sources for the cracking problem were investigated. These possibilities include foundation settlement, shrinkage cracking, and vibrations caused by the rail traffic passing by the jail on the adjacent tracks.

2.1 Foundation settlement: The foundation for the jail consists of a system of spread footings and belled piers placed in an active clay soil. An elevation survey was made of the second floor using standard surveying instruments and techniques. The floor surface was level within expected construction tolerances. Thus, settlement was eliminated as a possibile cause of the cmu cracking.

2.2 Shrinkage cracking: The only candidate for shrinkage cracking would be the mortar between the blocks. Further, this type of cracking occurs shortly after construction and the mortar has set. The cmu blocks themselves have cracked, many of the cracks continue to extend and widen, and new cracks are developing. Therefore, shrinkage cracking is also eliminated as a possibility.

2.3 Vibrations: Due to the nature of the cracks evident in the structure, the possibility of vibrations induced by passing trains was the focus of the investigation. Two identical seismographs (Dallas Instruments, Model ST-4D) were utilized to document the magnitude and waveforms of the vibrations. The primary function of these seismographs are to measure and record the vibrations from blasting activity. Therefore, the peak particle velocity was the measured magnitude.

During a one month period (March, 1987), various combinations of seismograph placements were made to obtain a wide range of data. For instance, one seismograph was placed in the ground adjacent to the tracks while the other was mounted on a second floor wall. Thus the forcing and response vibrations, respectively, were measured simultaneously. Other seismograph placement combinations include ground and floor, and in the ground at different track locations to compare track conditions.

3. RESULTS

The waveforms of the forcing vibrations can be described as basically sinusoidal with regular spaced pulses. The number of pulses per second or pulsing frequency varied from 0.33 hertz (hz) to 8 hz, depending on the velocity of the train. The magnitude of these vibrations were on the order of 0.2 inches per second (5.08 mm/sec). Similarly, the response vibrations were also of a pulsing nature with the magnitude on the order of 0.05 ips (1.3 mm/sec). However, the seismograph sensitivity was too low to precisely compare the waveforms of the response vibrations to the forcing vibrations. In addition to the pulsing frequency, each individual pulse had a much higher frequency - from 18 to 32 hz.

The pulsing nature of the rail traffic vibrations was believed to be the result of the train wheels impacting the uneven abutting rail sections. Therefore, it was recommended that the tracks be repaired. The recommended repair work included reworking the ballast and installing new ties and continuously welded rails. It was believed that this repair work would mitigate the vibrations to a non-damaging level.

Subsequent to the recommendations outlined above, a limited amount of remedial work was performed on the tracks. Most of the rail joints were welded, a few ties were replaced, and the spikes were re-driven. Additional seismic measurements were made in October, 1987, to evaluate the effectiveness of this remedial work. Only the forcing vibrations were measured in the subsequent evaluation. It was deemed not necessary to measure the structural response as in the initial investigation.

No reduction in the magnitude of the vibrations was detected. The seismic readings of the repair work evaluation were equal in magnitude and similar in waveform to that of the initial investigation.

4. CONCLUSION

It was determined that the masonry cracking in the jail can be solely attributed to the vibrations from the rail traffic on the adjacent tracks. Poor track conditions evident in the initial investigation was singled out as the primary factor. The limited amount of remedial work performed on the tracks, however, proved ineffective in mitigating the vibrations.

The natural frequency of the jail was estimated to be in the range of 0.5 hz to 10 hz. Certain components, such as the masonry walls, were estimated to have higher natural frequencies. With forcing frequencies in the ranges of 0.3 hz to 8 hz and 18 hz to 32 hz, there is some overlap with the natural frequency ranges. Therefore, depending on the train velocity and load, it is believed that resonance occurs.

An important factor influencing the response of the structure is the duration of the vibrations. Some of the longer trains take several minutes to pass by the jail. This is ample time for steady-state vibrations to occur.

ON SHOCK EFFECTS IN STRUCTURES DUE TO PILE DRIVING - CASE STUDY

Stanislaw Uminski
Designing Office for Maritime Structures Projmors, Gdansk

and

Zbigniew Cywinski
Technical University of Gdansk
Gdansk, Poland

ABSTRACT: For the design of necessary pile foundations in connection with the construction of a footbridge over an urban thoroughfare, certain simplified approaches related to Polish and German Democratic Republic (GDR) standards have been used to determine the expected hazardous zones of shock effects from pile driving. Therefrom the vibratory response of the particular buildings located near the bridge site was evaluated.

On the basis of certain theoretical calculations and with reference to the actual site conditions and configuration, specified soil conditions, and known characteristics of the pile driver used, the danger zones have been found and the behaviour of the eighteen existing buildings predicted. Because of the prevailing poor structural condition of the majority of the buildings concerned, it was found that the action of the pile driver might cause substantial damage. Consequently, as a preventive measure these buildings should be suitably strengthened. For this eventuality, construction measures have been suggested and admissible amplitudes of structural vibrations established. A test, to drive the piles without the costly preventive strengthening of buildings, showed the correctness of the anticipated performance. As a consequence, for the installation of the piles the initially assumed impact driving technology was then changed to one of drilling.

1. INTRODUCTION

Driving of foundation piles by means of pile driver or vibrator generates para-seismic shocks. Until now the problem of para-seismic waves propagating from such sources is not satisfactorily investigated and documented. The execution of works using pile drivers in built-up areas creates potential danger of damage to structures, caused by generated shocks or settlement and dislodging of the ground. In this report are presented the results of theoretical analysis of hazard caused by the use of the pile driver FUNDEX at the site of a road system connecting the centre of the town with a new housing estate.

2. PRELIMINARY DESIGNS AND THE CONDITIONS OF PILE INSTALLATION

The road system is situated in an area with substantial slope, built-up with apartment buildings. Two level crossings require that several footbridges be built above the road system. The construction of these footbridges is of prefabricated reinforced concrete with foundations on piles of "Vibro" type, diameter d = 520 mm and length l = 7.0 - 10.0 m. Under each bridge head, 18 battered piles with inclination 5:1 and 32 vertical piles are provided. The interbedded subsoil consists of clayey sands and sandy clays, with a consistency of plastic and hard-plastic. A pile driver FUNDEX with drop weight type Delmag D-22-02/03, has been employed. Characteristic of the drop weight is as follows [4]:

weight $Q = 22000$ kN,
energy of blow $E = 55000$ kNm,
frequency of blows $n = 40\text{-}60$/min.

For the installation of the first group of piles in the existing subsoil, the penetration of the pile per blow was 1 mm. The shocks generated during pile driving caused damage in several surrounding buildings. Cracks and fractures of walls and cracks of plasterworks on the ceilings were noticed. The pile driving was then stopped in order to investigate the dynamic influence of pile driving on the existing buildings.

3. ANALYSIS OF EFFECTS OF PARA-SEISMIC SHOCKS ON THE STRUCTURES

Analysis of the propagation of dynamic effects generated by pile driver and influence on the structures was performed on the basis of requirements contained in GDR standard JTB-75 [1], which are the result of investigations made by Forschungsanstalt fur Schiffart, Wasser-und Grundbau-Berlin. The estimation of hazards is based here on the assumption of subsoil vibrations considered acceptable (safe) for given building types, determined experimentally.

3.1 Classification of the structures: According to standard [1], the structures are divided into the following types, depending on their characteristics:

Type I - old structures, ashlar masonry,
- old structures, brick nogged timber wall,
- monumental structures and ruins.

Type II - apartment and office buildings with traditionally built brickwork, wooden floors; structures built of reinforced concrete; large panel and frame constructions; underground construction.

Type II is divided into two sub-types:

Type IIa - structures in poor condition,
Type IIb - structures in good condition,
Type III - industrial buildings constructed of monolithic concrete,
- steel construction,
- highway bridges.

3.2 Danger zones for structures caused by para-seismic shocks: There are 3 zones of danger caused by shocks:

Zone A - no damage,
Zone B - minor damage is acceptable e.g. cracks in the plaster,
Zone C - acceptable damage which does not endanger the stability of the building.

To each zone, according to the number of stories and the height of buildings, the permissible velocities of ground vibrations "V_d" and limit distances "R_g" are assigned (see Table 1). The limit distance closes off the zone of dynamic effects on the site. The range of danger zone determines the permissible distance of the pile driver from the building. According to the type of pile driver and the subsoil conditions, the range of danger zone "R_d" is defined by the formula:

$$R_d = \left(\frac{sf}{V_d}\right)^{1/k} \tag{1}$$

where: s = driving factor depending on pile driver and ground characteristic;
k = factor depending on group type;
f = factor depending on pile-driving procedure. For vertical piles $f = 1.0$;
V_d = permissible velocity of ground vibration.

Shocks caused during battered pile driving with the angle of flare of about 120° (see Fig. 1) have the strongest effect. The range of danger zones for this emission may be assigned according to formula (1) using a suitable multiplier factor "f". For pile inclination to 3:1, $f = 1.5$; to 1:1, $f = 3.0$. Intermediate values should be interpolated.

3.3 The zone endangered by ground settlement: Permissible distance, "R_o", of the pile from a building defines the range of the zone endangered by ground settlement (Fig. 2) according to the formula:

$$R_o = (l-h)\,\mathrm{ctg}\,(45^\circ + 0.5\,\Phi)\,, \qquad (2)$$

where: l - pile length,
h - depth of foundation,
Φ - angle of internal friction of the ground.

3.4 Determining the danger zones: In the region of road system construction are two-storey buildings with height 8.0 m, of types I, IIa and IIb, for which the limit distances according to Table 1 are:

Type I : $R_g = 200$ m
Type IIa : $R_g = 100$ m
Type IIb : $R_b = 40$ m

For the existing conditions of pile-driving, the following mean v[illegible]s of the factors were assumed according to [1]:

$s = 140$,
$k = 0.75$,
$f = 1.2$ for battered piles.

The range of danger zone for particular types of buildings according to formula (1) is:

Buildings type I:

Zone A : $V_d = 3$ mm/s , $R_d = 214$ m assumed $R_d = 200$ m
Zone B : $V_d = 5$ mm/s , $R_d = 108$ m
Zone C : $V_d = 7$ mm/s , $R_d = 70$ m

Buildings type IIa:

Zone A : $V_d = 5$ mm/s , $R_d = 100$ m
Zone B : $V_d = 10$ mm/s , $R_d = 43$ m
Zone C : $V_d = 15$ mm/s , $R_d = 25$ m

Buildings type IIb:

Zone A : $V_d = 10$ mm/s , $R_d = 43$ m assumed $R_d = 40$ m
Zone B : $V_d = 15$ mm/s , $R_d = 25$ m
Zone C : $V_d = 25$ mm/s , $R_d = 13$ m

The diagrams of the envelopes of para-seismic hazard zones are presented on Fig. 3.

4. ESTIMATION OF DAMAGE IN BUILDINGS FROM DYNAMIC ACTIVITY ACCORDING TO ZELLER SCALE AND AN ATTEMPT TO INTEGRATE IT WITH THE GDR STANDARD

According to Polish standard [2] and [3], the estimation of damage caused by shocks and vibrations should be made on the basis of determining the shock coefficient "κ". The degree of hazard is designated in the 8-grade Zeller scale depending on the value of the shock coefficient. The requirements are valid for brick buildings or buildings of frame construction in good structural condition.

The shock coefficient according to [2] is determined by the formula:

$$\kappa = 16\pi^4 n^3 A^2 \qquad [\mathrm{cm^2 s^{-3}}] \tag{3}$$

where: A = vibration amplitude
n = vibration frequency.

The shock coefficient as a function of vibration velocity is determined as follows:

$$\kappa = 4\pi^2 V^2 n\,. \tag{4}$$

On the basis of formula (4) in standard [1] the shock coefficients for admissible vibration velocities of the ground for appropriate danger zones have been determined and assembled in Table 2.

5. CONTROL MEASUREMENTS OF VIBRATIONS

For the control of hazards caused during pile driving, the method based on the measurement of vibration amplitude has been chosen. The vibration amplitude may be presented as a function of vibration velocity, V, or as a function of the shock coefficient, κ:

$$A = \frac{V}{2\pi n} \tag{5}$$

$$A = \frac{1}{4\pi^2}\sqrt{\frac{\kappa}{n^3}} \tag{6}$$

By means of formula (5) or (6) the permissible shock amplitude may be defined according to the required structure protection. Propagation of vibration in the ground according to [3] is defined by the formula:

$$A_r = \alpha A_o \rho \tag{7}$$

where: A_o = amplitude of forced vibrations
A_r = amplitude of vibrations at a distance "r" from the source of vibration
ρ = correction coefficient; for $\alpha < 10$ Hz; $\rho = 2$.

ρ is expressed by the formula:

$$\rho = \sqrt{\frac{r_o}{r}} - 0.4\,\frac{r_o}{r}\left(1 - \frac{r_o}{r}\right) \tag{8}$$

where: r = the distance from the source of vibration

$$r_o = \sqrt{\frac{F}{4\pi}} - \frac{d}{2}$$

where: f = area of pile footing,
d = pile diameter.

For the example of the building situated at distance r = 30 m from the pile driver, the permissible amplitude is calculated as follows:

Assumptions: Frequency of pile driver blows n = 1 Hz, pile diameter d = 0.52 m, r_o = 0.26 m.

$$\frac{r_o}{r} = \frac{0.26}{30.0} = 0.0087$$

$$\rho = \sqrt{0.0087} - (0.4)\cdot(0.0087)\,(1 - 0.0087) = 0.09$$

For zone A and V_d = 5 mm/s the permissible amplitude of ground vibrations near the building is:

$$A_r = \frac{V}{2\pi n} = \frac{5}{(2)(3.14)(1.0)} = 0{,}8 \text{ mm}$$

The permissible amplitude of ground vibrations near the pile driver is:

$$A_o = \frac{A}{\alpha\rho} = \frac{0.8}{(2)(0.09)} = 4{,}42 \text{ mm}$$

6. SUMMARY AND CONCLUSIONS

Eighteen buildings are located in the para-seismic hazard zone as a result of the installation of piles with the FUNDEX pile driver. The envelope of the hazard zone is presented on Fig. 3. Two buildings located in zone C are seriously imperilled and require special protection during pile driving.

Prevention against the effects of the pile driver is very difficult and expensive; therefore, the replacement of driven piles by drilled piles has been recommended.

Estimating the damage caused by dynamic effects to buildings using the Zeller scale according to [2] should be more accurately defined in further investigations. In particular, the range of shock coefficient value depending on the type and condition of the structure and the height of the building should be investigated.

REFERENCES

[1] Rammarbeiten-Berechnungsgrundlagen. Vermeidung von Schaden durch Rammarbeiten, Verkstandart JTB 75. VEB Kombinat Tiefbau Berlin, October 72.

[2] Polish standard PN/B-02170. Estimated harmful influences of vibrations and shocks on buildings.

[3] Polish standard PN-80/B-03040. Machine foundations and supporting structures. Calculation and design.

[4] Bestimmung der Tragfähigkeit für Beton-und Stahlpfähle mit Hilfe der Delmag- Rammformel für D 22-03/03 und D 30-02/03. DELMAG 2 RO 21003/0.

[5] Maciag, E. Interpretation of the building-ground system affected by seismic and para-seismic action. Theoretical and applied mechanics 1979, No. IV, Warsaw, Poland.

Table 1: Permissible velocities of ground vibration "V_d" and limit distances "R_g"

Structure Types	No. of Storeys	Structure Height	V_d [mm/s] Danger zones			Limit Distances R_g [m]
			A	B	C	
I	1 to 2	4 to 8	3	5	7	200
	3 to 4	12 to 16	5	7	10	100
	4	16	7	10	15	65
IIa	1 to 2	4 to 8	5	10	15	100
	3 to 4	12 to 16	8	15	25	55
	4	16	12	20	30	32
IIb	1 to 2	4 to 8	10	15	25	40
	3 to 4	12 to 16	15	25	30	25
	4	16	20	30	40	16
III	1 to 2	4 to 8	30	40	50	15
	3 to 4	12 to 16	50	60	70	15
	4	16	70	80	90	15

Table 2: Shock coefficients "κ" and Zeller scale Z.S.

Structure Types	Danger Zones								
	A			B			C		
	V_d	κ	Z.S.	V_d	κ	Z.S.	V_d	κ	Z.S.
I	3	3.55	II	5	9.87	II	7	19.34	III
IIa	5	9.87	II	10	39.48	III	15	88.83	IV
IIb	10	39.48	III	15	88.83	IV	25	246.7	IV

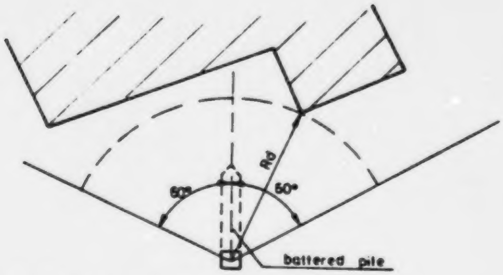

Figure 1: The range of the strongest dynamic emission by slant driven pile

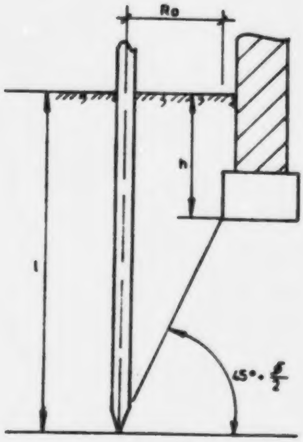

Figure 2: The permissible distance by ground settlement

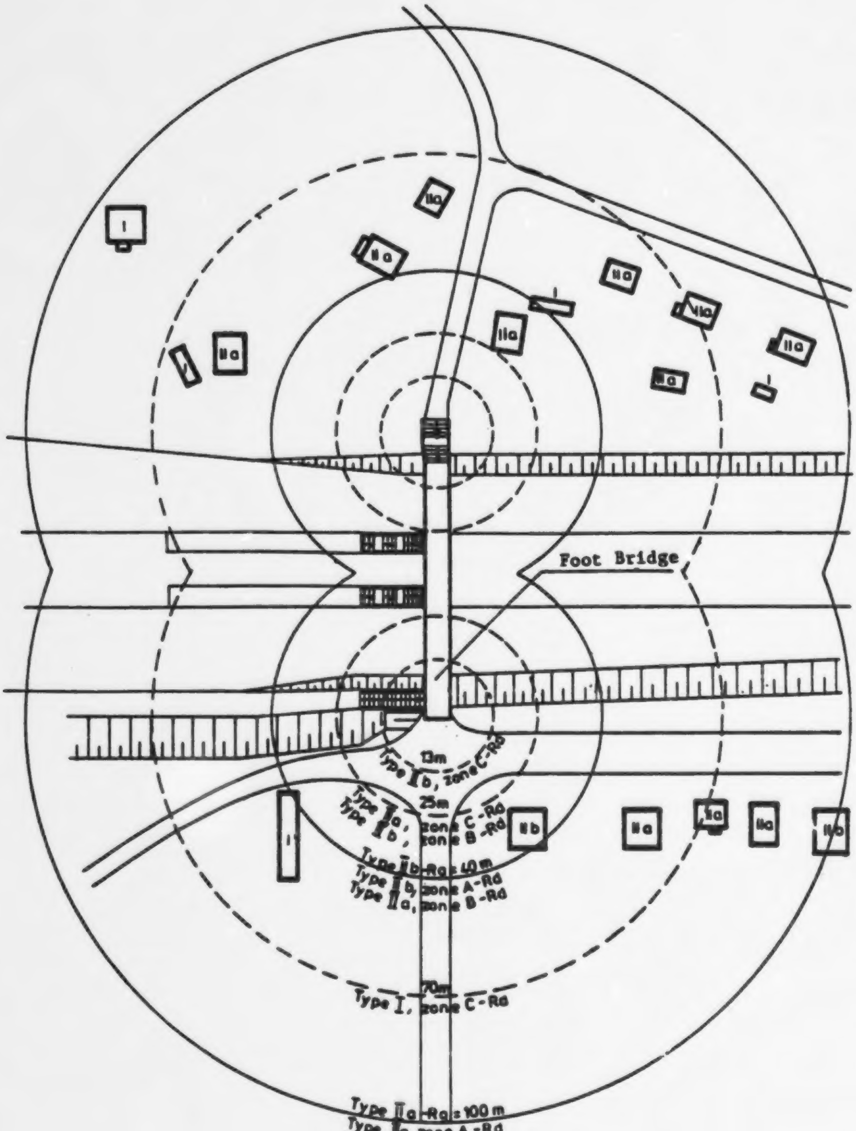

Figure 3: Envelope of para-seismic hazard zones

AUTHOR INDEX/INDEX DES AUTEURS

Page

Al-Noury, S.I. 152
Allen, D.E. 566,603
Allen, D.L. 575
Arumugasaamy, P. 378
Bachmann, H. 419
Bergmann, R. 293
Bljuger, F. 73
Brockbank, R.G. 101
Burghardt, G.J. 112
Burnett, E.F.P. 32
Chaiseri, P. 214
Chui, Y.H. 512,547
Ciesielski, R. 579
Cywinski, Z. 618
Dauenheimer, E.G. 360
Davenport, A.G. 181
Ebrahimpour, A. 451
Eriksson, P.-E. 497
Ferraro, V. 200
Frangopol, D.M. 49
Fujii, K. 228,260
Fujimoto, M. 270
Fujino, Y. 214
Gardner, N.J. 126
Ghosh, S.K. 124
Gillard, R.G. 62
Holicky, M. 19,166
Howe, B. 575
Hust, D.W. 242
Irwin, P.A. 200
Isyumov, N. 181
Itskovitch, M. 526
Jokela, J. 396
Jokinen, E.P. 112
Kanda, J. 260
Kawecki, J. 579
Kelly, P.F. 32
Knoll, F. 91
Kosugi, M. 228
Krywiak, G. 101
Law, K.T. 603
MacGregor, J.G. 3
Maciag, E. 579
Maebayashi, K. 589

Page

Mahmood, K. 152
Masciantonio, A. 181
Matthews, C.M. 465,533
Maurenbrecher, A.H.P. 603
Mehta, M.M. 124
Montgomery, C.J. 101,465,533
Morris, T.B. 615
Murray, T.M. 495
Najdanovic, D.B. 337
Nawar, G. 11
Nemestothy, É 348
Niu, H.P. 406
Ohkuma, T. 270
Ohlsson, S.V. 435,497
Onysko, D.M. 477
Pacheco, B.M. 214
Pernica, G. 566,603
Pinjarkar, S.G. 137
Raghu, D. 360
Rainer, J.H. 566,603
Robins, S. 411
Rosenthal, I. 526
Sack, R.L. 451
Salinas, J.J. 62
Sato, T. 228
Scanlon, A. 112
Schuring, J.R. 360
Shaikh, A.F. 124
Shioya, K. 589
Smith, I. 512,547
Smith, K.N. 86
Sommerstein, M. 323
Stephens, M.J. 101
Stone, G.K. 200
Sun, L.M. 214
Swamy, R.N. 378
Tamura, T. 270
Tamura, Y. 228,260
Tolaymat, R.A. 558
Tomasetti, R.L. 7
Uminski, S. 618
Visnovitz, Gy. 348
Wakahara, T. 228

Volume

2

National Research Council Canada
Conseil national de recherches Canada

PROCEEDINGS
VOLUME II

SYMPOSIUM/WORKSHOP ON SERVICEABILITY OF BUILDINGS (MOVEMENTS, DEFORMATIONS, VIBRATIONS)

May 16-18, 1988

University of Ottawa
Ottawa, Ontario, Canada

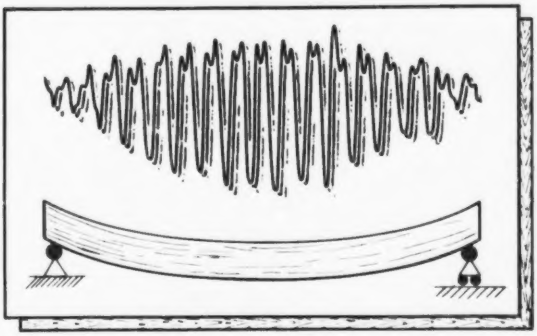

COMPTE RENDU
VOLUME II

COLLOQUE-ATELIER SUR LA TENUE EN SERVICE DES BÂTIMENTS (MOUVEMENTS, DÉFORMATIONS, VIBRATIONS)

16 au 18 mai 1988

Université d'Ottawa
Ottawa (Ontario), Canada

Canada

Sold by:

Publication Sales & Distribution
National Research Council Canada
Ottawa, ON, Canada
K1A OR6

Price: $50.00 (Vols. I & II)

DSS: NR15-31/1988E
ISBN: 0-660-12788-1 (set)
NRCC: 28822

Vendu par:

Vente et diffusion des publications
Conseil national de recherches Canada
Ottawa, ON, Canada
K1A OR6

Prix: 50,00 $ (Vols. I & II)

MAS: NR15-31/1988E
ISBN: 0-660-12788-1 (série)
CNRC: 28822

PROCEEDINGS

VOLUME II

SYMPOSIUM/WORKSHOP ON SERVICEABILITY OF BUILDINGS (MOVEMENTS, DEFORMATIONS, VIBRATIONS)

May 16-18, 1988

University of Ottawa
Ottawa, Ontario, Canada

Editor: D.E. Allen

COMPTE RENDU

VOLUME II

COLLOQUE-ATELIER SUR LA TENUE EN SERVICE DES BÂTIMENTS (MOUVEMENTS, DÉFORMATIONS, VIBRATIONS)

16 au 18 mai 1988

Université d'Ottawa
Ottawa (Ontario), Canada
Editeur: D.E. Allen

ORGANIZING COMMITTEE/COMITÉ ORGANISATEUR

D.E. Allen Co-chairman/Coprésident	National Research Council Canada, Ottawa Conseil national de recherches Canada, Ottawa
J.H. Rainer Co-chairman/Coprésident	National Research Council Canada, Ottawa Conseil national de recherches Canada, Ottawa
R. Bergmann	M.S. Yolles and Partners Ltd., Toronto
B. Ellingwood	The John Hopkins University, Baltimore
R. Green	University of Waterloo, Waterloo/Université de Waterloo, Waterloo
F. Knoll	Nicolet, Chartrand, Knoll & Assoc., Montreal
C.J. Montgomery	The Cohos Evamy Partners, Edmonton
M. Saatcioglu	University of Ottawa, Ottawa/Université d'Ottawa, Ottawa

SPONSORS/ORGANISMES PROMOTEURS

Institute for Research in Construction, National Research Council Canada/
Institut de recherche en construction, Conseil national de recherches Canada

University of Ottawa/Université d'Ottawa

Canadian Society for Civil Engineering/
Société canadienne de génie civil

American Society of Civil Engineers

Canadian Group of the International Association for Bridge & Structural Engineering/
Le groupe canadien de l'Association internationale des ponts et charpentes

International Council for Building Research (CIB)/
Conseil international du bâtiment pour la recherche (CIB)

SECRETARIAT/SECRÉTARIAT

Mike Boroczki
Conference Services/Service des conférences
National Research Council Canada/Conseil national de recherches Canada
Ottawa, Ontario, Canada K1A 0R6

Telephone/Téléphone: (613) 993-9009
Facsimile: (613) 957-9828
Telex/Télex: 053-3145

PREFACE

Lighter and more flexible building structures with fewer non-structural attachments have resulted in an increasing number of problems associated with movements, deformations and vibrations.

The Symposium/Workshop brought together designers, builders and researchers to review current experience with such problems, to exchange knowledge for avoiding such problems, and to make recommendations for the future. Volume I of the proceedings contains papers prepared for the symposium. This volume contains discussion and recommendations from workshop sessions, plus two additional papers, one containing additional case studies of floor vibrations and the other on the control of building vibration from ground-transmitted excitation.

The Volume starts with "Pay Now or Pay Later" summarizing a lively panel discussion on quality assurance.

PRÉFACE

L'avènement de structures de bâtiment plus légères et plus flexibles et comportant mains de pièces de fixation non structurales a donné lieu à un nombre croissant de problèmes associés aux mouvements, aux déformations et aux vibrations.

Le présent colloque-atelier met en rapport des concepteurs, des constructeurs et des chercheurs pour passer en revue l'expérience acquise jusqu'à ce jour en ce qui a trait à ces problèmes, pour échanger les connaissances acquises récemment pour éviter ce genre de problèmes et pour faire des recommandations pour l'avenir. Le volume I du compte rendu contient toutes les communications préparées pour le colloque. Le présent volume renferme les discussions et les recommandations découlant des séances d'atelier, ainsi que deux autres communications, l'une d'elle décrivant des études de cas supplémentaires sur les vibrations du plancher et l'autre portant sur le contrôle des vibrations causées par des excitations transmises par le sol.

Le volume débute par un résumé d'une discussion en panel animée sur l'assurance de la qualité s'intitulant "Payer maintenant ou payer plus tard".

TABLE OF CONTENTS/TABLE DES MATIÈRES

Page

Organizing Committee/Comité organisateur ii
Sponsors/Organismes Promoteurs ii
Secretariat/Secrétariat ii
Preface/Préface iii

Pay Now or Pay Later
R.G. Brockbank 1

Introduction to Workshop Discussions
D.E. Allen 4

Workshop A - General Serviceability 6

Workshop B - Deflections and Cracking 11

Workshop C - Wind Induced Vibrations 14

Workshop D - Differential Movement 17

Workshop E - Vibrations from Human Activities 21

Workshop F - Ground-transmitted and Machinery Induced Vibrations 25

Floor Vibrations - Two Case Studies
R. Cantieni 29

Control of Building Vibration from Ground Borne Excitation
D.L. Allen, [illegible] Howe 41

List of Participants 55

PAY NOW OR PAY LATER

by

R.G. Brockbank
PCL Construction Ltd., Edmonton, Alberta, Canada

Designers, owners and contractors should function as a team whose principal objective is to produce a serviceable building at an acceptable cost, within a reasonable time and in conformance with clearly stated requirements for quality. In return, each member of the team should expect to receive a fair profit proportional to effort and achievement.

Unhappily, this team approach is not often working as it should. Most of the problems in a team approach are caused by four factors:

1. The highly competitive nature of today's economic climate;
2. The narrow scope of the team members' interest;
3. The increasing scale and complexity of today's projects;
4. The lack of basic honesty among the players.

In today's difficult economic situation, designers often contract with the owner for less than full fees and, therefore, must do less than a complete job of the design so they can make some profit on their work. The contractor has now been squeezed to where the average builder makes a profit of less than 1%. All parties have to scramble to survive and have no surplus funds to help each other out of the inevitable design and construction problems that occur. We must all work to prove to the owner that, basically, he gets what he pays for.

A small increase in the bottom line for the designers and contractors pays handsome dividends in the end product the owner receives. Today, all members of the team play a charade - pretending they can deliver more than they intend to. We must state clearly and honestly what we mean - and be prepared to live with the costs of this clear definition.

Construction is based on a three party adversarial system where conflict between the owner, designer and contractor is encouraged by each party's narrowly defined and separate areas of responsibility. This is particularly evident in the area of innovation. Typically, the owner does not know how to encourage it. The designer is afraid of it because of potential liability and the contractor sees little immediate value because the low bidder gets the job.

The owner, designer and contractor can work effectively as a team to create an atmosphere that puts effort up front where it is needed. This is a far better solution than attempting to solve problems after they occur.

A quick look at a few of the problem areas may help to demonstrate some of the difficulties and may suggest possible solutions which would benefit all parties and which would result in more serviceable buildings.

CASE I

The owner may succeed in driving design fees to very low levels in a competitive market place. Carried to extremes, this can result in a less completely detailed design for the contractor or an over-designed project for the owner. This penny wise, pound foolish practice needs no further comment.

CASE II

The owner may elect to cut costs by omitting some inspection services by the designers. The contractor is then assigned these responsibilities by default. Not all contractors are capable of performing these functions effectively. The results of this process can be expensive in the long run.

Independent inspection of the manufacturing of precast exterior wall panels was omitted to save initial cost. The precaster was made responsible. He went broke about half-way through the work.

When the work was resumed by another precaster, the original work was found to have significant hidden structural defects. The costs of remedial work far outweighed the saving from the omitted inspection. Another question is posed by this example. What if the problems had not been caught before the panels were erected?

This example also demonstrates the problem of narrowly defined areas of responsibility. The structural engineer for the project had no assigned responsibility for this so-called "architectural" work other than for the connections to the building frame.

CASE III

The designer may specify tolerances that can only be achieved at great cost and which are far more stringent than necessary. The contractor then, in order to remain competitive, must decide what degree of compliance will actually be required.

An office building was designed with a structural steel frame, employing the stub girder framing system. The specifications contained no warning to the bidding contractors of the frightful consequences that ensue with this composite framing system. The specifications cited the CAN3-A23.1-M77 standard for floor tolerances. The successful contractor had to provide significant shoring during construction. The behaviour of the frame after construction made the tolerances impossible to achieve. The result of this was a shoring cost in excess of $1 per square foot, a remedial cost of $0.75 per square foot to level the floors and a reduced allowable live load for the floor, negating any possible savings for this innovative design.

CASE IV

The designer may be uncertain and may want to protect his position by getting others to assume his responsibilities. This may be done by adding a performance requirement to the specification, detailing how and with what something is to be done and how it is to perform. While this does appear to offer the designer some protection, it creates major problems for the owner and for the contractor.

A recent building design featured an attractive composite exterior wall system that could not possibly ever work properly. The bidding contractors had 12 working days to price the 40 million-dollar project. Most of the contractors were unqualified to recognize the design faults inherent in the design. The designer had incorporated a performance requirement for this wall system that effectively transferred financial responsibility to the contractor.

The successful contractor completely redesigned the wall resulting in a significant cost-saving and a wall that works. Who should be the designer?

CASE V

Minor substitutions deter achievement of quality and safety and put unnecessary pressure on designers, who are seldom reimbursed for the additional reviews required. The first meeting after the presentation of the budget for a project always deals with the developer's problem of getting the budget down to match the developer's proforma.

The contractor and his subcontractors then prepare a comprehensive shopping list of potential savings. This is called "value engineering". The designer then must spend a very considerable effort in wading through this material and evaluating it. Often, incorrect decisions result due to the attractiveness of immediate cost reduction and ignoring the long term cost impact.

CASE VI

The shop drawing process has evolved into a dangerous adventure.

In the past, shop drawings were thoroughly reviewed and responsibility for the review was taken. Today, the word "approval" has been forbidden by the legal advisors. We must be accountable for our actions and must stop trying to escape our responsibilities with cleverly constructed "weasel" clauses or the courts may decide the matter for us.

The Hyatt disaster in Kansas City serves to illustrate this point.

CASE VII

Fast track construction offers many benefits to the owner of the project. However, this process accentuates the problems described before.

The members of the team are only willing to accept responsibility for their own specific area. This leads to the current situation where things are starting to fall between the cracks.

It is essential that we change our direction and encourage an effective team approach. We must pay attention to detail. We must get back to the basics. A satisfactory building benefits everyone involved. We must recognize that if we don't pay now then we will have to pay later and more. An ounce of prevention is still better buy than a pound of cure, even at today's prices.

Introduction to Workshop Discussions

by D.E. Allen

There are a wide variety of building problems associated with movement, deformation and vibration of the building structure, and an even wider variety of design and repair solutions. Table 1 summarizes problems associated with structural deformation and indicates design approaches in preventing their occurrence, either by controlling structural movements by means of design criteria or by detailing (or construction procedures) to accommodate their effects.

Six workshops were held during the symposium devoted to the satisfactory performance of buildings as related to structural design. Topics included general serviceability, deflection and building vibration due to wind, human activities, machinery and ground-transmitted sources such as transportation and blasting. The following pages contain summaries of the workshop discussions and recommendations.

There was a common thread to many of the recommendations. These can be summarized as follows:

- Structural serviceability problems are becoming more widespread in practice due to changes in the design and use of buildings and adjacent transportation systems, as well as quality control problems associated with changing construction procedures.
- There is a need for better guidelines for structural practice containing recommended criteria which allow flexibility in application.
- Two-tiered criteria are needed: simple criteria to cover buildings in general (e.g. beam or slab deflection, walking vibration, lateral wind deflection), and more detailed criteria (possibly contained in Appendices) to take care of special problems (e.g. cantilevers supporting brick walls, floor vibration due to rhythmic activities, wind-induced motion in high-rise buildings).
- Criteria depend not only on physical phenomena (summarized in Table 1) but also on the expectations of users of buildings. Both aspects need to be addressed as indicated by the following diagram:

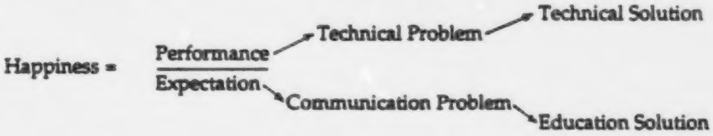

- Better communication is required between team players in any project (See "Pay Now or Pay Later"); communication between the designer and owner of the building is especially important.
- Reliable feedback is required to ensure that lessons learned are well-covered by the guideline information used by the design engineer.

TABLE 1. A SUMMARY OF PROBLEMS ASSOCIATED WITH STRUCTURAL DEFORMATION AND THEIR PREVENTION

	Problems with	Repair Cost	Prevention by: Design Criteria	Prevention by: Detailing, Construction Procedures	Give special attention to:
A.	*DEFLECTION AND ROTATION*				
1.	Cladding	C	✓	✓✓	cantilevers, shrinkage, creep or differential temperature
2.	Partitions	NC to C	✓	✓	long spans, wind distortion in tall buildings
3.	Roof	C	✓	✓✓	ponding, cantilevers, prestress, slab rotation at supports
4.	Floor	NC to C		✓	brittle finishes, differential deflection of adjacent members, unintentional supports or restraints
5.	Aesthetics	C	✓	✓	long spans, differential deflection of adjacent members
6.	Equipment	C	✓	✓	crane girders, overhead cranes, elevators
7.	Construction	NC to C		✓	differential deflection of adjacent members
B.	*DIFFERENTIAL MOVEMENT*				
1.	Cladding	NC to C		✓✓	masonry veneer, change in supports, roof expansion
2.	Roof and Top Storeys	C to VC		✓✓	shortening of tall concrete buildings and wood-stud walls
3.	Partitions	C		✓	shortening of prestressed planks
4.	Finishes	NC		✓	brittle finishes on concrete surfaces
5.	Services	NC		✓	vertical pipes in tall concrete buildings
C.	*DIFFERENTIAL SETTLEMENT*				
1.	Cladding	NC to VC	✓	✓	varying ground conditions, uncompacted backfill
2.	Partitions	C		✓	moisture sensitive clay soils under houses
3.	Services	NC		✓	ground-building junction
D.	*VIBRATION*				
1.	Annoyance	NC to VC	✓		sensitive occupancies, long spans, flexible frames
2.	Equipment			✓	location and isolation of sensitive equipment
3.	Building fabric	NC to C	✓		blasting
4.	Motion-induce noise	C		✓	very tall buildings

Notes:

NC	costs associated with minor repair or relocation
C	costs associated with major alteration of non-structural components
VC	costs associated with major alterations - structural and non-structural
✓✓	signifies extra attention to detailing and construction procedures

WORKSHOP A - GENERAL SERVICEABILITY

Session Chairman: R. Green
Workshop Report by: B.R. Ellingwood

Introduction

As a structural design problem, serviceability is concerned primarily with structural movement in the vertical and horizontal directions. This movement may be either static or dynamic in nature and may arise from loads due to building occupants, environmental effects such as wind, and self-straining actions of temperature, creep, shrinkage or differential settlement. Experienced structural designers have always known that they must provide in some way for serviceability to ensure a building that is functional as well as safe. And yet, they are unable to agree on what constitutes a serviceability limit state (unserviceability), how one can calculate it, who is responsible, and whether codes of practice should incorporate specific serviceability checks.

Participants in the workshop on general serviceability considered a number of issues, including the definition of serviceability; the scope of serviceability problems in modern building construction, including those trends that may cause them to increase; treatment of serviceability issues in current codes of practice; and future needs and recommendations. The following summary is organized about those points.

Unserviceability in Modern Construction

There was general agreement that serviceability is a significant issue and one that designers must consider in order to ensure adequate building performance. Partial or total structural collapses are (fortunately) rare. Instances of unserviceability comprise the majority of those problems requiring remedial action during the life of a building. Having agreed on these points, however, unserviceability proved difficult to define in a precise way. Serviceability appears to be as much an economic issue as a technical one; if a problem with a building is not costly to fix, it may be handled by routine maintenance rather than as a serviceability limit state that warrants explicit treatment in design.

Several trends in modern design and construction point toward serviceability being an increasing concern for engineers and architects. First, members are getting smaller and structures are becoming more flexible as a result of the use of high-strength construction materials, higher stresses at service loads and well-integrated structural systems. Second, new construction materials and components are continually being introduced and construction tolerances are changing. These new materials may be oversold in the market place before there is adequate experience with their service performance. Third, the use of traditional materials and components is continually evolving. Problems occasionally occur when these traditional components are adapted to modern technology or are used in non-traditional applications. One example involved a dressed stone building facade. Modern technology permitted the stone panels to be cut very thin. After the facade panels had been attached to the building, they distorted excessively and had to be downsized and re-attached at considerable expense. There had been no previous problem with this material in thicker sizes. Engineers and architects should know their materials well. Unfortunately, material science and the general interfacing of building components usually receives cursory attention in education and later in design.

Participants in this workshop did not reach a consensus on what precisely are the most significant serviceability problems in modern construction. Several participants mentioned serious serviceability problems in parking garages due in large part to the corrosive effects of chlorides used in de-icing. Cracking of concrete members and objectionable sagging or vibration of long-span floors were mentioned. The participants felt a need for improved construction practices and quality assurance and control programs to ensure acceptable building performance in service. However, it was generally agreed that a distinction should be made between quality assurance and serviceability; that while these share common features, they should be addressed separately in the design and construction process.

The fact that engineers are not trained adequately to deal with all facets of the serviceability problem was a recurrent theme. Engineering education is aimed at analyzing strength of individual members. One must consider the behaviour of the system as a whole to ensure serviceable performance. Many serviceability problems occur when construction materials and products are mixed on a project; evaluation of frame-cladding interactions, for example, requires that their performance as a system be considered.

Serviceability appears to be related closely to the expectations of the owner and building occupant regarding performance of the building, viewed as a consumer product. If the structure is thought of as a shelter, expectations generally are higher and the threshold of unserviceability is lower. The expectations of individuals differ, of course, which makes specific serviceability limits difficult to identify for code purposes.

Consumer expectations concerning performance of buildings are increasing as they have been with other consumer products. This increase in expectation affects the definition of unserviceability. There is a tendency to use the courts in resolving disputes. This increase in litigation affects the attitudes of engineers toward the need to consider serviceability in design. Paradoxically, at the same time there is pressure to remove serviceability requirements from codes. It is inappropriate to leave the resolution of serviceability issues to the courts, where they will be decided in a nontechnical context. There is a danger of this happening if the profession does not address the serviceability issue responsibly.

Serviceability in Current Codes

Treatment of serviceability in current codes and standards is uneven. Some requirements are in the form of deemed-to-satisfy clauses, such as span thickness ratios for slabs. Most two-way concrete slabs that have had deflection problems have failed to satisfy these minimum thickness requirements, so for the most part, these clauses have worked well. Specific requirements in the form of deflection limits as a percentage of span or storey height focus on minimum structural stiffness. These provisions also are satisfactory, provided that the unserviceability arises from excessive flexibility of the structure under static load. However, deflection limits are not always useful. They work poorly for cantilevered construction, for example, and are not meaningful when the building function is not hindered by deflections in excess of the prescribed limit. Moreover, they may be inadequate for serviceability problems related to vibration involving factors other than, or in addition to, stiffness.

Workshop participants agreed that serviceability guidelines ought to appear in some design document, but there was no consensus on which design document should contain them. Codes customarily address issues of public health and safety, and serviceability is more an economic than a safety issue. Options discussed ranged from including minimal mandatory serviceability requirements in the code itself, including such requirements in non-mandatory commentaries to the code, or including them in companion reports that are not part of the codes. The appropriate document might depend on the national or local building authority and regulatory climate. In countries where the building code is not a legal document, for example, there might be less resistance to incorporating serviceability requirements in the code itself. In the United States, on the other hand, sentiment is very strong against placing mandatory serviceability requirements in codes. By requiring serviceability limits to be enforced by code officials, the engineer/architect would lose much of the present flexibility in dealing with serviceability problems, which impact building economics more than safety.

From the designer's viewpoint, there is a professional obligation to provide for serviceability. While competent designers recognize this, it was observed that many designers do marginal work under pressures from developers to cut costs. Thus, the view was expressed that the code should contain some minimum requirements for all buildings that could be used in lieu of more involved calculations of unserviceability. For most buildings, code provisions consisting mainly of deemed-to-satisfy clauses would be adequate. With an additional accent on proper detailing, problems such as concrete cracking could be controlled without having to calculate maximum crack widths explicitly. An example of this indirect approach to serviceability checking is British Standard BS 8110.

The Evaluation of Serviceability Limit States

Problems in evaluating building serviceability were addressed by several of the papers presented during the day and in the workshop. Identification of appropriate serviceability limit states is not an easy task, as perceptions concerning what is acceptable performance differ from individual to individual. Often there is not a clear connection between building performance requirements set by the owner or architect and the structural response quantity needed to ensure adequate performance. Accurate computation of structural response is needed for comparison to serviceability limits when the latter can be agreed upon. In some instances, the computation of structural response with sufficient accuracy to make such serviceability checks meaningful may be difficult, e.g., deflections of reinforced concrete structures where creep, shrinkage and similar long-term effects are taken into account. Suitable structural loads and load combinations must be identified for serviceability checking. The load levels used in safety checks seldom would be appropriate, but it is still an unresolved question as to how much they should be reduced.

Future Needs and Recommendations

It was generally agreed that current procedures for dealing with serviceability need to be improved. Rather broad guidelines in the form of simple deflection checks help engineers avoid many troublesome situations simply through providing minimum structural stiffness. Although more comprehensive serviceability guidelines are needed, it is not practical or feasible to address each serviceability concern explicitly.

One of the most difficult and important tasks is taxonomic in nature, i.e., to define and classify serviceability limit states and to relate them to building performance requirements. This general classification ought to take place outside any of the material specifications. Serviceability checks that work well with one construction material may not be satisfactory for other materials. Moreover, problems may arise when materials are mixed without due regard to their different properties.

The method of implementing serviceability criteria in design must be decided. Options range from general performance requirements to prescriptive criteria, such as deflection or drift limits, span-to-depth ratios, and similar deemed-to-satisfy provisions. Most of these address the structural stiffness either directly or indirectly. There is a suspicion that some deemed-to-satisfy clauses are on the verge of being ineffective for new construction. Consideration should be given to devising a two-tiered serviceability criteria. The lower tier would consist mainly of deemed-to-satisfy provisions and would apply to the majority of ordinary buildings. The higher tier would contain a set of performance requirements and would require more complex checks of structural response quantities. Sensitivity studies would have to be performed to identify those classes of buildings and serviceability limit states requiring use of the higher tier provisions.

More thought needs to be given to the selection of structural loads and load combinations used in serviceability checking. The loads should be related to the nature of the limit state. Different loads probably should be used for checking permanent or irreversible limit states than for temporary, reversible limit states. Moreover, different load models are required to analyze deflection and vibration limit states.

Responsibility for serviceable buildings ought to be shared jointly by the structural engineer, architect, building contractor, and owner/developer. Many serviceability issues are best addressed at the conceptual or preliminary design stage, but the structural engineer may not become involved until later, when many of the parameters have already been determined. One participant noted that architects seem to be more concerned with the external appearance of the building than with its function. Such attitudes must be changed to enhance building performance.

Design codes are written with a limited amount of information. Feedback on code provisions is important; it is especially so for serviceability provisions, where there is a lack of agreement on exactly what constitutes unserviceability. Mechanisms need to be set up to obtain this feedback from practicing engineers on a regular and consistent basis. Those provisions that no longer are effective should be removed from the design codes.

Concluding Remarks

The workshop participants agreed on the following general points:

(1) Serviceability is easy to identify in the abstract as a problem requiring consideration in design but is difficult to deal with by specific prescriptive requirements.

(2) Most of the problems requiring attention in buildings are serviceability problems by definition, inasmuch as safety seldom is a consideration in a completed building.

(3) Serviceability limit states should be identified in codes and ought to receive further consideration by architects and engineers.

(4) Serviceability requirements should be reasonably flexible and should enable engineers to pursue a range of options in building structural design.

There was only limited discussion of specific serviceability measures, as these are difficult to identify outside the context of specific construction types at the present state-of-the-art. Serviceability limit states arising from deflections and differential movement and from vibrations due to occupant activities, wind and machinery are covered in other workshops.

WORKSHOP B - DEFLECTIONS AND CRACKING

Session Chairman: F. Knoll
Workshop Report by: F. Knoll and H. Bachmann

General Considerations Regarding Serviceability Problems

Serviceability defects such as deflections or the often related cracking can be evaluated in different ways reflecting different aspects of the problem:

The Owner's View

In the perception of the owner (buyer) of the product, i.e. the building or structure, deflections and cracks represent quality defects.

Perception and evaluation on the other hand, depend very much on the degree of pertinent information of which the owner is possessed, as well as many other influences. It is clear that, for example, a particular deflection value does not mean the same in different circumstances.

A deflection is of little concern as long as it can not be perceived by the human senses or does not cause trouble with building functions.

A crack of 1 mm width takes significance only when it causes leakage, or when it remains exposed to view. Sandblasting will dramatically exaggerate unsightly appearance or will even make cracks visible which were not before.

Excessive deflections or cracks may be perceived, rightly or wrongly, to indicate a lack of durability or safety which then becomes a public concern. What is perceived as excessive varies from case to case, depending on visibility and sensitivity of the viewer, in addition to the physical reality. Even matters unrelated to the structure, such as trouble with other structures, juxtaposition with similar but unrelated objects, colour, texture, or the geographical and social context may have their influence and may have to be considered when gaging the deflection behaviour of a proposed design, as far as it is predictable.

Compatibility

Besides the more intangible elements of perception such as unsightliness, an important relationship exists with other building elements such as doors, cladding, partitions, drainage, machinery, etc. To be compatible with the rest of the building components, a structure must not exceed certain limits of deflection which depend on the particulars of each case. On the other hand, the other building components may - perhaps at some expense - be adjusted in order to establish compatibility (modes of attachment, flexible joints, adjustment in case of long term movements, etc., with a deflecting structure). The establishment of compatibility and deflection behaviour then amounts to an optimization task which is part of the conceptual design. In particular, this means for the structural engineer, that he must participate and contribute to the concept of the building because it is his responsibility to share the information he (alone) possesses with the other members of the design team, as well as with the owner.

The view that deflection behaviour is part and parcel of the design concept, and therefore must respond to compatibility criteria, does not correspond with the traditional way that codes treat the subject of serviceability criteria, i.e. by stating numbers or expressions largely irrespective of the circumstances in which they will be used (e.g. deflection less than span/360).

There are, however, ways to accommodate this apparent contradiction, as for example by adding commentaries to Code rules. In the discussion it was felt that both aspects, i.e. simplified numerical rules as well as general requirements of compatibility, should be addressed by codes in the future. No unified numerical values necessarily apply in all countries, since building methods and quality expectations are different.

Also, the same deflection to span ratios do not appear to be appropriate for all span lengths.

Expectations and Performance

Owners (and other consultants) may not be aware of the laws of physics relating to deflection and cracking of structures. Expectations may therefore be unrealistic. It is the task of the consulting engineer to rectify the situation, explaining circumstances and relationships between design decisions, construction methods and effects, including uncertainties with the prediction of the behaviour of a building before it is built.

It is important to establish a reasonable equilibrium between expected and perceived performance and quality aspects. An informed client is a better client: After all, most clients still prefer to make the right decisions rather than prosecute the builders for inducing them to take the wrong ones.

Uncertainty

Substantial uncertainly exists in the prediction of deflection and cracking. Many important effects and parameters influencing serviceability behaviour cannot be accounted for in calculations, such as early loading or other features of construction history. Numerical methods based on stiffness values of concrete structures in many cases fail to yield predictions of real behaviour with useful precision. General experience must then be called upon to supply design criteria in some form, such as span/depth ratios or extrapolation from similar cases.

The trend to greater economy through reduction of material quantities has generally led to structures more susceptible to serviceability problems. This implies that all considerations cited previously are becoming more urgent and important. As more and more quality aspects become a matter of choice rather than of course, consciousness about these same matters must increase. It is doubtful whether codes can, by simply stating limits and citing calculation methods for serviceability related behaviour, provide a protective screen for designers and owners, especially in the adversary climate of North America. Great pressure may be directed towards engineers by profit-conscious clients, to dispense - largely at their own risk - with criteria stated in codes, and reduce dimensions to less than those stated by codes and handbooks which cannot, after all, protect a builder who does not want to be protected.

When stating deflection criteria, codes must indicate that uncertainties exist in order to remind the user that reality will differ from the models used for design and analysis.

WORKSHOP C - WIND INDUCED VIBRATIONS

Session Chairman: P. Irwin
Workshop Report by: P. Irwin, Masciantonio and J. Kanda

General

In this workshop, the design of buildings against wind-induced vibrations was discussed. Tall buildings are affected by wind-induced motions or vibrations in several ways. The motions can result in excessive deflections which may cause cracking of partitions or may result in problems with the exterior wall system. The deflections, particularly in torsion, may also be visible to occupants, causing them concern. The accelerations in buildings can be felt by the occupants in some cases under strong wind conditions and lead to dissatisfaction of tenants.

In this workshop, one objective was to discuss current criteria for acceptability of wind-induced vibrations that designers should try to meet. To meet given criteria, designers need methods of predicting at the design stage what the building's response to wind will be. Wind tunnel testing can be undertaken to do this, but for most buildings and for preliminary design an analytical approach is used based on formulae such as those in the Commentary to the National Building code of Canada (NBCC). During the workshop the use and accuracy of such formulae were discussed.

Finally, the important topic of how to reduce building motions was discussed. This discussion included tuned mass dampers, viscoelastic dampers, the increase of building stiffness and the recent application of tuned liquid dampers.

Criteria

Discussion began on the subject of what is the appropriate reference period to use when specifying criteria for building vibrations. One year was suggested as a reference period, e.g., the criterion for motion could be stated in terms such as the "probability of exceeding a particular acceleration level should be not more than 10% in one year". People find it easy to relate to a period of one year. Another popular measure is the return period wind speed that is given in the code, e.g., 10, 30, 100 years in the National Building Code of Canada. The two are related: a 10 year return period is in fact equivalent to assuming a probability of 10% in any one year. It was also suggested that the measure be expressed in terms of the number of hours per year that a given acceleration is exceeded.

The use of static deflection limits, e.g. height/500, was also discussed. How useful are they? Static deflection criteria are necessary for design of cladding and other secondary elements but are difficult to use for human comfort considerations. The appropriateness of a given deflection criterion depends on the nature of the secondary building elements. Therefore, while an all-encompassing deflection criterion has its limitations, some kind of deflection criterion is still necessary for each building. It was generally agreed that for the building components themselves, deflection criteria are needed but for human perception accelerations were more relevant.

Torsional building movements are more easily perceptible than sway movements and therefore more disturbing. It was agreed that torsional movements and other types of visual cues are subject areas requiring further research. Visual cues could be important in the light of the fact that physiological research has shown that visual cues alone could induce motion sickness, especially at low frequencies typical for tall buildings. How criteria might be adjusted to reflect people "learning" to accept or not accept motions, (the psychological factor), also needs study.

There is also a need to involve the building owner in decisions concerning building motions. If the owner wants a higher quality building and is prepared to pay the extra cost then the vibration criteria used could be made more stringent. A basic minimum standard to be met by all buildings will still be necessary to protect building occupants because some owners may be influenced more by economic considerations and because of the ownership possibly changing hands. Also owners do not necessarily understand the significance of the criteria.

Criteria for motion perception could be affected by differences in culture and attitudes from country to country. This raises a question: Is the International Standards Organization (ISO) approach of unification appropriate, considering these differences?

Formulae in NBCC Commentary for Estimating Acceleration

It was shown that the formulae currently in the NBCC Commentary frequently lead to overly pessimistic estimates of acceleration, as was evidenced in the paper of Irwin, Ferraro and Stone, and that this sometimes leads to building structural designs, particularly steel designs, dying on the drawing board before ever being wind tunnel tested. It was therefore recommended that the formulae be replaced by less conservative ones or that the designer be advised to undertake wind tunnel tests to obtain an accurate answer. The NBCC Commentary formulae can give unrealistic results in particular cases that differ by 50% or even 100% from the more accurate results obtained by a wind tunnel test. Therefore, some modifications of the commentary are certainly warranted on the subject of accelerations.

Methods of Reducing Vibration

The discussion of this subject was opened by commenting on the wide range of proposed methods of increasing damping, including tuned mass dampers (TMD), tuned liquid dampers (TLD), visco-elastic dampers and active control systems. However, in North America there are still very few buildings in which they have actually been used: The World Trade Center towers and Citicorp Building in New York, the John Hancock building in Boston, the Columbia Center in Seattle, and the CN Tower in Toronto. Most structural engineers appear reluctant to use these devices. This may be due partly to unfamiliarity with them, but also partly due to cost (for example, a $4.5M cost to install a damper on a building in 1982).

It was suggested that a TLD is a combination of a TMD and an impact damper. A TLD in which water is the liquid also has large space requirements, much more than needed by a TMD.

A TLD, however, was shown to be useful in a retrofit situation. As an example, the use of a TMD had been examined for a hotel building but ran into many difficulties. The solution using the TLD had, however, proved practical. Larger TLD's are in the planning stage, including a 150 tonne TLD for a highrise residential building in Japan with natural period 4.5 seconds.

It was pointed out that the right solution to a vibration problem depends on the building. In RWDI's aeroelastic wind tunnel investigation during design of the 72 storey Interfirst Plaza Tower in Dallas, vortex excitation was identified as the cause of excessive vibration near the top end of the design wind speed range. The options of adding a TMD and adding structural stiffness were compared and, for this case, adding stiffness proved the more cost beneficial. It was sufficient to move the vortex excitation to a higher wind velocity, above the design range. For other buildings the amount of structural stiffness to be added might be much greater and therefore the TMD (or TLD) would be the more attractive option.

Other methods were also discussed such as viscoelastic dampers used in the World Trade Center towers and in the Columbia Center. No one present had direct experience with these devices nor with their relative initial and maintenance costs compared with TMD's and TLD's. However, questions were raised about their durability. A paper by Mahmoud published by the ASCE in August 1987 discusses this in more detail.

Conclusions and Recommendations

There is a need for further research efforts aimed at refining wind-induced vibration criteria for human comfort. The roles of visual cues, torsional motion and "learning" effects are still not well understood. The owner should be involved in deciding on comfort criteria for his particular building but some minimum criteria to be met by all buildings are still needed. Cultural differences may be important in different countries, something to be borne in mind by those involved with international standards.

Static deflection criteria must be related to the properties of the secondary building elements attached to the main structural system. The criteria may need adjustments from building type to building type.

Current theoretical methods of estimating accelerations analytically are not well advanced. Because of this the current formulae in the 1985 NBCC Commentary give misleading results in some cases. They need to be revised and qualified and wind tunnel testing should be pointed to as the method for obtaining more accurate predictions.

The more wide-spread use of damping devices will hinge on further demonstrating their reliability and effectiveness in real situations. It appears that several economical types are now available or are being developed. It will also depend on close cooperation between the structural designers and those developing the damping systems.

WORKSHOP D - DIFFERENTIAL MOVEMENT

Session Chairman: R. Bergmann
Workshop Report by: R. Green

Movements of structures and the effect of these movements on structures and exterior cladding were the main topics of this workshop. The workshop, which was well attended, tended to focus more on problems of communication between the parties involved than on technical criteria.

Key words which might be associated with the workshop are JOINTS and CURTAIN WALLS.

Joints

Reinforced concrete or precast concrete buildings tend to pose more difficulty than structural steel buildings when movement and joints are considered in design. The reliable prediction of deformation is more difficult for a concrete structure than for a similar steel structure, mainly because time dependent shrinkage and creep characteristics of concrete building are uncertain. Concrete buildings may creep and shrink at various rates which are a function of size (exposed area) and they may have differing thermal masses and hence thermal movements from one portion to another. Exact predictions of creep, shrinkage or thermal movement are almost impossible. Ranges of movement should be considered in design.

The design engineer should develop procedures to resolve the design problem in spite of the inability to calculate movements precisely. Procedures worthy of consideration include:

i) The identification of different buildings, e.g., office, industrial or parking garages, each with structural members having different degrees of direct exposure to the environment.

ii) The recognition of transition zones where movements of the adjoining components may not be compatible.

iii) The use of closure strips between various construction stages, placed after shrinkage is well advanced.

iv) The use of prestress to control movement and limit cracking.

v) The use of joints where a clear separation is warranted between different structures or parts of the building (e.g., heated building and unheated ramp or garage).

Where joints are included in a system, care should be taken with respect to:

i) watertightness, as few if any joints are watertight, and

ii) assumed coefficients of friction at the joint surface.

Procedures for the replacement of joints and seals must be considered and should form part of the original design concept.

Curtain Walls

Discussion pertaining to differential movement and curtain walls tended to address the overall design and performance of the wall systems. It was felt that deformations could be calculated and serviceable walls are possible if coordination is encouraged between designers and contractors.

Three main problems were addressed in the discussion of design and performance of curtain walls. These were:

i) the assessment of inaccuracies and knowledge of typical tolerances associated with the construction of the structural frame supporting the wall panels

ii) the deformations associated with the frame and wall after completion of the structure due to permanent and short time loads

iii) the allowable movement tolerated by the wall or components of the wall.

Normally, the supporting frame of steel, precast concrete or cast-in-place concrete will be constructed to specified tolerances. However, these tolerances may not always be achieved during construction. Generally, the tolerances are less for steel construction than for either precast or cast-in-place concrete structures.

The inaccuracies of construction of the structural frame from the ideal tend to be less for steel construction than for concrete construction. The erection scheme for the curtain wall units must consider these inaccuracies of construction. For example, anchors attached to steel columns should be mounted at a lower than desirable elevation to permit the use of shims to achieve the desired elevation. The design and location of anchors into cast-in-place concrete spandrel beams should include tolerances for the uncertainty in prediciton of spandrel beam deflection due to creep and shrinkage.

The deformation of the frame and walls include column shortening, vertical deflection and rotation of the edge beam or slab supporting the curtain wall, lateral drift of the frame and deformatin of the curtain wall due to temperature gradients across the thickness of the wall. After the curtain wall has been installed with correct alignment, further deformations of the frame and the curtain wall are predictable within reasonable accuracy. For example, an edge beam may deflect 10 mm due to live load and accumulation of dead and live load creep. The horizontal joint between curtain wall panels should therefore be able to accommodate 10 mm as a differential movement. Permissible lateral deformation under live load is frequently determined by the window clearance details. A movement of 5-6 mm may be tolerated over the height of a window, so that, for a window which is half a storey high, a permissible lateral frame deformation of 10 mm is required.

Movements to be considered as part of the overall construction process include:

a) thermal gradients through small or large panels

b) the properties of the jointing materials used as sealers

c) the tolerable movements for various types of glazing within supporting frames.

Minor design changes can be used to reduce the restraints to thermal effects such as bowing in sandwich panels.

Successful curtain wall design, installation and long term performance should be a cooperative responsibility of the manufacturer and both the architect and structural engineer. The long term performance of a curtain wall is a function of the particular design philosophy and expertise of the manufacturer. The traditional approach is for architects or engineers to specify the frame deformations to be sustained by a curtain wall. Sufficient information, however, must be supplied so that the fabricator can make the necessary tradeoffs to ensure adequate performance of a given system. Alternatively, if a tendering system is used for larger buildings, this should include the preparation of a complete design including test results, and criteria for subsequent evaluation by the architect and engineer.

There is a possibility for confusion regarding the responsibility for curtain walls. Three groups may become involved with the design, selection and installation of curtain walls. These are the architects, the engineers, and the manufacturers or building envelope specialists. The main difficulties between these groups lie in the areas of communication and responsibility.

The view of many structural engineers with expertise in the design of building structures is that the curtain wall design, a complex design, should be completed by someone expert in curtain wall design taking into account manufacture, installation, and sealing materials. The structural engineer may provide data necessary for design for deformation. The alternative view is for the structural engineer to accept the responsibility for curtain wall design in a professional manner.

Serviceability problems seem to arise from the tendency to use large steel supporting frames upon which the exterior cladding is mounted to form a complete unit prior to site installation. These particular problems relate to maintenance and repair in cases where access to the back of the panel is restricted. Damage may develop because of thermal bridging and corrosion of the wall system. Such considerations should be taken into account at the design stage.

Frequently, wall systems which function well in a temperate climate are being utilized in Canada. Such systems, however, may not perform successfully in Canadian environmental conditions. Special care must be taken with movements of new cladding materials. For example, some fibre reinforced plastics exhibit movements which are an order of magnitude greater than for traditional concrete cladding. This must be taken into account in the design to avoid cracking of the glazing.

Conclusion

The structural engineer can provide the necessary expertise to ensure sound performance of joints and curtain walls. It is necessary to ensure that a framework for coordination exists for a given project and that any additional responsibility because of this coordination is recognized.

WORKSHOP E - VIBRATIONS FROM HUMAN ACTIVITIES

Session Chairman: B. Ellingwood
Workshop Report by: D.E. Allen and J.C. Swallow

Vibrations of floors, pedestrian bridges and stadia due to walking, aerobics, dancing, concerts, etc. was the topic of this workshop. The workshop was very well attended with active participation, a reflection of the increasing number of problems that have occurred in recent years. Volume I of the proceedings contains a wealth of information on the topic.

Problem identification, acceptable vibration limits, codes/guidelines and research/information needs were the main topics of discussion.

Where are the Problems?

Approximately 25 years ago complaints showed that the old stiffness rule (deflection under live load less than span/360) did not work for the new long-span floors with low damping, nor for residential floors with low stiffness perpendicular to the joists. Since then a number of design criteria have been recommended for use in practice, notably those based on heel impact response such as contained in an appendix to the Canadian standard for steel structures. More recently rock concerts and aerobics have become popular with ensuing problems for long-span floors; design criteria to control such vibration based on response of the simple spring-mass-damper model (SDOF) have started to appear, e.g. in the Commentary to the National Building Code of Canada (NBCC).

Experience so far indicates that the recommended criteria have been helpful in reducing the incidence of problems but that more needs to be done to minimize future occurrences and to reduce the cost of fixing problems. The following problem areas were identified:

- lightweight residential floors, particularly new lightweight systems with spans and spacings greater than traditional wood joists.
- shopping centres of structural steel floor systems exhibiting low damping.
- vibrations in occupancies where the vibration source is not immediately apparent (mixed occupancies, transmission of vibration to other parts of the building).
- cantilever beams and balcony areas
- pedestrian bridges
- gymnasia
- dance floors
- stadia

Vibration Limits

Recommended limits of acceptable vibration have recently been developed for buildings and are contained in British and draft ISO standards. These limits take into account occupancy, duration and repetition of vibration. They are expressed in terms of a multiple of a base curve of constant rms acceleration up to 8 Hz vibration frequency and constant rms velocity beyond. The range of limits is from approximately 0.2% g rms acceleration to approximately 5% g. Although useful for performance testing, care must be taken in interpreting them in design criteria; heel impact acceleration used in design criteria, for example, can be entirely different from walking accelerations that actually occur. It has been especially difficult to relate the limits to recommended design criteria for lightweight residential floors.

Experience shows that vibration limits depend strongly on the activity of the people who feel the vibration, their relationship to the source of vibration, auditory cues (e.g. china rattling), visual cues (e.g. motion of ceiling below dance floor disturbs people below), duration and repetition of vibration. Fear of safety has a strong influence on human reaction and reduction of this fear increases acceptance (getting used to it). On the other hand, people in quiet occupancies would generally prefer not to be 'vibrated' from time to time and their expectations are rising. People are especially disturbed when the vibration is caused by an unknown source.

Codes/Guidelines

Should design criteria to limit vibration be contained in building codes and standards? After all, given the problems that occur, it is generally agreed that serviceability is more important than strength. On the other hand, the wide variations in human reaction discussed above indicate that it may be difficult to specify such criteria.

Reasons for including vibration criteria in codes and standards are:

- it protects future owners of buildings, keeping in mind that consumer expectations are rising and that noticeable vibration has a negative effect on renting or selling.
- it forces the designer and developer to address vibration in design and not leave it to chance which, for the unlucky owner, may require expensive alteration.

Reasons against include:

- it is not a safety or health issue, but an economic one, and therefore should not be regulated but agreed to between designer and owner.
- there is a danger of establishing code criteria which will not be satisfied by a large number of existing floors that perform satisfactorily.
- criteria for special problems such as dance floors, gymnasia and stadia should not be part of a general building code.

The workshop discussion led toward a general consensus that the building code or standard should not contain criteria but should reference guidelines containing recommended design criteria. The designer would make use of the guidelines to design the structure to a level of vibration comfort acceptable to the owner or developer. This is to ensure awareness by the designers and, as well, by the developers and owners and yet not be restricted by regulatory requirements. Designers at the workshop recommended that the guidelines be separated into two parts, one dealing with general buildings where disturbing walking vibration may be a problem for which simple criteria would apply, and the other dealing with special problems such as gyms, dance floors, stadia, very sensitive use and occupancy and non-human vibration sources (e.g. vehicular traffic), all of which require a more detailed analysis.

Research/Informational Needs

If the loading and the properties of the structure are known, then the response can be predicted and compared with what will be acceptable. This ideal situation is generally too difficult to carry out fully in design, yet it can be approximated sufficiently to provide simple yet rational design criteria. So far, with the exception of the NBCC Commentary, vibration criteria for design are either fully empirical (traditional stiffness rule) or semi-empirical (heel impact criteria).

Some information on loading due to human activities has been obtained but more is needed, particularly for rhythmic events involving large groups of people. A problem recently occurred involving resonance at the third harmonic of jumping frequency; only the first two harmonics are taken into account in the NBCC Commentary.

Important parameters for determining structural response include natural frequency (usually, but not always, for the lowest vibration mode), modal mass and modal damping. Better information on how to predict these parameters is needed based on field tests, in particular damping of floor systems (including non-structural components), and natural frequency of two-way systems on flexible supports. It was suggested that damping determined from heel impact contains a geometric vibration dispersion component and is therefore approximately twice as large as modal damping.

In addition, simplified rational design criteria need to be checked out and demonstrated in practice based on field tests.

Lightweight floors whose natural frequencies are well above a significant harmonic of human activity (about 10 Hz) require special consideration. Stiffness under point load appears to be an important parameter in addition to the modal parameters already mentioned. Also ISO vibration limits should be reviewed as they relate to proposed design criteria and possibly human reaction testing specific to lightweight floors carried out.

The best information for developing better design guidelines, however, is feedback on problems that occur. This includes not only being aware of a problem that exists, but testing and analysis to relate the problem to existing guidelines. Such case studies are also very useful educational tools; a recent IABSE publication containing case studies by Bachmann is highly recommended [1]. A number of case studies are contained in Volume I [2,3] and two case studies by Cantieni are contained in this Volume[4].

Besides feedback another important information tool is communication between the designer and his client regarding floor vibration. There are a number of reasons for this. It makes the designer aware of any possible special activities (such as aerobics adjacent to sensitive occupancies) that are intended for the building. It makes the client aware of vibration levels that can be expected and provides the opportunity of establishing criteria by agreement. Finally the client will be educated about possible noticeable floor vibration during construction when there is little damping.

Finally, an important task is education of designers by seminars, etc. on recent guidelines, including design and repair implications, using case problems as examples.

References

[1] Bachmann, H. and Ammann, W. Vibrations in Structures Induced by Man and Machine. Structural Engineering Document No. 3e. IABSE, Zurich 1987. (Cases summarized in Proceedings of Symposium/Workshop on Serviceability of Buildings, Vol. 1, 1988, p. 419-434).

[2] Rosenthal, I. and Itskovitch, M. Vibration Response of Ribbed Slab Fllor to Dancing. Proceedings of Symposium/Workshop on Serviceability of Buildings, Vol. 1, 1988, p. 526-532.

[3] Matthews, C.M. and Montgomery, C.J. A Dance Floor with Unsatisfactory Dynamic Response. Proceedings of Symposium/Workshop on Serviceability of Buildings, Vol. I, 1988, p. 533-546.

[4] Cantieni, R. Floor Vibrations - Two Case Studies. Proceedings of Symposium/Workshop on Serviceability of Buildings, Vol. II, 1989, p. 26.

WORKSHOP F - GROUND-TRANSMITTED AND MACHINERY-INDUCED VIBRATIONS

Session Chairman: D.L. Allen
Workshop Report by: G. Pernica

Introduction

Five major topics were discussed by a group of about 12 participants. As the group was small, discussions were conducted on an extremely informal basis, and, as a result, it was a lively and informative session with a variety of opinions being voiced. Some of the discussions, however, ended with several of the questions raised during the discussion left unanswered. These are noted in the topic summaries which follow.

Damage Criteria for Transportation-Induced Vibrations

Damage criteria for vibrations produced by transportation sources are at the present time poorly defined in comparison to blasting. Blasting criteria are reasonably well established because of the large amount of experience and published data. However, blasting criteria are not suitable for transportation-induced vibrations because of large differences between the two types of excitations in frequency content and time duration. In comparison to traffic-induced vibrations, blasting vibrations are high frequency, short duration pulses.

The German Standard DIN 4150 recommends for transportation-induced vibrations a damage criterion of 5 mm/s peak for frequencies less than 10 Hz. After an extensive literature search, this criterion was recently used to assess damage to houses alleged to have been caused by train vibrations [1].

Damage criteria should also take into account the type of structure because different structural types behave differently to the same input. As an example, historic structures should have a lower damage criterion, perhaps 0.5 to 2 mm/s peak as is suggested in several European standards because of the perceived susceptibility of the construction to vibrations.

Three questions on damage criteria were discussed.

1. At what locations and in which directions within the building should measurements be taken to apply damage criteria?

It was noted that for blasting, measurements are generally taken on basement foundation walls. For traffic (road or rail) the location and direction will depend on whether the concern is human annoyance or structural damage. For human annoyance, vibrations should be measured in the vertical direction on floors; and for structural damage, vibrations should be measured not only in the vertical direction on floors but also in the horizontal directions at floor and ceiling levels.

2. How does one determine whether traffic-induced vibrations and not other factors, i.e. temperature, settlement etc., were the primary cause of damage to architectural components?

One has to carefully examine all the cracks and try to find a rationale to explain the presence of single cracks or groups of cracks. It is possible that certain cracks patterns might suggest certain damage mechanisms.

One could also approach the issue based on technical reasoning. The maximum strain sustained by the damaged components from each alleged mechanism could be estimated and compared to the maximum allowable strain. However, this approach which is technically sound, is impractical because of the number of parameters which must be estimated.

In practice, we use case studies to develop empirical criteria. However, the uncertainty still remains even if an extensive catalogue of case studies existed. We cannot prove conclusively what the actual damage mechanism was; we can only surmise what it most likely was.

3. If the primary cause of damage is uncertain how can criteria be realistically established from case studies?

More research is needed.

Washing Machine-Induced Building Vibrations

Case studies were presented by several participants. One study, which summarizes this discussion, concerns two commercial washing machines located on the eighth floor of a large highrise hotel.

Each machine weighed about 500 kg, had a dry load capacity of about 110 kg and a rotational frequency during the spin cycle of about 9.5 Hz. Although the machines were supported on air springs, vertical floor vibrations in nearby rooms were more than five times larger than the ISO perceptible level or in excess of 0.5 mm/s. Fundamental vertical frequencies of these floors were between 6 Hz and 11 Hz.

The participants felt that the problem was likely caused by the nearness of the rotational spin frequency of the washing machine to a natural frequency of the floor supporting the machine. One solution would be to increase the mass carried by the springs and thereby reduce the spring's transmissibility of forces. In effect, this is one of the ways to improve the effectiveness of the isolation system so that as little of the rotational forces produced by the washing machine enters the supporting floor system.

The conclusion drawn from the studies was that the spin cycle (water extract cycle) in large commercial washing machines can cause floor vibration problems in highrise buildings if the machines are not properly isolated from the structural floor slab.

Building Isolation for Ground-Induced Transportation Vibrations

Two questions arose for discussion.

1. Does building isolation work for ground-borne vibrations?

Unfortunately, there is very little information on this topic in the literature. Details of building isolation systems and their measured effectiveness is rarely published. There is some data which shows that 64 mm pads are effective for frequencies above 40 Hz. Pads 128 mm thick can give an additional 10 dB attenuation above 40 Hz and blocking masses without pads 14 dB attenuation (see paper on control of building vibration from ground-borne excitation by Allen and Howe in this Volume).

2. Has any building been isolated for traffic vibrations after it was built?

Many buildings have been modified (i.e. base isolation added) after they were built to isolate the structure from earthquake-induced lateral ground motions. However, there did not appear to be any buildings which were later modified to isolate the structure from traffic-induced vibrations. Instead, isolation techniques such as trenches, which do not alter the structure, have been used in several cases, but with limited success. A more efficient approach would be to control the amplitude and frequency content of the ground-induced vibrations by isolating the source of the vibrations. For rail traffic, this would mean isolating the track from its supporting base.

The use of slender piles in attenuating building vibrations by more effectively decoupling the foundation and the building from the ground was also discussed. Although some of the major factors affecting the amount of the decoupling are known, i.e. distance of the pile from the source of the ground vibration and whether the pile was placed in a sleeve, the degree of the decoupling for each of the factors is not known. More research in this area is required.

Problems Arising from Heavy Vehicular Traffic

Vibration problems (i.e. human annoyance, architectural damage) have been produced by heavy vehicles but incidents of these problems have been sporadic in nature. The problems have usually been associated with vehicles that produce low frequency airborne noise, roads with poor surface conditions and roads built on soft soils.

Low frequency noise from heavy vehicles can induce vibrations in buildings in conjunction with those produced by ground-borne vibrations from the same vehicles. What is not known is which of the two transmission paths (airborne or ground-borne) is the major contributor to structural vibrations and what is the variation of the two contributions with changes in structural, ground and environmental conditions.

It is known that road surface conditions play a large role in the generation of noise and vibration from heavy vehicles. Road surfaces should be flat and smooth to minimize the production of ground vibration and airborne noise at the tire-road interface. Pot holes which are the major source of truck-induced ground vibrations should be completely eliminated.

The participants concluded this topic by noting that more research is required in the following three areas: the contribution of low frequency airborne noise from heavy vehicles to structural vibrations; the development of a universal approach to solve traffic-induced vibration problems; and a better way of generalizing observations and conclusions from specific case studies.

Standards Governing Transportation-Induced Vibrations

There is a lack of standards (regulations) in Canada governing traffic-induced vibrations from road and rail sources. Some participants thought that this void might be tackled by the National Building Code of Canada (NBCC). However, it was noted that this assignment would be a difficult undertaking for the code because its primary function at the present time is building safety and not building serviceability.

The task, instead, could be assigned to an agency or department of the Government of Canada involved with transportation. Irrespective of the organization given the responsibility, the introduction of a standard would affect about 5% of all Canadians living beside major road or rail lines.

In Canada, a Canadian Standards Association (CSA) committee has recently begun preparing a measurement standard for transportation-induced vibrations. This committee noted that more fundamental research on damage and human annoyance criteria and predictive methods for ground-borne vibrations was needed before standards in these other three areas could be developed. Because of the impact and importance that these standards would have on the development of land abutting transportation right-of-ways, funding for this research should come from a senior level of government (provincial or federal).

Concluding Remarks

The session concluded by reviewing some of the areas which require more work. They are listed in the order presented by the session's chairperson and not in order of importance.

1. Human Response Criteria
2. Building Damage Criteria
3. Heavy Vehicles: Noise-Induced Structural Vibrations
4. Building Isolation for Transportation-Induced Vibrations
5. Vibration Mitigation Using Different Types of Foundations
6. Development of Vibration Standards

References

[1] Rainer, J.H., Pernica, G., Maurenbrecher, A.H.P., Law, K.T. and Allen, D.E., Effect of Train-Induced Vibrations on Houses - A Case Study. Proceedings of Symposium/Workshop on Serviceability of Buildings, Vol. I, 1988, p. 603-614.

FLOOR VIBRATIONS - TWO CASE STUDIES

by

R. Cantieni
EMPA, Swiss Federal Laboratories for Materials Testing and Research
CH-8600 Dubendorf, Switzerland

Abstract

This paper presents the results of experimental and theoretical investigations on the dynamic behaviour of a 12.8 m span steel floor of a two-storey office building and a 14.4 m span reinforced concrete floor of a two-storey gymnasium. In the case of the office building, corrective measures had to be taken to decrease the vibrations induced by human activities to an acceptable level. In the case of the gymnasium floor, corrective measurements were carried for strength only.

1. *Steel Floor of an Office Building*

A three-storey reinforced concrete building located in the City of Zurich was expanded by erecting a two-storey steel structure above the existing structure. The area of the new structure is smaller than that of the existing structure. Consequently, the columns of the new structure do not match the existing walls and a rather heavy steel bottom floor had to be introduced between the two structures (See Figures 1 and 2). The new structure, steel frames consisting of columns and stringers for the roof and intermediate floor of a 12.8 m span, is supported elastically by this steel bottom floor.

During erection of the intermediate floor, construction workers complained of excessive floor vibrations. Preliminary measurements yielded a fundamental natural frequency of the floor of 6 Hz. The necessary corrective measure was straightforward as there were no objections to the adding of supplementary columns between the intermediate and bottom floors; thus the floor's span was reduced to approximately 6 m.

Tests performed by EMPA on the structure before and after placing one row of additional columns included monitoring of the intermediate floor's response to impulsive loading and to people jumping and walking on the floor. In the impulsive loading tests, the structure was excited by the means of dropping an 8.6 kg wooden ball from a height of 0.6 m. These tests yielded information on the structure's natural behaviour, whereas the tests with people jumping and walking allowed determination of the floor vibrations under simulated actual service conditions. (After completion of the tests, a second row of columns was added, as shown in Figure 1).

The results of the impulsive tests are presented in Figure 3 together with those of an analytical investigation of natural frequencies and mode shapes. (Damping of the fundamental mode for the system without columns was determined to be 1% of critical). Experiments showed that the fundamental frequency increased from 5.85 Hz to 11.25 Hz after the columns were added to the structure. This increase was less than expected. Subsequent calculations showed that this is due to the fact that all columns are supported elastically, not rigidly. The structural model which was used for the analysis after several steps of optimization is shown in Figure 4.

The effect of the additional columns on the floor vibrations excited through one person jumping on the floor can be evaluated from the frequency spectra given in Figure 5. Jumping frequencies have been chosen to be one-third and one-half of the floor's fundamental frequency.

Figure 6 shows the time signals recorded during the walking of three persons on the floor. The time signals confirm what the frequency spectra show with full clarity; that is, the added columns eliminate the 5.85 Hz vibration from the floor response.

To evaluate the admissibility of the vibrations excited by occupants under normal service conditions, a number of codes were consulted. These included ISO 2631-1978 [1], VDI 2057 [2], DIN 4150 [3] and BS 6472:1984 [4]. Of these codes, only DIN 4150 and BS 6472 are directly applicable to floor vibrations of office buildings.

Processing of the data according to DIN 4150 yielded maximum KB-values (KB is a parameter representing intensity of human reaction to vibration) of KB = 13.5 and KB = 5.8 for the structure without and with additional columns respectively. Comparison with the admissible value of KB = 0.4 reveals that neither of the two floor vibrations would be acceptable for an office building.

Application of BS 6472 requires the determination of 1/3-octave spectra of walking vibrations shown in Figure 6. These are presented in Figure 7. It can be seen that adding of the columns to the structure shifts the 1/3-octave-band with maximum intensity to a higher frequency where human susceptibility is smaller, and also reduces the maximum intensity itself. As a result, the critical acceleration reaches curve 4 instead of curve 20.

Weighting of the 1/3-octave bands according to the provision given in BS 6472 yields values of the multiplying factor of 25.3 and 7.1 for the vibrations before and after installation of the columns respectively. Since the admissible value is 4, the possibility of complaints still exists for the floor with the columns. Nevertheless, no complaints have been registered after completion of the building. Thus, BS 6472 seems to provide a more reliable means of rating floor vibrations of office buildings than does DIN 4150.

Reinforced Concrete floor of a Gymnasium

The structural components of a 20 year old two-storey gymnasium located in the city of Bulach were checked analytically for their load carrying capacity. According to the provisions of the present Swiss code [5], the live load consisted of static loads only. It was found that the 14.4 m span intermediate floor had to be strengthened.

This floor consists of a 0.14 m thick slab of roughly 15 x 27 m overall dimensions and four 0.4 m wide girders of additional 0.6 m height, both of reinforced concrete (Figure 8). It was intended to increase the load carrying capacity by bonding steel plates onto the bottom side of the four girders.

Probably as a consequence of Prof. Bachmann's activities in this field [6], the engineer in charge also checked the dynamic properties, i.e. the fundamental frequency of the floor. According to the assumptions concerning the flexural stiffness of the girders (uncertain clamping and crack conditions), he calculated this frequency to lie between 3 Hz and 5 Hz which was substantially lower than the 7.5 Hz recommended in [6] and in the draft Swiss code [7].

Therefore, field tests were performed by EMPA to establish the actual fundamental frequency of the floor prior to strengthening. As this frequency proved to be not as low as calculated but still lower than recommended, additional tests had to be executed. These tests were to provide information on the response of the floor to people jumping rhythmically on its surface, and hence allow a reliable analytical treatment of various dynamic load cases.

The tests to determine the fundamental frequency made use of the impulse excitation technique. The girder under consideration was struck on its bottom side with an instrumented 6 kg hammer and its response was measured with four accelerometers located as shown in Figure 8. Figure 9 shows the transfer function calculated on site. From this function it can be seen that the fundamental frequency of the floor was 6.1 Hz. Determination of the mode shapes showed that all the natural modes with frequencies between 6.1 Hz and 18.6 Hz shown in Figure 9 have the same shape in the span direction, i.e. a half sine-wave over the span.

Two tests were then carried out where seven persons in the mid-span region of a girder jumped during approximately one to two minutes with a given jumping frequency. The jumping frequencies were 2.0 Hz and 3.0 Hz according to one-third and one-half of the floor's natural frequency. Instrumentation consisted of four accelerometers. Figure 10 shows the frequency spectra determined from these tests. The maximum velocities measured at mid-span were: 19.7 mm/s at 2 Hz jumping frequency and 33.6 mm/s at 3 Hz jumping frequency, with a maximum acceleration of 1.27 m/s^2 at 3 Hz jumping frequency.

The main results of these tests were that jumping with f = 3.0 Hz is critical and that damping of the fundamental mode (established from a free decay test) was approximately 3% of critical.

Subsequent theoretical analysis included the following steps:

- transforming of one of the girders into an equivalent SDOF system, representing the girder's fundamental mode of vibration.
- loading this mechanical model with "one 800 N person jumping at 3 Hz". The forcing function for this, shown in Figure 11, was separated into its three first harmonic terms [6].
- calculating the response for this load case by superimposing the results for the three load harmonics.
- expanding these results to the case of seven persons and comparing with the experimental results:

  $u = 1.2$ mm, $v = 37.8$ mm/s, $a = 1.31$ m/s^2

  v_{max} (theor.)/v_{max} (ex.) = 37.8/33.6 = 1.12

  a_{max} (theor.)/a_{max} (ex.) = 1.31/1.27 = 1.03

- being on the safe side, the theoretical model was then accepted for further calculations.

- calculating the load case "38 persons evenly distributed on the floor (1 person per 2 m^2), jumping at 3 Hz" resulted in:

  $u = 4.0$ mm, $v = 132$ mm/s, $a = 4.6$ m/s^2

The design engineer and the owner of the building then defined the following load cases for verification of the load carrying capacity and fatigue, respectively:

- load carrying capacity: 60 persons concentrated at mid-span and jumping with $f = 3$ Hz (15 persons per girder),

- fatigue: 100 persons evenly distributed on the floor and jumping with $f = 3$ Hz (25 persons per girder, 1 person per 3 m^2).

After calculating the corresponding forced vibrations the following equivalent static forces were determined: 134.4 kN per girder for the load carrying capacity and 1.89 kN/m^2 for fatigue.

The structure with the proposed repair proved to meet the design requirements and the repair described above was therefore carried out. The frequency of the repaired structure is not known, but no problem has so far occurred as far as human reaction is concerned.

References

[1] ISO 2631-1978; Guide for the evaluation of human exposure to whole-body vibration. International Organization for Standardization, 1978.

[2] VDI-Richtlinie 2057; Beurteilung der Einwirkung mechanischer Schwingungen auf den Menschen. Verein Deutscher Ingenieure, 1957 (Blatt 1, Entwurf), 1981 (Blatt 2), 1979 (Blatt 3, Entwurf).

[3] DIN 4150 (Vornorm); Erschuetterungen im Bauwesen. Deutsches Institut fuer Normung, 1975.

[4] BS 6472:1984; British Standard: Guide to evaluation of human exposure to vibration in buildings (1 Hz to 80 Hz). British Standards Institution, 1984.

[5] SIA 160 (1970); Norm fuer die Belastungsannahmen, die Inbetriebnahme und die Ueberwachung der Bauten, Schweizerischer Ingenieur- und Architekten-Verein, Zuerich, 1970.

[6] Bachmann, H., Ammann, W.; Vibrations in Structures Induced by Man and Machines, Structural Engineering Documents No. 3e, International Association for Bridge and Structural Engineering (IABSE), Zuerich, 1987.

[7] SIA 160E (1987); Einwirkungen auf Tragwerke (Entwurf), Schweizerischer Ingenieur- und Architekten-Verein, Zuerich, April 1987.

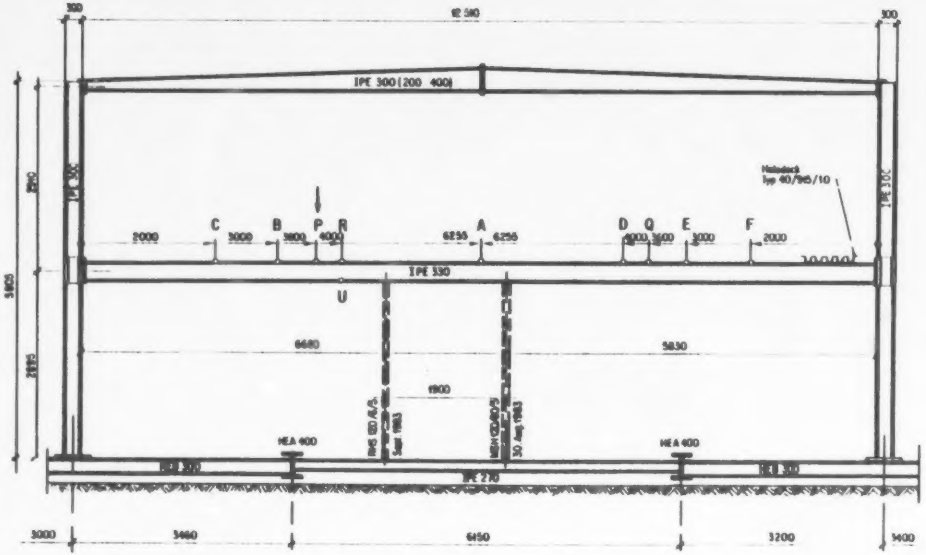

Figure 1. Section of new structure, showing loading and measurement points. The columns indicated by hatched lines were added to improve floor vibration.

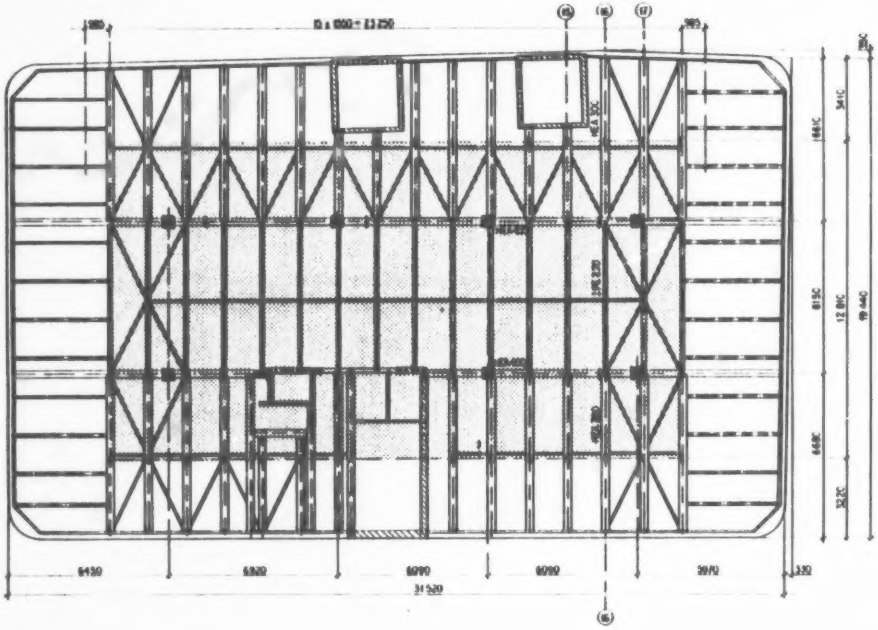

Figure 2. Steel floor between old and new structure. Shaded area shows location of new structure.

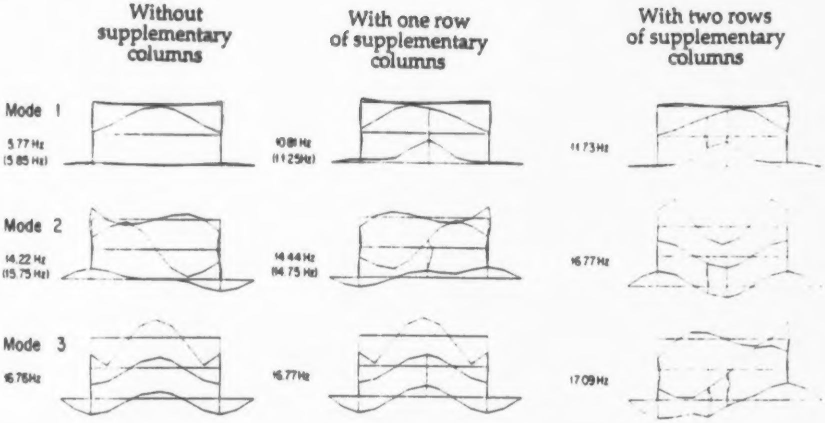

Figure 3. Calculated shapes and frequencies of the first three nodes. Measured frequencies are indicated in parentheses.

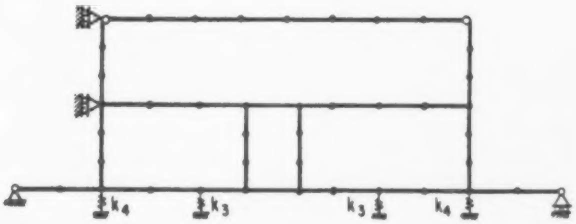

Figure 4. Model frame used for calculation of natural modes (129 degrees of freedom).

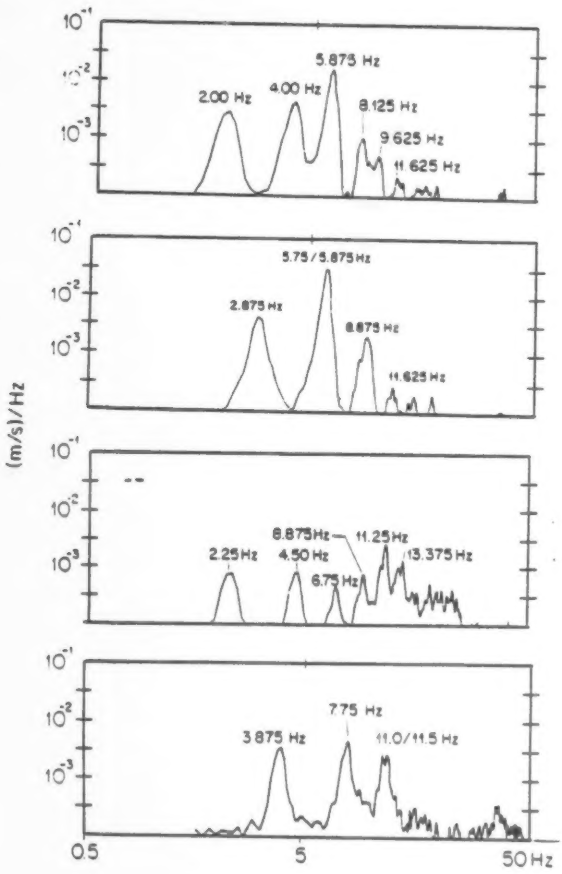

a) no additional columns
f = 2.0 Hz

b) no additional columns
f = 2.875 Hz

c) one row of columns added
f = 2.25 Hz

d) one row of columns added
f = 3.875 Hz

Figure 5. RMS spectra of velocity at R during tests with one person jumping at P (see Fig. 1).

a) no additional columns

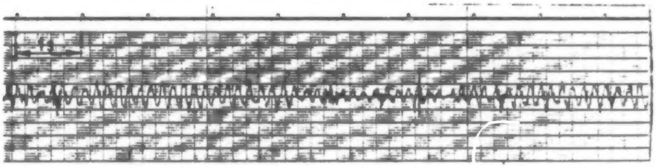

b) one row of columns added

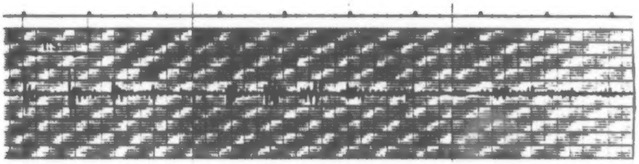

Figure 6. Time signals of acceleration measured at R (see Fig. 1) during the tests with three persons walking on the floor.

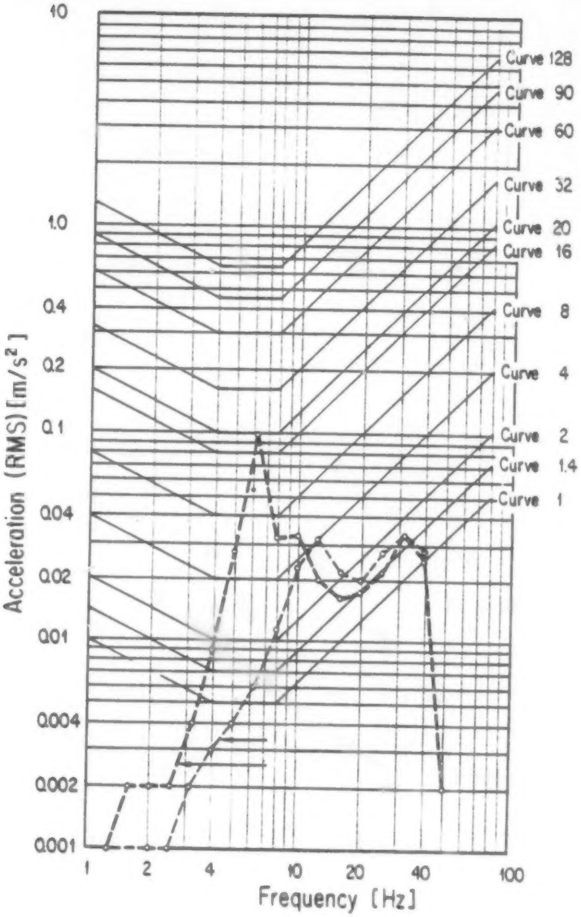

Figure 7. Third octave spectra of the acceleration time signals shown in Fig. 6 in comparison with criteria given in BS6472 [4].

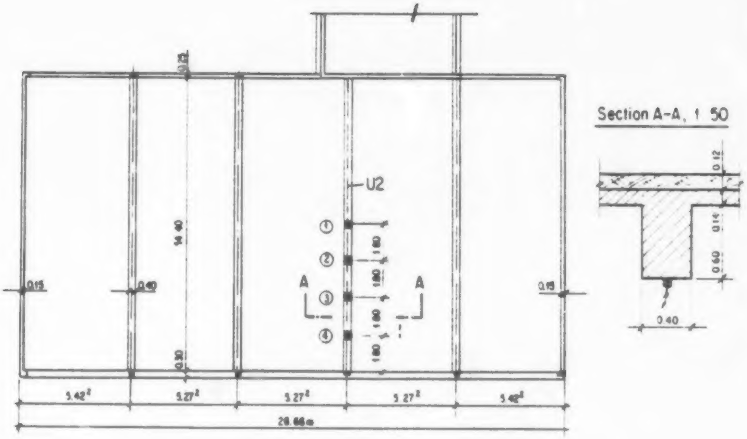

Figure 8. General plan and typical cross section of gymnasium floor (dimensions in m).

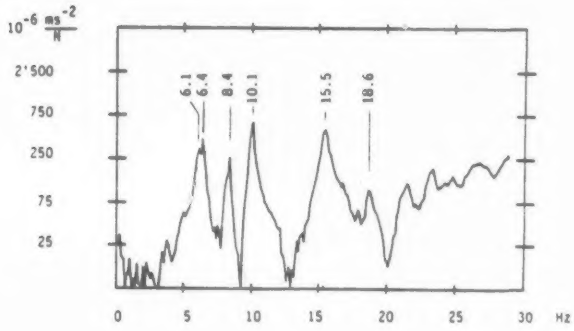

Figure 9. Transfer functions (acceleration/force) determined at point 2 in Fig. 8 from impulse excitation of girder.

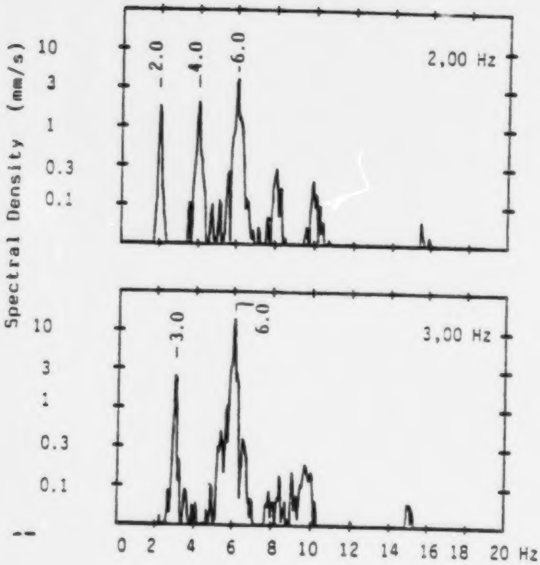

Figure 10. RMS-spectra of velocity measured at point 2 in Fig. 8 during tests with 7 persons jumping at frequencies of 2 Hz and 3 Hz at mid-span.

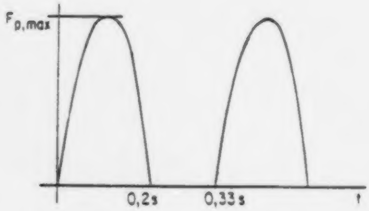

Figure 11. Forcing function used for analytical investigation.

CONTROL OF BUILDING VIBRATION FROM GROUND BORNE EXCITATION

by

D.L. Allen and B. Howe
Vibron Limited
Mississauga, Ont., Canada

Introduction

Buildings founded near or over subways and/or train tracks are vulnerable to ground borne vibration which can be transmitted to the building structure. Such a structural vibration can create a perceptible vibration or a radiated noise which can be disturbing to occupants. (Figure 1).

The successful control of building vibration and structurally radiated noise requires specific design of the foundation and building structural elements for adequate vibration mitigation. When building foundations alone cannot be designed to control ground-borne vibration to an acceptable degree, vibration isolation may be necessary.

This presentation addresses the design concepts needed to control vibration transmission into the foundation and structure of multi-storey buildings with specific emphasis placed on building location, environmental factors, structural/foundation design and the possible necessity for vibration isolation.

Environmental Factors

The degree to which ground borne vibration is transmitted to a structure is related to:

a) Rail type or subway tunnel, rail bed, train type, speed, number of cars.

b) Height separation between the rail bed and the building foundation. Subway structures can be beside or below building foundation. Train tracks can be on the same level or above the foundation. (Figure 2).

c) Soil type and its ability to transmit vibration from the point of excitation to the building foundation. (Figure 3).

d) Physical orientation of the building involving factors such as distance from the point of excitation, whether the building is founded on a subway structure (Figure 4), and the geometric orientation of the foundation with respect to the vibration excitation source (Figure 5).

Combinations of the above factors define the level of soil or subway structure vibration excitation input to the proposed building foundation. The strength of the source at the soil/foundation interface defines the need for vibration control measures and the degree to which vibration control is required. The building foundation type, wall and structural elements can often be conceived for adequate vibration control. Building vibration isolation may be necessary where structural design concepts cannot be chosen to provide adequate vibration reduction.

Structural Vibration Mitigation Using Conventional Foundation Design Concepts

Ground borne vibration from rail or subway tunnel excitation can have an impact upon a foundation through side walls or on the bottom of the foundation to a varying degree, depending upon whether the excitation is beside or below the foundation. Each source location has implications on the choice of building foundation.

Foundation Transmission

When the ground-borne excitation source is at or below the foundation supports, emphasis must be placed on the specific design of caissons, spread footings or possibly vibration isolation. Spread footings or caissons interfacing with and loaded on the soil can become springs which provide building isolation with respect to soil vibration (Figure 6). However, it is not the load on the column that provides vibration attenuation but it is the mass of the footing above the interface (i.e. blocking mass) which can provide optimum attenuation.

Often adequate vibration mitigation from an excitation at or below the foundation supports can be achieved by proper design of the caissons or spread footings alone.

Walls

A vibration excitation source beside or below a foundation can also transmit vibration into the foundation walls and structure to possibly propagate several storeys upward and cause an annoying structural vibration or radiated noise. Foundation wall vibration can also excite floor vibration modes which often fall within the frequency region of train/subway vibration excitation. As a result resonant modes can be amplified.

Foundation design for vibration mitigation requires thick walls facing the ground excitation, connected to thin floor slabs, creating an interface vibration impedance mismatch between the floor/wall elements (Figure 7). A better solution often dictates that the foundation wall adjacent to the ground excitation be disconnected from the structure by having independent interior columns near the wall to support the floor slabs (Figure 8). Vibration isolation between these columns and the disconnected foundation wall can support horizontal ground thrust loading while maintaining a superior structural impedance mismatch between the wall and the columns.

Interior shear walls close to a ground borne excitation from below can often transmit vibration upward unless similar floor/shear wall connections are designed with a structural impedance mismatch.

Interior Structural Design and Environmental Factors

Structural vibration diminishes with height above the excitation source. Often, the placement of noise insensitive occupancies such as parking and retail space closest to the foundation can be a good design strategy, provided the vibration/radiated noise levels are sufficiently low. Since structural vibration reduces with height, the design goal is then to reduce the vibration levels to an acceptable region at the first occupied office or residential floor.

Care must be taken to ensure that resonances are not excited to cause a floor to vibrate at a sufficiently high level to radiate an unacceptable noise on occupied floors. Structurally radiated sound, depending upon the building use, can be absorbed in acoustically soft rooms whereas the same vibration level may be bothersome for acoustically hard rooms such as bathrooms and kitchens in residential buildings. Light drywall panels tend to amplify vibration levels compared to the base building structure and become a source of radiated noise. Drywall panels near high vibration levels on the structure, must be designed to minimize amplification.

Vibration Isolation

If environmental factors, foundation types and structural elements cannot be conceived and designed to reduce building vibration to an acceptable level then vibration isolation may need to be considered (Figure 9). Alternatively, it may be more cost effective to install vibration isolation rather than specific and sometimes extensive foundation design for vibration mitigation. If it is not feasible to have buffer zones of parking and retail space in a building then possibly vibration isolation might be required.

Even though a building may be isolated, structural elements must still be designed to minimize vibration amplification. Column footings require blocking masses. Even with vibration isolation, the foundation wall/floor interface requires structural element impedance mismatches as does shear wall/floor connections.

Vibration isolation pad design requires that each load point has the correct stiffness and deflection for sufficient vibration isolation (Figure 10). The isolator material must be designed to have adequate longevity.

Overview

There are many factors involved in building foundation design for ground borne vibration mitigation. Environmental factors, foundation structural element design and possibly vibration isolation are all strategies which can be applied toward providing a cost effective approach to the reduction of building vibration.

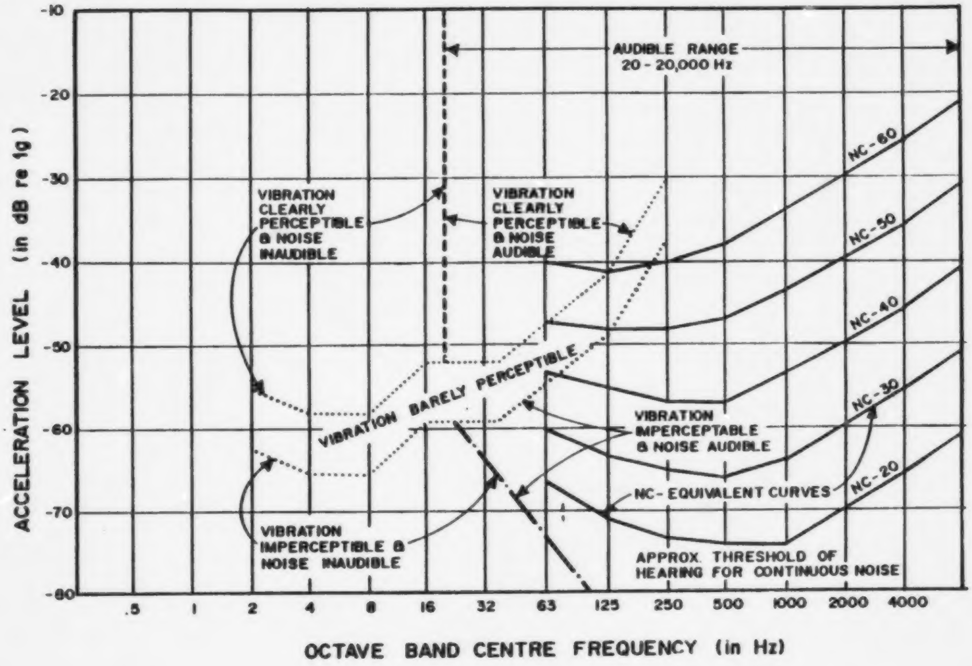

Figure 1. Relationship between the vibration amplitude and perceptibility as a function of frequency.

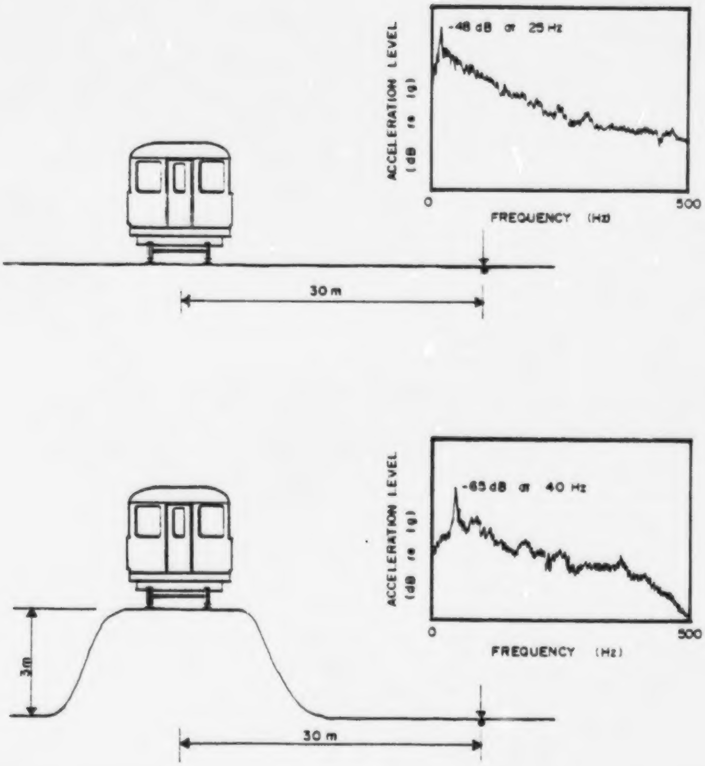

Figure 2. Typical effect of rail bed height

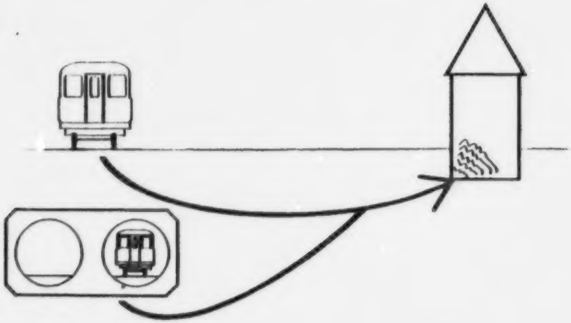

ELASTIC HALF SPACE

WAVE	RELATIVE ENERGY	DECREASE IN DISP. AMPLITUDE
RAYLEIGH	67%	$\frac{1}{\sqrt{r}}$
SHEAR	26 %	$\frac{1}{r}$ $\left(\frac{1}{r^2}\text{ SURFACE}\right)$
COMPRESSION	7%	$\frac{1}{r}$

VARIATION OF DISPLACEMENT AMPLITUDE WITH DISTANCE

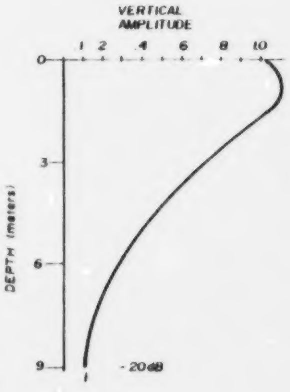

VARIATION OF AMPLITUDE OF RAYLEIGH WAVELENGTH WITH DEPTH

Figure 3. Typical effect of soil on vibration.

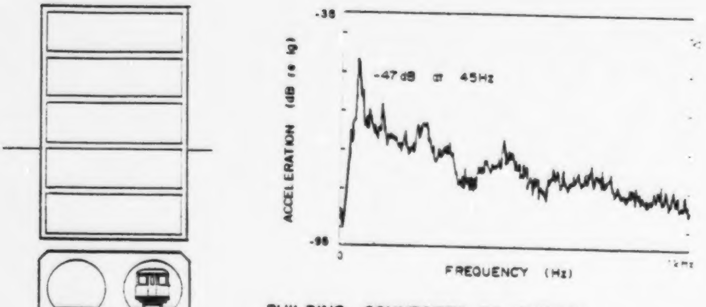

BUILDING CONNECTED TO SUBWAY

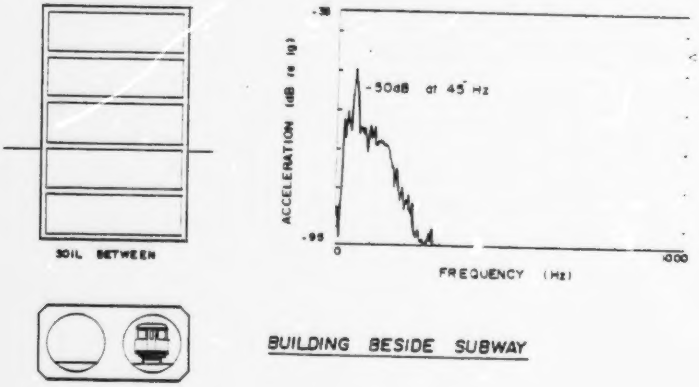

BUILDING BESIDE SUBWAY

Figure 4. Example of high frequency attenuation of ground vibration for a building connected to or beside a subway.

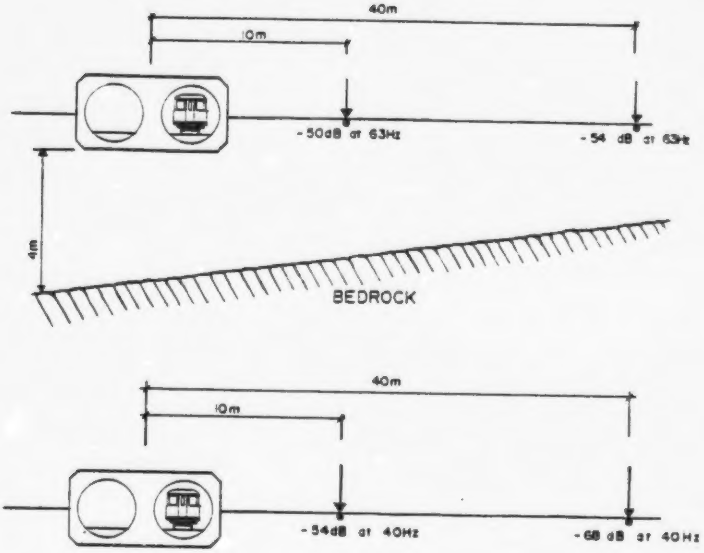

Figure 5. Effect of bedrock on vibration level.

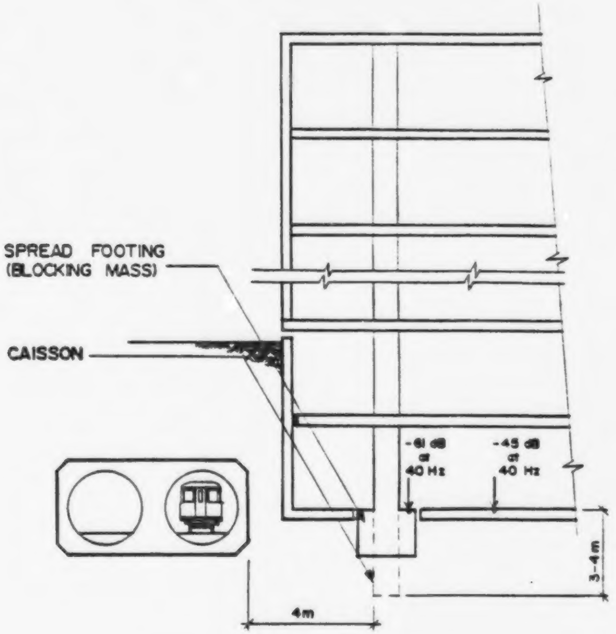

Figure 6. Spread footing and caisson foundations.

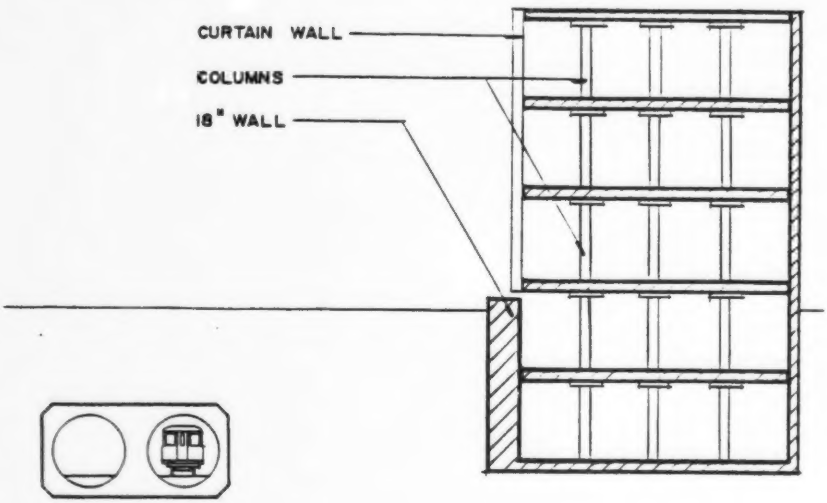

Figure 7. Improved foundation design for vibration control using thick walls.

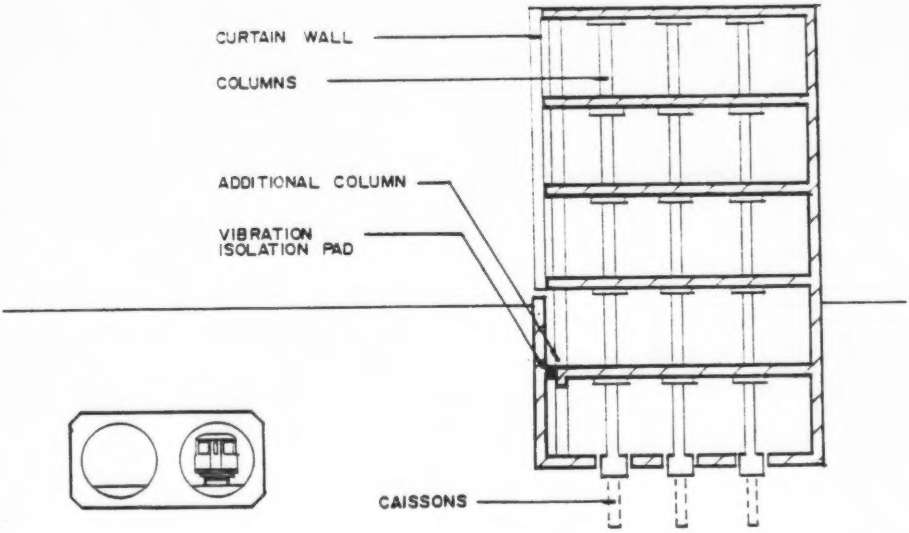

Figure 8. Foundation design for vibration control incorporating isolation pads and additional columns.

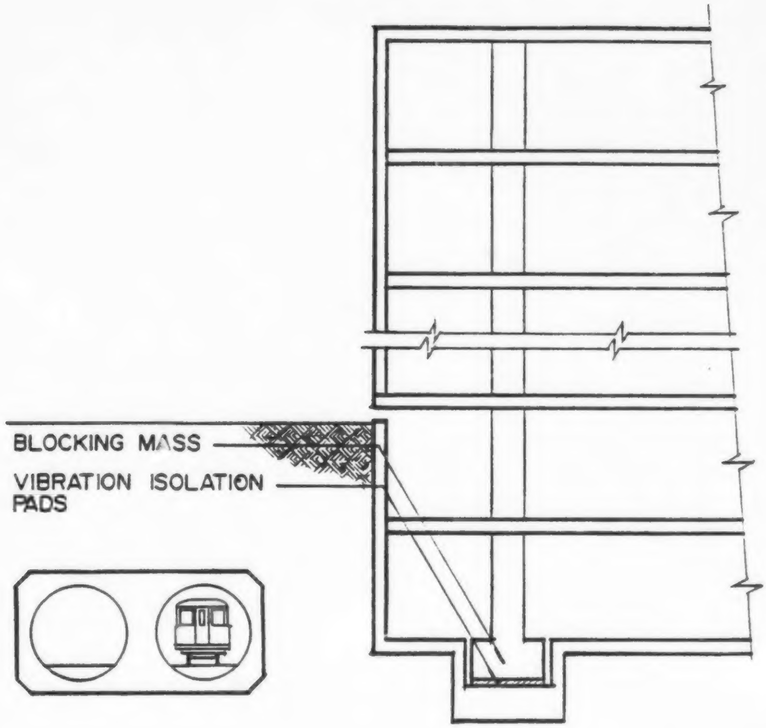

Figure 9. Building vibration isolation.

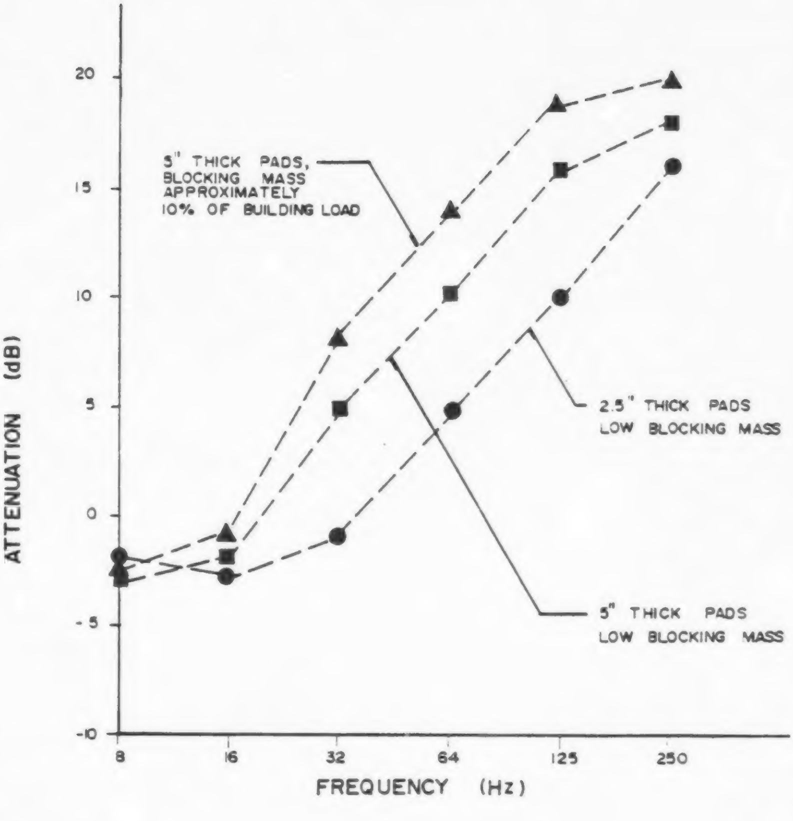

Figure 10. Typical characteristics for a vibration isolation system.

Symposium/Workshop on Serviceability of Buildings

May 16-18, 1988

LIST OF PARTICIPANTS

A

S.I. Al-Noury
Dept. of Civil Engineering
King Abdulaziz University
P.O. Box 9027
Jeddah 21413
Saudi Arabia

D.E. Allen
Institute for Research
in Construction
National Research Council
Ottawa, Ont.
Canada K1A 0R6

D.L. Allen
Vibron Limited
1720 Meyerside Drive
Canada L5T 1A3

B

H. Bachmann
Inst. f. Baustatik-Konstruktion
ETH-Hohggerberg
CH-8093 Zurich
Switzerland

R. Bergman
M.S. Yolles & Partners
85 Richmond Street W.
Suite 812
Toronto, Ont.
Canada M5H 2E6

F. Bljuger
Building Research Station
Israel Inst. of Technology
Haifa 32000
Israel

N.M. Brown
144 Front Street W.
Ste 510
Toronto, Ontario
Canada M5J 2L7

G. Burghardt
6207-179 Street
Edmonton, Alberta
Canada T5T 3B5

E.F.P. Burnett
Dept. of Civil Engineering
University of Waterloo
Waterloo, Ont.
Canada N2L 3G1

C

R. Cantieni
EMPA
Uberlandstr., 129
CH-8600 Duebendorf
Switzerland

J.R. Casas Rius
E.T.S. Enginyers de Camins
Calle Jordi Girona, 31
E-08034 Barcelona
Spain

E. Chien
Canadian Steel Construction
Council
201 Consumers Road
Suite 300
Willowdale, Ont.
Canada M2J 4G8.

S. Chu
Ontario Hydro
700 University Avenue
Toronto, Ont.
Canada M5G 1X6

Y.H. Chui
Dept. of Forest Engineering
University of New Brunswick
P.O. Box 4400
Fredericton, NB
Canada E3B 5A3

M.Z. Cohn
Dept. of Civil Engineering
University of Waterloo
Waterloo, Ont.
Canada N2L 3G1

M.P. Comeau
W.G. Campbell Engg. Ltd.
1730 Granville Street
Halifax, N.S.
Canada B3J 1X5

D

M.L. Daali
Dept. of Civil Engineering
Graduate Office
University of Waterloo
Waterloo, Ont.
Canada N2L 3G1

P. Desautels
17 Lascelles Blvd.
Suite 1203
Toronto, Ont.
Canada M4V 2X9

E

B.R. Ellingwood
Dept. of Civil Engineering
The Johns Hopkins University
3400 N. Charles Street
Baltimore, MD
USA 21218

M. Elnimeiri
Skidmore, Owings & Merrill
33 West Monroe Street
Chicago, IL
USA 60637

P.E. Eriksson
Division of Steel & Timber
Structures
Chalmers Univ. of Technology
S-412 96 Goteborg
Sweden

F

D. Frangopol
Dept. of Civil Engineering
University of Colorado
Boulder, CO
USA 80309-0428

J.A. Free
Dominion Bridge-Quebec
C.P. 500
Lachine, Que.
Canada H8S 4E7

K. Fujii
Inst. of Technology
Shimizu Corporation
4-17 Etchujima 3-Chome
Koto-Ku, Tokyo 135
Japan

Y. Fujino
Engineering Research Inst.
Faculty of Engineering
University of Tokyo
Bunkyo-Ku, Tokyo 113
Japan

D.K.W. Fung
Waterman Partnership
46-47 Blackfriars Road
London SE1 8PN
UK

G

A.S. Ghafeel
Republic Engin. Corp. Ltd.
7-D Kashmir-Egerton Road
Lahore
Pakistan

S.K. Ghosh
Portland Cement Association
1811 Cree Lane
Mount Prospect, IL
USA 60056

R. Green
Dept. of Civil Engineering
University of Waterloo
Waterloo, Ont.
Canada N2L 3G1

L.G. Griffis
Walter P. Moore & Associates
3131 Eastside, 2nd Floor
Houston, TX
USA 77098

H

J.C. Havard
Forintek Canada Corporation
800 Montreal Road
Ottawa, Ont.
Canada K1G 3Z5

J. Hofman
The Cohos Evamy Partnership
902-11th Avenue SW, Ste 200
Calgary, Alberta
Canada T2R 0E7

M. Holicky
Building Research Institute
Solinova 7
16608 Prague 6
Czechoslovakia

B. Howe
Vibron Limited
1720 Meyerside Drive
Mississauga, Ont.
Canada L5T 1A3

I

P.A Irwin
Rowan Williams Davies &
Irwin Inc.
650 Woodlawn Road, W
Guelph, Ont.
Canada N1K 1B8

N. Isyumov
Boundary Wind Tunnel
Dept. of Civil Engineering
University of Western Ontario
London, Ont.
Canada N6A 5B9

D. Ito
Housing Division
Asahi Chemical Industry Co.
21 Nishi-Shinjuku 1-chome
Meiho
Shinjuku–Ku, Tokyo 160
Japan

J

A.M. Jablonski
932 Elmsmere Road
Gloucester, Ont.
Canada K1J 7T6

D. Janssens
Canadian Wood Council
55 Metcalfe Street
Suite 1550
Ottawa, Ont.
Canada K1P 6L5

D.J. Jokela
Concrete & Silicate Lab
Technical Res. Center Finland
P.O. Box 26
SF-02151 Espoo
Finland

K

J. Kanda
Dept. of Architecture
Faculty of Engineering
University of Tokyo
7-3-1 Hongo
Bunkyo-Ku, Tokyo 113
Japan

P. Kelly
Adjeleian Allen Rubeli Ltd.
2221 Yonge Street, Suite 201
Toronto, Ont.
Canada M4S 1B5

J. Khan
Civil Engineering
Public Works Canada
Riverside Drive
Ottawa, Ontario
Canada K1A 0M2

K. Kimura
45 Mann Avenue
Suite 410
Ottawa, Ontario
Canada K1N 6Y7

A. King
Building Research Association
of New Zealand
Private Bag
Porirua, New Zealand

F. Knoll
Nicolet Chartrand Knoll & Ass.
1200 McGill College
Montreal, Que.
Canada H3B 4G7

J. Kong
Dept. of Civil Engineering
University of Waterloo
Waterloo, Ont.
Canada N2L 3G1

M. Kosugi
Dept. of Construction
Azusa Sekkey Company Ltd.
1-Chome Kuko
Ota-Ku, Tokyo
Japan

S. Kraemer
TUV Rheinland
2901 Bayview Avenue
Suite 208
North York, Ont.
Canada M2K 1E6

L

P.C. Lampman
Building Department
City of Hamilton
71 Main Street W.
Hamilton, Ont.
Canada L8N 3T4

A. Longinow
Wiss, Janney, Elstner
Assoc. Inc.
323N Taylor Avenue
Oak Park, IL 60302
USA

Z. Lounis
Civil Engineering Graduate
Office
University of Waterloo
Waterloo, Ont.
Canada N2L 3G1

M

J.G. MacGregor
Dept. of Civil Engineering
University of Alberta
Edmonton, Alberta
Canada T6G 2G7

W. Mak
Diand Technical Services
Public Works Canada
10 Wellington Street
Hull, Que.
Canada K1A 0H4

D. Mansell
Dept. of Civil and Agricultural
Engineering
University of Melbourne
Melbourne 3052
Australia

A. Masciantonio
Boundary Wind Tunnel
Dept. of Civil Engineering
University of Western Ontario
London, Ont.
Canada N6A 5B9

C. Matthews
Ctr. for Frontier Engineering
Research
University of Alberta Campus
C-FER Building
Edmonton, Alberta
Canada T6G 2E2

R.T. McBride
Geo Brandys & Assoc. Ltd.
5413 Doyle Street
Halifax, N.S.
Canada B3J 1H9

R. McGrath
Canadian Portland Cement
Association
116 Albert Street, Suite 609
Ottawa, Ont.
Canada K1P 6A1

W.E. McKevitt
4473 West 14th Avenue
Vancouver, B.C.
Canada V6R 2Y2

N. Mezlekia
Dept. of Civil Engineering
University of Waterloo
Waterloo, Ont.
Canada N2L 3G1

C.J. Montgomery
916 Rice Road
Edmonton, Alberta
Canada T6R 1A1

T.B. Morris
Morris Engineering
5952 Royal Lane, Suite 109
Dallas, TX
USA 75230

T. Murray
Virginia Technology
200 Patton Hall
Blacksburg, PA 24061
USA

N

D.B. Najdanovic
Gradjevinski FakultetIMK
Bulevar Revolucije, 73
11000 Belgrad
Yugoslavia

G. Nawar
University of New South Wales
Box 1
Kensington, NSW 2033
Australia

B. Neil
Adjeleian Allen Rubeli Ltd.
2221 Yonge Street, Ste. 201
Toronto, Ont.
Canada M4S 1B5

E. Nemestothy
Dept. of Strength of Materials
and Structures
Technical Univ. of Budapest
H-1521 Budapest
Hungary

S.H.P. Niu
Dept. of Civil Engineering
University of Missouri
600 W. Mechanic
Independence, MO 64050
USA

O

A. Oberti
2005 Dutrisac, Apt. 503
St-Laurent, Quebec
Canada H4L 4K8

S. Ohlsson
Dept. of Structural Engineering
Chalmers Univ. of Technology
S-412 96 Goteborg
Sweden

T. Okuma
Dept. of Architecture
Faculty of Mech. Engineering
Kanagawa University
3-27-1 Rokakubashi
Yokahama 221
Japan

D.M. Onysko
Forintek Canada Corporation
800 Montreal Road
Ottawa, Ont.
Canada K1G 3Z5

P

G. Pernica
Inst. for Research in
Construction
National Research Council
Ottawa, Ontario
Canada K1A 0R6

S.G. Pinjarkar
835 Midway Drive
Willowbrook, IL 60521
USA

R

D. Raghu
Dept. of Civil Environ. Engg.
New Jersey Inst. of Technology
Newark, NJ 07102
USA

J.H. Rainer
Inst. for Research in
Construction
National Research Council
M-20, Room 159
Ottawa, Ont.
Canada K1A 0R6

P. Riva
Dept. of Civil Engineering
University of Waterloo
Waterloo, Ont.
Canada N2L 3G1

S. Robins
McNeely Engineering &
Structures Ltd.
815 Princess Street
Kingston, Ont.
Canada K7L 1G6

I. Rosenthal
Building Research Station
Technion City, Haifa 32000
Israel

S

M. Saatcioglu
Dept. of Civil Engineering
University of Ottawa
Ottawa, Ont.
Canada K1N 6N5

R.L. Sack
Dept. of Civil Engineering
University of Idaho
Moscow, Idaho 83843
USA

M. Sacks
Tacet Engineering Ltd.
111 Ava Road
Toronto, Ont.
Canada M6C 1W2

J.J. Salinas
Dept. of Civil Engineering
Carleton University
Colonel By Drive
Ottawa, Ont.
Canada K1S 5B6

A. Scanlon
Dept. of Civil Engineering
Pennsylvania State University
University Park, PA 16802
USA

A. Schriver
Dept. of Civil Engineering
University of New Brunswick
P.O. Box 4400
Fredericton, NB
Canada E3B 5A3

F. Scott
3950 Hickmore Avenue
St-Laurent, Quebec
Canada H4T 1K2

R. Sheldon
W.P. Brown & Partners Pty Ltd
3 Lynch Street
Hawthorn, Victoria, 3122
Australia

K. Shioya
Inst. of Technology
Shimizu Corporation
4-17 Etchujima 3-Chome
Koto-Ku, Tokyo 135
Japan

I. Smith
Dept. of Forest Engineering
University of New Brunswick
Box 4400
Fredericton, NB
Canada E3B 5A3

K.N. Smith
McNeely Engineering &
Structures Ltd.
815 Princess Street
Kingston, Ont.
Canada L4J 4S2

M. Sommerstein
75 Green Acres Road
Thornhill, Ontario
Canada L4J 4S2

R.A. Strachan
3984 - 19th Avenue W
Vancouver, BC
Canada V6T 1W5

J.C. Swallow
Barman Swallow Associates
1 Greensboro Drive, Ste 401
Rexdale, Ontario
Canada M9W 1C8

K. Swensson
Stanley D. Lindsey &
Assoc. Ltd.
1906 West End Avenue
Nashville, TN
USA 37203-2371

T

Y. Tamura
Dept. of Architecture
Faculty of Mechanical
Engineering
Tokyo Inst. of Polytechnics
1583 Iiyama
Atsugi, Kanagawa
Japan

R. Tardao
21 Havelock Street
Toronto, Ont.
Canada M6H 3B4

R. Tolaymat
Le Messurier Consultants
P.O. Box 1124
Cambridge, MA
USA 02238

R. Tremblay
Engineering & Operations
Honco Inc.
1191 Chemin Industriel
Bernieres, Quebec
Canada G0S 1C0

R. Tuttle
Ottawa-Carleton Regional
Housing Authority
1545 Carling Avenue, Ste 700
Ottawa, Ont.
Canada K1Z 8R3

W

R. Wadzinski
Contract Glass & Metal
Division
AFG Glass Inc.
75 Doney Crescent
Downsview, Ontario
Canada L4K 1P6

R.L. Wardlaw
NAE-Low Speed
Aerodynamics
Lab
National Research Council
Ottawa, Ontario
Canada K1A 0R6

M.A. West
Computerized Structural
Design Inc.
8989 North Port Washington
Road
Milwaykee, WI 53217
USA

Y

Z.C. Yao
Dept. of Civil Engineering
University of British Columbia
Vancouver, BC
Canada V6T 1W5